

UNCLASSIFIED

AD NUMBER
AD921578
NEW LIMITATION CHANGE
TO Approved for public release, distribution unlimited
FROM Distribution authorized to U.S. Gov't. agencies only; Test and Evaluation; 28 AUG 1974. Other requests shall be referred to Air Force Flight Dynamics Lab., Wright-Patterson AFB, OH 45433.
AUTHORITY
AFFDL ltr, 28 Nov 1979

THIS PAGE IS UNCLASSIFIED

THIS REPORT HAS BEEN DELIMITED
AND CLEARED FOR PUBLIC RELEASE
UNDER DOD DIRECTIVE 5200.20 AND
NO RESTRICTIONS ARE IMPOSED UPON
ITS USE AND DISCLOSURE.

DISTRIBUTION STATEMENT A

APPROVED FOR PUBLIC RELEASE;
DISTRIBUTION UNLIMITED.

✓
AFFDL-TR-74-17

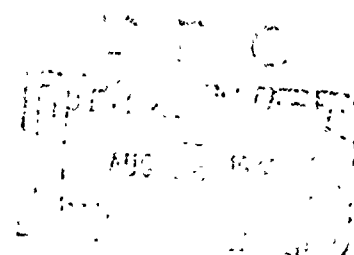
AD921578

**ADVANCED METALLIC AIR VEHICLE
STRUCTURE PROGRAM**

**PHASE II - DETAIL DESIGN AND ANALYSIS
SUMMARY REPORT - TECHNICAL**

C. E. HART, ET AL.

GENERAL DYNAMICS
Convair Aerospace Division
Fort Worth Operation



TECHNICAL REPORT AFFDL-TR-74-17

January 1974

26 AUG 1974

Distribution limited to U.S. Government Agencies only.
Reason: Test and Evaluation. Other requests for this
document must be referred to Air Force Flight Dynamics
Laboratory/FBA, Wright-Patterson Air Force Base, Ohio
45433.

Air Force Flight Dynamics Laboratory
Air Force Systems Command
Wright-Patterson Air Force Base, Ohio 45433

NOTICES

When Government drawings, specifications, or other data are used for any purpose other than in connection with a definitely related Government procurement operation, the United States Government thereby incurs no responsibility nor any obligation whatsoever; and the fact that the government may have formulated, furnished, or in any way supplied the said drawings, specifications, or other data, is not to be regarded by implication or otherwise as in any manner licensing the holder or any other person or corporation, or conveying any rights or permission to manufacture, use, or sell any patented invention that may in any way be related thereto.

Copies of this report should not be returned unless return is required by security considerations, contractual obligations, or notice on a specific document.

ADVANCED METALLIC AIR VEHICLE STRUCTURE PROGRAM

PHASE II - DETAIL DESIGN AND ANALYSIS SUMMARY REPORT - TECHNICAL

Distribution limited to U.S. Government Agencies only. *8 AUG 1974*
Reason: Test and Evaluation. Other requests for this
document must be referred to Air Force Flight Dynamics
Laboratory/FBA, Wright-Patterson Air Force Base, Ohio
45433.

FOREWORD

This report presents the results of Phase II - Detail Design and Analysis of a wing carrythrough structure for an advanced metallic moveable wing aircraft. The efforts reported herein were sponsored by the Air Force Flight Dynamics Laboratory (AFFDL) under joint management and technical direction of AFFDL and the Air Force Materials Laboratory, Wright-Patterson Air Force Base, Ohio.

This work was performed under contract F33615-73-C-3001 "Advanced Metallic Air Vehicle Structure" (AMAVS) as part of the Advanced Metallic Structures, Advanced Development Programs (AMS ADP), Program Element Number 63211F, Project Number 486U. John C. Frishett, Major, USAF, is the ADP Manager while Mr. Frank D. Boensch is the Project Engineer for the AMAVS Program.

Phase Ia of this program has been previously reported in AFFDL-TR-73-4, Volume I, Parts 1 and 2, and Volume II.

Principal Convair contributors to this report were:


C. E. Hart	- Program Manager
R. C. Bissell	- Deputy Program Manager
D. L. Duncan	- Non-Destructive Inspection
E. L. Hensley	- Design and Structures
J. W. Jennings	- Information Transfer
J. L. McDaniel	- Manufacturing Engineering
Dr. H. I. McHenry	- Fracture and Fatigue Analysis
R. E. Miller	- Stress Analysis
W. O. Sunafrank	- Manufacturing Engineering
J. M. Shults	- Materials Engineering
A. F. Stern	- Structural Design
W. M. Walker	- Test Coordination

This work was performed during the period 1 February 1973 to 9 November 1973. It was submitted by the authors in January 1974.

This technical report has been reviewed and is approved for publication.



Frank D. Boensch
Project Engineer



John C. Frishett, Major, USAF
Program Manager
AMS Program Office
Structures Division

A B S T R A C T

This report covers the design, analysis, manufacturing and testing done during Phase II, Detail Design, of the Advanced Metallic Air Vehicle Structure (AMAVS) program. The objectives of Phase II were to complete the detail design work for two configurations of a wing carrythrough structure for a movable-wing aircraft, to complete materials and component testing in support of the two configurations, to select one of the configurations for manufacture in Phase III and to continue design and manufacture of a fixture for full-scale testing of the carrythrough structure.

Additional trade studies and design optimization studies were conducted in the early part of Phase II for the two configurations selected in Phase Ib: Fail Safe Integral Lug (FSIL) and "No-Box" Box (NBB). An updated baseline data package was received during Phase II and the configurations were revised to meet the modified baseline requirements.

Material testing and component testing were completed. Beta annealed 6Al-4V and Beta C titanium and 10Ni steel (HY180) were used in these tests.

Some detail design work remains on the full-scale test fixture but manufacturing has started. Manufacture of the simulated fuselage structure has also begun.

The NBB configuration which utilizes the outstanding fracture toughness and good crack growth characteristics of 10Ni steel has been selected for manufacture in Phase III.

T A B L E O F C O N T E N T S

<u>Section</u>		<u>Page</u>
1	INTRODUCTION	1-1
2	TECHNICAL DISCIPLINES PROGRESS	2-1
2.1	Structural Design	2-1
2.1.1	"No-Box" Box	2-1
2.1.2	Fail-Safe Integral Lug Configuration	2-33
2.2	Structural Analysis	2-77
2.2.1	Design Loads	2-78
2.2.2	Node Point Loads for Math Models	2-105
2.2.3	NBB Stress Analysis	2-124
2.2.4	Fail Safe Integral Lug	2-126
2.2.5	Common and Miscellaneous	2-127
2.2.6	Stiffness Analysis	2-129
2.2.7	Effect of Updated Loads on Weight	2-129
2.2.8	Simulated Fuselage	2-131
2.3	Fatigue and Fracture Analysis	2-137
2.3.1	Fatigue Analysis	2-137
2.3.2	Fatigue Crack Growth Test Data	2-167
2.3.3	Crack Growth Analysis	2-183
2.3.4	Fracture Analysis of Selected Control Points	2-185
2.3.5	Fracture Control Plan	2-204
2.3.6	Finite Element Fracture Analysis	2-204
2.3.7	Fatigue Life Variability	2-216
2.4	Materials Engineering	2-222
2.4.1	Material Selection	2-222
2.4.2	Material Procurement	2-222
2.4.3	Materials Testing	2-226
2.4.4	Brazing Development	2-226
2.4.5	Welding Development	2-254
2.4.6	Adhesive Bonding Development	2-256
2.4.7	Materials and Process Specifications	2-256
2.4.8	Corrosion Prevention System	2-259

TABLE OF CONTENTS (Continued)

<u>Section</u>		<u>Page</u>
2.5	Weights	2-260
2.6	Configuration Ratings	2-265
2.7	Configuration Selection	2-268
3	TESTING	3-1
3.1	Material Testing	3-1
3.2	Component Testing	3-1
3.2.1	Test Results	3-2
3.3	Full-Scale Testing	3-12
3.3.1	Progress During Phase II	3-12
3.4	Aluminum-Manganese Coating for Steel Bolts	3-18
4	QUALITY ASSURANCE AND NDI	4-1
4.1	Bonding Evaluations	4-1
4.2	Brazed Joint Evaluations	4-6
4.2.1	NDI Development	4-6
4.2.2	Engineering Specimen Evaluation	4-11
4.3	Welded Joint Evaluations	4-15
4.3.1	NDI Specimen Design and Fabrication	4-15
4.3.2	Transducer Evaluation	4-15
4.3.3	Engineering Specimen Inspection	4-15
4.3.4	Shear Ultrasonic Techniques, 6Al-4V Titanium	4-17
4.3.5	Delta Ultrasonic Techniques, 6Al-4V Titanium	4-17
4.3.6	Pulse Echo Longitudinal Evaluation, 6Al-4V Titanium	4-17
4.3.7	Pulse Echo/Longitudinal Evaluation, 10 Nickel Specimen	4-19
4.3.8	Evaluation Summary	4-19

TABLE OF CONTENTS (Continued)

<u>Section</u>	<u>Page</u>
4.4 NDI Plans	4-22
5 MANUFACTURING DEVELOPMENT	5-1
5.1 Laminated Brazing Process Development	5-1
5.1.1 603FTB033 Test Specimen, Damage Tolerance, Braze Lower Plate Element	5-1
5.1.2 603FTB053 Braze Test Specimen Centerline Splice Lower Plate	5-5
5.1.3 603FTB035 Braze Lower Plate Damage Tolerance Test Specimen	5-5
5.2 Wide-Area Adhesive Bonding	5-48
5.3 Welding 10Ni Steel	5-59
5.3.1 Electron Beam Welding	5-59
5.3.2 Gas Tungsten Arc Welding	5-71
5.4 Metallurgical Evaluation of 10Ni Steel	5-78
5.4.1 Thermal Treatment	5-78
5.4.2 Microstructure Evaluation	5-80
5.4.3 Microhardness Tests	5-80
5.5 Machining	5-83
5.5.1 Machinability Evaluation of 10Ni Steel	5-83
5.6 Assembly of Group II Production Verifi- cation Test Specimens	5-96
5.6.1 603FTB052 Lower Lug to Rail Splice Assembly	5-96
5.6.2 603FTB053 Lower Plate Centerline Splice Assembly	5-99
5.6.3 603FTB035 Braze Lower Plate Assembly	5-103
5.7 Machining of 603FTB043 Upper Cover Group II Test Specimen	5-103

TABLE OF CONTENTS (Continued)

<u>Section</u>	<u>Page</u>
APPENDIX A	A-1

LIST OF ILLUSTRATIONS

<u>Figure</u>		<u>Page</u>
2-1	Plate Assembly - Pivot Lug, Lower	2-3
2-2	Bulkhead Installation - Y _F 932.00	2-9
2-3	Bulkhead Installation - Y _F 992, Wing Carrythrough	2-15
2-4	Cover Installation - Upper Y _F 932 to Y _F 992	2-23
2-5	Rib Installation - Centerline Y _F 932 to Y _F 992	2-29
2-6	Rib Installation - X _F 39, Wing Carrythrough	2-31
2-7	Rib Installation - X _F 84, Wing Carrythrough	2-35
2-8	Rib Installation - Outboard Closure	2-37
2-9	Lower Plate, Wing Carrythrough Assembly	2-43
2-10	Plate, Lower - Wing Carrythrough Assembly	2-47
2-11	Upper Plate Installation - Y _F 932 to Y _F 992	2-51
2-12	Bulkhead Installation - Wing Carrythrough, Y _F 932	2-57
2-13	Bulkhead Installation - Wing Carrythrough, Y _F 947	2-63
2-14	Bulkhead Installation - Y _F 977.00	2-65
2-15	Bulkhead Installation - Y _F 992	2-67
2-16	Rib Installation - Closure, X _F 119, Canted	2-71
2-17	Rib Installation - X _F 84.00	2-75

L I S T O F I L L U S T R A T I O N S (Continued)

<u>Figure</u>		<u>Page</u>
2-18	NARSAP-ASKA Math Model Interface Load Geometry Y _F 932 Bulkhead	2-85
2-19	NARSAP-ASKA Math Model Interface Load Geometry Y _F 992 Bulkhead	2-89
2-20	Wing Sweep Actuator Geometry	2-96
2-21	Main Landing Gear Fitting Geometry	2-97
2-22	Main Landing Gear Emergency Hyd. Actuator Cyl. Loads and Geometry vs. Gear Rotation	2-100
2-23	Fuel Tank Pressures - AMAVS	2-101
2-24	Y _F 932 Geometry for CAD Panel Point Loads Resolution	2-106
2-25	Y _F 992 Geometry for CAD Panel Point Loads Resolution	2-107
2-26	Geometry for Determination of WCTS Lug Loads	2-112
2-27	Simulated Fuselage Math Model	2-132
2-28	Forward Simulated Fuselage Shear Flow and Longeron Location Diagram - Y _F 891-932	2-135
2-29	Aft Simulated Fuselage Shear Flow and Longeron Location Diagram Y _F 992-1021	2-136
2-30	S-N Curves, 6Al-4V Titanium	2-138
2-31	S-N Curves, 6Al-4V Titanium	2-139
2-32	S-N Curves, 6Al-4V Titanium	2-140
2-33	Constant Life Fatigue Diagram for Beta Annealed 6Al-4V Titanium, $K_T = 2.4$	2-141

LIST OF ILLUSTRATIONS (Continued)

<u>Figure</u>		<u>Page</u>
2-34	Constant Life Fatigue Diagram for Beta Annealed 6Al-4V Titanium, $K_T = 5$	2-142
2-35	S-N Curves, 6Al-4V Titanium	2-143
2-36	S-N Curves, 6Al-4V Titanium	2-144
2-37	S-N Curves, 6Al-4V Titanium	2-145
2-38	S-N Curves, 10 Nickel Steel	2-146
2-39	S-N Curves, 10 Nickel Steel	2-147
2-40	S-N Curves, 10 Nickel Steel	2-148
2-41	Constant Life Fatigue Diagram for 10 Ni Steel, $K_T = 2.4$	2-149
2-42	Constant Life Fatigue Diagram for 10 Ni Steel, $K_T = 5$	2-150
2-43	S-N Curves, 10 Nickel Steel	2-151
2-44	S-N Curves, 10 Nickel Steel	2-152
2-45	S-N Curves, 10 Nickel Steel	2-153
2-46	S-N Curves, Beta C Titanium	2-154
2-47	S-N Curves, Beta C Titanium	2-155
2-48	S-N Curves, Beta C Titanium	2-156
2-49	S-N Curves, Beta C Titanium	2-157
2-50	S-N Curves, 10 Nickel Steel	2-159
2-51	S-N Curves, 10 Nickel Steel	2-160
2-52	S-N Curves, 10 Nickel Steel	2-161
2-53	Fatigue Data Summary	2-162

LIST OF ILLUSTRATIONS (Continued)

<u>Figure</u>		<u>Page</u>
2-54	S-N Curves, 10 Nickel Steel	2-163
2-55	Fatigue Crack Growth, 10 Nickel Steel	2-169
2-56	Fatigue Crack Growth, Beta C Titanium	2-170
2-57	Fatigue Crack Growth, Beta C Titanium	2-171
2-58	Fatigue Crack Growth, Beta C Titanium	2-172
2-59	Crack Growth Test, Beta Annealed 6Al-4V Titanium, FJT10940-153, Spec. 1	2-173
2-60	Crack Growth Test, Beta Annealed 6Al-4V Titanium, FJT10940-153, Spec. 2	2-174
2-61	Crack Growth Test, Beta Annealed 6Al-4V Titanium, FJT10940-153, Spec. 1	2-175
2-62	Crack Growth Test, Beta Annealed 6Al-4V Titanium, FJT10940-153, Spec. 1	2-176
2-63	Crack Growth Test, Beta Annealed 6Al-4V Titanium, FJT10940-153, Spec. 2	2-177
2-64	Crack Growth Test, Beta Annealed 6Al-4V Titanium, FJT10940-152, Spec. 1	2-178
2-65	Crack Growth Test, Beta Annealed 6Al-4V Titanium, FJT10940-152, Spec. 2	2-179
2-66	Crack Growth Test, 10 Nickel Steel, FJT10940-185, Spec. 1	2-180
2-67	Crack Growth Test, 10 Nickel Steel, FJT10940-186, Spec. 1	2-181
2-68	Crack Growth Test, 10 Nickel Steel, FJT10940-186, Spec. 2	2-182
2-69	Critical Crack Length vs. Gross Section Stress	2-188

L I S T O F I L L U S T R A T I O N S (Continued)

<u>Figure</u>		<u>Page</u>
2-70	FSIL Control Point 1; Upper Plate, Aft. Outboard Weld Line	2-190
2-71	FSIL Control Point 2; FSIL YF992 Bulkhead Attach Angle	2-191
2-72	FSIL Control Point 3; YF992 Bulkhead, Aft Lower, Outboard	2-192
2-73	FSIL Control Point 4; Lower Lug	2-193
2-74	FSIL Control Point 5; Lower Plate and Splice	2-194
2-75	FSIL Control Point 6; YF992 Bulkhead, Inboard	2-195
2-76	FSIL Control Point 7; YF932 Bulkhead, Lower Outboard Attach Angle	2-196
2-77	NBB Control Point 1; YF992 Bulkhead, Lower Plate	2-198
2-78	NBB Control Point 2; Lower Lug, Aft	2-199
2-79	NBB Control Point 3; Lower Plate, Lug	2-200
2-80	NBB Control Point 4; Lower Plate, Aft Outboard Cutout	2-201
2-81	NBB Control Point 5; YF932 Bulkhead Lower Flange	2-202
2-82	NBB Control Point 6; NBB Upper Aft, Outboard	2-203
2-83	Fracture Critical Parts List	2-205
2-84	Material Traceability Requirements for the AMAVS Program	2-207
2-85	A Four-Bay Brazed Panel With a Center Crack Under Uniform Tension	2-210

L I S T O F I L L U S T R A T I O N S (Continued)

<u>Figure</u>		<u>Page</u>
2-86	K_I and K_{II} vs. A of an Eccentrically Cracked Lower Panel Specimen	2-211
2-87	A Thru-Crack Embedded in the First Bay of the Lower Panel Specimen	2-212
2-88	A Typical Finite Element Simulation of the Brazed Lower Panel Specimen	2-213
2-89	K_I and K_{II} vs. a of A Center Cracked Lower Panel Specimen	2-215
2-90	Weibull Plot of Beta Annealed 6Al-4V Titanium Reliability Test Data	2-218
2-91	Weibull Plot of Beta C Reliability Test Data	2-219
2-92	Weibull Plot of 10 Nickel Steel Reliability Tests	2-220
2-93	Weibull Plot of Beta Annealed 6Al-4V Titanium, Single Ply and 2 Ply Braze, Reliability Test Data	2-221
2-94	603FTB035 Re-Braze	2-229
2-95	603FTB035 Re-Braze	2-230
2-96	603FTB035 Re-Braze	2-231
2-97	603FTB035 Re-Braze	2-232
2-98	603FTB035 Re-Braze	2-233
2-99	603FTB035 Re-Braze	2-234
2-100	603FTB035 Re-Braze	2-237
2-101	603FTB035 #2	2-239
2-102	603FTB035 #2	2-240
2-103	603FTB035 #2	2-241

L I S T O F I L L U S T R A T I O N S (Continued)

<u>Figure</u>		<u>Page</u>
2-104	603FTB035 #2	2-242
2-105	603FTB035 #2	2-243
2-106	603FTB035 #2	2-244
2-107	603FTB035 #2	2-246
2-108	AMAVS Brazing Cycle for 603FTB035 #2	2-247
2-109	Sustained Load Stress Corrosion Test Braze Single Lap Shear Specimens	2-251
2-110	Microsection of Braze Line of Stress Corro- sion Specimen 11-28 Removed from MR&D Panel No. 28, 750X	2-252
2-111	Microsection of Braze Line Removed from MR&D Panel No. 25A, 750X	2-252
2-112	Microsection of Braze Line Removed from 603FTB035 #1 Panel, 750X	2-253
2-113	Microsection of Braze Line Removed from 603FTB035 #2 Panel, 750X	2-253
2-114	AMAVS Brazing Cycle Time-Temperature Boundaries	2-255
2-115	Convair Aerospace Division Problem 005485-05	2-263
2-116	Convair Aerospace Division Problem 005485-06	2-264
3-1	Test Specimen - Damage Tolerance, Braze Lower Plate Element	3-3
3-2	Edge Cracked Crack Growth Test	3-5
3-3	603FTB035 Test Specimen in Test Fixture	3-7
3-4	Upper Cover Compression Test Specimen in the 1,000,000 Pound Test Machine	3-9

L I S T O F I L L U S T R A T I O N S (Continued)

<u>Figure</u>		<u>Page</u>
3-5	Test Specimen in Test Fixture	3-10
3-6	FSIL Centerline Splice Specimen in Fatigue Fixture	3-11
3-7	AMAVS Full Scale Test	3-13
3-8	Reassembly Sequence - Lower Fixture	3-14
3-9	Reassembly Sequence - Second Shipment of Hardware	3-15
3-10	Reassembly Sequence - Final Hardware Shipment	3-16
3-11	Taper-Lok Fasteners Installed in Titanium Specimens	3-19
3-12	Taper-Lok Fasteners Installed in Titanium Specimens	3-19
4-1	Typical Through Transmission C-Scan Recording of an NDI Sandwich Panel	4-4
4-2	Flat Bottom Holes and an Elox Slat Evaluated as Flaw Induction Methods	4-8
4-3	A "Good" Area Showed a Relatively Low Signal at the Gate	4-10
4-4	A Defective Area was Indicated by a Relatively High Signal in the Gate	4-10
4-5	The Schlieren System Indicates One Cross Section of the Soundbeam to be Strong	4-12
4-6	Because of a Malfunction in the Transducer Part of the Soundbeam is Missing	4-12
4-7	The Ultrasonic Inspection of 603FTB035-7 Recorded in a C-Scan Mode	4-13

LIST OF ILLUSTRATIONS (Continued)

<u>Figure</u>		<u>Page</u>
4-8	Ultrasonic Recording of 603FTB053-21	4-14
4-9	NDI Welded Specimens	4-16
4-10	6AL-4V(A) and 10 Ni(B) Flat Bottomed Hole References	4-16
4-11	Typical Pulse-Echo Recordings of 10 Ni Weld and Preliminary Reference Specimen	4-18
4-12	Variable Depth/Angle Delta Probe Fixture	4-18
4-13	Typical 6Al-4V B Weld Responses Using Pulse Echo Longitudinal Technique	4-20
4-14	Metallographic Sections of Flaws in Specimen H27(A) and H9(B)	4-20
4-15	Radiographic/Ultrasonic Comparisons for the Inspections of 10 Ni Specimen H9	4-21
4-16	Raw Material and Brazed NDI Specimens	4-23
4-17	EB and GTA Welding	4-25
4-18	Bonded Sandwich NDI Specimens	4-27
5-1	Titanium Details for 603FTB033 Braze Test Specimen	5-2
5-2	Titanium Details for 603FTB033 Braze Test Specimen Assembled in Braze Box	5-2
5-3	Prebraze Cycle for 603FTB033 Test Specimen	5-3
5-4	Braze Cycle for 603FTB033 Test Specimen	5-3
5-5	603FTB033 Brazed Test Specimen After Removal From Braze Box	5-4
5-6	Lower Plate Titanium Detail of 603FTB033 Test Specimen With Braze Alloy Tack Welded in Place	5-6

LIST OF ILLUSTRATIONS (Continued)

<u>Figure</u>		<u>Page</u>
5-7	Braze Cycle for 603FTB053 Run #1	5-7
5-8	Braze Cycle for 603FTB053 Run #2	5-7
5-9	Brazed Test Specimen 603FTB053 in Braze Box Tooling	5-8
5-10	Gas Fired Holden Pacific Furnace for Brazing 603FTB035 Test Specimens	5-9
5-11	Thermocouple Locations for 603FTB035 Test Part Preblaze Cycle	5-10
5-12	Preblaze Cycle for 603FTB035 Test Specimen Thermocouples 1, 2 and 3	5-11
5-13	Preblaze Cycle for 603FTB035 Test Specimen Thermocouples 4, 5, and 6	5-11
5-14	Tooling and Test Specimen Components of 603FTB035 Preblaze Cycle	5-12
5-15	Braze Cycle for 603FTB035 Test Specimen Run #1 Thermocouple No. 1	5-21
5-16	Braze Cycle for 603FTB035 Test Specimen Run #1 Thermocouple No. 2	5-21
5-17	Braze Cycle for 603FTB035 Test Specimen Run #1 Thermocouple No. 3	5-22
5-18	Braze Cycle for 603FTB035 Test Specimen Run #1 Thermocouple No. 4	5-22
5-19	Braze Cycle for 603FTB035 Test Specimen Run #1 Thermocouple No. 5	5-23
5-20	Braze Cycle for 603FTB035 Test Specimen Run #1 Thermocouple No. 6	5-23
5-21	Lay-Up of 603FTB035-3C Illustrating Dummy Panel, Center Lamina and 7-1/2 x 12" Test Specimen Locations	5-25

L I S T O F I L L U S T R A T I O N S (Continued)

<u>Figure</u>		<u>Page</u>
5-22	Tooling, Lay-Up and Thermocouple Entries for 603FTB035-3C	5-26
5-23	Braze Cycle for 603FTB035-3C Thermocouple #7	5-27
5-24	Braze Cycle for 603FTB035-3C Thermocouple #1	5-28
5-25	Braze Cycle for 603FTB035-3C Thermocouple #2	5-28
5-26	Braze Cycle for 603FTB035-3C Thermocouple #3	5-28
5-27	Braze Cycle for 603FTB035-3C Thermocouple #4	5-28
5-28	Braze Cycle for 603FTB035-3C Thermocouple #6	5-29
5-29	Braze Cycle for 603FTB035-3C Thermocouple #8	5-29
5-30	Braze Cycle for 603FTB035-3C Thermocouple #9	5-29
5-31	Braze Cycle for 603FTB035-3C Thermocouple #10	5-29
5-32	Braze Components for 603FTB035-(7A)	5-31
5-33	Braze Box Tooling Illustrating Thermo- couple Locations	5-32
5-34	Braze Box Tooling Illustrating Cant Sheets, Argon Lines, and Vacuum Line	5-32
5-35	Braze Box Illustrating Argon Gas Lines for Purging Lower Lamina Hog-outs	5-33
5-36	Braze Box Illustrating Titanium Lamina and Filler Blocks	5-33

L I S T O F I L L U S T R A T I O N S (Continued)

<u>Figure</u>		<u>Page</u>
5-37	Complete Lay-Up for 603FTB035-7A	5-34
5-38	Upper Titanium Detail for 603FTB035-7A Braze Test Specimen Immediately after Acid Clean	5-41
5-39	Lay-Up of Braze Alloy on Lower Plate of 603FTB035-7A Test Specimen	5-41
5-40	Placement of Center Titanium Detail After Lay-Up of Braze Alloy on Lower Titanium Detail - 603FTB035-7A	5-42
5-41	Lay-Up of Braze Alloy on Upper Surface of Center Titanium Plate (Top Braze Line) for 603FTB035-7A	5-42
5-42	Final Alloy Lay-Up on Center Titanium Detail of 603FTB035-7A	5-43
5-43	Insertion of Filler Blocks in Hog-Outs of Upper Titanium Detail of 603FTB035-7A	5-43
5-44	Placement of Cover Sheets on Top of Laid- Up Assembly of 603FTB035-7A	5-44
5-45	Welding Vacuum Sheet on Braze Box Retort for 603FTB035-7A	5-44
5-46	Heat-Up Rate Comparison of 603FTB035-3C and -7A	5-45
5-47	Braze Cycle for 603FTB035-7A Thermocouple #1	5-45
5-48	Braze Cycle for 603FTB035-7A Thermocouple #2	5-46
5-49	Braze Cycle for 603FTB035-7A Thermocouple #3	5-46

L I S T O F I L L U S T R A T I O N S (Continued)

<u>Figure</u>		<u>Page</u>
5-50	Braze Cycle for 603FTB035-7A Thermocouple #4	5-47
5-51	Braze Cycle for 603FTB035-7A Thermocouple #5	5-47
5-52	Upper Plate Surface of Brazed 603FTB035-7A	5-49
5-53	Lower Plate Surface of Brazed 603FTB035-7A	5-49
5-54	Brazed Test Specimen 603FTB035-7A Ready for Removal from Braze Box (Upper Surface)	5-50
5-55	Lower Surface of Braze Test Specimen 603FTB035-7A	5-50
5-56	Braze Surface of Center Titanium Plate for 603FTB035-7A	5-51
5-57	Liquidus/Solidus Curve for Braze Alloy used in 603FTB035-3C	5-52
5-58	Liquidus/Solidus Curve for Braze Alloy Used in 603FTB035-7A	5-52
5-59	Simulated 4 Ply Bulkhead Panel (Adhesive Bonded Beta C Titanium)	5-53
5-60	Chemically Etched Test Panel (1/8 x 36 x 40 Inch Beta C Titanium)	5-55
5-61	Overall Warpage of 1/8 Inch Beta C Test Panel from Chemical Etching	5-56
5-62	Warpage Resulting from Chemical Etching 0.060 Inch Deep Pockets in 1/8 Inch Beta C Titanium	5-57
5-63	Thickness Measurements Before and After Chemical Etching of Beta C Titanium Sheet	5-58

L I S T O F I L L U S T R A T I O N S (Continued)

<u>Figure</u>		<u>Page</u>
5-64	EB Weld Root of 1.6 Inch Thick 10 Ni Steel Showing Globular and Uniform Penetration	5-60
5-65	X-Ray of Weld Specimen from Figure 5-64 Showing Voids and Microfissures	5-60
5-66	Macro and Micro Structure of EB Welded .500 Inch Thick 10 Ni Steel (Weld No. H10)	5-62
5-67	Macros of EB Welds on 1.61 Inch Thick 10 Ni Steel Showing Typical Microfissures and Good Weld	5-63
5-68	Macro and Micro Structure of EB Welded .500 Inch Thick 10 Ni Steel (Weld No. H11)	5-64
5-69	Failed Tensile Specimens from EB Welded .500 Inch Thick 10 Ni Steel Showing Fracture	5-70
5-70	Test Plate J-Groove Configuration	5-72
5-71	Section of GTA Weld Fixture	5-72
5-72	Setup for Using Weld Tabs	5-73
5-73	Combination GTA and EB Weld Fixture for Welding Bulkhead Test Specimens	5-79
5-74	Comparison of Microstructure of 10 Ni Steel Using Various Etchants on Base and GTA Weld Metal (200X)	5-81
5-75	Microstructure of Solution Treated and Solution Treated and Aged 10 Ni Steel - 2% Nital Etchant (200X)	5-82
5-76	Macro and Micro Structure of Multipass GTA Welded and Reaged 10 Ni Steel (Etchant - 25% HNO ₃ + Ethanol)	5-85

L I S T O F I L L U S T R A T I O N S (Continued)

<u>Figure</u>		<u>Page</u>
5-77	10 Ni Steel Plate Used for Boring, Drilling and Reaming Tests	5-87
5-78	C15002-4844 Cobalt, 20 ⁰ Helix Drill	5-89
5-79	C15013-4844 HSS, 30 ⁰ Helix Drill	5-89
5-80	C15481 Carbide Tipped Reamer	5-89
5-81	C15014 Cobalt Reamer	5-89
5-82	Preliminary End Milling Tests on 10 Ni Steel - 1-1/2 Inch Diameter, 8 Flute, HSS Cutter	5-92
5-83	Profile Milling 10 Ni Steel, Thin Flange, Production Verification Test Part (603FTB052)	5-92
5-84	End Milling 10 Ni Steel Splice Plate (603FTb052 Production Verification Test Specimen)	5-92
5-85	Face Milling Cutter with Round Carbide Inserts	5-92
5-86	Flame Cutting Techniques for 2-3/8 Inch Thick 10 Ni Steel	5-95
5-87	Post Stress Relief Dimensional Survey	5-97
5-88	-A10 Subassembly Fixture for 603FTB052 Test Component	5-98
5-89	603FTB052 10 Ni Steel Details (Unpainted Part is 6Al-4V Titanium)	5-98
5-90	Fixture for Installing Bolts in 603FTB052-A1 Assembly (-A10 Assembly Side)	5-98

L I S T O F I L L U S T R A T I O N S (Continued)

<u>Figure</u>		<u>Page</u>
5-91	Fixture for Installing Bolts in 603FTB052-A1 Assembly (Opposite Side)	5-98
5-92	Partially Assembled 603FTB052 Test Component (-A10 Assembly Side)	5-100
5-93	Partially Assembled 603FTB052 Test Component (Opposite Side)	5-100
5-94	Completed 603FTB052 Test Component	5-100
5-95	Completed 603FTB052 Test Component (Opposite Side)	5-100
5-96	603FTB053 Detail Parts Ready for Sealing Application and Assembly	5-102
5-97	Drill Plate and Portable Equipment Kit Used to Power Ream Taper-Lok Holes in 603FTB053	5-102
5-98	Assembled 603FTB053 (Top Side and Bottom Side)	5-104
5-99	Assembled 603FTB035 Test Component	5-105
5-100	603FTB043 Upper Cover Group II Test Specimen	5-106

LIST OF TABLES

<u>Table</u>		<u>Page</u>
II-1	Overall Load Condition Summary	2-81
II-2	NARSAP Condition Number Description	2-82
II-3	Ultimate NARSAP 39 Sta. Wing Pivot Loads (4-23-73)	2-83
II-4	Y _F 932 Bulkhead Longeron Load Summary	2-84
II-5	Y _F 932 NARSAP Shear Flow Summary	2-86
II-6	Y _F 992 Longeron Loads Summary	2-87
II-7	Y _F 992 NARSAP Shear Flow Summary	2-90
II-8	NARSAP Ult. A/P Loads Applied to Box	2-93
II-9	Ultimate Loads Applied to Wing Sweep Actuator Fitting	2-94
II-10	Main Landing Gear Fitting Ultimate Loads	2-95
II-11	Ultimate Weapons Launcher Loads	2-98
II-12	Overwing Fairing and Supplementary Wing Sweep Actuator Loads from AFFDL 10-12-73	2-99
II-13	Summary of Bulkhead Shears, Moments, and Vertical Balance Load for Design Conditions	2-104
II-14	AMAVS Y _F 932 Bulkhead Shear Flow Summary	2-108
II-15	AMAVS Y _F 992 Bulkhead Shear Flow Summary	2-109
II-16	Summary of Applied In-Plane Lug Loads and Shear Link Loads	2-113
II-17	Summary of Applied Pivot Loads in Global Coordinate System	2-114
II-18	Panel Point Loads, Condition AS 2000	2-115

LIST OF TABLES (Continued)

<u>Table</u>		<u>Page</u>
II-19	NBB TN1 Log Current Design Load Conditions	2-125
II-20	FSIL TN1 Log Current Design Load Conditions	2-128
II-21	Effects of Updated Loads	2-130
II-22	Convair and NARSAP Shear Flows - Lbs./In.	2-133
II-23	Convair and NARSAP Longeron Loads - KIPS	2-134
II-24	Fatigue Allowables for Seven Spectra Representative of FSIL and NBB Lower Covers	2-165
II-25	Fatigue Allowables for Fail Safe Integral Lug Configuration	2-165
II-26	Fatigue Allowables for the No-Box Configuration	2-166
II-27	Spectrum-Environmental Crack Growth Tests	2-168
II-28	Design Allowables for Ti 6Al-4V	2-223
II-29	Design Allowables for 10Ni Steel	2-224
II-30	Design Allowables for 7050 Aluminum Alloy Plate	2-225
II-31	Brazed Assemblies	2-227
II-32	Braze Alloy	2-249
II-33	Design Allowables for Weld Joints	2-257
II-34	AMAVS Specifications	2-258
II-35	Convair Aerospace Division Problem 005485-05	2-261
II-36	Convair Aerospace Division Problem 005485-06	2-262
II-37	Efficiency Grade	2-265
II-38	Integrity and Reliability Grade	2-265

LIST OF TABLES (Continued)

<u>Table</u>		<u>Page</u>
II-39	Ilities Grade	2-266
II-40	Configuration Ratings	2-267
III-1	Full-Scale Test Fixture Status	3-17
IV-1	Bonded NDI Sandwich Panels	4-2
IV-2	Bonded NDI Laminate Specimens	4-3
IV-3	NDI Brazed Joint Specimen	4-7
V-1	Transverse Shrinkage of Electron Beam Welds with 1.1 Inch Thick 10 Ni Steel	5-66
V-2	Transverse Shrinkage of Electron Beam Welds with .500 Inch Thick 10 Ni Steel	5-67
V-3	Mechanical Properties of EB Welded .500 Inch Thick 10 Ni Steel Tensile Test Specimen	5-69
V-4	GTA Welding Schedule for 10 Ni Steel	5-75
V-5	Transverse GTA Weld Shrinkage Data 1/2" Thick 10 Ni Steel	5-77
V-6	Hardness Values of GTA Welded and Aged 10 Ni Steel 1/2 Inch Plate	5-84
V-7	Boring Test Data - 1 Inch Thick 10 Ni Steel	5-88
V-8	Drill Test Data - 1 Inch Thick 10 Ni Steel	5-90
V-9	Face Milling Tests on 10 Ni Steel	5-93

SECTION 1

INTRODUCTION

This report summarizes the design, analysis and test activities of Phase II, Detail Design, for the Advanced Metallic Air Vehicle Structure (AMAVS) Program. The work done in the first portion of Phase II is presented in the Second Interim Technical Report, AFFDL-TR-73-77. Data presented in the Second Interim Report will not be repeated in this report unless it is required for a clear presentation of subsequent data. This work was performed under contract to the AFFDL by the Convair Aerospace Division of General Dynamics at Fort Worth, Texas.

The two configurations chosen for detail design were refined through additional trade studies and further study. The two configurations are designated as:

- o Fail Safe Integral Lug (FSIL)
- o "No-Box" Box (NBB)

Updated baseline data was received during the course of Phase II and both wing carry through structure configurations and the test fixture requirements were revised in accordance with the new data. Revised loads and interface geometry requirements were based on the elimination of the wing intrusion, new load conditions, revised gross weight and revised fairing support requirements. The design and analysis of both configurations were completed using updated data.

The Development Test Program consisting of Material Testing, Component Testing, NDI Development and Manufacturing Development was completed. Two of the three new materials were retained in the final configurations. These materials are beta annealed 6Al-4V titanium and 10 Ni steel (HY 180). Beta C titanium was dropped from both configurations.

Critical features of both configurations were evaluated in the Group II component tests. Additional problems were identified and solved in the brazing development program. Manufacturing capabilities were demonstrated for both configurations.

The design and manufacture of the full scale test fixture were continued. Manufacture of the simulated fuselage was started. Orders were placed for long-lead time materials needed for Phase III.

A design review was held to review the drawings and test results for both configurations. The NBB was selected for manufacture in Phase III.

SECTION 2

TECHNICAL DISCIPLINES PROGRESS

2.1 STRUCTURAL DESIGN

The two wing carrythrough structure configurations selected for detail design during Phase II are described in this section and are identified as follows:

"No-Box" Box (NBB)

This configuration utilizes the superior fracture resistance and weldability characteristics of 10 Nickel steel to achieve damage tolerance and fabrication reliability.

Fail-Safe Integral Lug (FSIL)

This configuration is characterized by brazing of titanium plates into a symmetrical three-element lower plate with integral pivot lugs.

Both configurations achieved the program objectives with respect to weight, cost and structural integrity.

2.1.1 "No-Box" Box

The objectives of the original "No-Box" Box configuration was to achieve a cost and weight efficient structure by use of the following major design approaches:

1. Direct and distinct load carrying member arrangement
2. Safe life concept
3. Minimal redundant internal structure
4. Simplified assembly and detail construction
5. Reduced number of fasteners.

This objective was pursued throughout Phase I and established the basic configuration. The pivot lugs were designed to direct the major portion of the load to the forward and aft bulkhead cap members. 10 Nickel steel (HY 180) was selected as the principal structural material for its excellent toughness. The weight penalty due to the marginal strength/density ratio of the 10 Nickel steel had to be overcome by the design concepts. Internal structure was limited to that needed to react loads at

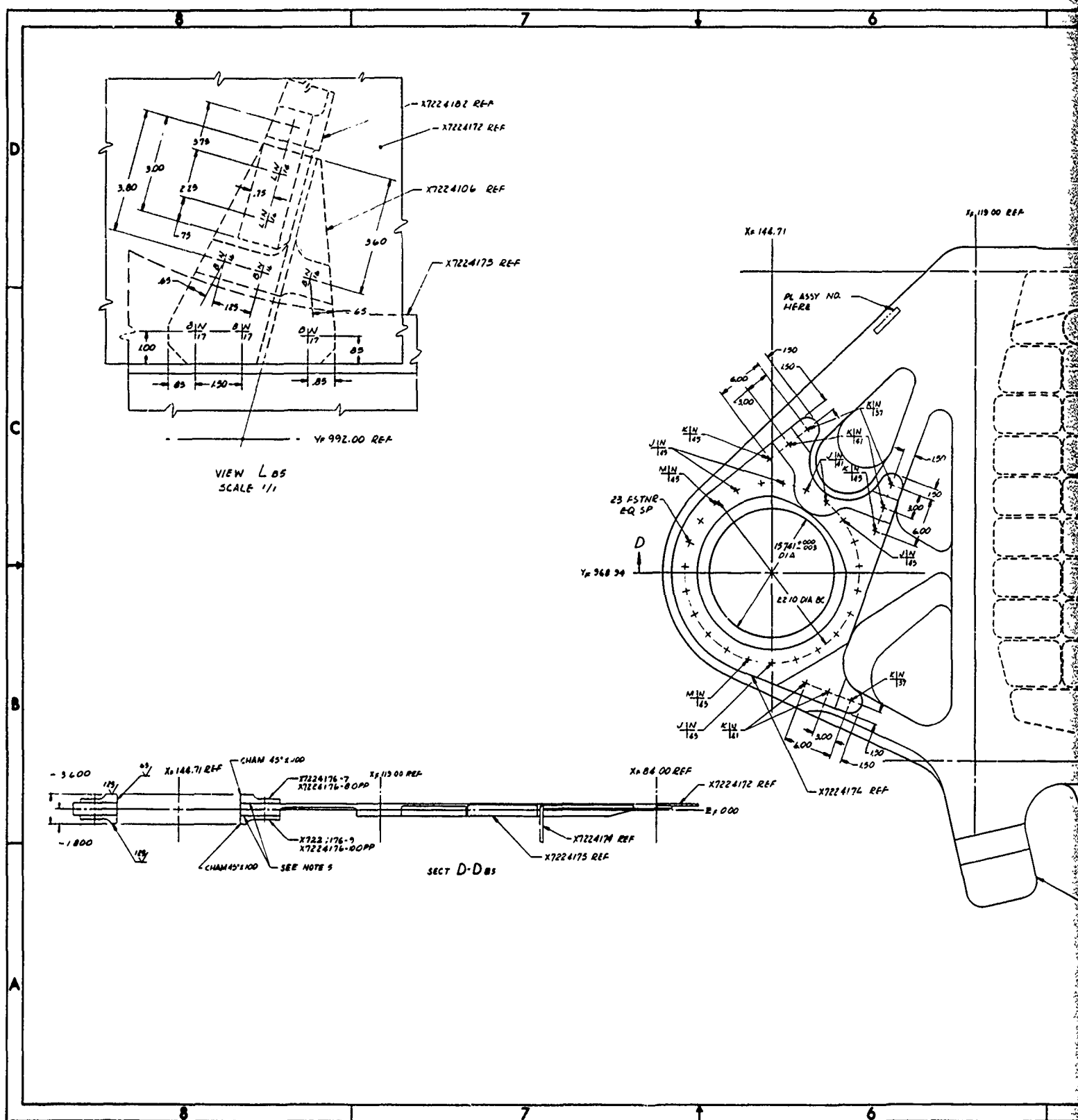
direction changes in the upper cover, the centerline fuel tank divider rib and structure for local interface load reactions. Machining time was minimized by using weldments to reduce the volume of metal removed and contour machining was confined to local areas of the bulkhead upper caps. The contour portion of the upper cover was confined to a single aluminum bonded panel. The reduced internal structure and direct load paths minimized the number of fasteners required.

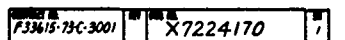
The Phase II design effort was concentrated on improving the implementation of these design objectives. However, certain compromises were required due to baseline load changes imposed midway through this phase. These will be discussed in detail in the following paragraphs.

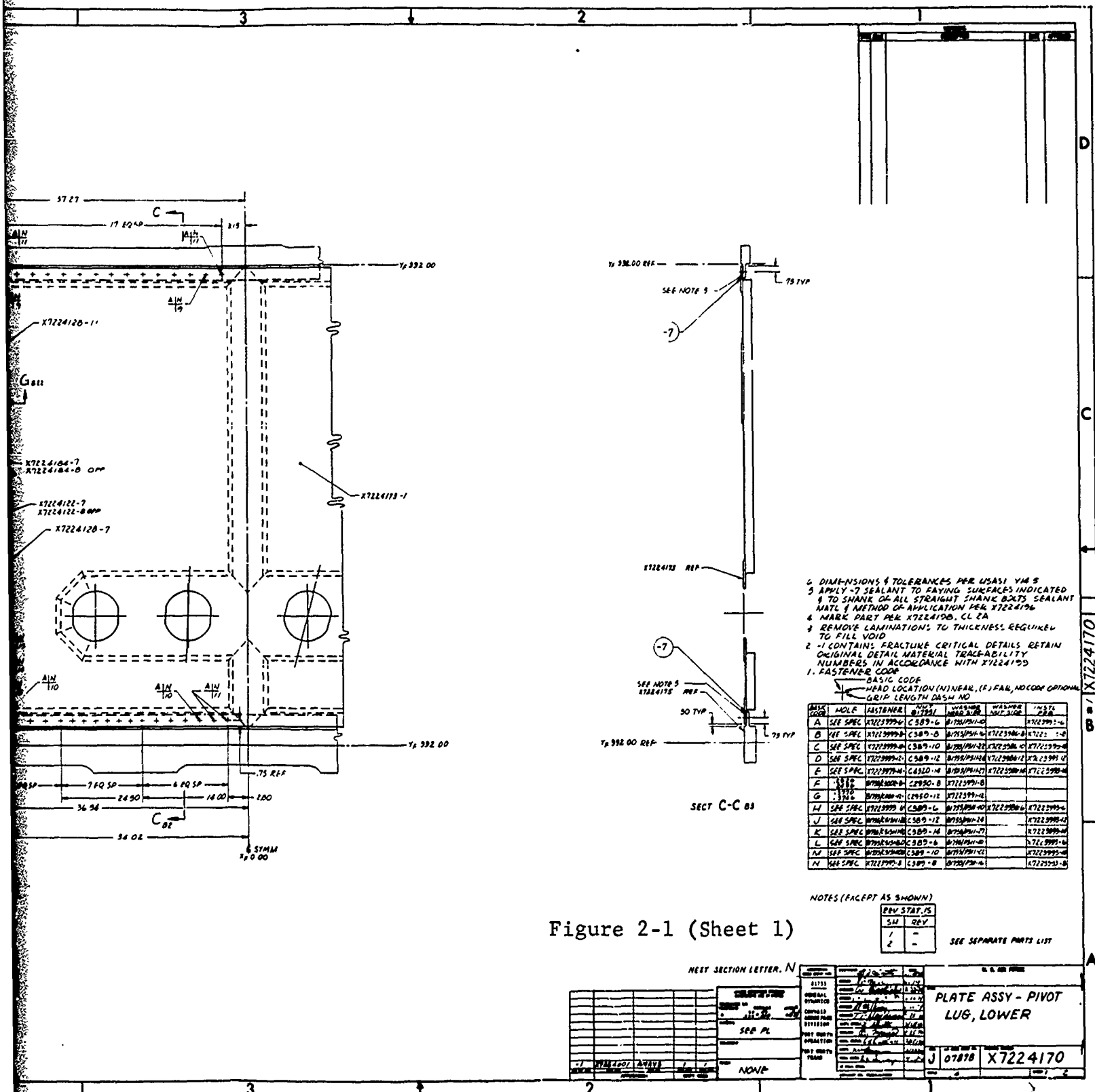
2.1.1.1 Lower Plate Assembly

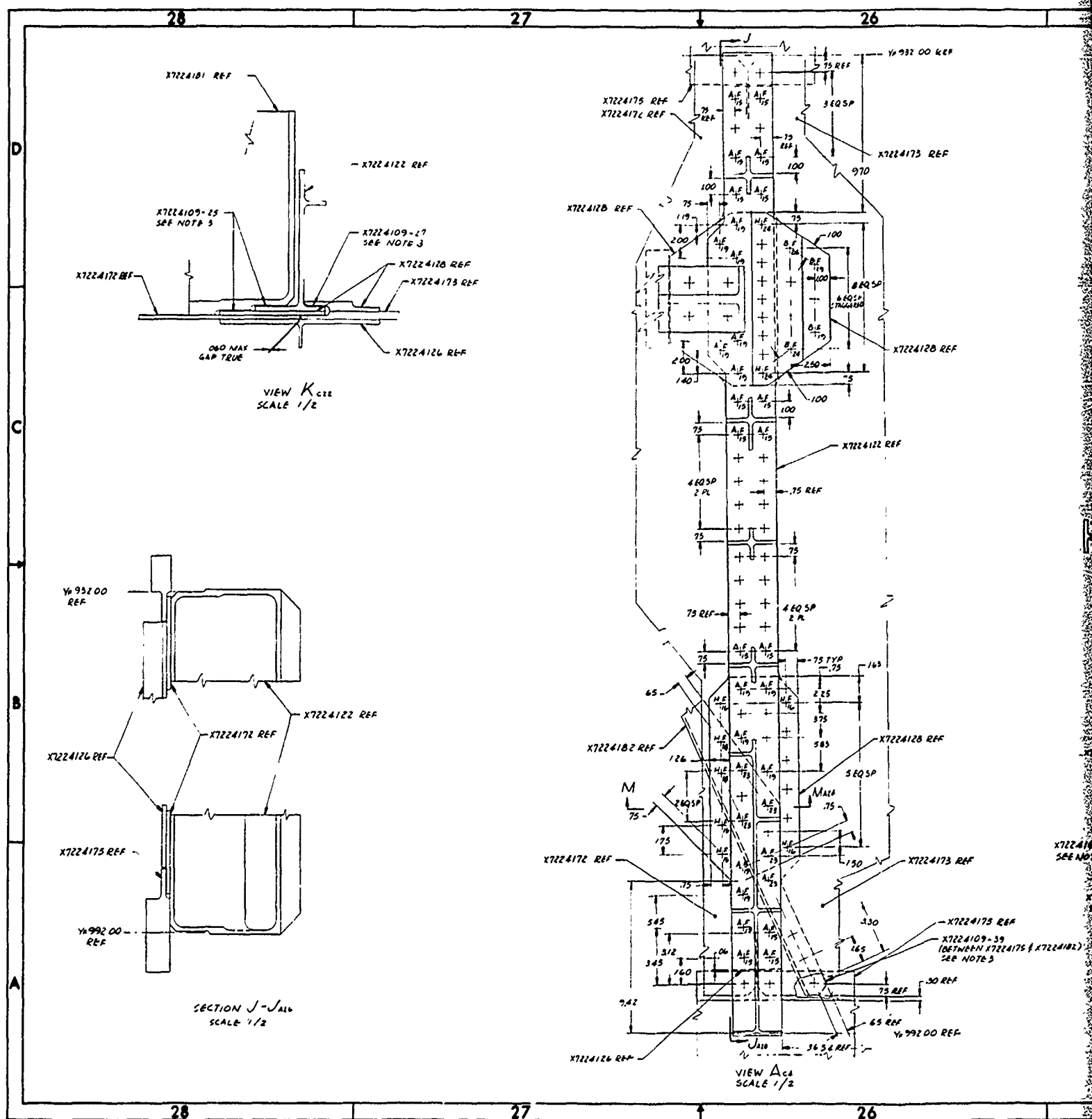
The original version of this configuration did not include a lower plate at Z_F0. The lugs were attached to the outboard caps of the forward and aft bulkheads. Shear and fuel pressure loads were carried by the lower contour panels. Late in Phase I, concern about relative deflections of the lug and lower panels resulted in a study to incorporate a full plate at Z_F0. Landing gear interface requirements also made this desirable. The highly loaded lug splice requirements were also of some concern. These considerations finally evolved into the configuration shown on Dwg. No. X7224170, Figure 2-1.

The lower plate assembly consists of a single 10 Nickel steel plate from pivot lug to pivot lug. A cut-out in the center leaves only rails inboard of the X_F84 rib. The area between the X_F84 and the closure rib is pocketed on the under side. The outboard aft longeron attachment provisions are machined in the basic plate. Three beta processed 6Al-4V titanium bonded sandwich panels are installed between X_F 84 and X_F84. These panels react shear, fuel pressure and the axial load not carried by the 10 Nickel steel rails. A machined aluminum (7050) beam is bolted to the under side of the steel plate at X_F95 to provide compression stability for negative loads. Machined 10 Nickel steel reinforcing plates are installed on the pivot lugs to provide additional reaction for pivot pin loads and meet the baseline lug thickness requirements. All fasteners through the 10 Nickel steel element are H11 steel Taper-loks.





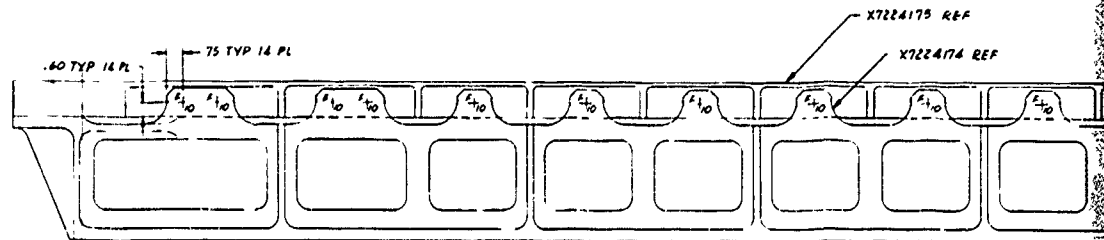




25

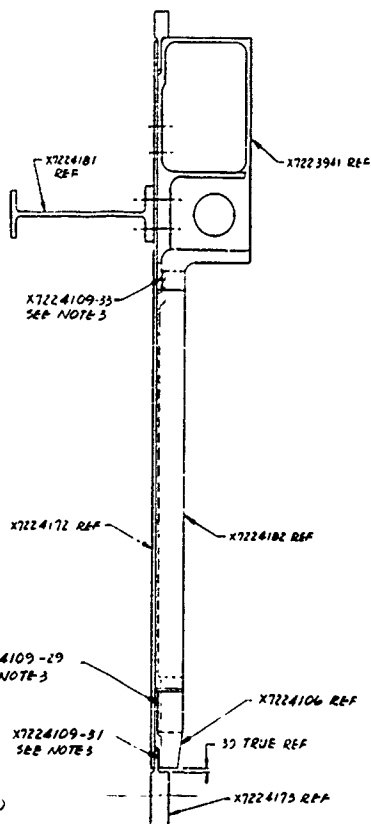
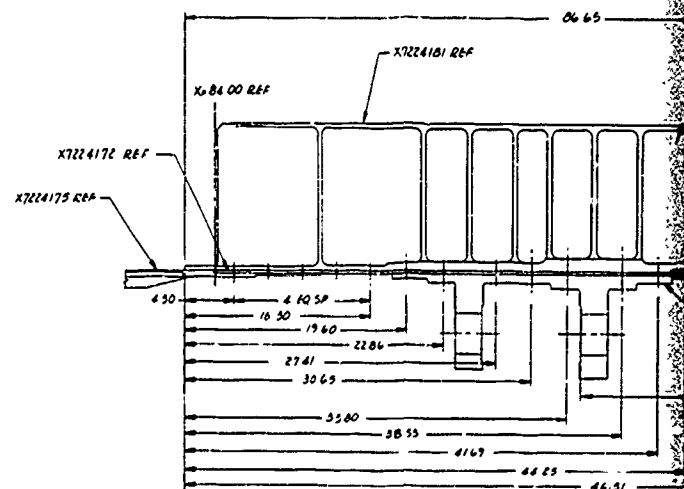
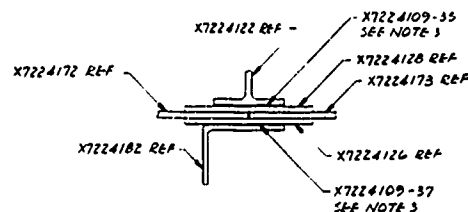
24

23



1/4 992.00 REF

SECTION B-B₀₅
SCALE 1/2
ROTATED 90° CLOCKWISE

SECTION H-H₀₅SECTION G-G₀₄

SECTION M-M₀₆
SCALE 1/2

PROJECT NO. F33615-73 C-3020
REV. 1, 2015
X7224170
2

25

24

23

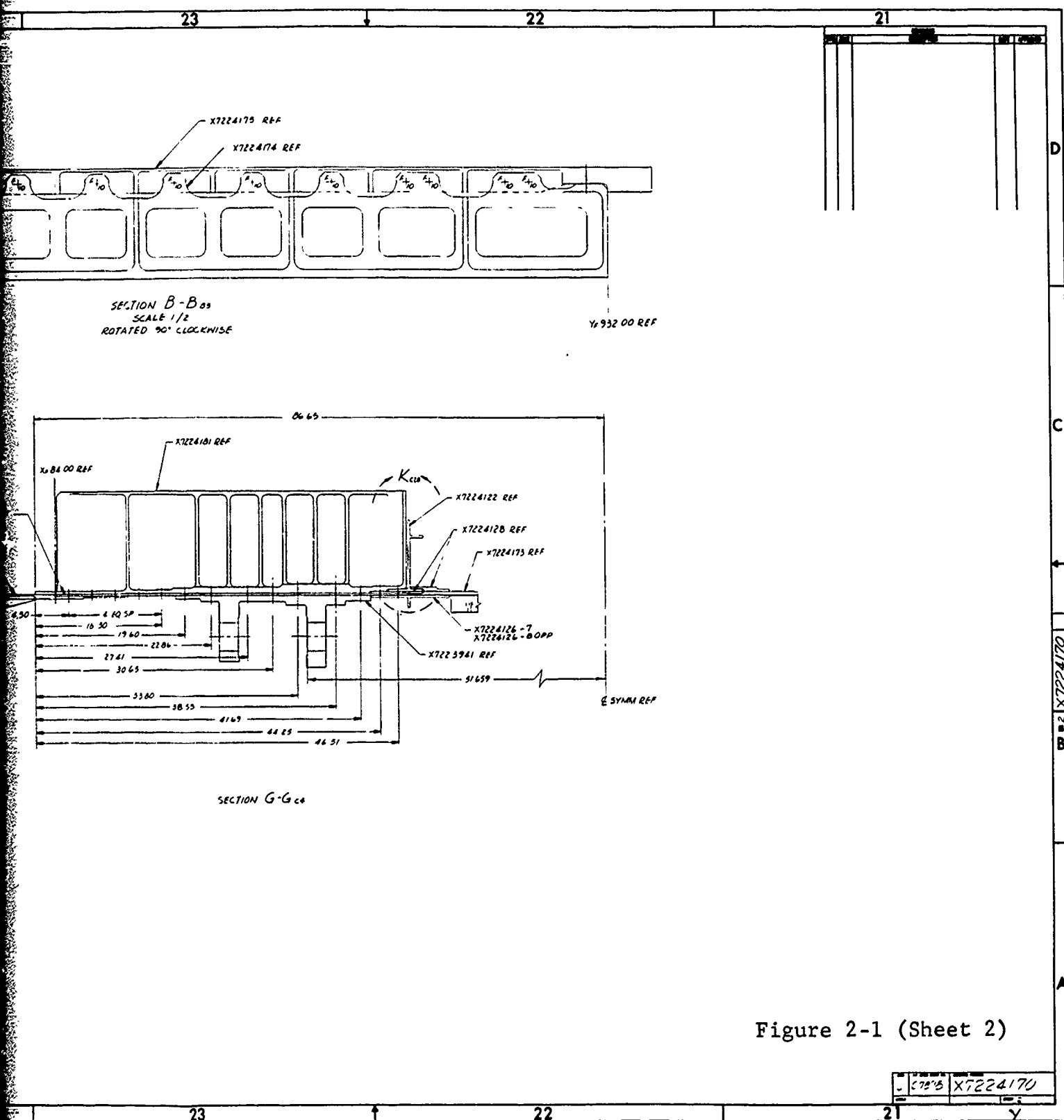


Figure 2-1 (Sheet 2)

2.1.1.2 Y_F 932 Bulkhead

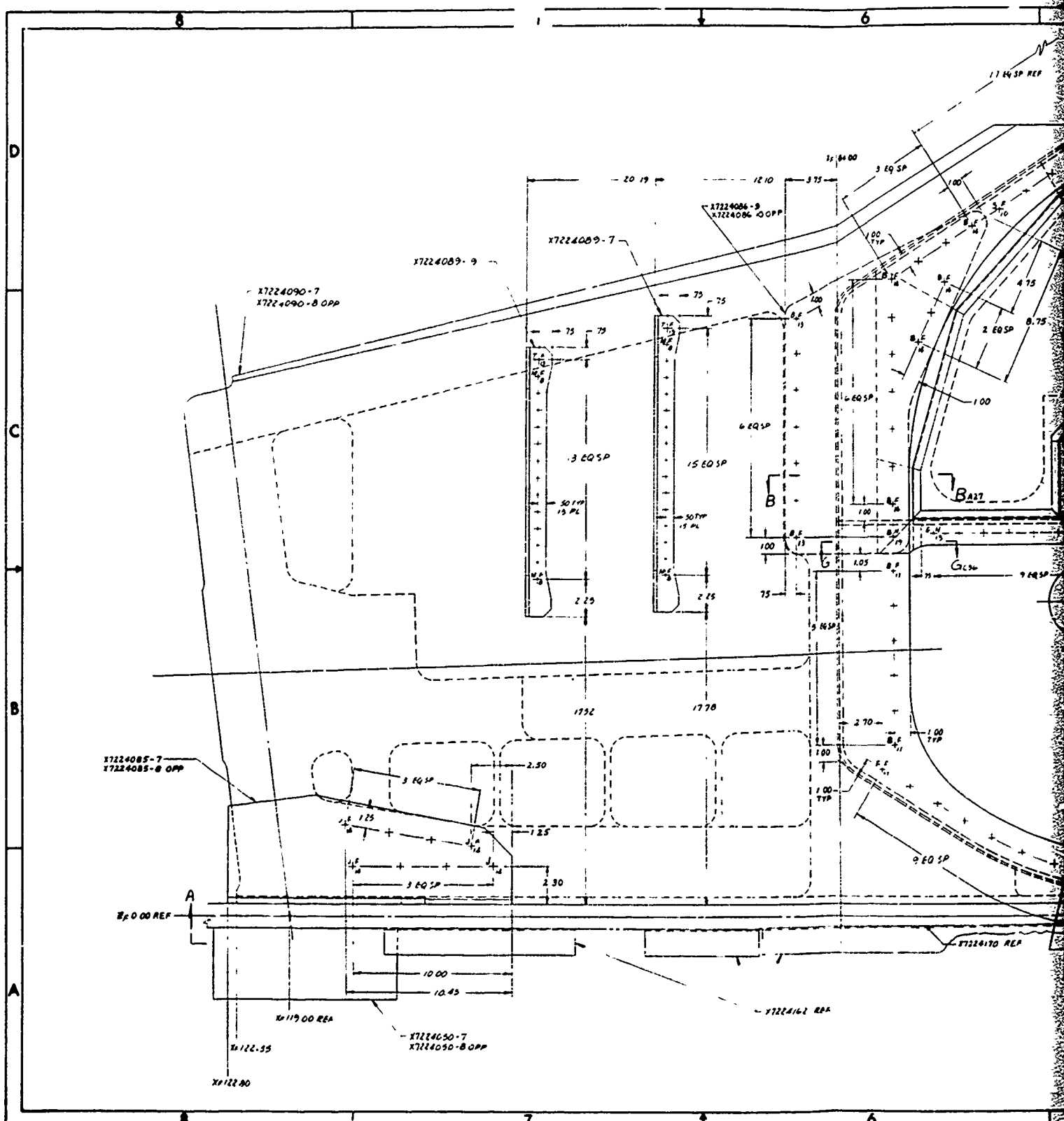
The forward bulkhead (Y_F 932) Dwg. No. X7224080, Figure 2-2, consists of six major elements. The L/R outboard sections are integrally machined from weldments of 10 Nickel steel plate and bar. The lower flange of the weldment extends inboard to the centerline. The upper flange extends inboard to X_F32. A machined 10 Nickel steel Tee section is mechanically spliced at these points to complete the upper flange. The lower flanges are spliced with a short 10 Nickel steel angle. The lower flange is attached to the lower plate with taper-loks which also pick up the lower fairing support angles. The intermediate bulkhead web area is a beta processed 6Al-4V titanium sandwich extending from approximately X_F84 to X_F39. This area is primarily designed to react shear & fuel pressure loads and local axial loads near the top and bottom edges. Locally high shear loads are also introduced by the forward end of the MLG drag load fitting. This panel was originally proposed to be an aluminum bonded sandwich. However, the local high load introduction areas required excessive thicknesses resulting in inefficient splice arrangements.

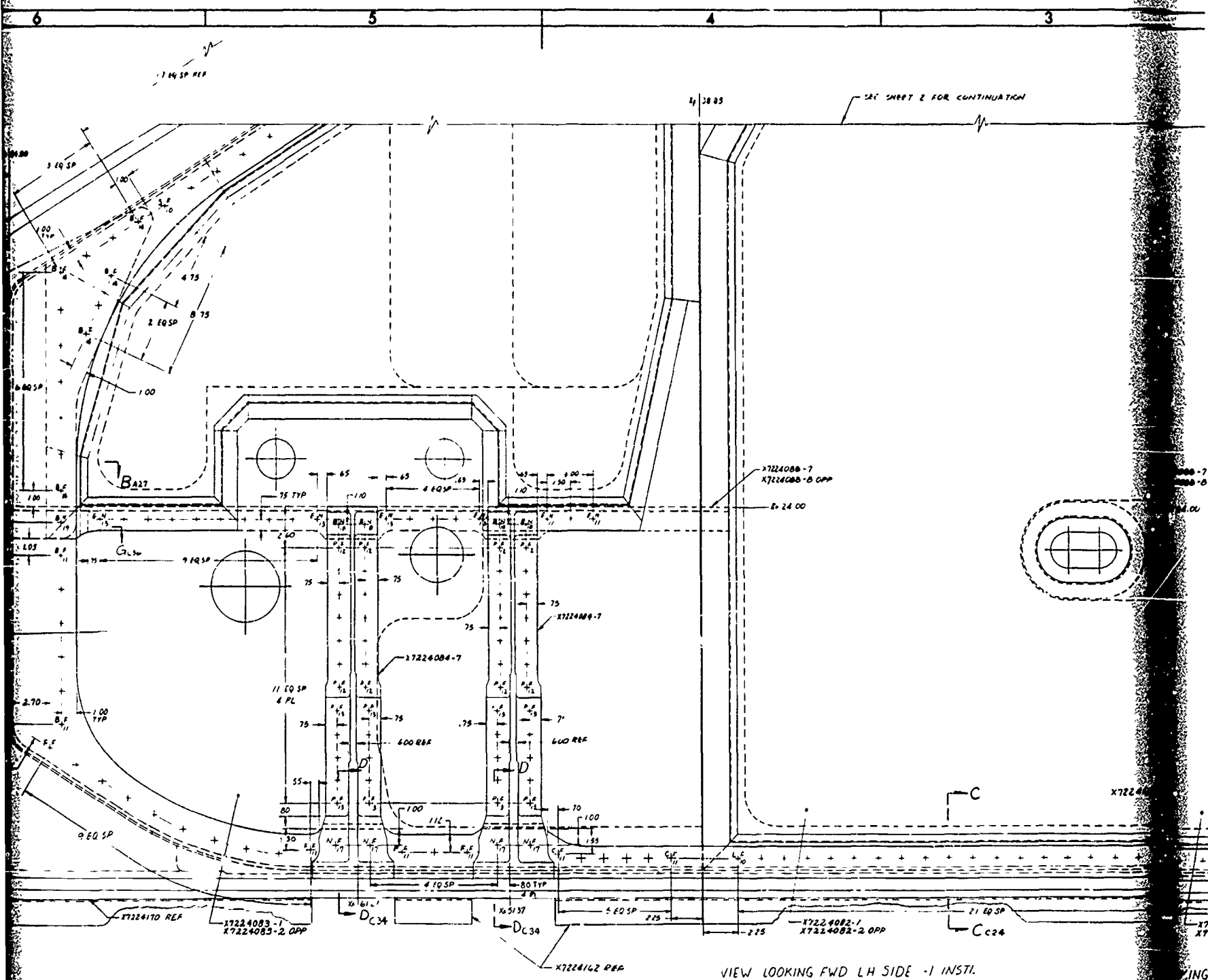
The inboard web area from X_F39 to X_F39 is a 2024 aluminum alloy bonded panel. The fuel pressure loading over the large flat panel makes this arrangement efficient.

2.1.1.3 Y_F 992 Bulkhead

The configuration of this bulkhead is essentially the same as the Y_F 932 bulkhead. The outboard webs, lower flange and upper cap is 10 Nickel steel. The main difference is that the bolted-on web is a one-piece beta processed 6Al-4V titanium bonded panel. Aluminum alloy was also originally considered for this panel. However, increased loads imposed during this phase made the titanium more efficient. An additional consideration in the selection of titanium was the more severe fatigue spectrum in the lower aft center area which would limit the allowable operating stress in the aluminum and thus penalize the steel lower plate rails.

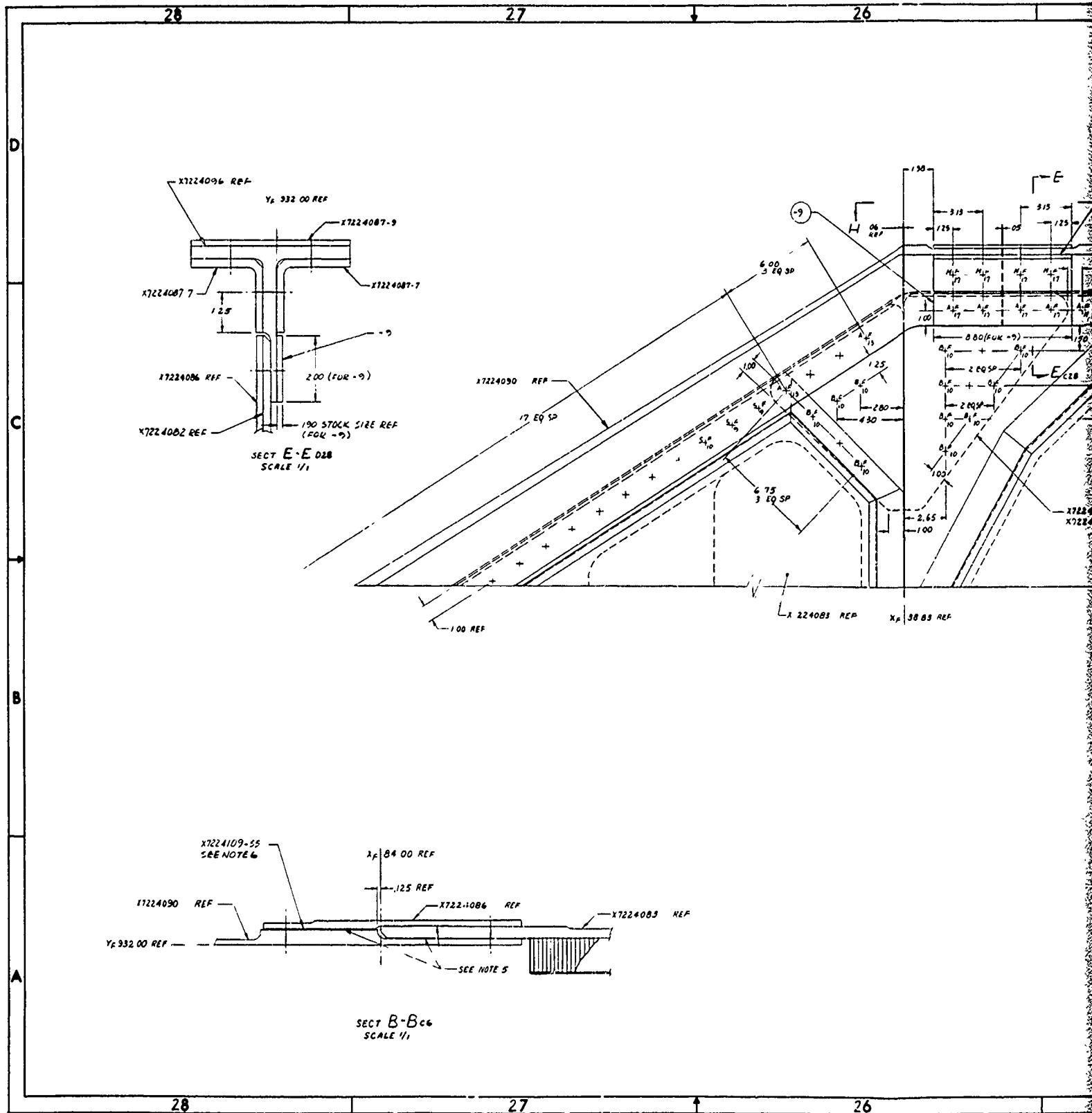
The general configuration of the bulkhead was established by the interface requirements: i.e., X_F 119 and X_F 103 shear web attachments, the entrance access provisions and the MLG trunnions, actuator bracket and side load fitting provisions. The bulkhead (Dwg. No. X7224060) is shown in Figure 2-3.

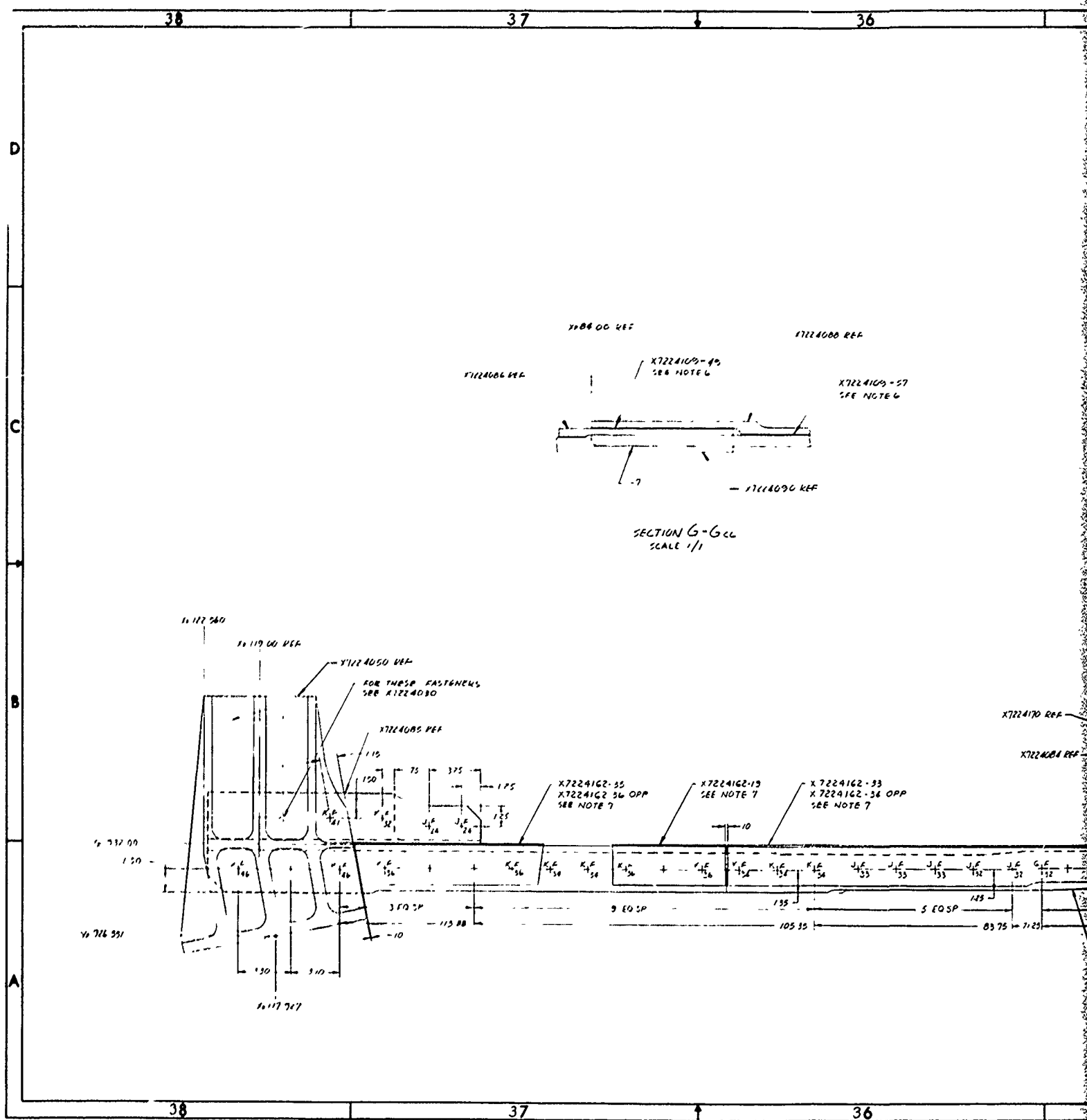




Fig

CONFIDENTIAL
F13615-13-C-3001
X7224080

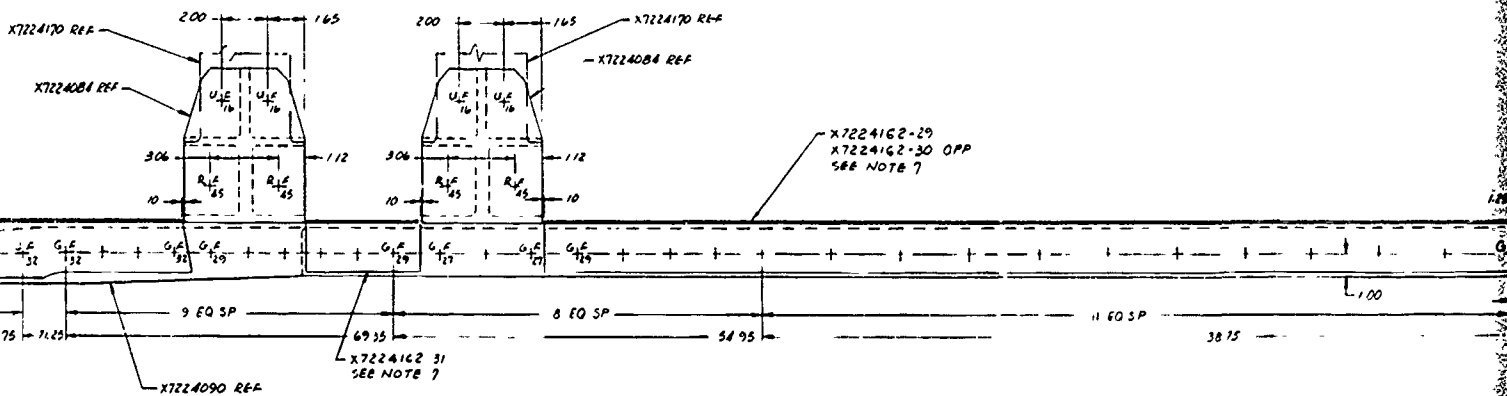
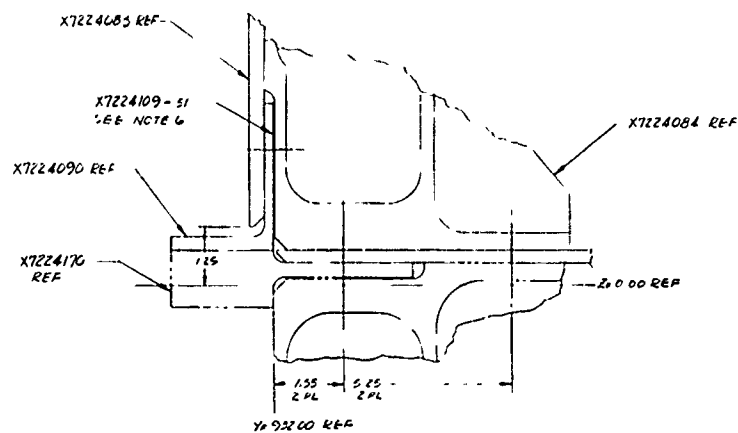




35

34

33



F 336/573 C 3001

X7224080

SEE FRONT VIEW FROM 1

35

34

33

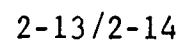
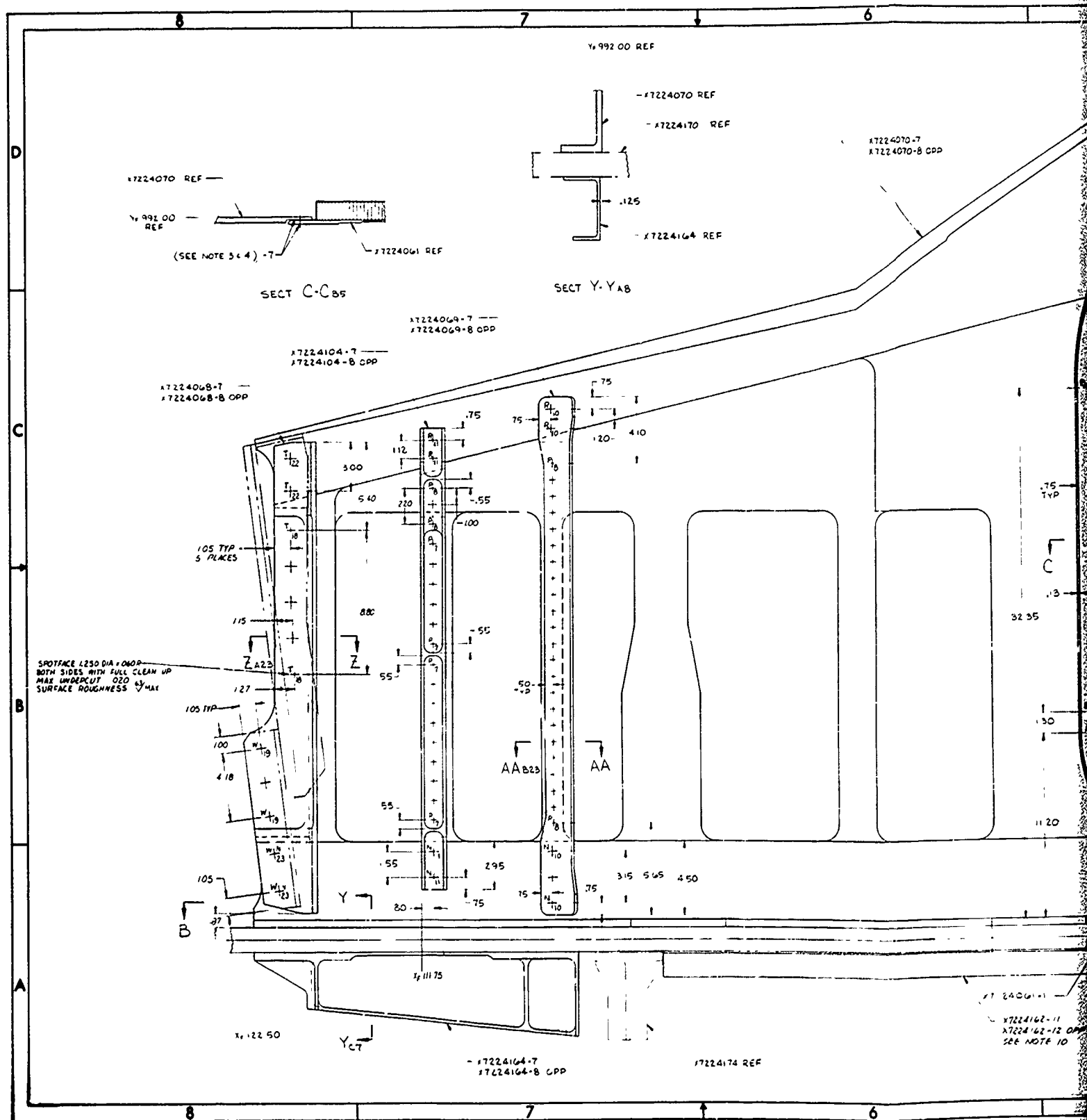
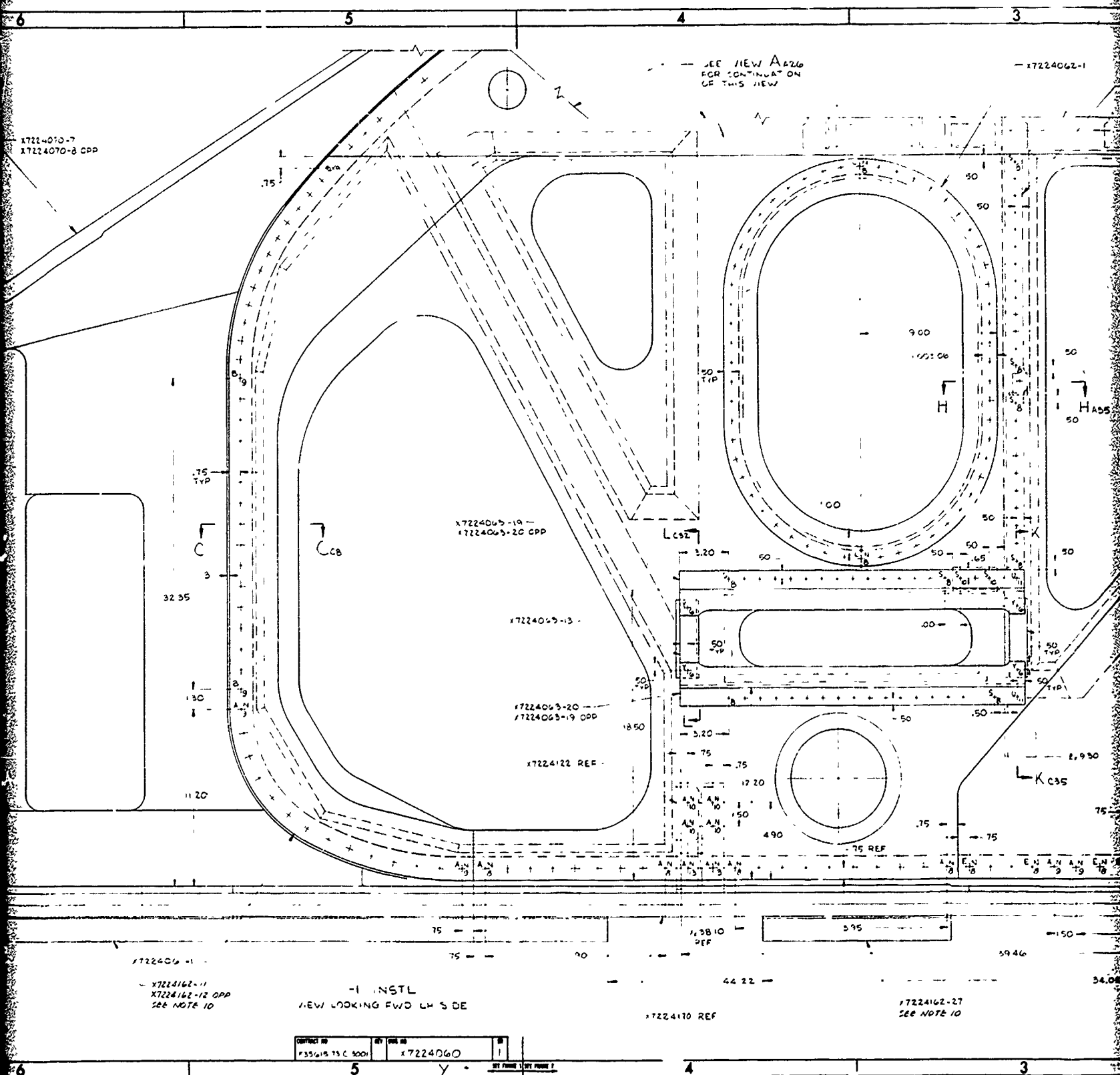


Figure 2-2 (Sheet 3)

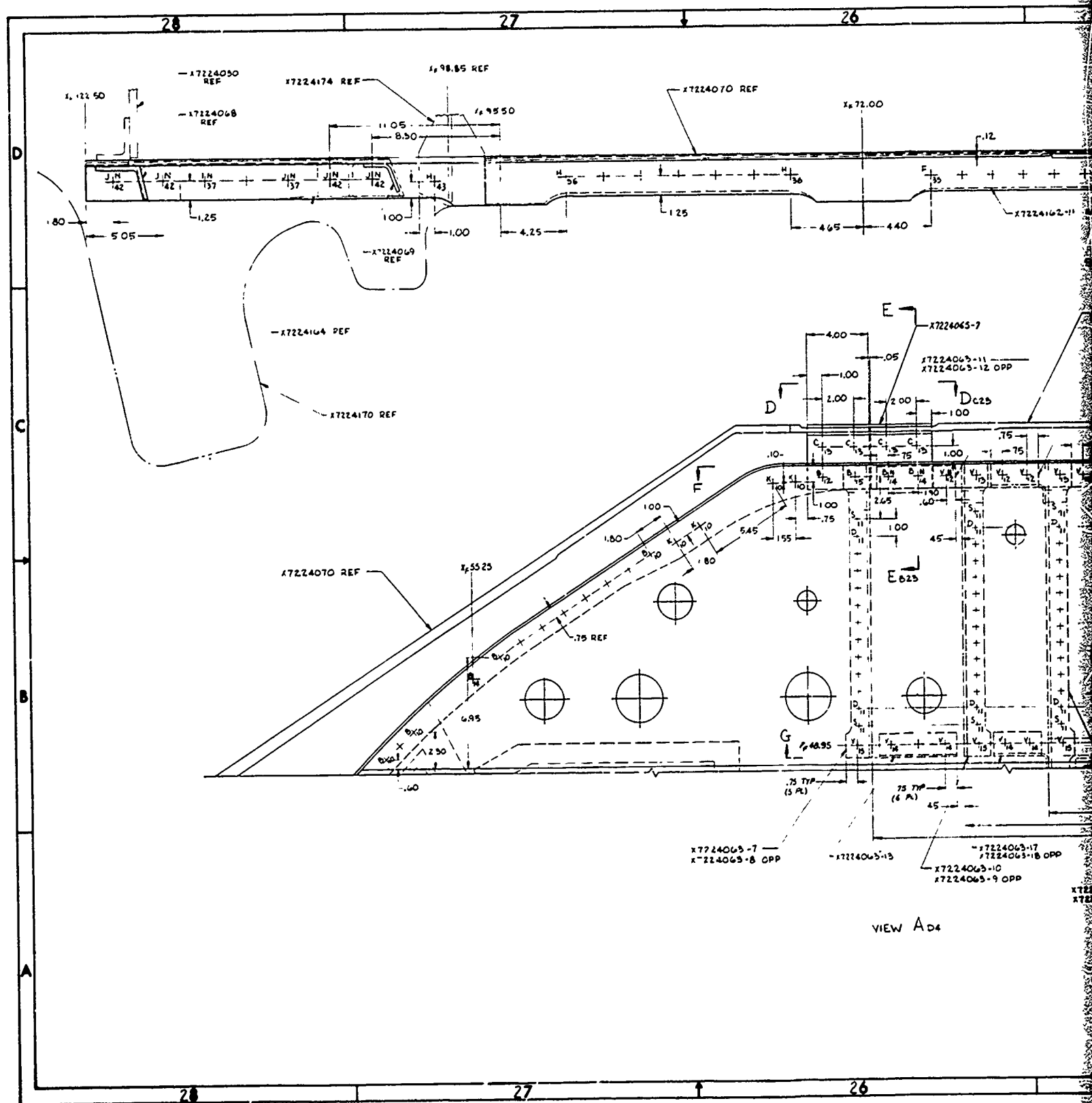


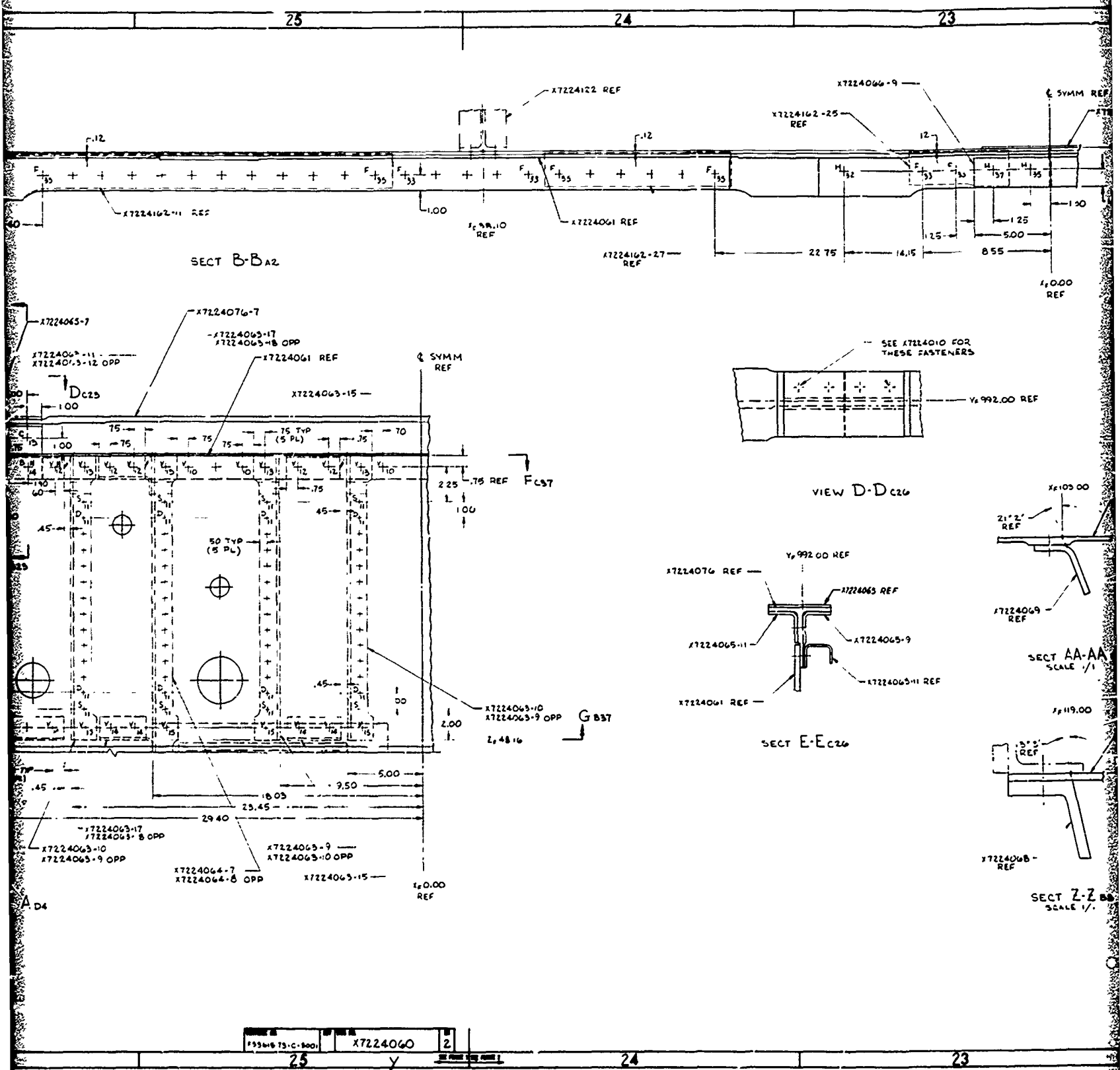


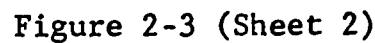


REV	-	-	-
SHEET	1	2	3
REVISION STATUS OF SHEETS			

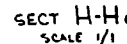
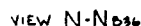
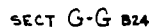
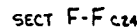
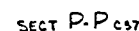
BULKHEAD INSTL-
YF99Z WING CARRYTHRU

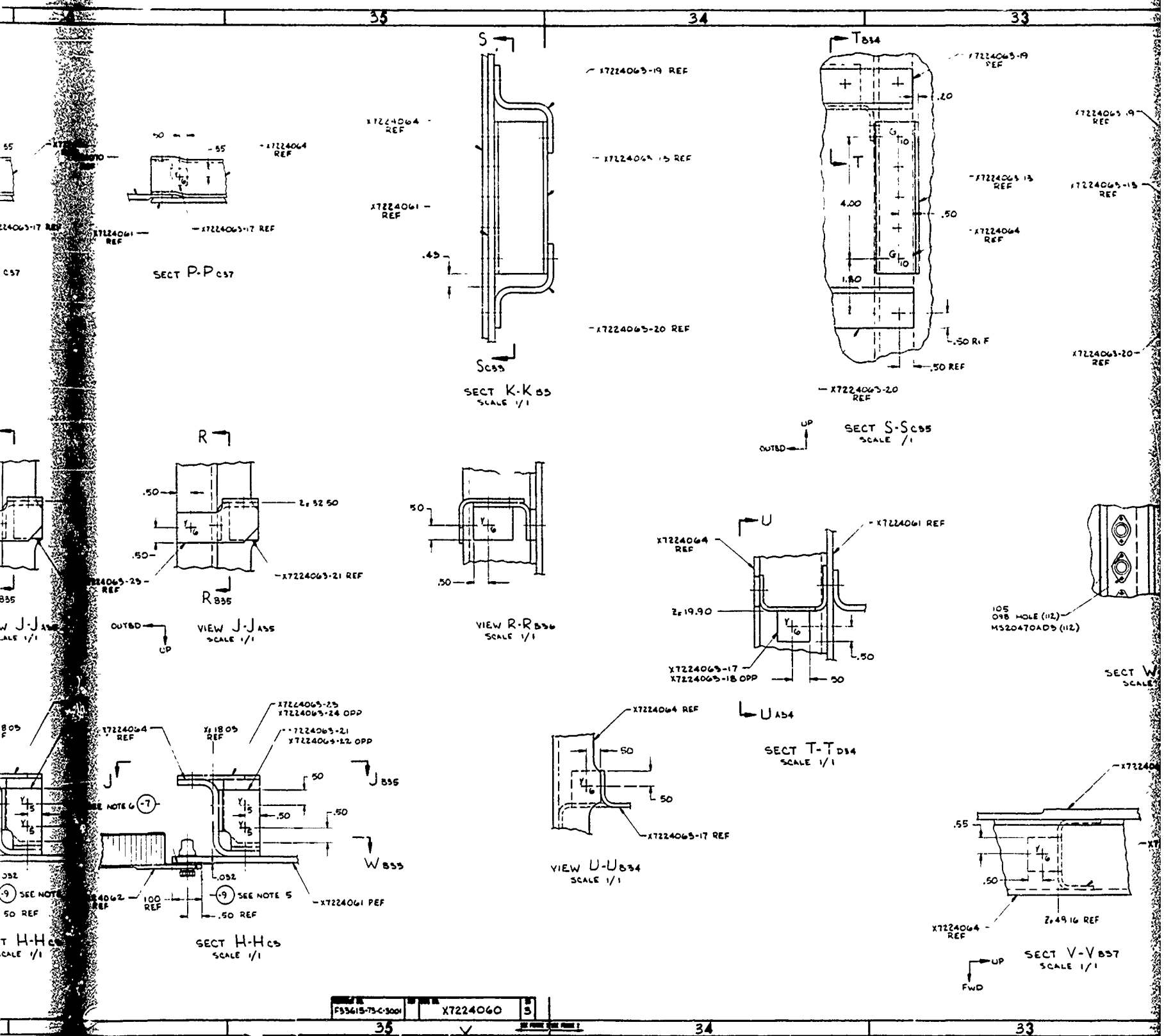






2-17 / 2-18





2.1.1.4 Upper Cover and Pivot Lugs

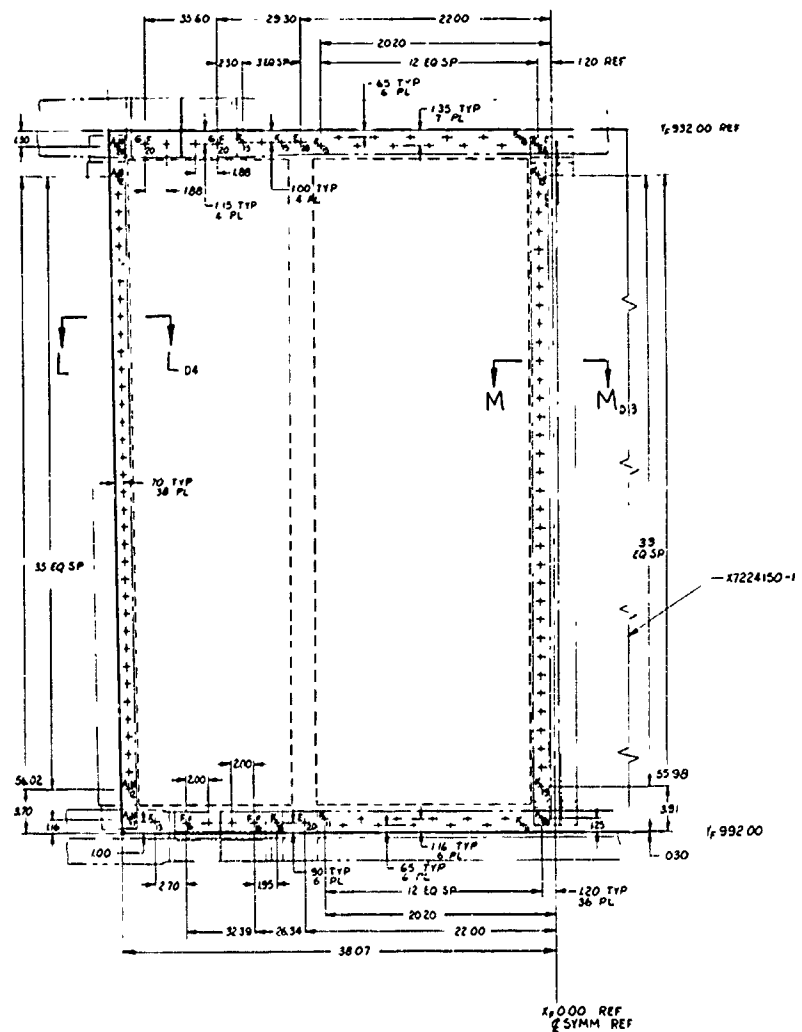
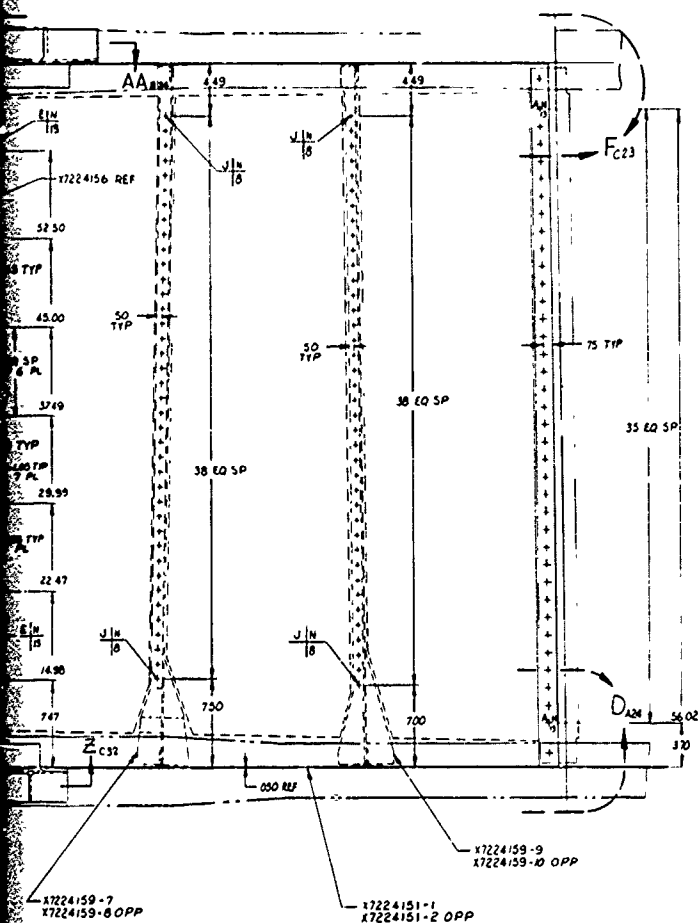
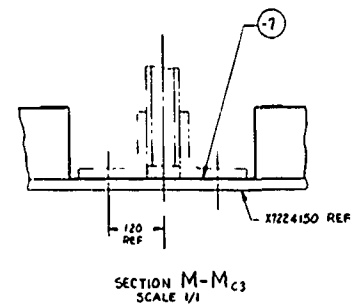
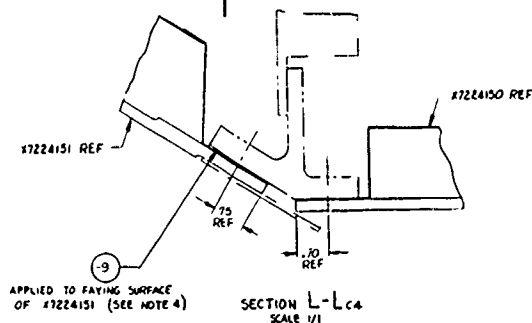
The upper cover, Drawing X7224010, Figure 2-4, is segmented into five components as it generally follows the air vehicle upper contour. The pivot lug and section outboard of X_F84 are integrally machined from a 10 Nickel steel plate that has been formed to accommodate the directional change required at the closure rib. This component transfers the majority of the axial load into the bulkhead caps by means of a single-shear bolted splice. The remaining axial load is transferred into aluminum sandwich panels which form the upper cover inboard of X_F84. These panels also react shear and fuel pressure loads. The left and right hand panels between X_F39 and X_F84 are contoured and partially form the external fuselage boundary. The outboard edge of these panels breaks below contour and forms an attach area for an aerodynamic fairing at the fuselage contour that extends outboard to approximately X_F 123. The panel inboard of X_F39 is not contoured, but functions as the lower surface of the routing tunnel.

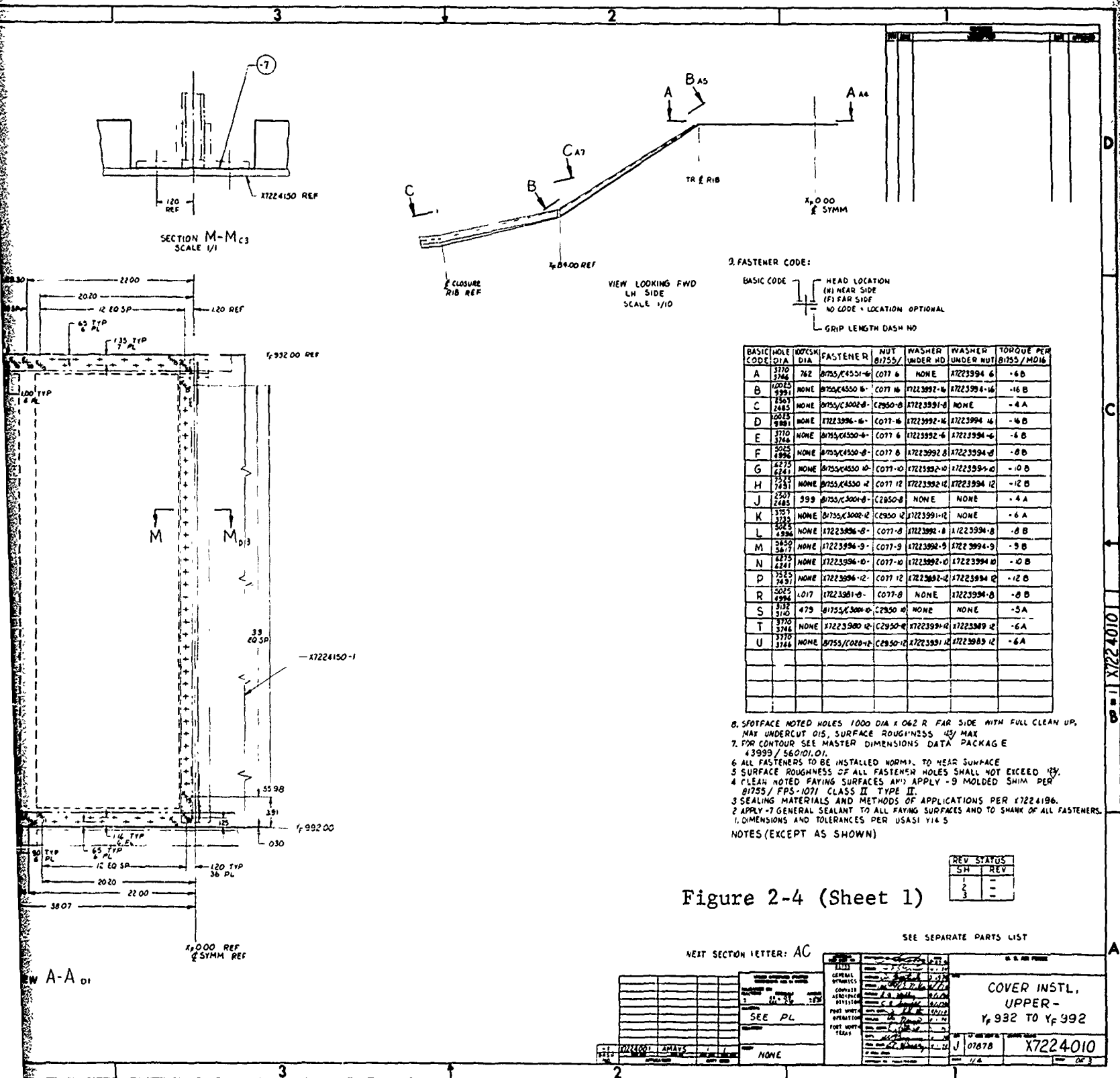
2.1.1.5 Centerline Rib

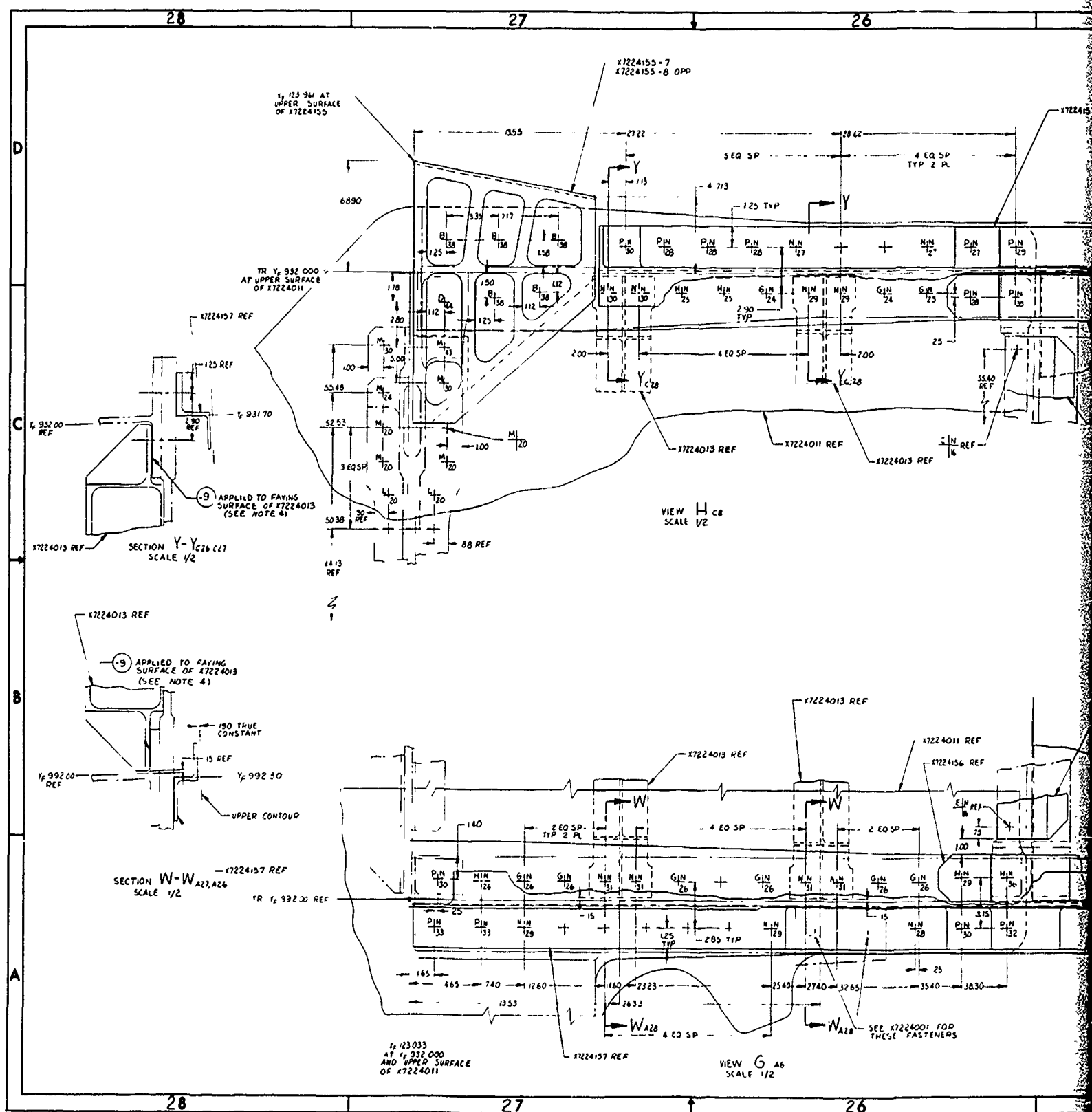
The centerline rib (Figure 2-5, Drawing X7224110) is an aluminum sandwich panel which divides the left and right hand fuel tanks and distributes the loads introduced by the interface structure. This panel utilizes slug type edge members with integral attaching flanges at Y_F 932 and Y_F 992 bulkheads. Separate bolt-on attach angles are required at the upper and lower plates. Reinforcing beams are required to react and distribute the local concentration of loads introduced by the weapons launcher and the MLG side load fitting. These beams, two per side, are machined from 7050 Aluminum and are located at approximately Z_F26 and Z_F44.

2.1.1.6 Inboard Intermediate Rib

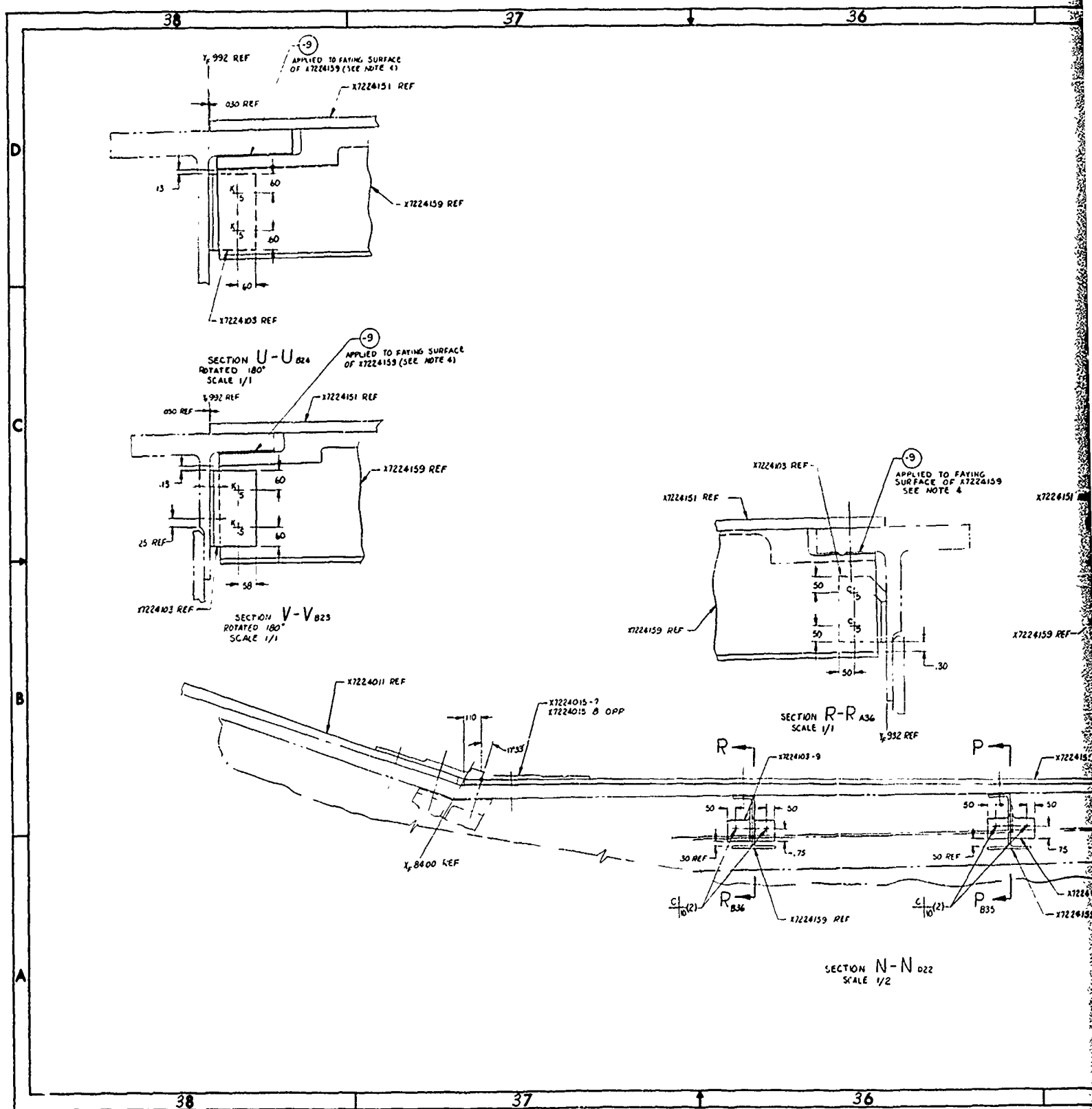
The inboard rib at X_F39 (Figure 2-6, Drawing X7224120) is an aluminum sandwich panel with bolt-on aluminum tee flanges for attaching and splicing the upper and lower covers and the bulkhead webs at Y_F 932 and 992. This rib distributes the loads resulting from the directional change in the upper cover and loads introduced by the MLG drag fitting back-up beam located at Y_F 947. An access opening is provided in the middle of the panel to allow entry to the outboard section of the box structure during fabrication, service maintenance, and inspection. Fuel flow and venting are also adequately provided.







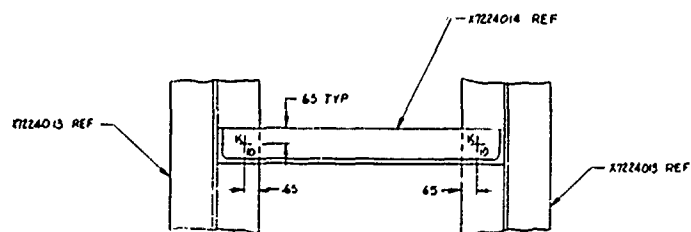




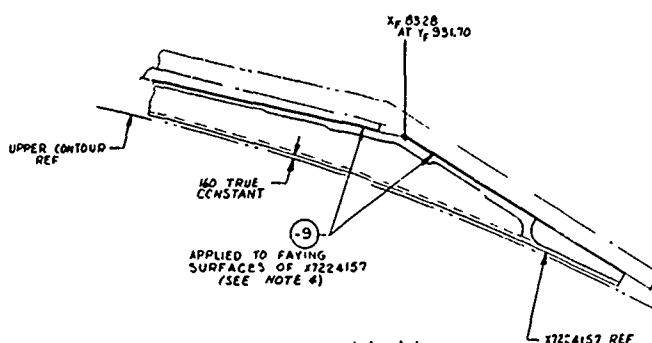
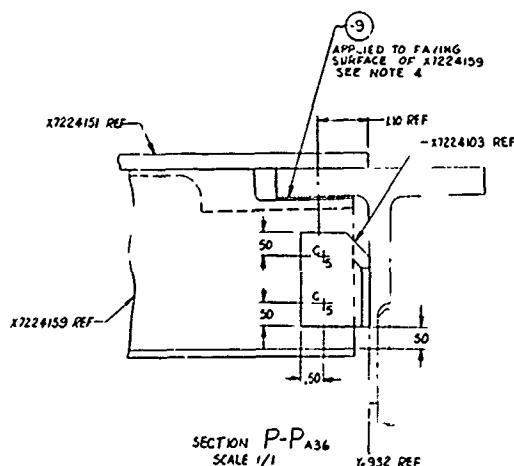
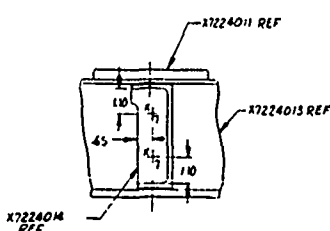
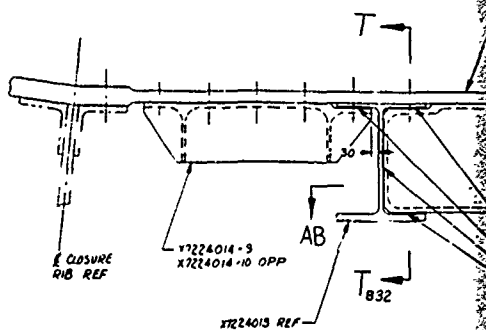
35

34

33



SECTION AB-AB A32

UPPER CONTOUR
(SEE NOTE 7)SECTION AA-AA C6
SCALE 1/2
ROTATED 32° CWSECTION P-P A36
SCALE 1/1SECTION S-S A33
SCALE 1/2SECTION J-J
SCALE 1/2

F33615-73-C-3001

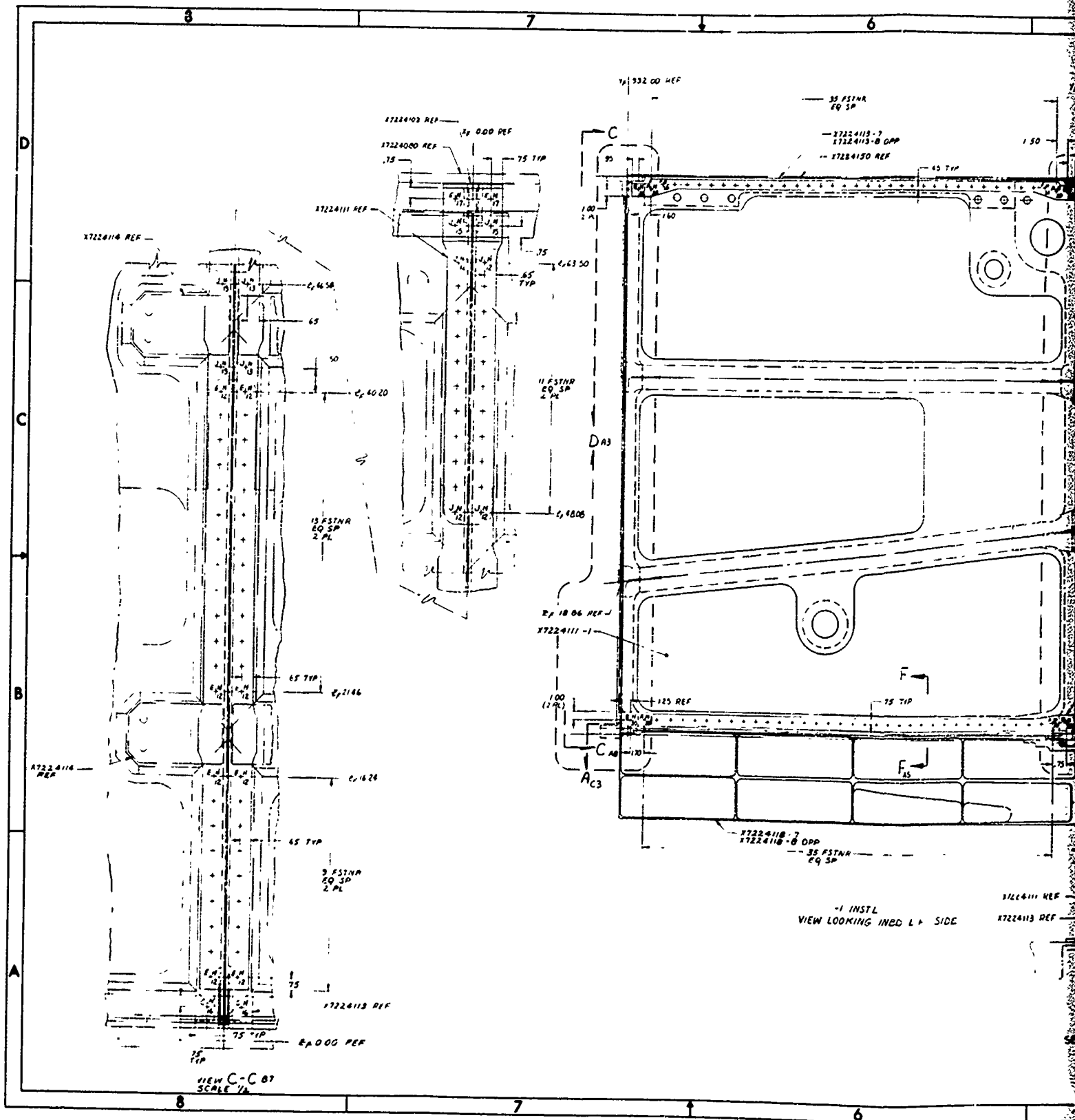
X7224010

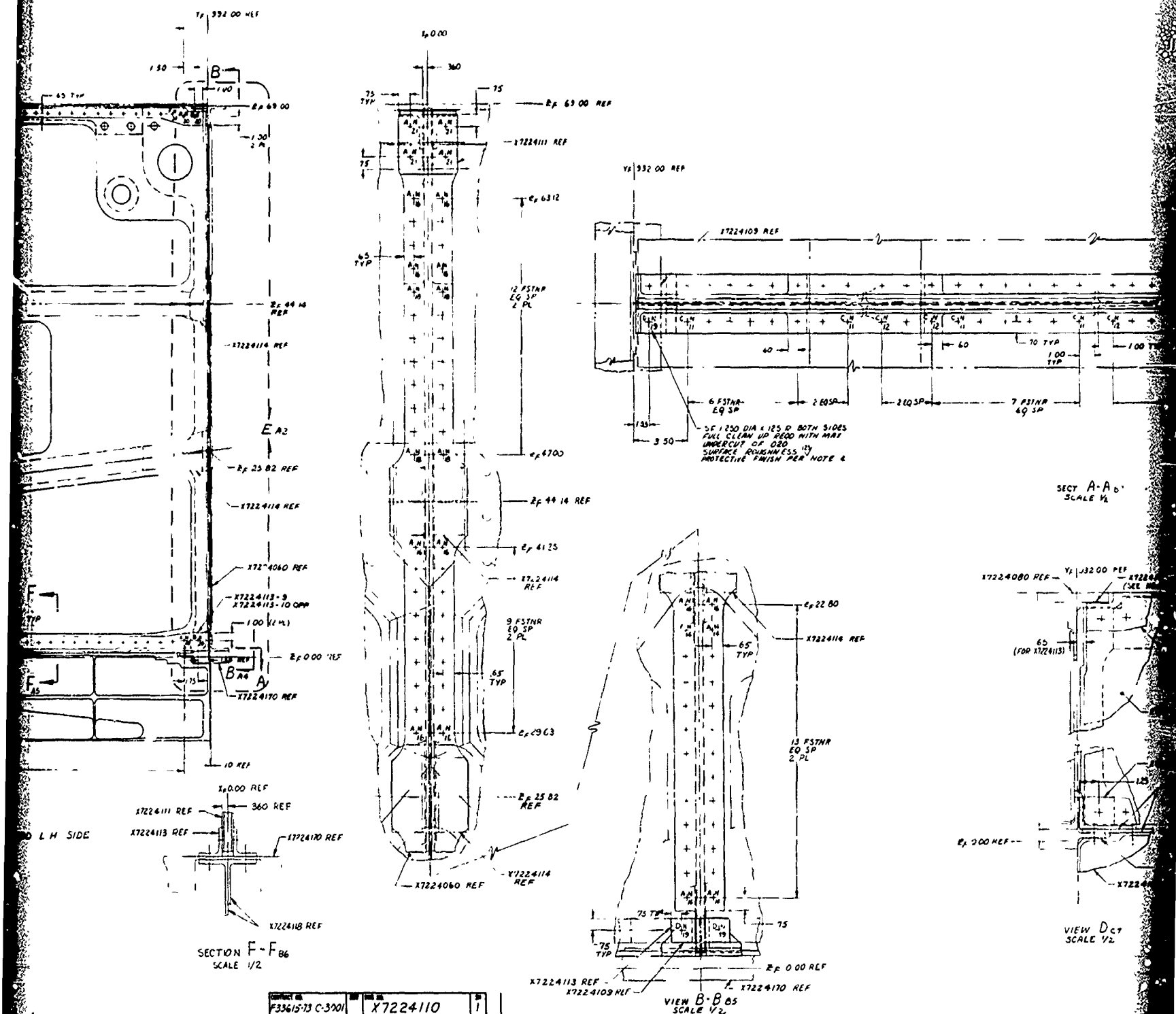
3

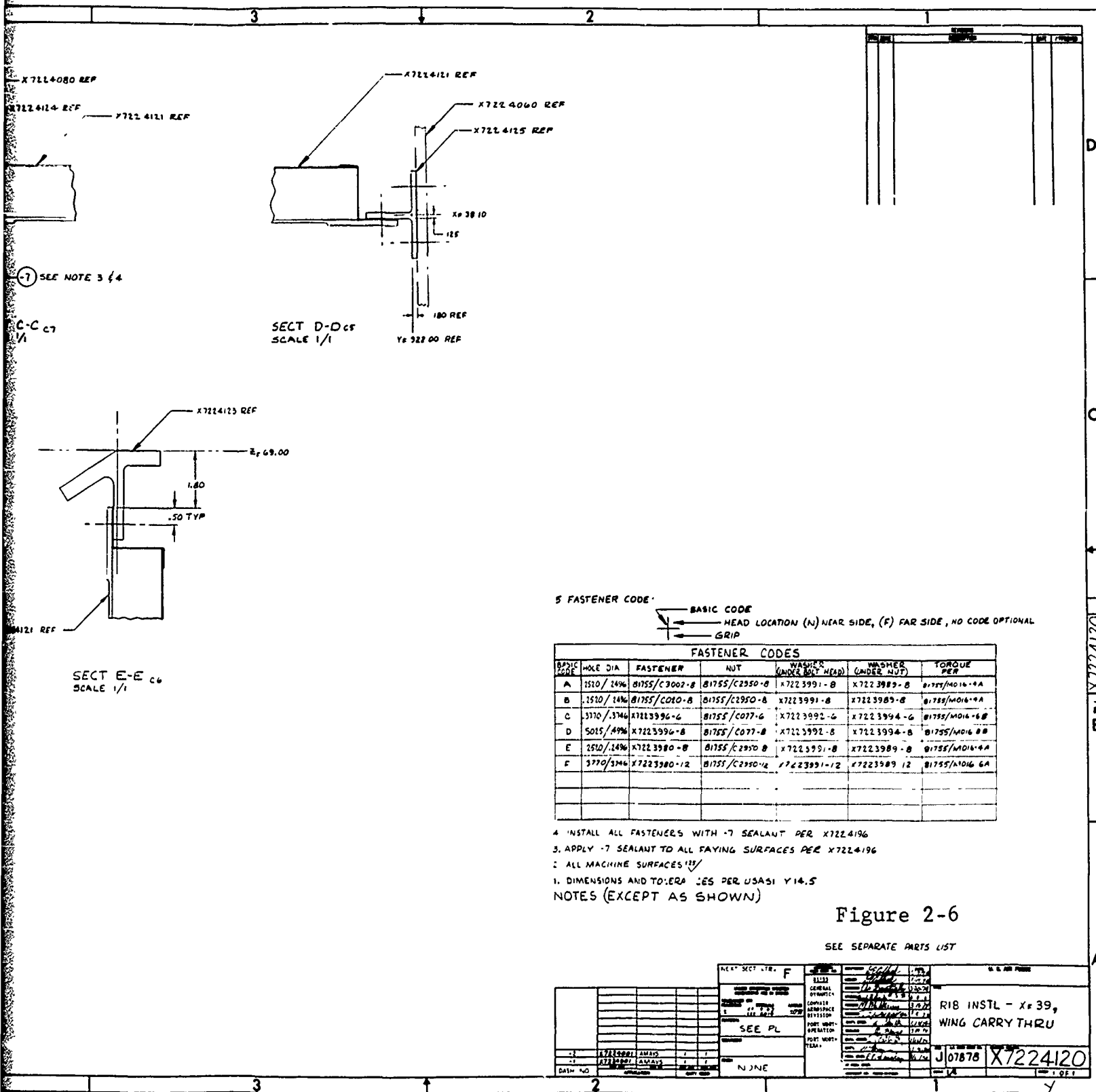
35

34

33







2.1.1.7 Outboard Intermediate Rib

The outboard rib at Xp84 (Figure 2-7, Drawing X7224130) is integrally machined from 7050 aluminum plate. This monolithic type construction was selected to efficiently distribute the torsional shear loads introduced by the pivot lugs, and to distribute the high concentrated reaction loads from the wing sweep actuator inboard attach bracket. This rib also supports the inboard end of the pivot lugs and splices them to the upper and lower cover sandwich panels. The kick load due to the directional change of the upper cover is also reacted by this rib. The outboard end of the Yp 947 beam is also supported by this rib. Provisions are made for access to the outboard area and for fuel flow and venting.

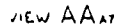
2.1.1.8 Outboard Closure Rib

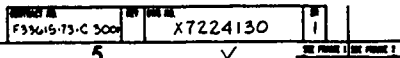
The outboard closure rib (Figure 2-8, Drawing X7224030) has been redesigned from an integrally machined 10 Nickel steel weldment into a beta annealed 6AL-4V titanium web reinforced with aluminum stiffeners and attached by titanium angle sections. Separate bolt-on titanium fittings are utilized to react and distribute the high concentrated load introduced by the wing sweep actuator bracket. The closure rib is designed to resist the torsional shear loads introduced by the pivot lugs and to distribute the wing sweep actuator bracket kick loads. Although 10 Nickel steel was originally selected due to its superior fracture toughness, the beta annealed titanium provides sufficient safe crack growth capabilities at lower weight and reduced cost.

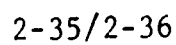
2.1.2 Fail-Safe Integral Lug Configuration

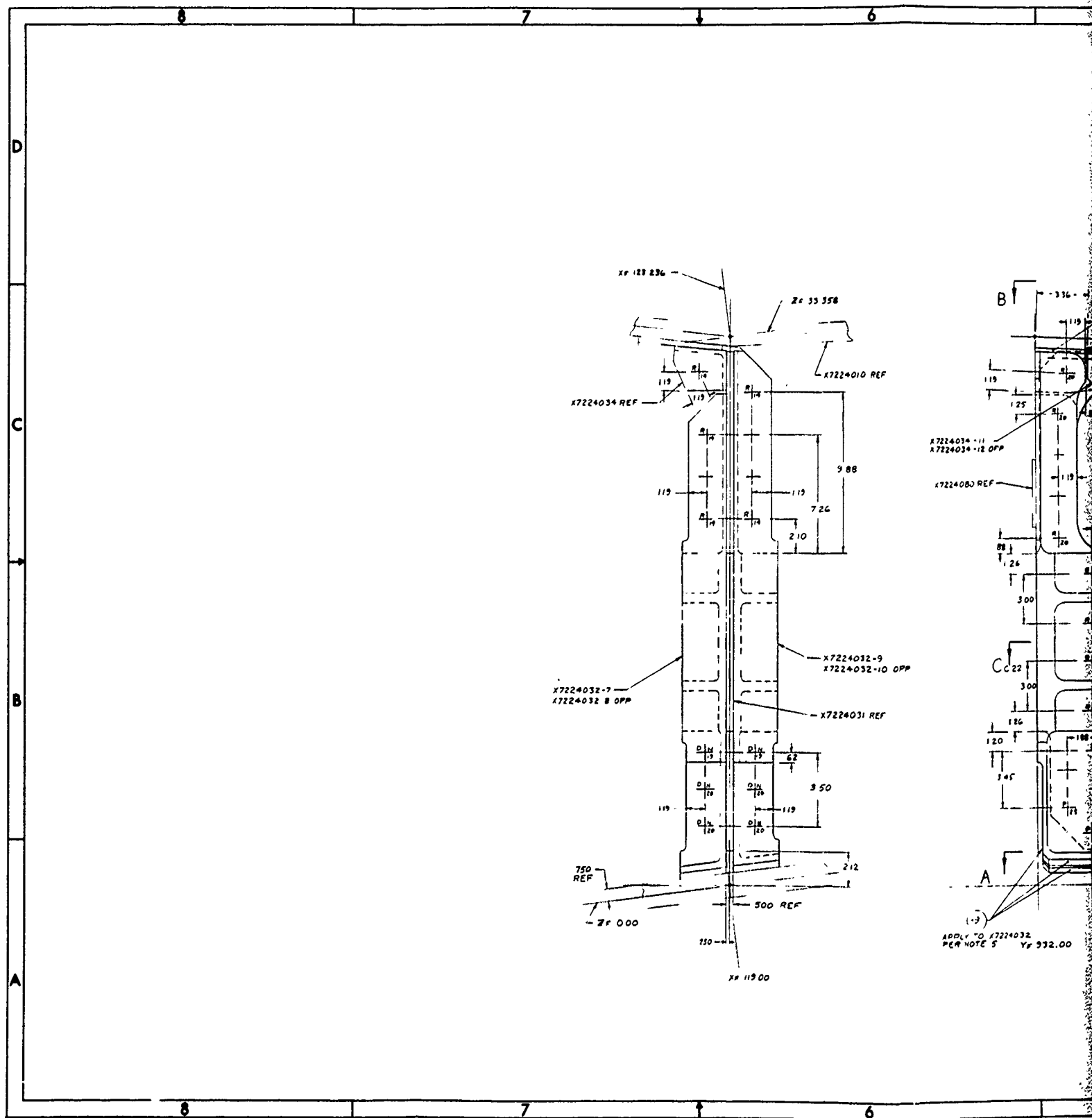
The fail-safe removable lug configuration of Phase Ib has been renamed to reflect the integral lug concept now employed for the lower plate. The objective of this configuration was to achieve a reliable fail-safe design with a minimum quantity of fasteners piercing the critical lower plate. In addition to minimizing fasteners, brazing functions as a crack arrestor to effectively increase the number of elements for additional fail-safe capability.

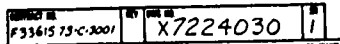
Other design changes incorporated during Phase II, in addition to the integral pivot lug, include the following:

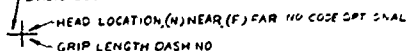












BASIC CODE	NOM INCH REF	HOLE SIZE SPEC	BOLT OR PIN P	NUT P	WASHER, HEAD SIDE	WASHER NUT SIDE	TORQUE IN-FT SPEC	INS-FT SPEC
A	1/2	SEE SPEC	X723399-8	81755/C280-8	81755/PEW-16	X722598-B	SEE SPEC	X7223997-B
B	9/16	SEE SPEC	X723399-9	81755/C280-9	81755/PEW-19	X723398-C	SEE SPEC	X7223997-B
C	5/8	SEE SPEC	X723399-10	81755/C280-10	81755/PEW-22	X723398-D	SEE SPEC	X7223998-10
D	3/4	SEE SPEC	X723399-12	81755/C280-12	81755/PEW-24	X723398-E	SEE SPEC	X7223998-12
E	7/8	SEE SPEC	X723399-14	81755/C280-14	81755/PEW-27	X723398-F	SEE SPEC	X7223998-14
F	1	2502 3436	X723398-B	81755/C2450-B	X723399-8	X723398-B	81757/ 3998-B	NCNC
H	5/8	3770 3766	X723398-12	81755/C2950-12	X723399-12	X723398-12	81757/ 3998-B	NCNC
K	1/2	5025 5296	X723398-16	81755/C2810-16	X723399-16	X722398-16	81757/ MOH-88	NONE
L	1/4	2502 2695	81755/C210-8	81755/C2910-8	X723399-8	X722398-8	81757/ MOH-88	NONE
M	1/2	5025 5296	X722398-B	81755/C010-B	X722399-8	X722398-B	81757/ MOH-88	NONE
N	3/4	5630 6617	X723396-9	81755/C011-9	X722399-9	X722399-9	81757/ MOH-88	NONE
P	5/8	5291	X723396-10	81755/C011-10	X722399-10	X722399-10	81757/ MOH-88	NONE
R	3/4	7526 7491	X723393-12	8165/C077-12	X7223992-12	X7233994-12	81757/ MOH-88	NONE
S	5/8	6275	X722398-11	8158/C077-11	NONE	X7223994-10	81757/ MOH-88	NONE

7 1.1. SMOJIN-2.0DD
8 1/2. CONTAIN FRACTURE CRITICAL DETAILS. RETAIN ORIGINAL DETAIL
9 MATERIAL. TRACEABILITY NUMBERS IN ACCORDANCE WITH X7224/19
10 CLEAN SURFACE OF NOTED PARTS AND APPLY -3 MOLDED SHIM PER
11 B155/PP1101 CLASS II TYPE II TO FILL VOID
12 4. ALL MACHINE SURFACES -101
13 1/4. SEALANT TO ALL PAYING SURFACES AND SHANKS OF STRAIGHT SHANK
14 FASTENERS. METHOD OF APPLICATION PER X7224/196
15 2. ALL FASTENERS EQUALLY SPACED BETWEEN END LOCATED FASTENERS. QUANTITIES
16 AS SHOWN
17 DIMENSIONS/TOLERANCES PER JAS1 Y14.5
18 NOTES (EXCEPT AS SHOWN)

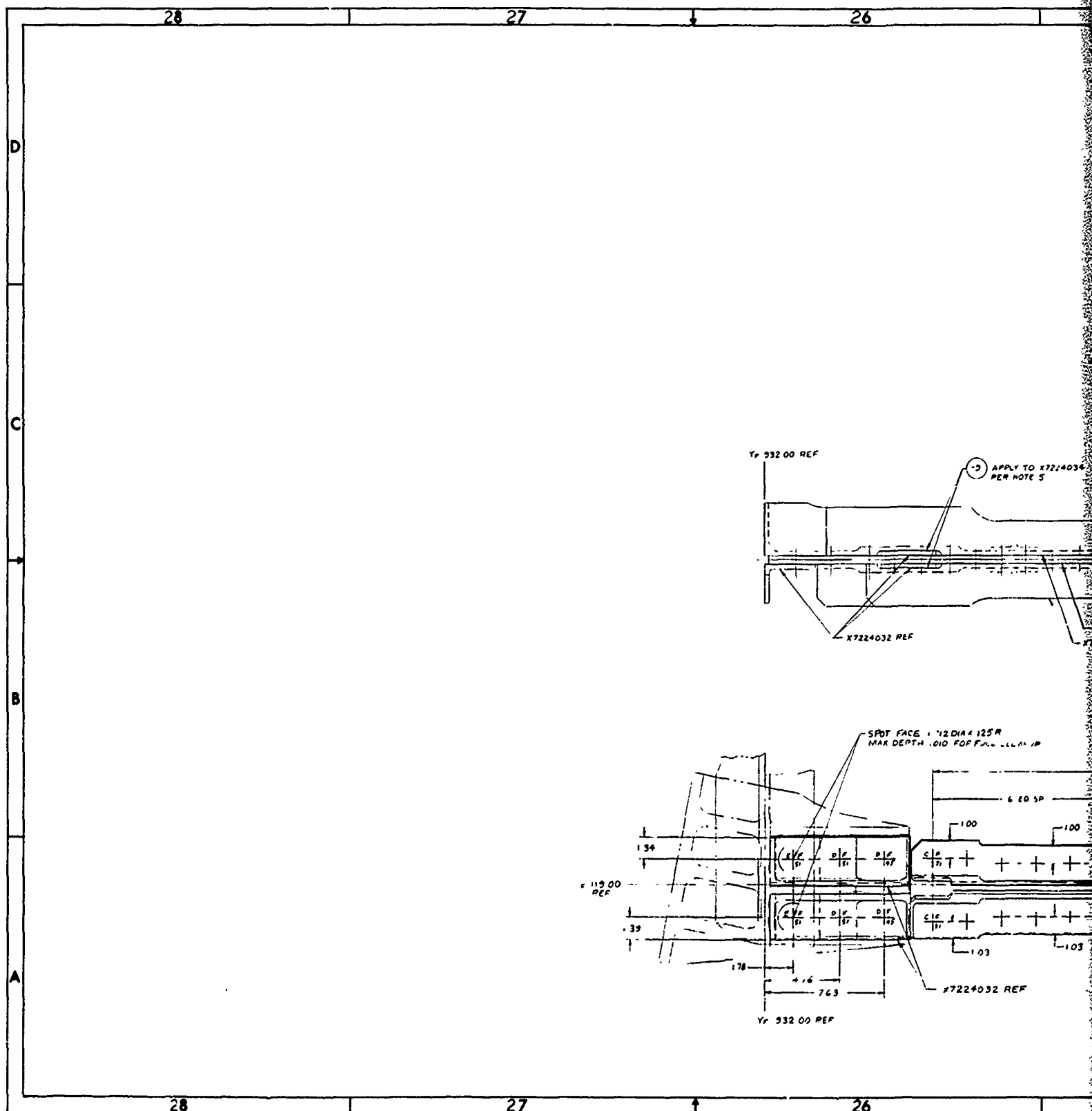
Figure 2-8 (Sheet 1)

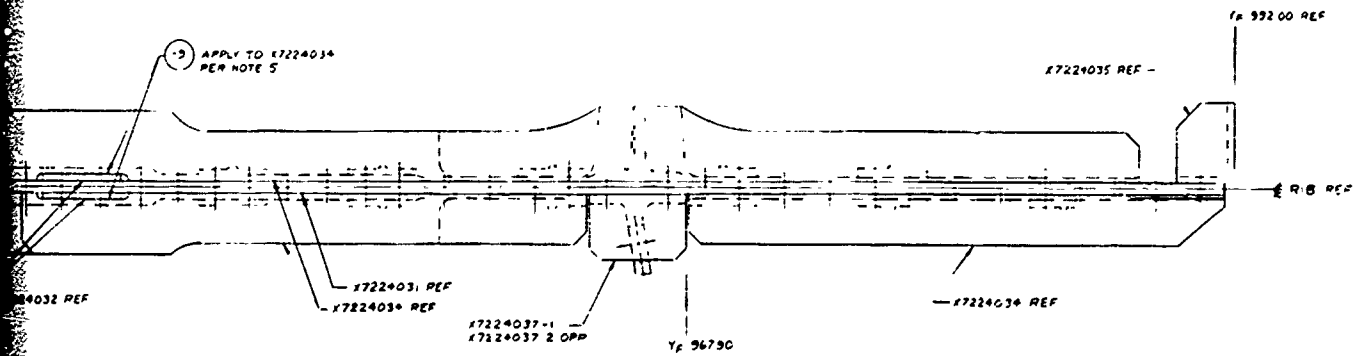
25V	STA-JS
3H	REV
1	—
2	—

SEE SEPARATE PARTS - 57

NEXT SECT LTR. F

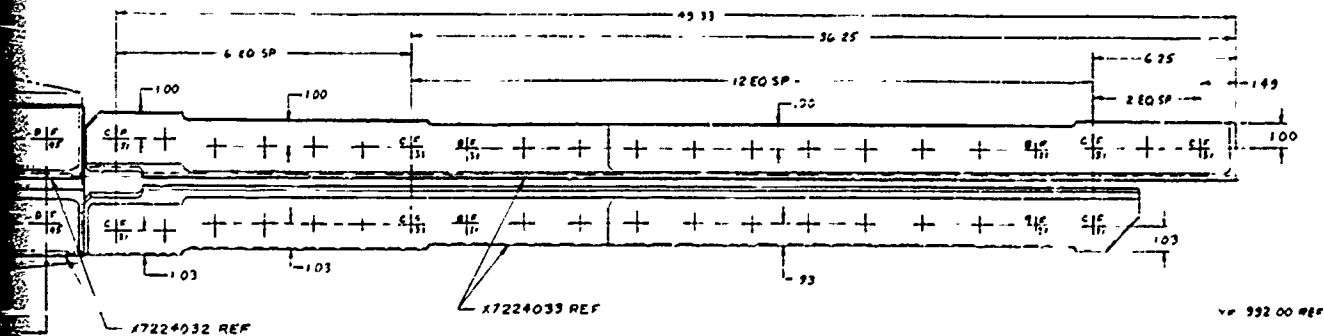
NAME (Last, first, middle) LAST FIRST MIDDLE 1 2 3		GRADE GRADE 1 2 3 4 5 6 7 8 9 10 11 12		DATE DATE 1 2 3 4 5 6 7 8 9 10 11 12	
ADDRESS ADDRESS 1 2 3 4 5 6 7 8 9 10 11 12		CITY CITY 1 2 3 4 5 6 7 8 9 10 11 12		STATE STATE 1 2 3 4 5 6 7 8 9 10 11 12	
PHONE PHONE 1 2 3 4 5 6 7 8 9 10 11 12		SEE PL SEE PL 1 2 3 4 5 6 7 8 9 10 11 12		RIB INSTL - GURBD CLOSURE 1 2 3 4 5 6 7 8 9 10 11 12	
2 STAIRS: ANKLE STAIRS: ANKLE 1 2 3 4 5 6 7 8 9 10 11 12		2 STAIRS: ANKLE STAIRS: ANKLE 1 2 3 4 5 6 7 8 9 10 11 12		2 STAIRS: ANKLE STAIRS: ANKLE 1 2 3 4 5 6 7 8 9 10 11 12	





VIEW B-B C3

SPOT FACE 1812 DIA R125R
MAX DEPTH .010 FOR FULL LENGTH



SECTION A-A A3
NORMAL TO FLANGES

FORM NO. 1
F93615-78-C-3001

X7224030

2

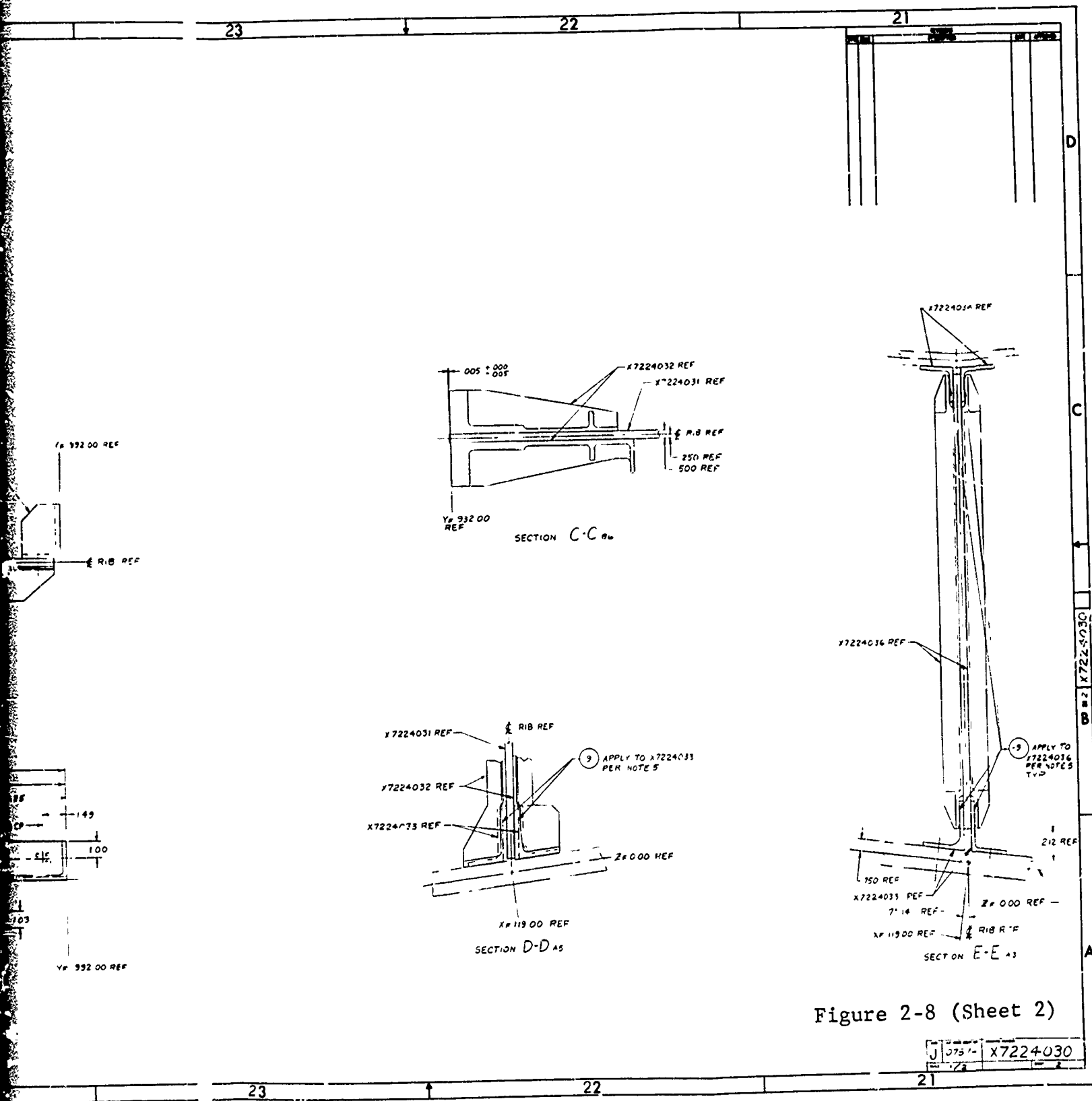


Figure 2-8 (Sheet 2)

- o symmetrically brazed three-element lower place
- o reconfigured internal bulkheads
- o material substitution and fabrication revision to the highly loaded shear webs.

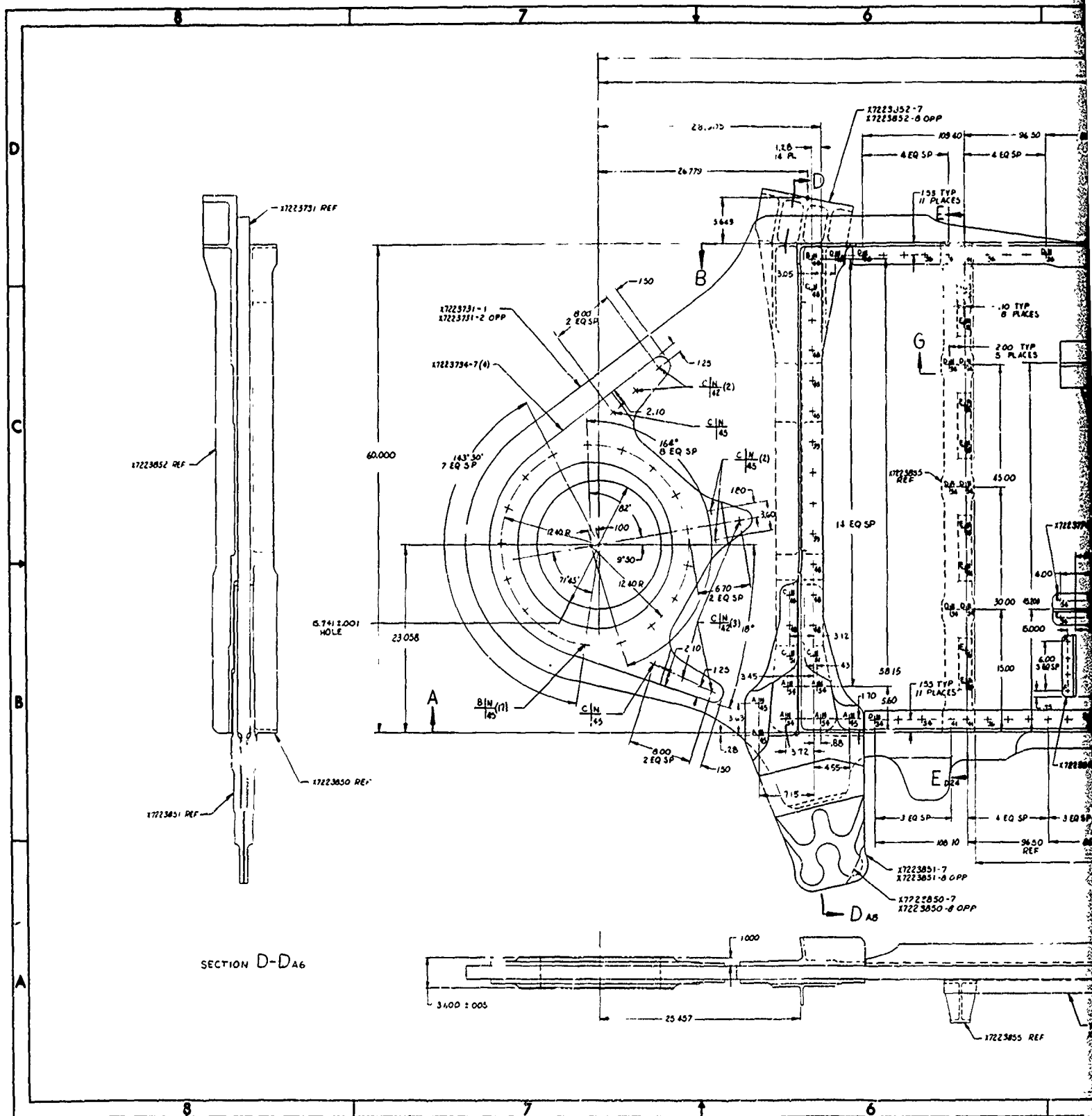
These changes along with a complete description of each major component are discussed in the following paragraphs.

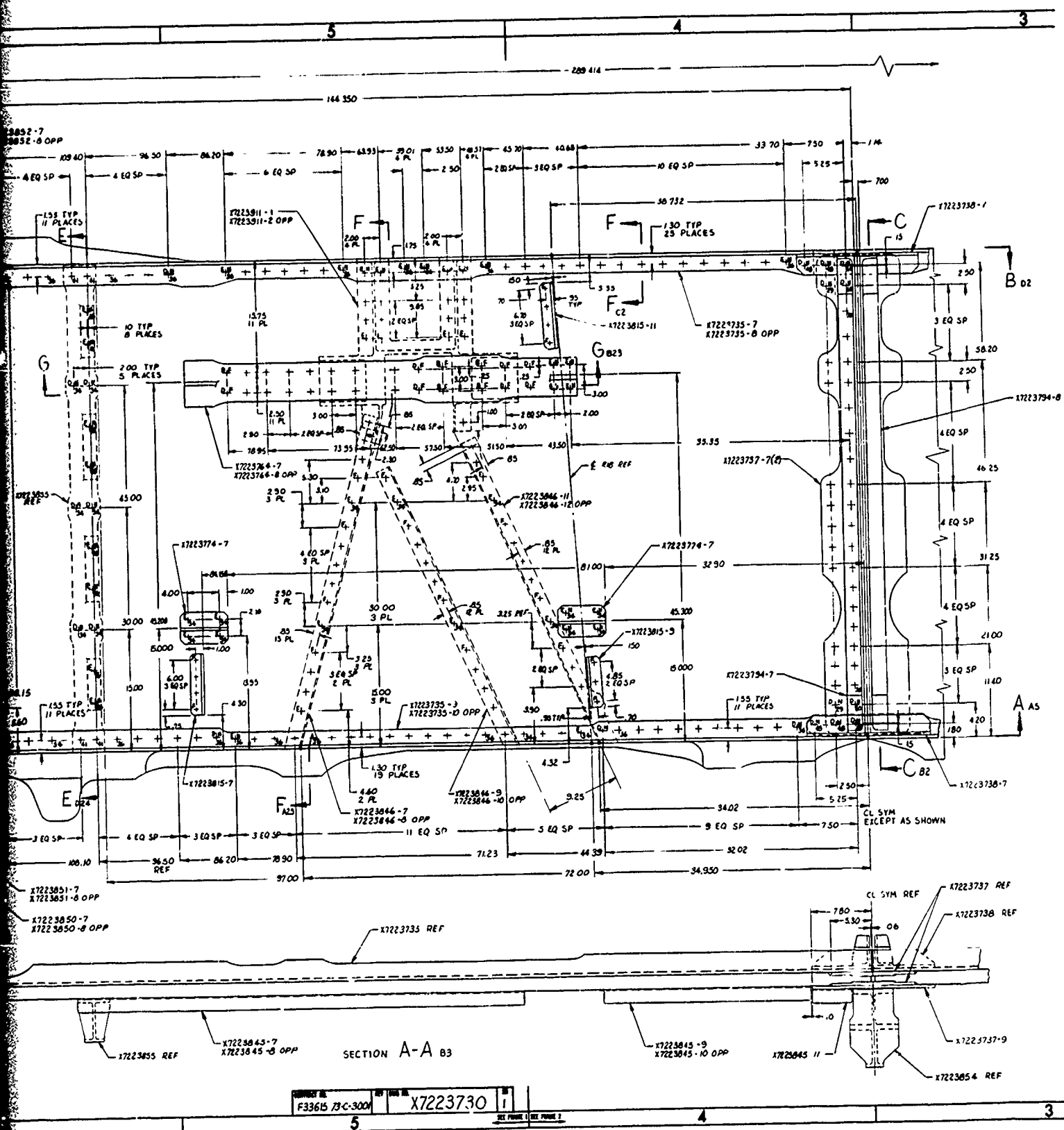
2.1.2.1 Lower Plate Assembly

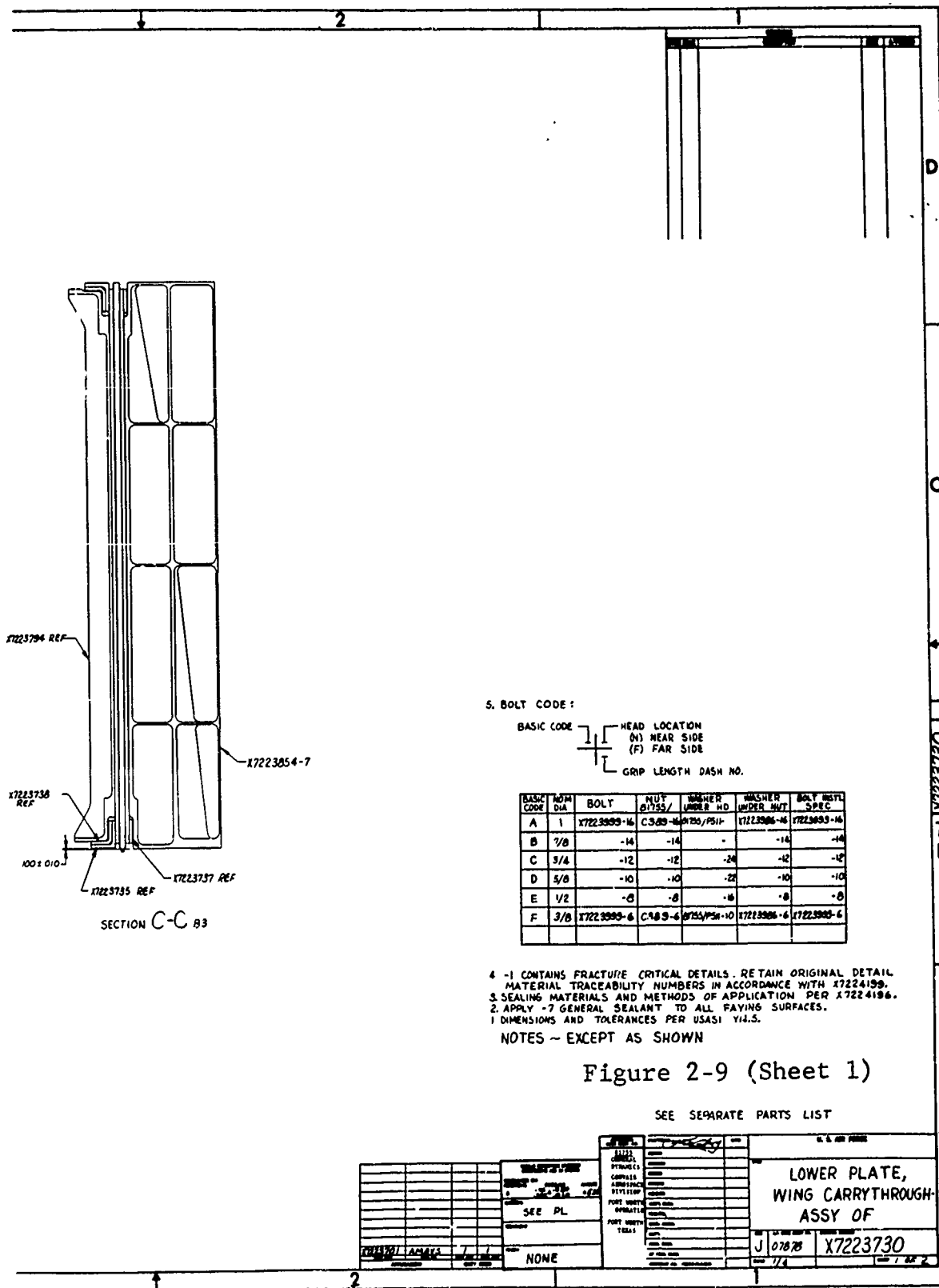
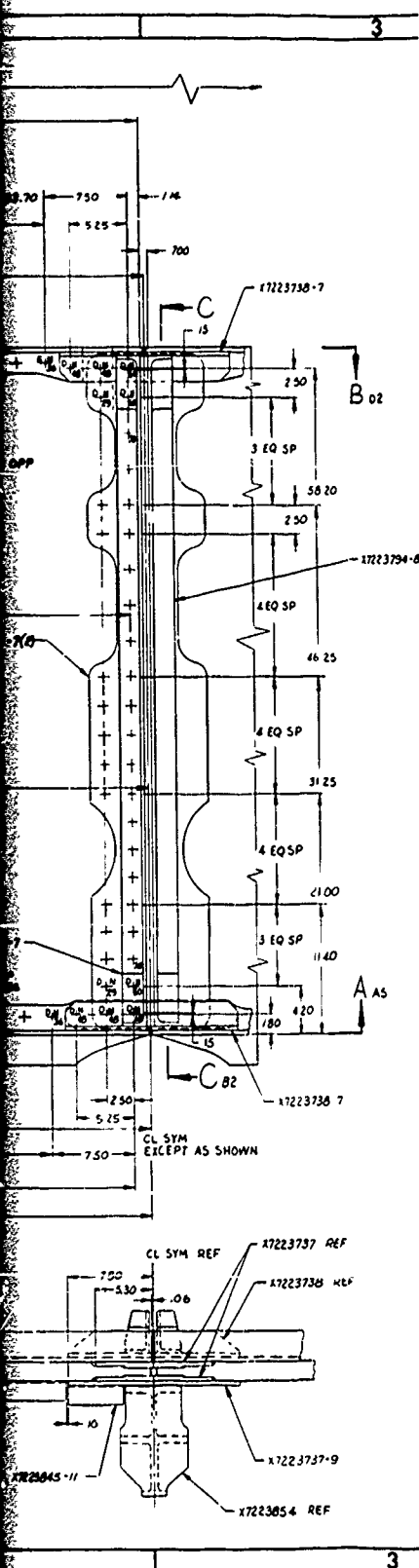
The lower plate assembly (Figure 2-9, Drawing X7223730) consists of two symmetrically brazed Titanium sub-assemblies with integral pivot lugs, lug reinforcing hubs, forward and aft bulkhead attach angles, outboard longeron splice fittings, stabilizing beam at X_F99, and centerline splice plates. These components are mechanically assembled using taper-lok fasteners for a minimal stress concentration intensity. The integral lug concept improves fabrication by eliminating the separate brazed assembly for the pivot lug and eliminates the critical fit between the lug and plate. The integral lug is also a more weight efficient configuration and improves structural reliability by deleting the dependence on mechanical fasteners for transferring the critical lug loads into the box structure. The symmetrically brazed concept permits the assembly to be used as either a left or right hand part, but requires separate bolt-on bulkhead attachment angles. Eccentric loading of the brazed joints is also minimized by the symmetrical design.

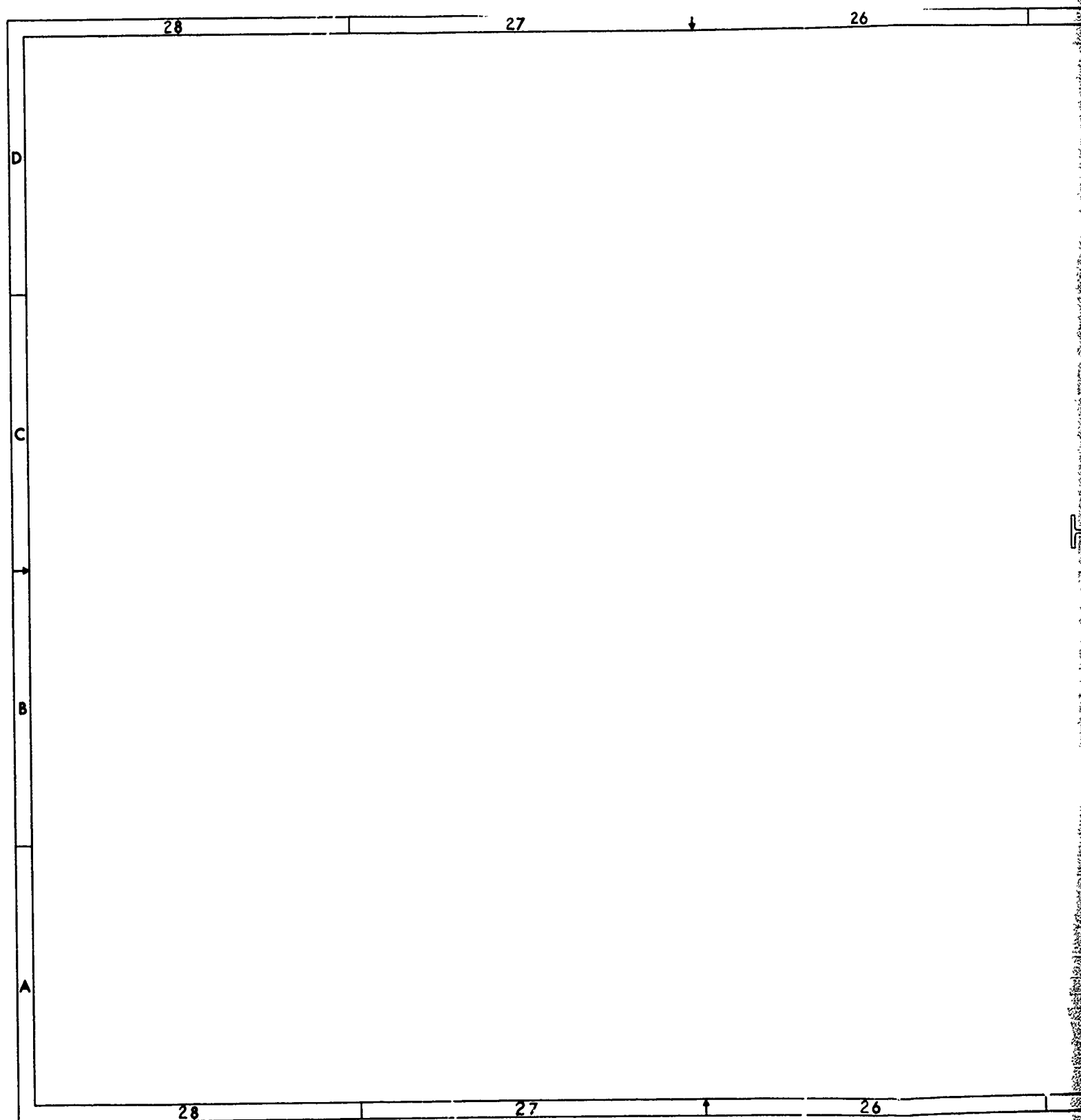
The brazed plate assembly shown in Figure 2-10 (Drawing X7223731) is constant thickness consisting of three lamina of beta-annealed 6AL-4V titanium which extend to include the pivot lug. The one-piece center lamina is a solid thin plate whereas the one-piece upper and lower elements are profiled into five crack stopper bars, inboard of the lug region. The plate assembly, as brazed, is symmetrical about its horizontal centerline. Local machining will be required after brazing to obtain identity as either a left or right hand part.

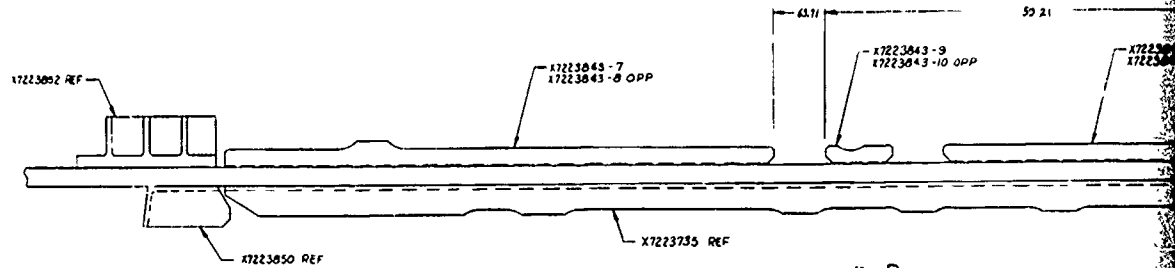
The aft longeron splice fitting consists of two elements of beta annealed 6Al-4V titanium, attached with fasteners to the brazed assembly. The upper element extends the full width of the plate and incorporates the vertical flange for attaching the closure rib. The lower element terminates after transferring the longeron load into the lower plate. This splice provides extra thickness to accommodate the baseline longeron interface



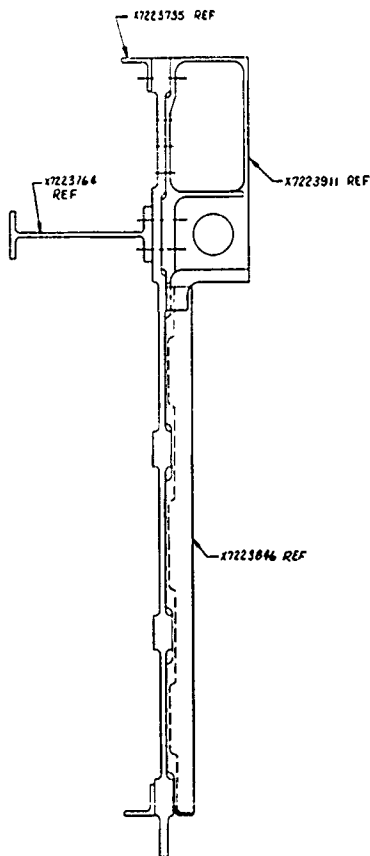




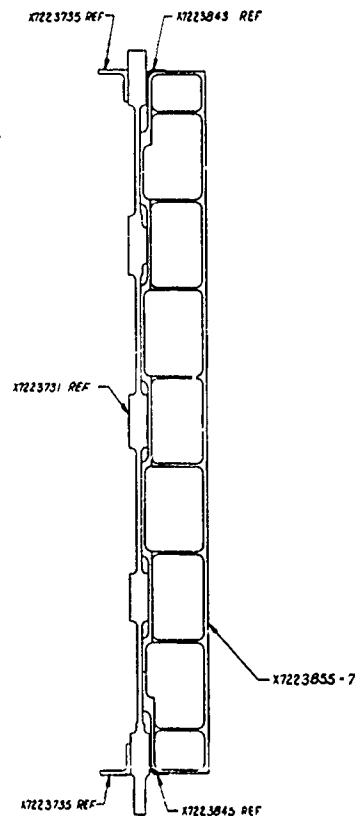




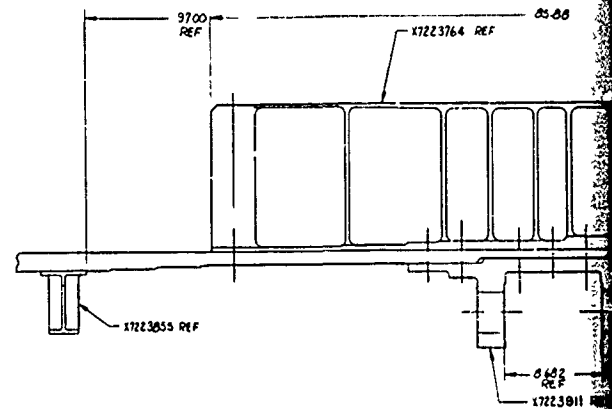
SECTION B-B



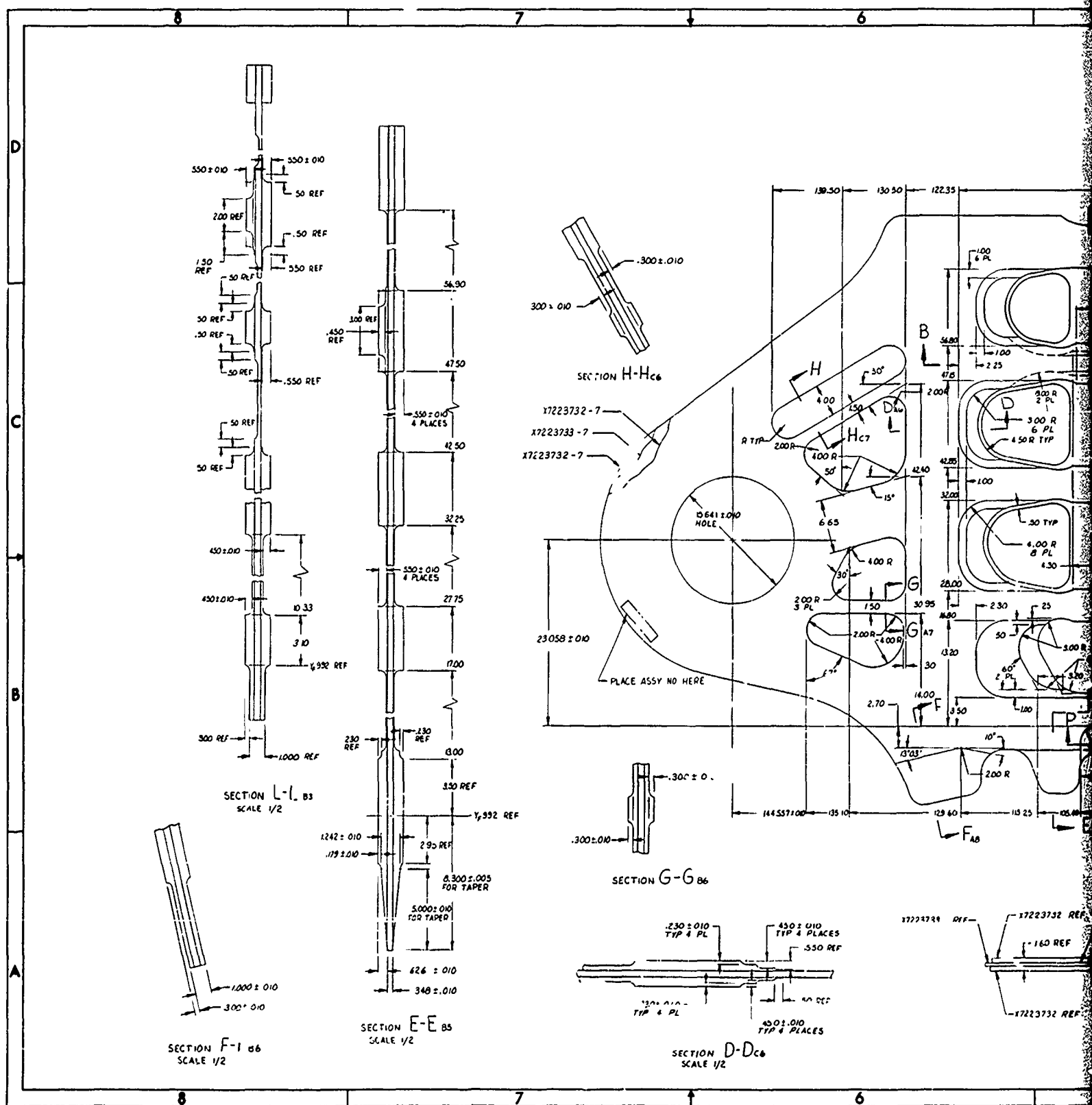
SECTION F-F

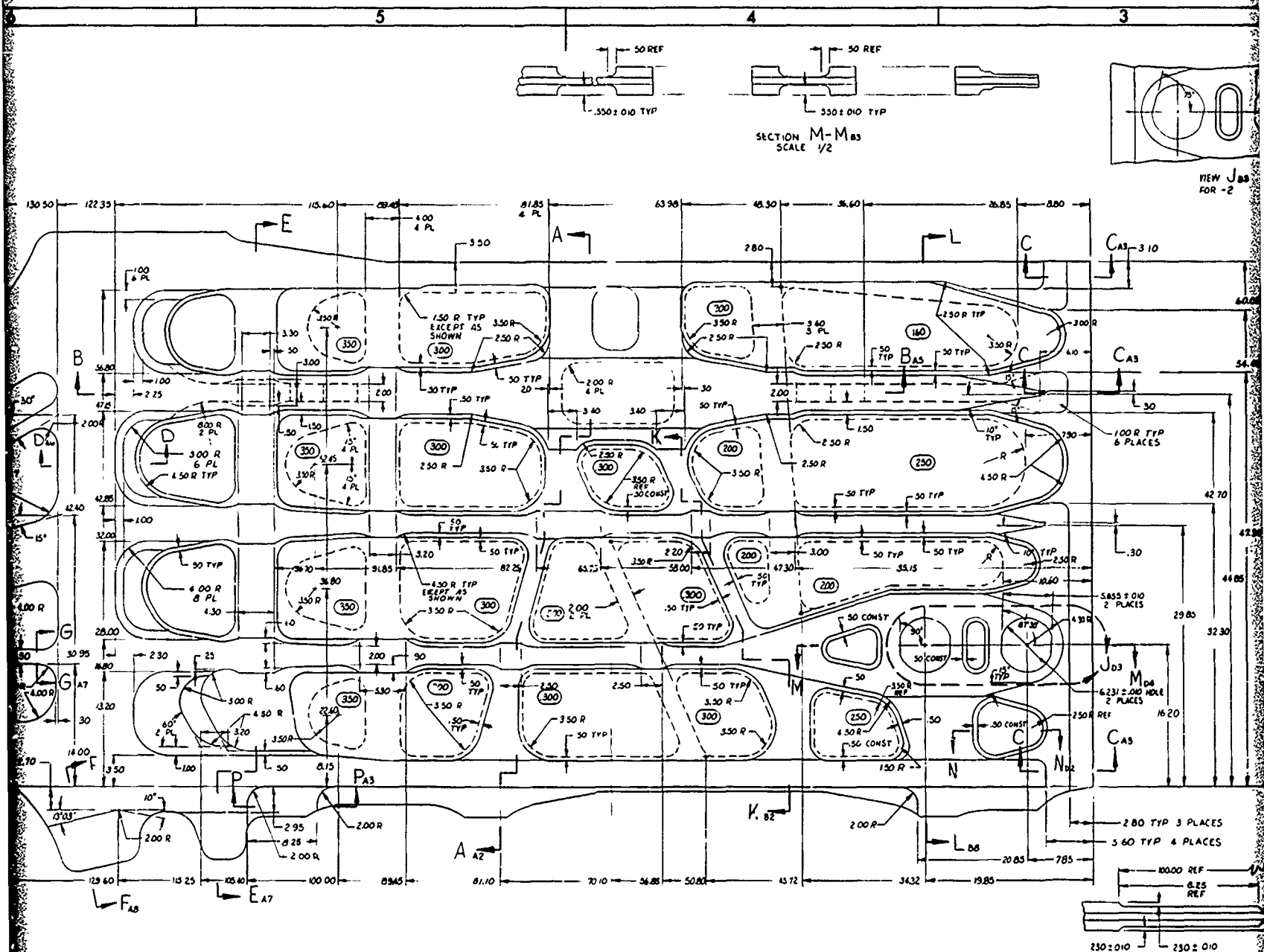


SECTION E-E

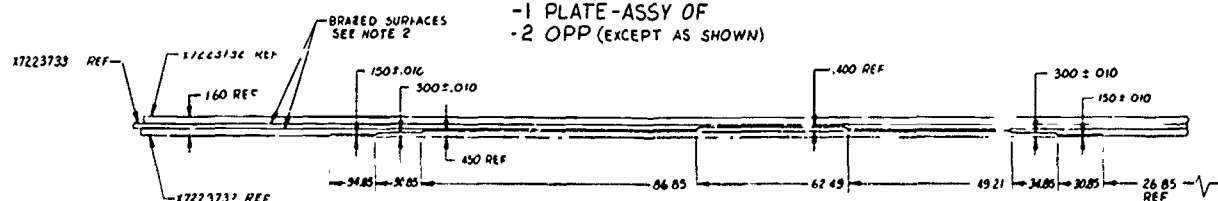


SECTION G-G



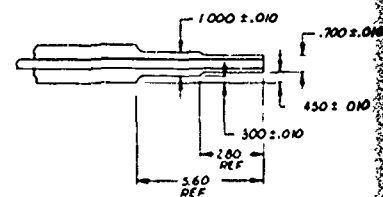


-1 PLATE-ASSY OF
-2 OPP (EXCEPT AS SHOWN)



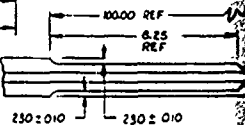
SECTION B-Bc4

CONTRACT NO. F33615-73-C-3001
REV. 1000 1000
17223731



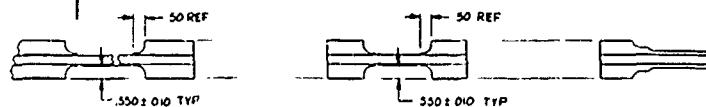
SECTION C-C 83,C3, D3
SCALE 1/2

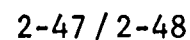
SECTION P-Pa5



VIEW J-B5
FOR -2

SECTION M-MB3
SCALE 1/2





3

requirement, and it reduces the material width required in the lower plate from 84 inches to 73 inches.

The forward longeron splice fitting is integrally machined from 7050 aluminum plate and is mechanically fastened to the lower surface of the brazed lower plate. The fitting extends the full width of the lower plate and includes a vertical flange for attaching the support structure for the lower contoured fairing.

Separate bolt-on lug reinforcements are required to supplement the strength capability of the brazed assembly, and to maintain baseline bearing thickness at the pivot hole. The attaching taper-lok bolts are located in relatively low stressed areas and provide a positive control against element delaminations.

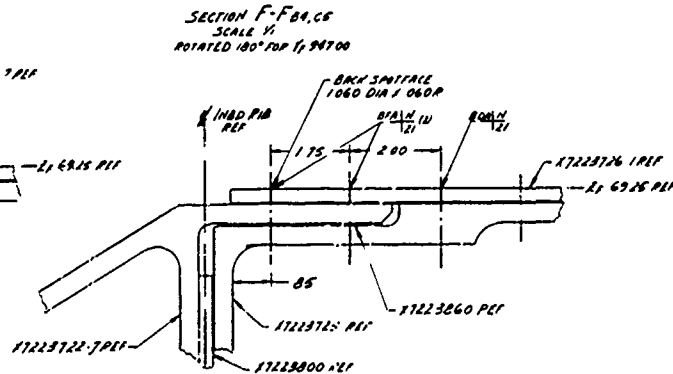
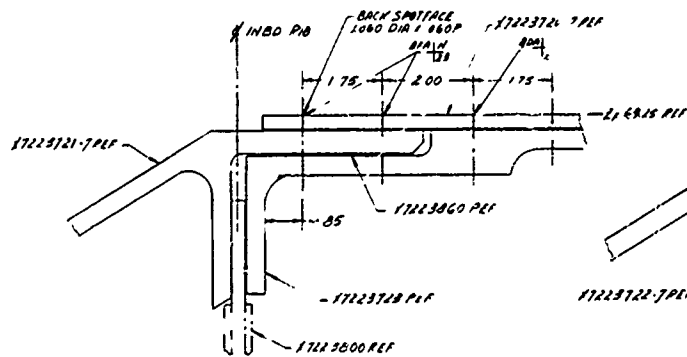
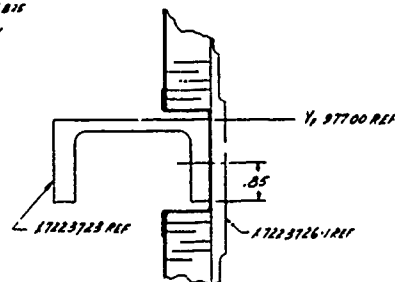
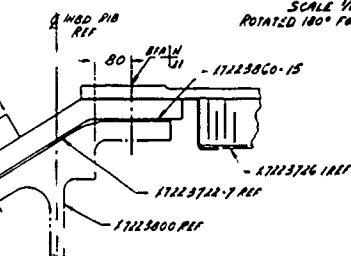
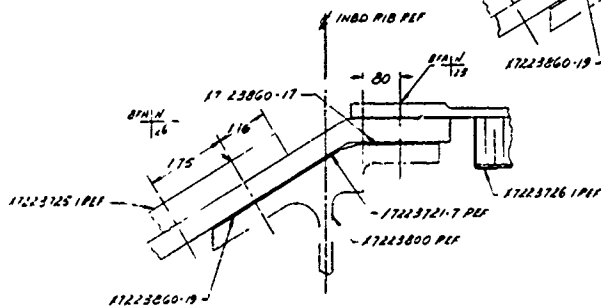
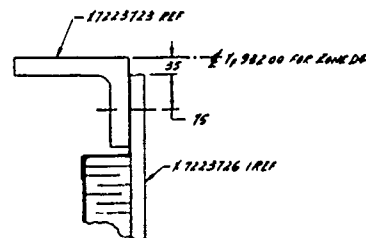
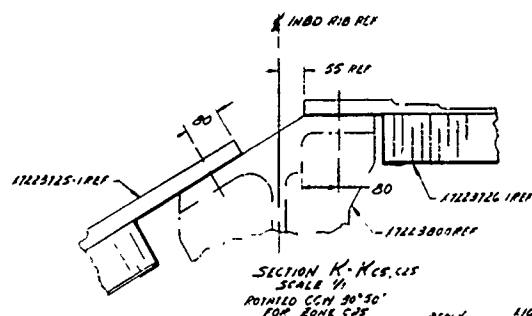
The reinforcement beams attached to the external surface of the lower plate at X_F99 are required for compression stability during negative loading conditions and extend to contour for support of the lower fairing. The beams have been redesigned from a built-up aluminum section to an integrally machined part of 7050 aluminum.

2.1.2.2 Upper Plate Assembly

The upper plate assembly (Drawing X7223720, Figure 2-11) reacts the compression load introduced into the box structure by the pivot pins. Since the primary loading is compression, no fail-safe features are required. This structure is critical in compression stability.

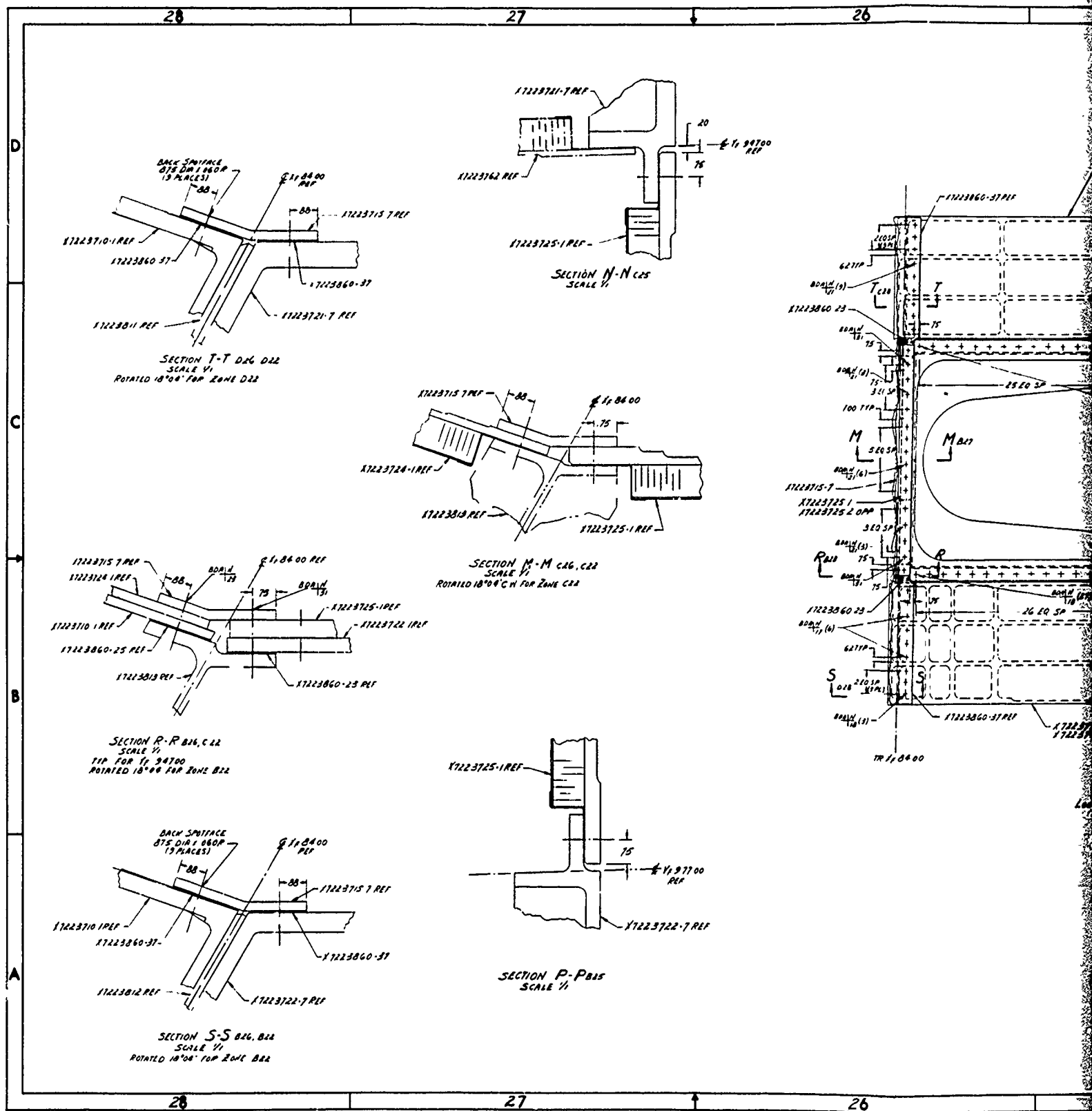
The section outboard of X_F84 consists of integrally machined details electron-beam welded together and a bolt-on sandwich panel. The welded assembly includes the pivot lug, forward and aft partial width plate elements, and an outboard plate rail in the area of the closure rib. Beta annealed 6Al-4V titanium material was selected for the weld assembly to obtain its high fracture toughness because of the critical nature of the pivot lug and integral aft longeron tab. Although compression is the primary load, the pivot lug will experience some local tensile stresses, while the longeron tab is loaded primarily in tension. The sandwich panel is made of 6Al-4V-2Sn titanium for maximum strength and stiffness.

The intermediate section (X_F39 to X_F84) consists of integrally machined forward and aft partial width plates connected by a bolt-on sandwich panel. Aluminum was selected for both the plate



SECTION H-H D/S, C/S
SCALE 1/4

SECTION L-L B/S
SCALE 1/4
TIP 2 PLACES



elements and the sandwich panel to minimize cost. The heavier gages used for the aluminum structure also reduces the stiffening requirements to prevent buckling. 7050 aluminum with its superior strength and above average fracture toughness was used for the integrally machined plate elements. The sandwich panel is fabricated from 2024 aluminum sheet, reinforced with 5052 aluminum core.

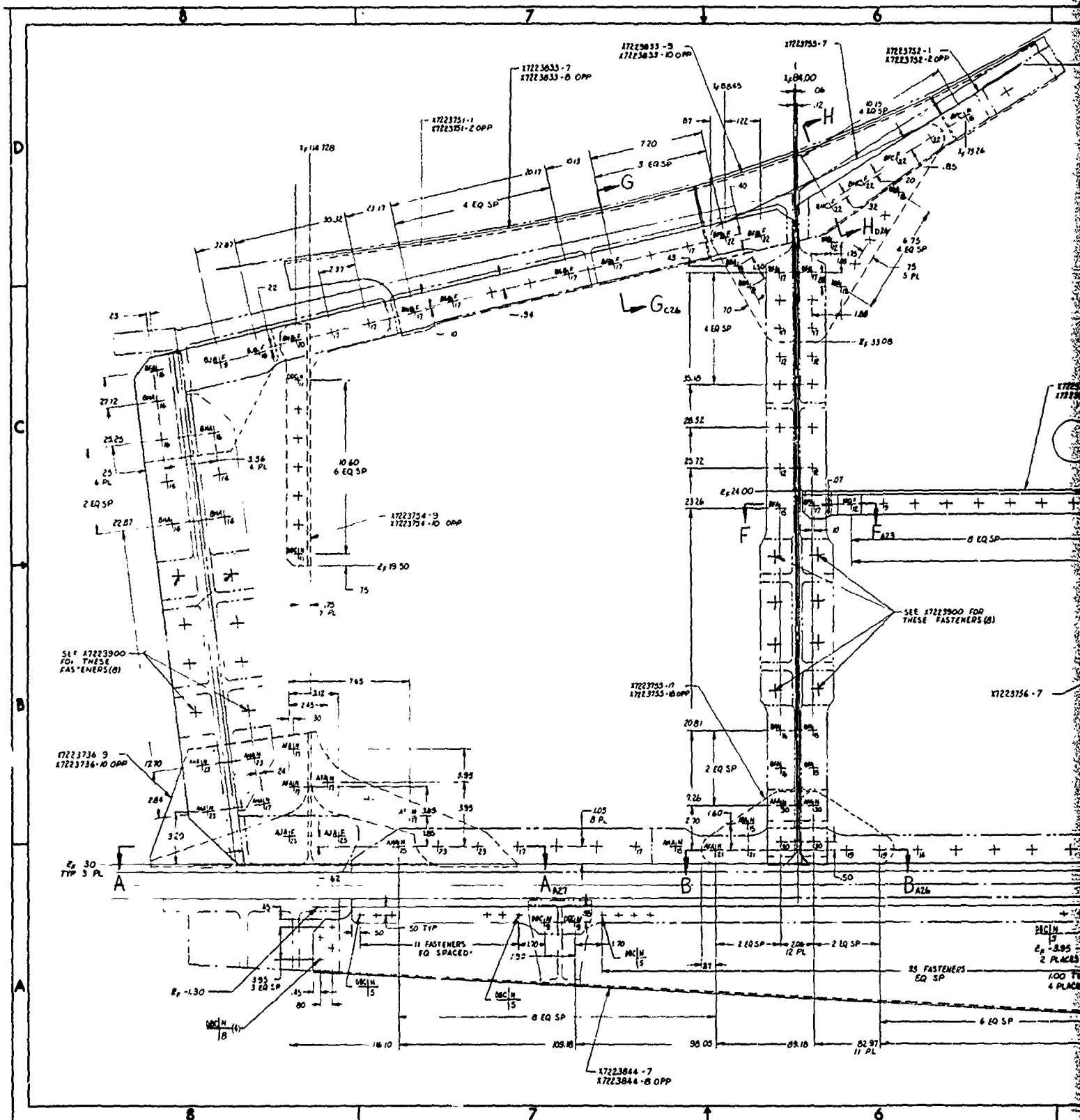
The area inboard of X_F 39 consists of a 2024 aluminum sandwich panel supported by 7050 aluminum rails at Y_F 932, Y_F 947, Y_F 977, and Y_F 992. Sandwich type construction is the most efficient structure in this region due to the low load density, the compression stability, and the fuel pressure requirements.

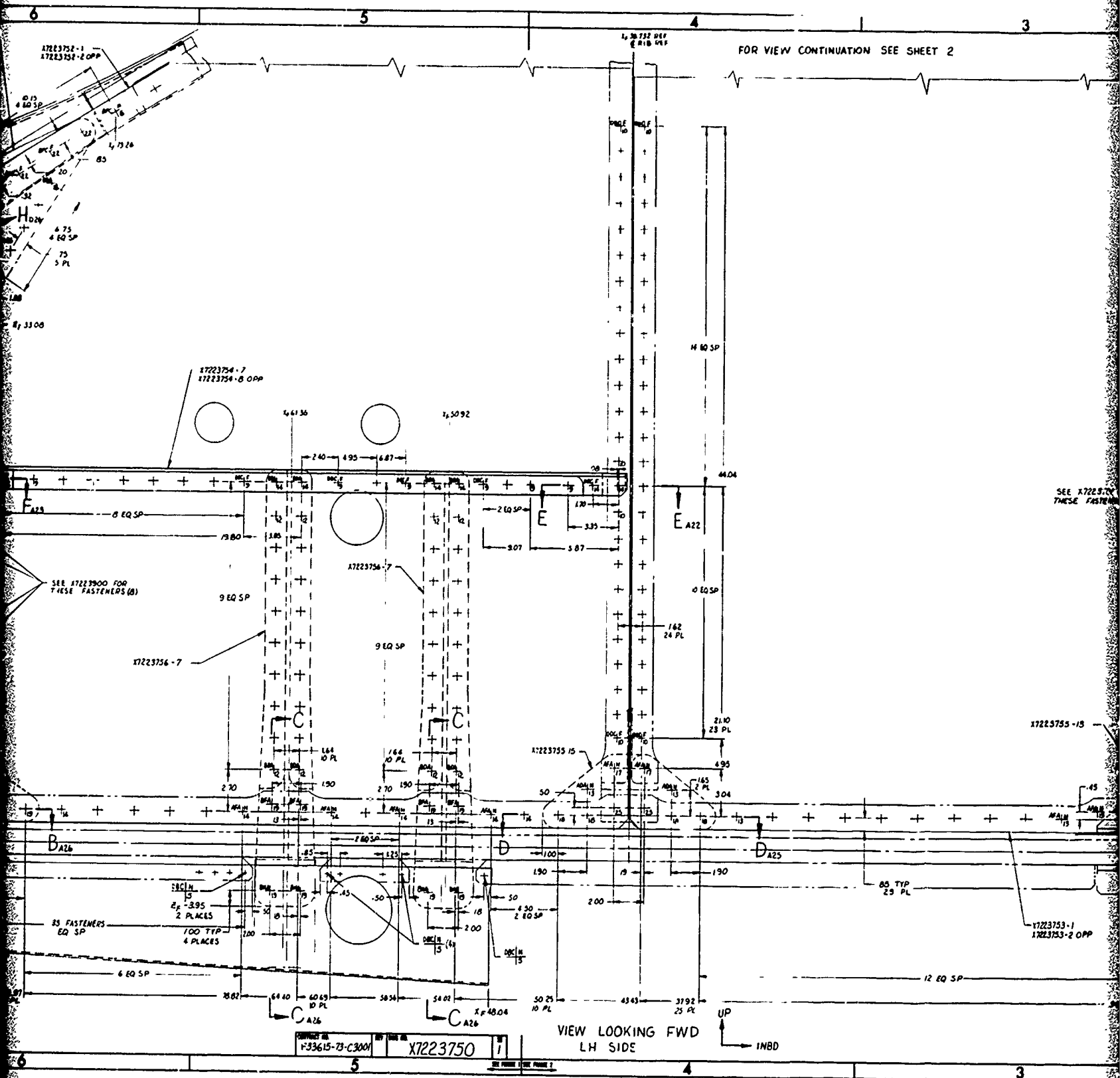
The intermediate section is mechanically attached to the outboard and inboard sections through tension splices which sandwich the ribs at X_F 39 and X_F 84. This type splice was employed to transfer the compressive loads through bearing, thus minimizing the fasteners requirement. Splices are required at these locations to accommodate the changes in direction of the upper surface. Integral flanges are provided for the attachment of the bulkheads and ribs. The upper plate has been configured to concentrate the axial load in the forward and aft plate elements to some extent. It is easier to stabilize this portion of the upper cover because of the bulkhead spacing.

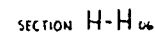
The intermediate section deviates from the baseline structure in that it is located below contour. This was accomplished to eliminate costs associated with part fabrication to a contoured surface. A separate, non-structural fairing is required to achieve fuselage contour.

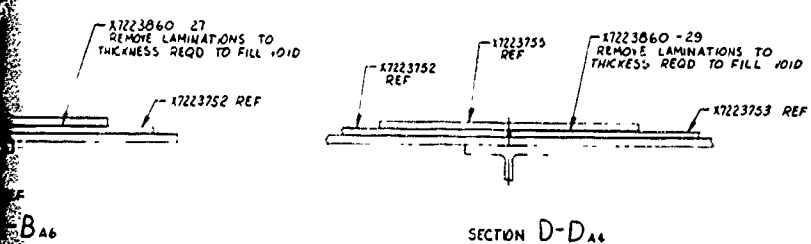
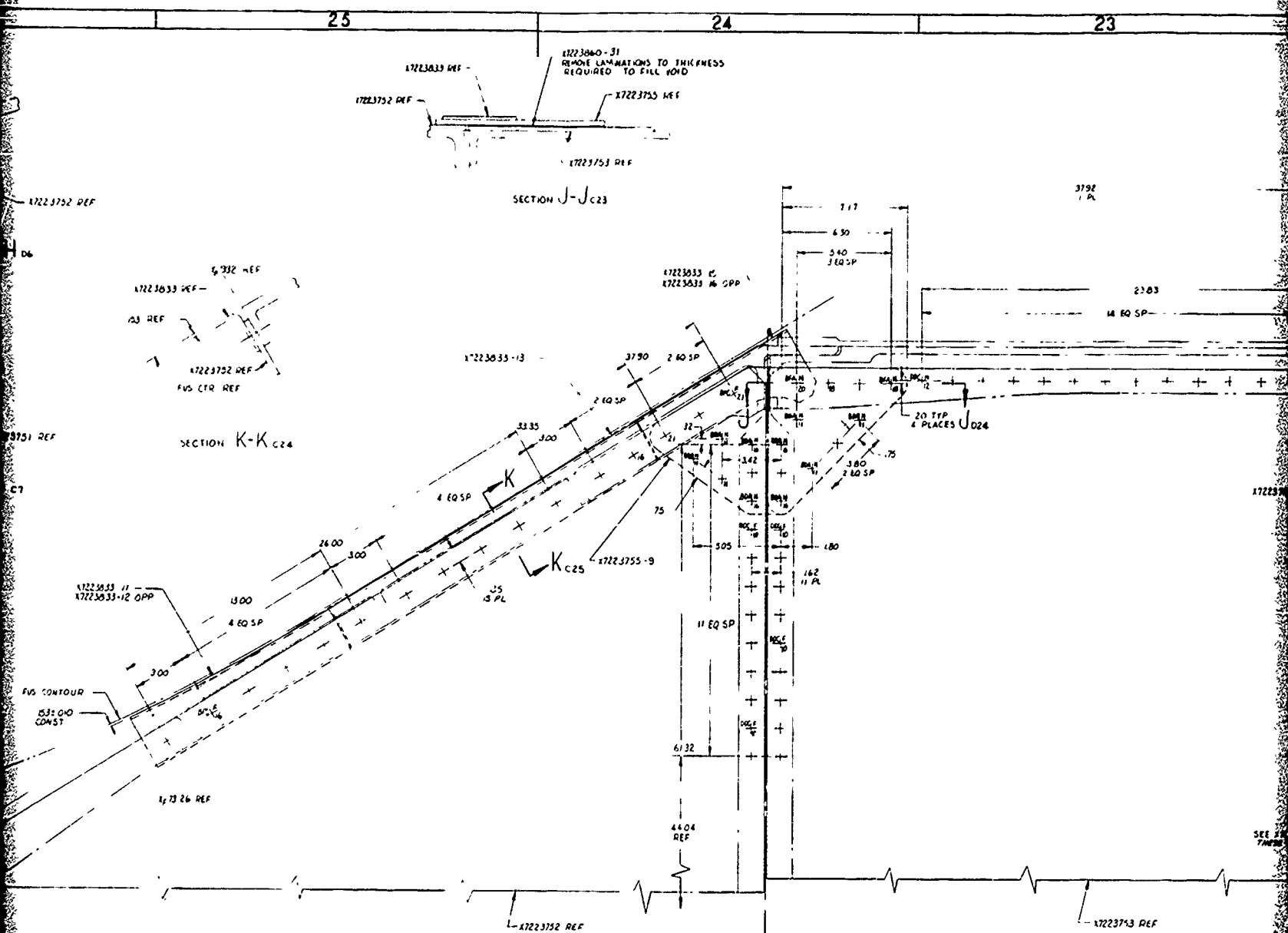
2.1.2.3 Y_F 932 Bulkhead

The forward bulkhead at Y_F 932 is shown in Figure 2-12 (Drawing X7223750). It reacts shear loads and fuel pressures, and distributes the inboard-outboard loads from the wing sweep actuator. The bulkhead also reacts the vertical kick loads from the MLG drag fitting. The two web elements outboard of X_F 39 consist of beta annealed 6AL-4V titanium reinforced with 5052 aluminum core. The Phase Ib design utilized laminated sheets of Beta "A" titanium adhesively bonded together. Test results, however, indicated the crack growth characteristics of Beta "C" sheet were inadequate. Aluminum was considered for this portion of the bulkhead web. However, the lower portion of the webs receive high tensile stresses from the lower plate and the fatigue

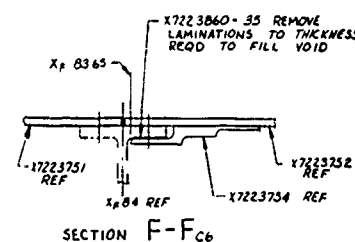








VIEW LOOKING FWD
LH SIDE



CONTRACT NO. F33615-73-C3001
X7223750
2

25

24

23

allowables for aluminum would not permit its use in conjunction with the titanium lower plate.

The panel inboard of Y_F 947 experiences relatively low load intensity, permitting the use of lower cost aluminum construction. 2024 aluminum sheet reinforced with 5052 core is used for this panel. This panel interfaces with the weapons bay wall and the rotary launcher fitting.

2.1.2.4 Internal Bulkheads

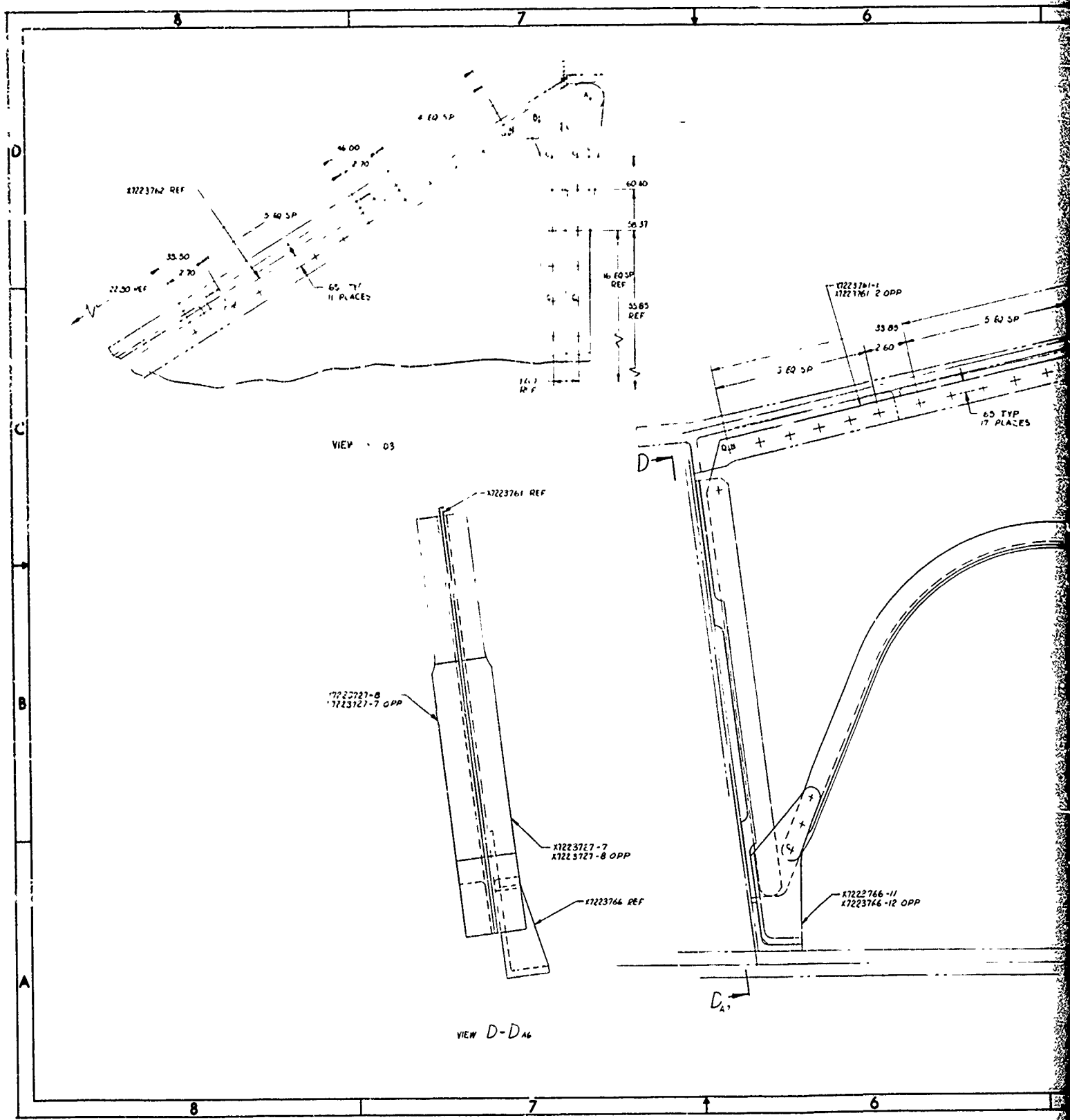
The internal bulkheads, located at Y_F 947 and Y_F 977, have been changed to "arched" configurations as shown in Figures 2-13 and 2-14 (drawing X7223760 and X7223770 respectively). The arched concept permits the use of lower cost aluminum construction by deleting the strain compatibility requirement with the titanium lower plate. Fastener reduction is also accomplished in the fatigue critical lower plate by eliminating the attachment of these bulkheads. The internal beam and its necessary attachments through the lower plate are still required, however, at Y_F 947 to support the MLG drag brace fitting.

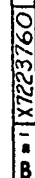
2.1.2.5 Y_F 992 Bulkhead

The aft bulkhead is shown in Figure 2-15 (Drawing X7223780) and is similar to the Y_F 932 bulkhead in type of material and fabrication. The only exception is the panel inboard of X_F39. Due to the higher axial stresses near the lower surface and the loads introduced by the MLG side load fitting, titanium was required for this panel. In addition to the MLG side load fitting, support is also provided to the MLG trunion fittings at X_F72 and X_F95.5. Access into the box structure is also provided in this bulkhead.

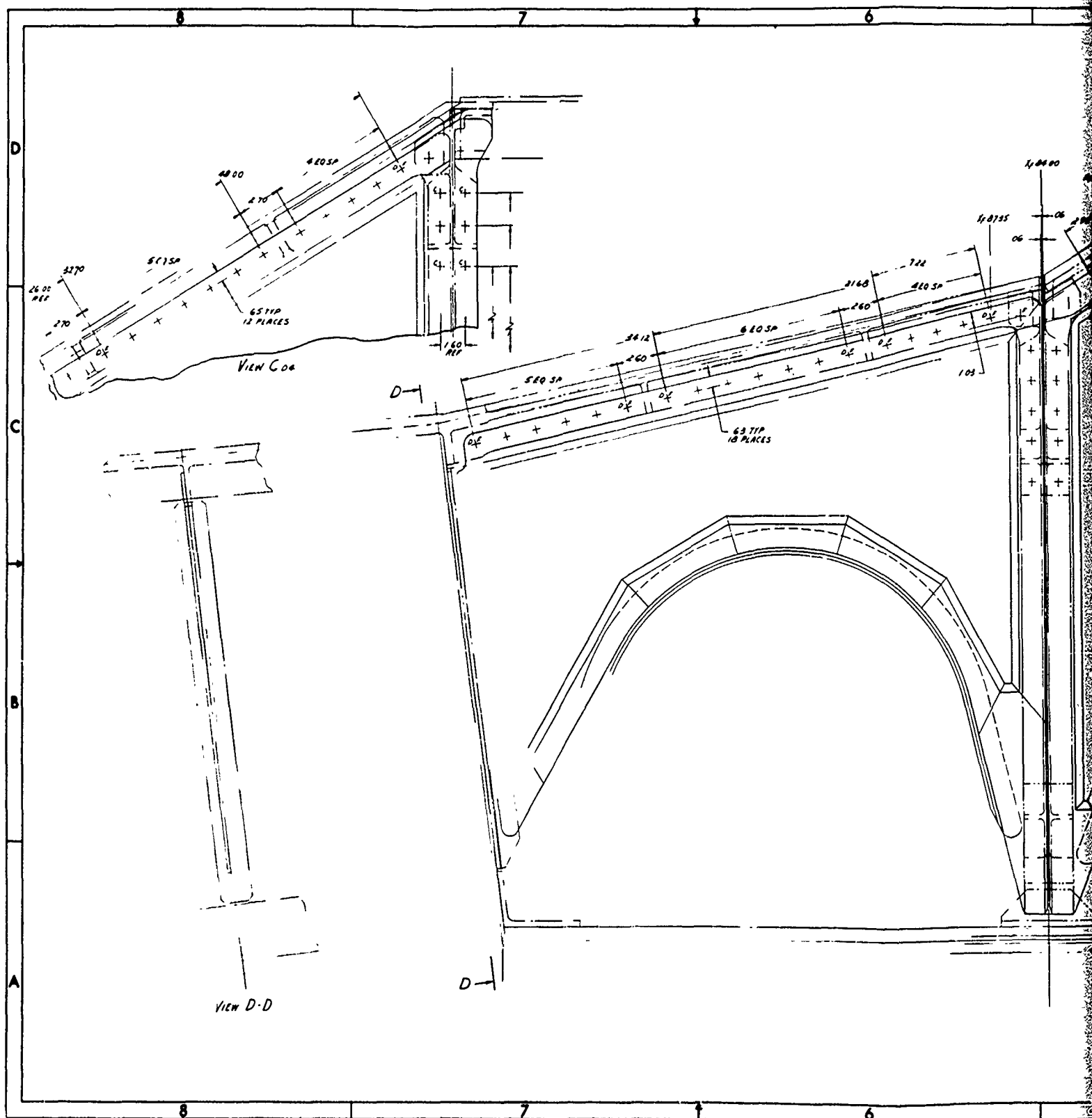
2.1.2.6 Outboard Closure Rib

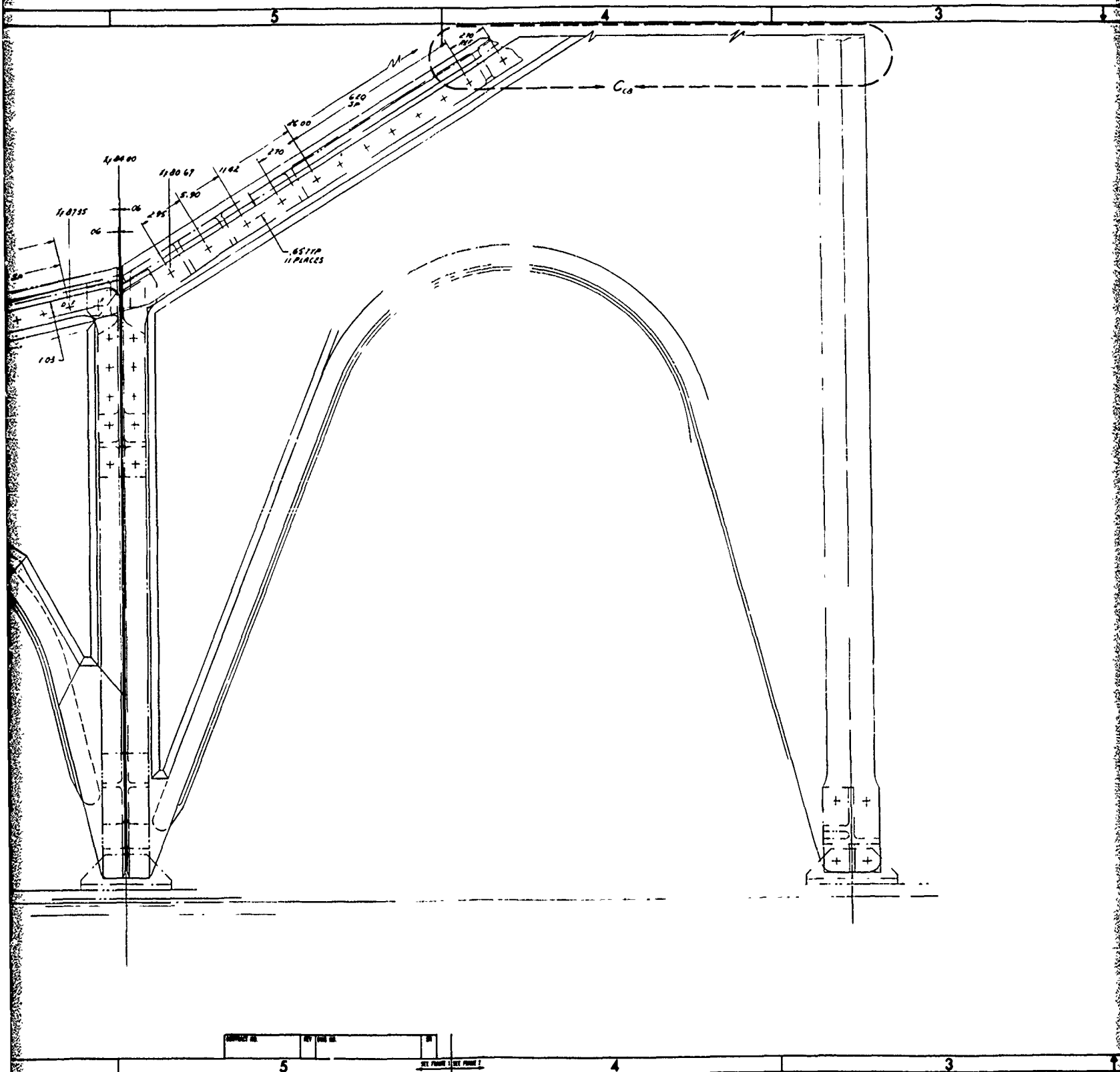
The outboard closure rib (drawing X7223820, Figure 2-16) is a fracture critical part designed to safe life requirements. The rib reacts torsional shear loads introduced by the pivot lugs, distributes the kick load from the wing sweep actuator attach fitting and resists fuel pressure loads. Beta annealed 6AL-4V titanium is used for the web and bolt-on fittings which distribute the actuator kick loads into the web. The web is reinforced with several bolt-on 7050 aluminum stiffeners.

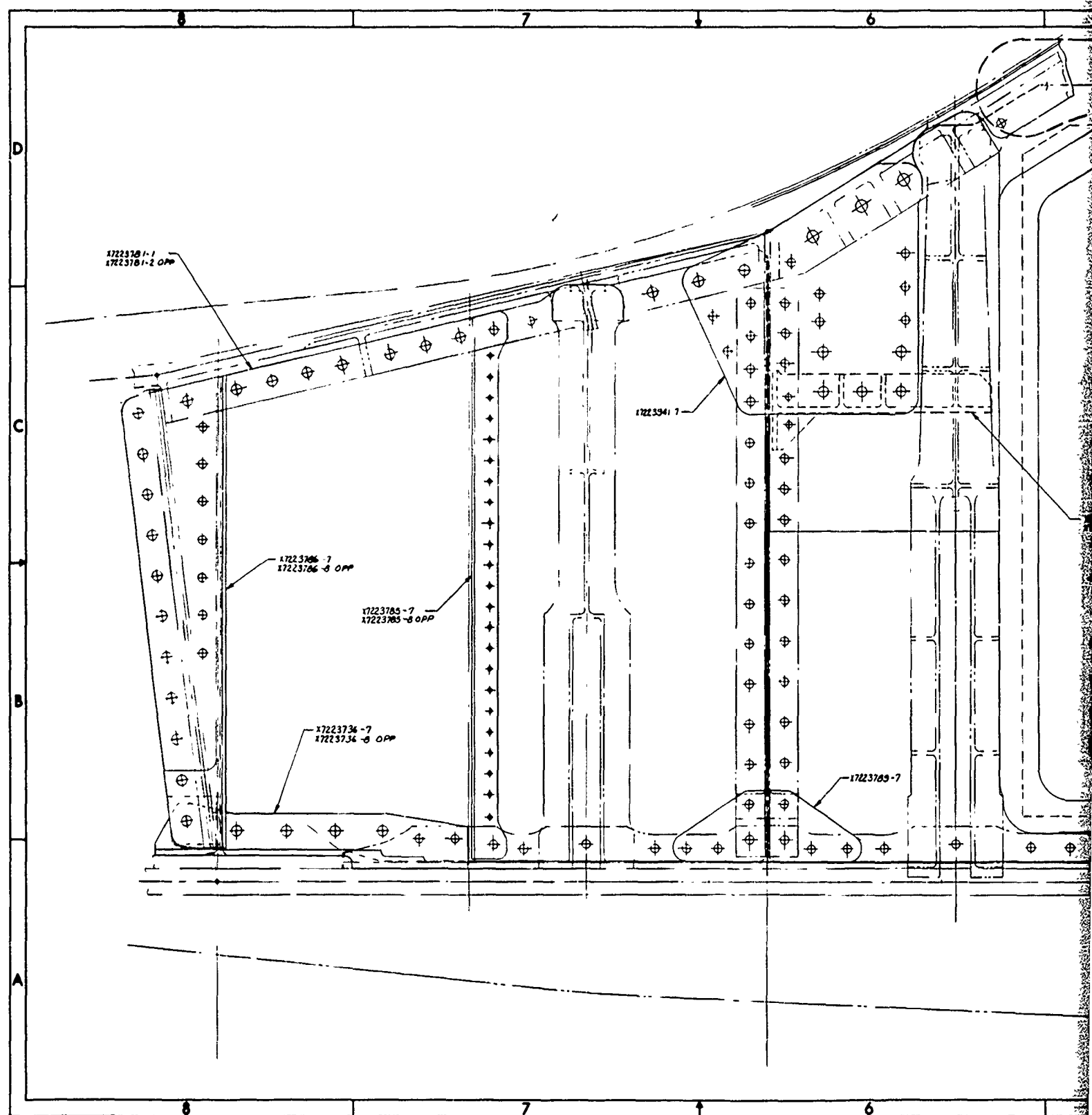


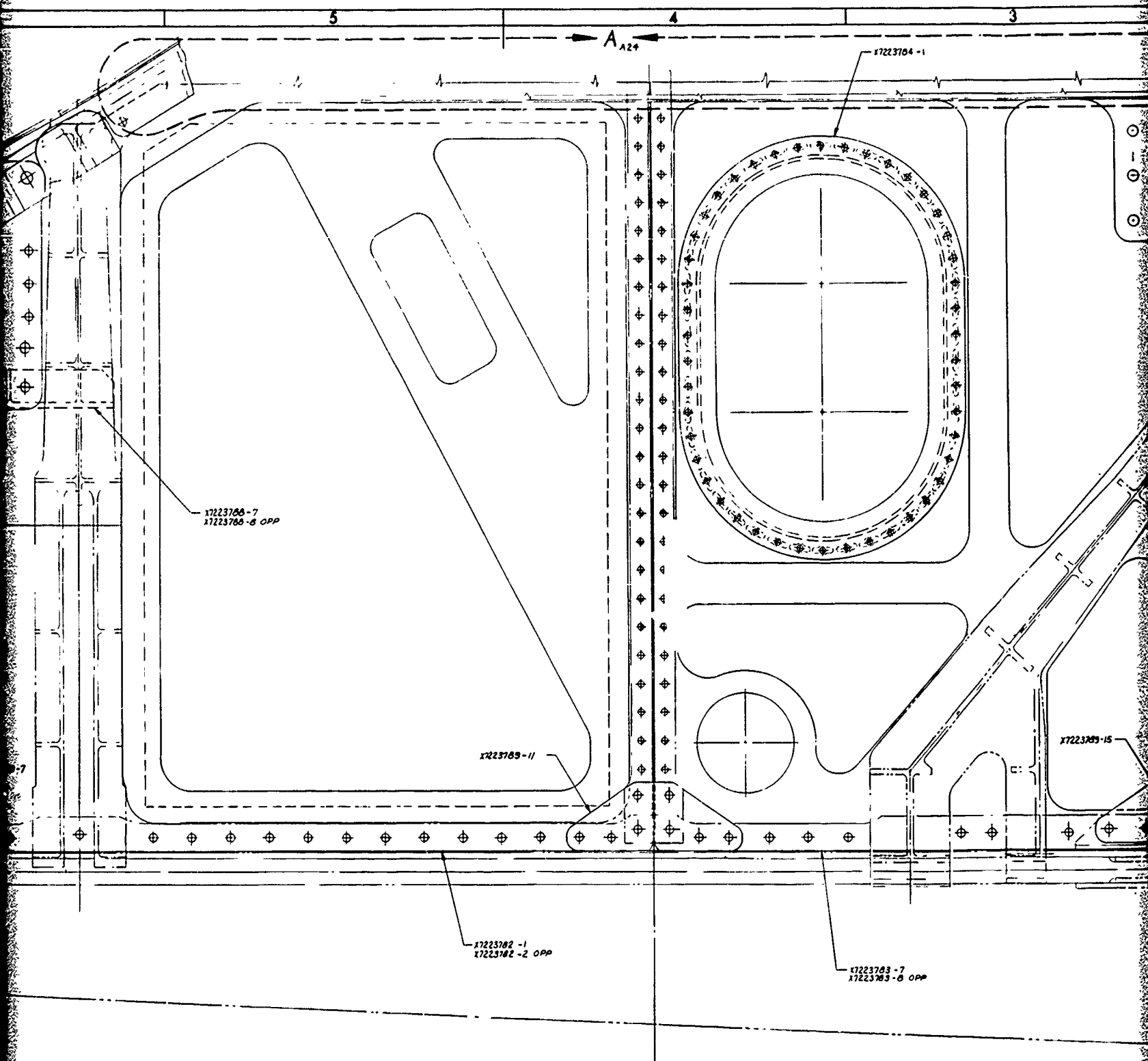


A









DRAWING NO. **F3561573 C-3001** |
 PART NO. **X7223780** |
 SHEET **1**

SEE FIGURE 1 FOR POINT 1

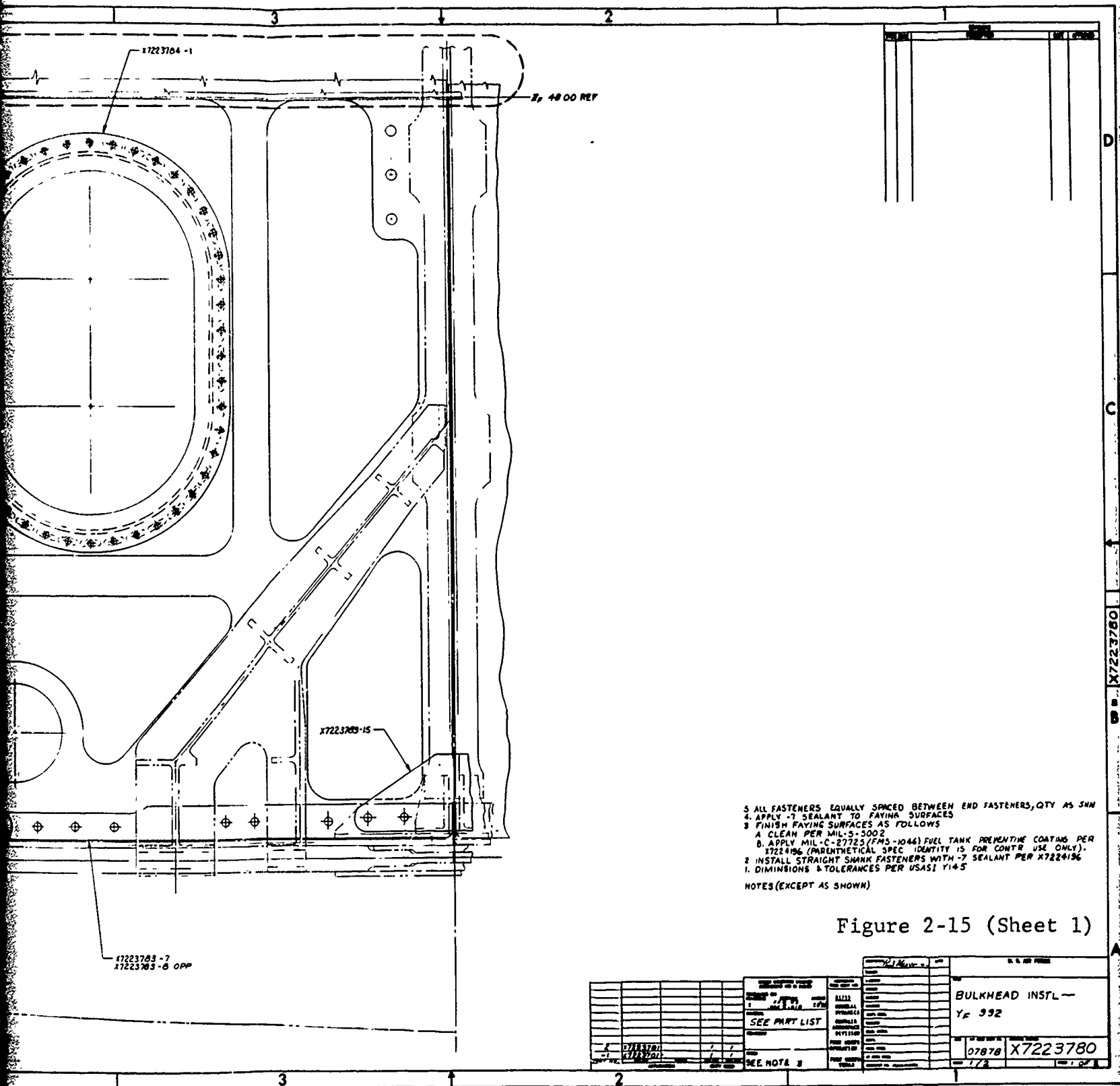
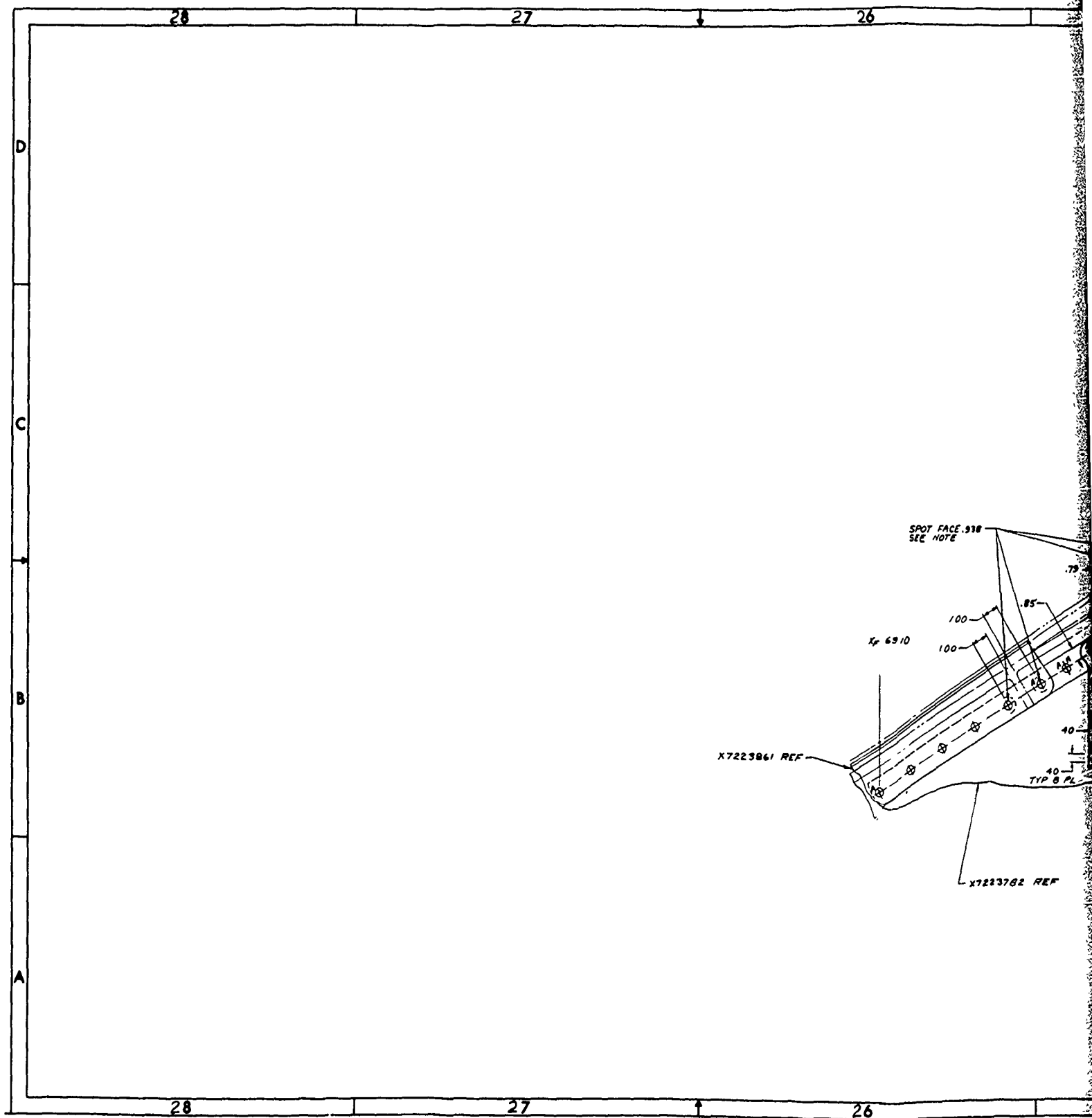


Figure 2-15 (Sheet 1)



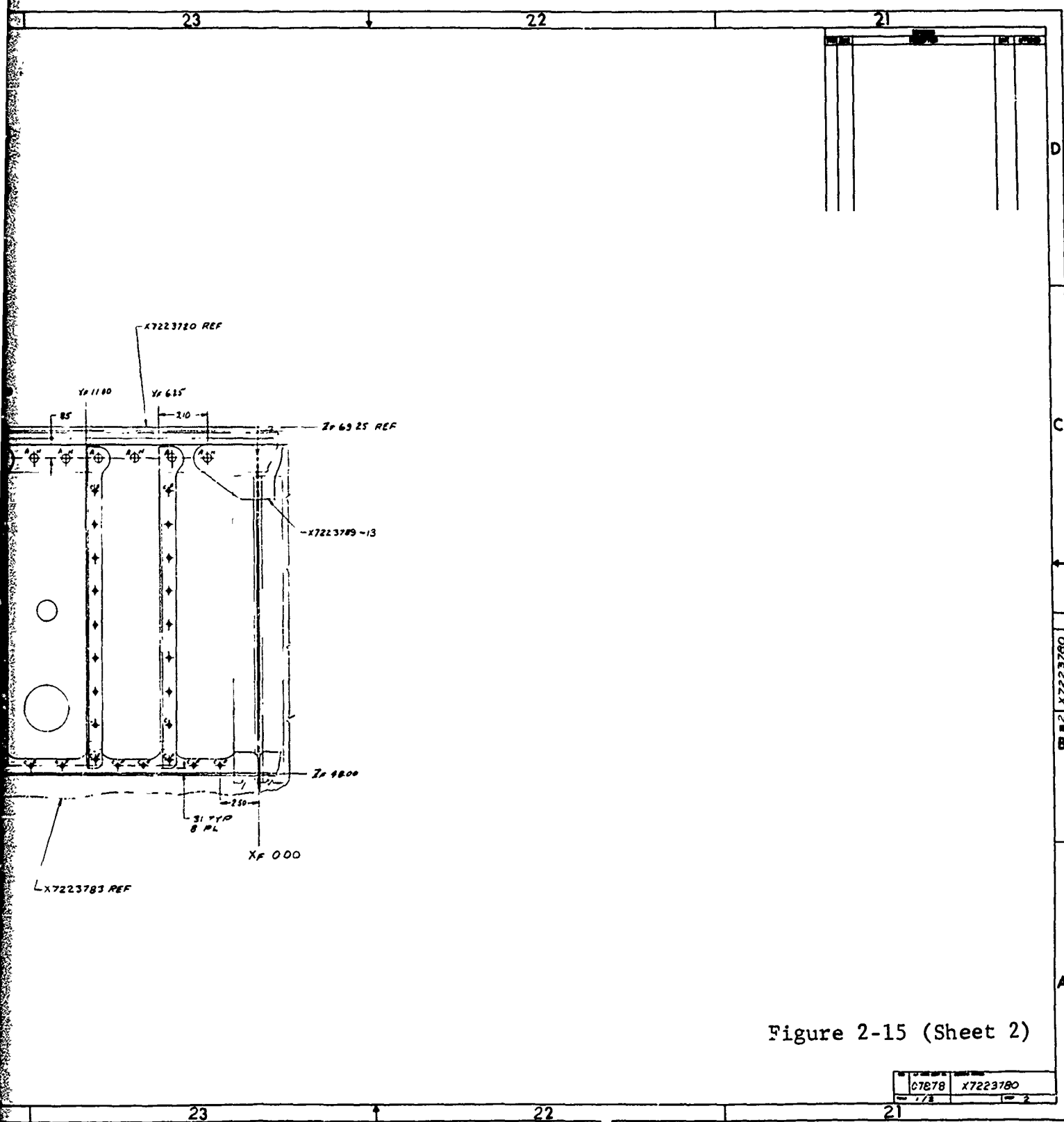
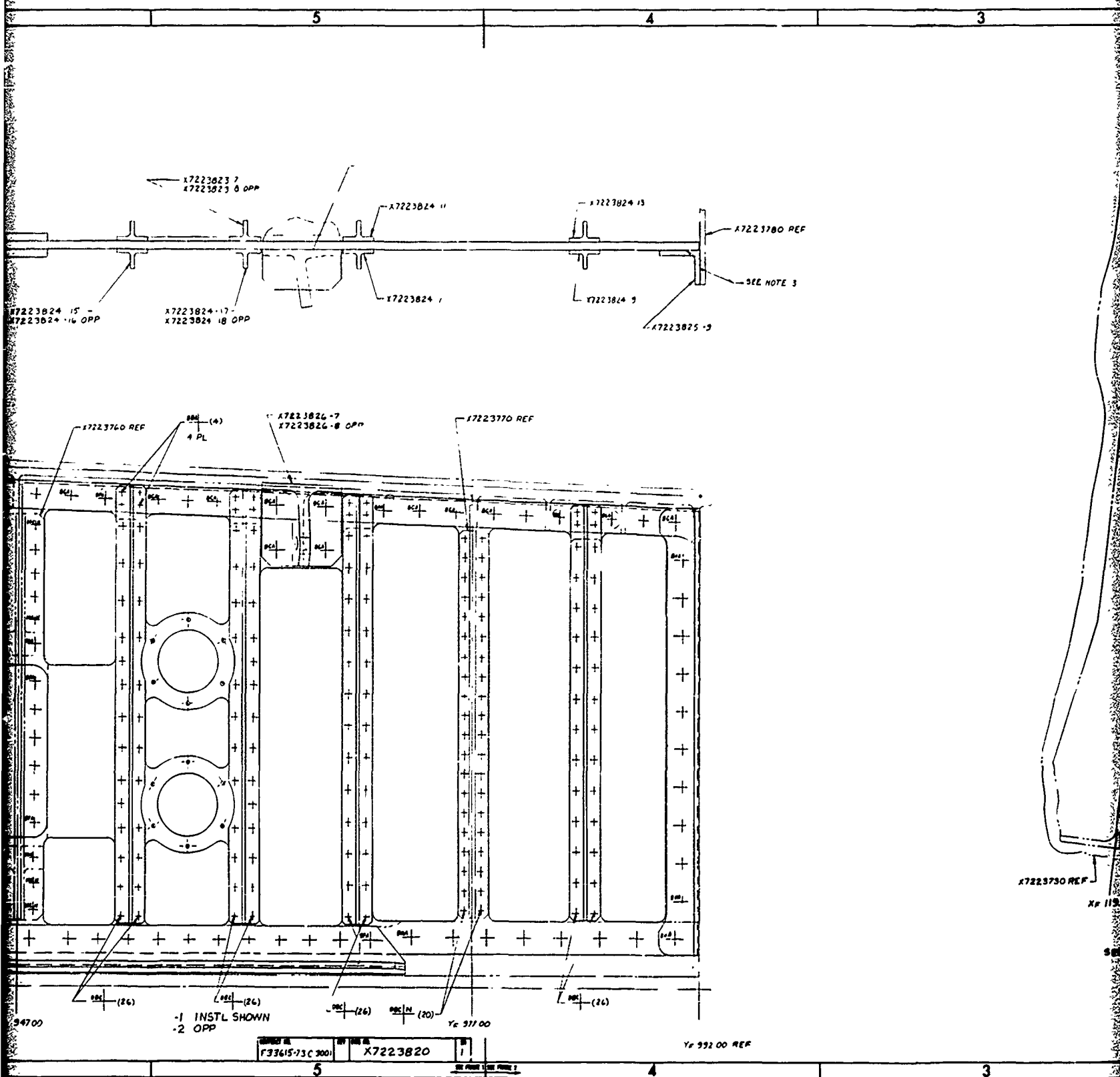


Figure 2-15 (Sheet 2)

07878	X7223780
1/8	2

2-69/2-70

3



2 1.2.7 Outboard Intermediate Rib

The outboard intermediate rib at X_F84 is shown in the box assembly drawing, X7223701, Figure 2-17. It is designed to react a combination of torsional shear loads, fuel slosh loads, kick loads due to the directional change of the upper plate, and the wing sweep actuator fitting load. This rib is a four element component configured to provide adequate access into the outboard portion of the box and to allow adequate fuel flow.

Aluminum construction satisfies the structural requirements of the rib and provides the minimum fabrication and material cost. The upper and lower center beams and the forward panel are integrally machined from 7050 plate. The aft panel is a sandwich panel consisting of a one-piece 7050 aluminum frame, 2024 aluminum face sheets and 5052 aluminum core.

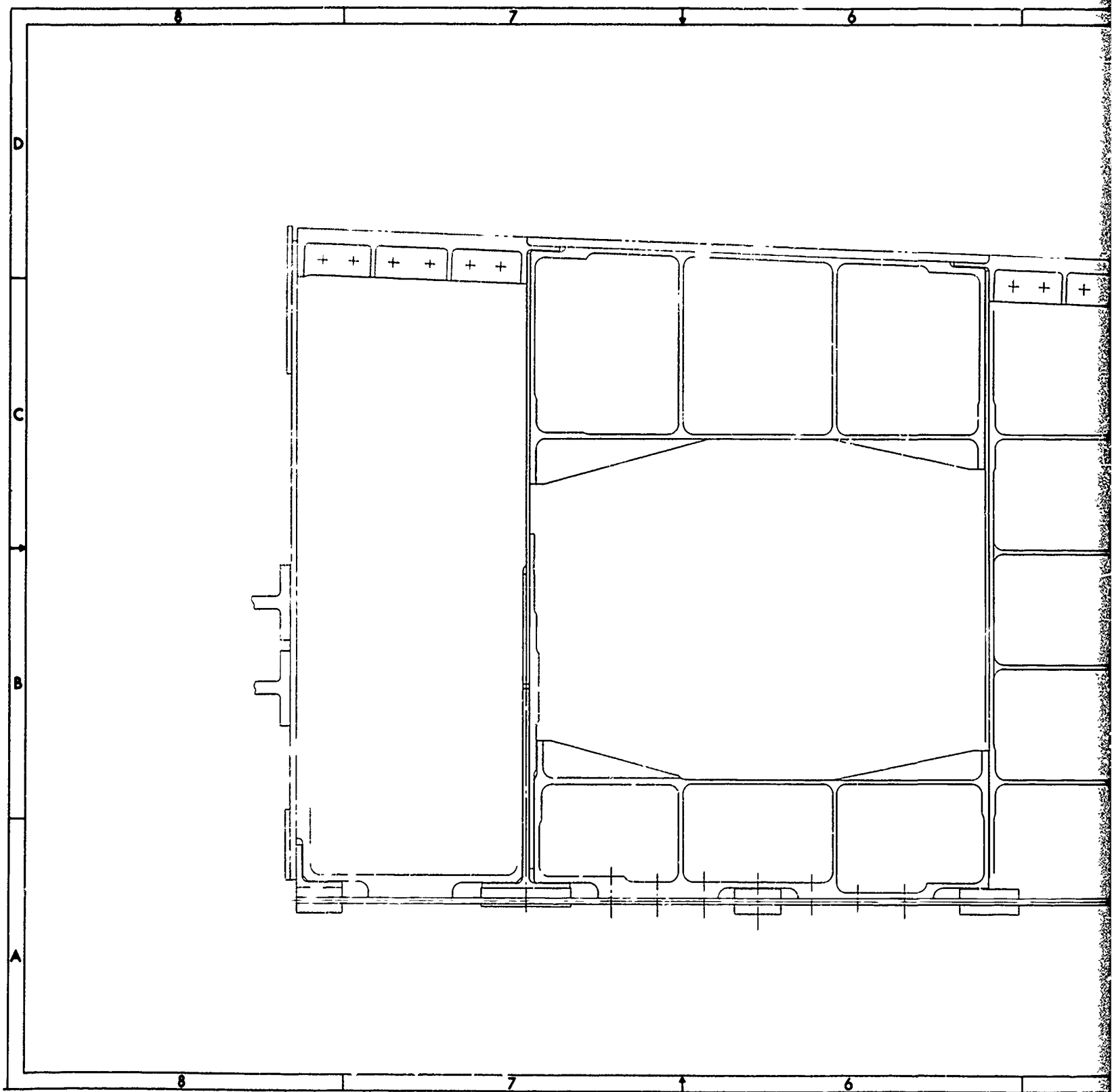
2.1.2.8 Inboard Intermediate Rib

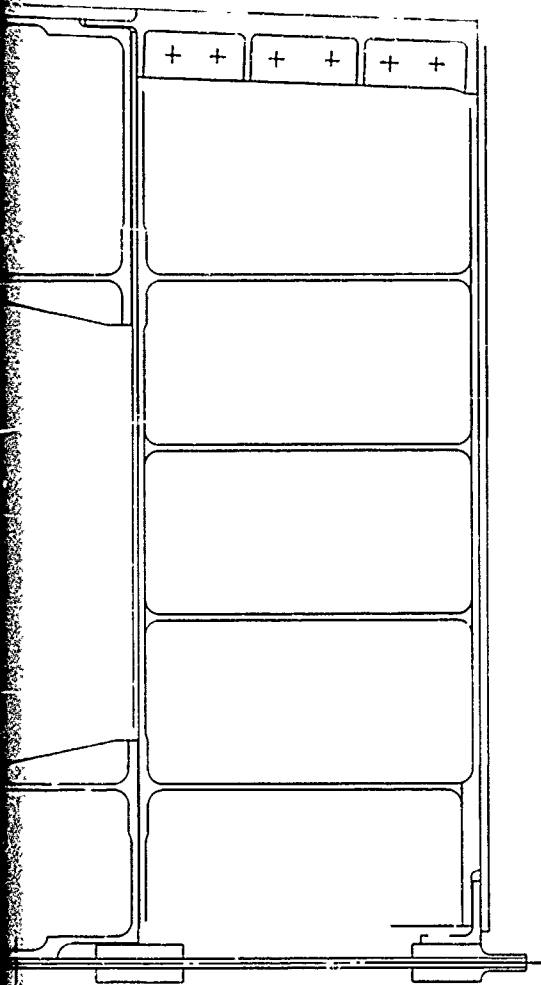
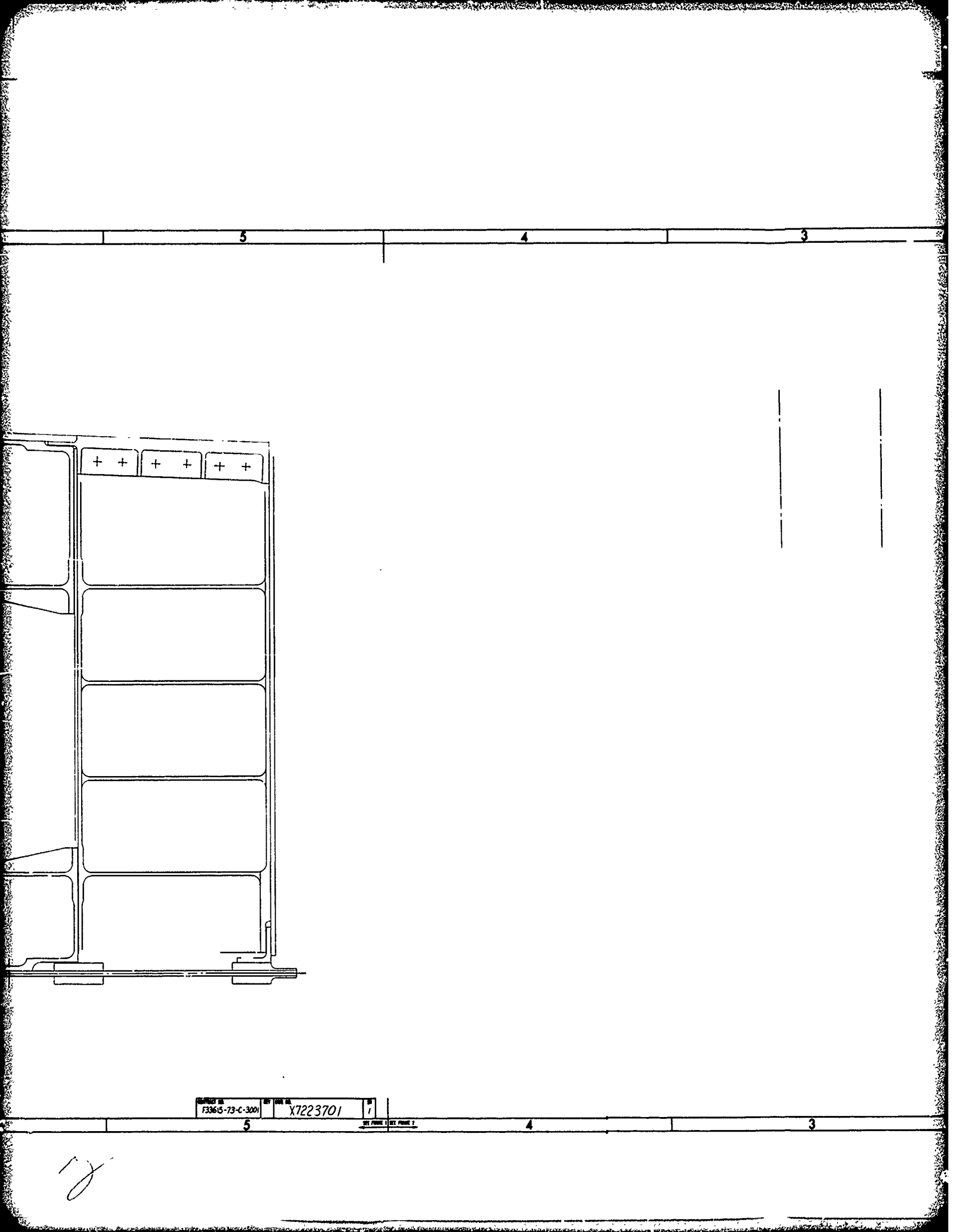
The inboard intermediate rib is also shown on the assembly drawing X7223701, Figure 2-17. The rib is located on the break of the upper cover (approximately X_F38) to react the resulting kick loads. In addition, the ribs experiences fuel slosh loads and secondary shear loads. The internal bulkheads terminate here, their load being transferred into the rib for redistribution. The rib is a four element component configured to provide adequate access into the outer portion of the box structure and to allow fuel flow.

The forward and aft sections are sandwich panels with 7050 aluminum slug type edge members and 2024 aluminum face sheets. The vertical attaching flanges are integral with the slug edge members. The upper and lower beams are integrally machined from 7050 aluminum plate.

2.1.2.9 Centerline Rib

The centerline rib is also shown on the assembly drawing, X7223701, Figure 2-17. This rib divides the left and right hand fuel tanks and, in addition to this fuel pressure loading, reaction is provided for the weapons launcher loads and kick loads from the MLG side brace fitting. The rib consists of an aluminum sandwich panel with 7050 slug type edge members. The forward and aft edge members are integrally machined with the attach flanges at Y_F932 and Y_F992. The skins are 2024 aluminum.





CONTRACT NO.
F33615-73-C-3001

REF. NO.
X7223701

REV. NO.
1

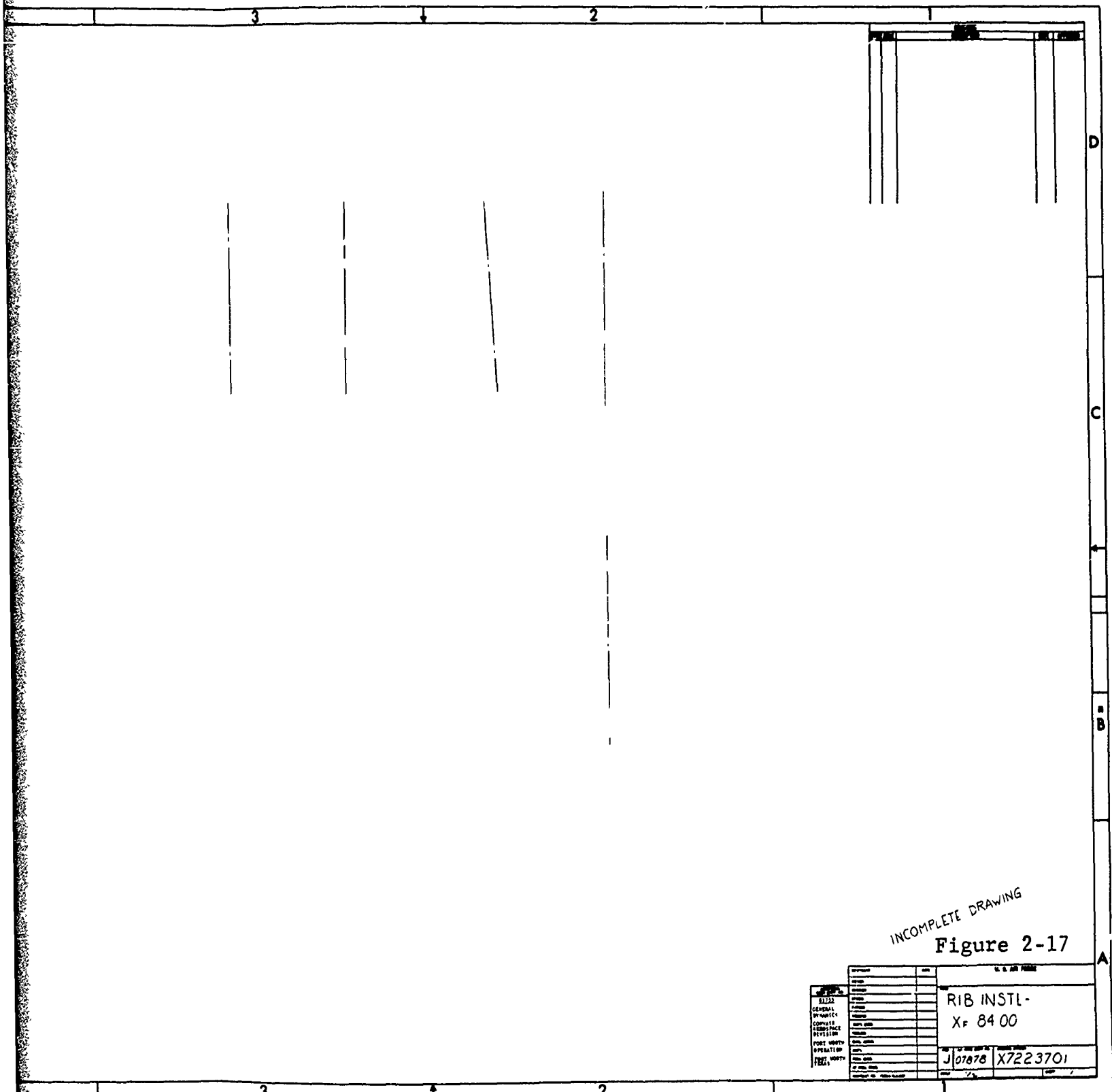
REV. NO. 1 REV. NO. 2

5

4

3

12



2.2 STRUCTURAL ANALYSIS

A variety of tasks were accomplished by stress analysis personnel during Phase II. The major accomplishments are summarized in the following list:

1. Converted updated design loads from the form furnished by Rockwell International to a form useable for Convair Aerospace finite element analysis, including determination of loads required for static balance.
2. Performed finite element analysis of the various FSIL and NBB configurations to determine internal loads and stresses for the complete carrythrough structure.
3. Performed additional fine grid finite element analysis for local areas to determine more detailed stress and load distributions and/or critical buckling loads.
4. Provided assistance to design personnel during final structural member sizing to assure adequate static and fatigue strength.
5. Provided stress data for fatigue and fracture analysis.
6. Continued stiffness studies.
7. Performed additional damage tolerance analyses for FSIL using finite element procedures.
8. Performed detailed stress analysis of parts shown on drawings being prepared for release for manufacture.
9. Participated in test planning, test part manufacture, testing, and interpretation of resulting data.
10. Performed finite element analysis of the simulated fuselage and fuselage test fixture to arrive at a configuration that would properly load the carrythrough structure during test.
11. Furnished internal loads from model of item 10. to test lab for design of upper test fixture structure.
12. Performed detailed stress analysis of simulated fuselage parts being released for manufacture.

13. Prepared inputs for necessary status and interim reports and the May and November, 1973 design reviews.

In many instances, the accomplishments represented a continuation of tasks begun in Phase Ib. Because of the large amount of computer data and manual stress analysis data generated, it is not feasible to include it in this report. The current data is retained on file by the contractor for review. In specific instances, in response to requests from AFFDL, data tapes were furnished to the interested parties through ADPO (Advanced Development Program Office). Where necessary for clarity of presentation, examples of data are included herein.

2.2.1 Design Loads

As noted in AFFDL-TR-73-40, Section 2.2.1, RI furnished loads data for 11 basic design conditions and two stiffness conditions. For the initial portion of the Phase II effort, the conditions described in Section 2.2.1 of AFFDL-TR-73-40 were used and, for brevity, they are not repeated here. For the latter portion of the design effort, updated technical data was provided which reflected deletion of the wing intrusion, increased pitching moments at the pivot and other load changes, and gross weight increase. For design purposes, the gross weight increase was covered through the stipulation by AFFDL that all flight loads be increased by 10% for analysis purposes. The 10% increase was considered where pertinent in the actual stress analysis, but it is not included in the loads actually used for finite element model input nor in loads summarized in this report.

The updated data was received in a period from approximately 8/23/73 to 10/15/73 and consisted of the following information:

1. Wing pivot loads shown in an excerpt from NARSAP 39 station Model data dated 4/23/73.
2. Interface loads contained in NA-73-510 NARSAP internal loads document.
3. Maximum gear actuator load obtained verbally - 250,000 lbs.
4. Main landing gear emergency hydraulic actuator loads in graphical form.
5. Wing sweep actuator vertical load and overwing fairing loads transmitted to Convair from ADPO.

6. Preliminary carrythrough box interface loads in the form of a Xerox copy produced from view graph presentation materials. Since these were only used for interim studies prior to receipt of NARSAP data, they are not reproduced in this report.

The final set of loads used for Phase II analysis was obtained from the following sources:

1. Shear flows - NARSAP values from NA 73-510 ratioed by
($\frac{1}{2} \text{ASKA} / \frac{1}{2} \text{NARSAP}$) TFD-72-838
2. Longeron loads - Based on NARSAP values from NA 73-510.
3. Wing pivot loads - From NARSAP 39 station model data dated 4/23/73.
4. Wing sweep actuator loads - Loads from TFD-72-835 and TFD-72-838, App. A, ratioed by $\frac{M_z \text{ NARSAP 39 Sta Data}}{M_z \text{ PH. Ib}}$, plus values from item 5. above.
5. Weapon launcher loads - Values from TFD-72-838 with Appendices A and B and TFD-72-835.
6. Landing gear loads - Values from TFD-72-838 with appendices for overall box analysis. These values were chosen rather than those presented in TFD-72-835 since the former were, presumably, those found by RI to be the most critical. The loads chosen apparently include no gear actuator loads. For local areas, values from TFD-72-835 were used.
7. Fuel pressures - Based on TFD-72-840 information.
8. Aerodynamic pressures - Values from TFD-72-835
9. Stiffness condition loads - Values from TFD-72-1176.
10. Overwing fairing loads - Values transmitted to Convair by ADPO.
11. Main landing gear emergency hydraulic actuator cylinder loads - Values from RI plots assumed to act separately for local design only.

12. Main landing gear actuator loads - Value noted previously taken as acting separately for local design only.

The data in TFD-72-835 (weapons launcher loads) and TFD-72-840 are not directly applicable to specific flight conditions because fuel and armament loadings for the design conditions were not made available.

A summary of load conditions used for overall box analysis is shown in Table II- 1. As noted, AS8C was used instead of AS8000 since insufficient data was available in NA-73-510 to allow breaking the latter down into symmetric and antisymmetric portions.

The revised baseline loads data is shown in Section 2.2.1.1. These loads do not include a 10% increase in gross weight. The internal loads represent the deletion of the wing intrusion and other changes.

2.2.1.1 Baseline Loads

1. Wing pivot loads from the NARSAP 39 station data are shown in Table II- 3.
2. Wing carrythrough structure - fuselage interface loads were supplied in the form of NARSAP math model internal loads data. The required interface loads were obtained or derived from this data. The interface loads are shown in Tables II- 4 through II- 7. The net NARSAP shears and moments are summarized for reference in Table II-8.
3. Wing sweep actuator loads derived from RI data are shown in Table II-9.
4. Landing gear loads are shown in Table II-10.
5. Weapons launcher loads are shown in Table II-11.
6. Main landing gear emergency hydraulic actuator cylinder loads are shown in Figure 2-22.
7. Wing sweep actuator vertical load and overwing fairing loads are shown in Table II-12.
8. The fuel pressures used in combination with the flight conditions are shown in Figure 2-23.
9. The upper cover aerodynamics pressures are as follows:

Table II-1 OVERALL LOAD CONDITION SUMMARY

CONVAIR ^{1,2,3} COND. NO.	NARSAP COND. NO.	CONDITION DESCRIPTION	WING POSITION
AS1000	660331	Abrupt Roll, 3G Limit	67.5°
AS1000A	660332		
AS2000	110021	Steady Pitch, 2G, Flaps Down	15
AS3000	161432	Steady Pitch, 3G	67.5
AS4000	110301	Steady Pitch, OG, Spoilers	15
AS5000	112120	Steady Pitch, 2G, Slats	15
AS6000	810012	2 Pt. Braked Roll, 1G	15
AS7000	880025	Taxi, 2G	15
AS8000 ⁴	880012	Ground Turning, 1G	15
AS8000A			
AS9000 ⁵	122222	Steady Pitch, 2G	25
AS10000	160337	Steady Pitch, 3G, Low Level	67.5
AS11000	160316	Steady Pitch, 1G	67.5

- NOTES:
1. PIVOT LOADS TAKEN FROM NARSAP 39 STA. DATA DTB. 4/23/73
 2. ARMAMENT AND LANDING GEAR LOADS ASSUMED TO REMAIN AS IN TFD-72-838 AND TFD-72-838 APP. A
 3. SWEEP ACTUATOR LOADS OBTAINED BY M_z RATIO USING TFD-72-835 AND TFD-72-838 APP. A AND NARSAP 39 STA. DATA DTD. 4/23/73
 4. ASKA 8C TO BE USED UNTIL ASKA DATA IS RECEIVED FOR AS8000
 5. NARSAP 122222 USED BECAUSE PIVOT LOADS EXCEEDED 122221
 6. SEE TABLE II-2 FOR NARSAP CONDITION NUMBER DESCRIPTION.

TABLE II-2 - NARSAP CONDITION NUMBER DESCRIPTION

6 DIGIT NUMBER - A B C D E S

A. TYPE CONDITION

- | | |
|--------------------------|------------------|
| 1. STEADY PITCH | 6. ROLL MANEUVER |
| 2. PITCHING ACCELERATION | 7. LANDING |
| 3. VERTICAL GUST | 8. TAXI |
| 4. LATERAL GUST | 9. NUCLEAR BLAST |
| 5. YAW MANEUVER | |

B. WING POSITION -

- | | |
|--------------------------|---------------|
| 0. EXTENDED OR UNDEFINED | 4. 45° |
| 1. 15° | 5. 55° |
| 2. 25° | 6. 65 - 67.5° |
| 3. 35° | |

C. ALTITUDE

- | | |
|------------------------------------|-------------------|
| 0. SEA LEVEL TO 9999' OR UNDEFINED | |
| 1. 10000 - 19999' | 4. 40000 - 49999' |
| 2. 20000 - 29999' | 5. 50000 - 59999' |
| 3. 30000 - 39999' | 6. 60000'+ |

D. VELOCITY - MACH NO.

- | | |
|----------------------|----------------|
| 0. ZERO OR UNDEFINED | 4. 1.00 - 1.49 |
| 1. 0.01 - 0.69 | 5. 1.50 - 1.99 |
| 2. 0.70 - 0.84 | 6. 2.00 - 2.19 |
| 3. 0.85 - 0.99 | 7. 2.20+ |

E. LOAD FACTOR 'g'

0. ZERO OR UNDEFINED
 1. — 8. APPROXIMATE 'g' LEVEL
 9. NEGATIVE 'g' LEVEL

S. SEQUENCE NUMBER

0. NORMAL
 1. — 9. IF THERE ARE SIMILAR CONDITIONS

TABLE II-3 - ULTIMATE NARSAP 39 STA. WING PIVOT LOADS (4-23-73)

CONDITION	P _Z KIPS	M _X IN. LB./10 ⁶	M _Y IN. LB./10 ⁶	M _Z IN. LB./10 ⁶
AS 1000	67.5			
1000A	67.5	264.28	-74.16	-12.68
AS 2000	15	344.26		
AS 3000	67.5		-26.79	-4.24
AS 4000	15	233.50	-70.57	-5.06
AS 5000	15	-96.26	6.52	24.45
AS 6000	15	294.86	-12.83	-22.20
AS 7000	15	-43.15	2.72	-7.53
AS 8000	15	-74.34	4.42	0
8000A	15	-37.17	2.21	0
AS 9000	25	314.01		
AS 10000	67.5		-31.65	-4.49
AS 11000	67.5	298.15	-88.33	-12.55
		20.82	-1.87	24.00

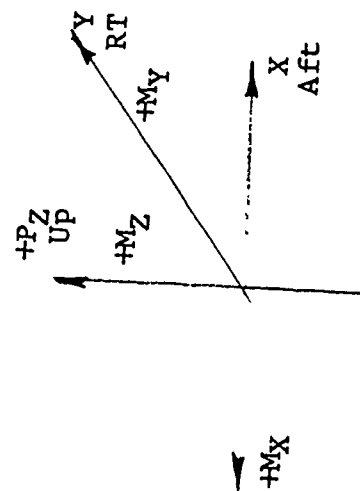
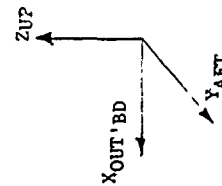





TABLE II-4
Y_F 932 Bulkhead Longeron Load Summary

Condition		①			②			③			⑥			⑦			⑨		
NARSAP	Convair	F _x	F _y	F _z	F _x	F _y	F _z	F _x	F _y	F _z	F _x	F _y	F _z	F _x	F _y	F _z	F _x	F _y	F _z
660331,2	1000S	0	68889	0	4513	23786	0	46720	246217	-18516	1909	-62168	1436	2035	-158727	4233	0	-117998	787
660331,2	1000A	0	4269	0	2412	12712	0	2943	15512	-1167	290	-9443	218	62	-4809	128	0	0	0
110021	200C	0	213869	0	45183	238121	0	19854	104630	-7868	2836	-92387	2134	3563	-277963	7413	0	-186286	1243
161432	3000	0	72294	0	3154	16621	0	49013	258302	-19424	1881	-61279	1416	2075	-161870	4317	0	-124067	828
110301	4000	0	4455	0	-9313	-49081	0	-12372	-65200	4903	-853	27797	-642	-638	49776	-1328	0	32254	-215
112120	5000	0	162451	0	41608	219279	0	16227	85518	-6431	2648	-86264	1993	2968	-231549	6175	0	-149434	997
810012	6000	0	-120889	0	16249	85632	0	8158	42994	-3233	462	-15052	348	507	-39566	1055	0	-40888	273
880025	7000	0	80647	0	23050	121477	0	4757	25071	-1885	920	-29952	692	1525	-118993	3174	0	-78250	522
880012S	8S	0	37937	0	14378	75773	0	-1953	-10291	774	422	-13756	318	549	-42821	1142	0	-46842	312
980012A	8A	0	22487	0	17585	92676	0	10423	54931	-4131	-815	26535	-613	-333	26006	-694	0	0	0
122222	9000	0	176364	0	36091	190205	0	22287	117453	-8832	2464	-80258	1854	3089	-240967	6427	0	-162797	1086
160337	10000	0	90576	0	5426	28593	0	62857	331261	-24911	2525	-82251	1900	2698	-210428	5612	0	-157752	1052
160316	11000	0	56451	0	990	5217	0	-8951	-47172	3547	-250	8346	-193	181	-14138	377	0	-8704	58

NOTES: 1) F_y values obtained from NARSAP data (NA-73-510 & TFD-72-838); F_x and F_z values derived from longeron geometry.
 2) All loads are lbs. ult.
 3) Longerons ⑨ on Q_L listed as 1/2 of total load.
 4) Positive sign convention per sketch.
 5) See Fig. 2-18 for longeron locations.



- NOTES:
1.  LONGERON
 2.  DUMMY LONGERON
 3.  SHEAR PATH NODE
 4. NUMBERS IN PARENTHESES ARE NARSAP LONGERON AND SHEAR FLOW DESIGNATIONS; ALL OTHERS ARE ASKA DESIGNATIONS.
 5. SHEAR FLOW DIRECTION COINCIDES WITH NARSAP CONVENTION.

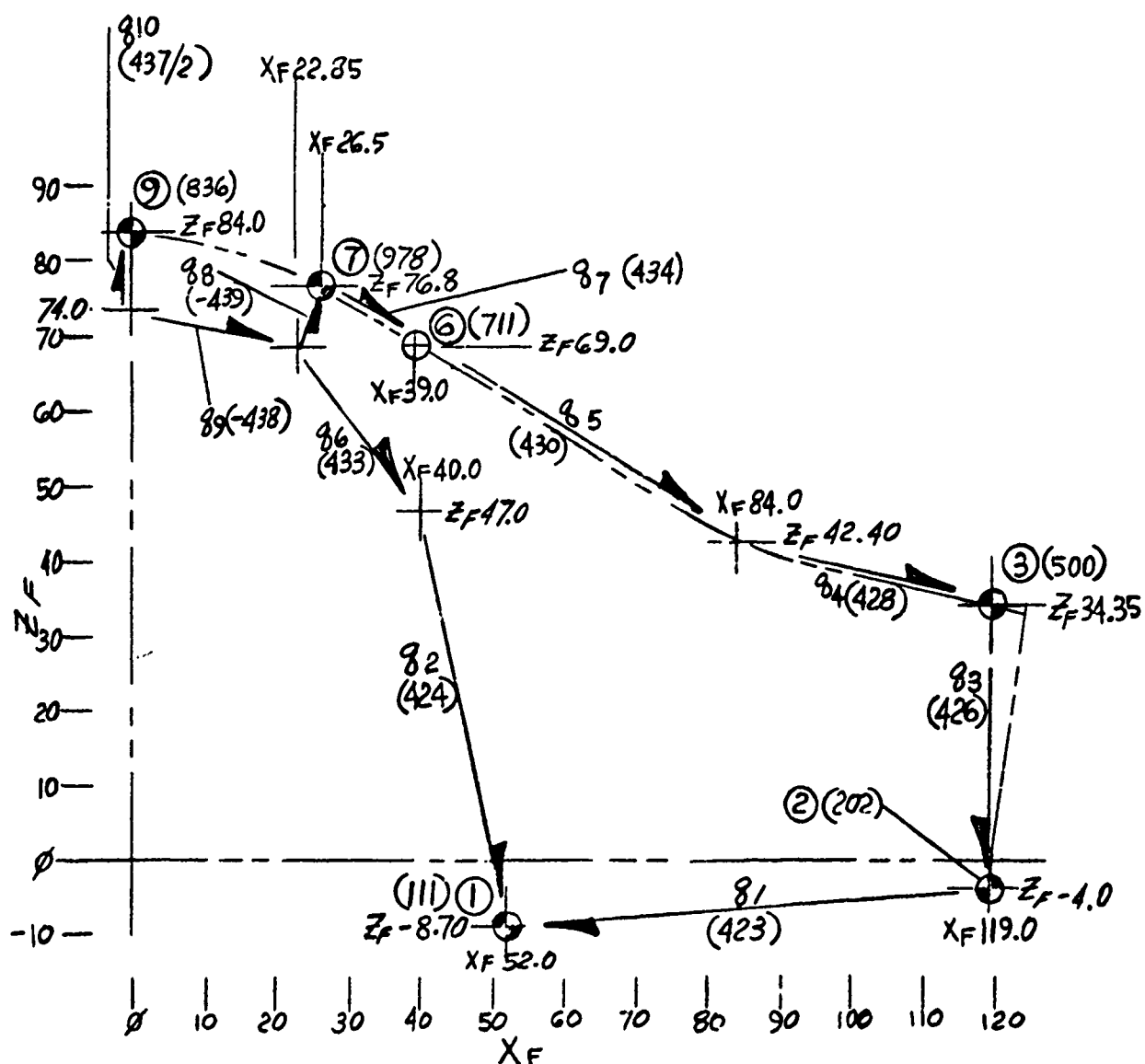


Figure 2-18 NARSAP-ASKA MATH MODEL INTERFACE LOAD GEOMETRY Y_F 932 BULKHEAD

TABLE II-5
Y_F 932 NARSAP Shear Flow Summary

NARSAP	Condition	Convair	q ₁	q ₂	q ₃	q ₄	q ₅	q ₆	q ₇	q ₈	q ₉	q ₁₀
660331,2	1000S		140.7	-201.52	-1166.49	1774.25	1774.25	-277.26	1097.77	-76.26	-103.69	-17.10
660331,2	1000A		-8.81	37.81	-157.82	25.02	25.02	38.62	-216.76	-152.62	-72.58	0
110021	2000		466.9	102.9	917.5	2162.8	2162.8	30.9	1459.7	-633.9	-160.2	-30.6
161432	3000		151.25	-239.84	-1315.98	1745.95	1745.95	-320.28	1108.95	-51.84	-107.46	-18.2
110301	4000		-139.76	168.98	-306.33	-936.23	-936.23	206.21	-530.86	-124.76	32.9	1.38
112120	5000		278.94	5.94	689.78	1817.20	1817.20	-66.26	1075.4	-461.43	-147.26	-20.05
810012	6000		-306.51	-391.41	714.03	826.48	826.48	-223.34	761.68	58.03	-18.46	-13.685
880025	7000		179.5	700.7	997.2	875.6	875.6	754.9	651.7	-967.5	-25.0	-29.2
880012S	8 S		57.50	211.74	637.85	299.65	299.65	331.59	260.74	-273.71	267.60	-436.98
880012A	8 A		66.16	-100.04	151.16	338.61	338.61	-143.41	543.94	382.29	96.65	0
122222	9000		363.9	9.6	517.5	1968.7	1968.7	-72.2	1357.9	-444.9	-142.0	25.1
160337	10000		186.9	-231.4	-1596.0	2318.0	2318.0	-330.1	1426.7	-150.9	-136.7	-24.0
160316	11000		-26.28	99.63	-49.40	-373.47	-373.47	105.13	-90.17	-142.61	-6.62	-2.70

Notes: 1) All loads are lbs/in Ult.
2) q₁₀ on q₁ listed as 1/2 of total shear flow
3) Positive sign convention and location for shear flow depicted on Figure 2-18
4) Values from NA-73-510 & TFD-72-838

TABLE II-6 Y_F 992 LONGERON LOADS SUMMARY Sheet 1

Condition		(11)			(12)			(15)			(16)			(17)		
NARSAP	Convair	F _x	F _y	F _z	F _x	F _y	F _z	F _x	F _y	F _z	F _x	F _y	F _z	F _x	F _y	F _z
660331,2	1000 S	0	-64347	0	0	994	0	303883	-1310464	-21990	72622	-188815	-3168	-215113	927649	-1633
660331,2	1000 A	0	0	0	0	0	0	53409	-230322	-3865	38886	-101102	-1696	-63493	273805	-482
110021	2000	0	-76268	0	0	2285	0	201789	-870194	-14602	70038	-182097	-3056	-83197	358778	-631
161432	3000	0	-66700	0	0	1457	0	329740	-1421968	-23861	75983	-197553	-3315	-230441	993752	-1749
110301	4000	0	27187	0	0	2188	0	-38457	165842	2783	-25019	65048	1092	31575	-136163	240
112120	5000	0	-75030	0	0	-201	0	118325	-510263	-8562	55635	-144650	-2427	-49564	213741	-376
810012	6000	0	-130164	0	0	-8986	0	129697	-559306	-9385	56116	-145899	-2448	-71389	307856	-542
880025	7000	0	-100476	0	0	-5242	0	130657	-563445	-9455	58679	-152564	-2560	-73703	317834	-532
880012 S	8 S	0	-71,850	0	0	417	0	46,452	-200,319	-3361	28,148	-73,184	-1228	-16,440	70,897	-125
880012 A	8 A	0	0	0	0	0	0	35,766	-154,238	-2588	16,919	-43,989	-738	-1386	5977	-11
122222	9000	0	-71112	0	0	2096	0	204359	-881274	-14788	65468	-170215	-2856	-98092	423012	-745
160337	10000	0	-78379	0	0	2025	0	406900	-1754710	-29444	94972	-246925	-4143	-286869	1237092	-2177
160316	11000	0	5468	0	0	3212	0	10608	-45745	-768	-8924	23202	389	7418	-31988	56

NOTES: (1) F_y values obtained from NARSAP data (NA 73-510 and TF072-838);

F_x and F_z values derived from longeron geometry.

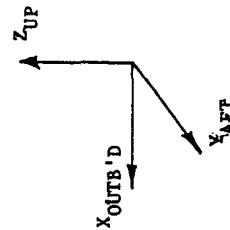
(2) F_y values do not include balance load contribution.

(3) All values are lbs ult.

(4) Values for longerons on \bar{c} are listed as 1/2 of total.


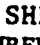
(5) Positive sign convention per sketch.

(6) See Fig. 2-19 for longeron locations.



TAB 11-6 YF 992 LONGERON LOADS SUMMARY Sheet 2

	(18)			(21)			(22)			(23)			(24)			(25)		
	F _x	F _y	F _z	F _x	F _y	F _z	F _x	F _y	F _z	F _x	F _y	F _z	F _x	F _y	F _z	F _x	F _y	F _z
Convair																		
2000 S	-22487	53468	6151	0	52008	-1035	0	178964	0	0	66539	0	0	250326	2013	0	28681	0
1000 A	-1350	3511	369	0	7004	-139	0	12137	0	0	-3292	0	0	0	0	0	0	0
2000	-8231	21402	2252	0	86457	-1720	0	227698	0	0	85908	0	0	304258	2446	0	41772	0
3000	-24056	62540	4580	0	57740	-1149	0	195952	0	0	71478	0	0	272513	2191	0	30791	0
4000	1055	-2742	-288	0	-6848	136	0	-38052	0	0	-14034	0	0	-56938	-458	0	-5489	0
5000	-2667	6934	730	0	56475	-1124	0	161427	0	0	55443	0	0	208561	1677	0	27563	0
6000	-8733	22706	2389	0	49159	-978	0	171591	0	0	18752	0	0	192362	1547	0	1702	0
7000	-15050	39131	4117	0	54794	-1090	0	173730	0	0	31393	0	0	190802	1534	0	14043	0
8 S	-5004	13,011	1369	0	22,148	-441	0	112,143	0	0	1374	0	0	129,575	1042	0	-4212	0
8 A	1596	-4151	-437	0	-1236	25	0	16,755	0	0	-3907	0	0	0	0	0	0	0
9000	-9589	24933	2623	0	78945	-1571	0	207176	0	0	77180	0	0	272412	2190	0	36845	0
10000	-28803	74888	7879	0	64939	-1292	0	235334	0	0	89208	0	0	337269	2712	0	39261	0
11000	181	-470	-49	0	19010	-378	0	15446	0	0	5961	0	0	2058	17	0	3846	0

- NOTES: 1.  LONGERON
 2.  SHEAR PATH NODE
 3. NUMBERS IN PARENTHESIS ARE NARSAP LONGERON AND SHEAR FLOW DESIGNATIONS; ALL OTHERS ARE ASKA DESIGNATIONS.
 4. SHEAR FLOW DIRECTION COINCIDES WITH NARSAP CONVENTION.

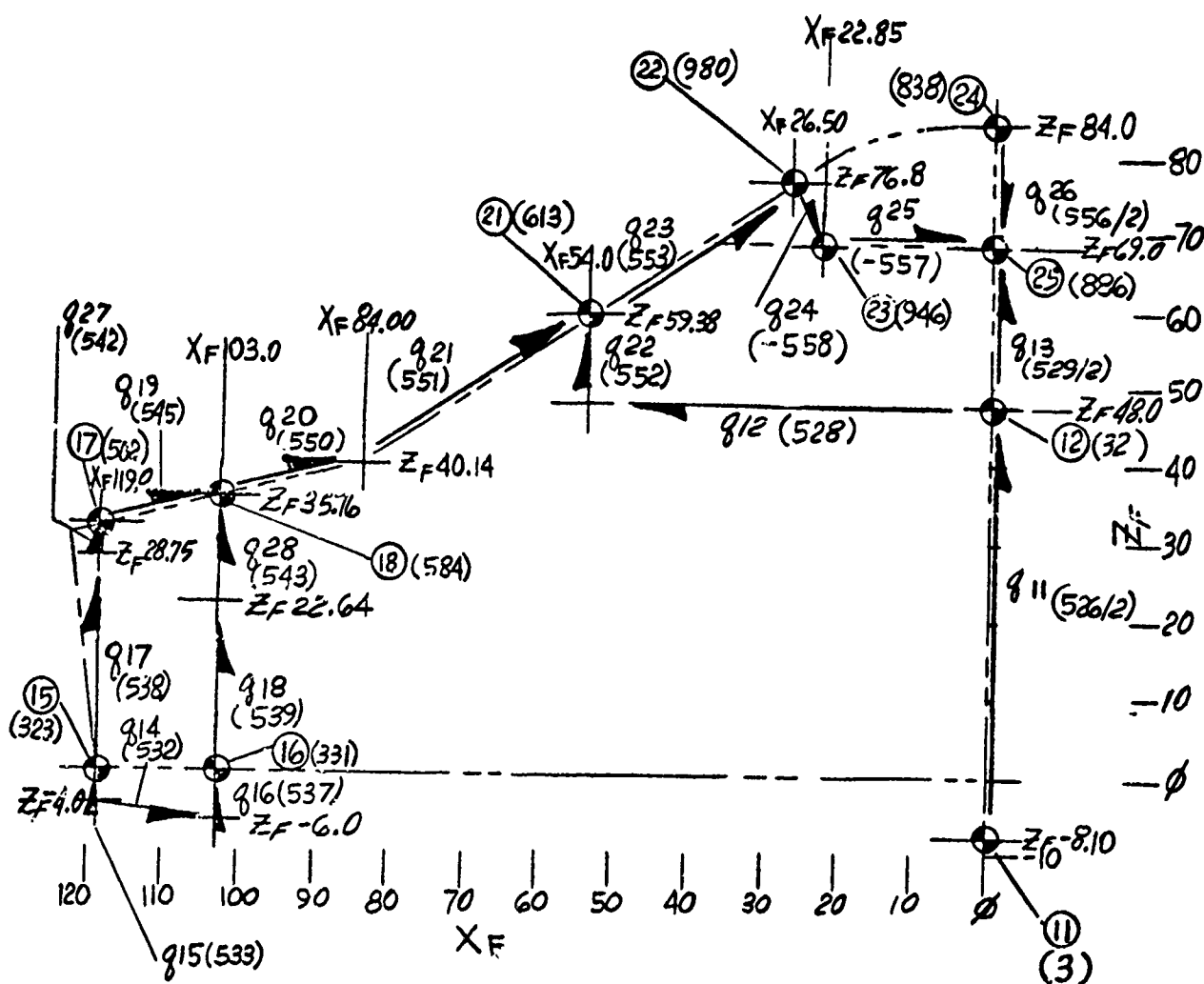


Figure 2-19 NARSAP-ASKA MATH MODEL INTERFACE LOAD GEOMETRY Y_F 992 BULKHEAD

TABLE II-7 SHEET 1
YF 992 NARSAP SHEAR FLOW SUMMARY

NARSAP	Condition		q ₁₁	q ₁₂	q ₁₃	q ₁₄	q ₁₅	q ₁₆	q ₁₇	q ₁₈
		Convair								
660331,2	1000	S	-249.97	-27.37	-115.85	-825.58	9729.17	2480.21	-8439.48	-174.40
660331,2	1000	A	0	-503.18	0	682.18	685.45	1570.13	-2958.79	60.73
110021	2000		-303.2	-134.9	-174.5	904.4	5757.6	3073.6	-5196.5	482.6
161432	3000		-490.31	2.97	-125.70	-443.53	10550.38	2608.74	-9074.97	-175.04
110301	4000		317.86	131.45	17.82	-328.92	-635.63	-1203.01	1446.47	-231.18
112120	5000		-762.54	-168.25	-222.33	559.11	2833.12	2498.9	-3621.6	394.45
810012	6000		-1886.29	-475.03	-477.25	208.38	4246.14	1577.33	-2443.24	-719.62
880025	7000		-685.75	-274.2	-442.0	304.6	4089.2	1550.3	-2941.5	-941.2
880012 S	8	S	-561.40	-271.82	-343.13	41.57	1828.64	680.09	-668.10	-489.52
880012 A	8	A	0	63.54	0	-65.41	1399.46	346.35	-418.15	-306.99
122222	9000		-289.7	-97.5	-180.2	661.6	5763.5	2785.3	-5731.4	365.7
160337	10000		-285.3	-5.0	-113.2	-796.1	12621.4	3401.1	-11470.6	-114.6
160316	11000		145.2	143.48	-71.38	-217.74	518.87	-499.18	-453.04	-115.34

NOTES: (1) All loads are lbs/in ult.

(2) Values for shear flows on \bar{q} are listed as 1/2 of total.

(3) Positive sign convention and locations for shear flows depicted on Fig. II-19

(4) Values from NA-73-510 and TFD-72-838.

TABLE II-7 SHEET 2
Y_F 922 NARSAP SHEAR FLOW SUMMARY

Condition		q ₁₉	q ₂₀	q ₂₁	q ₂₂	q ₂₃
NARSAP	Convair					
660331,2	1000 S	1388.48	962.44	962.44	-185.65	-562.09
660331,2	1000 A	-56.97	-35.22	-35.22	-416.03	471.05
110021	2000	-1567.7	-584.8	-584.8	-216.4	-399.8
161432	3000	1527.57	1031.54	1031.54	-179.54	641.63
110301	4000	62.98	-150.82	-150.82	84.74	-42.48
112120	5000	-1620.23	-754.89	-754.89	-161.98	-666.47
810012	6000	1225.40	344.86	344.86	-650.60	67.63
880025	7000	837.6	33.4	33.4	-565.8	-188.4
880012 S	8 S	627.28	-2.45	-2.45	-408.93	-209.04
880012 A	8 A	137.94	-67.20	-67.20	19.38	-72.05
122222	9000	-1351.3	-529.8	-529.8	-183.9	-383.4
160337	10000	2032.9	1417.1	1417.1	-216.9	920.4
160316	11000	-878.37	-709.99	-709.99	100.36	-454.15

TABLE II-7 SHEET 3

Y_F 992 NARSAP SHEAR FLOW SUMMARY

Condition		q ₂₄	q ₂₅	q ₂₆	q ₂₇	q ₂₈
NARSAP	Convair					
660331, 2	1000 S	-92.36	-788.46	-667.16	-8439.48	-174.40
660331, 2	1000 A	-174.80	209.44	0	-2958.79	60.73
110021	2000	-586.1	694.4	-607.85	-5196.8	482.6
161432	3000	-67.89	861.13	-720.99	-9074.97	-175.04
110301	4000	21.34	-183.53	174.64	1446.47	-231.18
112120	5000	-482.07	380.79	-225.56	-3621.6	394.45
810012	6000	788.5	761.89	-31.69	-2443.24	-719.62
880025	7000	433.5	645.3	-89.3	-2941.5	-941.2
880012 S	8 S	690.37	437.05	199.73	-562.31	-544.45
880012 A	8 A	185.47	98.97	0	-325.07	-309.05
122222	9000	-530.9	626.0	-512.7	-5731.4	365.7
160337	10000	-58.	1088.9	-985.0	11470.6	-114.6
160316	11000	-286.47	-126.03	176.47	-453.04	-115.34

TABLE II - 8 NARSAP ULT. A/P LOADS APPLIED TO BOX

CONVAIR NO.	NARSAP NO.	STA 932					STA 992						
		FWD LB	SHEAR SIDE LB	VERTICAL LB	PITCHING MOMENT	YAWING MOMENT	ROLLING MOMENT	FWD LB	SHEAR SIDE LB	VERTICAL LB	PITCHING MOMENT IN LB	YAWING MOMENT IN LB	ROLLING MOMENT IN LB
1000	060331	0	-7950	-28,238	-37,264,378	-6,169,861	-1,247,127	0	9,530	384,171	-153,691,102	-8,505,683	-17,545,966
2000	110021			-261,654	-85,179,070					302,532	-139,980,022		
3000	161432			-9,320	-37,816,322					408,054	-166,296,840		
4000	110301			-71,136	12,737,960					-67,108	28,079,361		
5000	112120			-194,536	-71,283,787					277,323	-93,399,775		
6000	810012	175,539	0	-70,855	-10,653,008			-160,455	0	283,189	-89,953,927		
7000	880025			-275,259	-36,210,178					317,878	-95,830,749		
8000	880012	0	-68,739	-119,591	-13,439,030	-24,040,657	7,019,259	0	79,245	158,939	-47,915,364	-31,802,619	-3,416,067
9000	122222			-199,698	-71,962,921					343,513	-132,972,792		
0000	160337			-37,928	-49,231,786					496,506	-204,432,574		
1000	160316			19,455	-6,745,465					90,478	-4,463,323		

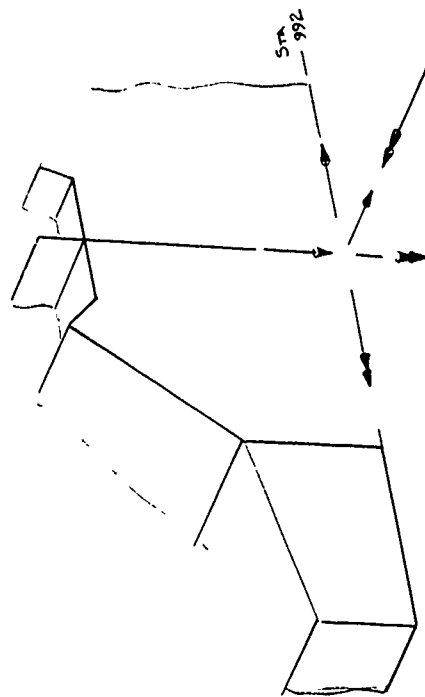
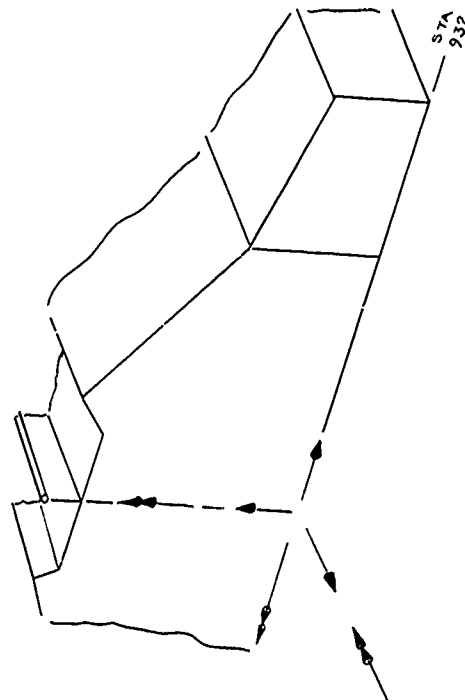


TABLE II-9

ULTIMATE LOADS APPLIED TO WING WEEP ACTUATOR FITTING

CONVAIR COND.	NAR COND.	∧ DEG.	F _X LBS ULT	F _Y LBS ULT	F _Z LBS ULT	RESULTANT LBS ULT
AS 1000S	660331	67.5	-215,895	-156,390	7950	-266,705
AS 1000A	660332		-78,840	- 57,840	2895	-97,392
AS 2000	110021	15	-80,685	- 7770	2655	-81,102
AS 3000	161432	67.5	-84,615	- 61,290	3120	-104,527
AS 4000	110301	15	491,970	47,250	-16,095	494,496
AS 5000	112120	15	-448,380	-43,200	14,715	-450,697
AS 6000	810012	15	-151,200	-14,565	4965	-151,981
AS 7000	880025	15	-390	-45	0	-392
AS S	880012	15	-195	-15	0	-196
AS A			0	0	0	0
AS 9000	122222	25	-78,615	-16,151	2621	-80,300 REF. NOTE 1
AS 10000	160337	67.5	-285,887	-207,074	10,524	-353,160 REF. NOTE 1
AS 11000	160316	67.5	669,585	485,010	-24,630	827,155

NOTES:

- (1) LOADS REVISED PER NAR LOADS PACKAGE RECEIVED 4 SEPT. 1973
- (2) POSITIVE RESULTANT LOAD INDICATES ACTUATOR IS IN TENSION
- (3) LOADS APPLIED AT X_F 122.75, Y_F 917.0, Z_F 14.748 -- Ref. Fig. 2-45
- (4) EFFECT OF PIVOT FRICTION NOT INCLUDED.

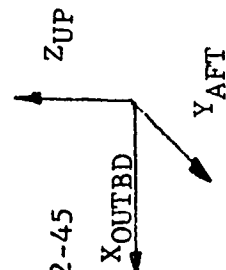


TABLE II-10

MAIN LANDING GEAR FITTING ULTIMATE LOADS

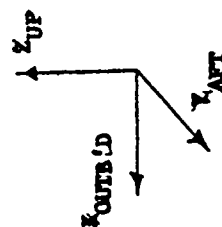
CONDITION	OUTER TRUNNION LBS X 10 ³			INNER TRUNNION LBS X 10 ³			SIDE BRACE LBS X 10 ³			DRAG BRACE LBS X 10 ³		
	F _X	F _Y	F _Z	F _X	F _Y	F _Z	F _X	F _Y	F _Z	F _X	F _Y	F _Z
ASKA 6	0	-153.369	312.524	0	-114.233	312.568	-236.130	-81.558	272.869	236.130	558.178	-622.562
7	0	-162.51	432.549	0	-77.855	222.874	-119.164	-41.286	137.7	119.164	281.669	-314.166
8	0	31.99	-150.708	0	-117.436	346.692	-177.288	-56.933	204.865	60.226	142.357	-158.782
8A	0	41.356	-177.538	0	-118.069	349.06	-180.446	-58.277	208.514	57.099	134.966	-150.538
POSITION OF LOAD APPLICATION	X _F 95.5	Y _F 1000	Z _F 1.0	X _F 72	Y _F 1000	Z _F 1.0	X _F 23	Y _F 1000	Z _F 1.0	X _F 56.0	Y _F 947.5	Z _F -4.5

NOTES:

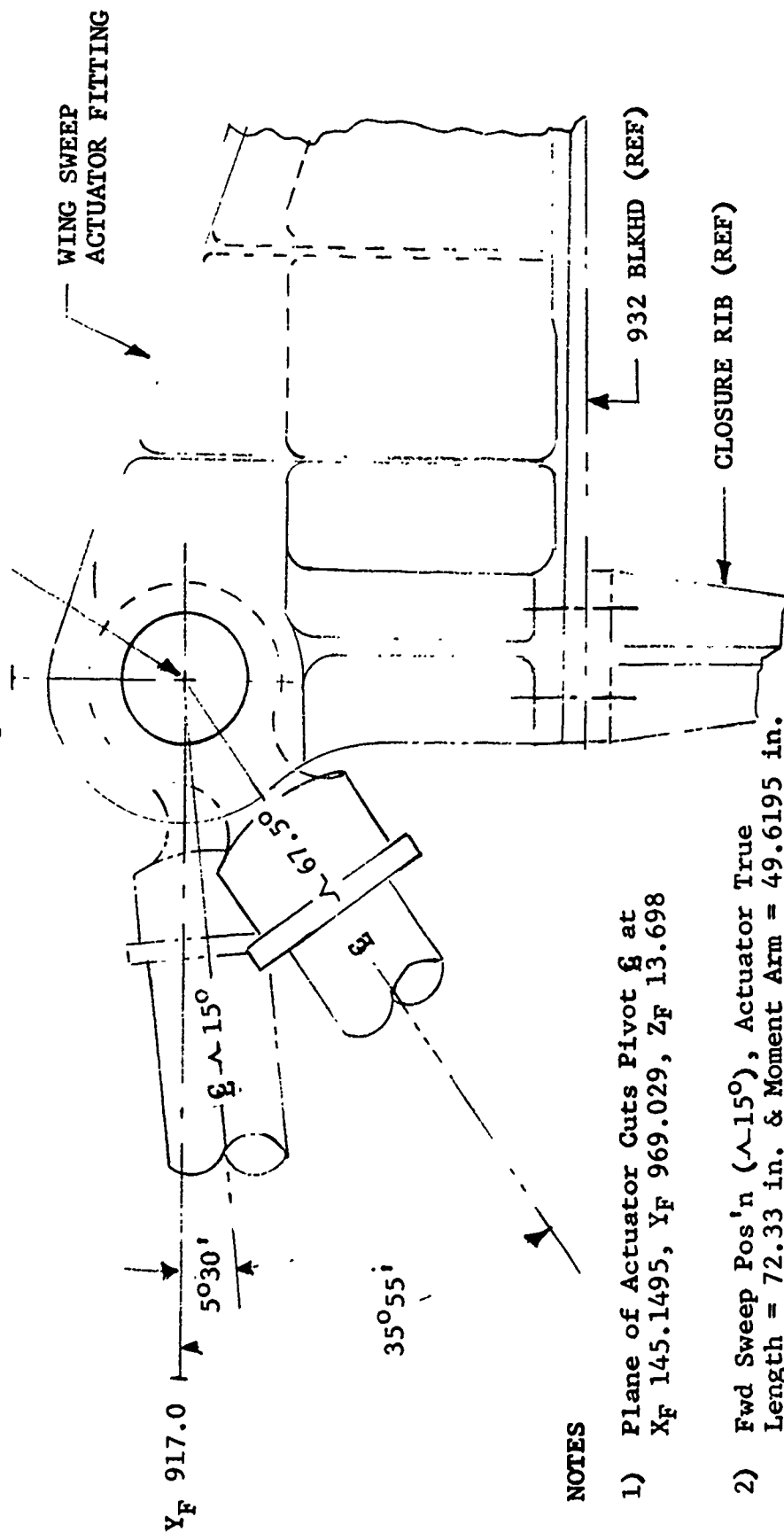
(1) Loads Listed as Applied to CTE Fittings --- One Side --- Per TFD-72-838

(2) Loads Are in "ASKA" Model Reference System (Ref. Sketch)

(3) "A" Designates Anti-symmetric Portion of Unsymmetrical Load Condition



X_F 122.750 - ξ Lug @ Z_F 14.748



NOTES

- 1) Plane of Actuator Cuts Pivot ξ at X_F 145.1495, Y_F 969.029, Z_F 13.698
- 2) Fwd Sweep Pos'n ($\sim 15^{\circ}$), Actuator True Length = 72.33 in. & Moment Arm = 49.6195 in.
- 3) Aft Sweep Pos'n ($\sim 67.5^{\circ}$), Actuator True Length = 109.0426 in. & Moment Arm = 29.0 in.

FIGURE 2-20

WING SWEEP ACTUATOR GEOMETRY

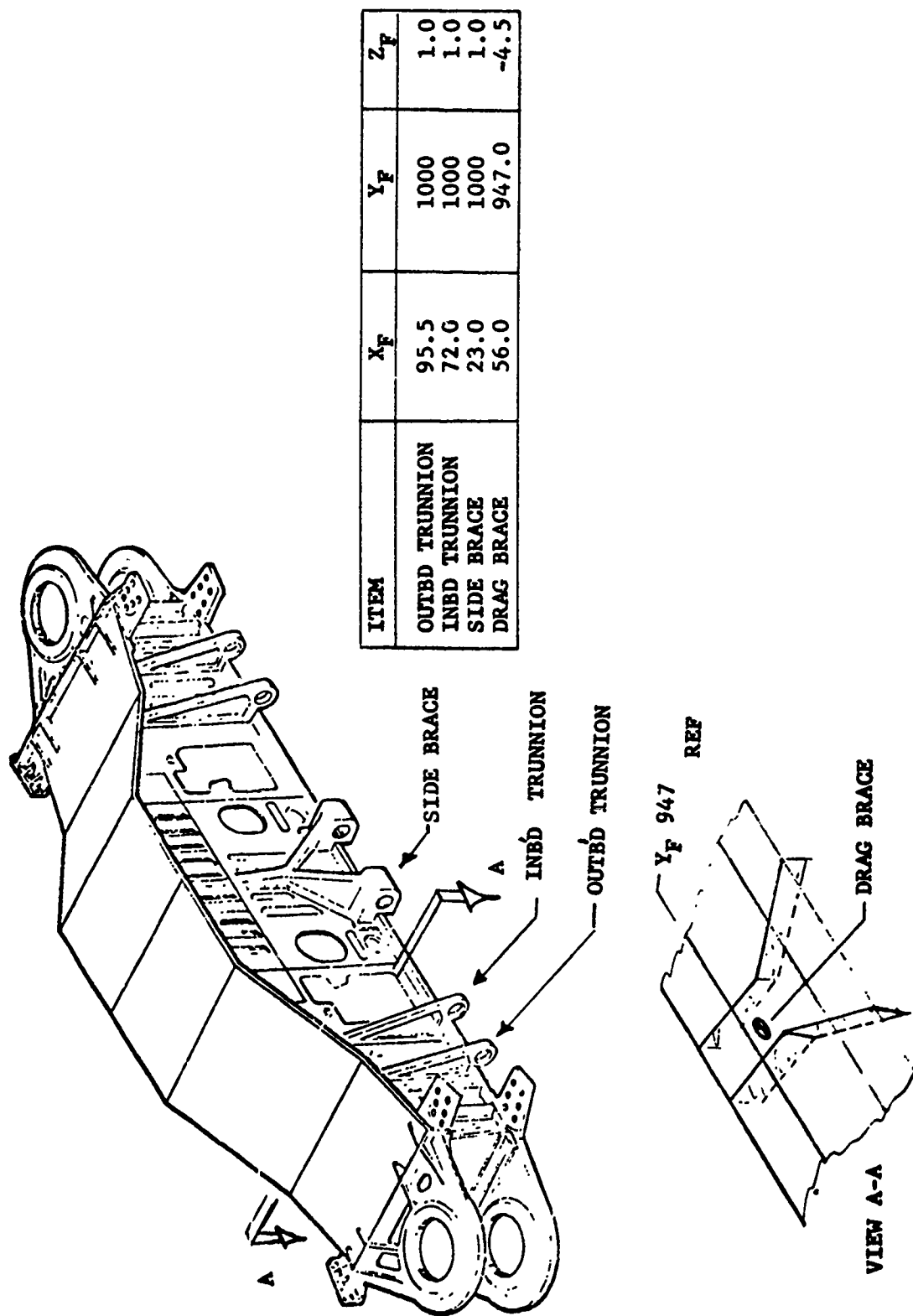
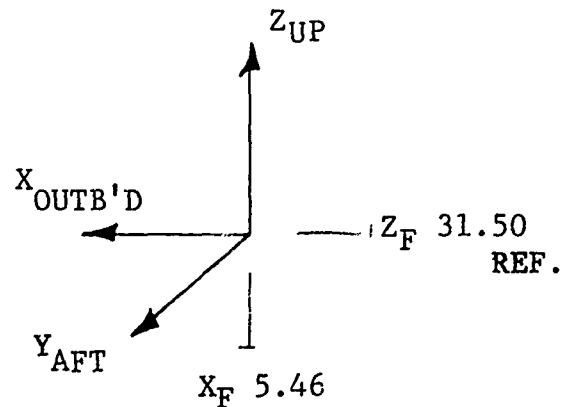


FIGURE 2-21 MAIN LANDING GEAR FITTING GEOMETRY

TABLE II-11

ULTIMATE WEAPONS LAUNCHER LOADS
(HALF BOX)

CONDITION	F _X LBS	F _Y LBS	F _Z LBS
ASKA 1000S	0	0	0
1000A	0	0	0
2000	0	0	-13,462
3000	0	0	-20,193
4000	0	0	0
5000	0	0	-13,462
6000	0	0	-5,040
7000	0	0	-13,427
8S	0	0	-6,731
8A	0	0	0
9000	0	0	-13,462
10000	0	0	-20,193
11000	0	0	-6,731



- NOTES: 1) Loads listed as applied to CTB --- One Side ---
Per TFD-72-838
- 2) Loads are in "ASKA" Reference System (Ref Sketch)
- 3) "A" Designates anti-symmetric portion of unsymmetrical load condition.

Table II-12

OVERWING FAIRING AND SUPPLEMENTARY WING SWEEP ACTUATOR LOADS FROM
AFFDL 10/12/73

<u>ITEM</u>	<u>LOCATION</u>				<u>VALUE</u>	
	X_F	Y_F	Z_F	F_Z	M_Y	
OVERWING FAIRING LOADS						
FORWARD UPPER	138.9	944.1	23.75	21,500 lbs	491,000 in. lbs	
AFT UPPER	149.6	988.01 ⁽¹⁾	30.00	15,195	—	
LOWER	138.9	944.1	-6.5	10,700	289,000	
SWEEP ACTUATOR DESIGN LOAD	SEE TABLE II-9				30,000	0

NOTES: (1) Given as 998.026
in original data.
(2) All loads ultimate



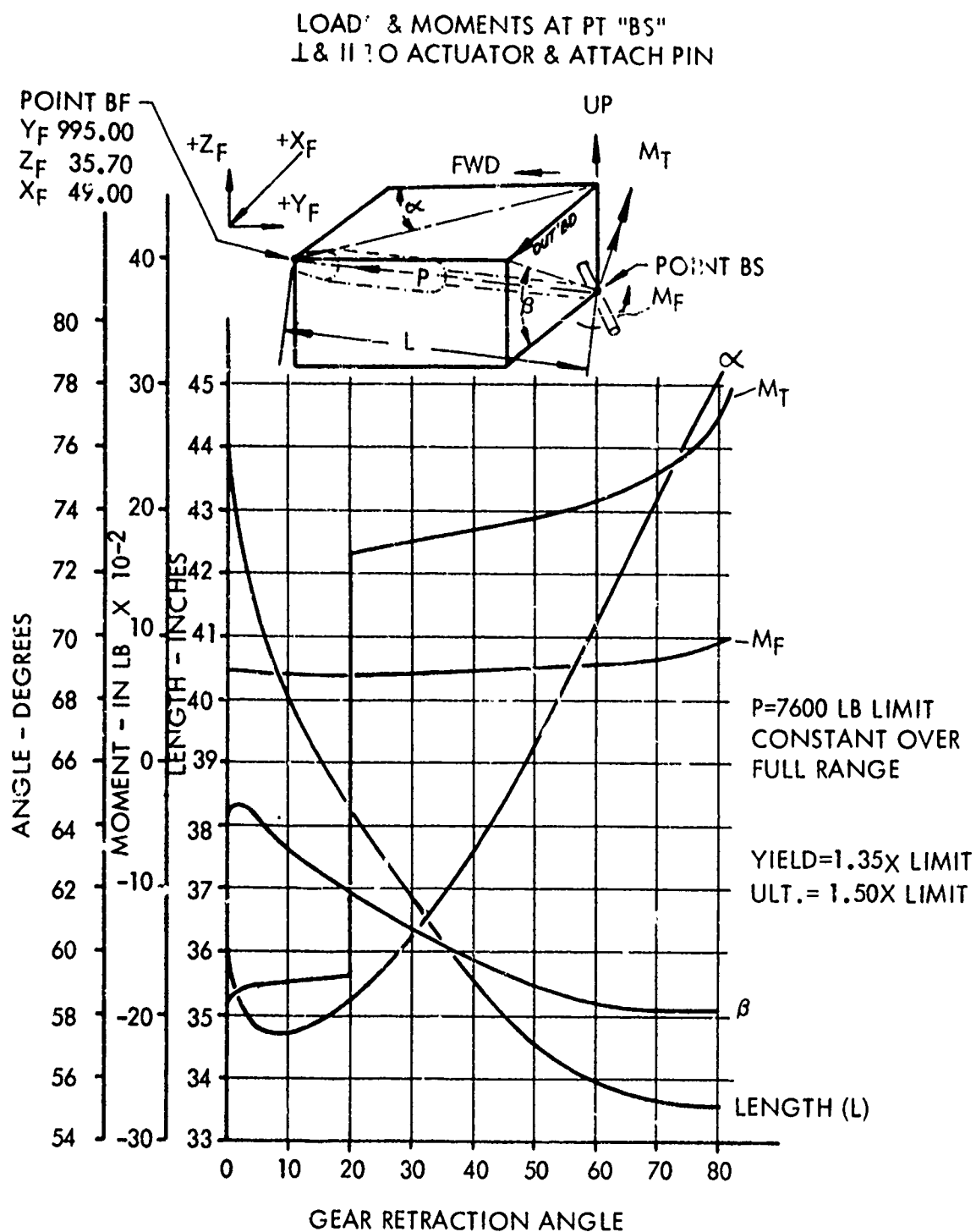
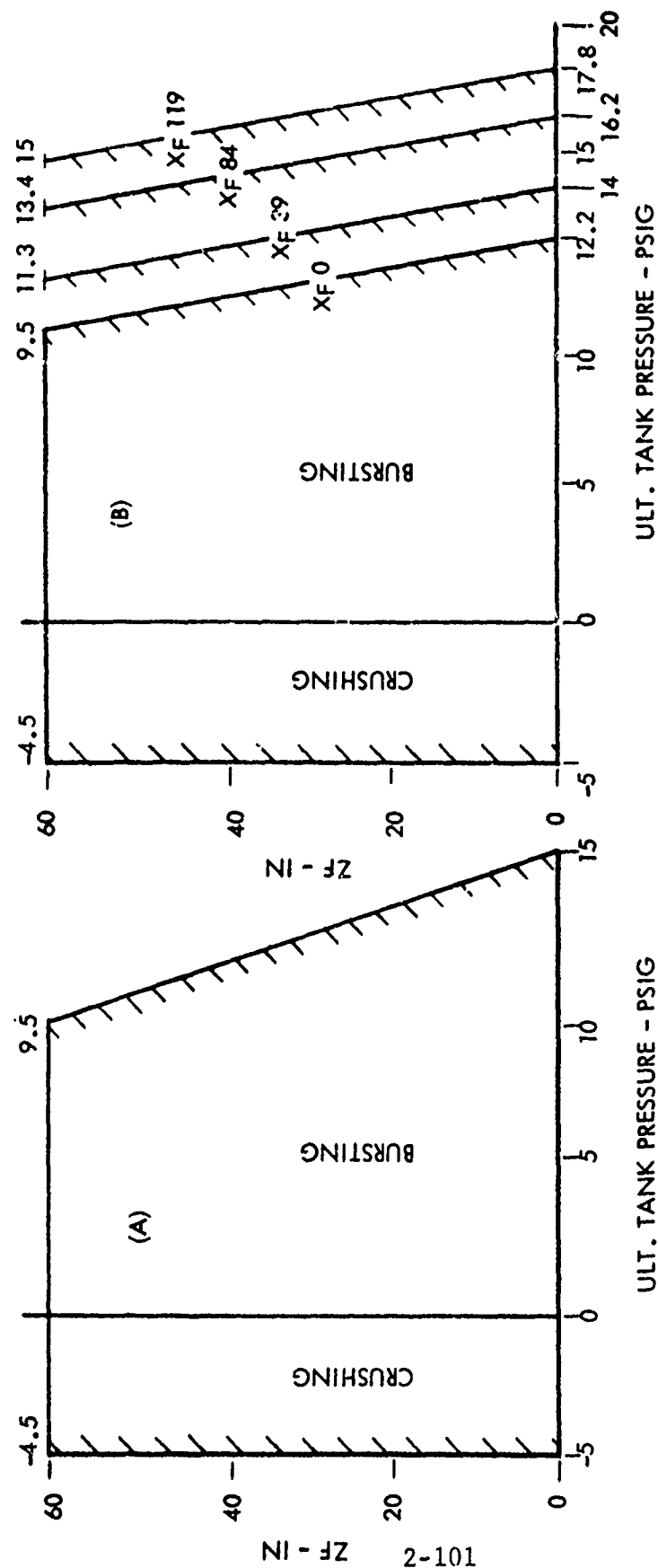


Figure 2-22 MAIN LANDING GEAR EMERGENCY HYD. ACTUATOR
CYL. LOADS & GEOMETRY VS. GEAR ROTATION



- NOTES:
1. USE (A) FOR COMBINATION WITH FLT. CONDS. ON TANK BOUNDARIES. ALL XF & YF EXCEPT FOR OG WHERE MAX. BURSTING PRESSURE IS TO BE 8.25 PSIG. (REFUELING)
 2. USE (B) VALUES ACTING SEPARATELY FOR LOCAL DESIGN OF TANK BOUNDARIES. ALL YF.
 3. FOR SLOSH PRESSURE USE 2.25 (F-III DATA)
 4. ALL PRESSURES ULTIMATE

Figure 2-23 FUEL TANK PRESSURES - AMAVS

	ϵ	Y_F 115
ASKA 2	.75 PSI	1.80 PSI
ASKA 3	2.55	2.55
ASKA 10	3.0	4.5

As specified in TFD-72-835, room temperature was used for all design conditions.

2.2.1.2 Static Balance

The application to the carrythrough box of all of the design loads supplied by RI does not result in a statically balanced structure. This fact was recognized by RI as has been previously discussed on page 2-179 of AFFDL-TR-73-40.

Small additional unbalances are present in the Convair model because of geometric differences such as longeron load application points at estimated longeron centroids instead of at the NARSAP longeron load locations. The balancing procedure used by Convair was as follows:

1. Symmetrical conditions or symmetrical portions of unsymmetrical conditions - The vertical force and pitching moment unbalance at Y_F 992, resulting from applying the design loads, was determined utilizing the HP9820 calculator. A force equal and opposite to one-half of the vertical unbalance was applied at the launcher fitting on Y_F 932 and to the inboard trunnion location (X_F 72, Y_F 992). The net remaining pitching unbalance was nullified by altering the fore and aft components of the Y_F 992 longeron loads in a manner similar to that used by RI. Since the fore and aft adjustment loads are small compared to the fore and aft (F_Y) longeron loads, no attempt was made to adjust the vertical and horizontal components of the longeron load (F_X , F_Z).

Condition AS6000 produces a fore and aft load unbalance as well as a pitching unbalance. Equilibrium was achieved by adjusting the longeron loads at 992 for both pitching moment and longitudinal force balance. The balance loads were determined as follows:

- (a) The incremental longeron loads produced by Y_F 992 AS6000 moment were obtained by multiplying the longeron loads for a pure moment conditions AS10000 by the moment ratio, $M_{AS6000}/M_{AS10000}$.

- (b) The incremental longeron loads produced by axial load were obtained by subtracting the incremental load due to moment obtained in (a) from the total AS6000 longeron load.
- (c) Adjusted moment longeron loads were obtained by multiplying the values of (a) by $M_{REQ'D AS6000}/P_{AS6000}$.
- (d) The incremental longeron loads required for fore and aft force balance were obtained by multiplying the values of (b) by $REQ'D P_{AS6000}/P_{AS6000}$.
- (e) The results of (b), (c), and (d) were added together to obtain the final longeron loads at 992 for overall balance.

A final overall force and moment summation including adjusted loads was made with the HP9820 to assure that equilibrium existed.

2. Antisymmetric conditions - Conditions AS1000A and AS8A are the antisymmetric portions which combine with AS1000S and AS8S to form the two asymmetrical design load conditions. For the antisymmetrical cases, static balance must be achieved in the yaw (M_z), roll (M_y) and lateral (F_x) directions. A simplified balancing procedure was developed which forced equilibrium by altering the lug loads. This alteration was deemed acceptable because the incremental lug loads resulting from balancing AS1000A and AS8A are insignificant compared to the critical lug design conditions. Yaw (M_z) balance was achieved by adding couple loads at the lugs and the centerline longerons. The yaw couple was created in the Z_F 15.0605 plane and the couple forces were then beamed out to the lugs and longerons. The lateral load unbalance was reacted with an equal and opposite load on the lugs. This load was divided equally between the upper and lower lugs. Finally, roll unbalance (including the effects of the lateral balance load) was nullified with a lateral couple load on the lugs.

A summary of the final fuselage shears and moments and the required vertical balance load for each condition is given in Table II-13. It should be noted that these values are for a total WCTS and combine the symmetric and antisymmetric portion of AS1000 and AS8 to yield total load conditions.

TABLE II-13

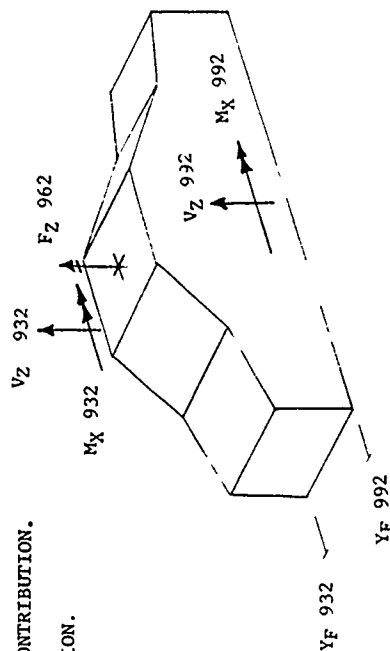
SUMMARY OF BULKHEAD SHEARS, MOMENTS, AND VERTICAL BALANCE LOAD FOR DESIGN CONDITIONS

CONDITION	DESCRIPTION	Δ	V_Z 932	M_X 932X10 ⁻⁶	V_Z 992	M_X 992X10 ⁻⁶	F_Z 962 (BAL)
AS 1000	ABRUPT ROLL	67.5°	-25,012	-35,721	-429,888	158,056	-20,954
AS 2000	2G FLAPS DOWN	15°	-261,394	-83,138	-307,544	140,849	-92,980
AS 3000	3G, 11,000 FT.	67.5°	-5,878	-36,217	-443,640	168,601	22,802
AS 4000	OG, SPOILERS OPEN 70°	15°	70,880	12,300	83,056	-24,793	38,692
AS 5000	2G, SLATS OPEN 20°	15°	-194,288	-69,601	-318,666	95,155	-50,308
AS 6000	2 PT. BRAKED ROLL	15°	-71,314	-10,532	-389,894	88,227	6,812
AS 7000	2G TAXI	15°	-276,172	-35,405	-321,246	97,754	-184,848
AS 8	GROUND TURNING	15°	-138,402	-17,986	-161,176	49,261	-63,300
AS 9000	2G, 20,000 FT.	25°	-198,970	-70,142	-348,038	134,082	-55,091
AS 10000	3G, S.L.	67.5°	-33,604	-47,173	-502,292	214,630	-20,200
AS 11000	1G, S.L.	67.5°	19,238	-6,729	-84,208	9,615	36,894

NOTES: (1) SHEARS ARE POUNDS ULT. AND MOMENTS ARE IN.- POUNDS ULT. FOR TOTAL CTB

(2) LISTED SHEARS AT Y_F 932 and Y_F 992 ARE INTERFACE SHEARS AND DO NOT INCLUDE ARMAMENT OR LANDING GEAR LOADS.(3) LISTED MOMENTS AT Y_F 992 INCLUDES BALANCE CONTRIBUTION.

(4) REFERENCE SKETCH FOR POSITION SIGN CONVENTION.



2.2.2 Node Point Loads for Math Models

In order to apply the design loads to the carrythrough structure math model, it was necessary to convert the basic RI loads data of paragraph 2.2.1 to panel point loads. The panel point loads were developed initially for the FSIL model. For use on the NBB model they were modified as necessary to match the loading points where commonality did not exist.

The first step consisted of geometry definition. The following assumptions were made in the geometry selection:

1. Longerons act at the estimated centroid of the RI longeron material based on RI drawings.
2. Shear flows act at the intersection of the actual fuselage webs and skins with the carrythrough structure as shown on RI drawings.

Figures 2- 24 and 2- 25 show the basic Convair Aerospace geometry used at Y_F 932 and Y_F 992 for panel point load computation.

The geometry shown in Figures 2-25 and 2-25 gives shear path lengths and directions that are somewhat different from the NARSAP model. For this reason and because the updated shear flow data was furnished in NARSAP rather than ASKA form, the following shear flow adjustments were made:

1. NARSAP shear flows shown in Tables II- 5 and II- 7 which are average panel values, were corrected to ASKA values using the ratios between NARSAP and ASKA values found in TFD-72-838 (Section 2.2.1).
2. The shear flows of item 1. were further adjusted to yield vertical force sums at Y_F 932 and Y_F 992 that were equal to the corresponding RI sums (prior to static balance corrections discussed in 2.2.1.2).

These adjustments were accomplished using HP9820 procedures. The results are summarized in Tables II-14 and II-15. The horizontal force sums at Y_F 932 and Y_F 992 were approximately the same as the corresponding RI sums.

The NMAVS shear flows along with the NARSAP longeron loads from Tables II-4 and II-6 were then entered into another HP 9820 program which computes the forces due to shear flows, distributes

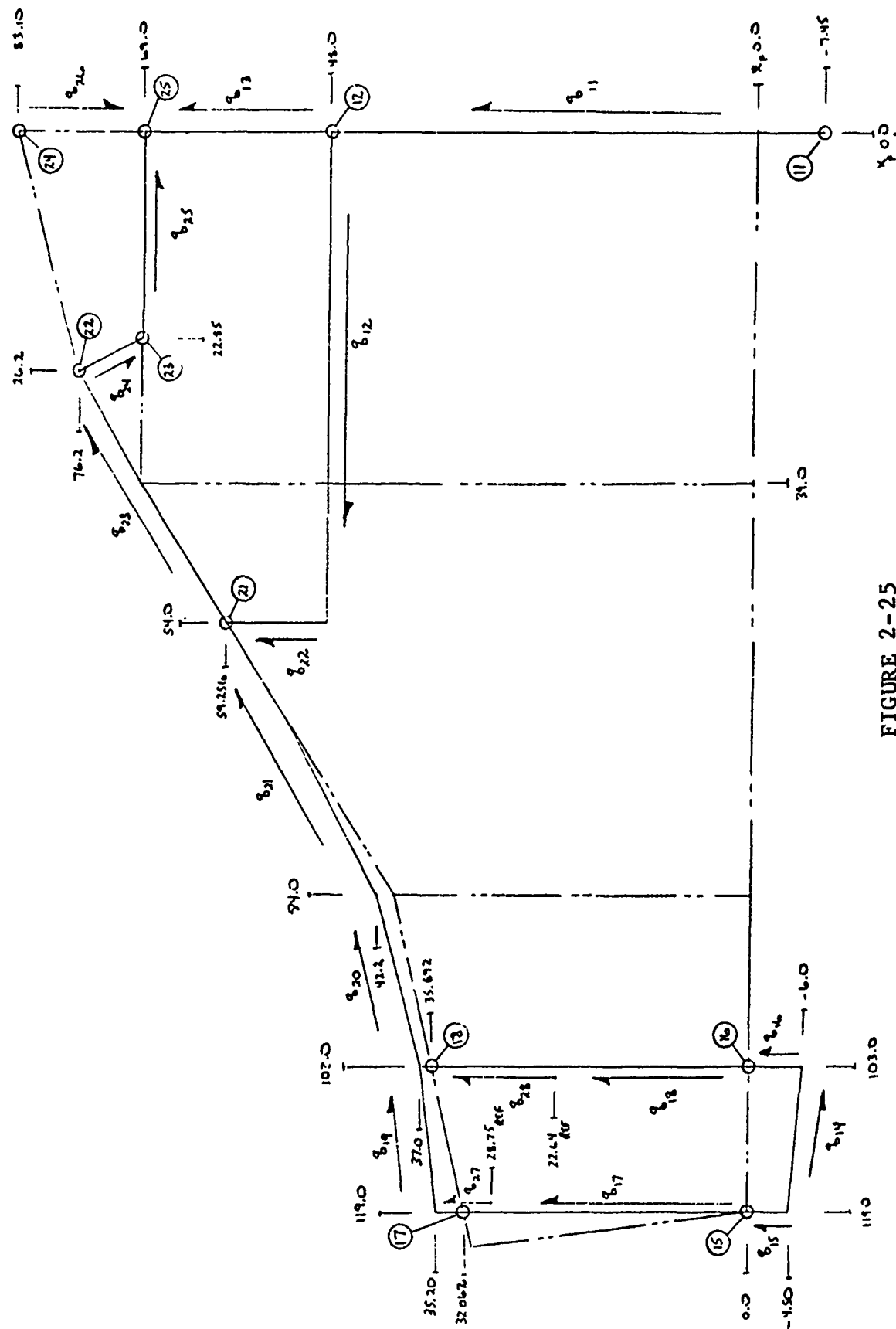


FIGURE 2-25
Y_F 992 GEOMETRY FOR CAD PANEL POINT LOADS RESOLUTION

TABLE II-14

AMAVS Yf932 Bulkhead Shear Flow Summary

Input for Node Point Distribution

Convair Condition	q1	q2	q3	q4	q5	q6	q7	q8	q9	q10
1000 S	330.64	-204.15	-1104.81	2363.35	1745.72	-285.06	1210.48	-93.74	-103.69	-19.29
1600 A	-20.70	33.30	-149.47	33.33	24.62	39.71	-239.01	-187.61	-72.58	0
2000	1097.21	104.24	868.98	2880.91	2128.02	31.77	1609.57	-779.22	-160.20	-34.51
3000	355.44	-242.97	-1246.39	2325.66	1717.88	-329.29	1222.81	-63.72	-107.46	-20.53
4000	-328.43	171.19	-290.13	-1247.09	-921.18	212.01	-585.36	-153.36	32.90	1.56
5000	655.51	5.56	653.30	2420.56	1787.98	-68.12	1185.83	-567.21	-147.26	-22.62
6000	-720.30	-396.52	676.27	1100.90	813.19	-229.62	839.88	71.33	-18.46	-15.44
7000	421.82	709.84	944.47	1166.33	861.52	776.13	718.61	-1189.30	-25.00	-32.94
8 S	135.13	315.80	604.12	399.14	294.83	340.88	286.97	-336.46	267.61	-492.89
8 A	155.48	-101.35	143.17	451.04	333.17	-147.43	599.80	469.93	96.67	0
9000	854.46	7.7	490.13	2622.37	1937.04	-74.23	1497.32	-546.89	-142.00	-28.31
10000	439.21	-234.42	-1511.60	3087.65	2280.73	-339.38	1573.18	-185.49	-136.70	-27.07
11000	-61.76	100.93	-46.79	-497.47	-367.46	108.09	-99.43	-175.30	-6.52	-3.05

NOTES: (1) All values are lbs/in ult.

(2) Values for shear flow on ξ are listed as 1/2 of total.

(3) Positive sign convention and location for shear flows depicted on Fig. 2-24.

TABLE II - 15
AMAYS YF992 BULKHEAD SHEAR FLOW SUMMARY Sheet 1

Conveyor Condition	q ₁₁	q ₁₂	q ₁₃	q ₁₄	q ₁₅	q ₁₆	q ₁₇	q ₁₈	q ₁₉
1000 S	-251.18	-27.37	-118.10	-2225.00	8727.07	3343.65	-6785.93	-144.05	7096.83
1000 A	0	-503.18	0	1838.53	614.85	2116.74	-2379.07	50.16	-291.19
2000	-304.66	-134.90	-177.89	2437.43	5164.57	4143.61	-4178.35	398.60	-8012.86
3000	-492.68	2.97	-128.14	-1195.35	9463.69	3516.92	-7296.91	-144.57	7807.75
4000	319.39	131.45	18.17	-886.47	-570.16	-1621.81	1163.06	-190.94	321.90
5000	-766.22	-168.25	-226.65	1506.85	2541.31	3368.84	-2912.02	325.80	-8281.35
6000	-1895.39	-475.03	-486.53	561.60	3808.79	2126.45	-1964.54	-594.37	6263.29
7000	-689.06	-274.20	-450.60	820.92	3668.01	2090.01	-2365.17	-777.38	4281.16
8 S	-564.12	-271.82	-349.79	112.03	1640.29	916.85	-537.20	-404.33	3206.16
8 A	0	63.53	0	-176.31	1255.32	466.92	-336.22	-253.56	705.04
9000	-291.10	-97.50	-183.70	1783.06	5169.86	3754.95	-4608.45	302.05	-6906.79
10000	-286.68	-5.00	-115.40	-2145.55	11321.40	4585.12	-9223.17	-94.65	10390.60
11000	145.90	143.48	-72.7	-586.83	465.43	-672.96	-364.28	-95.27	-4489.54

NOTES: (1) All loads are lbs/in ult.

(2) Values for shear flow on q₂ are listed as 1/2 of total.

(3) Positive sign convention and location for shear flows depicted on Figure 2-25

TABLE II - 15
AMAVS Yf992 BULKHEAD SHEAR FLOW SUMMARY Sheet 2

Convair Condition	q ₂₀	q ₂₁	q ₂₂	q ₂₃	q ₂₄	q ₂₅	q ₂₆	q ₂₇	q ₂₈
1000 S	345.14	864.04	-177.01	-611.24	-100.02	-788.46	-749.07	-10471.37	-262.56
1000 A	-12.63	-31.62	-396.68	512.24	-189.31	209.44	0	-3671.15	91.43
2000	-209.72	-525.01	-206.33	-434.76	-634.74	694.40	-682.48	-6447.98	726.57
3000	369.92	926.08	-171.19	697.73	-73.52	861.13	-809.51	-11259.86	-263.53
4000	-54.09	-135.40	80.80	-46.19	23.11	-183.53	196.08	1794.72	-348.05
5000	-270.71	-677.71	-154.44	-724.75	-522.08	380.79	-253.25	-4493.54	593.86
6000	123.67	309.60	-620.33	73.54	853.94	761.89	-35.58	-3031.47	-1083.41
7000	11.98	29.99	-539.48	-204.87	469.48	645.30	-100.26	-3649.70	-1417.00
8 S	-.88	-2.20	-389.90	-227.33	747.67	437.05	224.25	-697.69	-819.68
8 A	-24.10	-60.34	18.47	-78.36	200.86	98.97	0	-403.34	-465.28
9000	-189.99	-475.63	-175.34	-416.92	-574.96	626.00	-575.64	-7111.29	550.57
10000	508.19	1272.22	-206.81	1000.88	-62.81	1088.90	-1105.93	-14233.26	-172.53
11000	-254.61	-637.40	95.69	-493.86	-310.24	-126.03	198.14	-562.11	-173.65

these to the node points, and adds the X and Z components of the longeron loads to the shear flows where applicable.

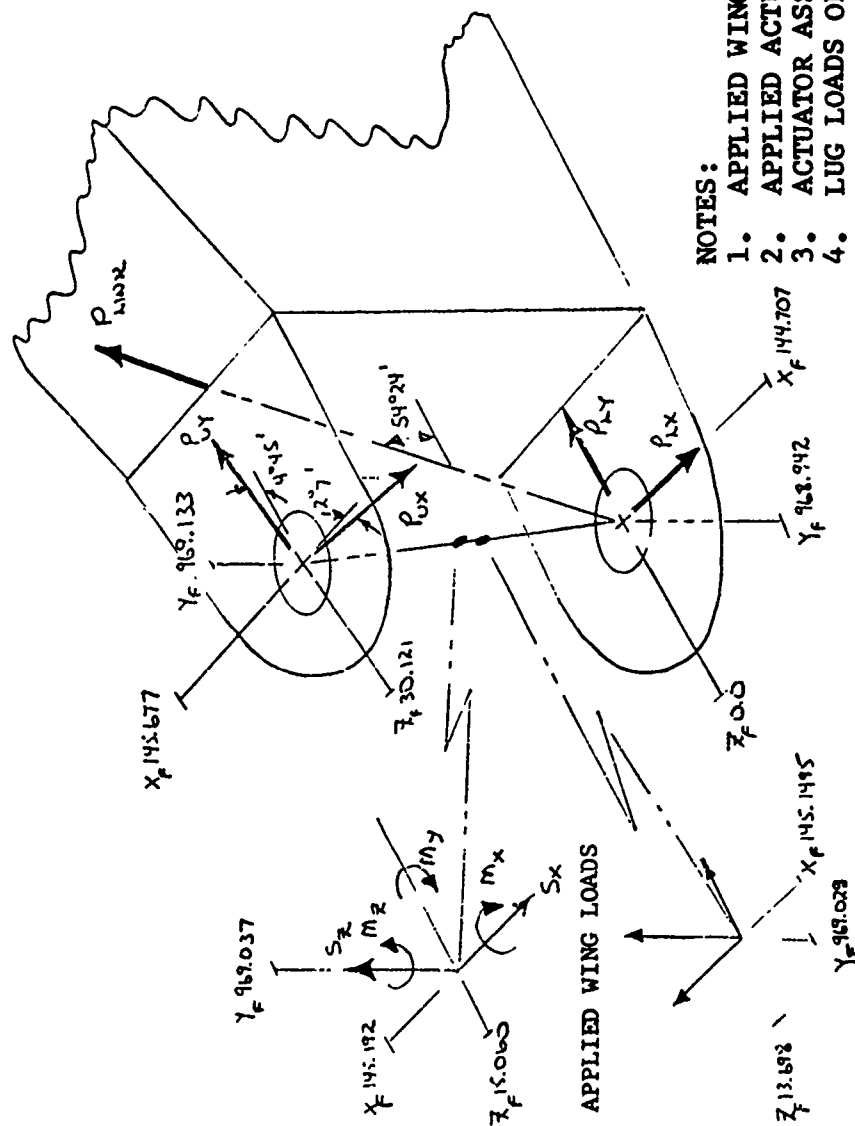
Using the pivot loads from Table II-3 and sweep actuator loads from Table II-9 simultaneous equations were written and solved to obtain lug loads in the place of the lugs and shear link load. The problem is statically determinate from the six force and moment equations available, but the number of equations was reduced to five by utilizing the sweep actuator loads from Table II-9 as known values rather than utilizing M_2 from Table II-3 and formulating the problem with the sweep actuator load as an unknown. A sketch of the geometry used is shown in Figure 2-26. The results are summarized in Table II-16. The inplane values were then resolved in the math model global coordinate system. A summary of the resolved loads is shown in Table II-17. These loads were then distributed over the lug panel points. Only the X and Y components of the upper lug loads were applied to the math model because the required Z boundary restraints of TN1 produced Z components. (See AFFDL-TR-73-40.) Sweep actuator loads applied to the actuator pivot point were beamed in a rational manner to panel points on the closure rib and on the X_F 84 rib.

Link loads were applied at a panel point coincident to the closure rib and the upper cover at X_F 123.06, Y_F 969.5, Z_F 31.985.

Landing gear loads were beamed in a rational manner to appropriate panel points.

All of the panel point loads for a given condition were then applied to a freebody of the wing carrythrough structure and forces and moments were summed, with the moment center being Y_F 992, Z_F 0. Utilizing the results of this operation (i.e., net WCTS unbalance), balance loads were calculated and applied as discussed in Section 2.2.1.2. After integrating the balance loads into the panel point loads, the balance was rechecked. A set of panel point loads for a typical condition (AS2000) are shown in Table II-18.

In using procedure TN1, forces cannot be applied to nodes which have been put in boundary. Consequently, force components in the direction of boundary restraints at boundary nodes were not entered as applied loads in the TN1 input. The omitted values are circled on the AS2000 data sheets presented.



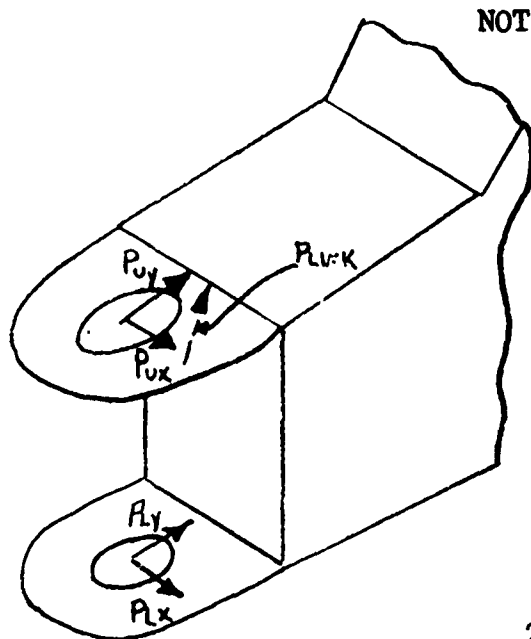
APPLIED WING SWEEP ACTUATOR LOADS

Figure 2-26 GEOMETRY FOR DETERMINATION OF WCTS LUG LOADS

TABLE II-16

SUMMARY OF APPLIED IN-PLANE LUG LOADS AND SHEAR LINK LOADS

CONVAIR COND.	Λ	P_{UX} LBS.ULT.	P_{UY} LBS.ULT.	P_{LX} LBS.ULT.	P_{LY} LBS.ULT.	P_{LINK} LBS.ULT.
AS 1000	67.5°	-2,114,632	1,263,002	2,269,787	-1,508,652	58,129
1000A	67.5°	-252,646	74,596	309,616	-158,950	9883
AS 2000	15°	-887,383	3,373,592	894,619	-3,464,658	36,416
AS 3000	67.5°	-2,317,083	1,287,388	2,376,995	-1,395,188	47,017
AS 4000	15°	195,488	-1,022,949	-242,745	1,503,300	14,394
AS 5000	15°	-407,444	2,909,325	450,378	-3,365,895	30,002
AS 6000	15°	82,890	-459,645	-97,002	311,963	-8606
AS 7000	15°	146,922	-650,758	-146,796	659,071	-18,538
AS 8000	15°	73,476	-325,376	-73,413	329,532	-9269
8000A	15°	0	0	0	0	0
AS 9000	25°	-1,045,068	3,185,941	1,060,580	-3,260,942	11,640
AS 10000	67.5°	-2,841,164	1,585,370	3,046,589	-1,902,974	63,309
AS 11000	67.5°	-282,831	458,220	-202,482	215,047	-3675



- NOTES: (1) POSITIVE CONVENTION SHOWN
 (2) LUG LOADS ARE IN PLANE OF LUG
 (3) LOADS INCLUDE EFFECT OF WING SWEEP ACTUATOR
 (4) SHEAR LINK LOADS SHOWN ARE AS APPLIED TO WCTS; SKETCH INDICATES COMPRESSIVE LINK LOAD

TABLE II-17

Summary of Applied Pivot Loads in Global Coordinate System

Convair Condition	Δ	UPPER LUG			LOWER LUG			SHEAR LINK		
		F _x	F _y	F _z	F _x	F _y	F _z	F _x	F _y	F _z
1000 S	67.5°	-1,258,670	-2,113,194	182,683	1,508,652	2,269,787	0	-33,797	0	47,294
1000 A ∇	67.5°	-7,576	-241,876	9,568	132,162	320,214	0	-5,746	0	13,981
2000	15°	-3,362,021	-886,780	312,138	3,464,658	894,619	0	-21,173	0	29,628
3000	67.5°	-1,282,972	-2,315,507	192,178	1,395,188	2,376,995	0	-27,336	0	38,254
4000	15°	1,019,440	195,355	-91,930	-1,503,300	-242,745	0	-8,369	0	11,711
5000	15°	-2,899,346	-407,167	255,968	3,365,895	450,378	0	-17,443	0	24,410
6000	15°	458,068	82,834	-41,124	-311,963	-97,002	0	5,004	0	-7,002
7000	15°	648,526	146,822	-59,315	-659,071	-146,796	0	10,778	0	-15,083
8 S	15°	324,260	73,426	-29,658	-329,532	-73,413	0	5,389	0	-7,541
8 A ∇	15°	-42,770	-26,027	4,516	51,636	-26,027	0	0	0	-4,516
9000	-25°	-3,175,013	-1,044,357	302,422	3,260,942	1,060,580	0	-6,768	0	9,470
10000	67.5°	-1,579,932	-2,839,232	236,209	1,902,974	3,046,589	0	-36,808	0	51,509
11000	67.5°	-456,648	-282,639	48,390	-215,047	-202,482	0	2,137	0	-2,990

NOTES: (1) All loads are lbs ult.

(2) Loads include effect of wing sweep actuator.

(3) Loads are listed as applied to WCIS.

(4) Reference sketch for positive sign convention.

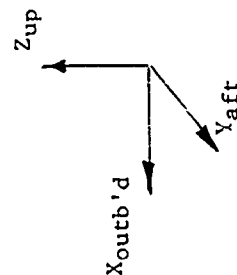
(5) ∇ asymmetric conditions include balance loads applied to lugs.

Table II-18 PANEL POINT LOADS, CONDITION AS 2000

I LUG LOADS

UPPER LUG LOADS

NBB MODEL
COND AS

2000

DATE

90573

TOTAL LUG FX=
-3362021
TOTAL LUG FY=
-886780

LOWER LUG LOADS

NBB MODEL
COND AS

2000

DATE

90573

TOTAL LUG FX=
3464658
TOTAL LUG FY=
894619

NODE +FX ACTS OUTBD
+FY ACTS AFT

FX4=
882 -531199.318
FX5=
883 -726196.536
FX6=
885 -847229.292
FX7=
886 -726196.536
FX8=
887 -531199.318

FY1=
901 -140111.240
FY2=
880 -191544.480
FY3=
881 -223468
FY4=
882 -191544.480
FY5=
883 -140111.240

END COND AS

NODE +FX ACTS OUTBD
+FY ACTS AFT

FX10=
896 547415.964
FX11=
908 748366.128
FX12=
916 873093.816
FX1=
884 748366.128
FX2=
907 547415.964

FY7=
874 141349.802
FY8=
875 193237.704
FY9=
876 225443.988
FY10=
896 193237.704
FY11=
903 141349.802

II SHEAR LINK

NODE	F _x	F _y	F _z
751	-10587	0	14814
753	-10587	0	14814

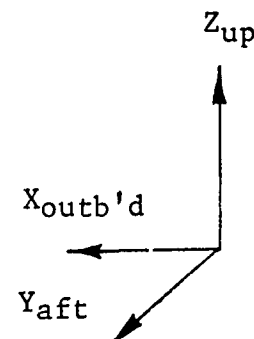
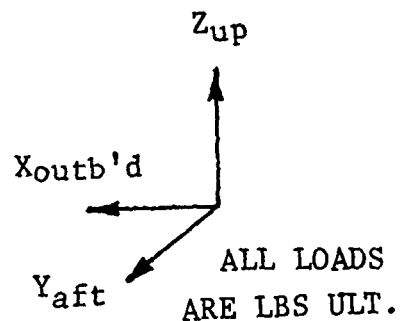


TABLE II - 18 Cont'd.

NODE POINT LOADS

COND 2000
MODEL N.B.B.III WING SWEEP ACTUATOR FITTING LOADS

NODE	F _x	F _y	F _z
737	-39439	-20338	1382
739	-41246	-20690	1382
510	0	16604	-54
513	0	16604	-54



NOTES:

1. These values for use with TN1 program.
2. Values shown are loads fitting applies to CTB.
3. Revised 17 May 73 for latest geometry.

IV LANDING GEAR FITTINGS

TRUNNIONS	NODE	F _x	F _y	F _z
	606	0	0	0
OUTBOARD	627	0	0	0
INBOARD	L.G.	0	0	0
	BAL.	0	0	-23245
		<hr/>	<hr/>	<hr/>
	467	0	0	-23245
	420	0	0	0

TABLE II - 18 Cont'd.

MODE POINT LOADS

COND. 2000
MODEL N.B.B.IV CONT.

SIDE BRACE FITTING	NODE	F _X	F _Y	F _Z
Lo L/H	296	0	0	0
Lo R/H	291	0	0	0
Up G _L :LD GR SHEAR	X	0	0	0
	X	0	0	-3549
TOTAL	116	0	0	-3549

DRAG BRACE:

NODE	F _X	F _Y	F _Z
476	0	0	0
257	0	0	0
277	0	0	0
317	0	0	0
279	0	0	0
347	0	0	0
390	0	0	0
397	0	0	0
398	0	0	0

TABLE II - 18 Cont'd

NODE POINT LOADS

COND. 2000
MODEL N.B.B.

V ARMAMENT LOADS.

NODE	LOAD SOURCE	F _X	F _Y	F _Z
14	ARM	0	0	-6731
	BAL.	0	0	-11623
		<hr/>	<hr/>	<hr/>
		0	0	-18354
17	ARM	0	0	-6731
	BAL.	0	0	-11623
		<hr/>	<hr/>	<hr/>
		0	0	-18354

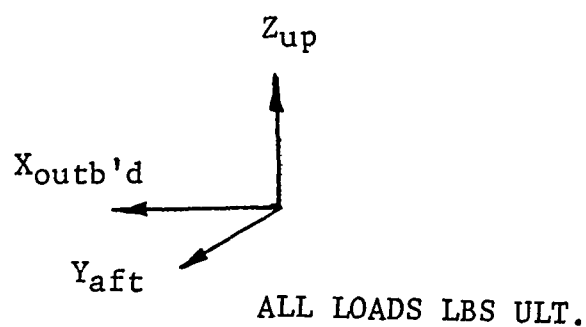
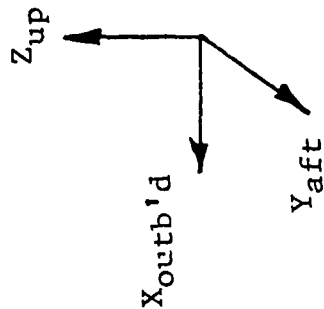


TABLE II - 18 Cont'd.

YF 932 FW BLKHD NODE POINT LOADS		COND. 2000		NBB (ALL LDS ULT)	
9820	NODE NO.	NODE NO.	F _X	F _Y	F _Z
1		3	0	-186286	1086
2		9	-921	0	42
3		35	-1687	0	+313
4		92	-1955	0	-2943
5		95	12925	-277953	-1187
6		162	26361	-92387	-8630
7		231	27154	0	-16237
8		359	24132	0	-12321
9		461	20216	0	-9534
10		499	20814	0	-7142
11		545	18351	0	-3918
12		601	16940	0	-3601
13		626	20512	0	-4379
14		646	17170	0	-3659
15		685	5647	0	-2844
16		714	0	104630	-7868
16 1/2		716	19854	0	0
17		678	0	0	-4166
17 1/2		761	0	0	-4489
18		687	0	0	-10793



$$\sum F_x = 240,690$$

$$\sum F_y = -13$$

$$\sum F_z = -130,697$$

ALL LDS LB ULT.

XX IN BOUNDARY

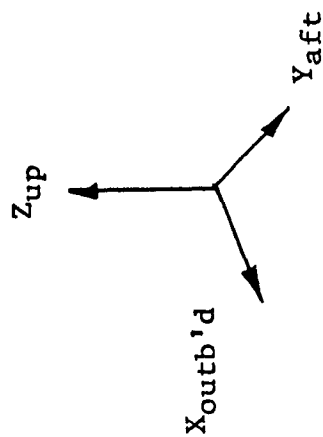
TABLE II - 18 Cont'd

YF 932 FWD BLKHD NODE POINT LOADS Cont'd		COND. 2000			NBB (ALL LDS ULT)	
9820 NODE NO.	NODE NO.	Fx	Fy	Fz		
19	688	0	0	-8307		
20	719	0	0	-41128		
21	743	45183	0	0		
21	733	0	238121	34246		
22	710	-955	0	-2412		
23	690	-2919	0	-203		
24	663	-3489	0	-247		
25	602	-2875	0	-203		
26	586	-3116	0	-219		
27	516	-4169	0	-291		
28	448	-5486	0	-384		
29	382	-5684	0	-400		
30	315	-2662	187737	-567		
31	266	288	26135	-1637		
32	251	630	0	-2481		
33	237	432	0	-1482		

TABLE II - 18 Cont'd

Y_F 992 AFT BLKHD NODE POINT LOADS

COND. 2000 NBB (ALL LDS ULT)



9820 NODE NO.	NODE NO.	F _X	F _Y	F _Z	
1	207	0	(-77257)	(-1135)	
2	220	0	0	-2963	
3	181	0	0	-5286	
4					
5					
6	55	0	0	-3123	
7	26	(-287)	2315	-1839	
8	30	0	0	-1868	
9	36	(-1476)	42314	3945	
10	21	0	(308205)	7257	
11	48	-3472	0	0	
12	70	-4253	0	0	
13	88	-4462	0	0	
14	85	-1142	87022	2285	
15					
16	33	-1500	0	0	
17	66	-1710	0	0	
18					

F_x = 214,700F_y = 0.0F_z = 153,772

All loads are lbs. ult.

(xx) In Boundary

1 F_y modified to
to force balance

TABLE II - 18 Cont'd.



YF 992 AFT BLKHD NODE POINT LOADS Cont'd		COND. 2000 NBB (ALL LDS ULT.)		
9820 NODE NO.	NODE NO.	FX	FY 	FZ
19	123	-1069	0	0
20	174	-1248	0	0
21	235	-1032	0	0
22	267	-438	0	-1161
23	94	3784	230651	720
24	164	4630	0	-5495
25	201	3326	0	-2117
26	258	4301	87578	-5619
27	371	4725	0	-2809
28	418	4988	0	-2636
29	542	4356	0	-1996
30	594	1992	0	-545
31	642	16813	0	-3464
32	686	31250	0	-7212
33	715	15224	0	-13585
34	724	-83197	363432	-24069
35	736	0	0	-30720
36	725	0	0	-32382

TABLE II - 18 Cont'd

Y _F 992 AFT BLKHD NODE POINT LOADS Cont'd.		COND. 2000 NBB (ALL LDS ULT.)		
9820 NODE NO.	NODE NO.	F _X	F _Y 	F _Z
37	732	0	0	-40112
38	763	199991	-881481	-28052
39	731	-7008	0	10731
40	712	-16063	0	-1828
41	708	-3436	0	0
	668	-9078	0	11492
42	660	69122	-184459	11766
43	658	0	0	3827
44	657	0	0	3886
45	638	0	0	5466
46	641	-8231	21680	5703

2.2.3 NBB Stress Analysis

The stress analysis of the "No-Box Box" configuration during Phase II consisted of three primary areas of effort:

1. Finite element modeling of the complete carrythrough box.
2. Finite element and other computer based analysis for local areas.
3. Manual stress analysis conducted as a continuing part of the support of on-board design and production drawing analysis.

Where buckling or static strength considerations governed fastener or member sizes, a 10% positive margin of safety was maintained to allow for the gross weight increase (Section 2.2.1). In areas where fatigue was critical, reduced allowable ultimate stresses were used (Section 2.3). Material properties were taken from standard sources such as MIL-HDBK5 and from data generated specifically for the less common materials used for AMAVS design (Section 2.4).

2.2.3.1 Overall Box Analysis

To obtain a consistent set of internal loads and stresses for the overall carrythrough box, finite element models were constructed for use with Convair Computer Procedure TN1 (Ref. AFFDL-TR-73-40, Par. 2.2.2.1). Membrane and bar elements were used. The models had approximately 868 nodes and 1942 elements. Because of relatively major changes in the configuration and load updating, several model iterations were made. The current conditions run with the model available during drawing sign out are summarized in Table II-19. An updated model will be developed when production drawings are substantially completed in order to verify or revise the final design prior to fabrication.

2.2.3.2 Local Areas - Computer Analysis

Local area analyses using finite element procedures included the following:

1. Upper lug stability checks - NASTRAN procedure.
Includes upper lug and upper plate inboard to X_F 84.
2. Closure rib stability checks - NASTRAN procedure.

TABLE II-19

NBB TN1 LOG
CURRENT DESIGN LOAD CONDITIONS

RUN DESIGNATION	JOB NO.	DATE	CHARGE TIME	CONDITIONS
NBB 4-1	18495	9/14/73	48.22 MIN	AS 2000, 7000, 9000, 10000
NBB 4-2	185362	9/21/73	48.58 MIN	AS 4000, 5000, 6000, 11000
NBB 4-3	185363	9/21/73	71.13 MIN	AS 1000 L/H, 1000 R/H, 3000

3. Lower lug stress distribution - TLO linear strain procedure. (See AFFDL-TR-73-40 Par. 2.2.2.2 for TLO description.)
4. Lower aft outboard longeron tab stress distribution - TLO procedure.
5. Lower plate material distribution studies - TR4 procedure (essentially same as TN1).
6. Y_F 992 bulkhead transition radius stress distribution - TLO procedure.
7. Sandwich panel load introduction studies - TN1.

2.2.3.3 Detailed Manual Stress Analysis

The computer analyses discussed in Sections 2.2.4.1 and 2.2.4.2 were supplemented by conventional manual stress analyses in the following general areas. Where feasible, the HP 9820 capability was used to make various standard solutions. Internal loads were ~~derived~~ from the finite element models in most cases.

1. Determination of net section stresses.
2. Fastener pattern checks.
3. Computation of margins of safety.
4. Stability analyses for plates, sandwich panels, and stiffeners.
5. Splice analyses.
6. Fitting analyses.

2.2.4 Fail Safe Integral Lug

As in the case of the NBB configuration, the stress analysis of the FSIL configuration consisted of three primary areas of effort (See 2.2.3). Although the NBB configuration was chosen for production, the FSIL was also analyzed during Phase II since both configurations were carried well into the final design stage before configuration selection.

2.2.4.1 Overall Box Analysis

Convair procedure TN1 was used with finite element models of the overall box. Membrane and bar elements were used. The models had approximately 801 nodes and 1790 elements. Several model iterations were made. A summary of the last set of conditions run prior to configuration selection is shown in Table II-20.

2.2.4.2 Local Areas - Computer Analysis

Local area analyses using finite element procedures included the following:

1. Lower lug stress distributions - TLO linear strain procedure.
2. Upper lug stability checks - A3S procedure (Ref. Par. 2.2.2.5, AFFDL-TR-73-40).
3. Upper forward outboard plate stability check - NASTRAN and A3S procedures.
4. Lower plate damage tolerance studies - overall TN1 model with elements cut to simulate crack.
5. Braze shear and peel stress studies - TLO linear strain procedure.

2.2.4.3 Detailed Manual Stress Analysis

The discussion for NBB para. 2.2.4.3, is generally applicable to FSIL also.

2.2.5 Common and Miscellaneous

2.2.5.1 Common Items

Stress analyses using conventional methods were performed for the sweep actuator fitting, the MLG drag brace fitting, the MLG side brace fitting and the MLG inboard and outboard trunnion fittings. These items were substantially common to both configurations. Additional analyses were performed to assure that changes made to tailor the parts for NBB were structurally adequate.

TABLE II-20
FSIL TNI LOG
CURRENT DESIGN LOAD CONDITIONS

RUN DESIGNATION	JOB NO.	DATE	CHARGE TIME	CONDITIONS	REMARKS
FSIL-6-1	184936	9/14/73	31.90 MIN.	AS 2000, 7000, 9000, 10000	QUAD ELEMENTS SIMULATED WITH RECTANGULAR ELEMENTS (SEE BELOW)
FSIL-6-2	184944	9/14/73	32.50 MIN.	AS 4000, 5000, 6000, 11000	SAME AS 6-1
FSIL-6-3	184948	9/24/73	45.43 MIN	AS 1000 L/H, 1000 R/H, 3000	SAME AS 6-1
FSIL-6-1	184936	9/26/73	34.06 MIN	AS 2000, 7000, 9000, 10000	RERUN TO CORRECT ELEMENT SIMULATION (SEE NOTES)

NOTES: QUAD ELEMENTS ON QUAD END OF F 932 BULKHEAD INCORRECTLY IDENTIFIED IN TNI PROGRAM AS RECTANGULAR ELEMENTS. FSIL-6-1 CONTAINS CRITICAL LOAD CONDITIONS FOR THIS STRUCTURE AND WAS RERUN TO OBTAIN CORRECT INTERNAL LOADS. OTHER CONDITIONS NOT CRITICALLY AFFECTED BY THIS SITUATION.

2.2.5.2 Miscellaneous

The following items were included in miscellaneous analyses:

1. 603FTB052 test specimen (Manual).
2. 603FTB053 test specimen (Manual).
3. 603FTB035 test specimen (TNI)
4. Studies of grid size effects (NASTRAN).
5. 603FTB004 test specimen (TLO).

2.2.6 Stiffness Analysis

As discussed in Para. 2.2.7 of AFFDL-TR-73-40, a stiffness requirement was furnished in the form of allowable stored elastic energy ($.0739 \times 10^8$ in.lbs.). The value found for the FSIL 5-3 model was $.0848 \times 10^8$ in.lbs. and for the NBB3-3 model it was $.0661 \times 10^8$ in.lbs. New runs were not made for the wing intrusion deletion configuration because ASKA stiffness conditions were not furnished to Convair. A review of box torsional deflections as reflected in relative Y deflections for the upper and lower lugs was made for AS10000 and AS10. The deflections were found to be larger for AS10000, but when the deflections were normalized on pitching moment, it was found that the NBB4 and FSIL 6 series models deflected less per inch-pound than the earlier models, i.e. they were stiffer. It was concluded, therefore, that with the deletion of the wing intrusion less virtual energy storage would occur than before so that FSIL would approach the requirement more closely while NBB would have an even greater stiffness margin.

2.2.7 Effect of Updated Loads on Weight

TNI models were run and the first cycle resized weights were obtained in order to gain some insight into the effect of the deletion of the wing intrusion and the load updating. The results obtained are shown in Table II-21. It may be seen that for the 67.5° condition, the weight increase on the FSIL is 284 lbs./AP and 336 lbs./AP for the NBB. It should be noted that the model box input weights are to be considered in a relative manner only. The effects of the 10% gross weight increase are not included in these values.

Table II-21 EFFECTS OF UPDATED LOADS

MODEL RUN	CONDITION	INPUT WEIGHT	RESIZED WEIGHT	WEIGHT CHANGE 1/2 BOX	WT. CHG. AP
FSIL-5-1 No. 2	ASKA 2	3853 lbs./1/2 box	2111 lbs./1/2 box	-4 lbs.	Neg.
FSIL-6-1	AS2000	3853	2107		
FSIL-5-1 No. 2	ASKA 10	3853	1784		
FSIL-6-1	AS10000	3853	1926	+142	+284 lbs
NBB-3-1 No. 2	ASKA 2	4424	2438		
NBB-4-1	AS2000	4424	2435	-3	Neg.
NBB-3-1 No. 2	AS10	4424	2039		
NBB-4-1	AS10000	4424	2207	+168	+336

Notes: 10% Gross Wt. Change Not Included

2.2.8 Simulated Fuselage

The structure referred to as the simulated fuselage consists of the two components of the test fixture which are adjacent to the WCTS. These components extend forward to Y_F 850 and aft to Y_F 1050. The simulated fuselage is designed such that loads applied to the WCTS are similar to the RI NARSAP math model results. In addition to required stiffness, sufficient strength is provided for static and fatigue loadings.

Several TNI math models of the upper test fixture - simulated fuselage - carrythrough structure combinations were set up and iterated to obtain longeron loads and shear flows to compare with the NARSAP results. These models are similar to the Phase Ib models (See AFFDL TR-73-40) except for the following differences:

1. Models with both FSIL and NBB boxes were run.
2. The simulated fuselage plate elements were changed to "shear only plate" which is the same type of element used in the NARSAP model.
3. The bulkhead at Sta. 1050 was changed from a full fuselage cross section planform to a configuration that reflects the cut out for the landing gear.
4. Longeron and web materials, areas, and thicknesses were adjusted on an iterative basis to obtain NARSAP load distributions.
5. Wing intrusion provisions were removed.

A computer drawing of a typical model is shown in Figure 2-27. The comparison of the two Convair models and the NARSAP model are shown in Table II-22 and Table 2-23. Figures 2-28 and 2-29 give the location of the math model load points referred to in the tables. For an overall review of the test set up see Section III.

The load comparisons indicate relatively good agreement for longeron loads and shear flows in the high load carrying regions.

Where appropriate, reduced ultimate material allowables were used to assure adequate fatigue life. Where required, allowance was also made for the required 10% gross weight increase effect.

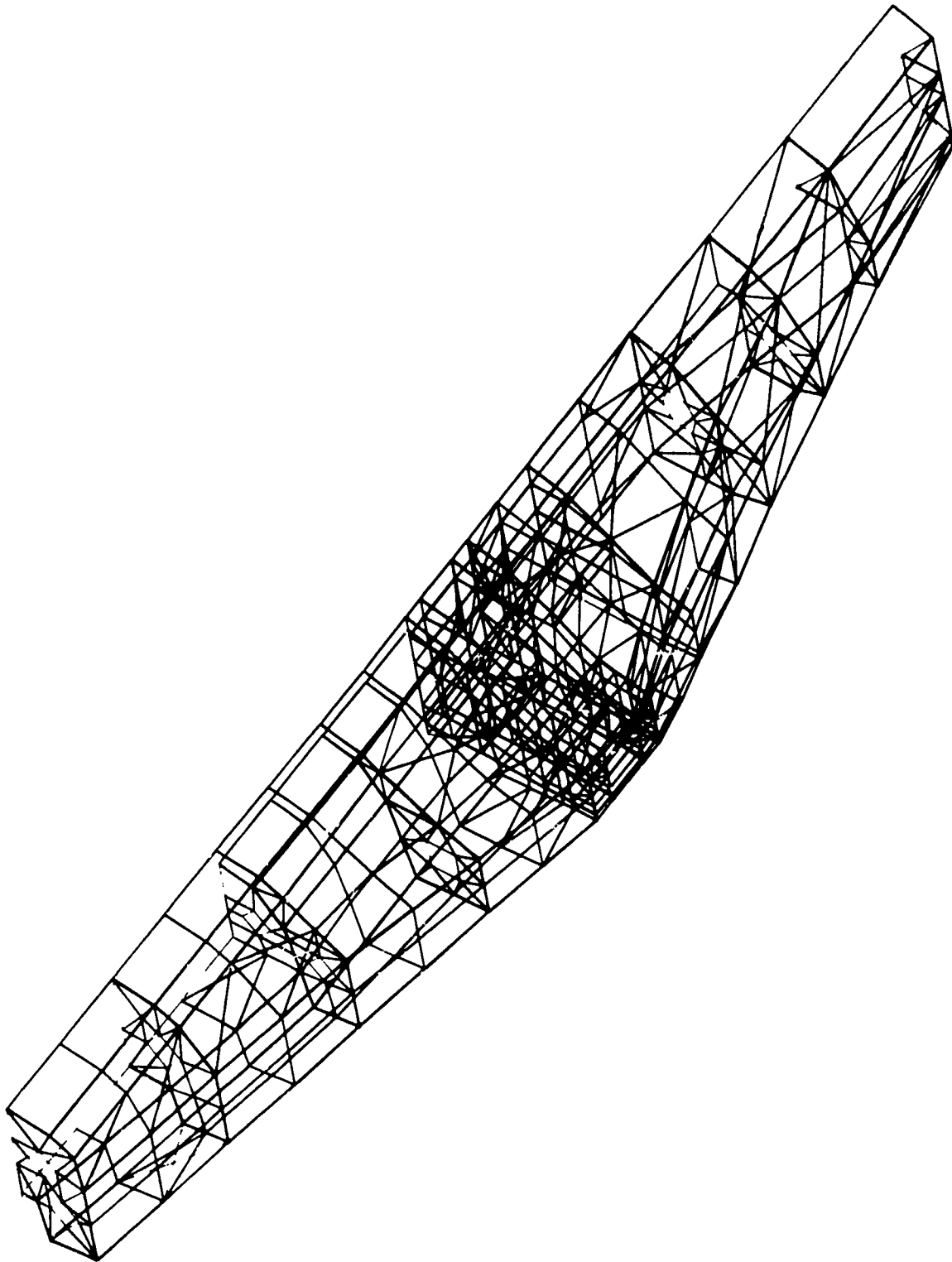


Figure 2-27 SIMULATED FUSELAGE MATH MODEL

Table II-22 CONVAIR AND NARSAP SHEAR FLOW - LBS./IN.

As 2000			AS 7000			AS 9000			AS 10000			
FSIL	NBB	NARSAP	FSIL	NBB	NARSAP	FSIL	NBB	NARSAP	FSIL	NBB	NARSAP	
1	455	409	467	-180	-115	179	475	410	364	714	545	187
2	-108	-54	103	807	844	701	-170	-132	8	-341	-348	-231
3	709	912	917	1097	905	997	255	503	517	-1837	-1379	-1596
4	2136	1852	2163	515	582	876	1949	1670	1969	2075	1754	2318
5	2386	2058	2163	553	628	876	2193	1869	1969	2437	2038	2318
6	-61	14	31	949	989	755	-139	-83	-72	-333	-324	-330
7	941	1115	1460	455	502	652	857	999	1358	914	1020	1427
8	670	505	634	375	407	967	574	411	445	462	250	151
9	650	565	160	82	84	25	592	515	142	632	561	137
10	100	-100	-61	-604	-316	-58	146	-32	-50	288	120	-48
11	2267	2422	-606	-1910	-2040	-1371	1878	2020	-579	1576	1625	-571
12	370	533	-135	-650	-803	-274	294	418	-97	-396	-337	-5
13	1758	1630	-349	-994	-710	-884	1440	1364	-360	1572	1816	-226
14	2415	440	904	-647	-685	305	1790	189	662	-1517	-1617	-796
15	-1611	445	5757	1185	1272	4089	-951	721	5764	3639	3762	12621
16	3578	-161	3074	437	307	1550	2963	-57	2785	929	710	3401
17	-6909	-7228	-5197	-1517	-1827	-2941	-6942	-7205	-5731	-10570	-10583	-11470
18	469	495	483	-1571	-1450	-941	193	183	366	-1132	-1214	-114
19	-4492	-3926	-1568	1209	1111	838	-3807	-3368	1351	748	385	2032
20	-2024	-1385	-585	472	426	33	-1615	-1064	-530	1554	1650	1417
21	-2049	1614	-585	-103	-106	33	-1734	-1366	-530	687	742	1417
22	225	367	-216	-602	-741	-566	170	277	-184	-173	-299	-217
23	-536	-612	-400	-57	-191	-188	-452	-532	-383	596	460	920
24	476	350	694	-706	-730	645	349	233	626	-295	-460	1089
25	-212	-389	-694	-917	-949	-645	-252	-404	-626	-970	-1106	-1089
26	-2346	-2078	-1216	632	494	-179	-1966	-1728	-1025	-2002	-1846	-1970

Table II-23 CONVAIR AND NARSAP LONGERON LOADS - KIPS

	AS 2000			AS 7000			AS 9000			AS 10000		
	FSIL	NBB	NARSAP	FSIL	NBB	NARSAP	FSIL	NBB	NARSAP	FSIL	NBB	NARSAP
141	-123	-140	-214	-47	-56	-81	-105	-117	-176	-78	-71	-94
146	199	202	186	82	86	78	174	176	163	159	159	158
148	302	293	278	114	119	119	264	255	241	237	223	210
150	102	77	92	24	25	30	91	67	80	90	64	82
157	-227	-173	-105	3	-20	-25	-239	-182	-117	-433	-356	-331
162	-253	-259	-238	-177	-154	-121	-185	-198	-190	25	-19	-29
256	291	280	304	206	199	191	263	253	272	319	315	337
257	40	26	42	-4	-9	14	34	20	37	12	-4	39
258	1	-6	2	-10	-14	-5	0	-7	2	-7	-18	2
259	274	282	228	190	197	174	249	256	207	289	303	235
260	76	77	86	31	32	31	68	68	77	72	70	89
262	97	79	86	69	66	55	89	73	79	85	85	65
266	51	75	21	57	56	39	60	83	25	139	167	75
267	274	334	359	254	279	318	345	399	423	1296	1300	1237
275	-812	-934	-870	-543	-577	-563	-832	-935	-881	-1822	-1842	-1755
282	-174	-110	-182	-122	-120	-153	-164	-114	-170	-236	-242	-247
286	-120	-103	-77	-127	-109	-100	-111	-96	-71	-148	-133	-78

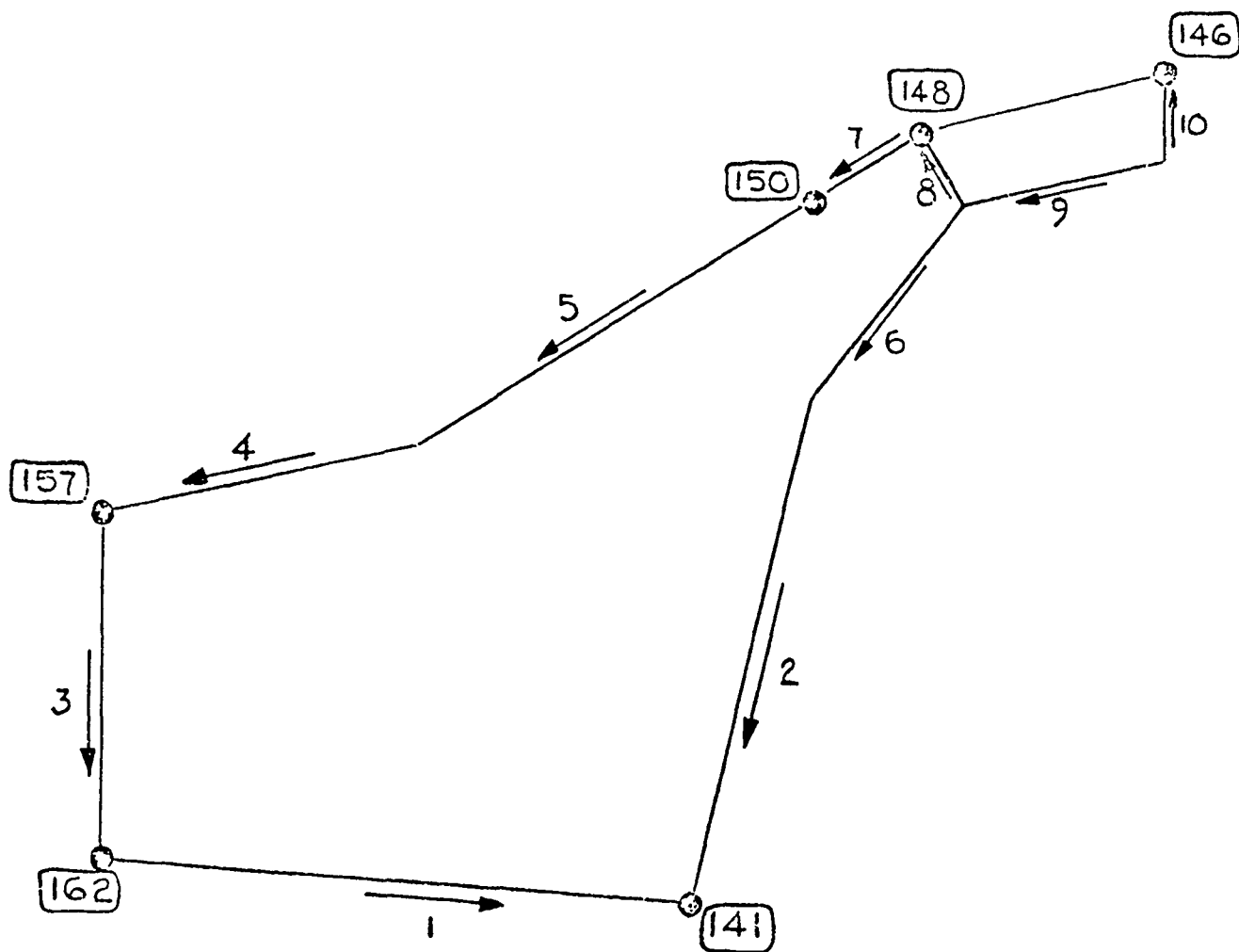


Figure 2-28 FORWARD SIMULATED FUSELAGE SHEAR FLOW AND LONGERON LOCATION DIAGRAM - Y_F891-932

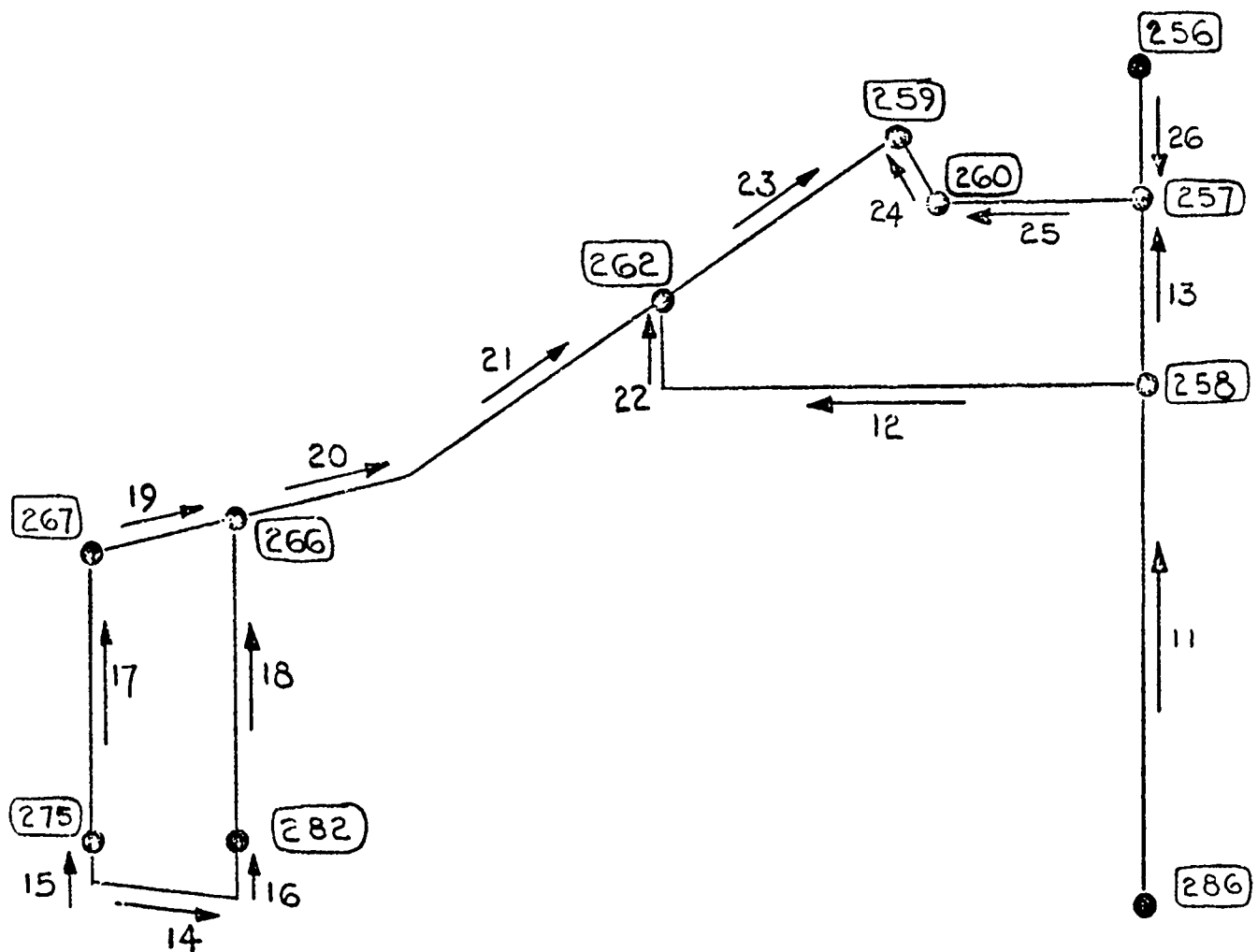


Figure 2-29 AFT SIMULATED FUSELAGE SHEAR FLOW AND LONGERON LOCATION DIAGRAM YF992-1021

2.3 FATIGUE AND FRACTURE ANALYSIS

Fatigue and fracture analyses were conducted to substantiate the ability of the FSIL and the NBB designs to meet the fatigue and fracture requirements specified for the baseline aircraft. The fatigue loads spectrum, the fatigue requirements, and the fracture mechanics design requirements are summarized in report AFFDL-TR-73-1.

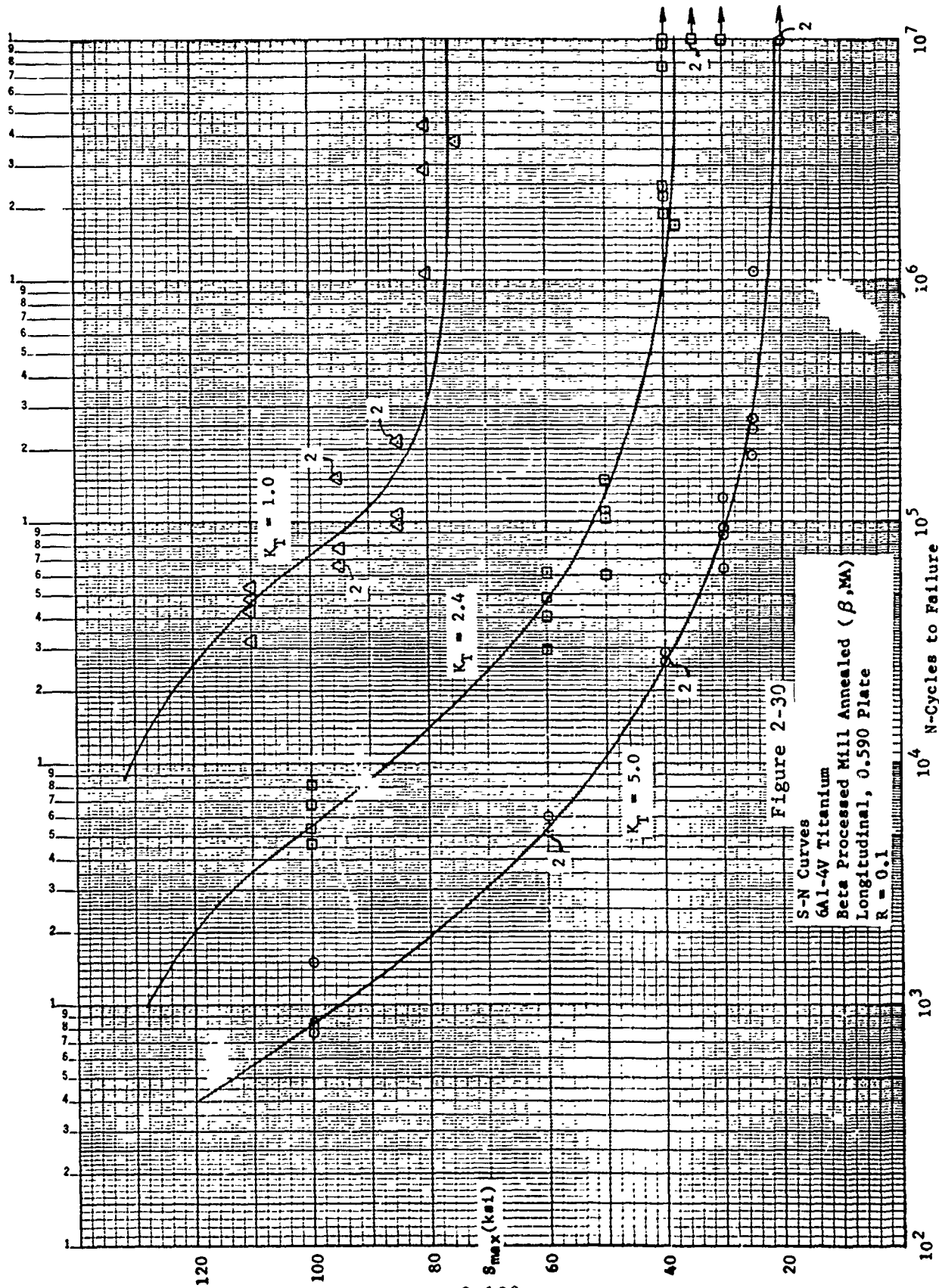
2.3.1 Fatigue Analysis

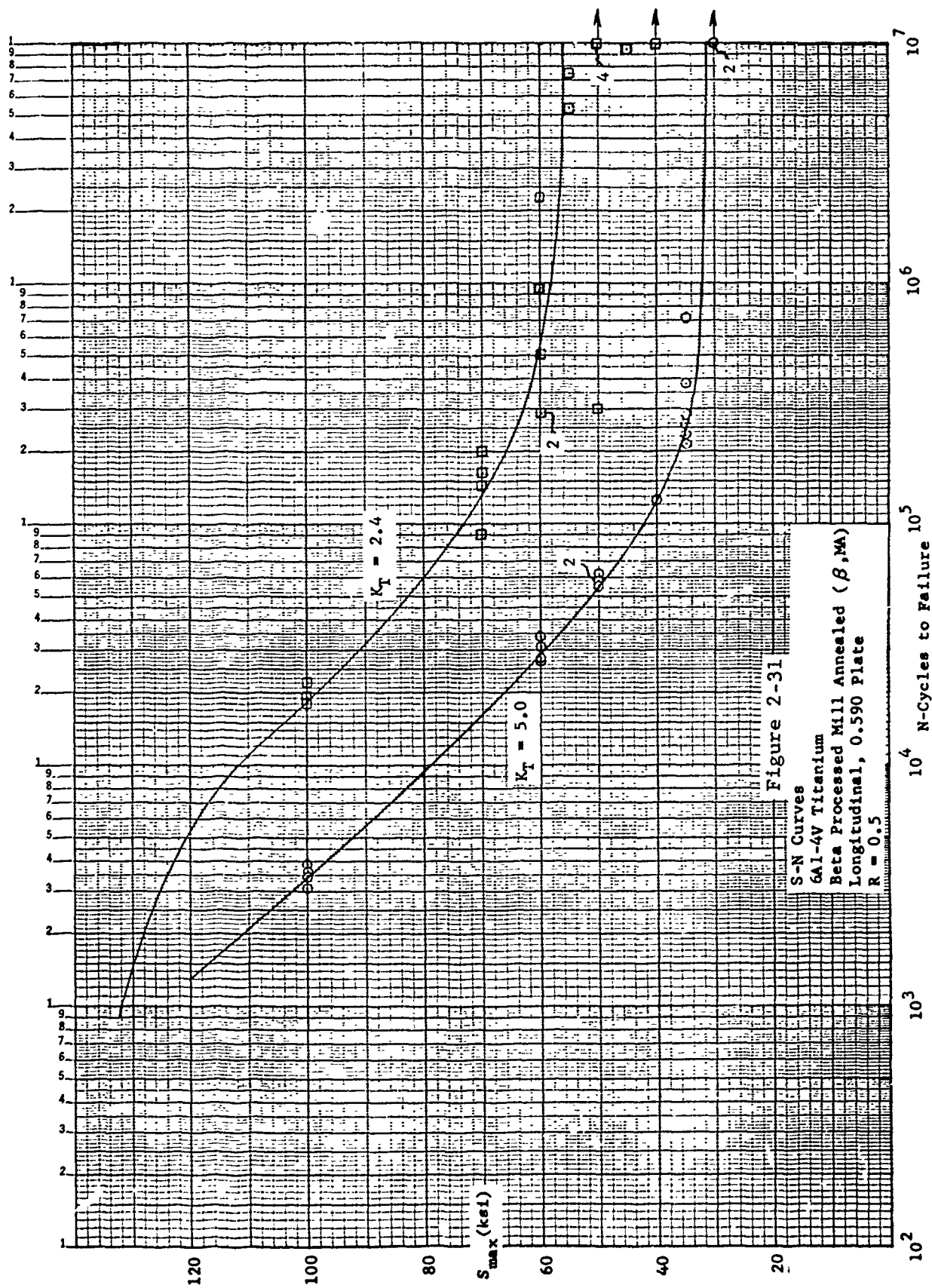
Fatigue allowables were determined for both WCTS designs using the results of the stress analysis, the fatigue loads spectrum, and fatigue S/N test data. The fatigue analysis method is based on Miner's theory of cumulative damage. Fatigue allowables are based on net section effective (Von Mises yield criterion) stresses.

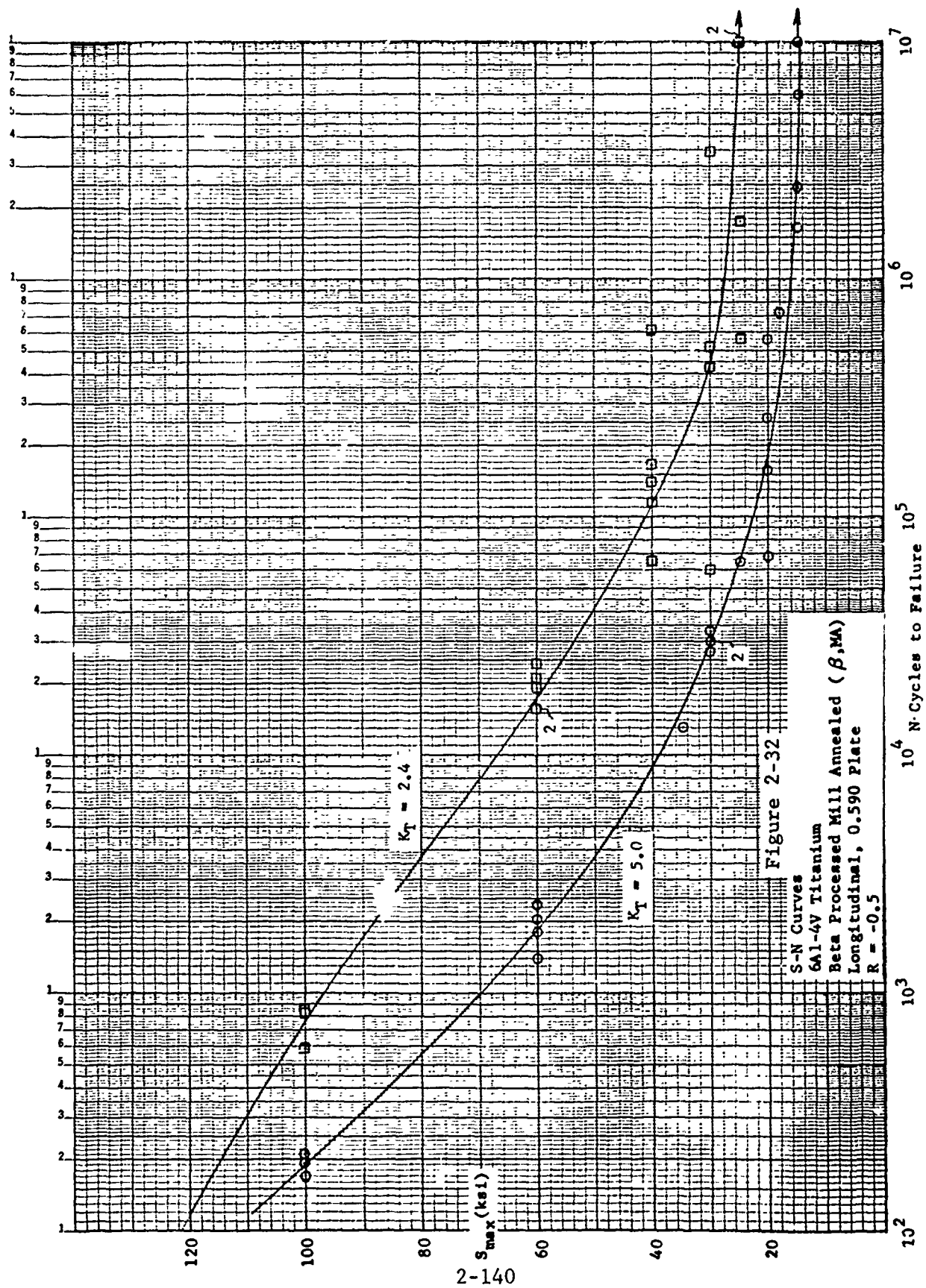
2.3.1.1 Fatigue Test Data - Basic Materials

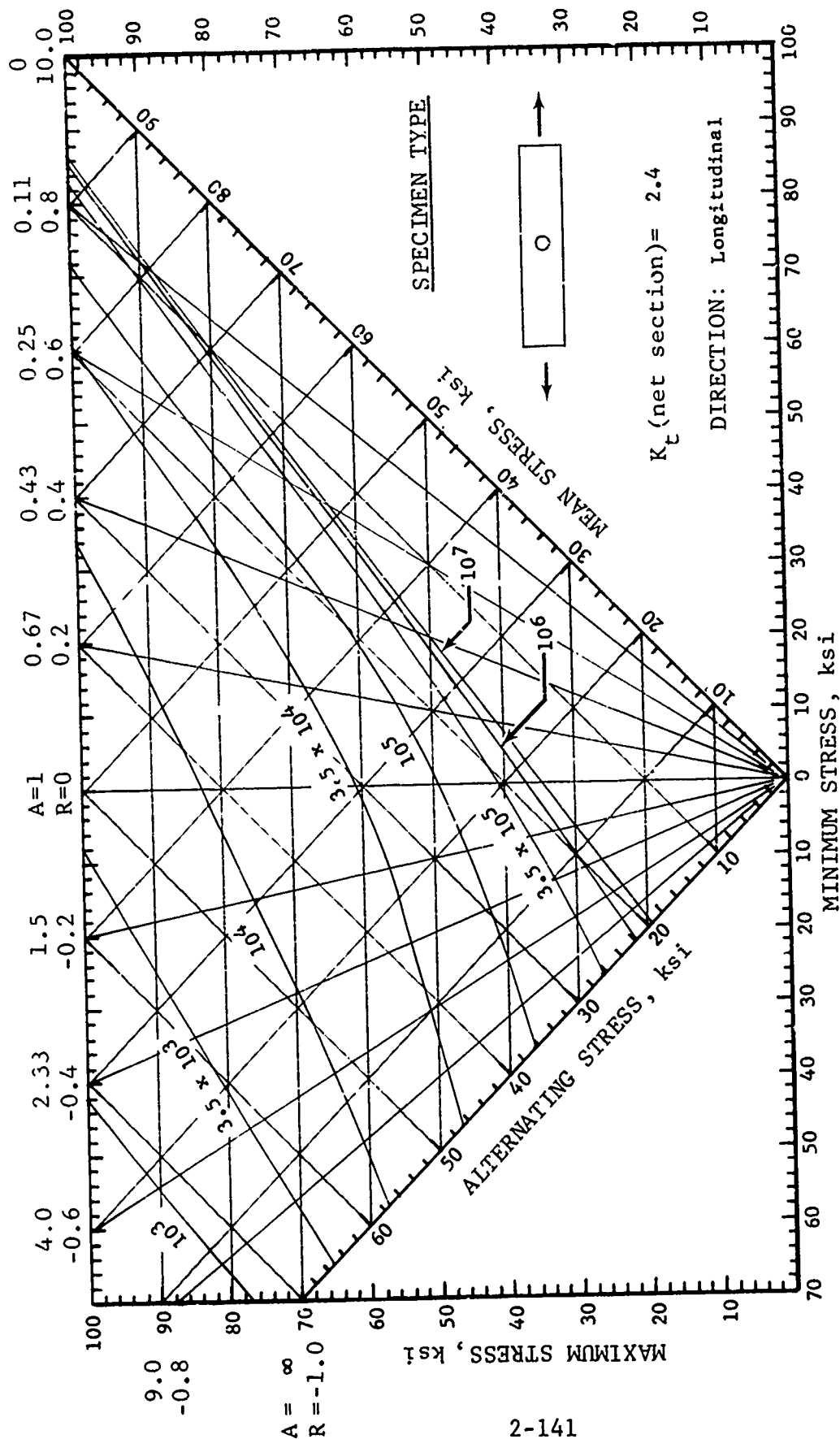
Conventional S/N fatigue tests were conducted on beta annealed 6Al-4V titanium plate, 10 Nickel steel plate, and Beta C titanium sheet. Flat specimens of three configurations were used: smooth ($K_T = 1$), center hole ($K_T = 2.4$), and edge notched ($K_T = 5.0$). Tests were conducted at three R ratios: $R = 0.1$, 0.5 , and -0.5 . Twenty specimen S/N curves were developed for K_T of 2.4 and 5.0 at each R ratio and for $K_T = 1$ at $R = 0.1$. Material was oriented in the longitudinal grain direction. Fatigue properties in the longtransverse direction were spot checked by testing 5 LT specimens at each of two stress levels for $K_T = 2.4$, $R = 0.1$, and $K_T = 5.0$, $R = 0.1$.

The fatigue test data were reduced to a form suitable for computer input by constructing constant life fatigue diagrams for $K_T = 2.4$ and 5.0 . Subsequently, these diagrams were used to construct a family of fatigue curves: alternating stress, S_A , vs cycles to failure, N , for a series of mean stress levels, S_M . The results are summarized in Figures 2-30 thru 2-49 as follows:









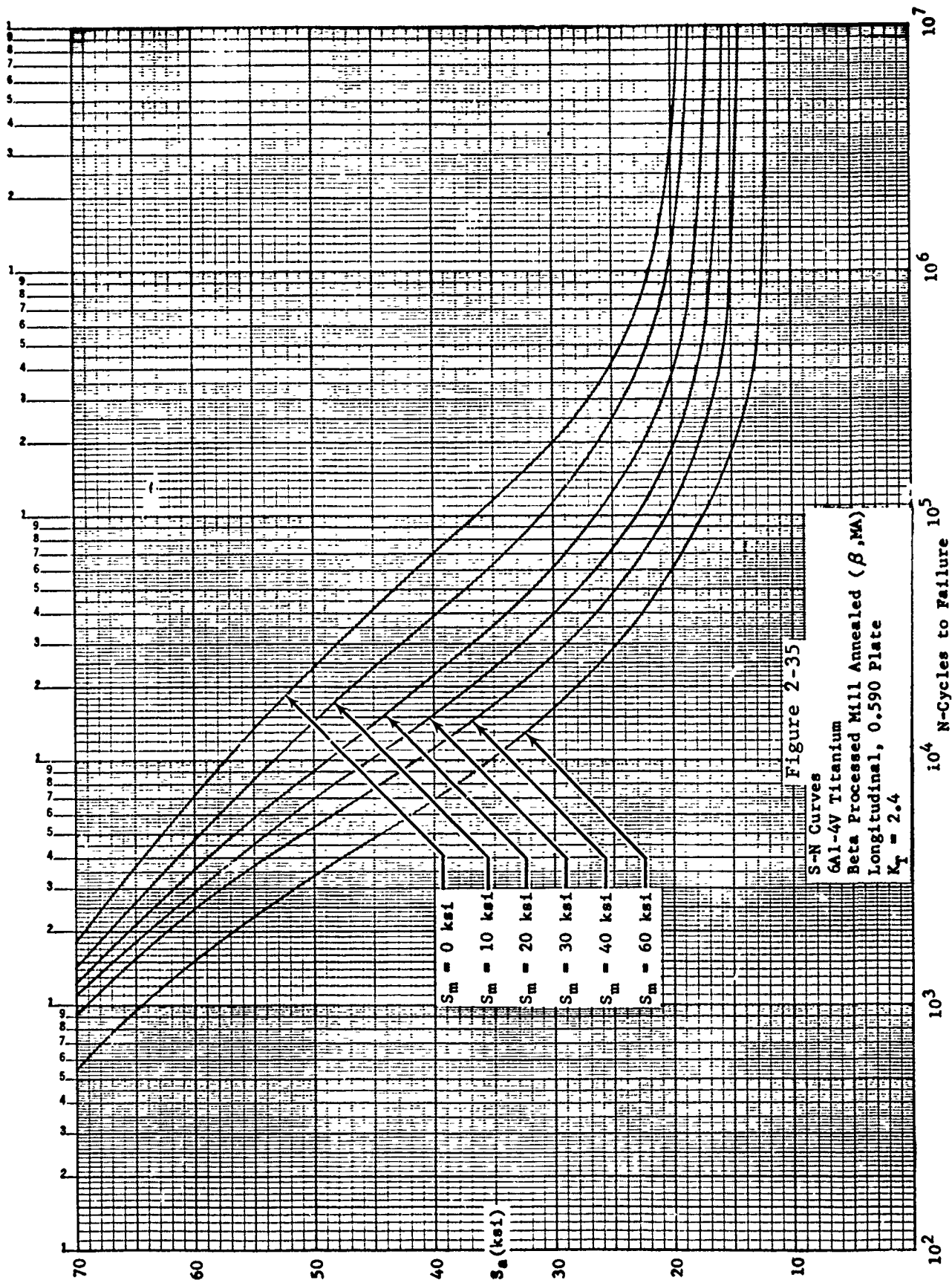
MATERIAL: 6Al-4V Ti $F_{tu} = 130$ $F_{ty} = 116$
 Beta Process Mill Anneal (β , MA)
 FORM: 0.590 Plate $F_{ntu} = 133$ % EL = 9

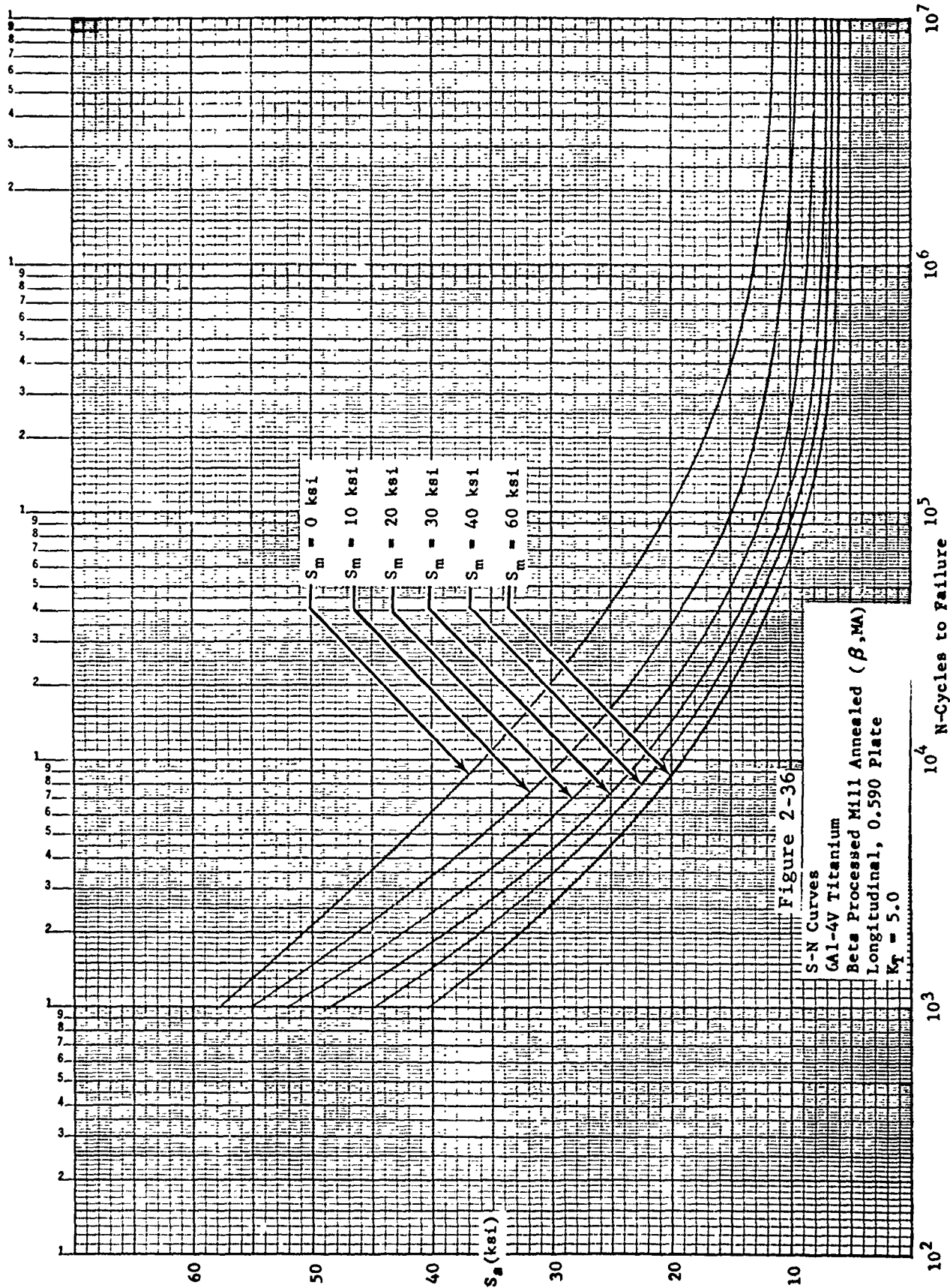
TEST CONDITIONS

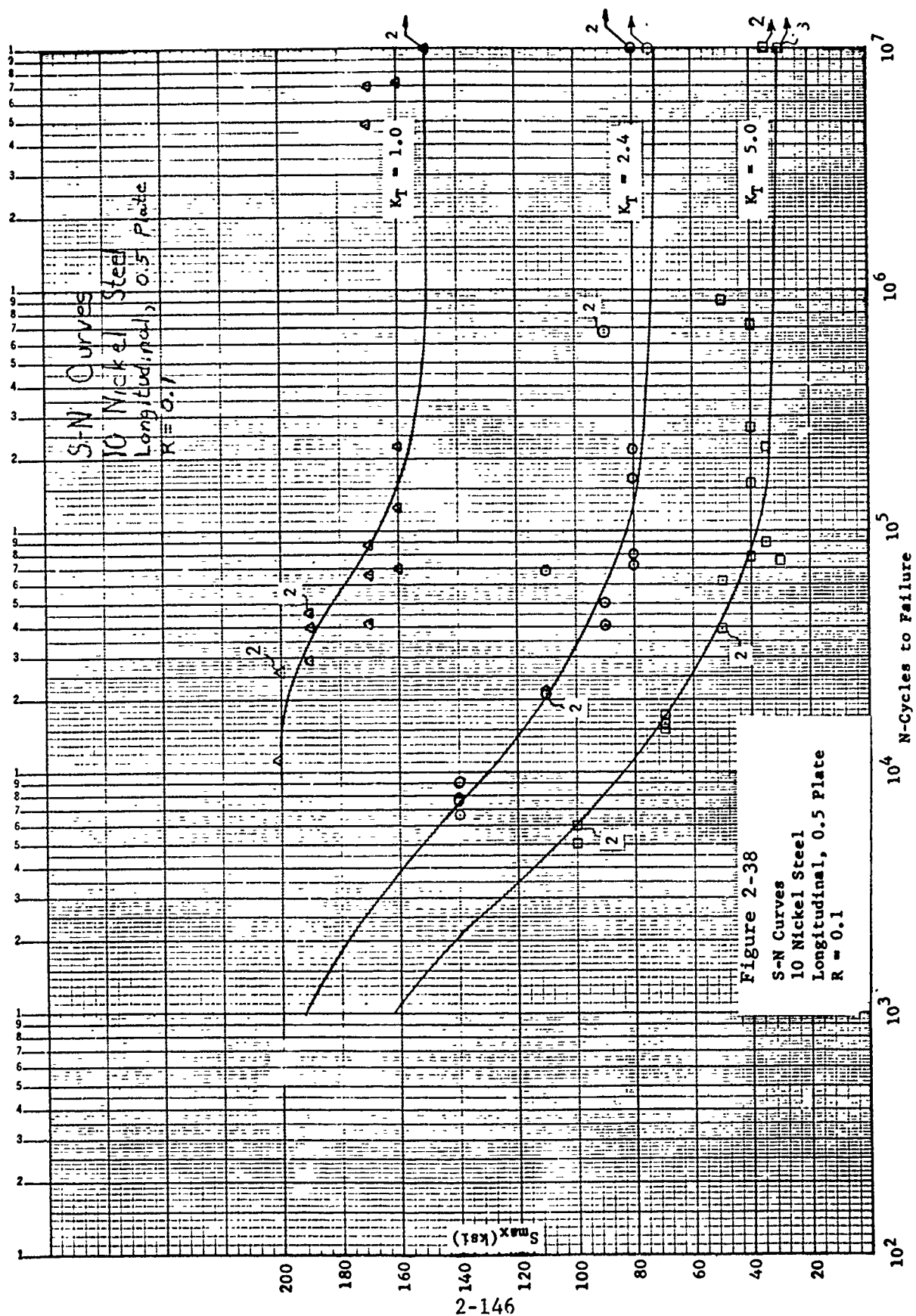
CYCLIC RATE: 1800 cpm
 TEMPERATURE: Room

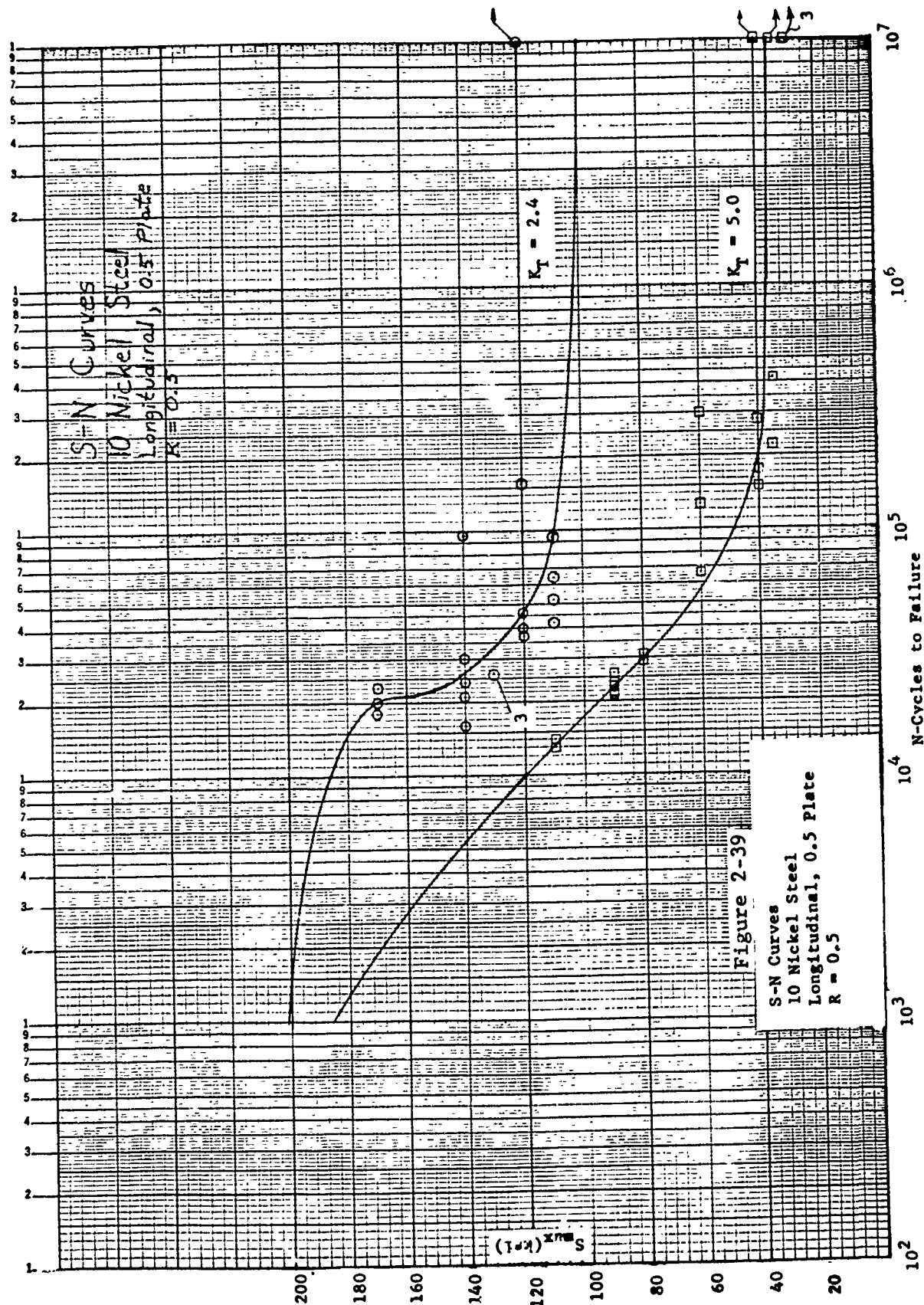
Date: October 1973

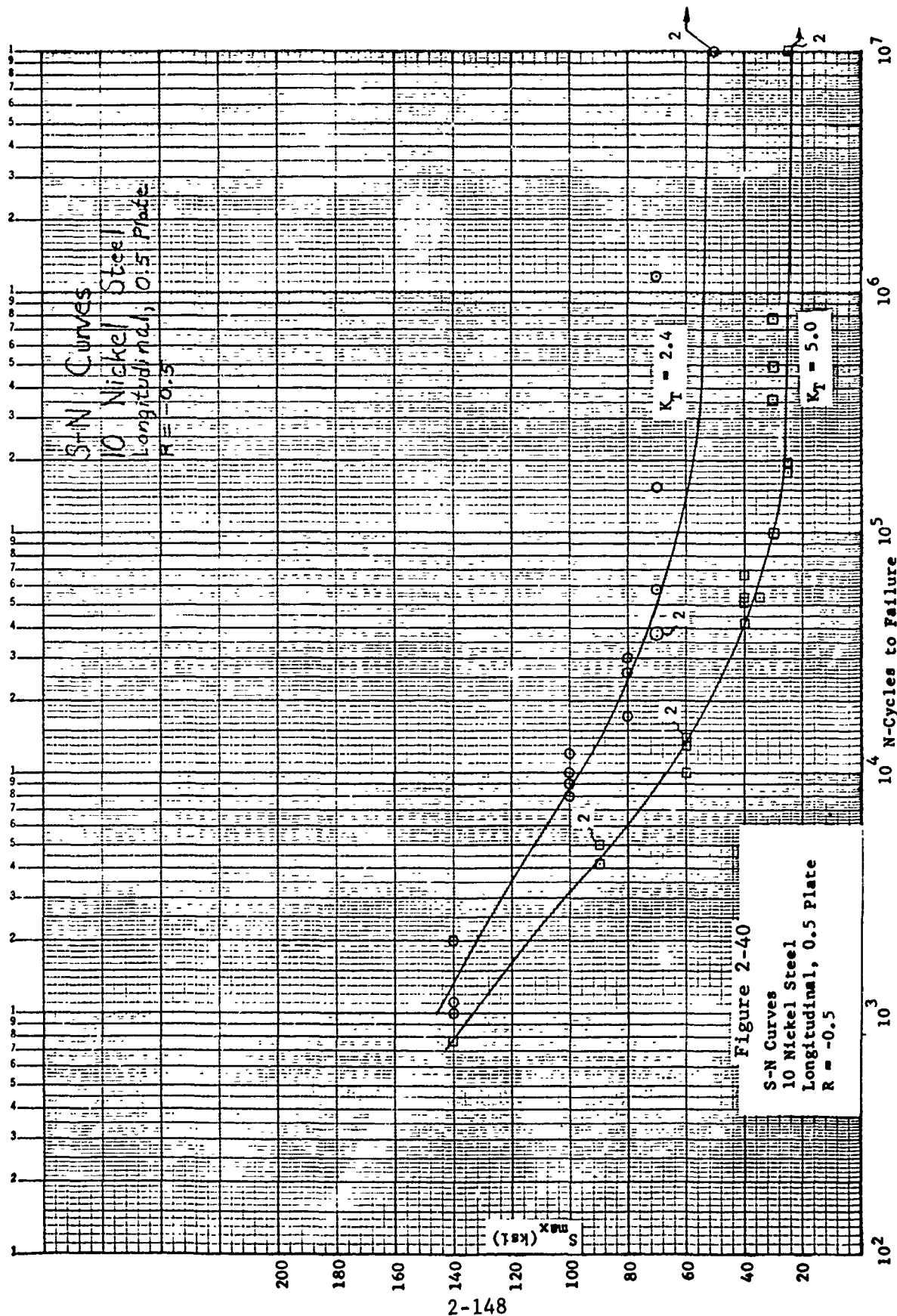
DATA SOURCE: AMAVS
 Figure 2-33 CONSTANT LIFE FATIGUE DIAGRAM FOR BETA ANNEALED
 6Al-4V TITANIUM $K_T = 2.4$

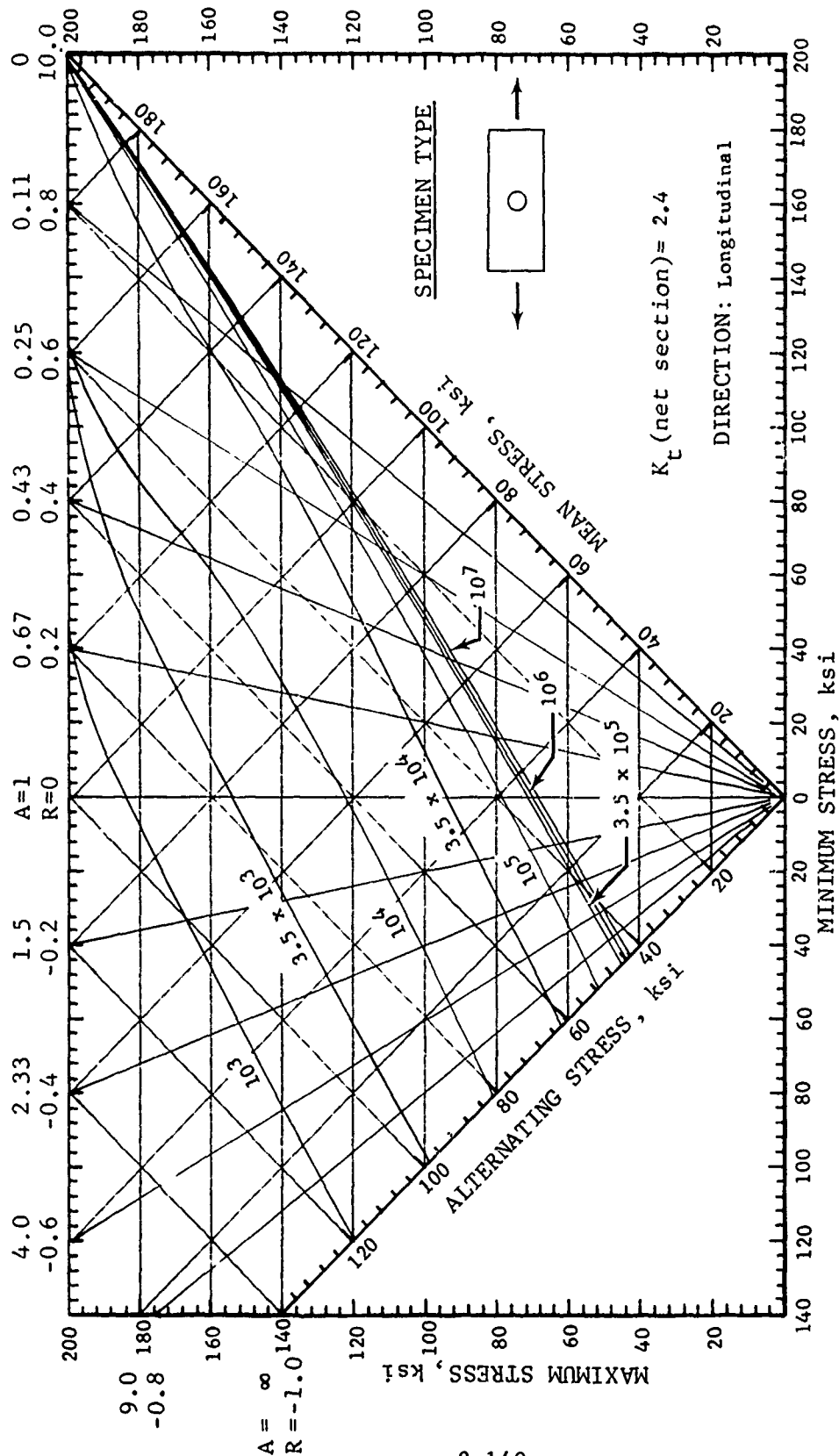












TEST CONDITIONS

CYCLIC RATE: 1800 cpm
TEMPERATURE: Room

MATERIAL: 10 Ni Steel $F_{tu} = 197$ $F_{ty} = 183$
FORM: 0.5 Plate $F_{ntu} = 202$ % El. = 16

DATA SOURCE: AMAVS

Date: October 1973

Figure 2-41 CONSTANT LIFE FATIGUE DIAGRAM FOR 10 NI STEEL, $K_T = 2.4$

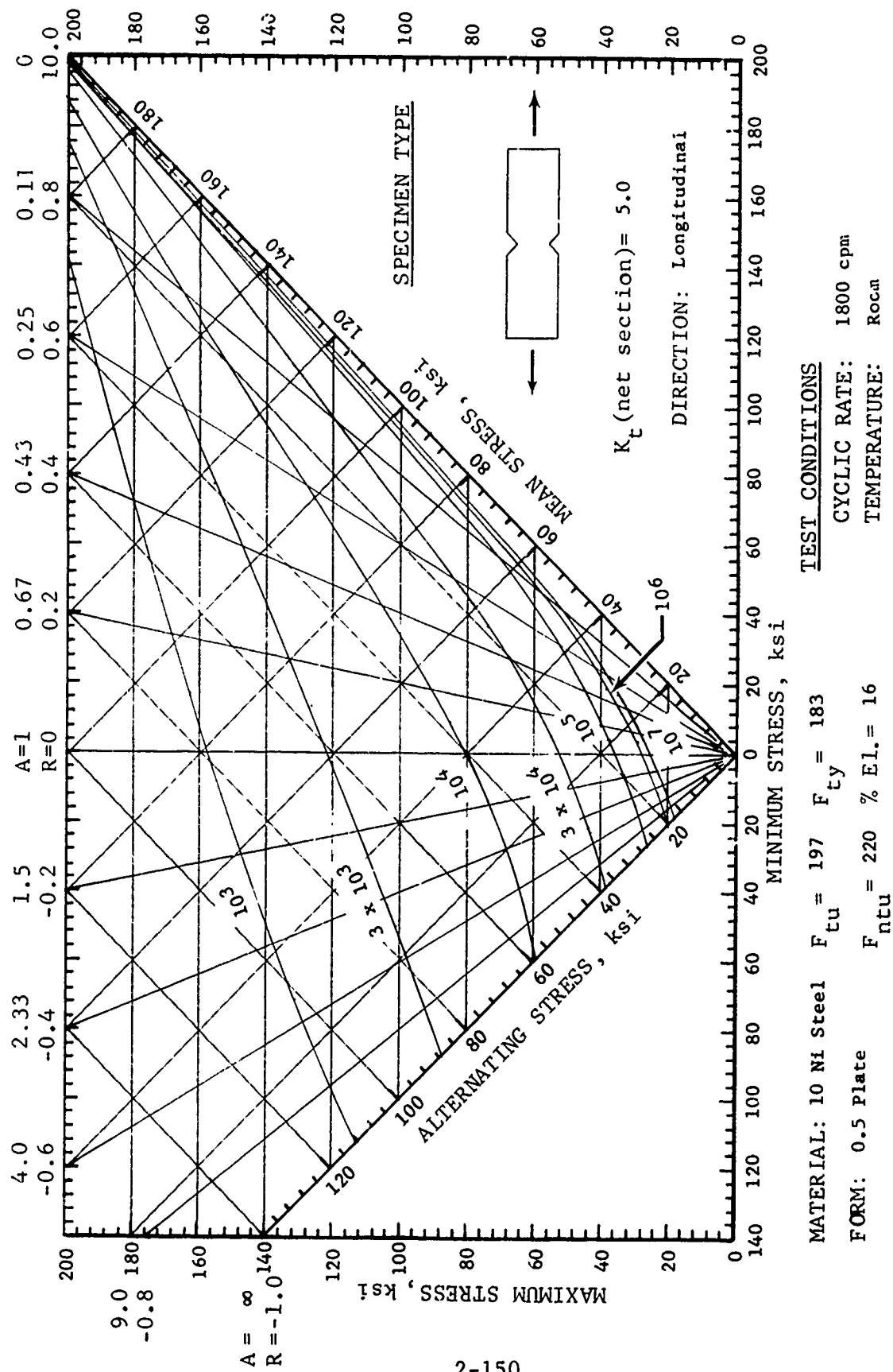
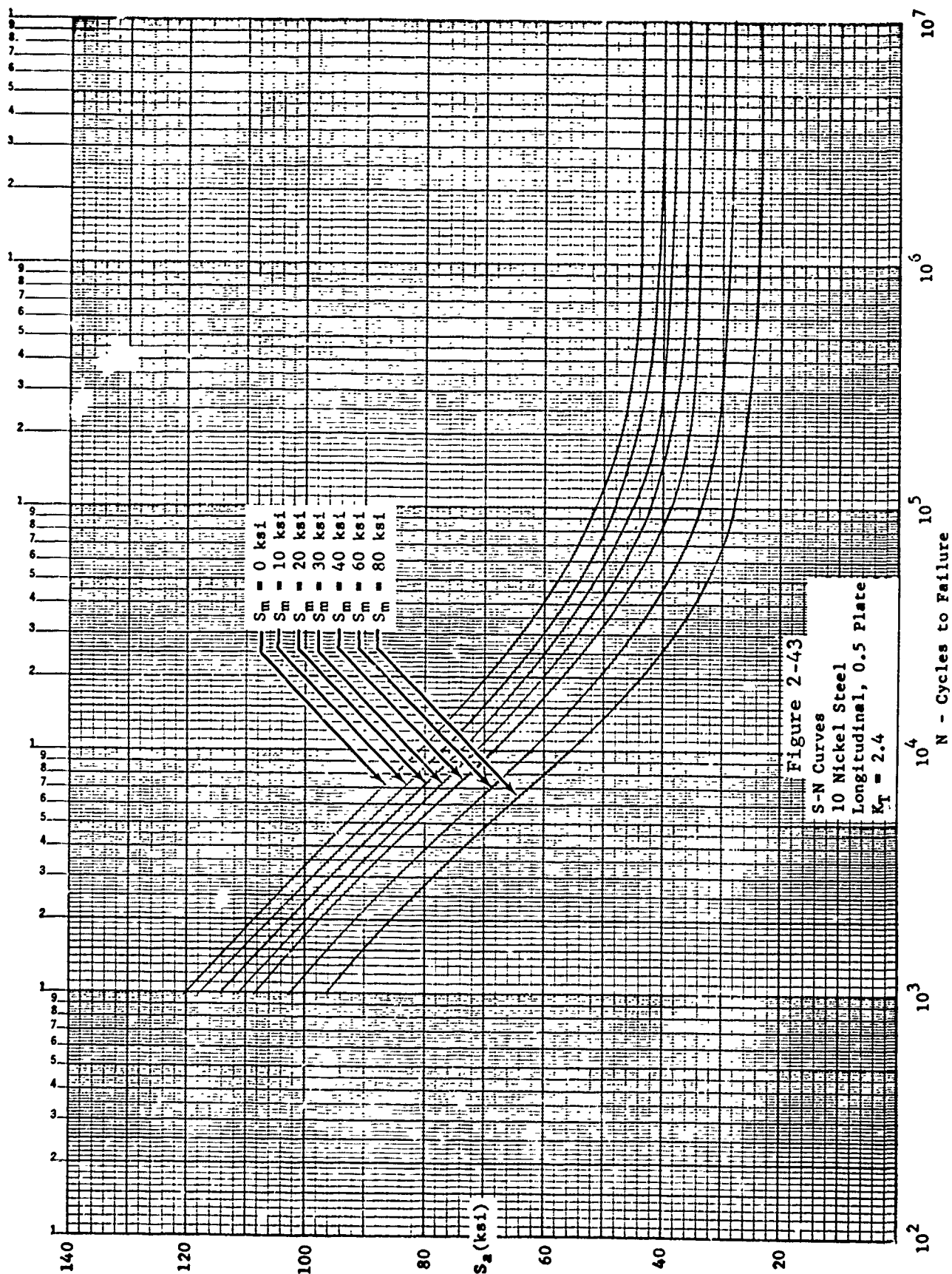
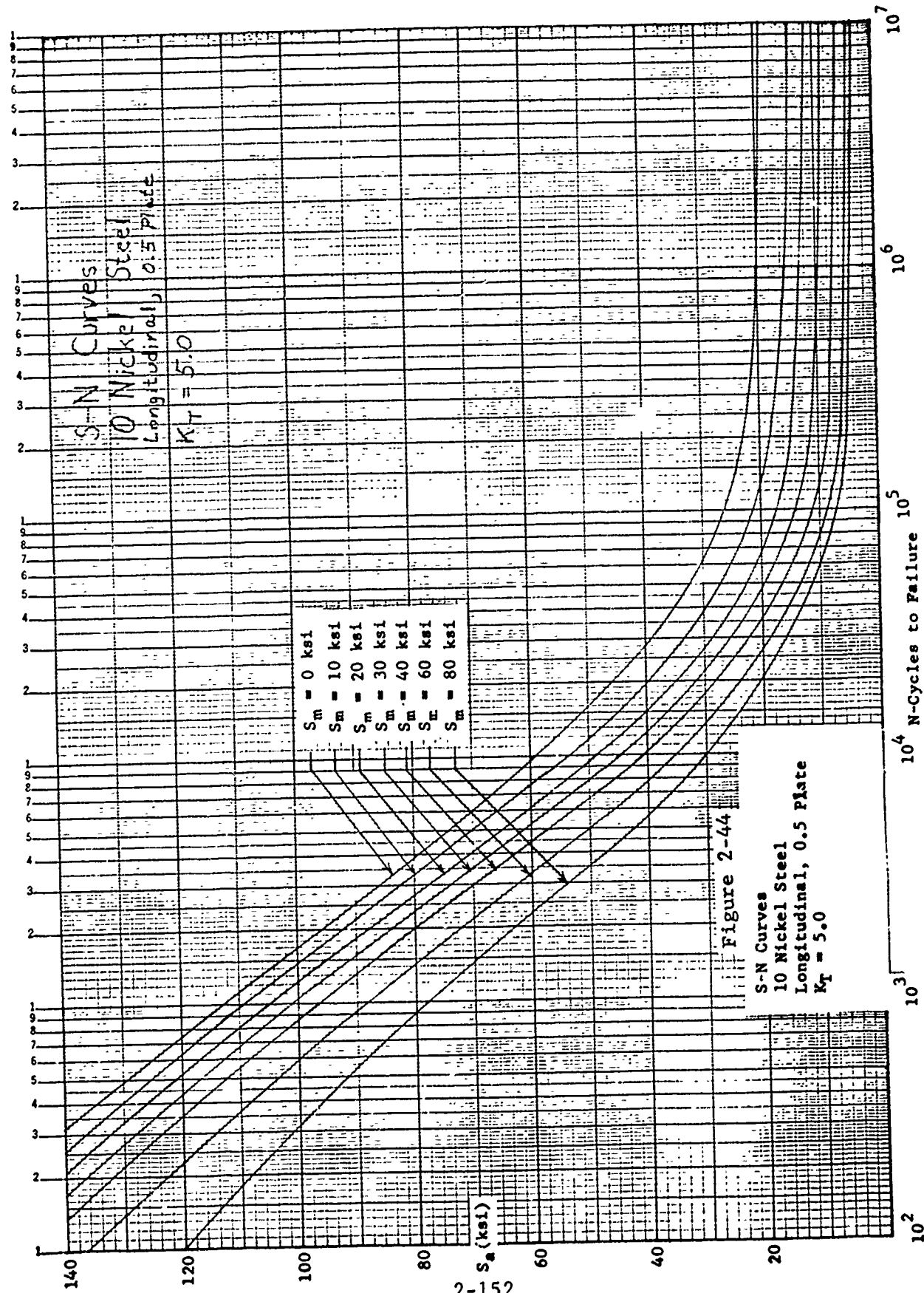
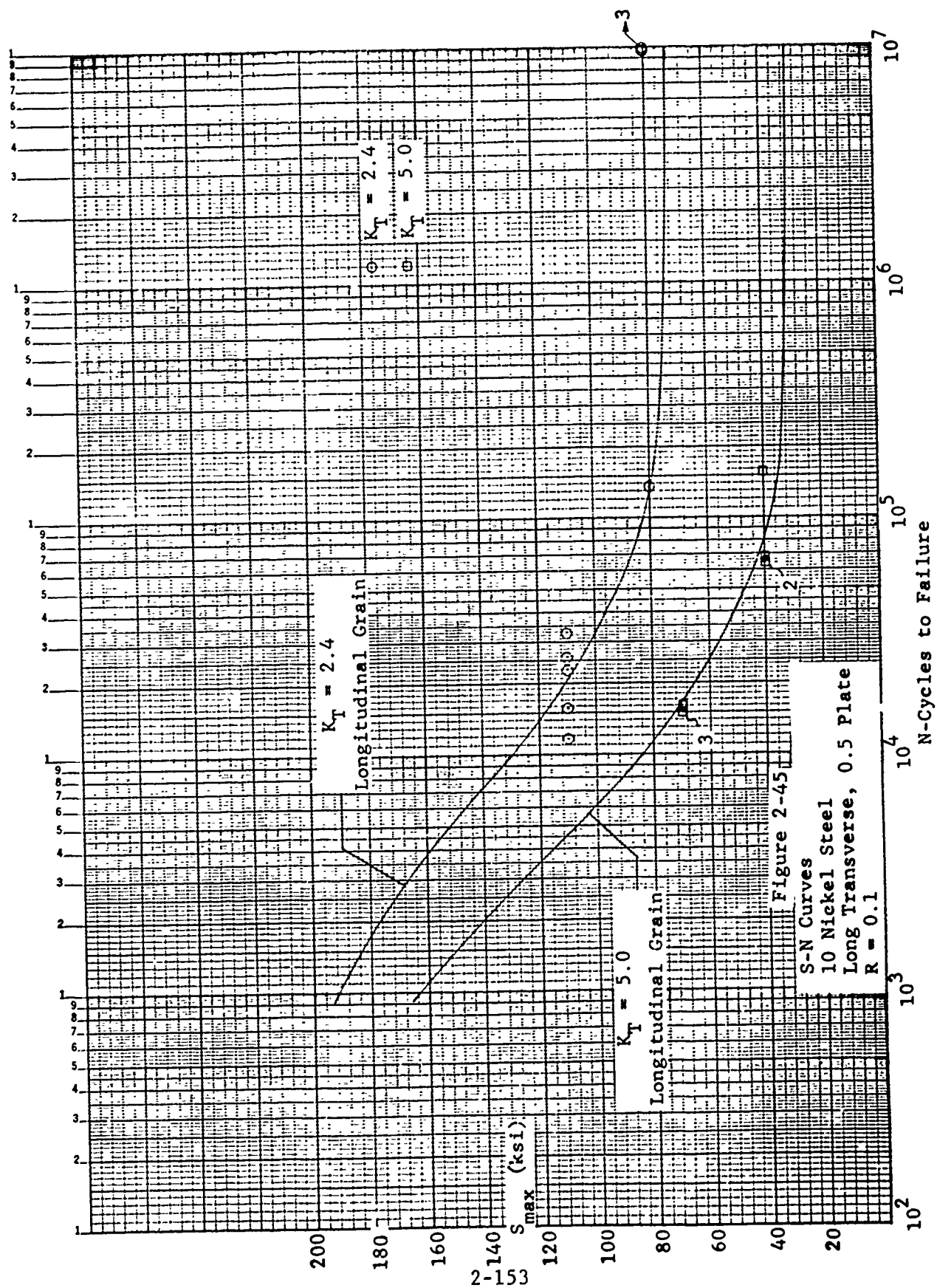
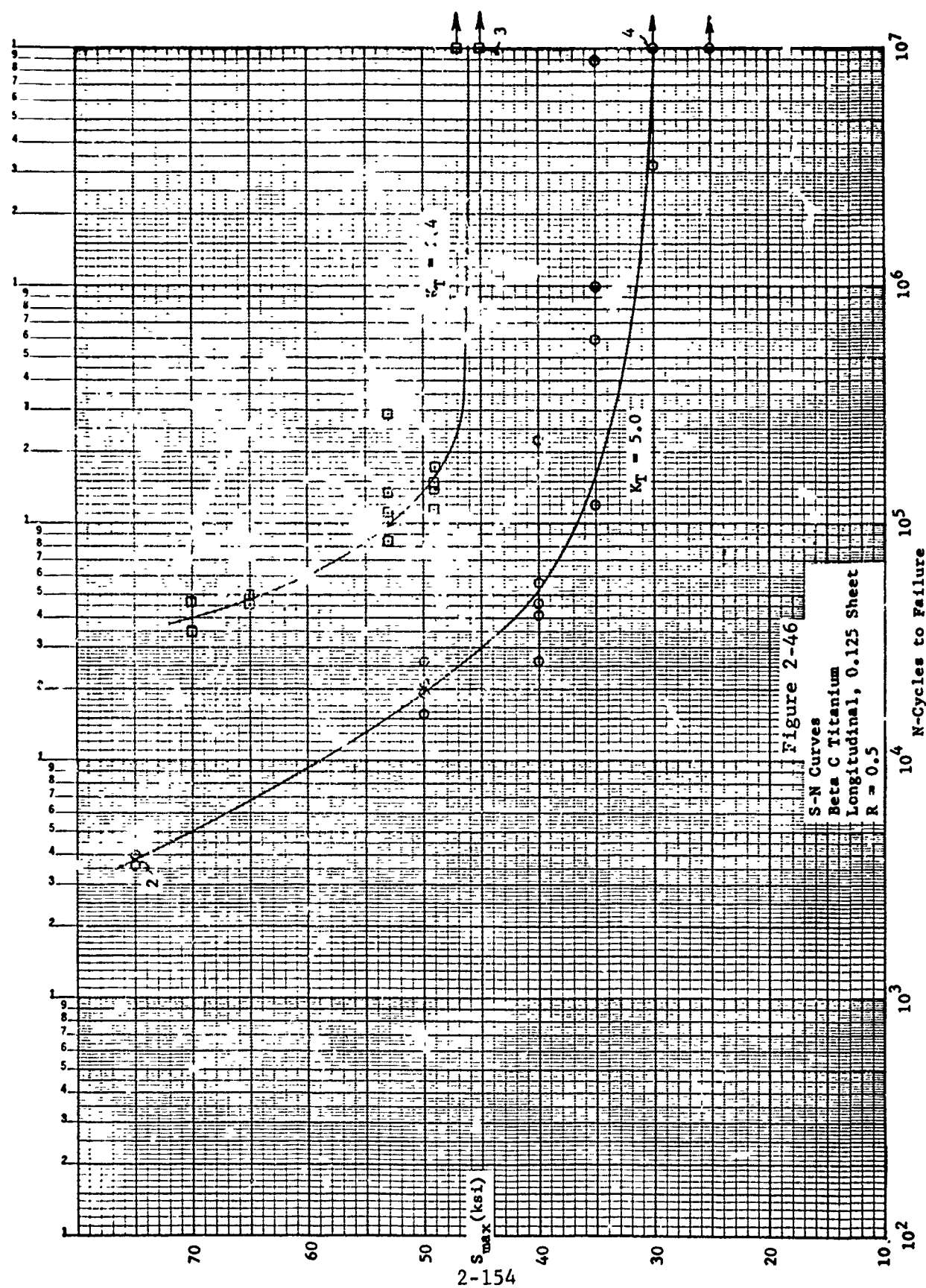


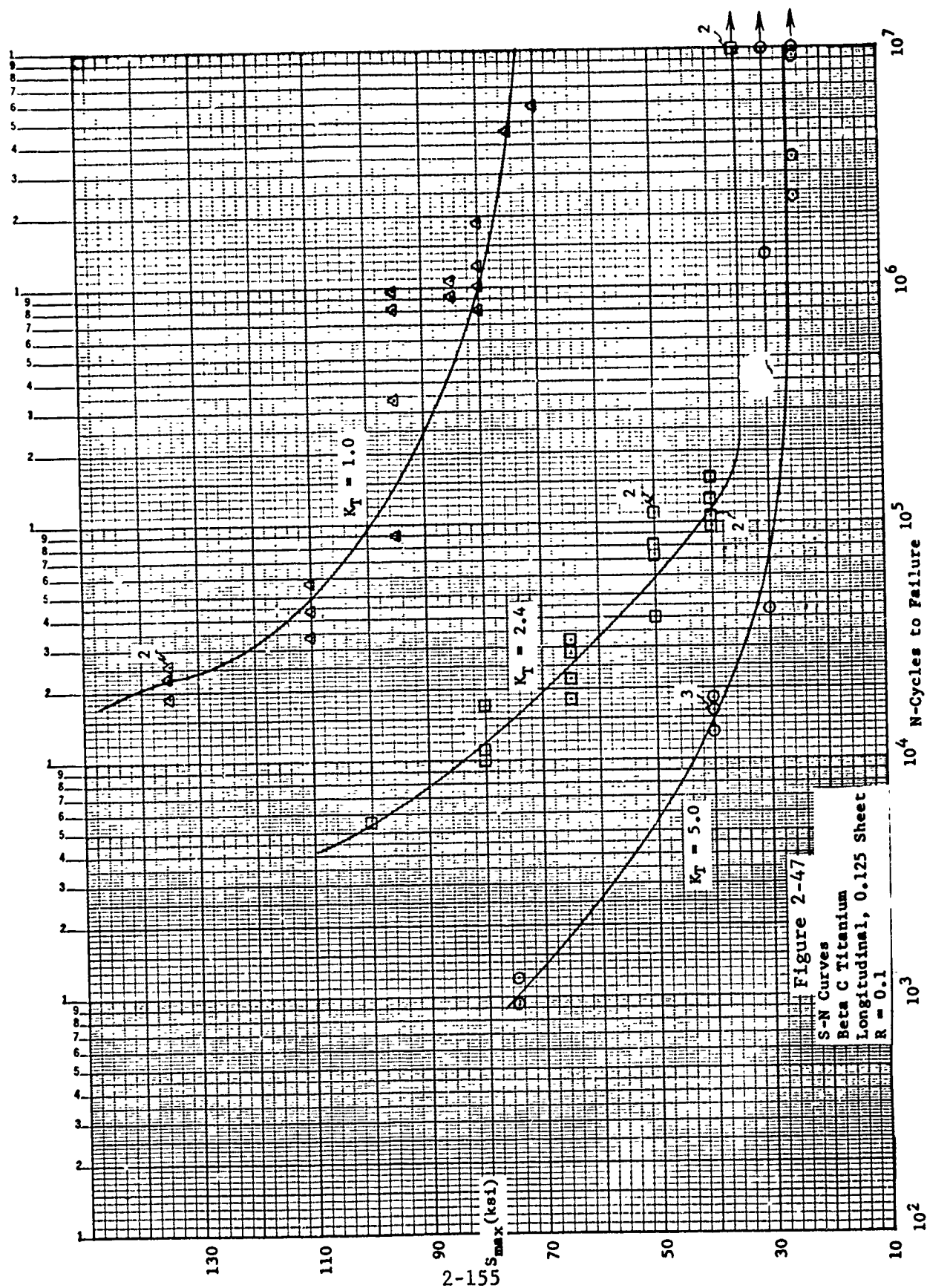
Figure 2-42 CONSTANT LIFE FATIGUE DIAGRAM FOR 10 NI STEEL, $K_T = 5$
 Date: October 1973

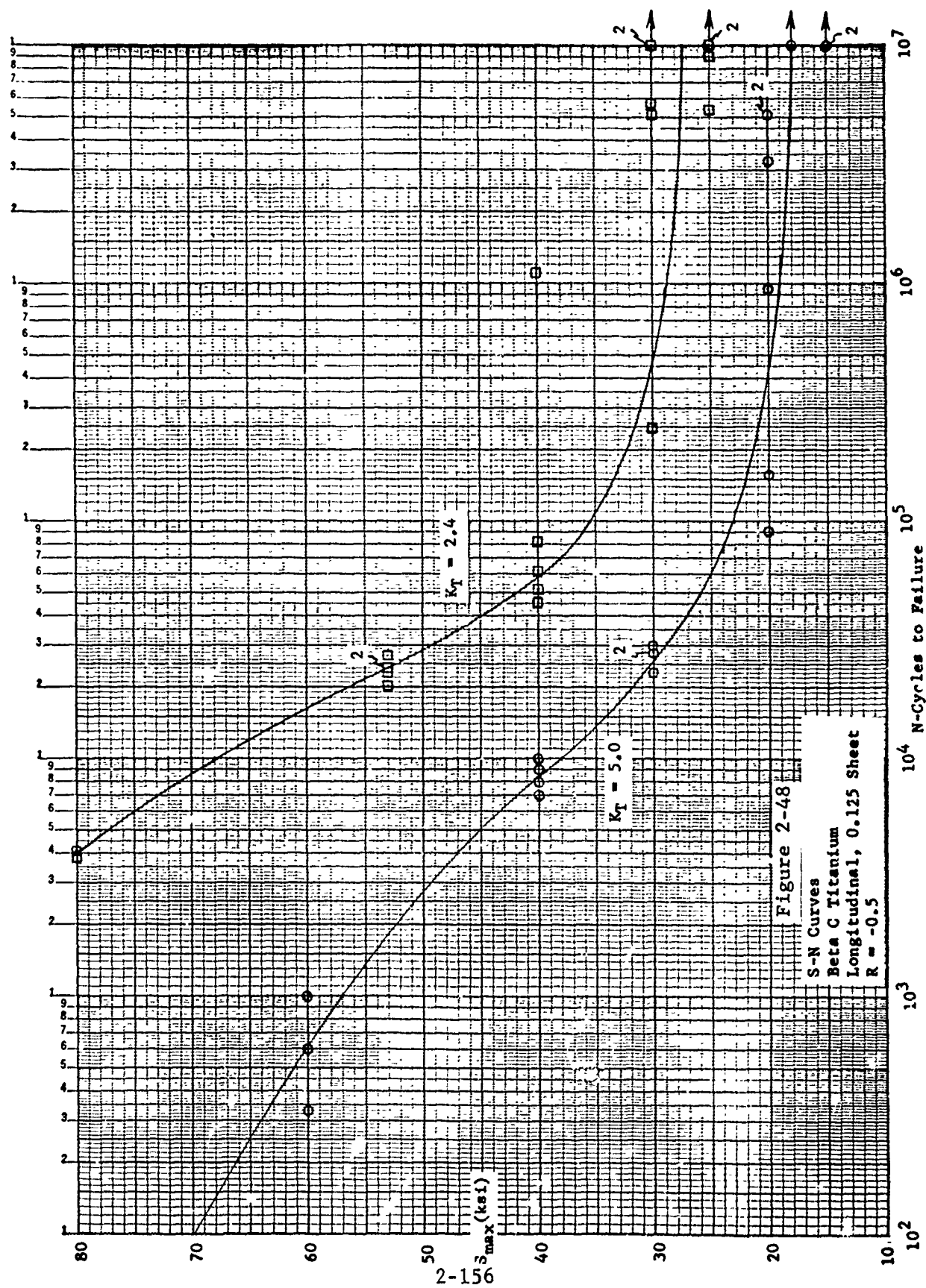


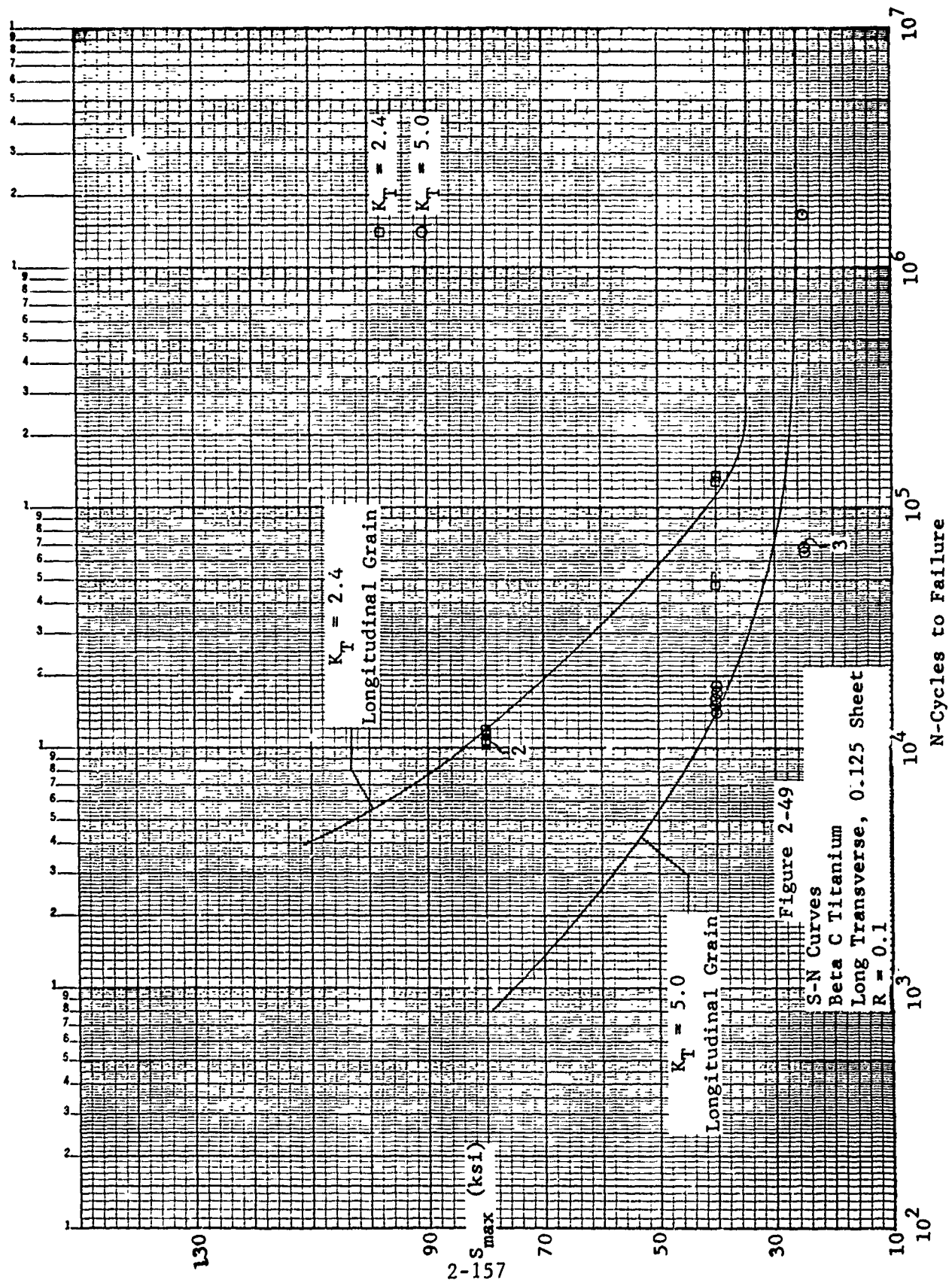












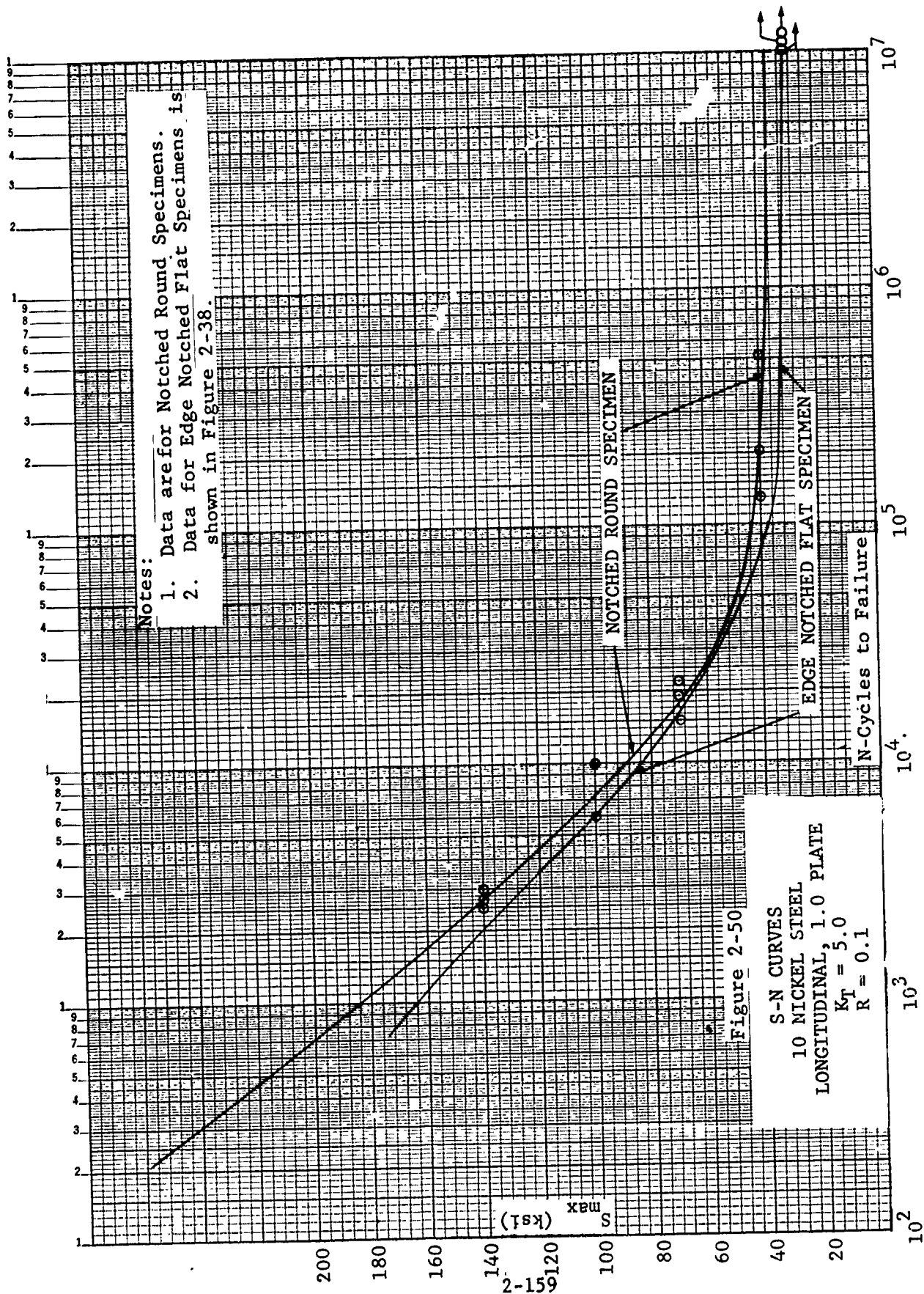
Material	Type	Figures
Ti 6Al-4V (β ,MA)	S/N Data	2-30, 2-31, 2-32
"	Constant Life Diagrams	2-33, 2-34
"	S_A vs N Curves	2-35, 2-36
"	Long Transverse Data	2-37
10 Ni Steel	S/N Data	2-38, 2-39, 2-40
"	Constant Life Diagrams	2-41, 2-42
"	S_A vs N Curves	2-43, 2-44
"	Long Transverse Data	2-45
Beta C	S/N Data	2-46, 2-47, 2-48
"	Long Transverse Data	2-49

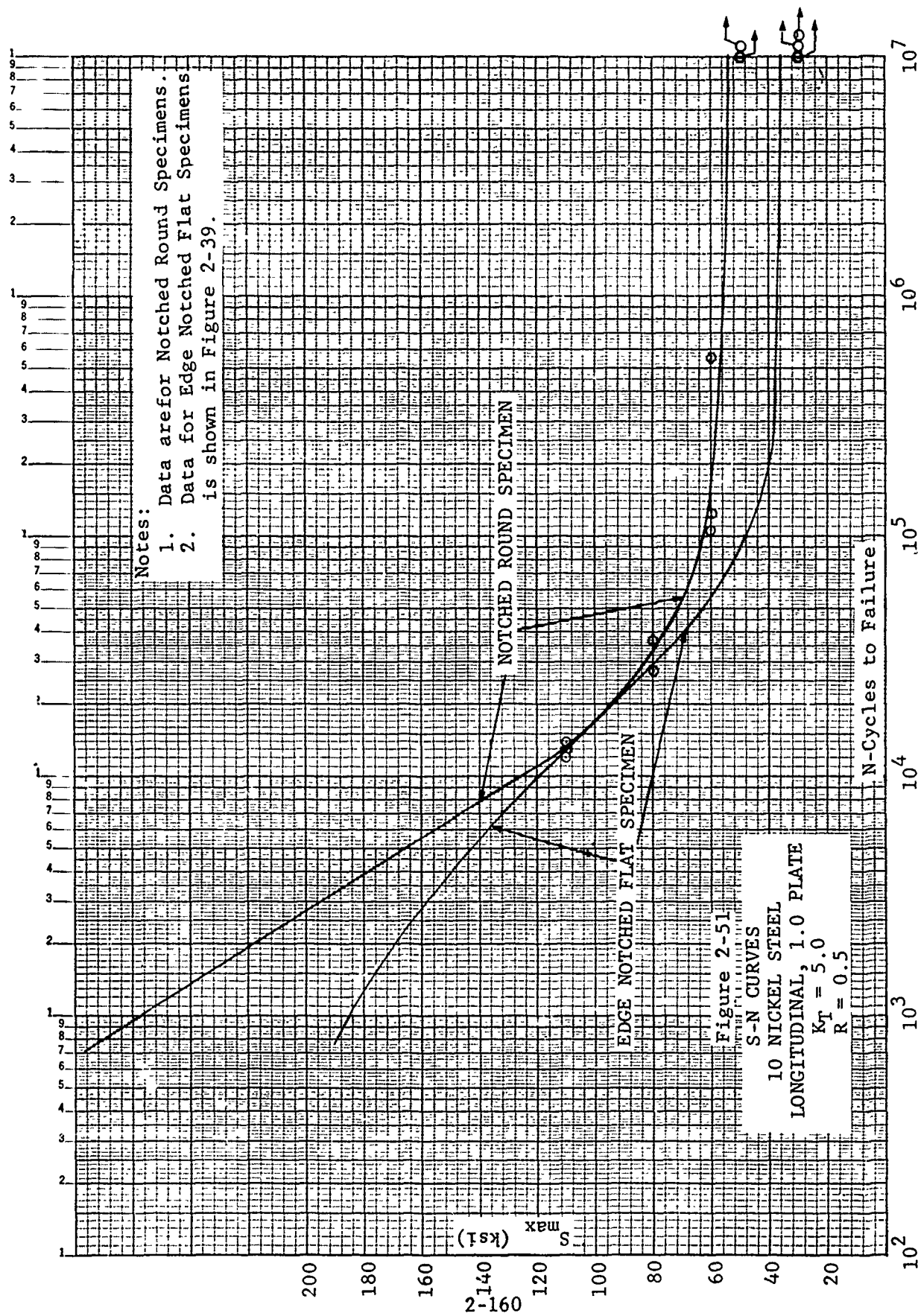
The 10 Ni steel fatigue data at $K_T = 5.0$ were significantly lower than expected. Tests on round notched specimens with $K_T = 5$ were conducted to determine if the edge notched specimens were more severe at a given K_T level than the round notch specimens commonly used. As shown in Figures 2-50, 51, and 52, the test data from round and flat specimens are essentially the same at $R = -0.5$ and $R = 0.1$; however, at $R = 0.5$ the endurance limit of the round specimens is 55 KSI vs 35 KSI for the flat specimens.

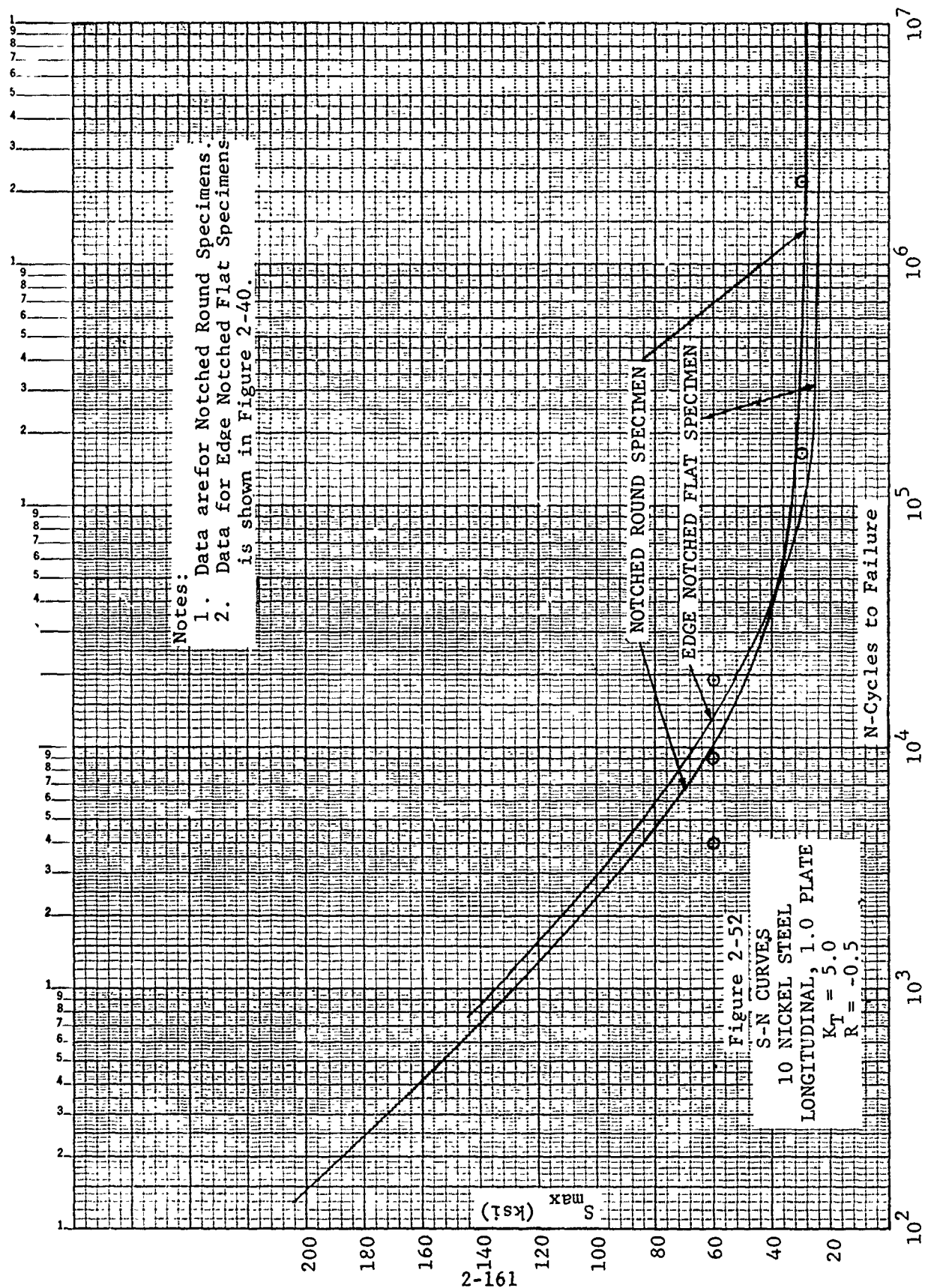
2.3.1.2 Fatigue Test Data - Weldments

Fatigue tests were conducted on EB welds in beta annealed 6Al-4V titanium (1/2, 1 and 2 in. thick) and GTA welds in 10 Nickel steel plate (.625 in. thick). Flat specimens with $K_T = 1$ were tested at $R = 0.1$ and $R = 0.5$ (10 Ni only). The weld line was located normal to the applied load in the center of the test section.

The fatigue test data were compared with data obtained for the base metal. Comparison plots are shown in Figure 2-53 for EB welded titanium and in Figure 2-54 for GTA welded steel. Notice that in both cases welding does impair the $K_T = 1$ fatigue resistance, but the welded specimens have better fatigue lives than the open hole specimens.







• EB WELDED Ti6Al-4V (β , MA)

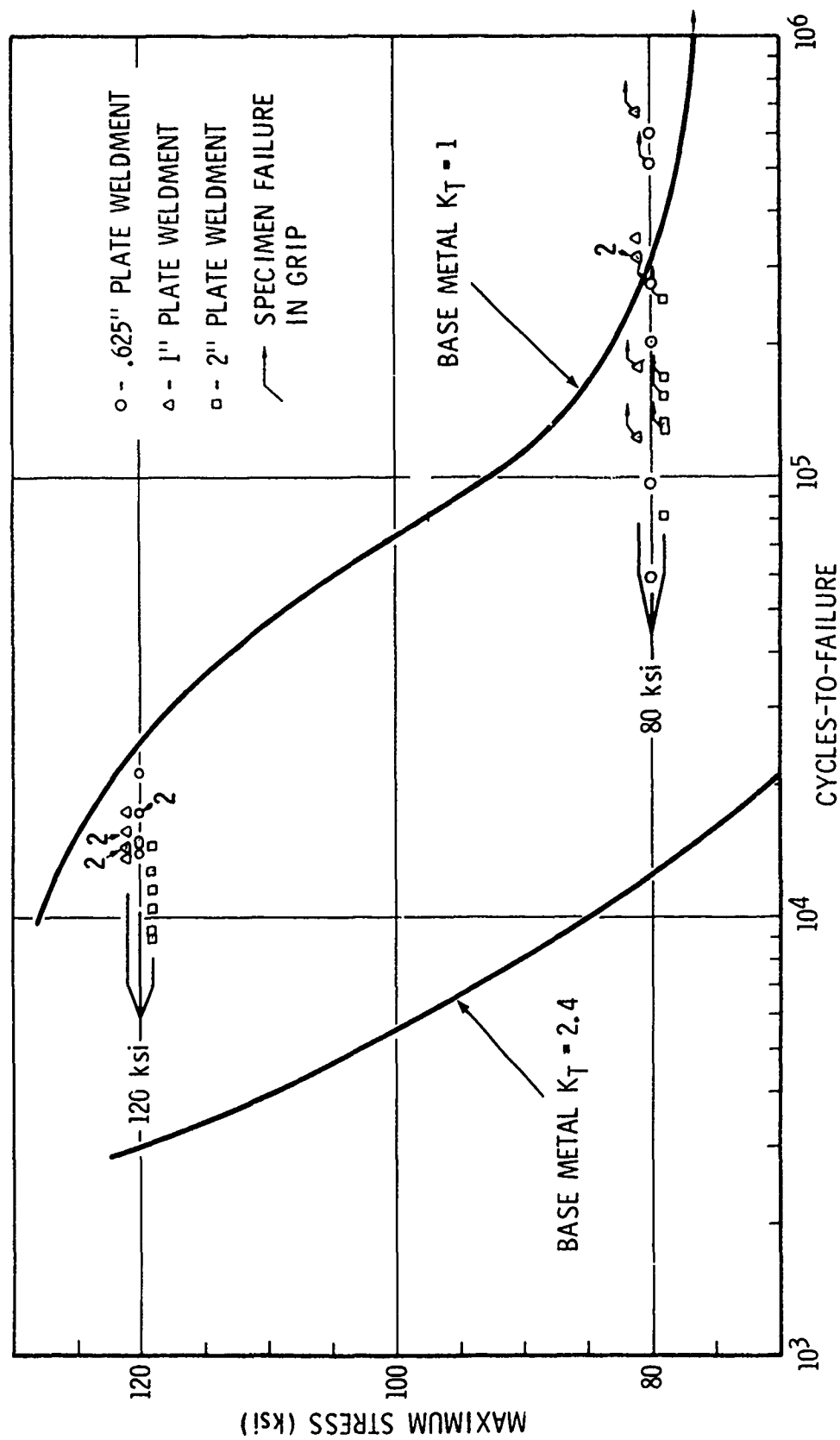
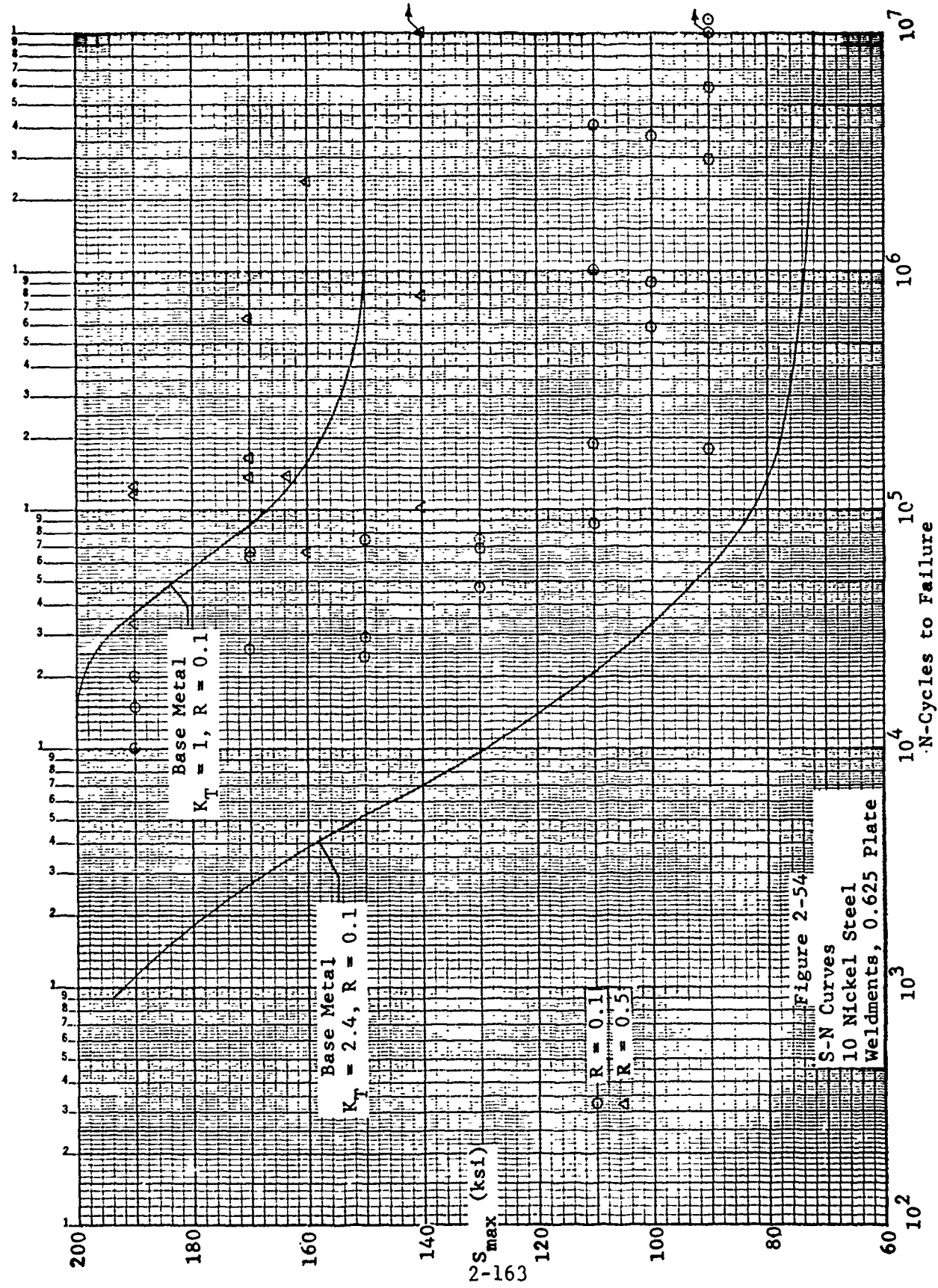


Figure 2-53 FATIGUE DATA SUMMARY



2.3.1.3 Fatigue Allowables

Fatigue allowables were determined for beta annealed 6Al-4V titanium and 10 Ni steel subjected to seven representative stress spectra. The spectra represent parts of the WCTS which are critical in forward sweep (spectra 1, 3 and 6), 25° sweep (spectrum 2), aft sweep (spectra 5 and 7), and ground (spectrum 4) conditions. The results for $K_T = 2.4$ and 5.0 are summarized in Table II-24. Notice that at $K_T = 2.4$ both materials can be worked to their static strength. Based on the $K_T = 2.4$ results, the fatigue allowable for these materials at all locations where $K_T \leq 2$ were set equal to the static strength of the material. The fatigue allowables at $K_T = 5$ ranged from 55 to 70% of F_{tu} for both materials. The $K_T = 5$ allowables were used for lugs, splices, and open holes. Whenever the stresses exceeded the $K_T = 5$ allowable, Taper-lok fasteners were required. Allowables for structural areas where holes with Taper-lok fasteners are the principal stress concentration points were intermediate between the $K_T = 2.4$ and $K_T = 5$ values: 100 KSI for beta annealed 6Al-4V titanium and 150 KSI for 10 Nickel steel. Aluminum allowables were established using the preliminary design allowables methodology discussed in AFFDL-TR-73-40 for the specific alloys of interest, 2024-T851 and 7050-T7351.

Fatigue allowables for the lugs were based on sizing procedures successfully applied during the F-111 program. The net section stress is determined using the maximum applied load and the minimum cross-sectional area. The maximum allowable net section stress was determined from fatigue analysis using $K_T = 5$ S/N data and a lug stress spectrum. The lug stress spectrum was developed assuming that the minimum lug cross-section receives the highest stress in each of the flight configurations, i.e., at different wing sweeps the critical location remains the same. It was further assumed that the limit stresses for each flight condition in the fatigue spectrum (ASKA 2, 10, 5, 9) were equal and the minimum applied stress was equal to zero. Using these procedures, the lug stress allowables were 77 KSI for FSIL and 131 KSI for the NBB.

Fatigue allowables for welded joints were based on the design requirement that all welds be located remote from stress concentrations. A factor of .85 on F_{tu} was used for the weld joint allowable. This is considered conservative because all weld fatigue test data were superior to the open-hole data. Fatigue analysis based on open-hole ($K_T = 2.4$) data indicates that both materials can be worked to 100% F_{tu} .

Fatigue allowables used in final design are summarized in Table II-25 (FSIL) and Table II-26 (NBB).

Table II-24 FATIGUE ALLOWABLES FOR SEVEN SPECTRA
REPRESENTATIVE OF FSIL AND NBB LOWER COVERS

SPECTRUM NO.	RELATIVE STRESS				TI6AL-4V(β_1 MA)		10 NI STEEL	
	ASKA* 10	ASKA 2&5	ASKA 9	ASKA 7	$K_T=2.4$ KSI	$K_T=5$ KSI	$K_T=2.4$ KSI	$K_T=5$ KSI
1	.45	1.0	.73	0	130	81	190	115
2	.58	.88	1.0	-.34	↑	82	↑	110
3	.76	1.0	.84	-.20		84		123
4	.68	1.0	.83	-.56		75		113
5	1.0	.78	.81	-.06		87		120
6	.81	1.0	.90	-.13		81		112
7	1.0	.86	.66	-.14	130	85	190	112

Table II-25 FATIGUE ALLOWABLES FOR FAIL SAFE
INTEGRAL LUG CONFIGURATION

<u>Material</u>	<u>Part</u>	<u>Allowable</u>
Ti 6Al-4V (β_1 MA)	Lower Lug	77 KSI (Net Section Stress)
	Centerline Splice	80 KSI
	All Welds	106 KSI
	Other Tension Members ($K_T \geq 2$)	100 KSI
	Upper Out'bd Longerons Splice	90 KSI
	Other Structure	Static Design
7050	All Tension Member ($K_T > 2$)	45 KSI
2024	Other Parts	Static Design

Table II-26 FATIGUE ALLOWABLES FOR THE
NO-BOX CONFIGURATION

<u>Material</u>	<u>Part</u>	<u>Allowable</u>
10 Ni Steel ↓	Lower Lug	131 KSI (Net Section Stress)
	All Welds	166 KSI
	Upper Out'bd Longeron Splice	130 KSI
	Other tension members $K_T > 2$	150
	Other structure	Static Design
7050 2024 ↓	All tension members $K_T > 2$	45 KSI
	Other Parts	Static design
Ti 6Al-4V (β , MA) ↓	Splices @ $X_F 39, Z_F 0$	87 KSI
	Splices @ $X_F 84, Z_F 0$	77 KSI
	Other Tension Members ($K_T > 2$)	100 KSI
	Other Structure	Static Design

2.3.2 Fatigue Crack Growth Test Data

The crack growth analysis is based on data for the two materials of principal interest: beta annealed 6Al-4V titanium and 10 Ni steel. Constant amplitude tests were conducted in dry air at 360 cpm and in sump tank water at 6 and 60 cpm. Spectrum tests were conducted using tensile panels with either surface flaws in open structure or quarter circle cracks extending from one edge of a hole. Specimens were tested using four distinct spectra representing two control points and two truncation levels.

2.3.2.1 Constant Amplitude Tests

Constant amplitude fatigue crack growth tests were conducted on beta annealed 6Al-4V titanium plate, 10 Nickel steel plate, and Beta C titanium sheet. The test data for beta annealed 6Al-4V titanium plate were presented in AFFDL-TR-73-77. For 10 Ni steel, 10 of 13 crack growth curves were presented in the same report. The other three tests are shown along with the curves of the equations used in the crack growth analysis in Figure 2-55. Notice that the analysis lines are conservative interpretations of the test data, particularly at growth rates below 2×10^{-6} inch per cycle where the cracks grow slower in sump tank water than in dry air. The test data for Beta C titanium are presented in Figures 2-56, 57, and 58; a single Forman equation fits all of the test data for both dry air and sump tank water:

$$\frac{da}{dN} = \frac{2.3 \times 10^{-7} \Delta K^{2.63}}{(1-R) 70 - \Delta K}$$

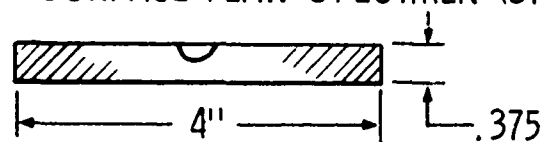
2.3.2.2 Spectrum Load Tests

The results of the spectrum environmental test program are summarized in Table II-27. Crack growth analyses based on the Wheeler model were conducted to develop an analytical correlation for each set of test data. Available data and preliminary analytical correlations were presented in AFFDL-TR-73-77. The analytical correlations for beta annealed 6Al-4V titanium were modified in accordance with the procedures outlined in Section 2.3.3; the test data and correlations are presented in Figures 2-59 - 2-65. The analytical correlations for 10 Ni Steel have remained unchanged; the test data obtained since the Second Interim Report are shown in Figures 2-66, 2-67 and 2-68.

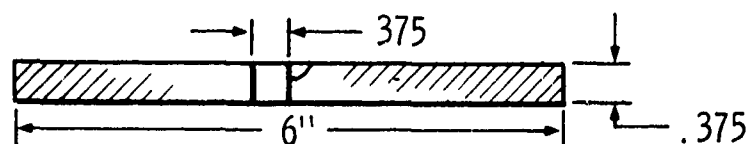
Table II-27 SPECTRUM-ENVIRONMENTAL CRACK GROWTH TESTS

MATERIAL	ENVIRONMENT	SPECTRUM	SPECIMEN	RESULTS m =
Ti6Al-4V(β ,MA) ↓	DRY AIR	1	SF	1.8
	DRY AIR	2	SF	1.6
	DRY AIR	1	CH	1.4
	DRY AIR	2	CH	0.7
	SUMP TANK WATER {	1	SF	1.9
		1*	SF	1.7
		2*	SF	1.8
	10 Ni Steel ↓	1	SF	0.8
		2	SF	0.8
		1	CH	0.9
		2	CH	0.7
		1*	SF	0.5
		2*	SF	0.6
	SUMP TANK WATER {	1	SF	1.0
		1*	SF	0.8
		2*	SF	1.2

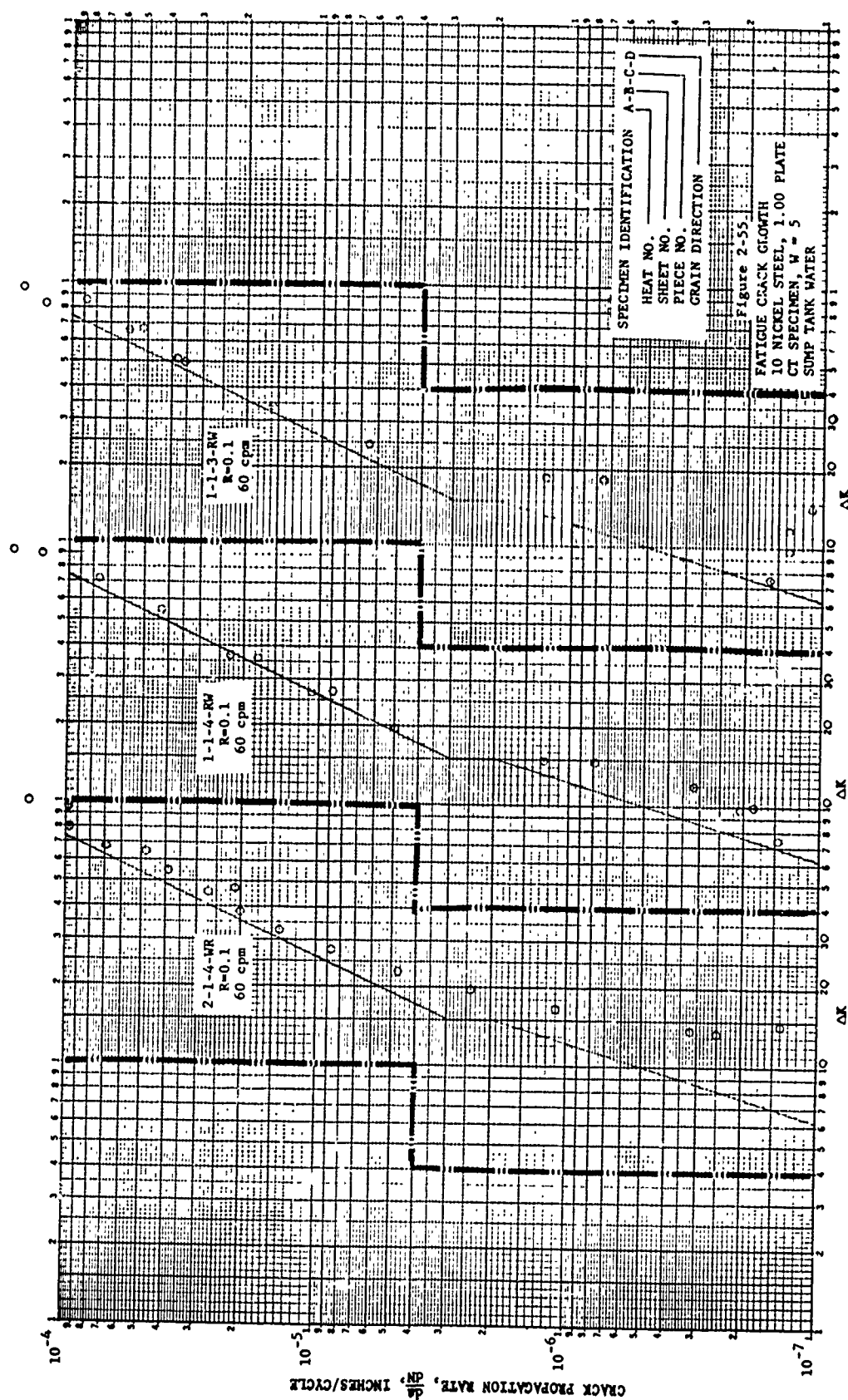
• SURFACE FLAW SPECIMEN (SF)



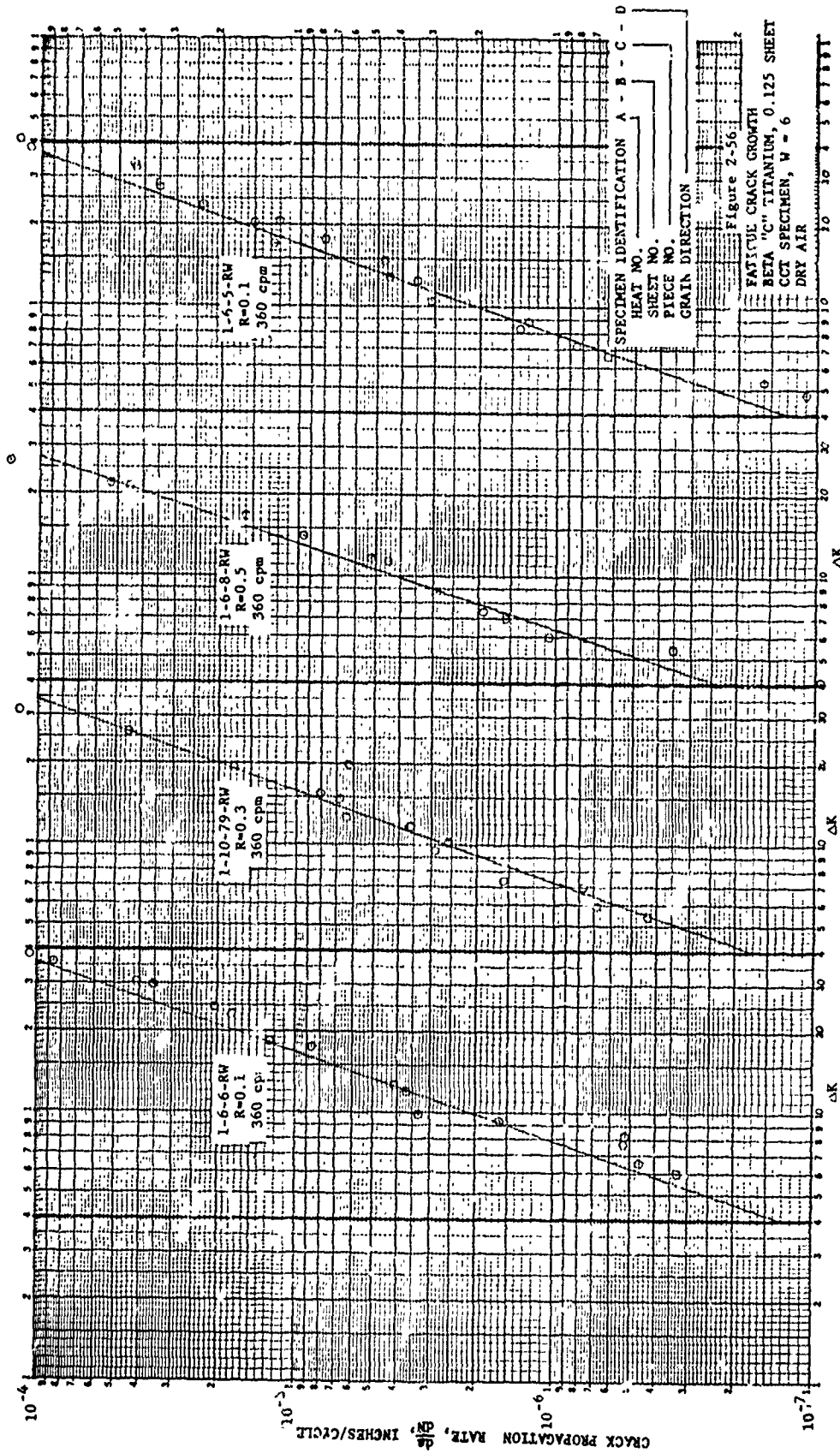
• CRACKED HOLE SPECIMEN (CH)

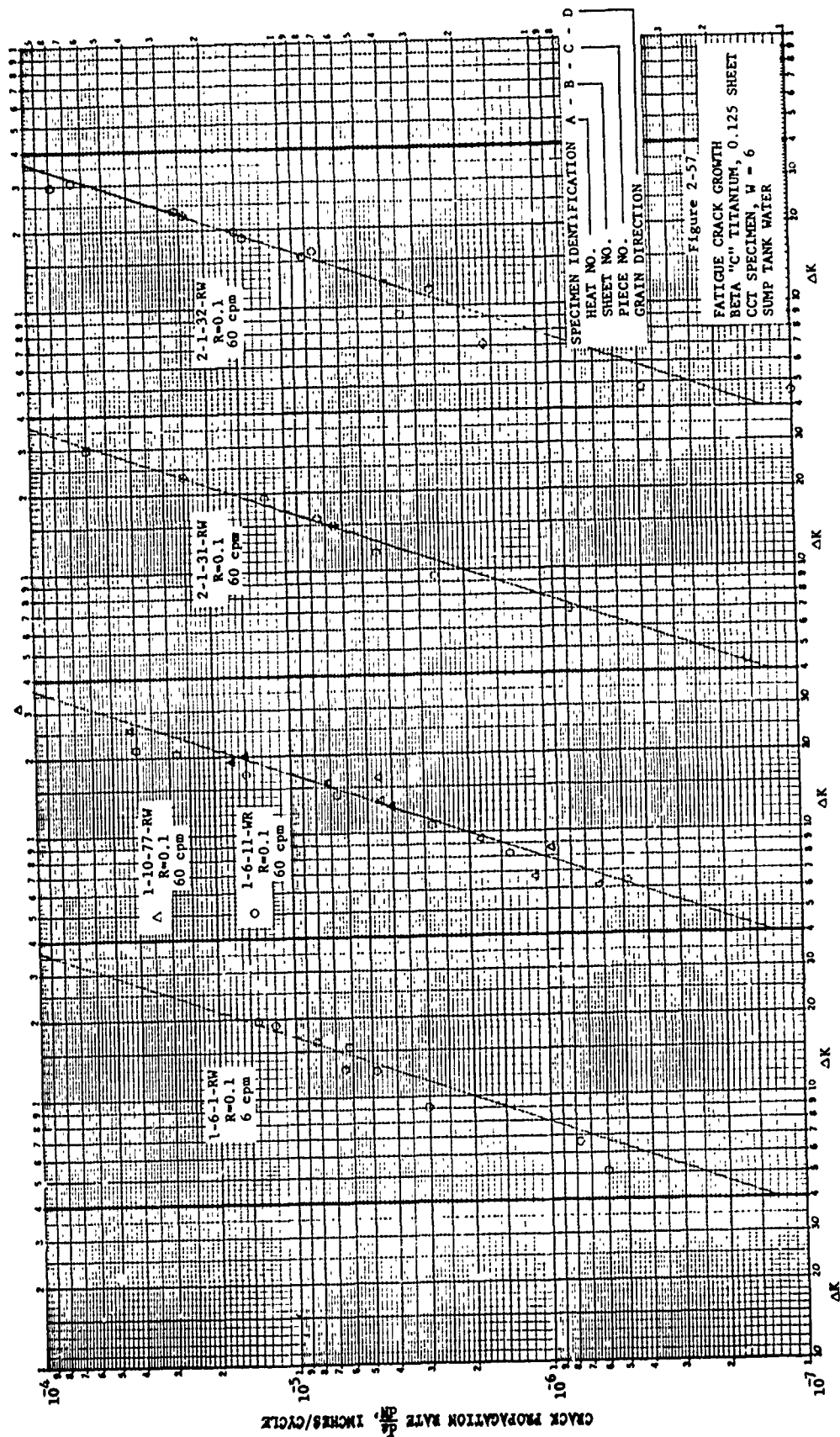


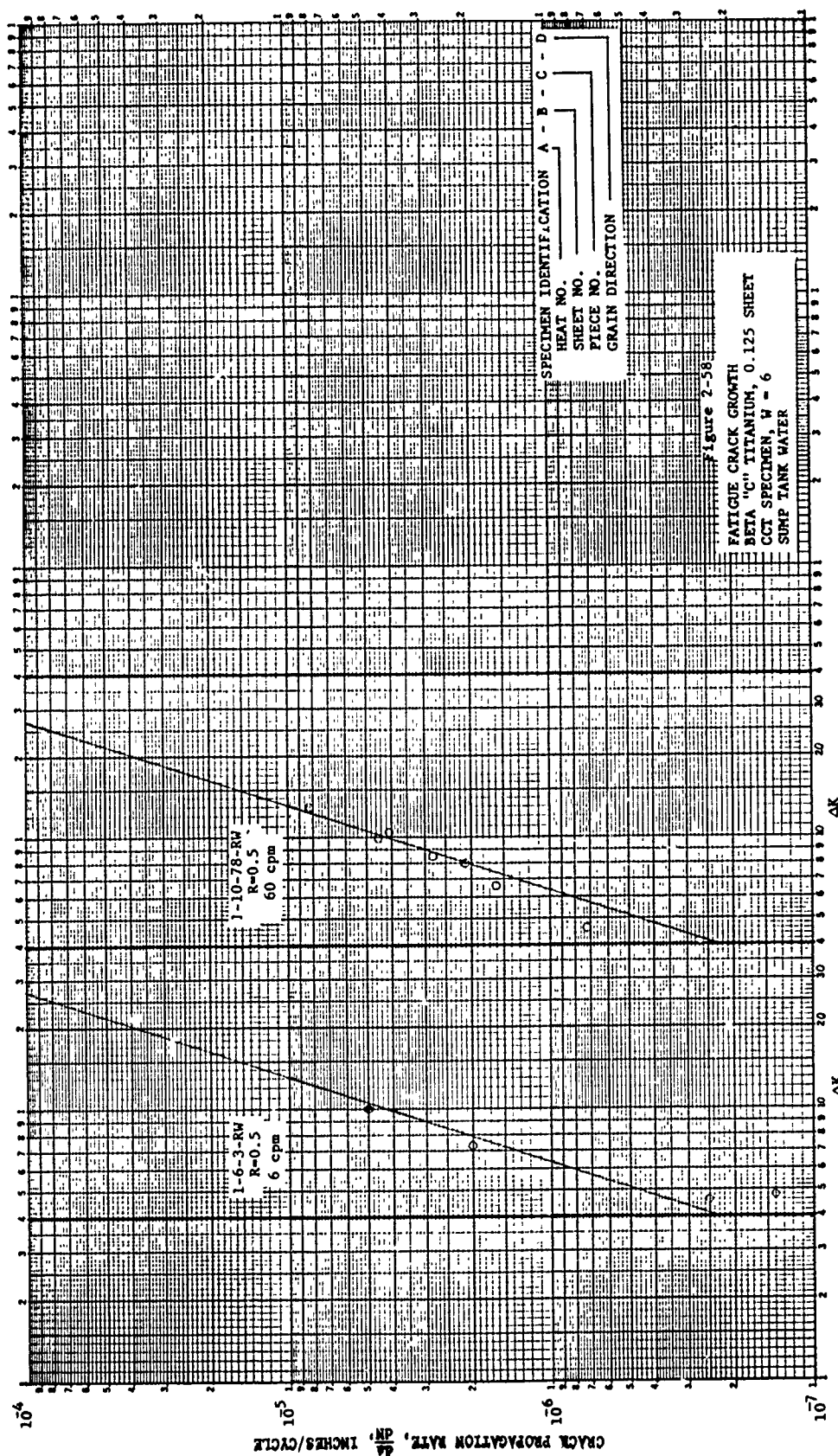
Note: Spectra 1* and 2* are untruncated versions of Spectra 1 and 2, respectively



Note: Lines represent Forman equations used in the crack growth analysis.







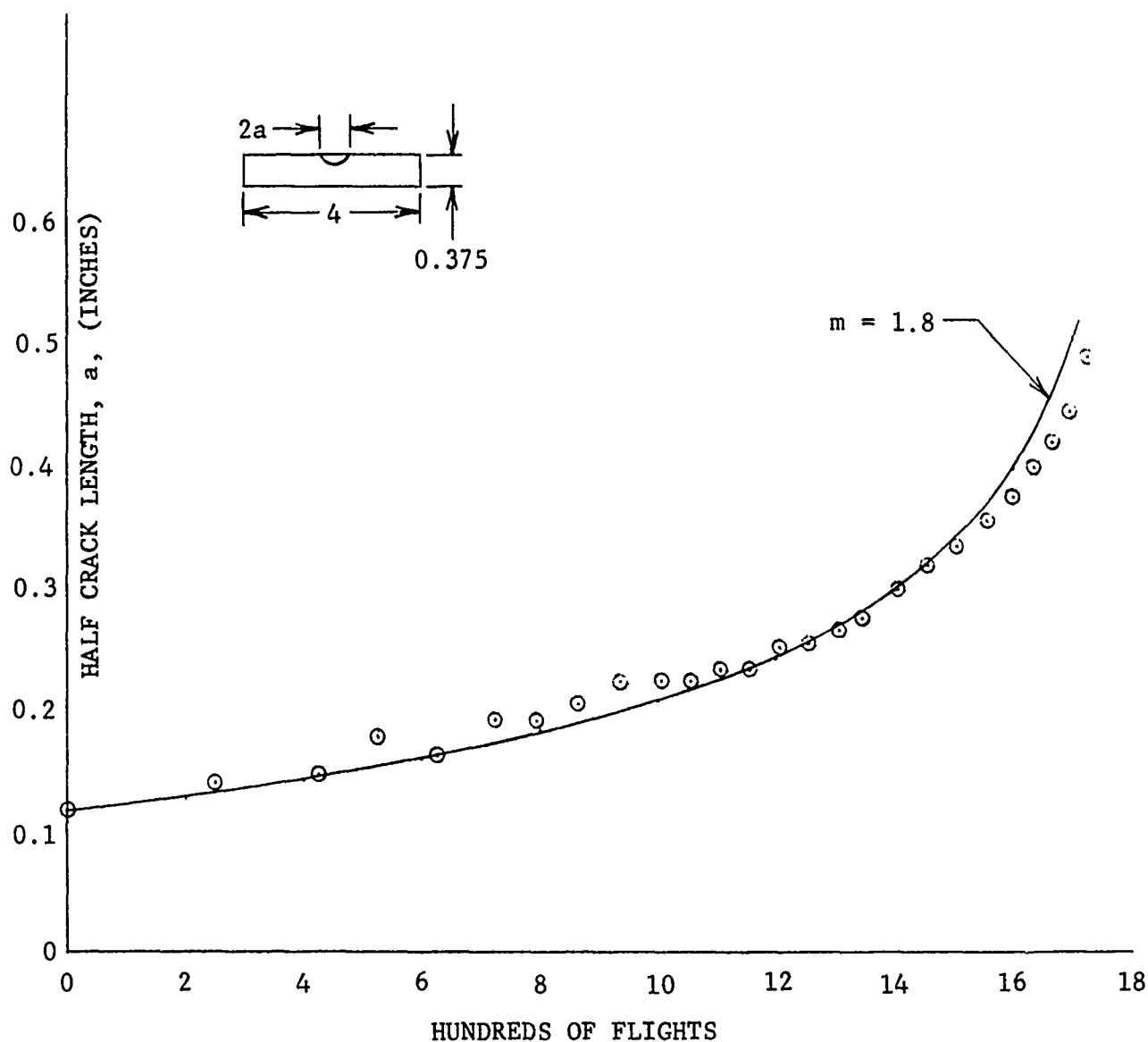


Figure 2-59
 CRACK GROWTH TEST
 BETA ANNEALED 6AL-4V TITANIUM
 FTJ10940-153
 SPECTRUM NO. 1 ($\sigma_{\max} = 79.82$ KSI)
 DRY AIR
 SEMICIRCULAR SURFACE FLAW

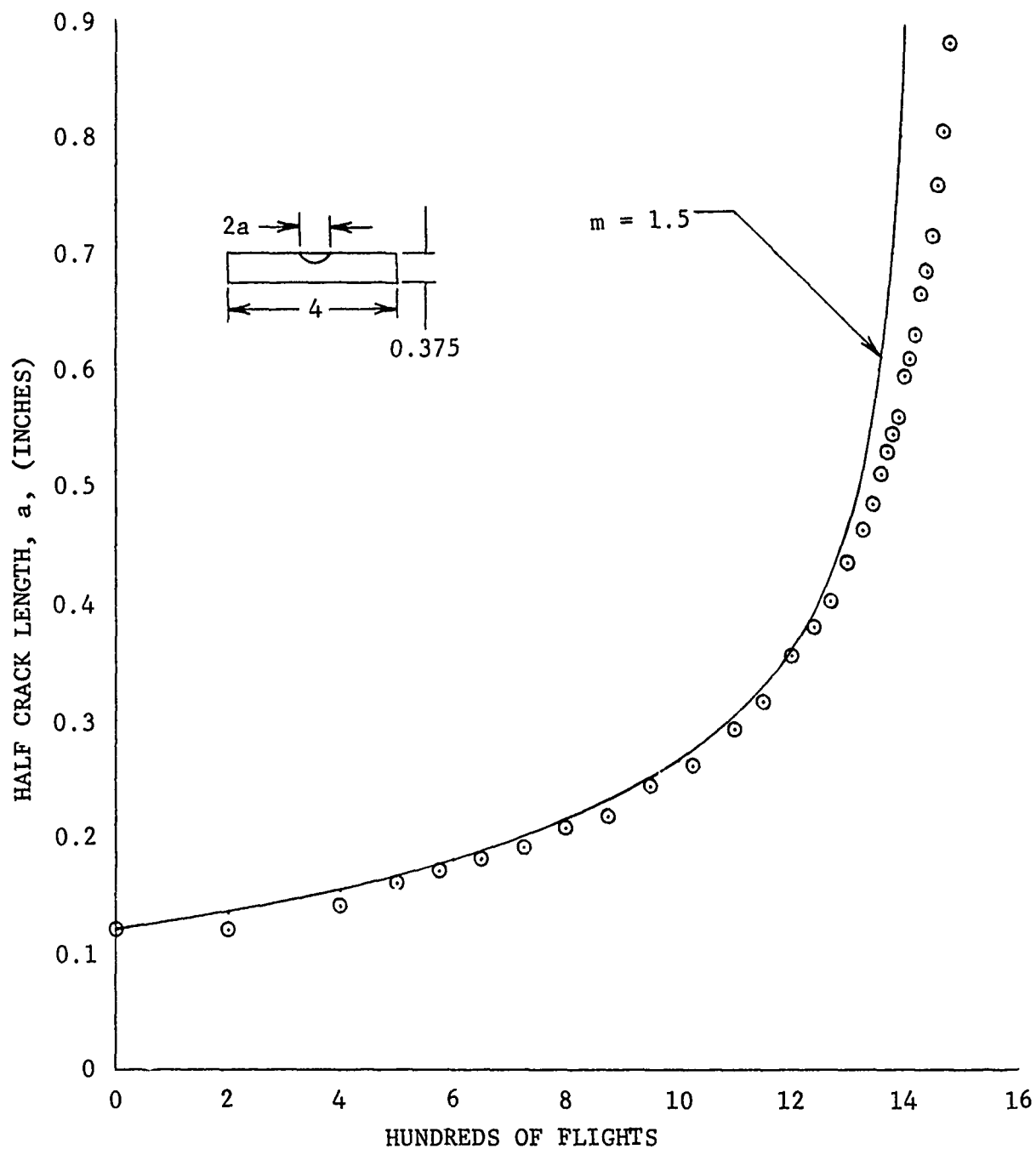


Figure 2-60

CRACK GROWTH TEST
 BETA ANNEALED 6AL-4V TITANIUM
 FTJ10940-153
 SPECTRUM NO. 2 ($\sigma_{\max} = 68.89$ KSI)
 DRY AIR
 SEMICIRCULAR SURFACE FLAW

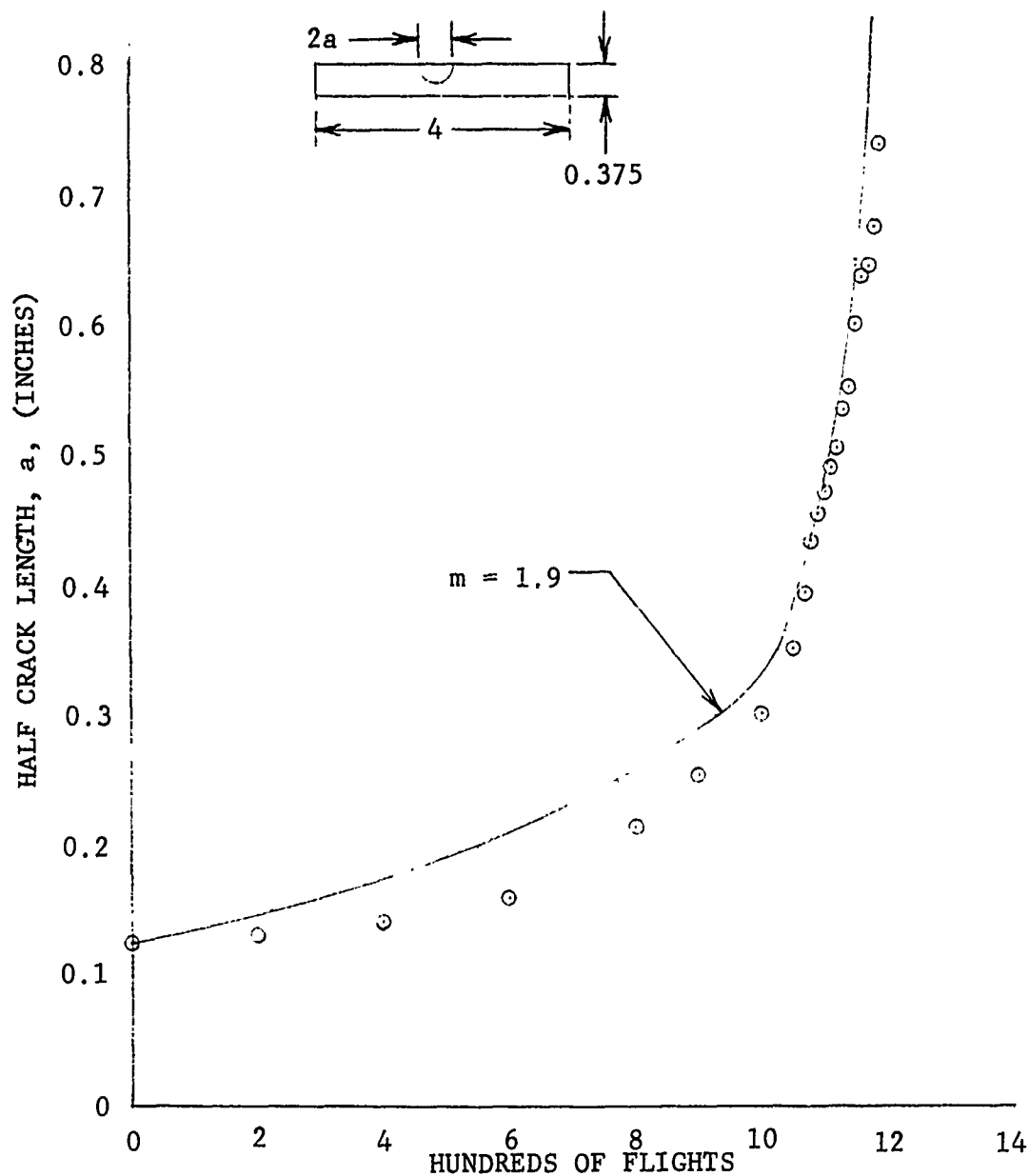


Figure 2-61

CRACK GROWTH TEST
 BETA ANNEALED 6AL-4V TITANIUM
 FTJ10940-153
 SPECTRUM NO. 1 ($\sigma_{\max} = 79.82$ KSI)
 SUMP TANK WATER
 SEMICIRCULAR SURFACE FLAW

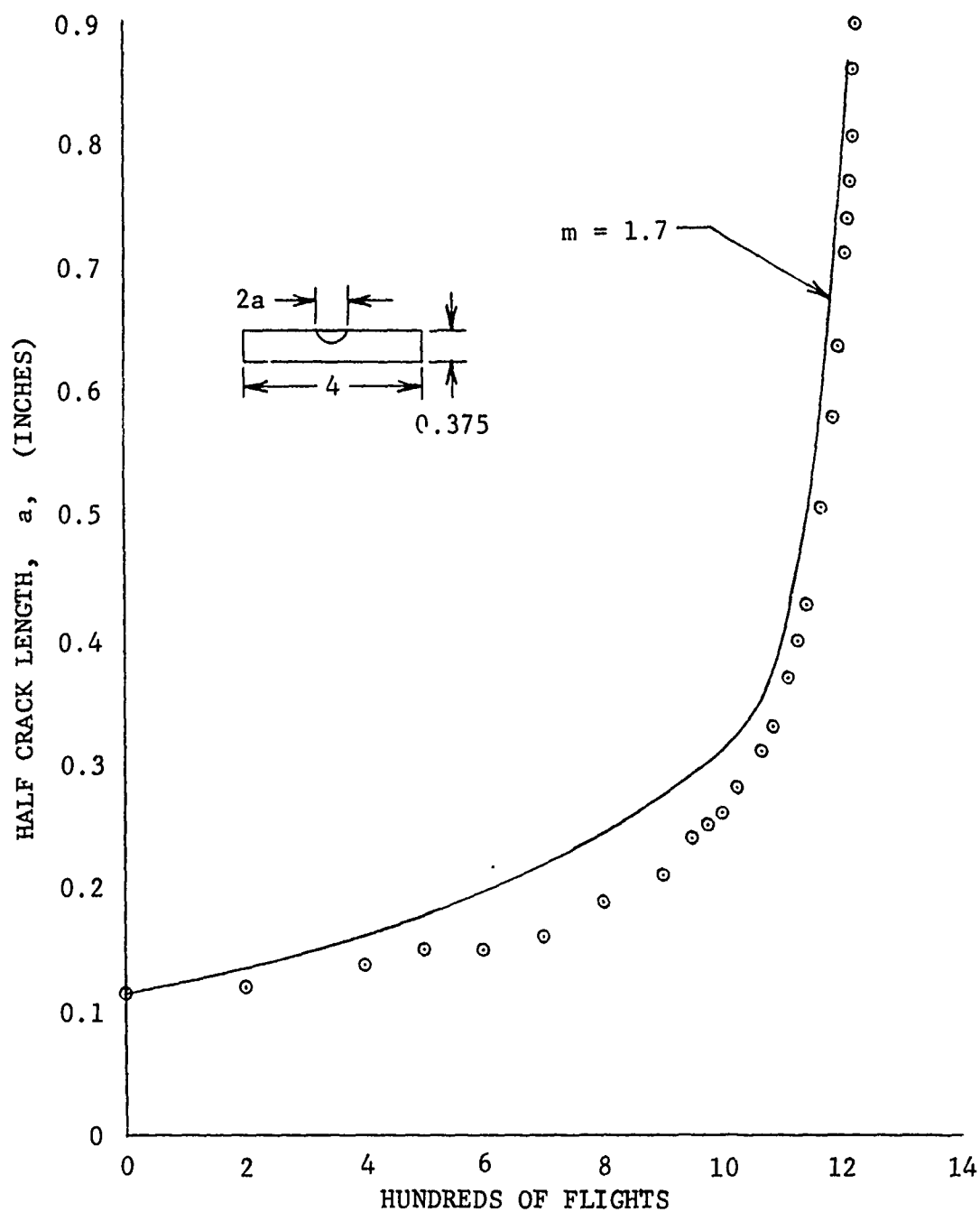


Figure 2-62

CRACK GROWTH TEST
 BETA ANNEALED 6AL-4V TITANIUM
 FTJ10940-153
 SPECTRUM NO. 1 * ($\sigma_{\max} = 79.82$ KSI)
 SUMP TANK WATER
 SEMICIRCULAR SURFACE FLAW

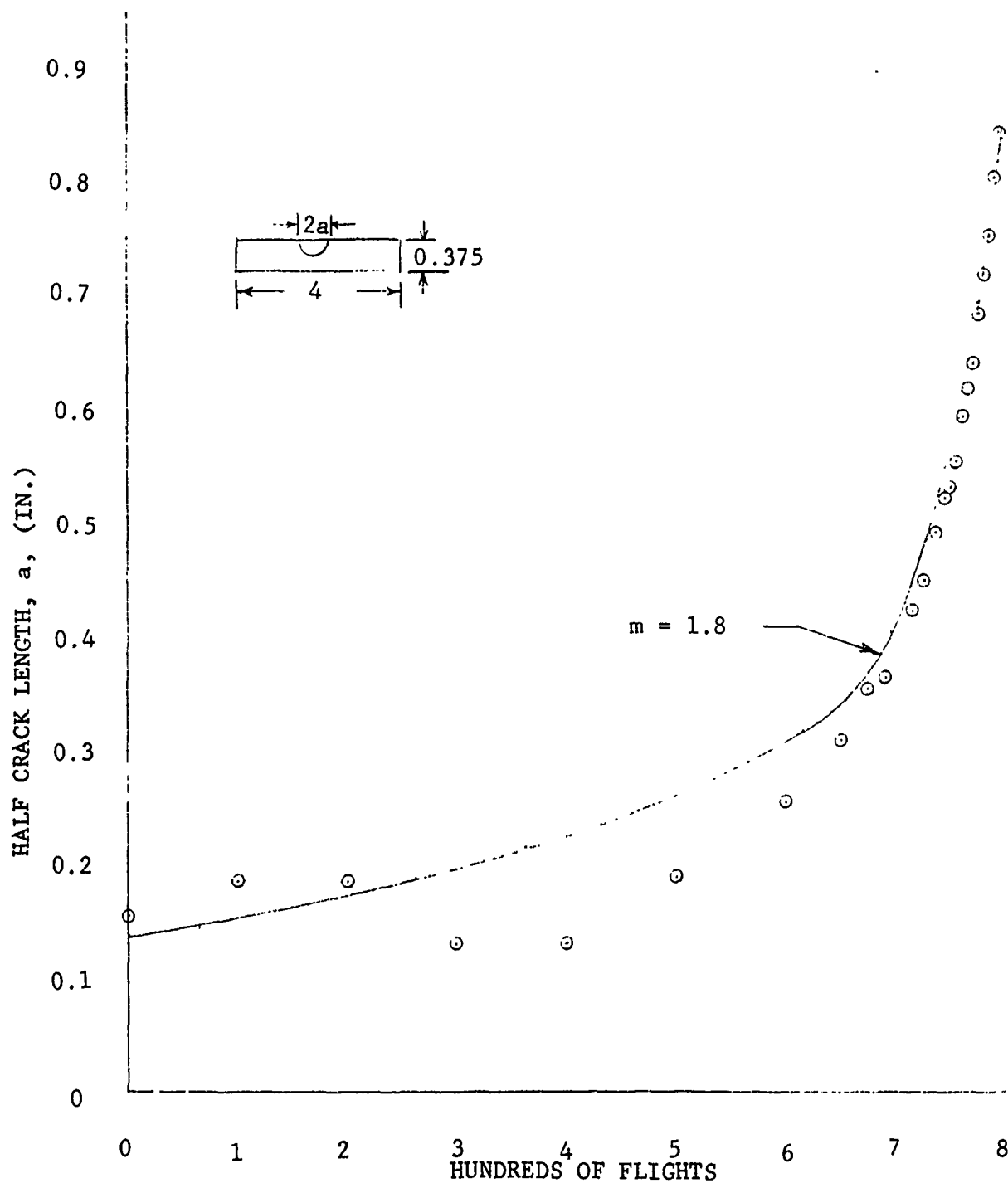


Figure 2-63

CRACK GROWTH TEST
 BETA ANNEALED 6AL-4V TITANIUM
 FTJ10940-153
 SPECTRUM NO. 2 * ($\sigma_{\max} = 68.89$ KSI)
 SUMP TANK WATER
 SEMICIRCUIAR SURFACE FLAW

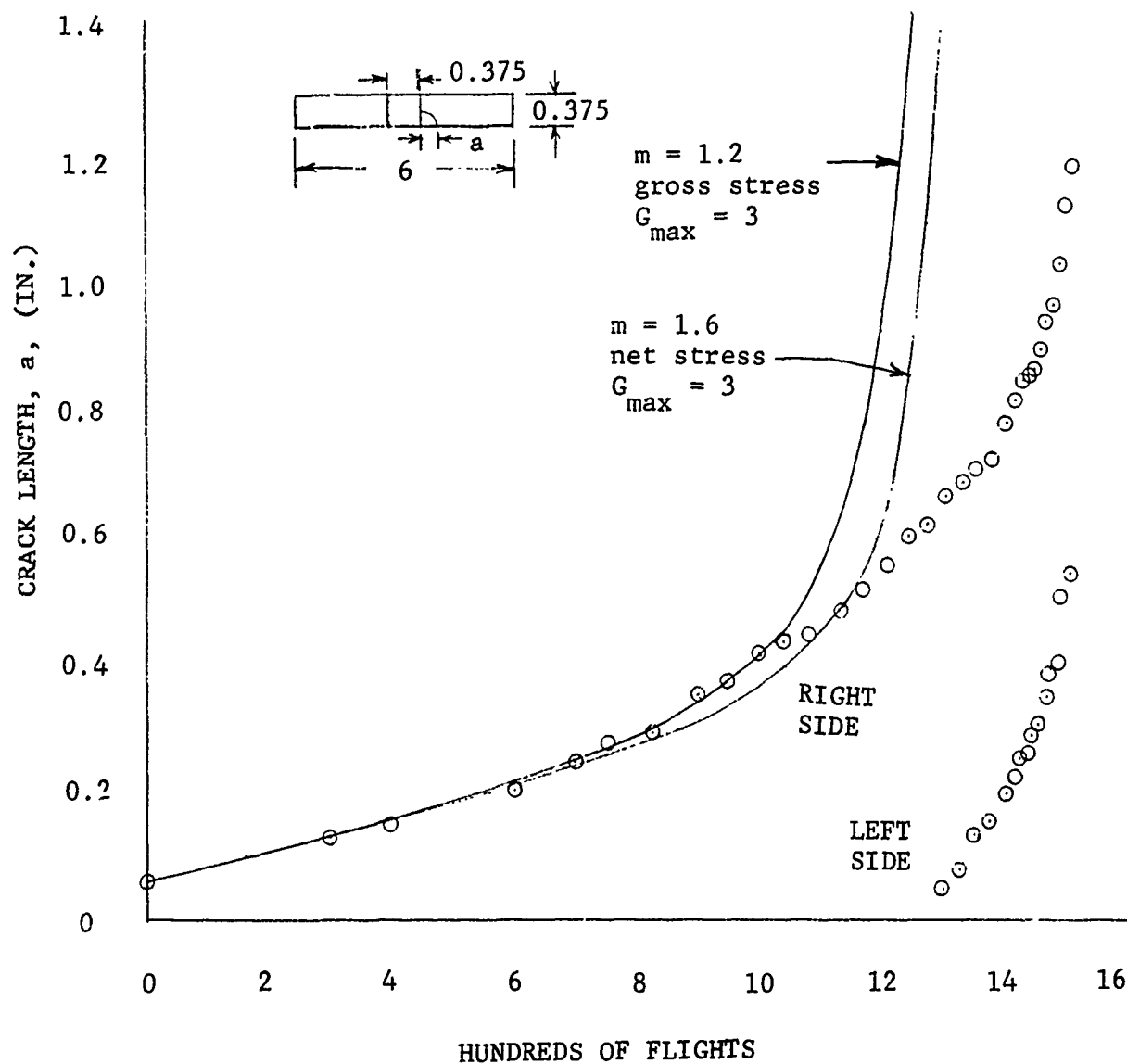


Figure 2-64
 CRACK GROWTH TEST
 BETA ANNEALED 6AL-4V TITANIUM
 FTJ10940-152
 SPECTRUM NO. 1 ($\sigma_{\max} = 79.82$ KSI)
 DRY AIR
 QUARTER CIRCULAR CORNER CRACK

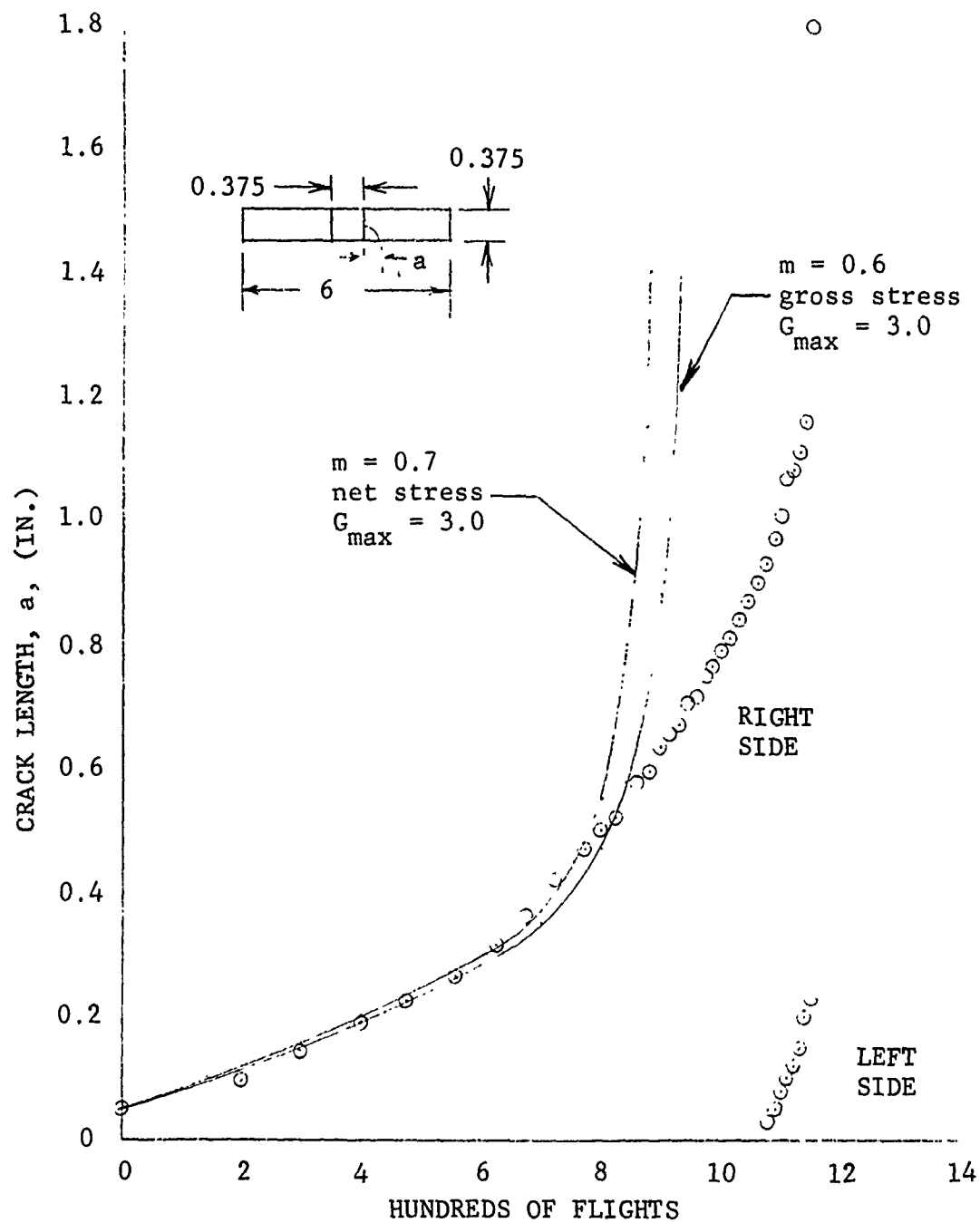


Figure 2-65

CRACK GROWTH TEST
 BETA ANNEALED 6AL-4V TITANIUM
 FTJ10940-152
 SPECTRUM NO. 2 ($\sigma_{\max} = 68.89$ KSI)
 DRY AIR
 QUARTER CIRCULAR CORNER CRACK

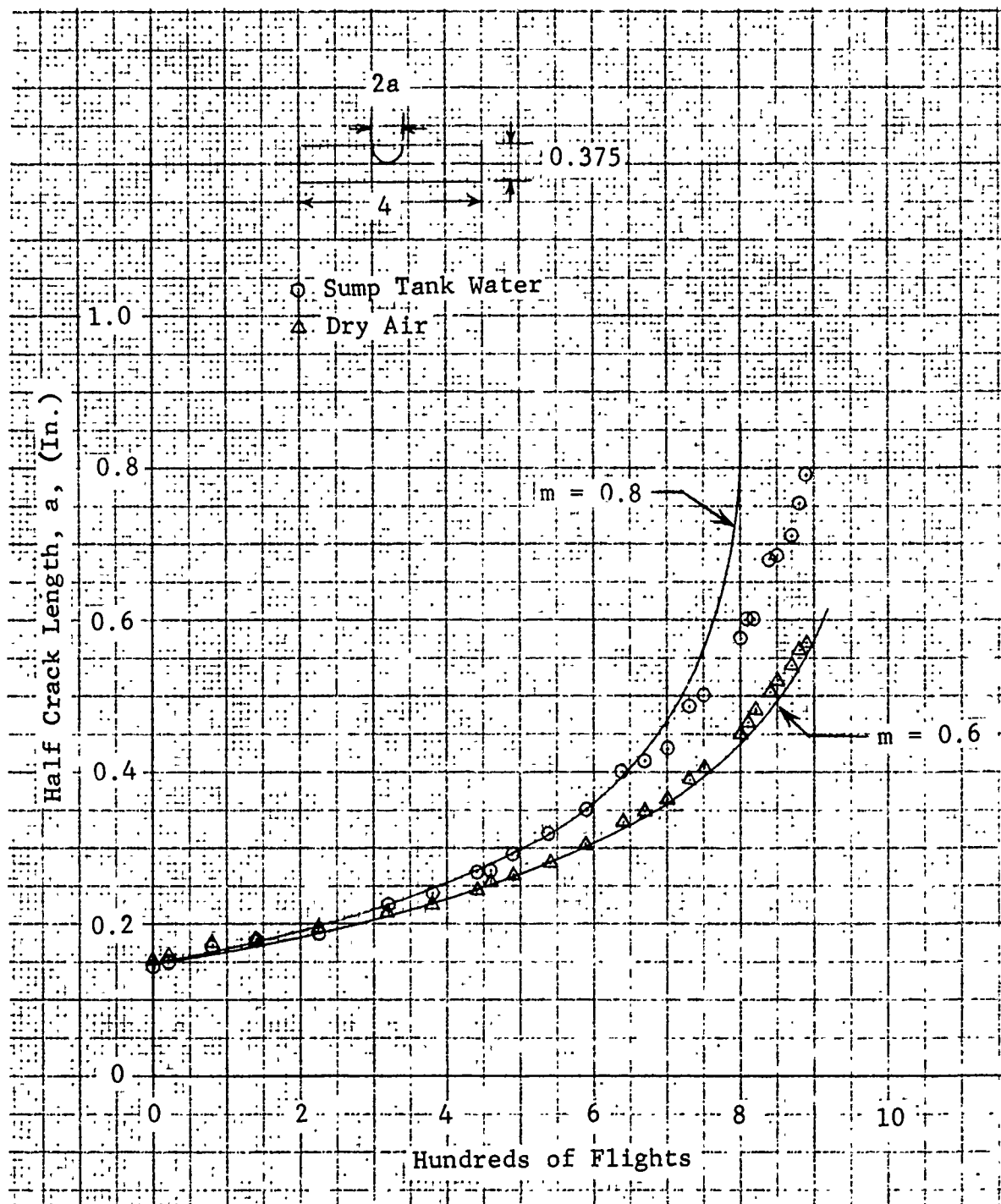


Figure 2-66
 CRACK GROWTH TEST
 10 NICKEL STEEL
 FTJ10940-185
 SPECTRUM NO. 1 * ($\sigma_{\max} = 120$ KSI)
 SEMICIRCULAR SURFACE FLAW

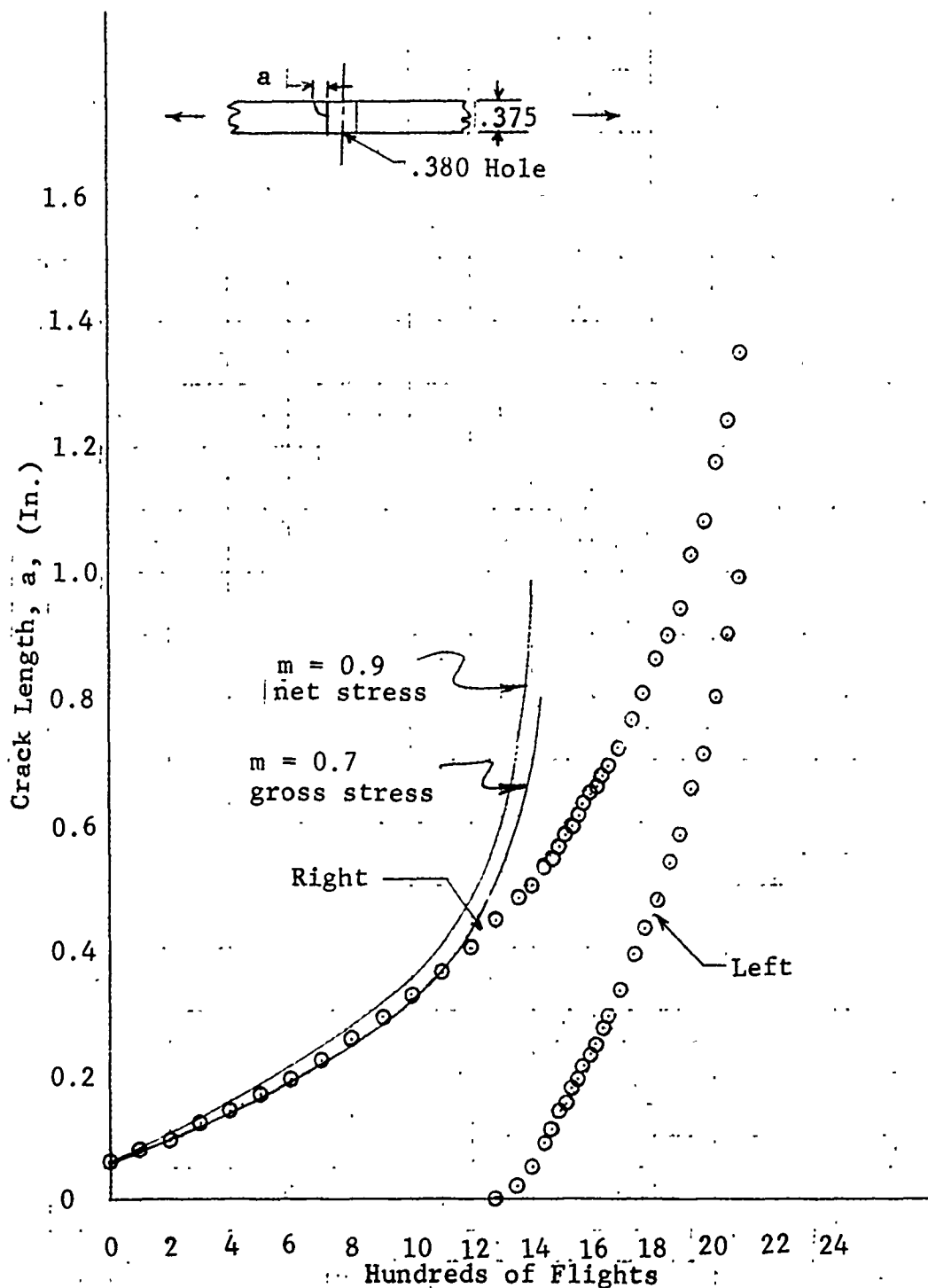


Figure 2-67

CRACK GROWTH TEST
10 NICKEL STEEL
FTJ10940-186
SPECTRUM NO. 1 ($\sigma_{\max} = 120$ KSI)
DRY AIR
QUARTER CIRCULAR CORNER CRACK
2-181

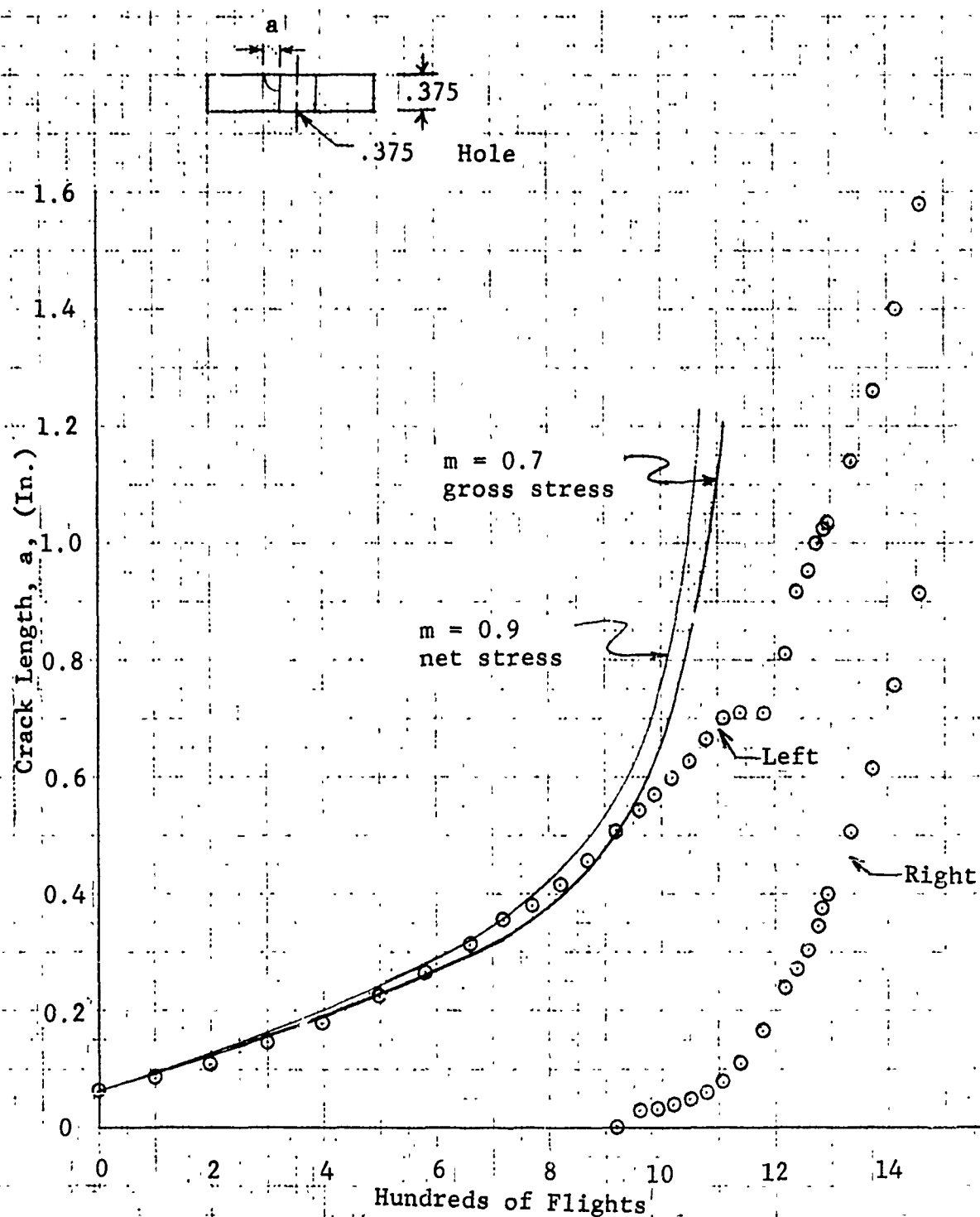


Figure 2-68

CRACK GROWTH TEST
 10 NICKEL STEEL
 FTJ10940-186
 SPECTRUM NO. 2 ($\sigma_{\max} = 103.6$ KSI)
 DRY AIR
 QUARTER CIRCULAR CORNER CRACK
 2-182

2.3.3 Crack Growth Analysis

Crack growth analyses were conducted on both WCTS designs using the results of the stress analysis, the fatigue loads spectrum and fracture mechanics test data. The Wheeler retardation model was used to account for spectrum retardation and environmental effects to the extent observed in the spectrum-environmental test program.

A modified version of the Air Force computer program CRACKS was used for the crack growth analyses. The modifications are discussed in report AFDDL-TR-73-1. The CRACKS program is based on a linear accumulation of incremental crack growth, i.e.

$$\frac{da}{dN} = f(\Delta K) \quad (1)$$

$$a_n = a_o + \sum_{i=1}^n \left(\frac{da}{dN} \right)_i \quad (2)$$

where a_o = initial crack length

a_n = crack length after n cycles

The functional relationship between crack growth rate da/dN , and the stress intensity range, ΔK , is established empirically from the constant amplitude crack growth test data. As presented in Section 2.3.2.1, this relationship is expressed in terms of one or more equations of either the Paris or the Forman type. Environmental enhanced crack growth is accounted for by use of the appropriate da/dN data.

The Wheeler model was used to account for spectrum retardation effects, i.e., the growth rate reduction following a peak overload. The Wheeler model was incorporated into the CRACKS program by modifying Equation 2 as follows:

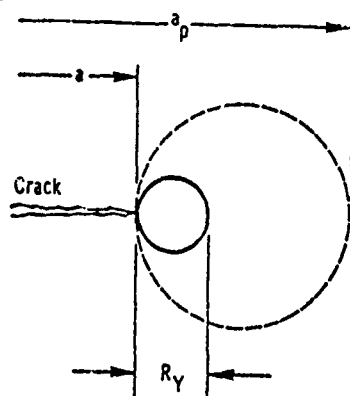
$$a_n = a_o + \sum_{i=1}^n C_{Pi} \left(\frac{da}{dN} \right)_i \quad (3)$$

Where C_{Pi} is the spectrum retardation factor

$$C_{Pi} = \left[\frac{R_Y}{a_p - a} \right]^m \quad \text{for } a + R_Y < a_p$$

$$C_{Pi} = 1 \quad \text{for } a + R_Y \geq a_p$$
(4)

where a , a_p and R_Y are defined in the sketch



$$R_Y = \frac{1}{6\pi} \left(\frac{K}{\sigma_{ys}} \right)^2$$

The retardation exponent, m , is an empirical constant determined on the basis of the spectrum environmental crack growth tests discussed in Section 2.3.2.2. The best-fit m value is obtained by generating a family of crack growth curves using the test spectrum, the appropriate da/dN data and a series of m values. The analysis curve that most closely approximates the experimental data sets the m value. The analysis curves shown in Figures 2-59 through 2-68 represent the best-fit m values for beta annealed 6Al-4V titanium and 10 Ni steel.

Equation (3) implies cycle-by-cycle summation of the incremental crack growth. To improve efficiency, the CRACKS program uses a Runge Kutta integration of the da/dN curves over an interval of fatigue cycles at a constant load level within the fatigue spectrum. This procedure is extremely accurate but requires several computational steps. Further efficiency improvements were achieved for the AMAVS program by using a single-step integration procedure, i.e.

$$a_n = a_o + \sum_{i=1}^{EN} C_{Pi} \left(\frac{da}{dN} \right)_i \Delta N_i$$
(5)

where ΔN_i is the number of cycles in the i^{th} spectrum load level and the incremental crack growth within each load level is summed over the range of load levels applied ($i = 1$ to EN).

Use of Equation 5 resulted in a four-fold savings in computer run time, however, computer run times were still too long. Satisfactory length computer runs (approx. 1 minute per 1280 flights) were achieved by converting the flight-by-flight spectrum to a 10 flight block spectrum. Comparative runs indicated that crack growth rates were essentially the same for both spectra. The block spectrum was slightly conservative because more retardation occurred in the flight-by-flight spectrum.

2.3.4 Fracture Analysis of Selected Control Points

Fracture analyses were conducted on 10 control points in the FSIL WCTS and 9 in the NBB configuration. Primary tensile-loaded elements of the WCTS were identified as control points based on the evaluation of finite element math model stresses, stress analysis results and design details. Surveys of the stress distributions for the five fatigue spectrum conditions (ASKA Conditions 2, 10, 5, 9 and 7, representing post-takeoff, TFR, prelanding, climb/cruise, and ground/taxi, respectively) were considered in the selection of control points.

A worksheet was prepared for each control point showing a sketch of the location and dimensions of the control point, part identification, material, damage tolerance category, and inspectability category. These control point data are supplemented with tabulated information which includes the stresses (maximum principal and effective) for each condition in the fatigue loads spectrum; maximum spectrum, limit, net ultimate, and allowable stress levels; initial and critical crack sizes; and type of crack (cracked hole, surface crack, etc.) considered at each control point.

Areas of the WCTS approaching and/or exceeding the following established gross section limit stress levels were selected as primary fracture control points.

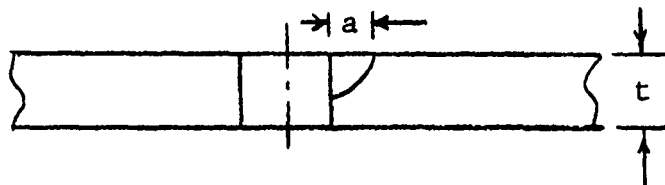
o Ti 6Al-4V (β ,MA)	67 ksi - maximum 53 ksi - typically
o 10 Ni Steel	100 ksi - maximum 80 ksi - typically
o 7075 Al 2024 Al	30 ksi - maximum

Using the gross section limit stress levels noted above, critical crack sizes, a_c were calculated using the following crack models.

- o For part thru cracks adjacent to holes:

$$K_{IC} = \sigma \sqrt{\frac{\pi a_c}{Q}} M_K G_{KT}$$

$$a_c = \frac{Q}{\pi} \left[\frac{K_{IC}}{M_K \sigma G_{KT}} \right]^2$$

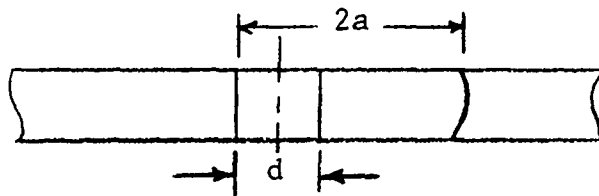


where Q = Flaw Shape Factor = $2.46 - .212 (\sigma/\sigma_{ys})^2$
 M_K = Back Face Correction Factor
 G_{KT} = Stress Gradient Factor

- o For thru-the-thickness cracks adjacent to holes:

$$K_{IC} = \sigma \sqrt{\frac{(a_c + d)}{2}} G_{KT}$$

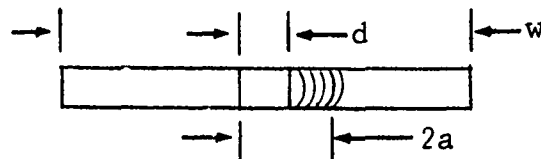
$$a_c = \frac{2}{\pi} \left[\frac{K_{IC}}{G_{KT} \sigma} \right]^2 - d$$



- o For thru-the-thickness cracks with a finite width correction.

$$K_{IC} = \sigma \sqrt{\pi a} \sqrt{\sec \frac{\pi a}{w}}$$

$$a_c = \frac{1}{\pi} \left(\frac{K_{IC}}{\sigma} \right)^2 \frac{1}{\sec \frac{\pi a}{w}}$$



The following material properties were used in developing critical crack sizes:

10 Ni Steel

$$K_{IC} = 200 \text{ ksi} \sqrt{\text{in}}$$

$$\sigma_{ys} = 175 \text{ ksi}$$

$$E = 28.0 \times 10^6 \text{ psi}$$

Ti 6AL-4V (β , MA)

$$K_{IC} = 80 \text{ ksi} \sqrt{\text{in}}$$

$$\sigma_{ys} = 115 \text{ ksi}$$

$$E = 16.3 \times 10^6 \text{ psi}$$

Critical crack sizes were calculated using stress levels corresponding to the maximum service spectrum stress or the limit load stress whichever was the greatest. For the control points considered herein, the highest stress was consistently the limit load stress; i.e., 2/3 ultimate gross section stress. Figure 2-69 shows a typical critical crack length, in this case a thru-the-thickness crack, for gross section limit stresses of 60 ksi to 130 ksi. For control points in the WCTS, a_c typically was less than 4.0 inches. For cases where $a_c > 4$ inches, it was assumed that other factors such as structural geometry, loads redistribution, etc., would dominate.

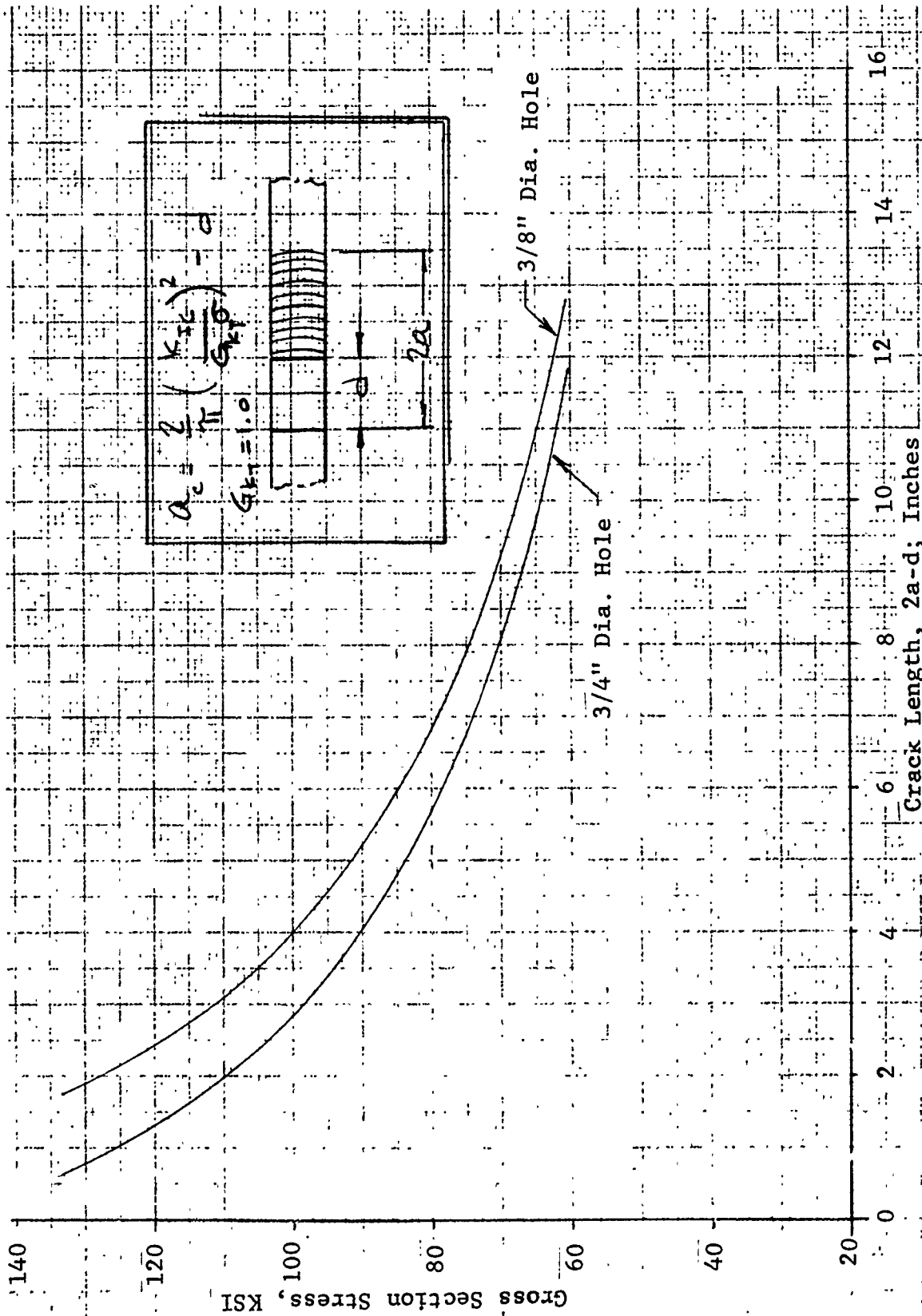


Figure 2-69 CRITICAL CRACK LENGTH VS. GROSS SECTION STRESS
 THRU THE THICKNESS CRACK IN
 10 NI STEEL; $K_{IC} = 200$ KSI IN.

2.3.4.1 FSIL Fracture Analysis

Fracture analyses were conducted on the following 10 FSIL configuration control points.

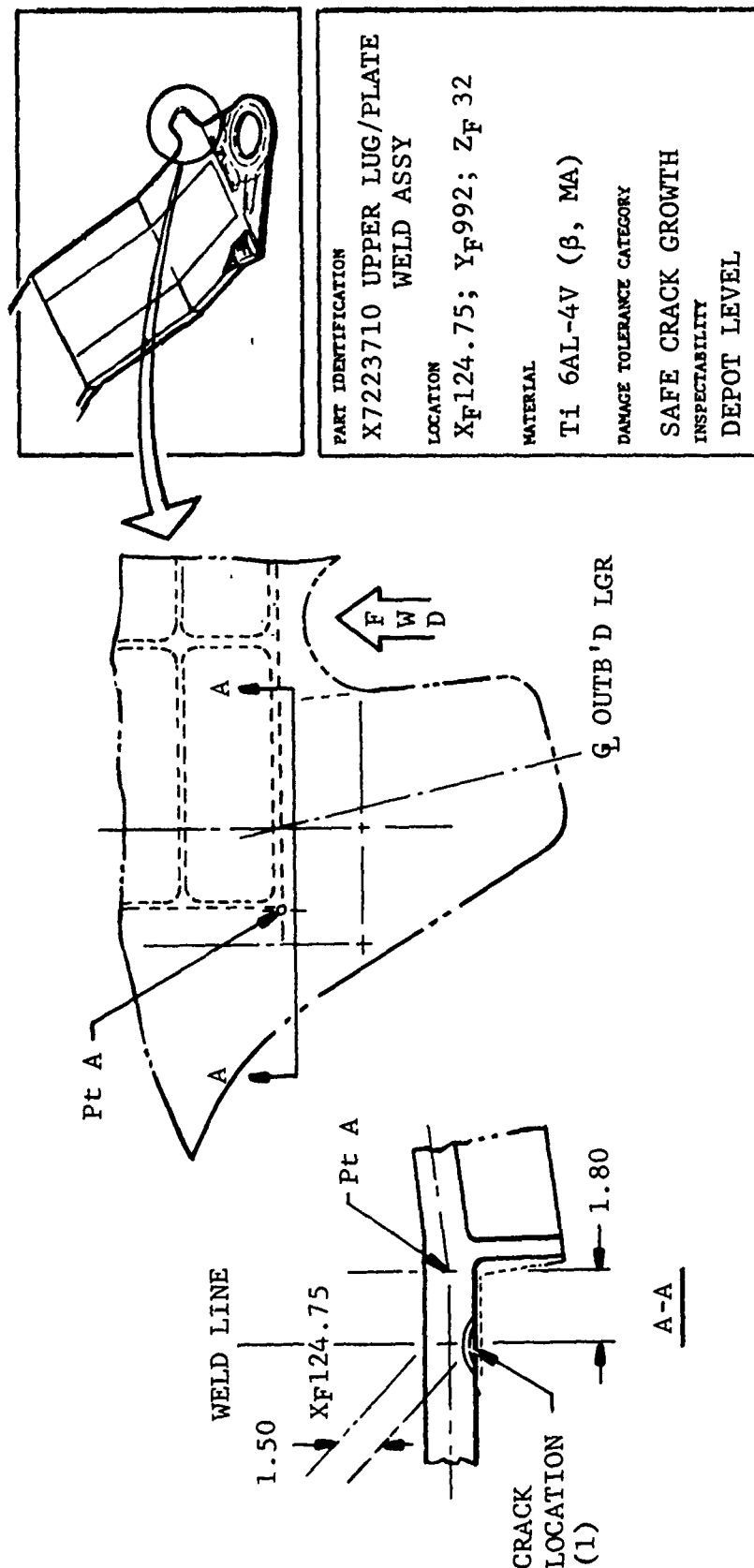
1. Control Point 1, Figure 2-70, Aft Outboard Corner, Upper Plate at Weld Line.

Crack growth analyses were conducted at the X_F 124.75 weld line using EB da/dN data. A 0.15-inch initial crack length, a crack retardation exponent, $m = 0$, and a sump tank water environment were used for these analyses. Results indicated that the initial crack length was less than 0.15-inches for 100% and 90% stress levels of the five fatigue spectrum conditions. An initial crack length greater than 0.15-inches with a critical length of 1.00-inches was calculated for an 80% stress level. Further work is needed to qualify this location.

2. Control Point 2, Figure 2-71, Y_F 992 Bhd, Outboard, Lower Attach Angle.

A crack growth analysis was conducted for a cracked hole at X_F54 using an 0.15-inch initial crack length, a crack retardation exponent $m = 0.7$, and a sump tank water environment. A critical crack length of 0.87 inches was calculated.

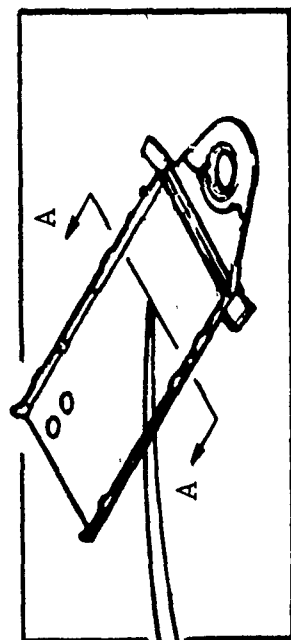
3. Control Point 3, Figure 2-72, Lower Plate, Aft Longeron, Outboard Lower
4. Control Point 4, Figure 2-73, Lower Plate, Lug
5. Control Point 5, Figure 2-74, Lower Plate, Centerline Splice
6. Control Point 6, Figure 2-75, Y_F992 Bhd, Inboard, Fuel Transfer Hole, X_F39
7. Control Point 7, Figure 2-76, Y_F932 Bhd, Forward Outboard, Lower Attach Angle
8. Control Point 8,
 - o Rib (X_F 119)
 - o Sweep Actuator Fitting
 - o Sweep Actuator Fitting Support



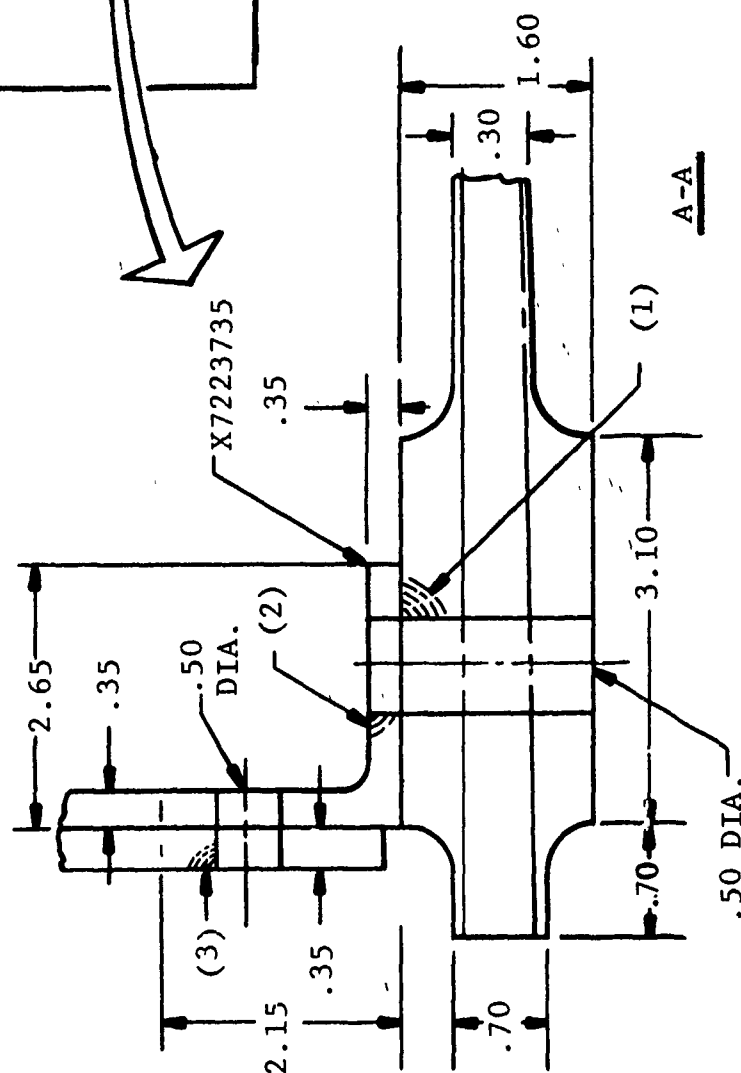
CRACK LOCATION	* ANALYSIS	GROSS SECTION ULTIMATE DESIGN STRESSES FOR ASRA CONDITIONS IN FATIGUE SPECTRUM, KSI					STRESS, KSI			CRACK SIZE, INCHES		CRACK TYPE		
		**	2	5	9	7	MAXIMUM SPECTRUM*	GROSS SEC LIMIT*	NET SECT. ULTIMATE*	ALLOWABLE	INITIAL		CRITICAL	
{ (1)	FRAC-TURE	M	-25	106	-44	-17	28	46.7	70.7	N.A.	> 80	<.15	0.72	SC

* Gross section principal stresses used for fracture analysis.
Net section effective stresses used for fatigue analysis.
** Type stress--M: Maximum Principal Stress
E: Effective Stress

Figure 2-70 FSIL CONTROL POINT 1; UPPER PLATE, AFT OUTBOARD WELD LINE



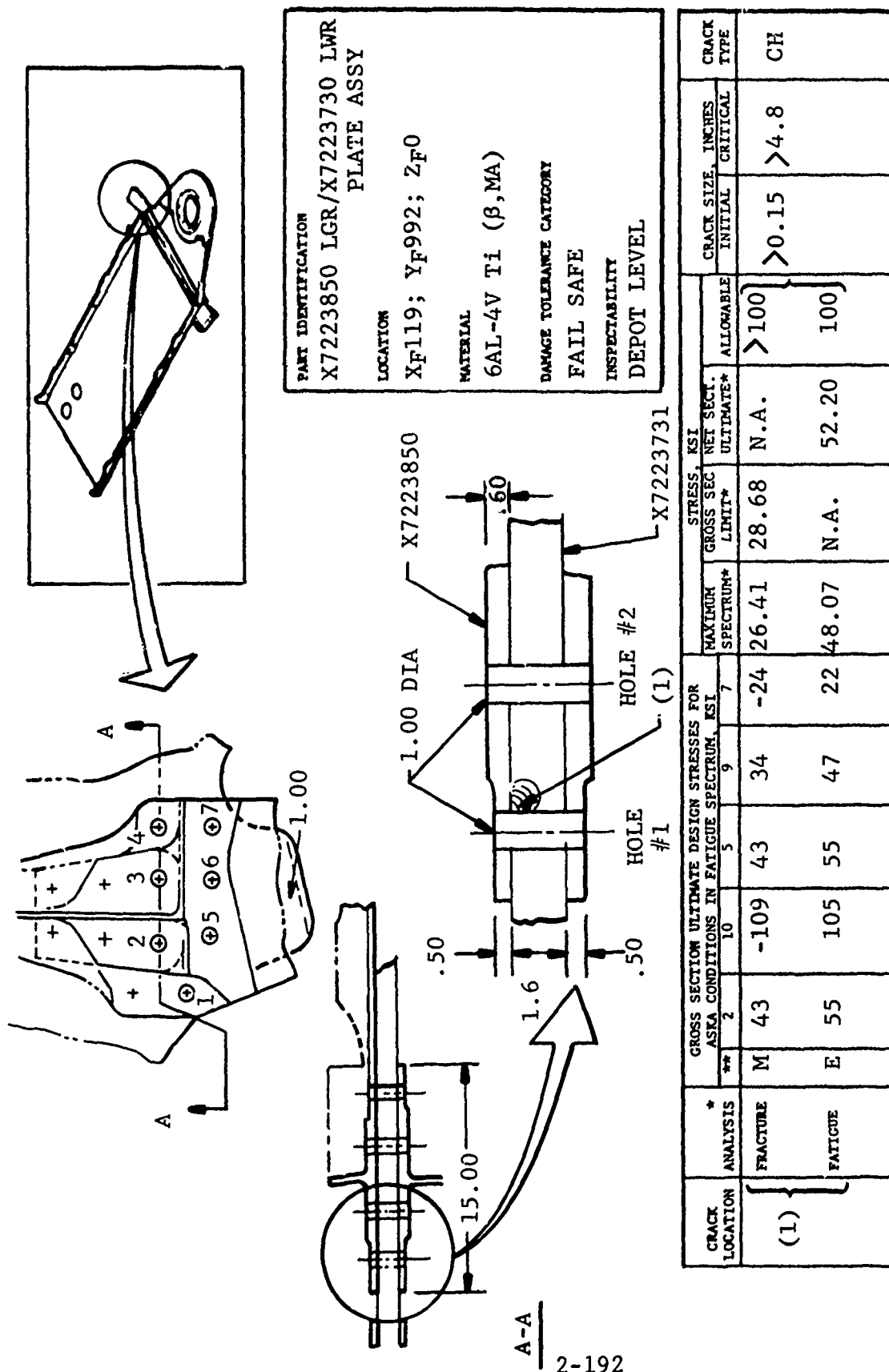
PART IDENTIFICATION	
X7223735 ATTACH ANGLE	
LOCATION	X7223735
MATERIAL	6AL-4V Ti (β , MA)
DAMAGE TOLERANCE CATEGORY	(1), (2) FAIL SAFE (3) SAFE CRACK GROWTH INSPECTABILITY
DEPOT LEVEL	



CRACK LOCATION	* ANALYSIS	GROSS SECTION ULTIMATE DESIGN STRESSES FOR ASKA CONDITIONS IN FATIGUE SPECTRUM, KSI						STRESS, KSI				CRACK SIZE, INCHES		CRACK TYPE
		**	2	10	5	9	7	MAXIMUM SPECTRUM*	GROSS SEC LIMIT*	NET SECT. ULTIMATE*	ALLOWABLE	INITIAL	CRITICAL	
(1)	{ FRACTURE	M	81.07	34.75	81.07	73.02	2.35	49.80	54.07	N.A.	{ >100	-	-	CH
(2)		E	81.07	34.75	81.07	73.02	2.35	60.26	N.A.	98.09		-	-	CH
3												100	>0.15	0.870

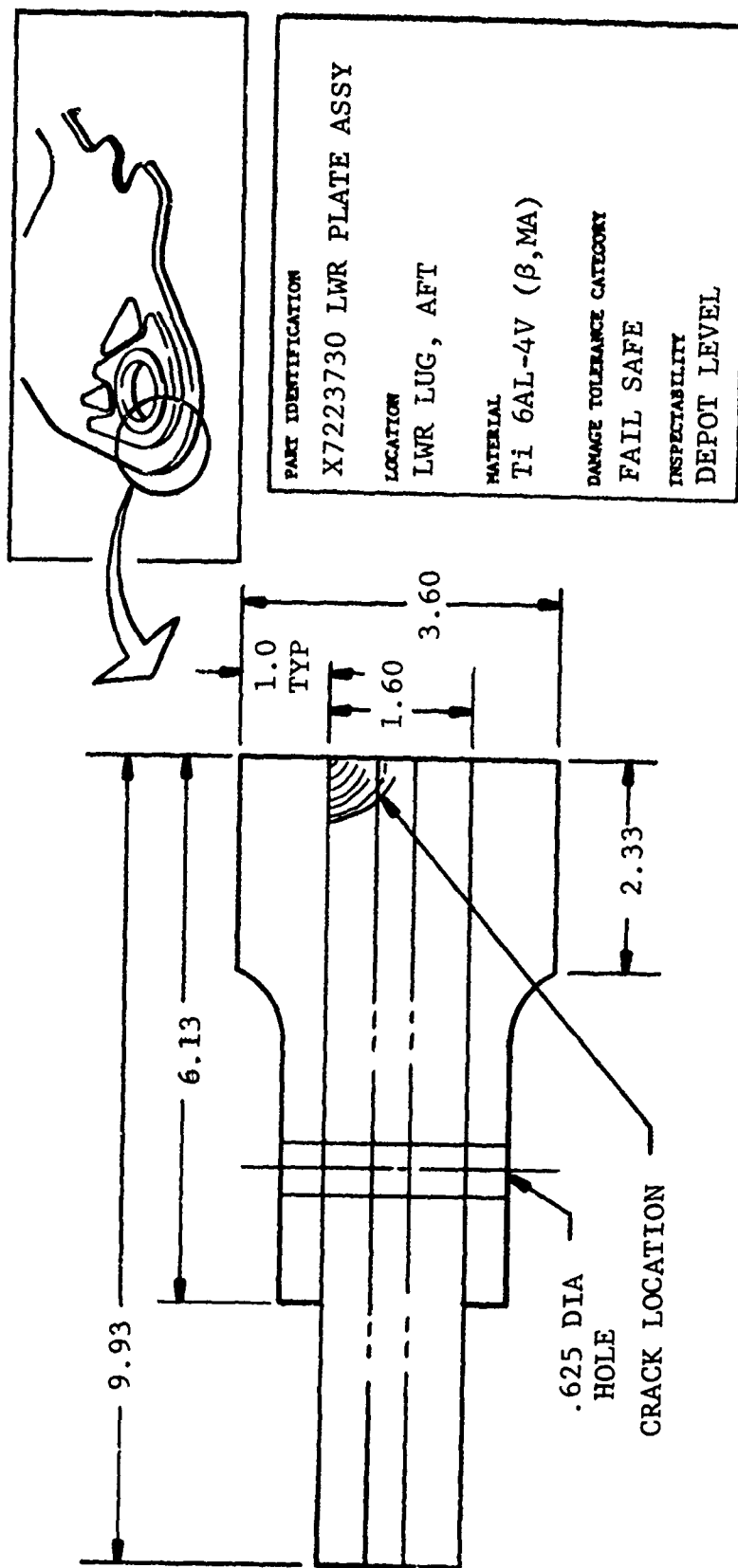
* Gross section principal stresses used for fracture analysis.
 Net section effective stresses used for fatigue analysis.
 ** Type stress--M: Maximum Principal Stress
 E: Effective Stress

Figure 2-71 FSIL CONTROL POINT 2; FSIL YF 992 BULKHEAD ATTACH ANGLE



* Gross section principal stresses used for fracture analysis.
 Net section effective stresses used for fatigue analysis.
 ** Type stress--M: Maximum Principal Stress
 E: Effective Stress

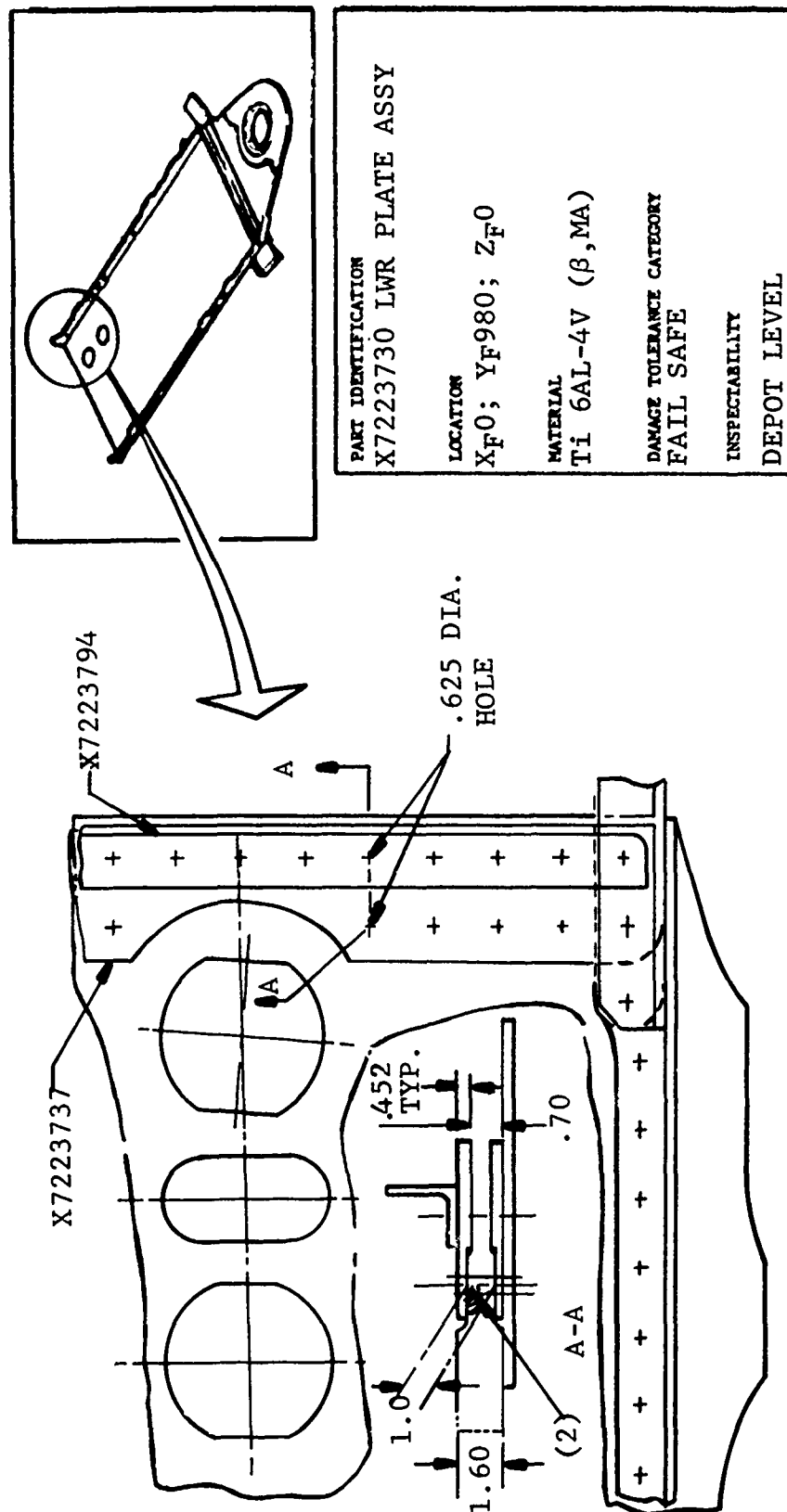
Figure 2-72 FSIL CONTROL POINT 3; YF 992 BULKHEAD, AFT LOWER, OUTBOARD



CRACK LOCATION	* ANALYSIS	GROSS SECTION ULTIMATE DESIGN STRESSES FOR ASKA CONDITIONS IN FATIGUE SPECTRUM, KSI							STRESS, KSI		ALLOWABLE	CRACK SIZE, INCHES		CRACK TYPE
		**	2	10	5	9	7	MAXIMUM SPECTRUM*	GROSS SEC LIMIT*	NET SECT. ULTIMATE*		INITIAL	CRITICAL	
(1)	FRACTURE	m	105	70	101	100	-4	62	70	N.A.	>78	>.15	-	EC
	FATIGUE	e	60	66	54	58	-5	66	N.A.	71	78			

* Local gross section principal stresses used for fracture analysis.
Average net section effective stresses used for fatigue analysis.
** Type Stress . . . m: local max principal stress
e: average net section effective stress

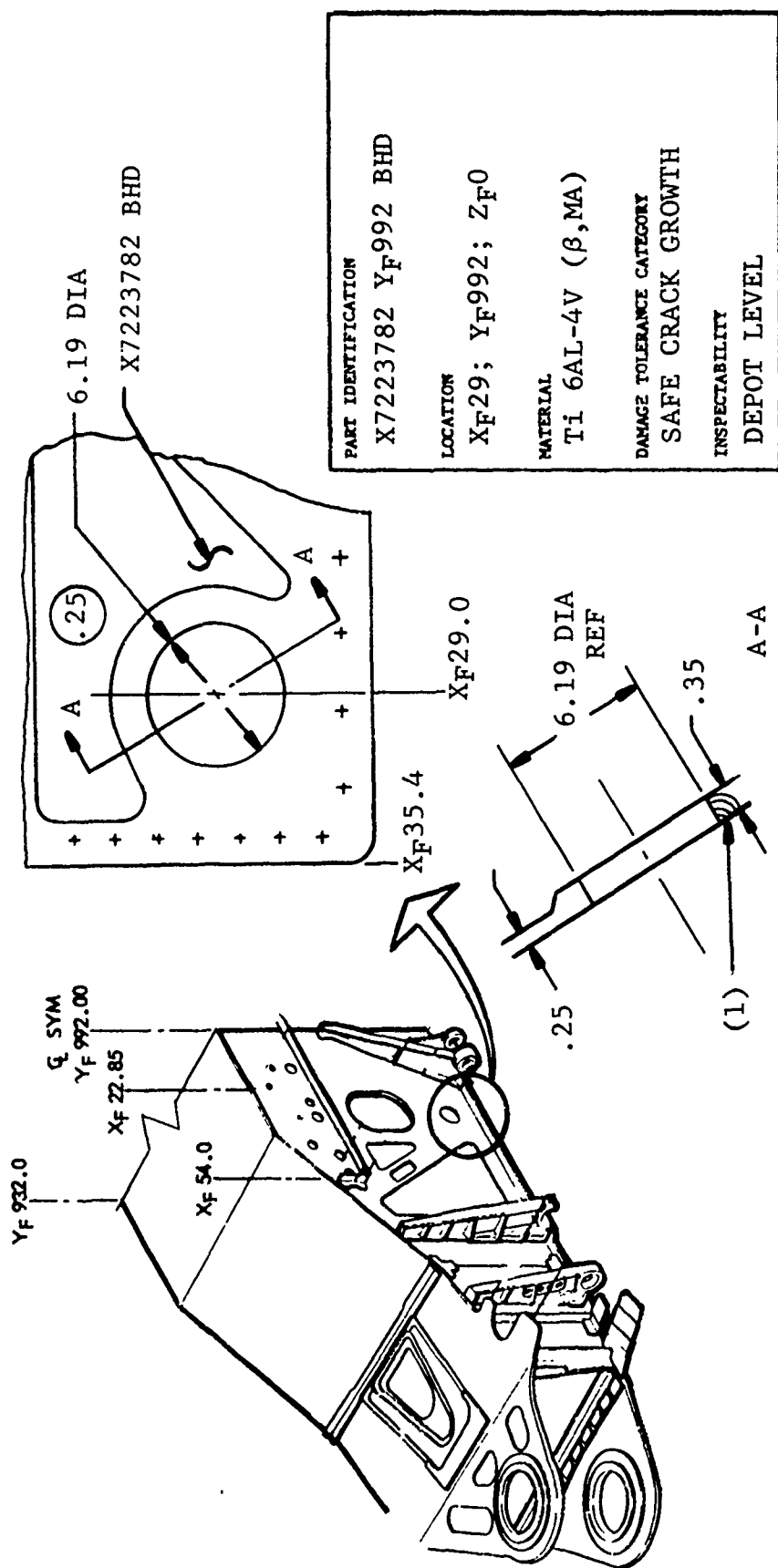
Figure 2-73 FSIL CONTROL POINT 4; LOWER LUG



CRACK LOCATION	ANALYSIS	GROSS SECTION ULTIMATE DESIGN STRESSES FOR ASKA CONDITIONS IN FATIGUE SPECTRUM, KSI							STRESS, KSI		ALLOWABLE	CRACK SIZE, INCHES		CRACK TYPE
		**	2	10	5	9	7	MAXIMUM SPECTRUM*	GROSS SEC LIMIT*	NET SECT. ULTIMATE*		INITIAL	CRITICAL	
(1)	FRACTURE	M	54.88	33.78	51.50	48.27	2.36	31.64	36.60	N.A.	>80	-	-	CH
	FATIGUE	E	54.88	33.78	51.50	48.27	2.36	40.18	N.A.	60.70	>0.15	>4.0	-	CH
											80	-	-	CH

* Gross section principal stresses used for fracture analysis.
 Net section effective stresses used for fatigue analysis.
 ** Type stress--M: Maximum Principal Stress
 E: Effective Stress

Figure 2-74 FSIL CONTROL POINT 5; LOWER PLATE AND SPLICE

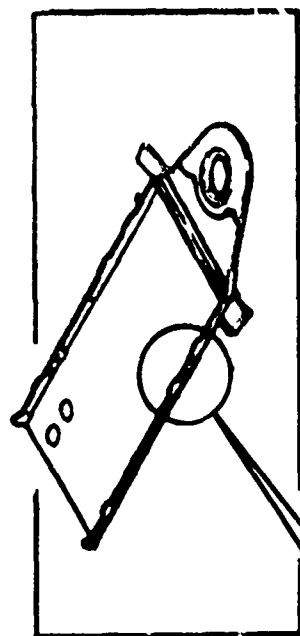


PART IDENTIFICATION	
X7223782 YF992 BHD	
LOCATION	XF29; YF992; ZF0
MATERIAL	Ti 6AL-4V (β , MA)
DAMAGE TOLERANCE CATEGORY	SAFE CRACK GROWTH
INSPECTABILITY	DEPOT LEVEL

CRACK LOCATION	ANALYSIS	GROSS SECTION ULTIMATE DESIGN STRESSES FOR ASKA CONDITIONS IN FATIGUE SPECTRUM, KSI						STRESS, KSI		ALLOWABLE	CRACK SIZE, INCHES		CRACK TYPE
		**	2	10	5	9	7	MAXIMUM SPECTRUM*	GROSS SEC LIMIT*		INITIAL	CRITICAL	
(1)	FRACTURE	M	72	44	65	65	10	40.87	48.02	N.A.	>80	>0.15	0.63 EC
	FATIGUE	E	72	44	65	65	10	48.23	N.A.	56.67	80		

* Gross section principal stresses used for fracture analysis.
 Net section effective stresses used for fatigue analysis.
 ** Type stress--M: Maximum Principal Stress
 E: Effective Stress

Figure 2-75 FSIL CONTROL POINT 6; YF 992 BULKHEAD, INBOARD



YF932

(1) CRACK LOCATION

YF935.75 .50 DIA.

X7223735 ATTACH
ANGLE



PART IDENTIFICATION

X7223735 ATTACH ANGLE

LOCATION

YF91-95; YF932; ZF0

MATERIAL

Ti 6AL-4V (β , MA)

DAMAGE TOLERANCE CATEGORY

FAIL SAFE

INSPECTABILITY

DEPOT LEVEL

CRACK LOCATION	* ANALYSIS	GROSS SECTION ULTIMATE DESIGN STRESSES FOR ASME CONDITIONS IN FATIGUE SPECTRUM, KSI					STRESS, KSI				CRACK SIZE, INCHES		CRACK TYPE	
		**	2	10	5	9	7	MAXIMUM SPECTRUM**	GROSS SEC LIMIT*	NET SECT. ULTIMATE*	ALLOWABLE	INITIAL		CRITICAL
(1) {	FRACTURE	M	51	58	38	49	-9	28.95	38.69	N.A.	} >80	} >0.15	0.94	CH
	FATIGUE	E	70	79	52	67	-13	39.71	N.A.	79.46				

* Gross section principal stresses used for fracture analysis.

Net section effective stresses used for fatigue analysis.

** Type stress--M: Maximum Principal Stress

E: Effective Stress

Figure 2-76 FSIL CONTROL POINT 7; YF 932 BULKHEAD, LOWER OUTBOARD ATTACH ANGLE

- o X7223821 - Web-Closure Rib, Outboard.
Based on gross section limit stresses below 60 ksi at localized areas; the closure rib was considered not to be fracture critical.
- o X7223822 Actuator Support Fitting
Low stress levels in the support fitting did not deem critical crack length calculations of this part.
- o X7223901 Sweep Actuator Fitting
Based on gross section limit stresses below 60 ksi, the actuator fitting was not considered critical.

9. Control Point 9, MLG Trunnion, Fittings

A survey of MLG trunnion fitting stresses indicated that these fittings are not fracture critical.

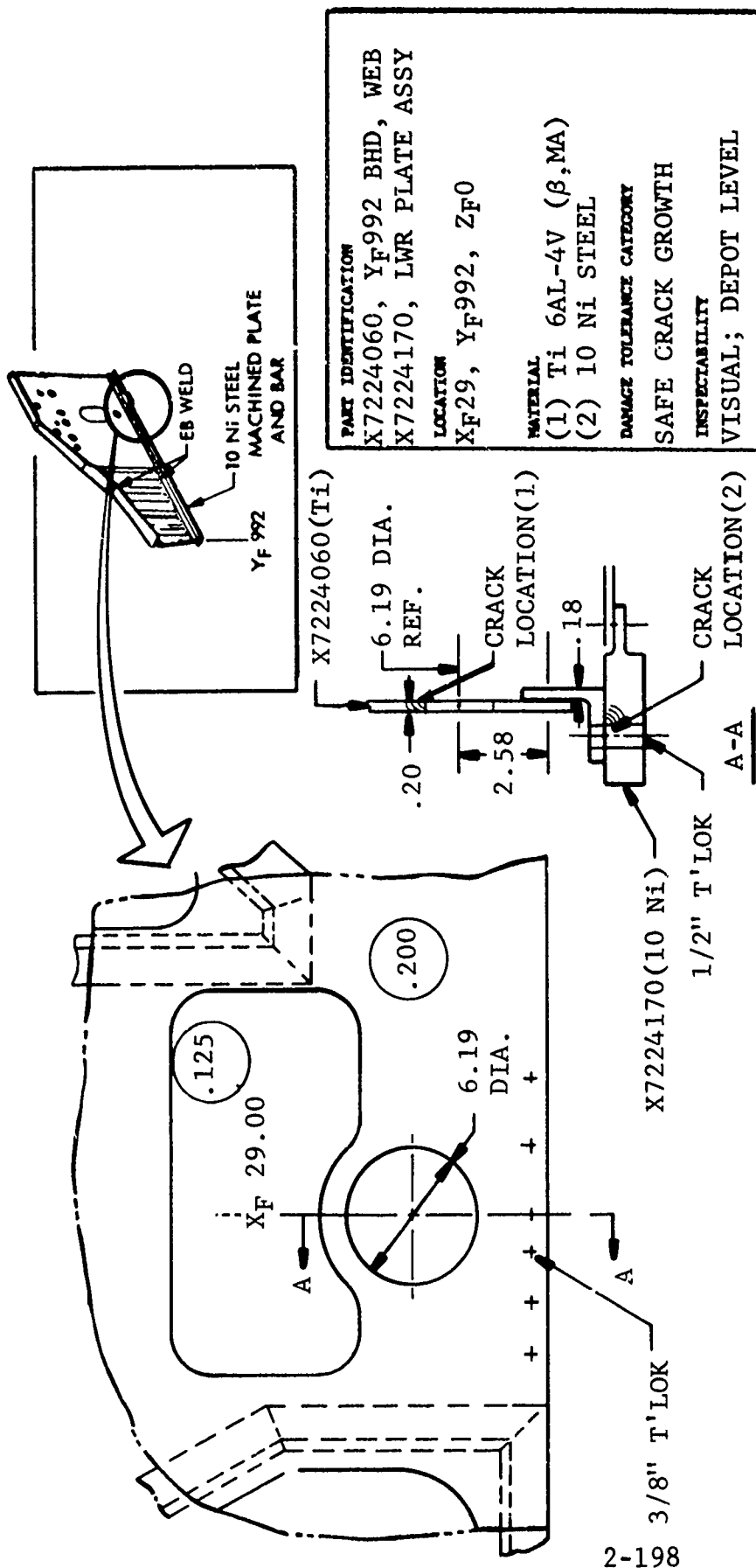
10. Control Point 10, Lower Plate, Fwd. Longerons, Outboard Lower

This control point is similar to Control Point 3. Based on lower stresses (approximately 56%) in comparison to control point 3, this area was not considered critical.

2.3.4.2 NBB Fracture Analysis

Fracture analyses were conducted on nine NBB configuration control points. A listing of these points follows.

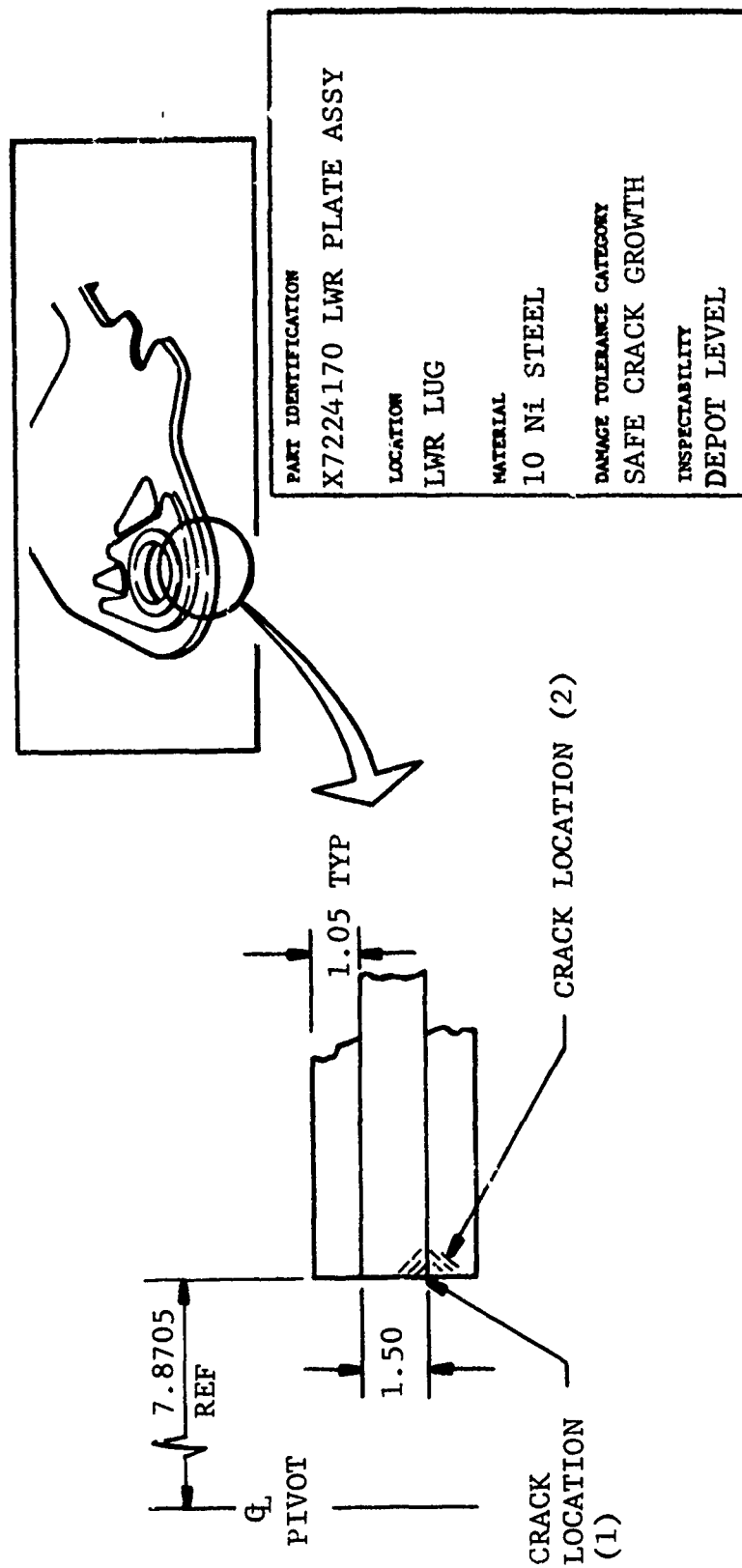
1. Control Point 1, Figure 2-77, Y_F 992 Bhd. Inboard, Fuel Transfer Hole, X_F 29.
2. Control Point 2, Figure 2-78, Lower Plate, Lug - Wing Pivot Bore
3. Control Point 3, Figure 2-79, Lower Plate, Fwd Inboard, Bolt Hole
4. Control Point 4, Figure 2-80, Lower Plate Assembly; Aft. Outboard Cutout, X_F 68-72; Y_F 992, Z_F 0
5. Control Point 5, Figure 2-81, Y_F 932 Bhd, Lower Attach Angle, X_F 65, X_F 72; Z_F 0
6. Control Point 6, Figure 2-82, Upper Lug Installation, Aft Corner, X_F 119



CRACK LOCATION	* ANALYSIS	GROSS SECTION ULTIMATE DESIGN STRESSES FOR ASKA CONDITIONS IN FATIGUE SPECTRUM, KSI							STRESS, KSI		ALLOWABLE	CRACK SIZE, INCHES		CRACK TYPE
		**	2	10	5	9	7	MAXIMUM SPECTRUM*	GROSS SEC LIMIT*	NET SECT. ULTIMATE*		INITIAL	CRITICAL	
(1)	FRACTURE	M	41.9	26.9	39.9	36.6	8.0	24.55	27.92	N.A.	> 80	>0.15	0.71	EC
	FATIGUE	E	41.9	26.9	39.9	36.6	8.0	46.62	N.A.	69.86	80	>0.15	0.71	EC
(2)	FRACTURE	M	71.9	46.2	68.6	62.9	13.8	42.18	47.96	N.A.	>150	>.015	2.89	CH
	FATIGUE	E	71.9	46.2	68.6	62.9	13.8	80.09	N.A.	120	150	>.015	2.89	CH

* Gross section principal stresses used for fracture analysis.
 Net section effective stresses used for fatigue analysis.
 ** Type stress--M: Maximum Principal Stress
 E: Effective Stress

Figure 2-77 NBB CONTROL POINT 1; YF 992 BULKHEAD, LOWER PLATE

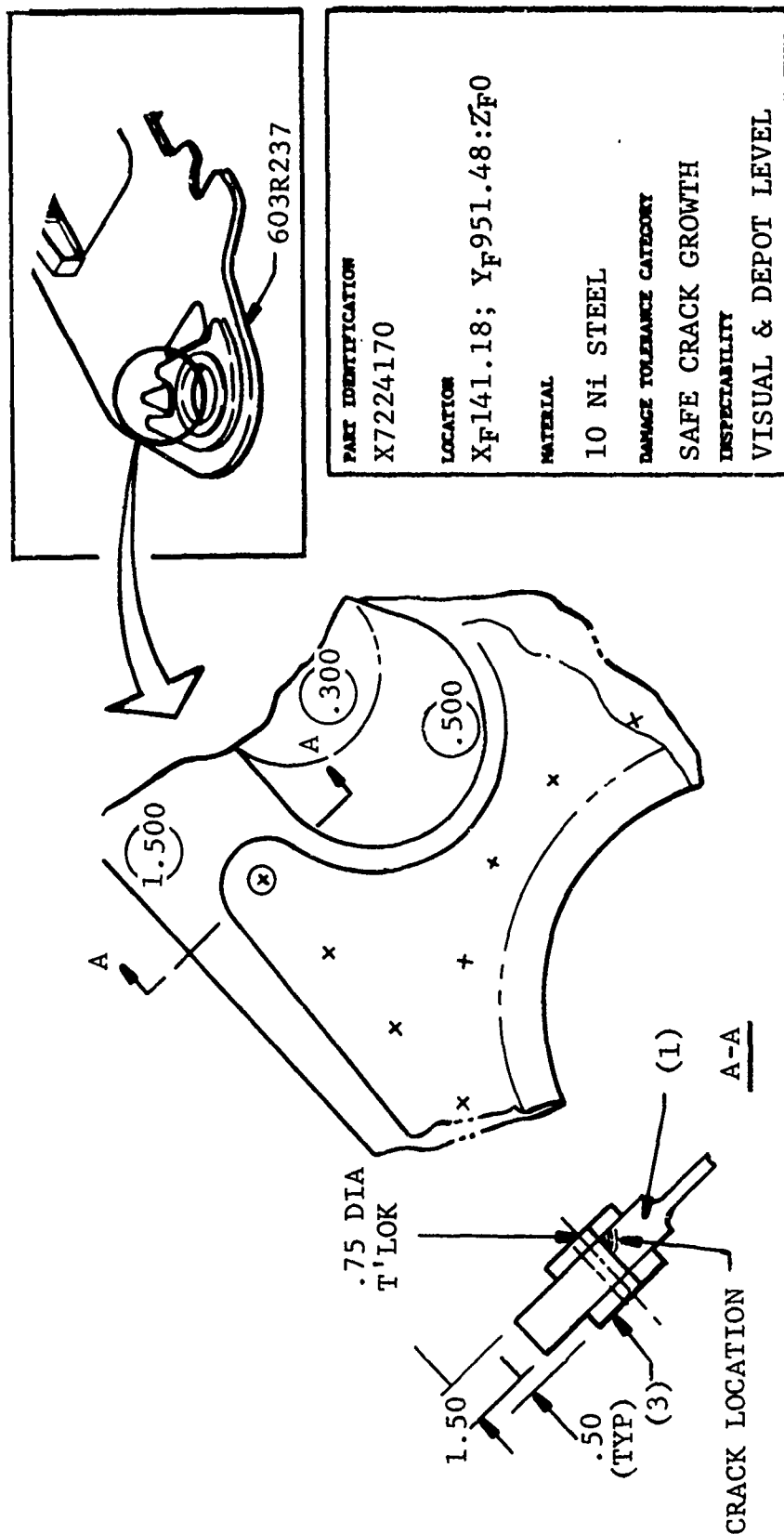


CRACK LOCATION	* ANALYSIS	GROSS SECTION ULTIMATE DESIGN STRESSES FOR ASKA CONDITIONS IN FATIGUE SPECTRUM, KSI						STRESS, KSI		ALLOWABLE	CRACK SIZE, INCHES		CRACK TYPE
		**	m	e	10	5	9	7	MAXIMUM SPECTRUM*	GROSS SEC LIMIT*	NET SECT. ULTIMATE*	INITIAL	CRITICAL
(1)	FRACTURE	137	35	140	118	4	86	93	N.A.	-	#	#	EC
(2)	FATIGUE	110	47	109	97	-6	67	N.A.	110	131	-	-	-

* Local gross section principal stresses used for fracture analysis.
Average net section effective stresses used for fatigue analysis.
** Type Stress . . . m: local max principal stress
e: average net section effective stress

Fine grid analysis not complete.

Figure 2-78 NBB CONTROL POINT 2; LOWER LUG, AFT

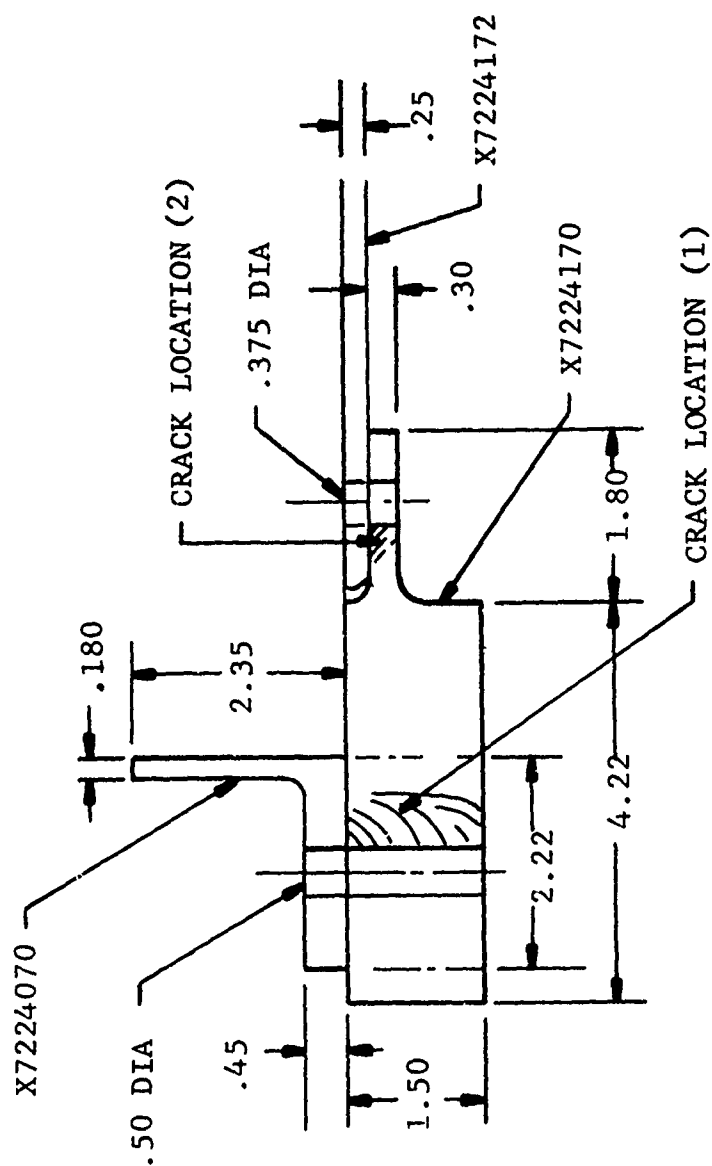


PART IDENTIFICATION	
X7224170	
LOCATION	XF141.18; YF951.48; ZF0
MATERIAL	10 Ni STEEL
DAMAGE TOLERANCE CATEGORY	SAFE CRACK GROWTH
INSPECTABILITY	VISUAL & DEPOT LEVEL

CRACK LOCATION	* ANALYSIS	GROSS SECTION ULTIMATE DESIGN STRESSES FOR ASKA CONDITIONS IN FATIGUE SPECTRUM, KSI							STRESS, KSI			CRACK SIZE, INCHES		CRACK TYPE
		**	2	10	5	9	7	MAXIMUM SPECTRUM**	GROSS SEC LIMIT*	NET SECT. ULTIMATE*	ALLOWABLE	INITIAL	CRITICAL	
(1)	FRACTURE	M	114	121	100	106	-16	64.71	80.71	N.A.	>150	>.15	>4.0	CH
	FATIGUE	E	113	121	99	105	16	77.65	N.A.	145.2	150			

* Gross section principal stresses used for fracture analysis.
 Net section effective stresses used for fatigue analysis.
 ** Type stress--M: Maximum Principal Stress
 E: Effective Stress

Figure 2-79 NBB CONTROL POINT 3; LOWER PLATE, LUG

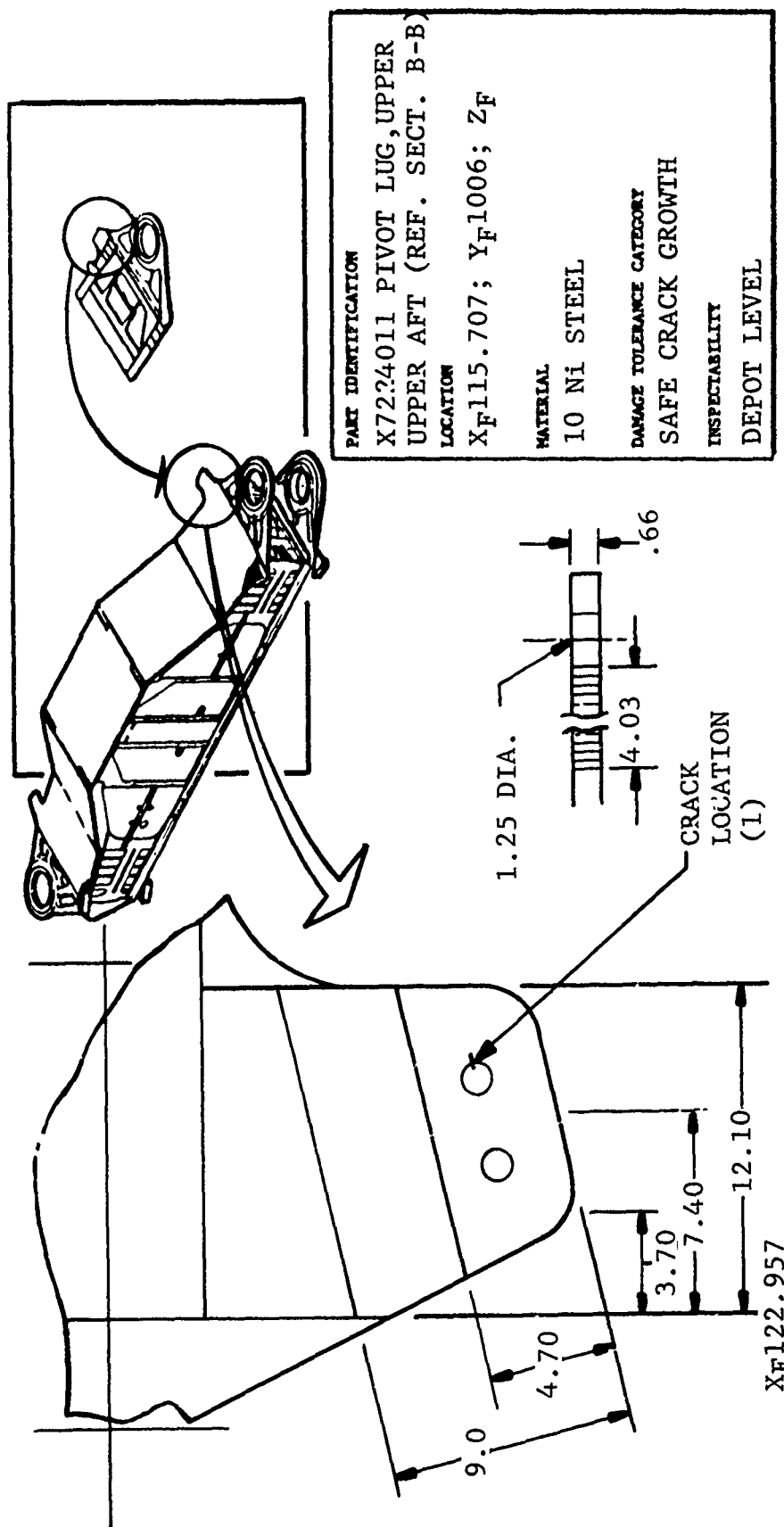


PART IDENTIFICATION	
X7224170 LWR PLATE ASSY	
X7224172 LWR PLATE, WEB	
LOCATION	
X _F 68; Y _F 992; Z _F 0	
MATERIAL	
10 NI STEEL	
DAMAGE TOLERANCE CATEGORY	
SAFE CRACK GROWTH	
INSPECTION	
DEPOT LEVEL	

CRACK LOCATION	* ANALYSIS	GROSS SECTION ULTIMATE DESIGN STRESSES FOR ASKA CONDITIONS IN FATIGUE SPECTRUM, KSI							STRESS, KSI				CRACK SIZE, INCHES		CRACK TYPE
		**	2	10	5	9	7	MAXIMUM SPECTRUM*	GROSS SEC LIMIT*	NET SECT. ULTIMATE*	ALLOWABLE	INITIAL	CRITICAL		
(1)	FRACTURE	M	127.1	60.5	122.7	110.5	14.9	75.37	84.78	N.A.	>150	>.15	>1.82	CH	
(2)	FATIGUE	E	125.4	59.6	121.0	108.7	20.2	88.94	N.A.	150	150	>.15	0.92	SC	

* Gross section principal stresses used for fracture analysis.
 Net section effective stresses used for fatigue analysis.
 ** Type stress--M: Maximum Principal Stress
 E: Effective Stress

Figure 2-80 NBB CONTROL POINT 4; LOWER PLATE, AFT OUTBOARD CUTOUT



PART IDENTIFICATION	
X7224011 PIVOT LUG, UPPER	
UPPER AFT (REF. SECT. B-B)	
LOCATION	XF115.707; YF1006; ZF
MATERIAL	10 Ni STEEL
DAMAGE TOLERANCE CATEGORY	SAFE CRACK GROWTH
INSPECTABILITY	DEPOT LEVEL

CRACK LOCATION	* ANALYSIS	GROSS SECTION ULTIMATE DESIGN STRESSES FOR ASKA CONDITIONS IN FATIGUE SPECTRUM, KSI							STRESS, KSI				CRACK SIZE, INCHES		CRACK TYPE
		**	2	10	5	9	7	MAXIMUM SPECTRUM*	GROSS SEC LIMIT*	NET SECT. ULTIMATE*	ALLOWABLE	INITIAL	CRITICAL		
{ (1) }	FRACTURE	M	-84.8	84.8	-85.7	-44.4	31.3	37.0	56.6	N.A.	>150	>.15	>4.0	CH	
	FATIGUE	E	107.4	86.0	103.0	91.4	29.8	49.8	N.A.	114	150				

* Gross section principal stresses used for fracture analysis.
 Net section effective stresses used for fatigue analysis.
 ** Type stress--M: Maximum Principal Stress
 E: Effective Stress

Figure 2-82 NBB CONTROL POINT 6; NBB UPPER AFT, OUTBOARD

7. Control Point 7, X7224130 X_F 84 Rib Assembly

A survey of maximum gross section stresses indicated very low stress distributions in the X_F 84 rib. The maximum limit stress was 25 ksi. The rib assembly was not considered fracture critical.

8. Control Point 8, X7224030 X_F 119 Closure Rib Assembly

A survey of stress levels in the closure rib indicated low stress distributions. The areas considered for this analysis are loaded by the sweep actuator fitting support attachment bolts and are therefore primarily loaded in shear. The maximum gross limit stress in the closure rib is 66 KSI.

9. Control Point 9, X7224170 Lower Plate, Forward Outboard Cutout; X_F 68-72; Y_F 940

This area is similar to control point 4. Since stress levels were lower than at Y_F 992 (control point 4) this area was not considered a primary control point.

2.3.5 Fracture Control Plan

The fracture control plan was prepared and published (FZM-6068, 1 Feb. 1973) during Phase Ib. A brief overview of the plan was presented in the AMAVS Phase Ib Technical Report. During Phase II, steps were taken to implement the Fracture Control Plan prior to start of production. The Fracture Critical Parts List, Figure 2-83, was updated and the detailed Traceability requirements, Figure 2-84, were defined.

2.3.6 Finite Element Fracture Analysis

2.3.6.1 The Assumed Stress Hybrid-Model Finite Element Method

The computer procedure (Convair code name UD1) based on the assumed stress hybrid-model finite element method for fracture mechanics analysis has been completely programmed and checked out. Improvements have also been made in efficiency, versatility, and applicability of the computer procedure during the Phase II reporting period of the AMAVS Program. The computer procedure calculates the crack tip stress intensity factors, then the nodal displacements, and finally the element stresses. For the assumed stress hybrid-model elements, element stresses at four corners are

FSIL Configuration

X7223730-1	Lower Plate Assembly
31-1/2	" " Brazed Assembly
32-7	" " Doubler
33-7	" " Web
34-7	" Lug Doubler
35-7/-8,-9/-10	Y _F 932 & Y _F 992 BHD Attach Angles
36-7/-8,-9/-10	Y _F 932 & Y _F 992 Gussets
37-7	Lower Plate \bar{C} Splice
X7223850-7/-8	Closure Rib Attach Angle
51-7/-8	O.B. Aft Longerons Adapter
52-7/-8	Fwd Lower O.B. Longerons Fitting
X7223751-7/-8	Y _F 932 BHD Web, O.B.
X7223752-7/-8	Y _F 932 BHD Web, X _F 39-84
X7223765-7/-8	Y _F 947 BHD Lower Beam
X7223781-7/-8	Y _F 992 BHD Web O.B.
82-7/-8	Y _F 992 BHD Web X _F 35-84
83-7/-8	Y _F 992 BHD Web I.B.
X7223710-1/-2	Upper Lug/Plate Weld Assembly
11-7/-8	Upper Lug
12-7/-8	Upper Plate - O.B. Fwd
13-7/-8	Upper Plate - O.B. Aft
14-7/-8	Upper Plate - O.B. Ctr
X7223853-7/-8	Fwd Upper O.B. Longerons Fitting
X7223821-7/-8	Web - Closure Rib
22-7/-8,-9/-10	Support - Actuator, Closure Rib

No-Box Box Configuration

X7224011-7/-8	Pivot Lug - Upper
60-1/-2	Y _F 992 Bhd Assembly
61-7/-8	Y _F 992 Bhd-Inboard Web
70-7/-8	Y _F 992 Bhd-Outboard Segment (Machined)
71-1/-2	Y _F 992 Bhd-Outboard Segment (Welded)
73-7/-8	Y _F 992 Bhd-Outboard Lower Cap
75-7/-8	Y _F 992 Bhd-Outboard Web
77-7	Y _F 992 Bhd-Inboard Lower Cap
65-7/-8	Y _F 992 Bhd-Lower Cap Splice
X7224080-1/-2	Y _F 932 Bhd Assembly
90-7/-8	Y _F 932 Bhd - Outboard Segment (Machined)
91-1/-2	" " " " " (Welded)
93-7/-8	" " " " Lower Cap
95-7/-8	" " " " Web
97-7	" " " - Inboard Lower Cap
85-7/-8	" " " - Outboard Gusset
87-7/-8	" " " - Lower Cap Splice

Figure 2-83 FRACTURE CRITICAL PARTS LIST

No-Box Box Configuration (Continued)

X7224155-7/-8	Longeron Fitting - Upper Forward
X7224170-1/-2	Lower Plate Assembly
72-7/-8	" " Panel XF 39-84
73-7/-8	" " " XF 39R-39L
75-7/-8	Pivot Lug Lower
76-7/-8	" " " - Reinforcement
77-7	Lower Plate Splice - YF 992
78-7	Lower Plate Splice - YF 932
X7224180-7/-8	Beam, MLG Drag Brace YF 947
X7224141-7/-8	Closure Rib (Machined)
43-7/-8, -9/-11	Closure Rib (Details)
44-7/-8	Support - Actuator, Closure Rib Inbd.
47-7/-8	" " " " Outbd.

Fittings

X7223900-1/-2	Wing Sweep Actuator Support Assy.
01-7/-8	" " " " "
11-1/-2	MLG Drag Strut Support Assy
12-7/-8	" " " " Inbd. Lug
13-7/-8	" " " " Outbd. Lug
14-7/-8	" " " " Extensions
15-7/-8	" " " " Splice
X7223920-1/-2	" " " Side Brace Support Assy.
21-7/-8	" " " " " Outbd Lug
22-7/-8, -9/10	" " " " " Web
23-7/-8	" " " " " Beam
X7223930-7/-8	" " " Trunnion XF 72
32-7/-8	" " " Cap XF 72
31-7/-8	" " " Trunnion XF 95.5

Figure 2-83 FRACTURE CRITICAL PARTS LIST (Continued)

APPLICATION			REVISIONS																																		
NEXT ASSY	USED ON	LTR	DESCRIPTION	DATE	APPROVED																																
<p>This drawing establishes the traceability requirements for Advanced Metallic Air Vehicle Structure parts when specifically called for on the Engineering Drawing.</p> <ol style="list-style-type: none"> 1. Raw Material Information Material for parts that require traceability will be purchased to specifications that define all traceability information which must be supplied by the producer. 2. Material Storage Materials procured specifically for the AMAVS program requiring material traceability will be stored separately from materials procured for other programs. 3. Material Allocation Plan (MAP) A material allocation plan (MAP) will be prepared by AMAVS Engineering for each sheet, plate or bar of incoming material requiring material traceability. 4. Material Serial Numbers The MAP will assign each piece of incoming material a serial number coded as follows: <div style="margin-left: 40px;"> <div style="display: inline-block; text-align: center; vertical-align: middle;"> X ↑ Material Code </div> <div style="display: inline-block; text-align: center; vertical-align: middle; margin-left: 20px;"> X ↑ Heat Number Code </div> <div style="display: inline-block; text-align: center; vertical-align: middle; margin-left: 20px;"> X ↘ Sheet, Plate or Bar Number </div> </div>																																					
			<table border="1" style="width: 100%; border-collapse: collapse;"> <tr> <td style="width: 15%;">REV</td> <td style="width: 15%;">-</td> <td style="width: 15%;">-</td> <td style="width: 15%;"></td> <td style="width: 15%;"></td> </tr> <tr> <td>SH</td> <td>1</td> <td>2</td> <td></td> <td></td> </tr> </table>			REV	-	-			SH	1	2																								
REV	-	-																																			
SH	1	2																																			
			REVISION STATUS OF SHEETS																																		
<p>UNLESS OTHERWISE SPECIFIED DIMENSIONS ARE IN INCHES TOLERANCES ON FRACTIONS DECIMALS ANGLES ± .XX ± .XXX ±</p>			<table border="1" style="width: 100%; border-collapse: collapse;"> <tr> <td style="width: 20%;">DRAFTSMAN <i>J. E. Stern</i></td> <td style="width: 20%;">DATE <i>7-10-73</i></td> <td colspan="2" style="text-align: center;">U.S. AIR FORCE</td> </tr> <tr> <td>CHECKER <i>D. J. Bostick</i></td> <td><i>8-10-73</i></td> <td colspan="2" rowspan="2" style="text-align: center;"> Figure 2-84 Material Traceability Requirements for the AMAVS Program </td> </tr> <tr> <td>ENGINEER <i>N. J. Kelly</i></td> <td><i>8/10/73</i></td> </tr> <tr> <td colspan="2">A F PROJ ENGR</td> <td colspan="2"></td> </tr> <tr> <td colspan="2">CONTRACT NO F33615-73-C-3001</td> <td colspan="2"></td> </tr> <tr> <td colspan="2">A F DESIGN ACTIVITY AUTHENTICATION</td> <td colspan="2"></td> </tr> <tr> <td colspan="2" style="vertical-align: bottom;"><i>E. K. ...</i></td> <td> <table border="1" style="width: 100%; border-collapse: collapse;"> <tr> <td style="width: 15%;">SIZE A</td> <td style="width: 35%;">AF CODE IDENT NO. 07878</td> <td style="width: 50%;">DRAWING NO. X7224199</td> </tr> </table> </td> </tr> <tr> <td colspan="2"></td> <td>SCALE</td> <td>SHEET 1 of 2</td> </tr> </table>			DRAFTSMAN <i>J. E. Stern</i>	DATE <i>7-10-73</i>	U.S. AIR FORCE		CHECKER <i>D. J. Bostick</i>	<i>8-10-73</i>	Figure 2-84 Material Traceability Requirements for the AMAVS Program		ENGINEER <i>N. J. Kelly</i>	<i>8/10/73</i>	A F PROJ ENGR				CONTRACT NO F33615-73-C-3001				A F DESIGN ACTIVITY AUTHENTICATION				<i>E. K. ...</i>		<table border="1" style="width: 100%; border-collapse: collapse;"> <tr> <td style="width: 15%;">SIZE A</td> <td style="width: 35%;">AF CODE IDENT NO. 07878</td> <td style="width: 50%;">DRAWING NO. X7224199</td> </tr> </table>	SIZE A	AF CODE IDENT NO. 07878	DRAWING NO. X7224199			SCALE	SHEET 1 of 2
DRAFTSMAN <i>J. E. Stern</i>	DATE <i>7-10-73</i>	U.S. AIR FORCE																																			
CHECKER <i>D. J. Bostick</i>	<i>8-10-73</i>	Figure 2-84 Material Traceability Requirements for the AMAVS Program																																			
ENGINEER <i>N. J. Kelly</i>	<i>8/10/73</i>																																				
A F PROJ ENGR																																					
CONTRACT NO F33615-73-C-3001																																					
A F DESIGN ACTIVITY AUTHENTICATION																																					
<i>E. K. ...</i>		<table border="1" style="width: 100%; border-collapse: collapse;"> <tr> <td style="width: 15%;">SIZE A</td> <td style="width: 35%;">AF CODE IDENT NO. 07878</td> <td style="width: 50%;">DRAWING NO. X7224199</td> </tr> </table>	SIZE A	AF CODE IDENT NO. 07878	DRAWING NO. X7224199																																
SIZE A	AF CODE IDENT NO. 07878	DRAWING NO. X7224199																																			
		SCALE	SHEET 1 of 2																																		

REVISIONS			
SYM	DESCRIPTION	DATE	APPROVED
<p>4. (Cont)</p> <p>The serial number shall be marked on incoming material prior to being placed in storage. The marking procedure will be specified on the MAP.</p> <p>4.1 Material Codes:</p> <ul style="list-style-type: none"> A - Beta Annealed 6Al-4V titanium B - 2024 or 2124 aluminum alloys C - 10 Nickel Steel D - Beta C titanium E - 7050 aluminum <p>4.2 Heat Number Code</p> <p>For each material, successive heats will be coded consecutively starting with the number one (1). Quality Assurance will maintain a record that correlates heat number and code number. The vendor and the full heat number will be recorded on the MAP.</p> <p>4.3 Sheet, Plate or Bar Number</p> <p>For each heat of material, each sheet, plate and/or bar will be consecutively numbered starting with the number one (1).</p> <p>5. Part Traceability Number</p> <p>Part traceability number is the piece serial number defined in step 4 along with the item number to identify the specific part, i.e.:</p> <div style="margin-left: 40px;"> <p><u>X - X - X</u> - X</p> <p>Piece S/N Item Number</p> </div> <p>This traceability number must be marked on the part during layout for the first cut operation and prior to material release.</p> <p>6. Material Release</p> <p>Production planning for traceable parts will specifically refer to the part traceability number as designated by the MAP. Material release for production of traceable parts will be by part traceability number.</p> <p>7. Maintenance of Part Traceability Number</p> <p>The part traceability number must be maintained on the part through all stages of manufacture and assembly. Loss of this identification at any stage of manufacture is cause for rejection of the part.</p> <p>8. Traceability Records</p> <p>For each traceable part, complete data documenting the heat number, material certification, production planning, inspection records, processing data sheets, discrepancy reports, etc., will be recorded, collected and maintained by Quality Assurance. These records will provide complete traceability from raw material through the completed assembly.</p>			

Figure 2-84 Sheet 2

CODE IDENT NO.	SIZE	Material Traceability Requirements for the AMAVS Program
07878	A	
SCALE	2-208	SHEET 2 of 2

calculated and printed. Triangular elements and general quadrilateral elements are based on conventional displacement assumptions and only the average stresses within the elements are calculated and printed. The computer procedure UDI was re-programmed to improve the overall efficiency in the following areas: (1) the maximum number of nodes in a structural simulation was increased from 250 to 350, (2) the maximum node separation was increased from 28 to 35, and (3) the solution algorithm of the program was improved.

2.3.6.2 Design Analysis by Computer Procedure UDI

In addition to a number of fracture analysis problems which have been reported in the First and Second Interim Reports of the AMAVS Program (AFFDL-TR-73-1 and AFFDL-TR-73-77), the following problems have been solved during Phase II, Final Design.

- (1) A four-bay brazed lower plate with a center crack under uniform tension was analyzed. The stiffened panel shown in Figure 2-85 has a center crack in the web material with the center stiffener still remains intact. Figure 2-85 also shows the variation of crack tip stress intensity, K_I , versus half crack length, a . The center stiffener is assumed to be completely delaminated from the web material in the analysis.
- (2) A fracture analysis was conducted on the brazed lower plate specimen, Drawing 603FTB035 "D". The test specimen is composed of a 0.5 inch web and two 0.6 inch stiffener panels brazed to the web plate. External loads of $P = 2000$ kips are applied to the structure along a line which is 4° off the centerline of the structure as shown in Figures 2-86 and 2-87.

The finite element simulation is composed of hybrid-model finite elements, triangular elements and general quadrilateral elements. A typical finite element simulation of the test specimen is shown in Figure 2-88. Note that a crude simulation was used for the test fixtures. K_I and K_{II} were calculated at both crack tips and stresses were calculated throughout the entire panel. The following fracture analyses were made:

- (1) A thru-crack embedded in the second bay of the lower panel specimen was analyzed. Figure 2-86 shows the structural arrangement as well as results from UDI analyses with $a = 2$ inch, 4 inch, 5 inch and 6 inch. Both K_I and K_{II} vs. a were plotted in Figure 2-86. Note that the values plotted are for the crack tip on the right-hand side which are slightly greater than K_I

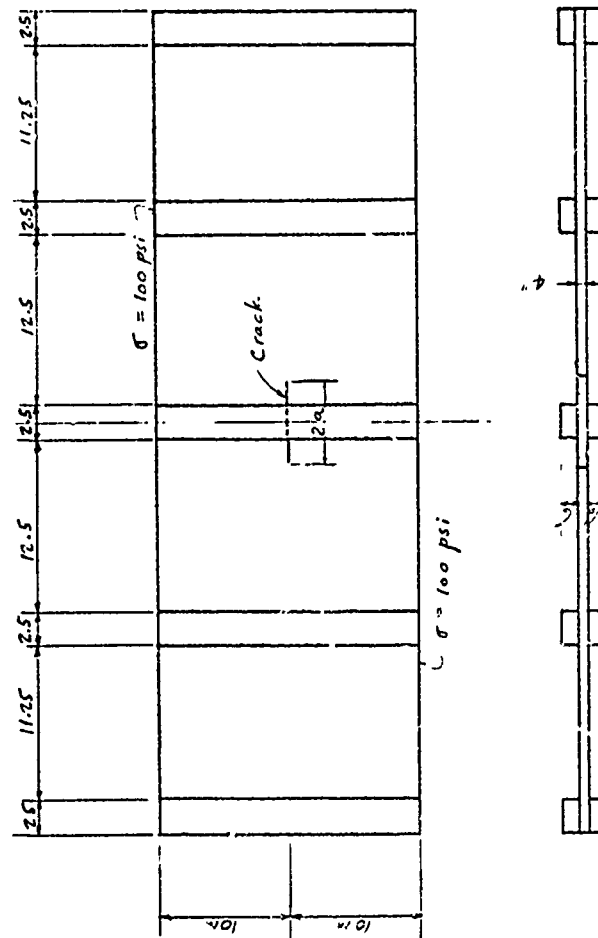
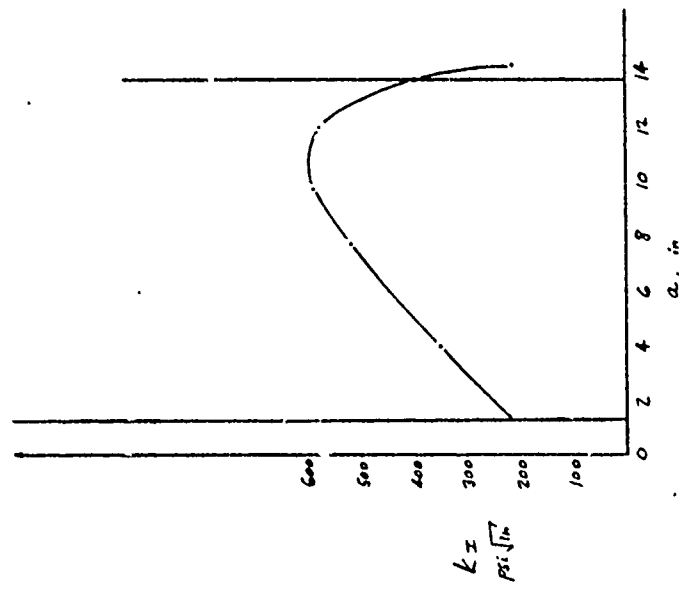


Figure 2-85 A FOUR BAY BRAZED PNL WITH A CENTER CRACK UNDER UNIFORM TENSION

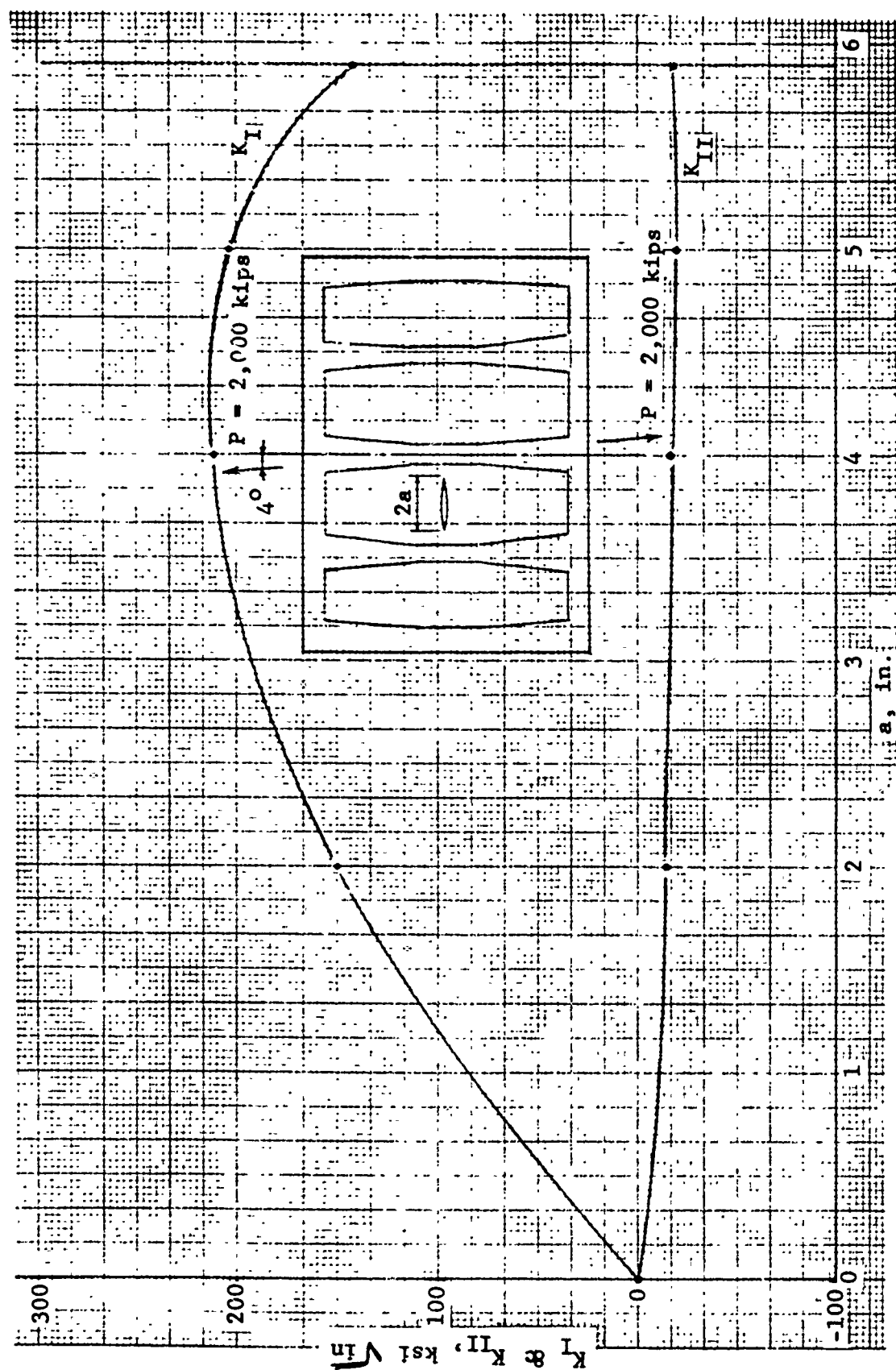


Figure 2-86 K_I and K_{II} vs. a of an Eccentrically Cracked Lower Panel Specimen

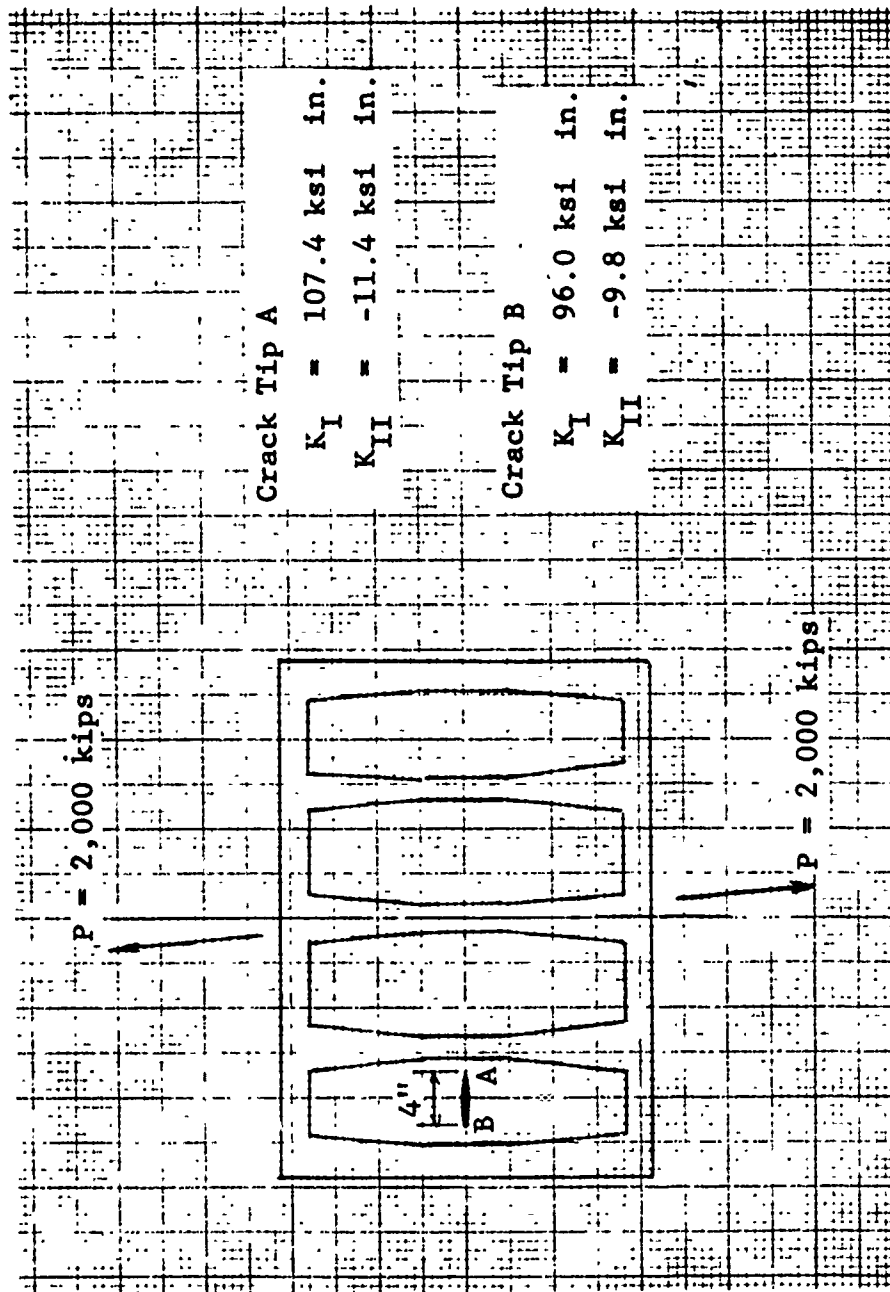


Figure 2-87 A Thru Crack Embedded in the First Bay of the Lower Panel Specimen

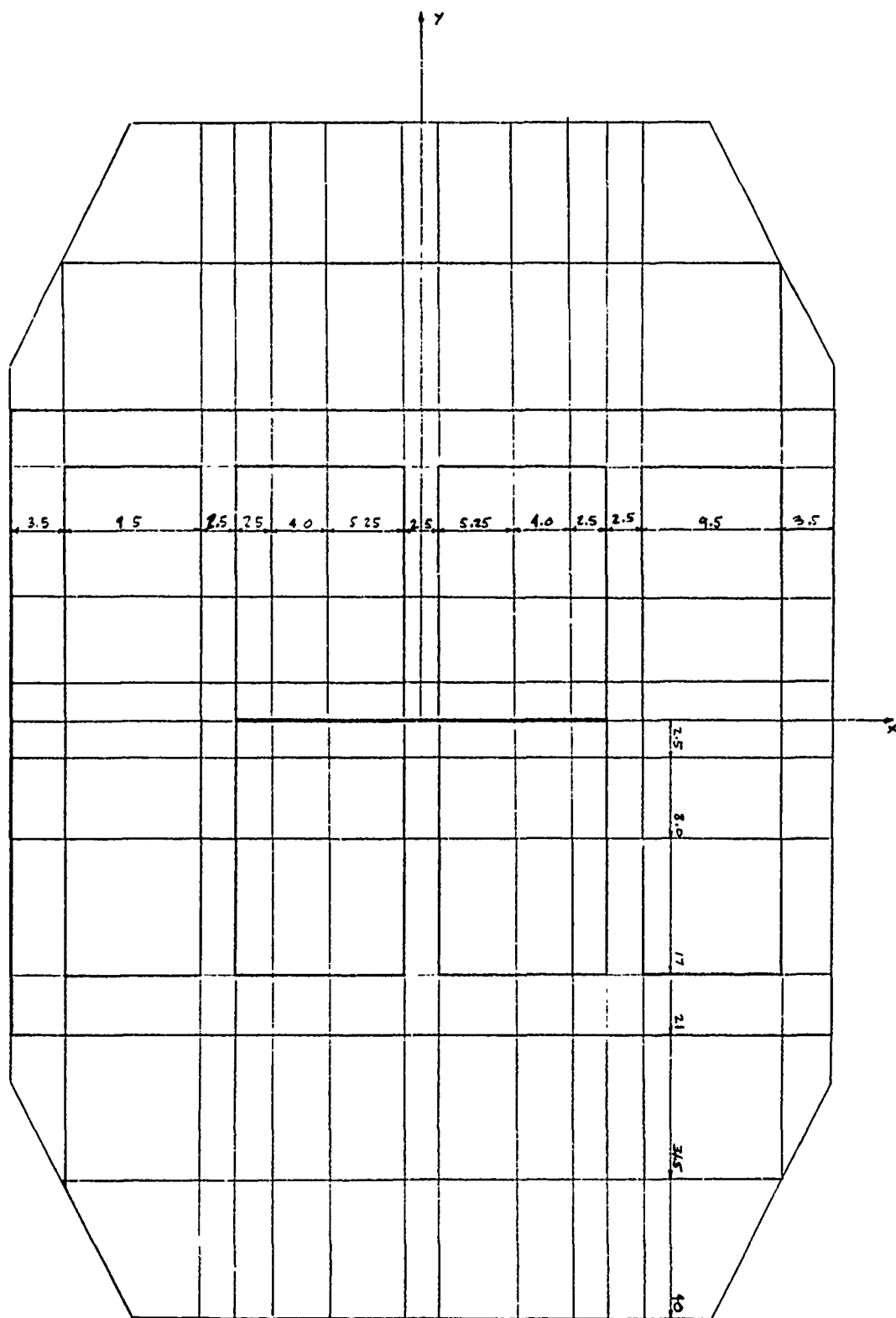


Figure 2-89 A TYPICAL FINITE ELEMENT SIMULATION OF THE BRAZED LOWER PLATE SPECIMEN

and K_{II} of the crack tip on the left-hand side due to the eccentricity of the crack.

(2) A thru crack embedded in the first bay was analyzed. Only one problem was solved for a 4 inch crack. The results are shown in Figure 2-87.

(3) A center thru-crack embedded in the lower panel test specimen was analyzed. The structural arrangement and the results of K_I and K_{II} vs. a computed by UD1 are shown in Figure 2-89.

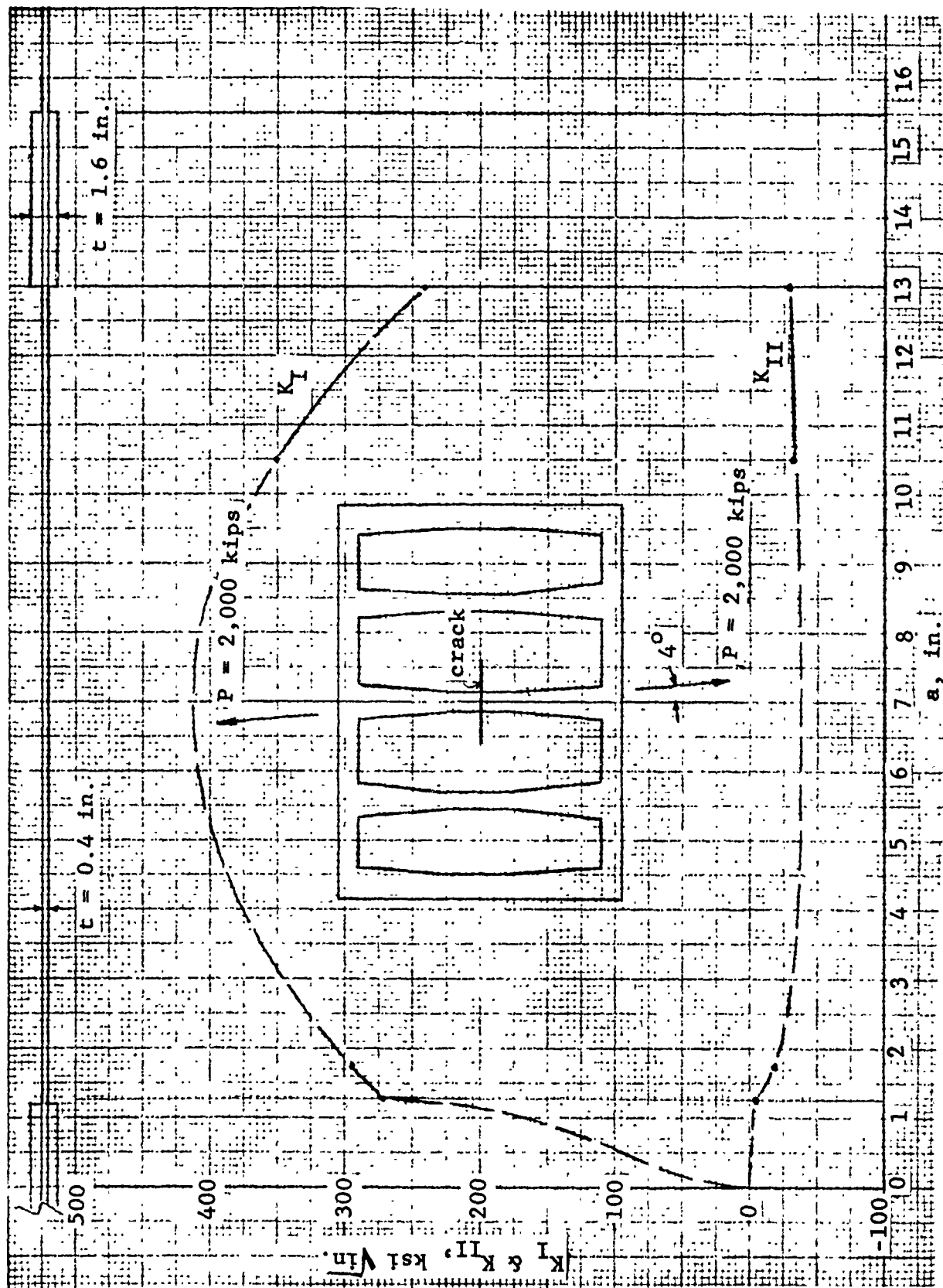


Figure 2-89 K_I and K_{II} vs. a of A Center Cracked Lower Panel Specimen

2.3.7 Fatigue Life Variability

The fatigue life variability of the following materials was evaluated:

- 10 Ni Steel Plate
- Beta Annealed 6Al-4V Titanium Plate
- Beta C Sheet
- Silver-Brazed Beta Annealed 6Al-4V Titanium

For each material, a series of 20 specimens was flight-by-flight fatigue tested to establish the fatigue life distribution. The resulting test data (Figures 2-90 thru 2-93) were analyzed using maximum likelihood estimates (MLE) methods to determine the Weibull parameters. The shape parameter, α , is a measure of the degree of variability and the characteristic life, β , is the number of flights for a 63.2% failure rate as defined by the untruncated Weibull distribution function:

$$F(t) = 1 - \exp [-(t/\beta)^\alpha]$$

where t = the fatigue life in cycles

$F(t)$ = the fatigue life distribution

The test results indicate that Beta Annealed 6Al-4V Titanium and 10 Ni Steel have virtually identical characteristic fatigue lives when fatigue cycled to the same percentage of F_{tu} , 6126 and 6060 flights, respectively. However, the fatigue scatter was greater for 10 Ni Steel ($\alpha = 2.05$) than for the 6-4 Titanium ($\alpha = 3.06$). The characteristic fatigue life of Beta C, 2601 flights, was significantly lower than that of Ti 6Al-4V (β , MA) using the same stress spectrum, despite the greater strength of the Beta C ($F_{tu} = 185$ KSI for Beta C vs 125 KSI for 6-4 Titanium). However, there was less scatter in the fatigue data for Beta C ($\alpha = 5.86$) than for 10 Ni Steel or Ti 6Al-4V (β , MA).

For silver alloy brazed pairs of Ti 6Al-4V (β , MA), the fatigue life variability ($\alpha = 7.96$), and the characteristic life ($\beta = 4563$ flights) were significantly lower than observed in single ply specimens. This was attributed to first-of-two type failures of parallel elements which tend to reduce scatter and decrease life. The decreased fatigue life was predicted to be 4803 flights for random pairs taken from the 20 single-ply specimens. Thus, most of the decrease in fatigue life can be attributed to a first-of-two failure mode as opposed to a degradation in fatigue strength due to brazing.

The fatigue life variability data were used to conduct a cursory evaluation of the two WCTS designs using the Whittaker reliability analysis model presented in AFML-TR-69-65. For the NBB, a location with a computed fatigue damage ($\sum n/N$) of .061, the reliability in a four-service life test program is .60. If there were four such points in the WCTS (i.e. with computed damage $\geq .061$) the computed reliability would be .36. For a fleet of 200 aircraft, the time to first failure would be 91 flights with a 50% probability. These predictions are considered unsatisfactory and are attributed to extrapolation of the Weibull plot to failure values not observed in the test program.

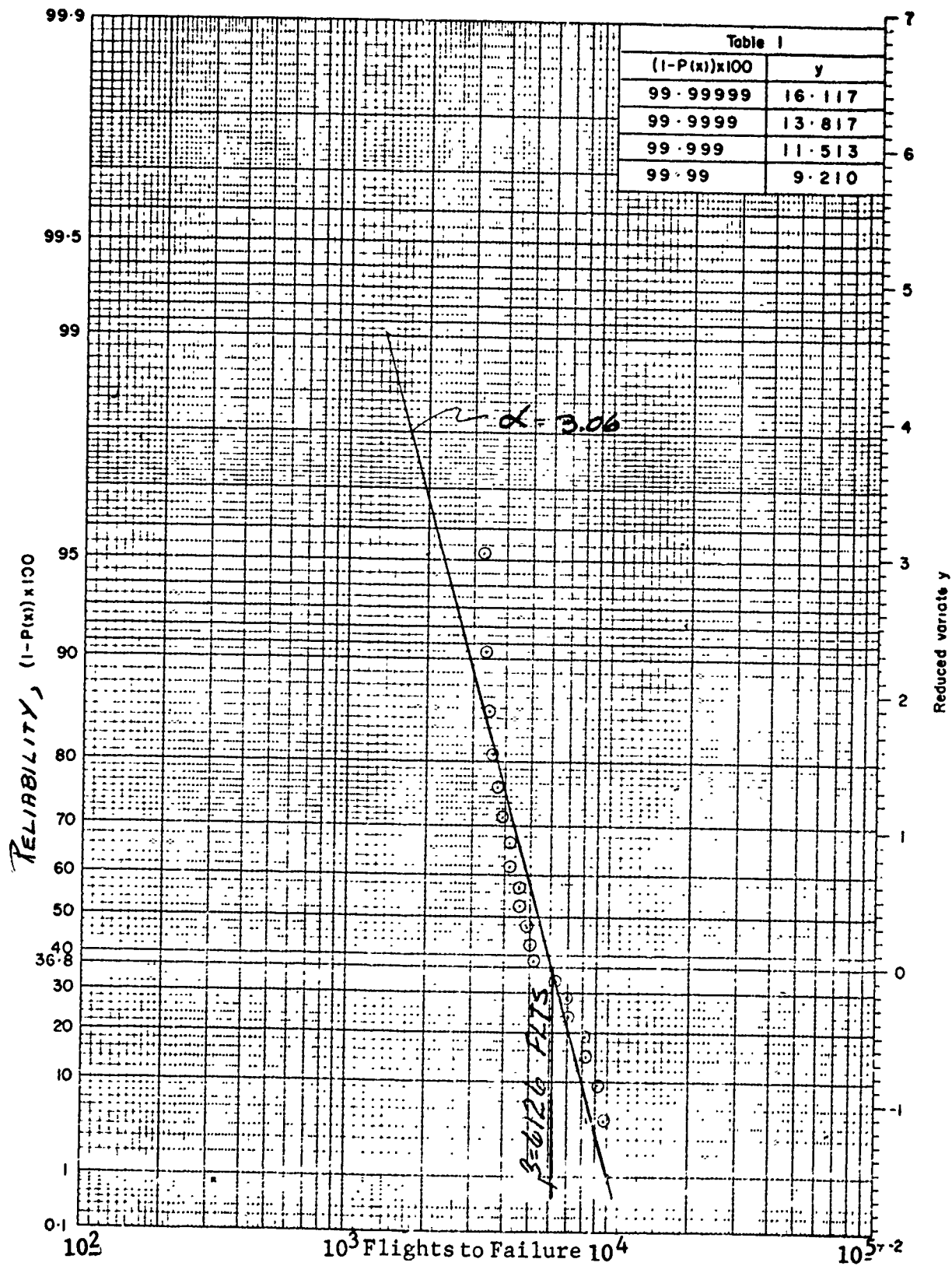


Figure 2-90 WEIBULL PLOT OF BETA ANNEALED 6AL-4V TITANIUM RELIABILITY TEST DATA

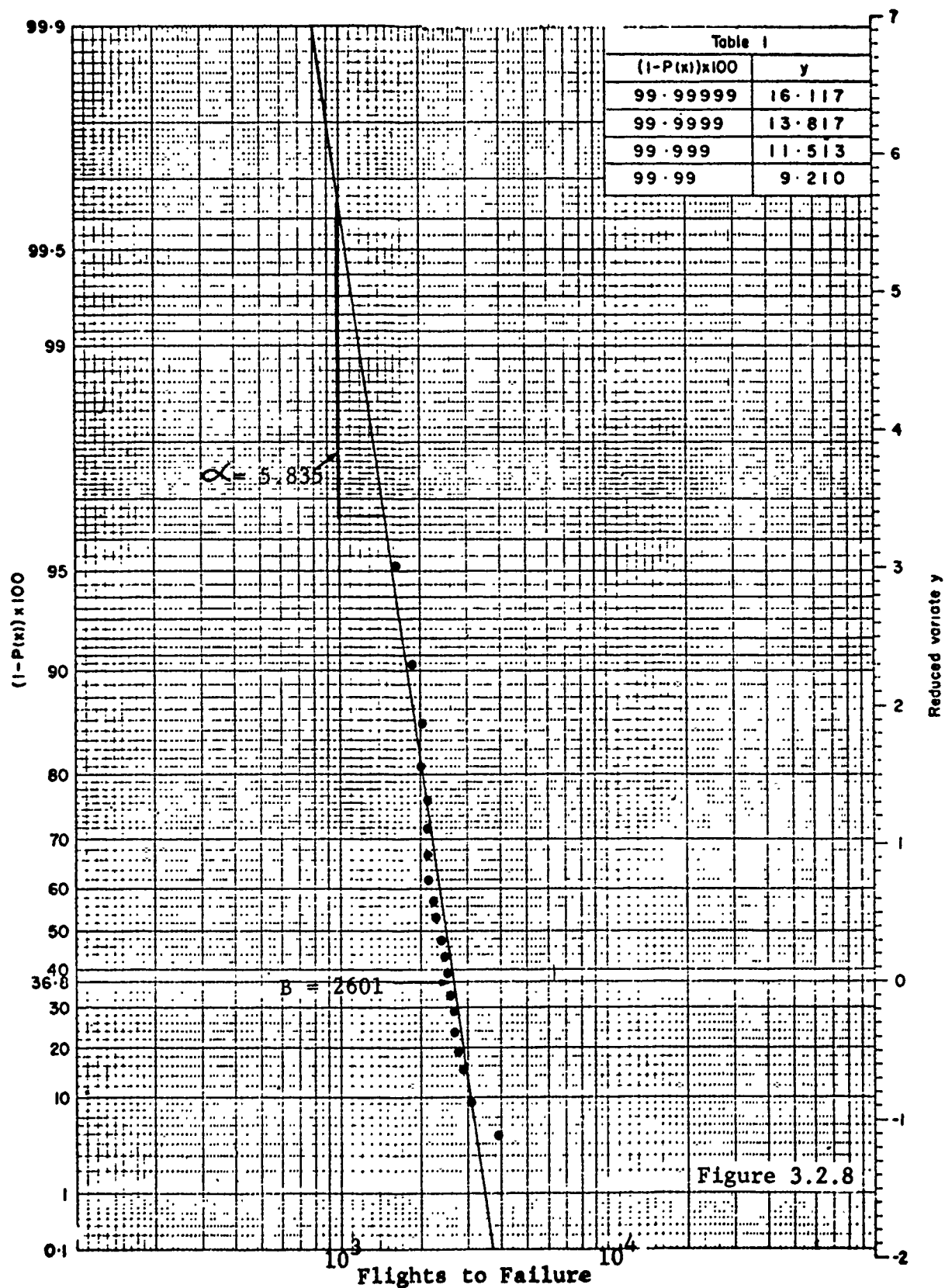


Figure 2-91 WEIBULL PLOT OF BETA C RELIABILITY TEST DATA

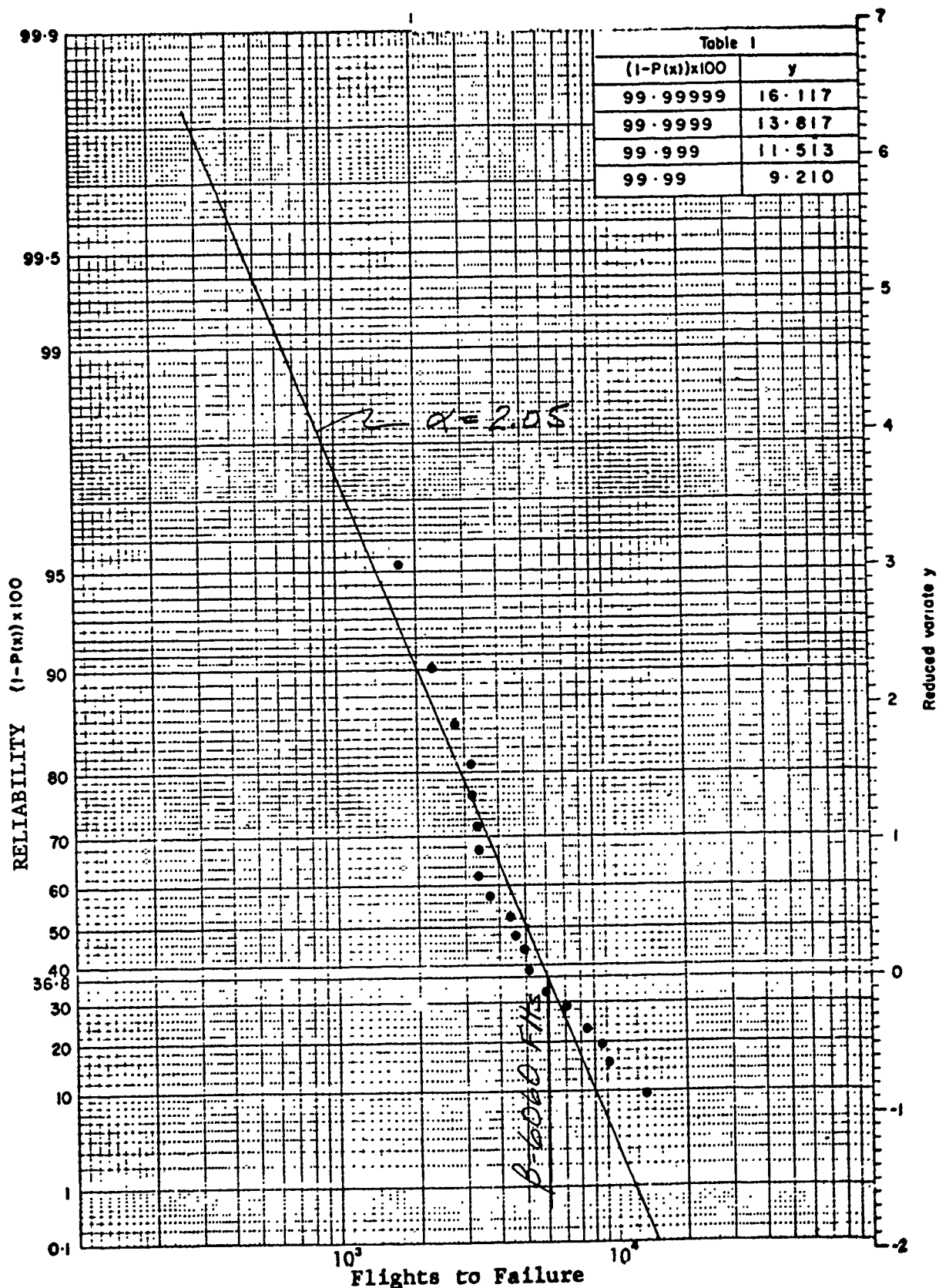


Figure 2-92 WEIBULL PLOT OF 10 NICKEL STEEL
RELIABILITY TESTS
2-220

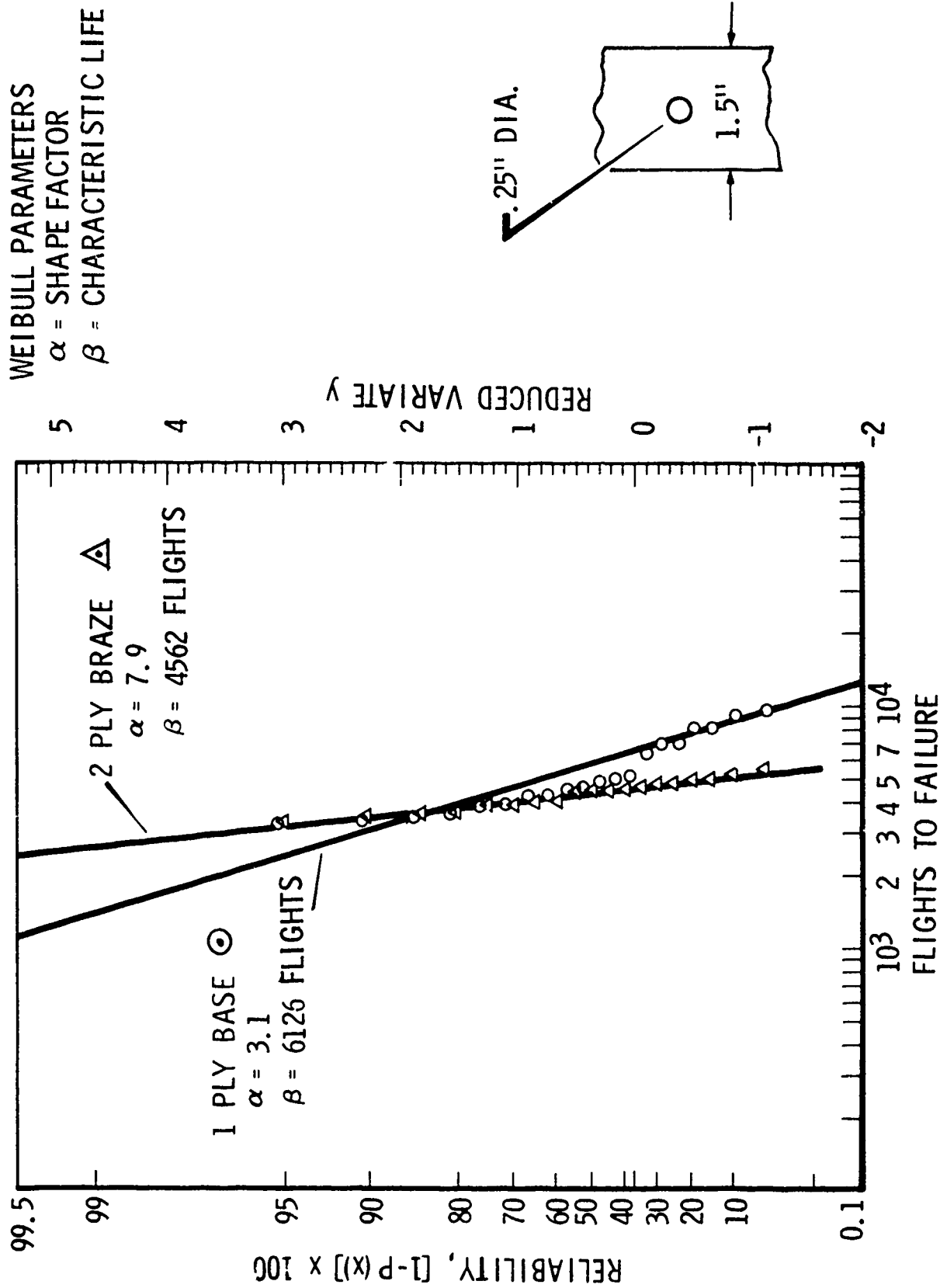


Figure 2-93 WEIBULL PLOT OF BETA ANNEALED 6AL-4V TITANIUM,
 SINGLE PLY AND 2 PLY BRAZE, RELIABILITY TEST DATA

2.4 MATERIALS ENGINEERING

2.4.1 Material Selection

The primary materials selected for use in the "No-Box" Box design are beta annealed 6Al-4V titanium, 10 Nickel steel and 7050 aluminum plate. Final design allowables based on test data, specification requirements, and vendor guarantees are shown in Tables II-28, II-29 and II-30, respectively.

2.4.2 Material Procurement

Beta Annealed 6Al-4V Titanium - Orders for all materials required for the FSIL design were placed during July and August and are scheduled for delivery during the last of December and the first half of January. Partial shipments have been received. Two vendors are participating in supplying this material, Reactive Metals Incorporated and Titanium Metals Corporation of America. The material on order for the FSIL configuration is more than adequate to support the "No-Box" Box design.

10 Nickel Steel - Orders for the material required to support the "No-Box" Box design were placed in September and first deliveries are scheduled to be received in January with completion in March. United States Steel Corporation is presently the only source for this material, with U. S. Steel doing the rolling and forging of the material and Latrobe Steel Company double vacuum melting (VIM plus VAR) of the ingot.

7050 Aluminum - Orders for the material required to support either configuration were placed in September, with delivery promised in early January. This material is a product of ALCOA and is being used in all applications requiring a starting thickness of 1.5 inches or greater.

Other Materials - Orders for long lead time items, such as 2024 aluminum, are being placed on an expedited basis. All orders for the 2024 aluminum required were placed during September and October and the majority of the requirements are being filled from warehouse stock. Orders for aluminum honeycomb core, adhesives, and other miscellaneous materials are in the process of being prepared.

Table II-28
DESIGN ALLOWABLES
 For Ti 6Al-4V
 Beta Annealed Condition
 (Ref. FMS-1109A)

PLATE						
FORM	THICKNESS (Inches)	.188 - .500	.501 - 1.000	1.001 - 2.000	2.001 - 2.500	2.501 - 4.000
PROPERTY:						
F_{tu} (KSI)		130	127	125	122	120
F_{ty} (KSI)		115	115	112	110	110
F_{cy} (KSI)		121	121	118	116	116
F_{su} (KSI)		87	85	83	81	80
F_{bru} (KSI)						
e/D = 1.5		208	203	200	195	192
e/D = 2.0		267	260	256	250	246
F_{bry} (KSI)						
e/D = 1.5		140	140	136	134	134
e/D = 2.0		170	170	166	163	163
%Elong(L or LT)		10	10	8	8	8
E (10 ⁶ psi)				16.0		
E _c (10 ⁶ psi)				16.4		
K _{IC} (KSI ^{1/2} inch)				90 (TYP) 80 (MIN)		
K _{Isc} (KSI ^{1/2} inch) typ				60+		
ρ (lbs/in ³)				.160		

Table II-29
DESIGN ALLOWABLES
For 10 Nickel Steel
(Ref. FMS-1111)

THICKNESS (Inches)	.375 - 2.00	2.01 - 4.00	4.01 - 8.00
PROPERTY:			
F_{tu} (PSI)	190	190	190
F_{ty} (KSI)	175	175	170
F_{cy} (KSI)	184	184	179
F_{su} (KSI)	121	121	121
F_{bru} (KSI)			
$e/D = 1.5$	274	274	274
$e/D = 2.0$	368	368	368
F_{bry} (KSI)			
$e/D = 1.5$	245	245	240
$e/D = 2.0$	291	291	282
% Elong	15	12	10
Charpy V-Notch (@ 0°F (Ft.-Lbs.))	60	50	40
E (10^6 psi)	28.0		
E_C (10^6 psi)	28.0		
ρ (lbs/in ³)	.284		
K_{IC} (KSI $\sqrt{\text{inch}}$)	> 180		
K_{Isec} (KSI $\sqrt{\text{inch}}$)	> 150		

Table II-30
DESIGN ALLOWABLES
7050 ALUMINUM ALLOY PLATE

TEMPER	7050-T7651	7050-T73651
THICKNESS	1.01- 2.00	2.01- 3.00 3.01- 4.00 4.01- 5.00 5.01- 6.00
F _{tu} (KSI)	77 78	71 72 71 72 69 70 66 67 63
F _{ty} (KSI)	69 67	63 63 60 60 58 59 54 56 53
F _{cy} (KSI)	68 69	61 64 59 61 57 63 60 63 59 61 57
F _{su} (KSI)	44	41 42 41 41
F _{bru} (KSI) e/r = 1.5 e/D = 2.0	115 150	110 144 111 142 108 137 105 133 129
F _{bry} (KSI) e/D = 1.5 e/D = 2.0	96 112	94 109 96 112 95 109 93 106 92 105
% Elong.	7 7	9 6 9 6 6 2 2 2 8 5 2
E (10 ⁶ psi) E _C (10 ⁶ psi) P (lbs/in ³) KIC (KSI in.) (Typ) K _{Isc} (KSI in)	10.3 10.5 .102 32 (L-T) 27 (T-L) 24 (S-L) Resistant in T73651 temper 90-95% of KIC	

TENSILE DATA BASED ON ALCOA GREEN LETTER GL220(4-73)

2.4.3 Materials Testing

The status of the materials testing program is being reported in other sections of this report and is essentially complete. The data generated is being compiled in the Materials Property Data Report which is prepared and submitted incrementally at the end of each phase of the AMAVS program. The Phase Ib report (General Dynamics, Convair Aerospace Division Report FZM-6148) was submitted in April 1973 and the Phase II report is scheduled for submittal in January 1974. The design allowables noted in paragraph 2.4.1 and 2.4.5 and in subsection 2.3 were based on this test program.

2.4.4 Brazing Development

2.4.4.1 Brazing

Brazed assemblies processed during this phase are shown in Table II-31. As a result of the problems encountered with the first 603FTB035, a braze improvement program was initiated. This program consisted of a series of time-temperature laboratory tests and manufacturing tests to improve retort atmosphere and conditions of all components.

The "Braze Improvement Program" and observations of the first 603FTB035 FSIL Specimen Brazing Operation led to the following conclusions:

- (1) Layup time from cleaning to braze needed to be reduced
- (2) Glass cloth used as a stop off in the retort contributed to the contamination
- (3) Silver braze alloy cleaning was not a major factor
- (4) Improved purging was necessary
- (5) Heat up rate to the brazing temperature needed to be improved
- (6) Temperature reading near the braze line was necessary

Table II-31

BRAZED ASSEMBLIES

(Braze Since 15 July 1973)

PANEL NO.	BRAZE		BZ ALLOY			BZ DATE	REMARKS
	TIME (MIN)	TEMP (°F)	VAC ("Hg)	ARGON (CFH)	THICKNESS (in)		
603FTB035 #1 Pre Braze Cycle	--	1540 1580	15	10	None	No	8/7/73
603FTB035 #1	10	1540 1585	15	10	.005	.002 x .125	8/20/73 No BZ
603FTB053 #1	10	1580	15	10	.005	.002 x .125	8/23/73 Excellent BZ Good Fillets
603FTB053 #2	10	1580	15	10	.005	.002 x .125	8/29/73 Excellent BZ Good Fillets
603FTB035 #1 $\frac{1}{2}$ Panel ReBZ	20	1605 1620	15	10	.005	.002 x .125	9/22/73 Marginal BZ
603FTB035 #2	7	1598	15	10	.005	.002 x .125	10/4/73 Excellent BZ 100% Fillets

Layup time can be reduced by organization and planning, such as, pre-cutting and pre-cleaning the braze alloy. Glass cloth was removed from the retort and was replaced by stop off. The stop off was baked at 700°F after application to tools to remove moisture and the carrier vehicle. Silver braze alloy cleaning was proven to be a minor factor but to insure consistency, all braze alloy foil is sanded and degreased.

Improved purging was obviously necessary due to atmosphere entrapment in the pocket areas of 603FTB035#1. On the -035 #1 argon was introduced through a 1/4" tube inside the barrier. The bottom pockets showed more discoloration than the top pockets. In order to insure purging, a tube with holes was placed in a groove in the base plate (See Figures 2-94, 2-95, 2-96 and 2-97). The holes provide argon in the center of the pocket areas to remove the atmosphere with a continuous flow. To improve the top pocket purging a tube with small holes was placed at the side of the titanium laminate so argon would flow through the slots on the other side (See Figures 2-98 and 2-99). This system was implemented for the rebraze operation of half of the 603FTB035#1 panel.

The strength of the Ag-Al-Mn brazements was shown to be dependent on the heating rate during brazing. At the lower brazing temperatures, slow heating rates produced low strength brazements. These brazements appeared spongy or grainy. Their microstructures revealed large void areas and incomplete melting along the central braze line.

A study of the experimental results in conjunction with the silver-aluminum and titanium-aluminum phase diagrams offered a metallurgical explanation to this heating rate dependence. The Ag-Al phase diagram shows that the liquidus temperature for this alloy system rises very rapidly from 1500°F to 1675°F with variations in the aluminum content from 5.5% to 2.0%. Microstructural and electron microprobe analyses of braze joints showed that a heterogeneous reaction takes place between the base titanium and the aluminum-rich molten portion of the braze alloy while heating through the liquid and solid region (1400-1600°F). This causes a wide compositional gradient to develop within the braze line. Given sufficient time, the aluminum content along the titanium interface region (gamma layer) rises to 36-44% with a corresponding drop in the central braze line

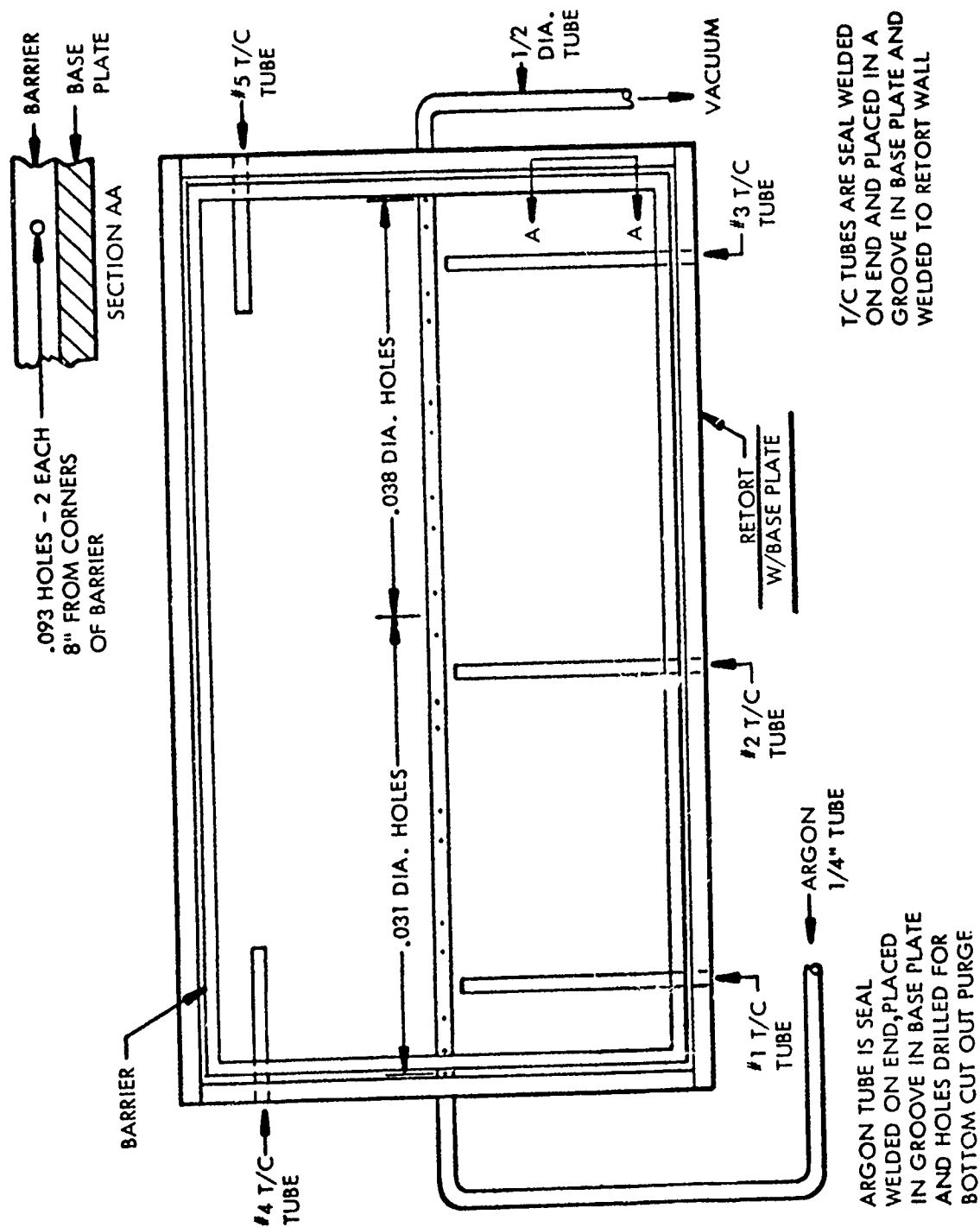
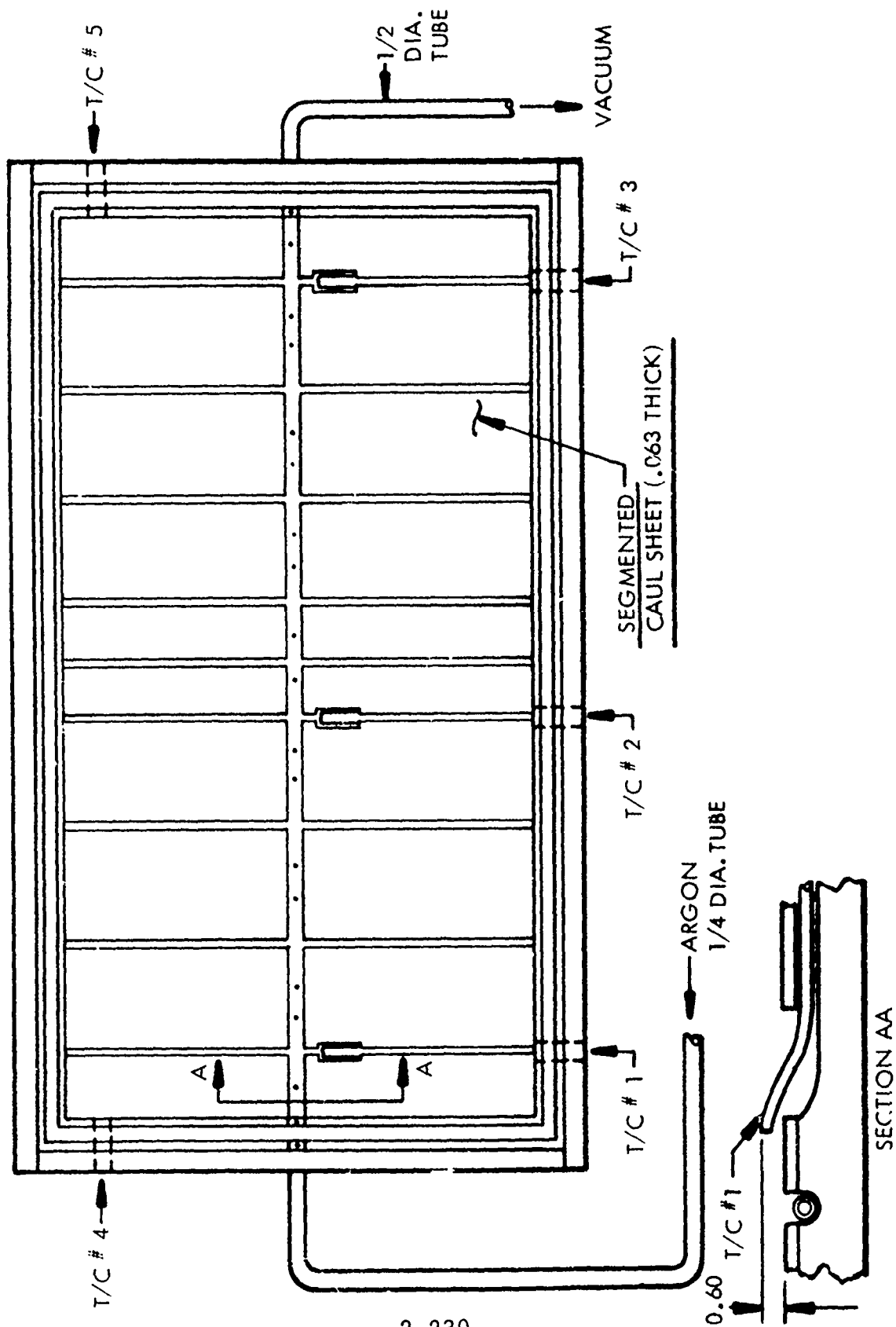


Figure 2-94 603FTB035 RE-BRAZE



2-230

Figure 2-95 603FTB035 RE-BRAZE

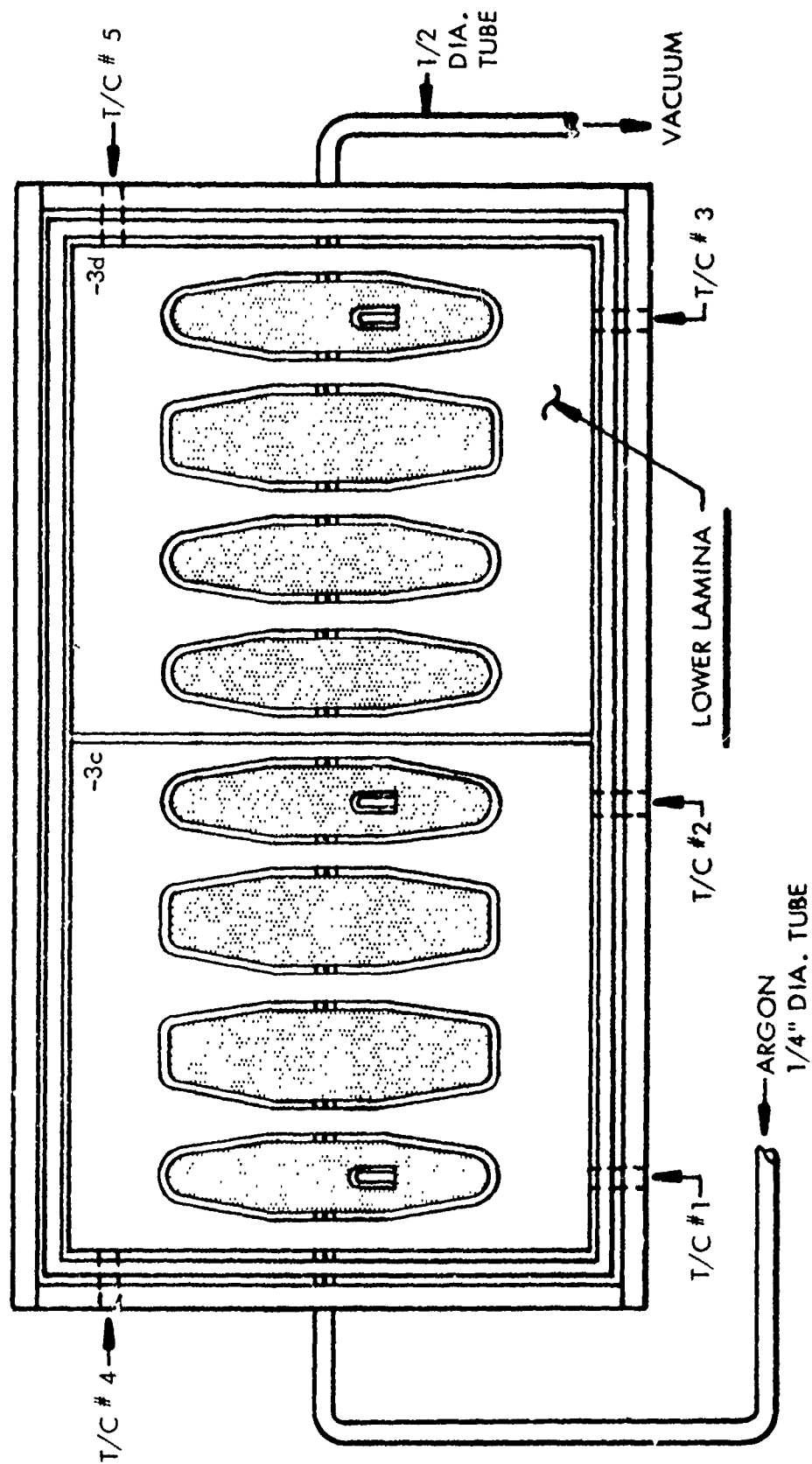


Figure 2-96 603FTB035 RE-BRAZE

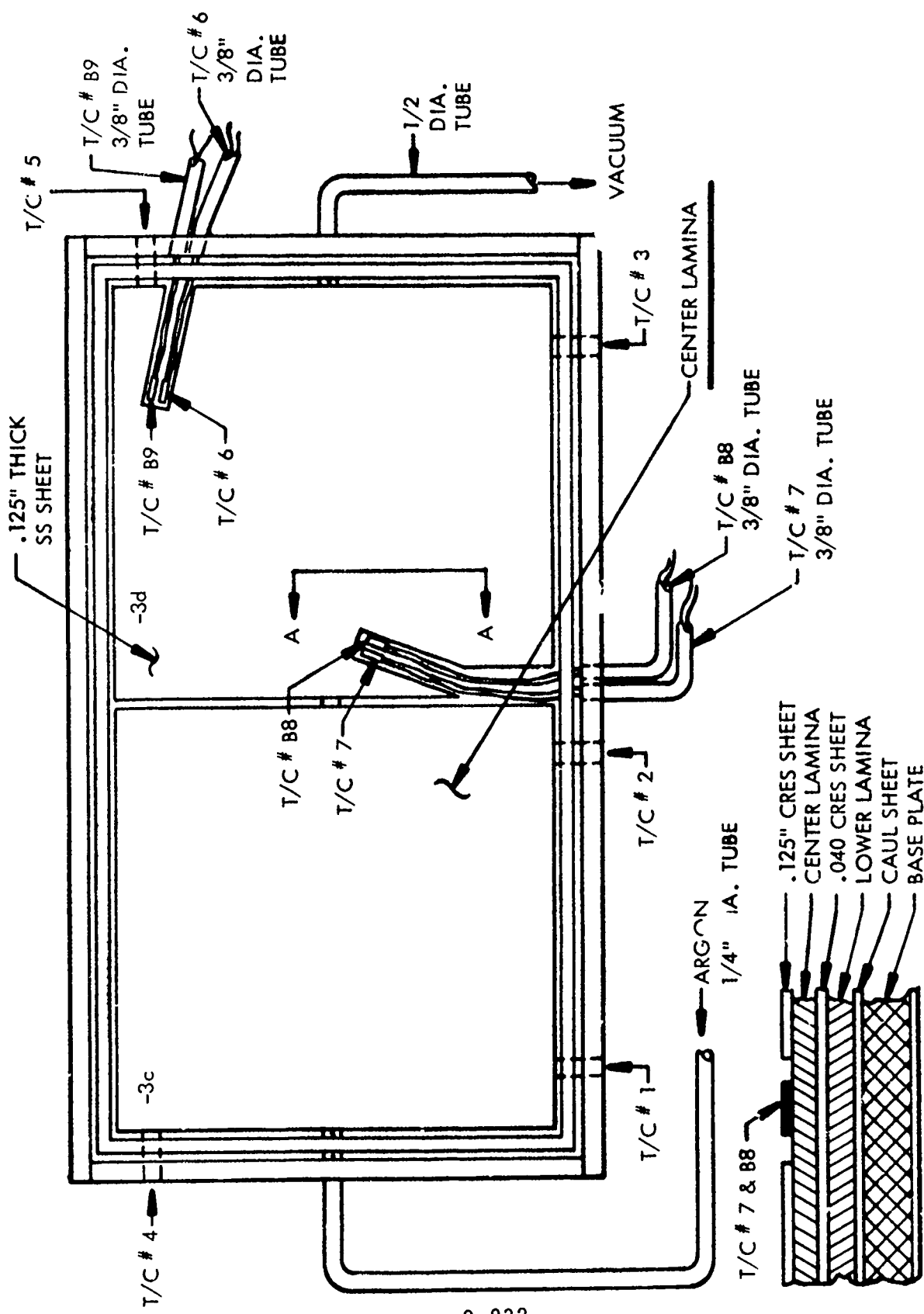
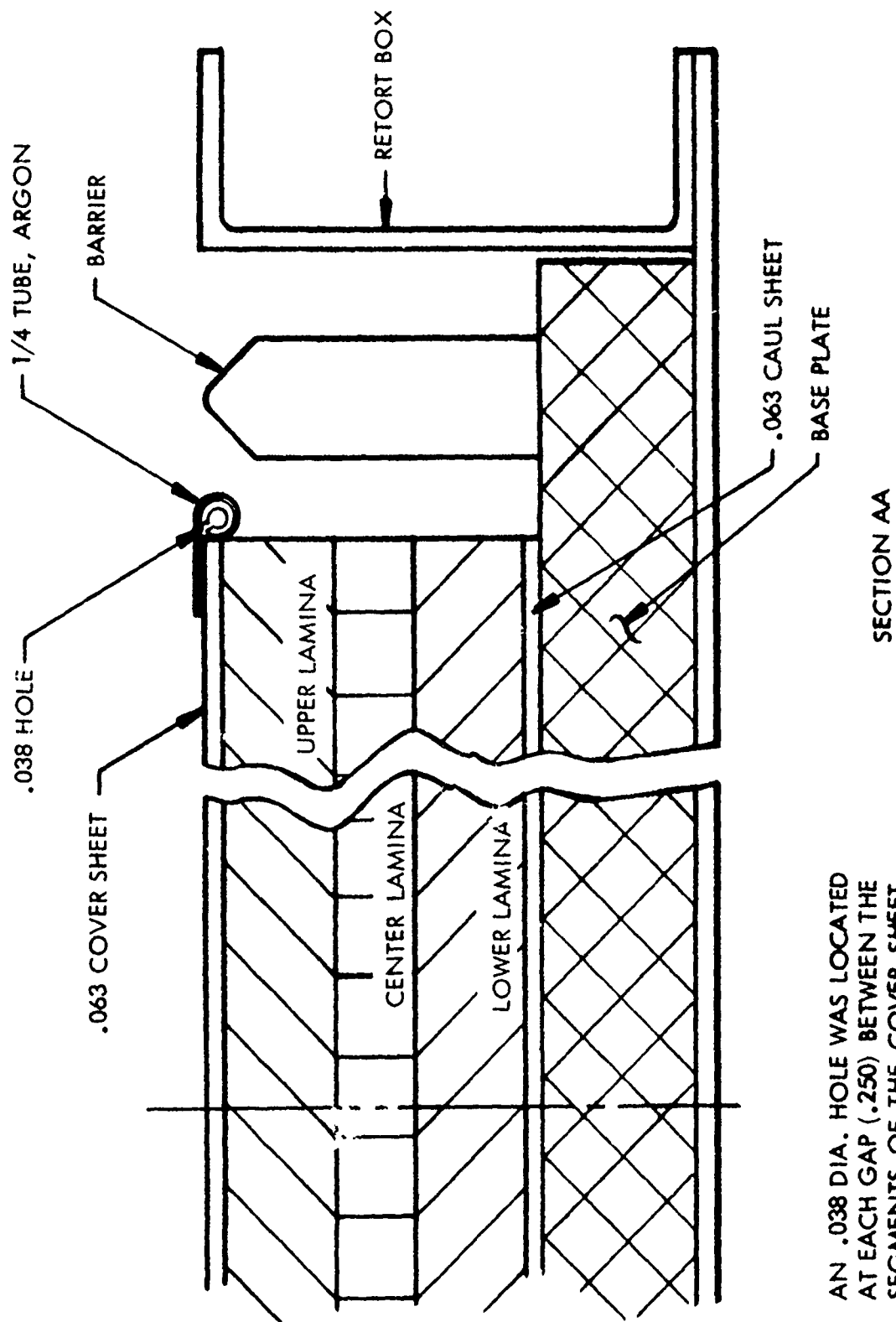


Figure 2-97 603FTB035 RE-BRAZE



AN .038 DIA. HOLE WAS LOCATED AT EACH GAP (.250) BETWEEN THE SEGMENTS OF THE COVER SHEET. THE HOLE WILL BE POINTED UP AT 45° \angle TOWARD THE VACUUM SHEET.

Figure 2-99 603FTB035 RE-BRAZE

to 2%. The phase diagram shows that an alloy with this low aluminum content will require a braze temperature of 1675°F to go fully liquid. If the chosen braze temperature is below this value the central braze line with its low aluminum content will not go fully liquid. A spongy, low-strength braze will be produced. The experimental results showed that with heating times of 60 minutes or more in the 1400-1600°F range, this condition was produced. It could be minimized by either reducing the heating time (less aluminum depletion) or increasing the maximum brazing temperature (to exceed the new liquidus temperature).

The furnace was raised to 1200°F prior to insertion for re-brazing the -035#1 half panel. Insulation was left on the top of the panel to insure uniform heating. Uniform heating was thought to be necessary to prevent warpage in the braze assembly. The furnace control was set at 1625°F and the re-braze package heated to the braze temperature faster than the initial -035 braze package. From room temperature the initial -035 took five hours - 40 minutes to reach a braze temperature of 1550°F. The re-braze package heating time from room temperature to 1600°F was four hours - 10 minutes. The time to heat from 1400°F to the top braze temperature was 80 minutes for the re-braze package compared to 70 minutes for the initial effort. The quality of the re-braze was better than the original though still marginal. The void content of the braze line was high and the flow was practically non-existent since the braze alloy did not change form. The braze joint was in excess of 0.005 inch thick and fillets did not exist. Microscopic examination of the braze joint indicated spongy appearance related to the high void count.

Temperature readings were suspect on the initial -035 braze operation since the thermocouples (T/C) were placed in the base plate. One T/C was embedded in a steel block on top of the vacuum sheet with the insulation removed in that area. The T/C's placed in the base plate were placed in CRES steel tubes seal welded on the end and welded to the retort wall. This allowed the sheathed T/C to be readily placed in position and removed. Also this arrangement minimized the number of tubes to be handled and mechanically sealed around the T/C. For the 603FTB053 #1 and #2 brazed assemblies the T/C CRES steel tube was formed up through a cut in the caul sheet and placed adjacent to the center Titanium lamina in a pocket. See Figure 2-95.

The #1 and #2 603FTB053 braze assemblies were of excellent quality with the braze alloy changing form - going from a foil sheet to a liquid. Wetting was excellent and fillets were consistently formed.

For the -035 rebraze half panel the T/C arrangement was modified. (See Figures 2-95, 2-96, 2-97, 2-98 and 2-100). T/C's #1, 2 and 3 were placed in tubes formed to end adjacent to the lower surface of the center lamina. T/C #4 and 5 were left in the base plate. Since only half of the -035 #1 was to be rebrazed the other half was used to dummy load the retort. In place of silver braze foil, CRES steel sheet was used to interleave the titanium lamina. (See Figure 2-97). By using 1/8 CRES steel sheet at the top braze line, it was possible to cut out slots and place sheathed T/C #6 and 7 geometrically opposite T/C 5 and 2. (See Figure 2-97).

To check sheathed T/C readings, unsheathed glass cloth coated T/C #B8 and #B9 were routed through exterior tubes to adjacent locations with T/C #7 and #6, respectively. The fragile nature of the glass cloth and routing through the holes and slots necessary to reach the T/C #7 and 6 location shorted out T/C #B8 and #B9. T/C #5 was lost due to a leak in the tube and had to be seal welded at the retort wall. Correlation between the remainder of the T/C's was very good. The T/C #6 and #7 indicated a slower heating rate than #4 and #2 which led to the conclusion that the Ti braze assembly was being heated primarily from the bottom. The insulation blanket is very efficient.

The rebraze half of -035 #1, as noted above, was not of desirable braze quality but the rebraze operation produced information on the heating rate and purging system.

Prior to the rebraze operation of -035 #1, a wood mock up of half of the -035 panel was fabricated. Using plexiglas as a cover sheet and smoke in place of argon, the flow from the tube purging system could be observed. Smoke was injected into the tube system after a partial vacuum was pulled on the mockup retort. The smoke flow indicated the desired flow of the argon.

After the rebraze of -035 #1 it was observed that the argon tube in the base plate injecting argon into the center of the pocket slots was much more effective than the tube at the side of the titanium laminate.

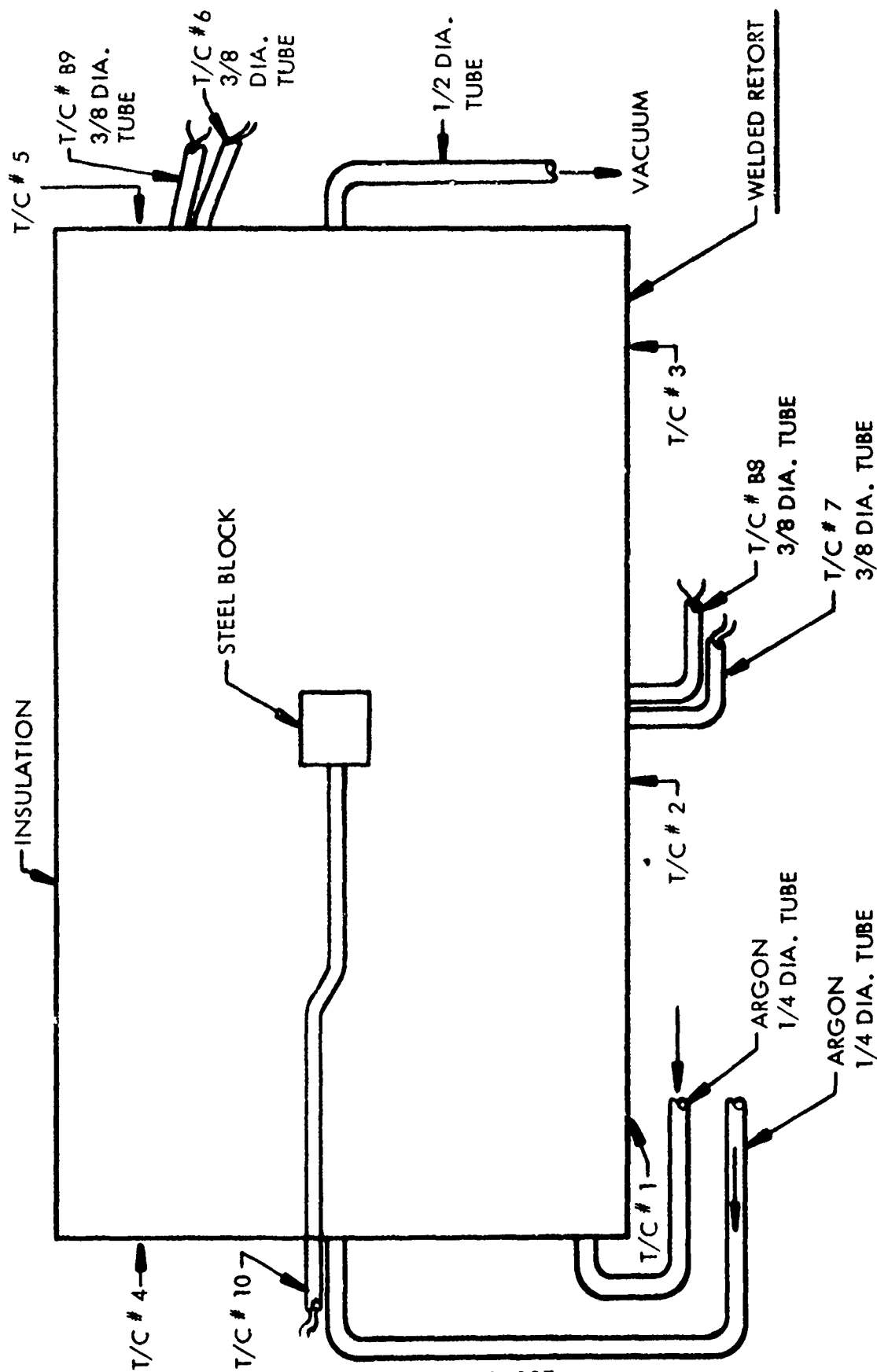


Figure 2-100 603FTB035 RE-BRAZE

Another observation was the discoloration of an area adjacent to the first two holes in the lower argon tube indicating improper cleaning of the argon tubing. All tubing is now degreased with 150°F trichloroethylene.

Two .250/.250 X 7.5 X 12 Ti panels were placed in the first and fourth slot, from the argon input end of the -035 rebraze panel. (See Figure 2-98). The titanium material in these panels was new. Some runout of the silver braze alloy was observed and the lap shear strength was 20 to 24 ksi. The microscopic examination indicated a general spongy appearance and fairly wide braze joint although not as spongy as the -035 rebraze panel. Small compression type shear specimens from the corners of the rebraze panel indicated a shear strength of 4 to 24 ksi. With small specimens, a wide variation can be expected. NDI results indicate greatly improved quality compared to the -035 #1 braze. The lower braze joint had estimated 45% void in the upper braze joint.

The analysis of the -035 #1 braze operation, the -035 #1 rebraze operation and the Braze Improvement Program Specimen Testing indicated the following changes for the -035 #2 braze operation.

- (1) Minimize the penetrations of the retort
- (2) Improve cleaning procedures
- (3) Improve the Argon Purging System
- (4) Increase the heat up rate (Target heat up rate 4°F/min)

The use of only five internal T/C's and one on top in a steel block reduced the penetrations of the retort and improved the handling of the retort considerably. (See Figures 2-100, 2-101, 2-102 and 2-103). Improved cleaning procedures were initiated as noted above.

The Argon System was changed primarily by shifting the top argon tube to the center of the retort. (See Figures 2-100, 2-101, 2-102, 2-103, 2-104, 2-105 and 2-106).

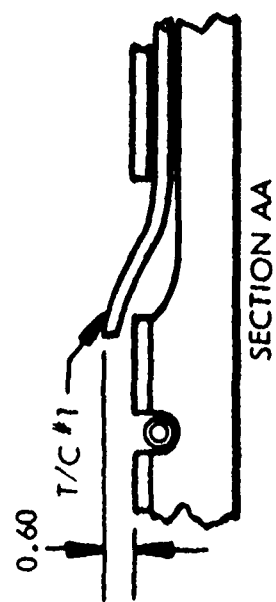
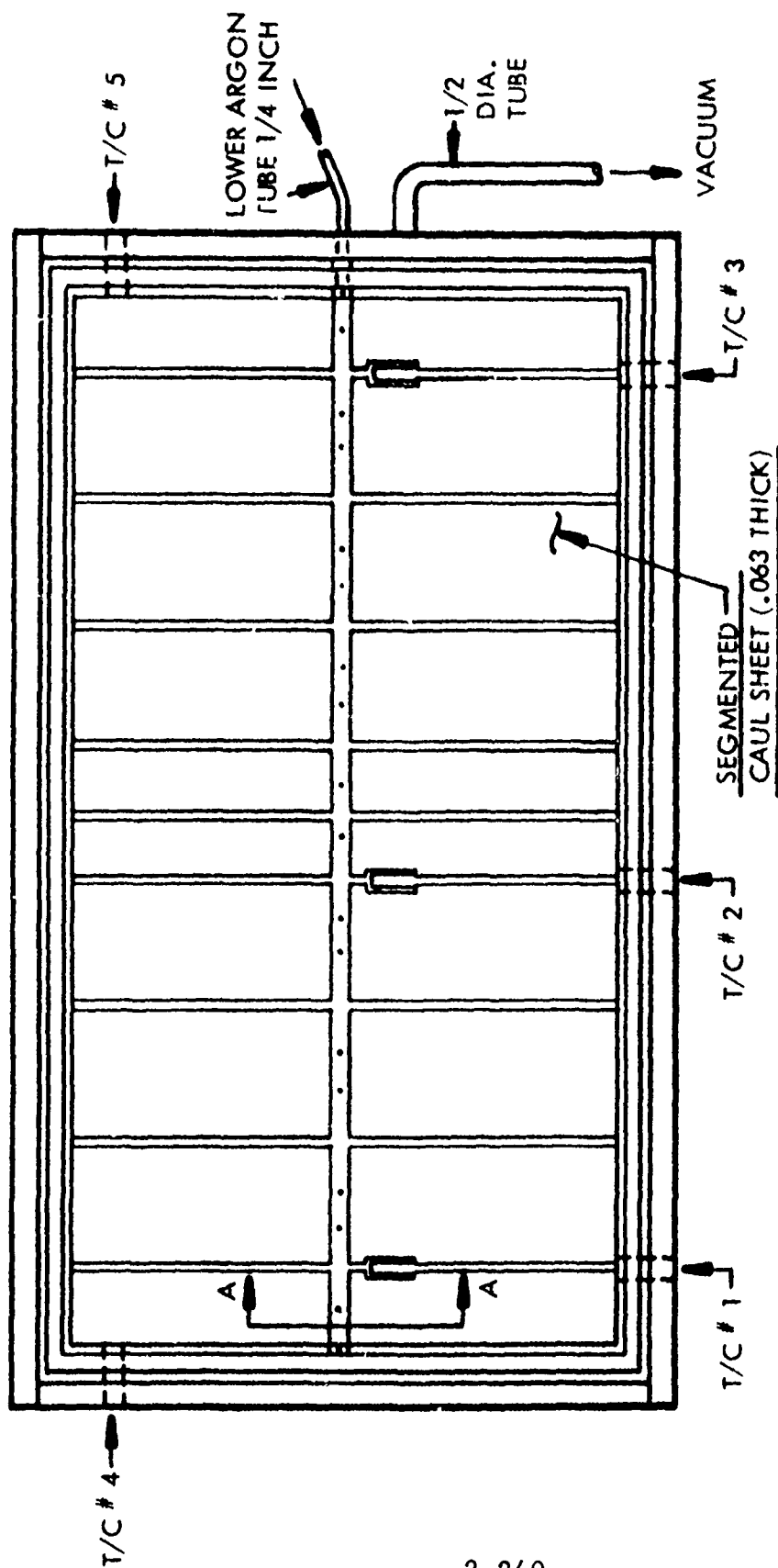


Figure 2-102 603FTB035 #2

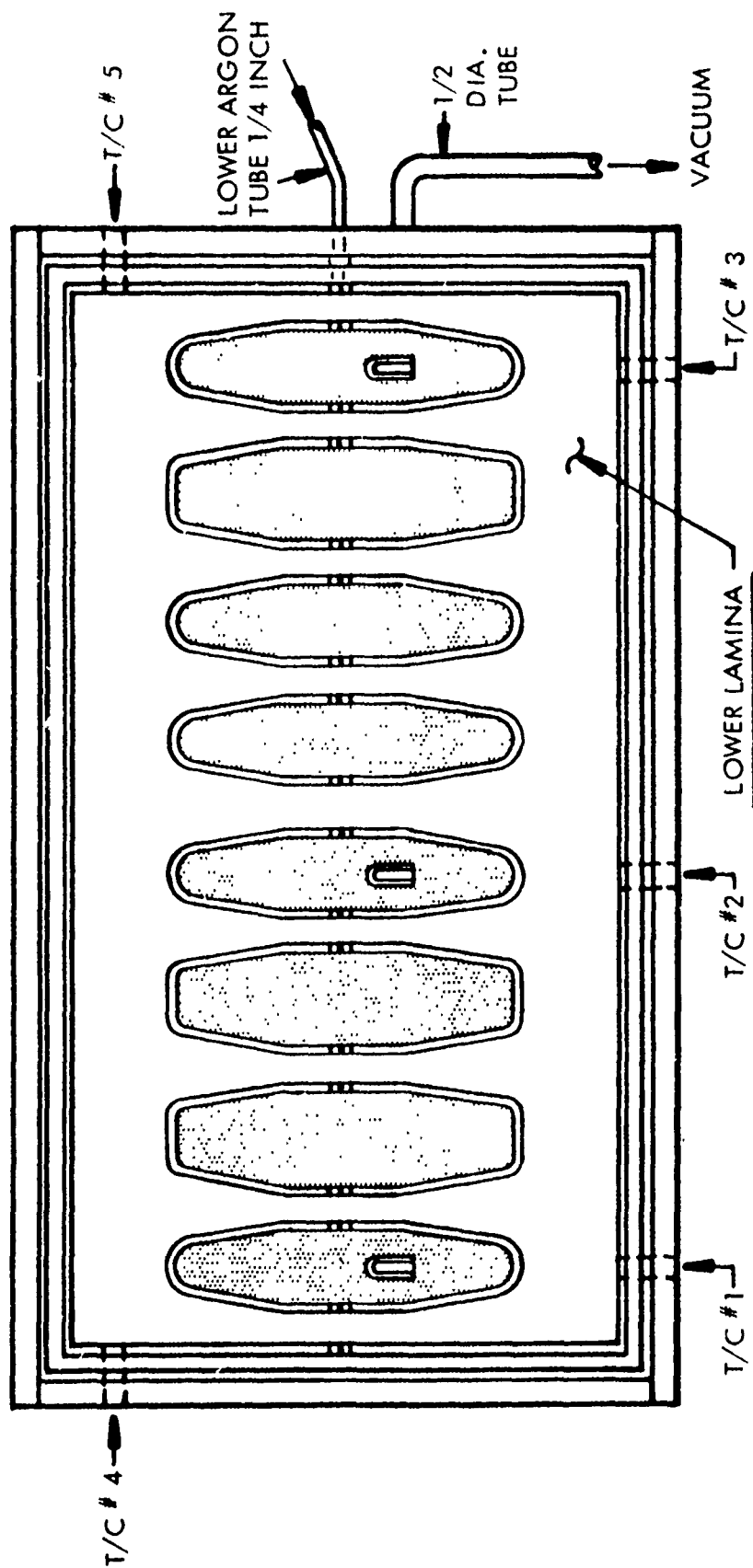


Figure 2-103 603FTB035 #2

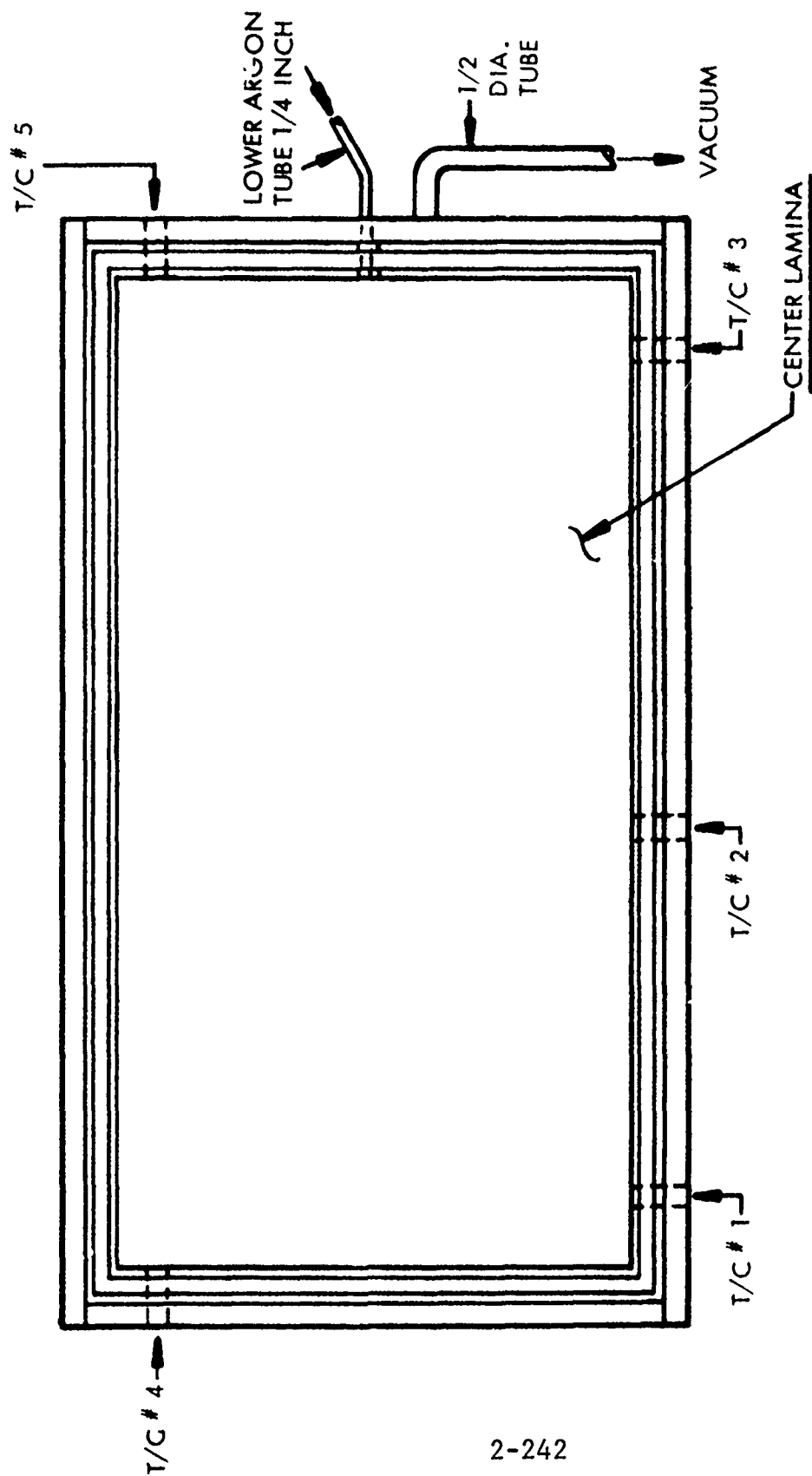
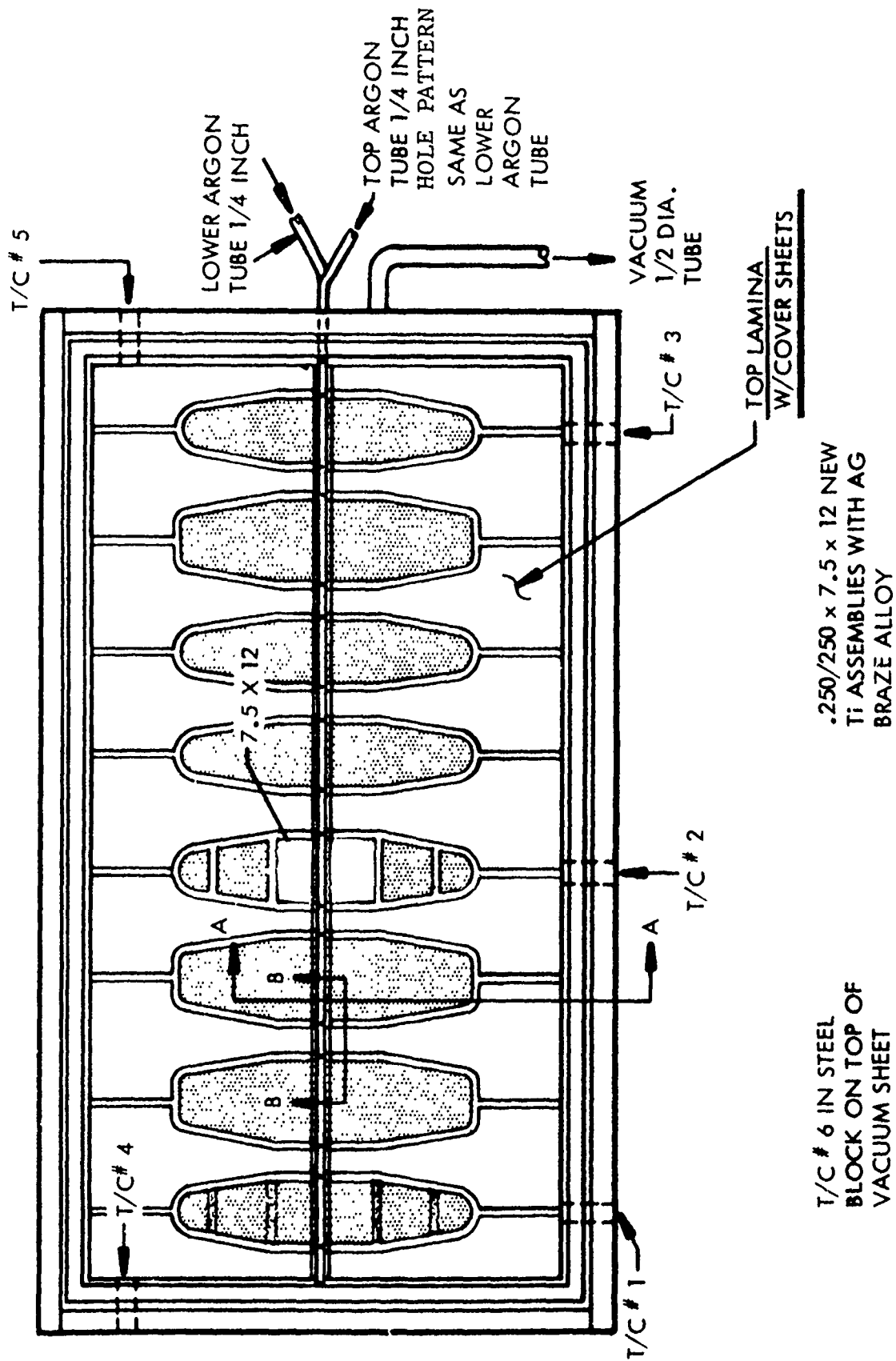
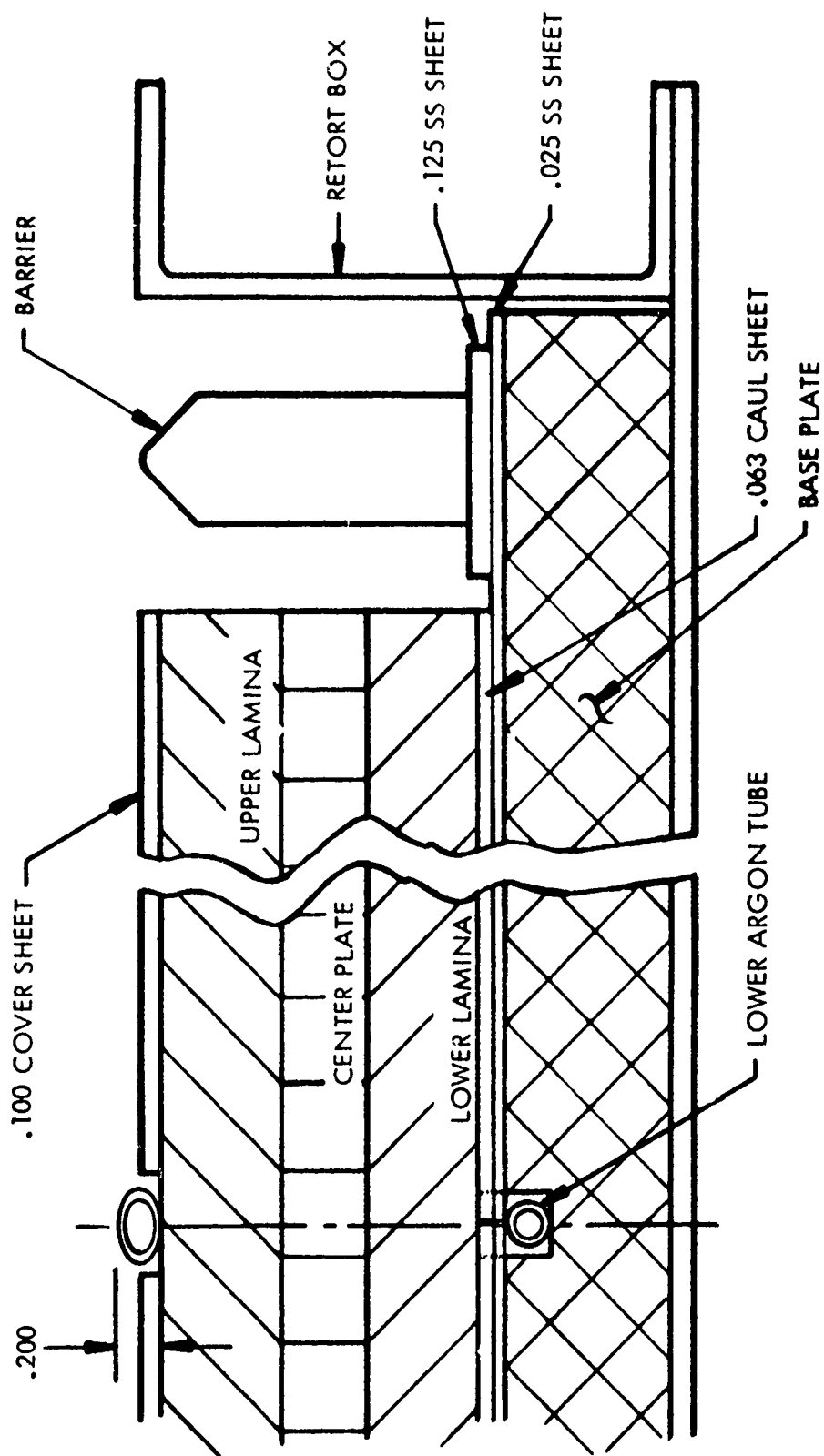


Figure 2-104 603FTB035 #2



2-243

Figure 2-105 603FTB035 #2



SECTION AA

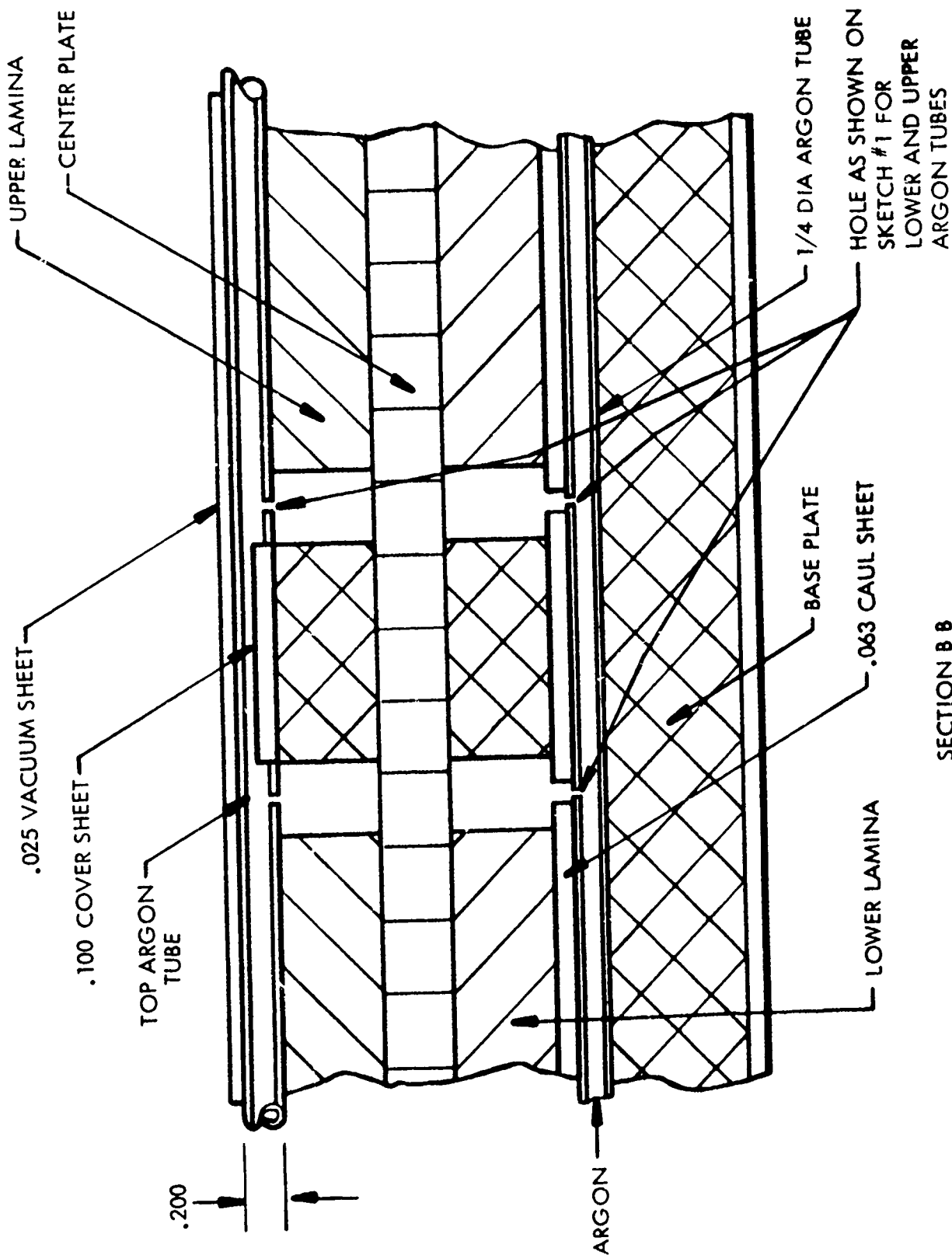
Figure 2-106 603FTB035 #2

The concern over the effect of the argon tube on the vacuum sheet was minimized by flattening the 1/4" tube to an oval shape which enhanced the formability at the ends of the -035 panel. Introduction of Argon at the center of each center slot position produced an argon flushing action to the purging system. The majority of the Argon gas is introduced into the inside of the barrier. The holes in the barrier for the argon to flow from the inside to the outside were placed in the opposite end of the retort from the vacuum tube. The argon tubes were placed on the same end as the vacuum tube to minimize the length and handling. (See Figures 2-104 and 2-107). The changes improve the purging action. These changes were checked out with the wood mockup prior to brazing -035 #2.

To increase the heatup rate the insulation blanket was removed from the top of the retort. The insulation is used primarily to prevent warpage of the Ti braze assembly due to the rapid cooling of the CRES steel retort edges and rapid cooling of the top Ti lamina. The insulation was left off during the braze operation and two layers were placed on the retort after removal from the furnace (1350°F). Only one layer was necessary, however, since the panel cooled from the bottom due to the efficiency of the insulation and a slight bow was noticed in the -035 #2 braze assembly. With the removal of the insulation preheating of the furnace to 1400°F and setting the controls on 1650°F (maximum on this furnace) the package heated rapidly. For a time-temperature plot of 603FTB035#2, see Figure 2-108.

From the braze improvement program specimens and review of previous successful braze packages (603FTB053, etc.) it was evident a heat up rate from 1400°F to the braze temperature would need to be near 4°F/min.

The actual time from 1400°F to 1598°F (#2 T/C) was 53 minutes or approximately 3.8°F/min. This heat up rate was approximately 5°F/min. through the solidus to liquidus range of the braze alloy. The results were that the braze alloy changed form completely going from a foil sheet (.005 thick) to a liquid and produced excellent wetting. Fillets were found in the pockets (100% top and bottom). For wetting of this nature to occur, very good cleaning was obvious and purging was the best obtained to date.



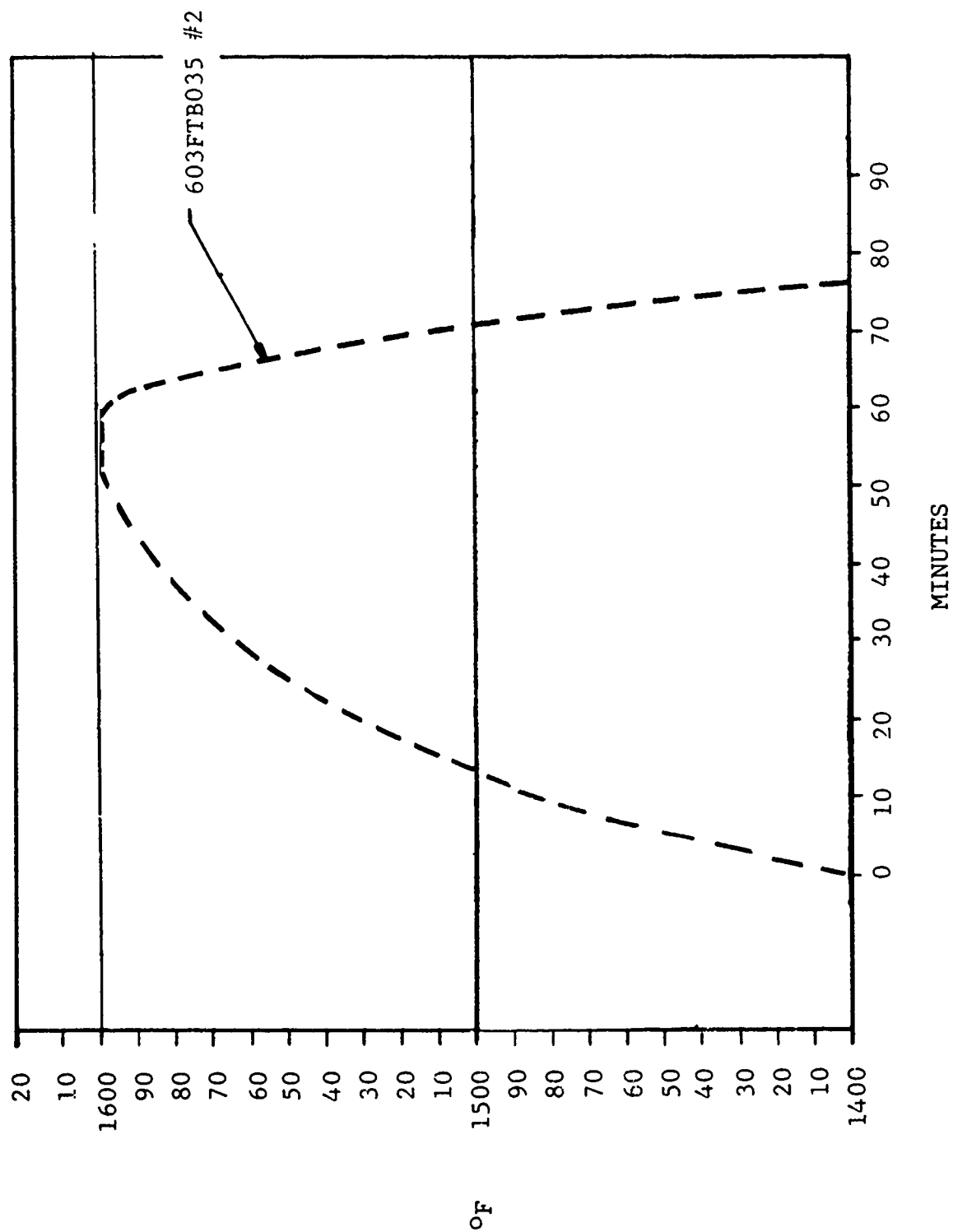


Figure 2-108 AMAVS BRAZING CYCLE FOR 603FTB035 #2

Lap shear specimen from the .250/.250 X 7.5 X 12 panel placed in the cutout produced an average of 20 KSI plus. Compression shear strength from a corner of the actual panel was 24 KSI plus. The microanalysis indicated a .003 to .004" thick braze joint and a minimum of voids and an excellent reaction area between the silver and titanium. NDI results indicate 90% minimum braze on both top and bottom braze joints.

2.4.4.2 Brazing Alloy

The Ag-Al-Mn brazing alloy used to braze all titanium laminates and assemblies was procured from Western Gold and Platinum Company, 525 Harbor Blvd., Belmont, California, 94002. The silver alloy foil was produced in approximately 100 troy ounce lots supervised by their laboratory personnel using extra care to control the manganese content. The quality of the foil was generally good except for a small percentage of the first foil produced which had oxide scale rolled into the surface. The producer eliminated this problem as soon as it was brought to his attention.

During the lay-up of the first 603FTB035 assembly, a feature of the braze foil was noticed that had escaped attention previously. Due to the size, 4 foot x 10 foot, of each braze joint, the .005" X 3.00" X random length foil was layed in strips in the 10 foot length. It was noticed that the strips of foil were not straight. If the strips were pulled straight parrallel to the 10 foot edge of the titanium, wrinkles resulted. To minimize the wrinkles the foil was cut in approximately 2 foot lengths. Discussion with the producer indicated the cause of the strips of foil being crooked was uneven tension on the roller that pulled the foil through the slitte. This problem is unique to large braze joint areas and has been corrected.

A compilation of pertinent data on the braze foil is found in Table II-32. Good uniformity in chemistry results in uniformity in solidus (1410 to 1440°F) and liquidus (1495 to 1525°F) melting temperature. Lot 19042 is excluded since the thickness was .002 and was never used in other than 3 inches X 3 inches specimens.

2.4.4.3 Stress Corrosion of Brazed Joints

Beta annealed 6Al-4V titanium brazed with Ag-Al-Mn alloy is subject to sustained load stress corrosion delamination in a sump tank water environment. Delamination occurs at the braze

Table II-32

BRAZE ALLOY

0.005 x 3 x Random Length Silver Alloy Foil

*LOT NO.	QUANTITY (TROZ)	Analysis						SOLIDUS (°F)	LIQUIDUS (°F)
		Vendor		Convair Check		AL	Mn		
		Ag	AL	Mn	Ag				
20608	166.135	93.67	5.62	.71	94.00	5.48	.52	1410	1495
20616	63.542	93.89	5.62	.49	93.70	5.64	.66	1430	1525
20682	(93.95	5.51	.54	94.00	5.48	.52	1410	1515
20683	222.148	93.56	5.57	.67	94.00	5.49	.51	1420	1510
20684	(93.71	5.61	.68	93.75	5.76	.49	1420	1505
20685	(93.55	5.79	.66	94.10	5.39	.51	1420	1500
20743	97.709	94.24	5.21	.55	94.20	5.30	.50	1425	1520
20811	295.104	94.14	5.27	.59	93.80	5.73	.47	1430	1520
**19042	148.321	94.41	5.02	.57	94.8	4.76	.44	1415	1540
19455	71.260	93.87	5.33	.55	93.80	5.55	.65	1440	1515
18897	195.275	94.18	5.16	.66	94.30	5.03	.67	1425	1510
19577	(94.09	5.34	.57	94.10	5.20	.70	1435	1495
19579	312.281	93.81	5.49	.70	93.60	5.60	.80	1430	1510
19576	(94.07	5.34	.59	93.60	5.80	.60	1440	1500
19578	(93.78	5.63	.59	93.70	5.70	.60	1420	1500

*Western Gold and Platinum Lot Numbers

**.002" Thick Foil

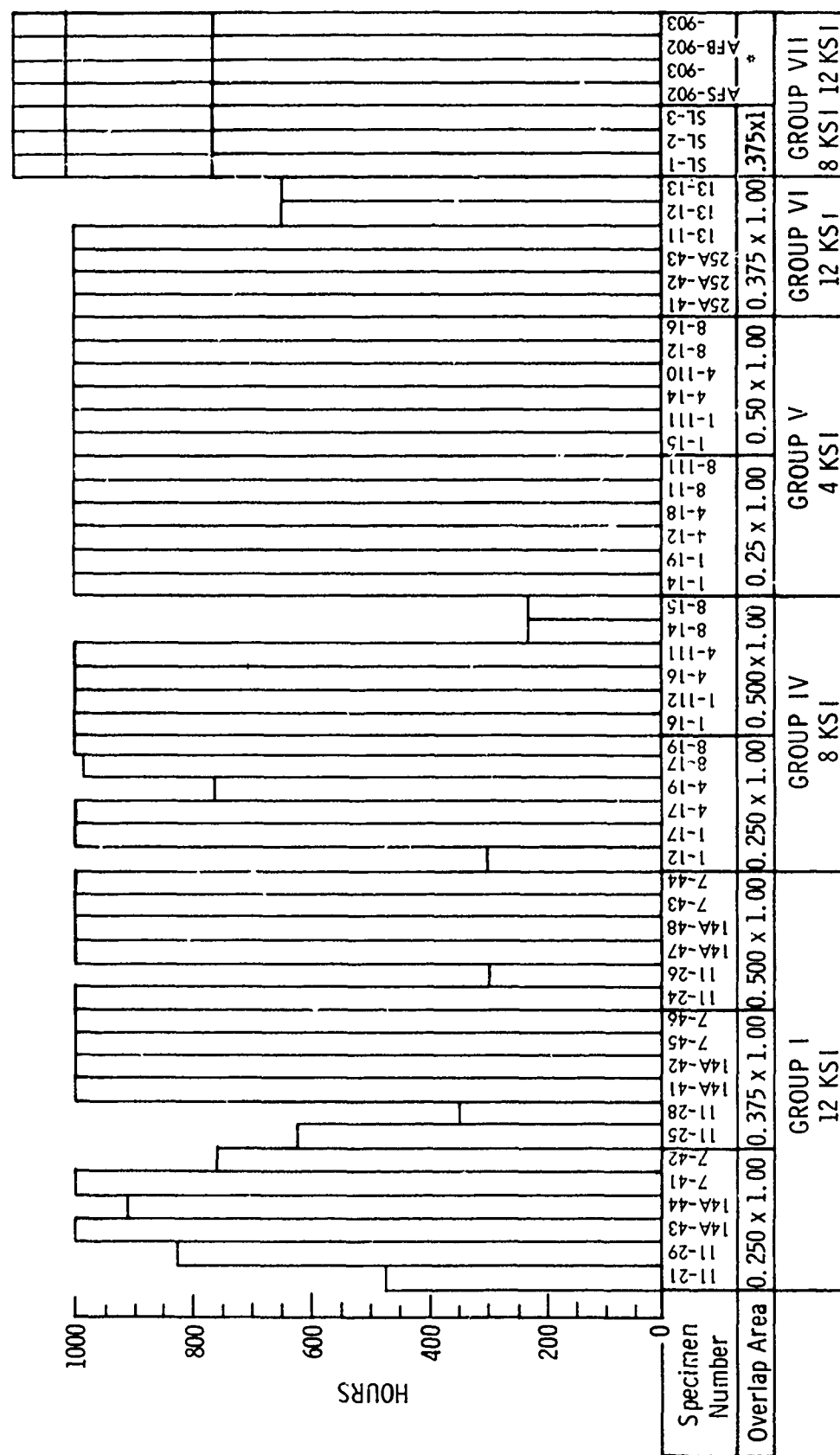
Note: Convair check analysis was made on the Ag and Mn and Al obtained by mathematical deduction.

interface. No evidence of base metal cracking has been observed. Results from 51 single lap shear specimens brazed using a wide range of processing variables indicate that the stress corrosion threshold is at least 4 ksi as shown in Figure 2-109.

Metallurgical studies suggest that the threshold level may be a function of braze interface concentration (of Ag and Al) gradients. Minimum concentration gradients and the best stress corrosion delamination resistance occurred in panels with extensive reaction between the braze alloy and the base metal. Fast thermal cycles maximized susceptibility and vice versa.

Microsections of stress corrosion test (SCC) specimens from MR&D brazed panels #11 and #25A and 603FTB035 #1 and #2 brazed component test assemblies are shown in Figures 2-110 thru 2-113, respectively. The microsection from panel #11 (Figure 2-110) indicates a minimal reaction zone between the braze alloy and titanium showing some γ phase with no apparent α zone. This panel was brazed at 1550°F and was above 1400°F only 28 minutes. The heating rate between 1400 and 1500°F was 10°F/min. Sustained load SCC testing (see Group I) at 12KSI in sump tank water failed 5 of the 6 specimens prior to 1000 hours. The microsections from panel #25A and 603FTB035#2 have a specific α and γ zone and a wide reaction area between the braze alloy and titanium. Panel #25A was brazed at 1550°F with a total time above 1400°F of 55 minutes. The 603FTB035#2 panel was brazed at 1598°F with a total time above 1400°F of 75 minutes. The heating rate of #25A and -035#2 between 1400 and 1500°F was 3.8°F/min. and 7.15°F/min., average, respectively. SCC specimens from #25A and -035#2 endured for 1000 hours at 12 and 8KSI sustained load, respectively. Some evidence of SCC attack was found on the interface region of some of the brazed joints. The extent of actual stress corrosion attack was complicated by small void areas in some specimens.

The braze thermal cycle used to produce the -035#2 test component is close to the optimum thermal cycle. Specimens taken from the .250/.250 X 7.5 X 12 panel brazed with this component have satisfactory corrosion delamination resistance. Three specimens were tested at 8KSI for 1096 hours (as noted above). Upon completion of the test, the specimens were loaded statically to failure and examined for evidence of sub-critical stress corrosion delamination. The lap shear strengths were 22.9 KSI, 22.3 KSI and 14.3 KSI with the latter showing some evidence of corrosive attack at the braze joint.



MR&D Panel BZ 11 Fast Heating Cycle
 Number and BZ 14A 30 Min. @ BZ Temp
 Test Condition BZ 7 Good BZ
 BZ 1 No Buttons, 63 RMS

BZ 4 Sanded Details (63 RMS)
 BZ 8 Low Pressure
 BZ 25A Good BZ
 BZ 13 Double Cycle Preform

*Vac. Furnace
 BZ - Small Spcm.
 from AFML

Figure 2-109 SUSTAINED LOAD STRESS CORROSION TESTS
 BRAZED SINGLE LAP SHEAR SPECIMENS

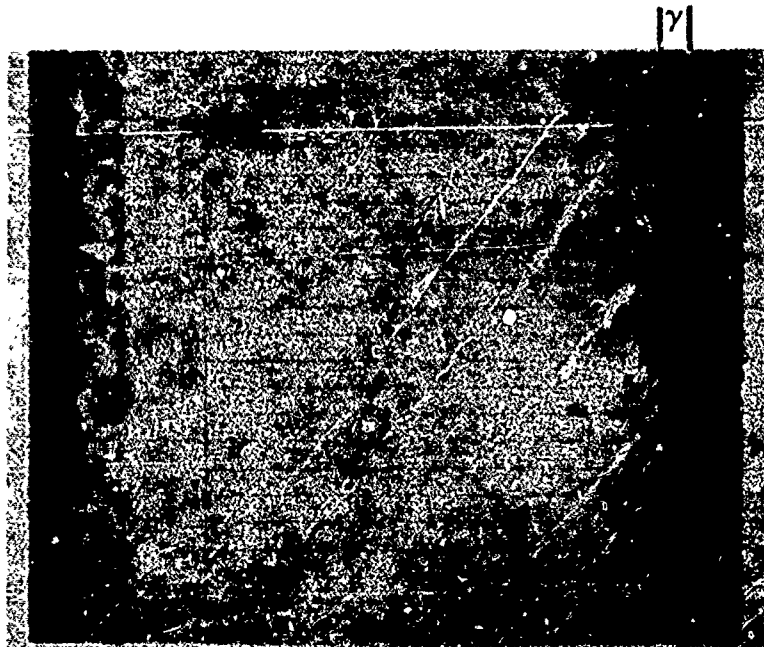


Figure 2-110 MICROSECTION OF BRAZE LINE OF STRESS CORROSION
SPECIMEN 11-28 REMOVED FROM MR&D PANEL NO. 28, 750X

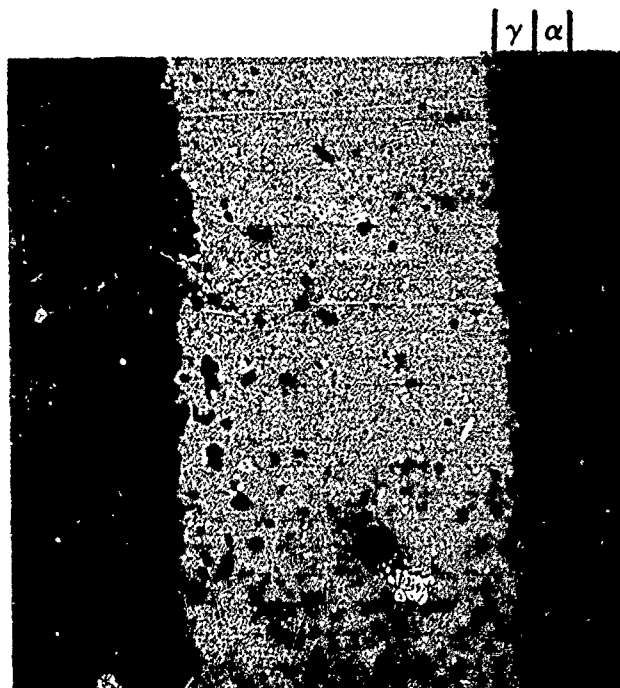


Figure 2-111 MICROSECTION OF BRAZE LINE REMOVED FROM
MR&D PANEL NO. 25A, 750X



Figure 2-112 MICROSECTION OF BRAZE LINE REMOVED FROM
603FTB035 #1 PANEL, 750X

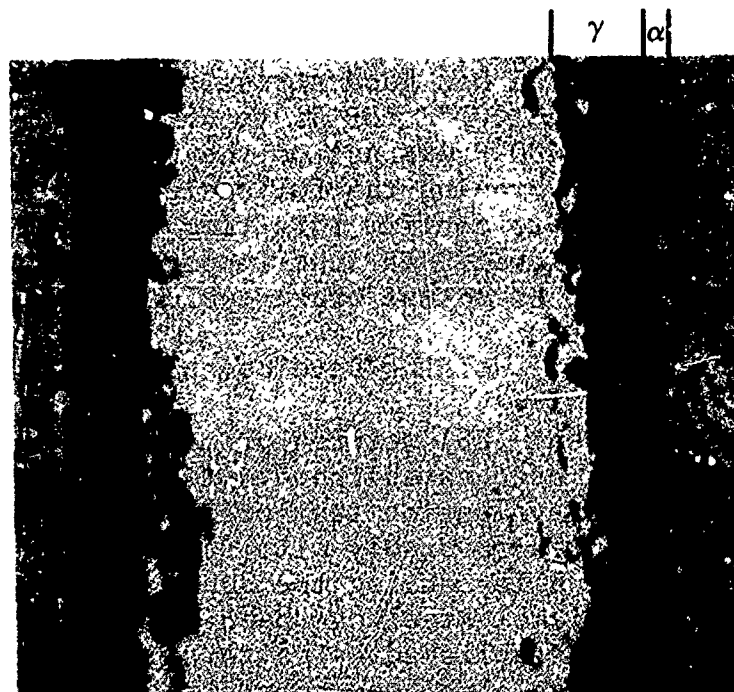


Figure 2-113 MICROSECTION OF BRAZE LINE REMOVED FROM
603FTB035 #2 PANEL, 750X

2.4.4.4 Brazing Thermal Cycle

The braze thermal cycle required to consistently provide braze joints with excellent shear strength and stress corrosion delamination is shown in Figure 2-114. The boundaries in Figure 2-114 define acceptable heat rate, braze temperature, hold time and cooling rate. The heating rate up to 1400°F and the cooling rate below 1400°F are assumed to have little effect on the resulting braze joint.

To heat a large heavy retort package, preheating the furnace to the braze temperature is recommended to achieve a sufficient heating rate in the range of 1400°F to 1580°F. The time-temperature (T-T) boundaries shown in Figure 2-114 were established using the T-T curves from the brazed assemblies and the SCC test data. Faster heating rates than 8°F/minute produce wetting of the silver braze alloy on the titanium (See Figure 2-112) and adequate shear strength, however, the stress corrosion delamination resistance is very low. Heating rates slower than 3.8°F/minute between 1400°F and 1500°F do not produce a braze joint of acceptable quality and shear strength (See Figure 2-112). To ensure complete melting of the brazing alloy, the minimum temperature was set at 1580°F. As explained in Section V, the melting point of the alloy increases as the heating rate decreases. The total time above 1400°F was set at 55 minutes minimum because panels 25A, 14A, 4 and 7 which had good stress corrosion delamination resistance were above 1400°F for 55 to 65 minutes. The 90 minute maximum time above 1400°F was set on the basis of the anticipated cycle achievable for brazing the fullscale lower plate but no tests were conducted to confirm this time interval. The T-T braze curve for 603FTB035#2 is superimposed on Figure 2-114 to show the relation of an actual braze cycle to establish boundaries.

2.4.5 Welding Development

The electron beam (EB) welding process for beta annealed 6Al-4V titanium has been established. Test assemblies have been welded and the evaluation test program has been completed. The test data compares favorably with data generated by Boeing Company on the same alloy during the Supersonic Transport Program. GTA welding of 10 Nickel steel has been accomplished and a production process established. The test program for this process on 10 Nickel steel has also been completed. The data for both of EB welded titanium and the GTA weld 10 Nickel steel is being included in the Materials Property Data Report and static design

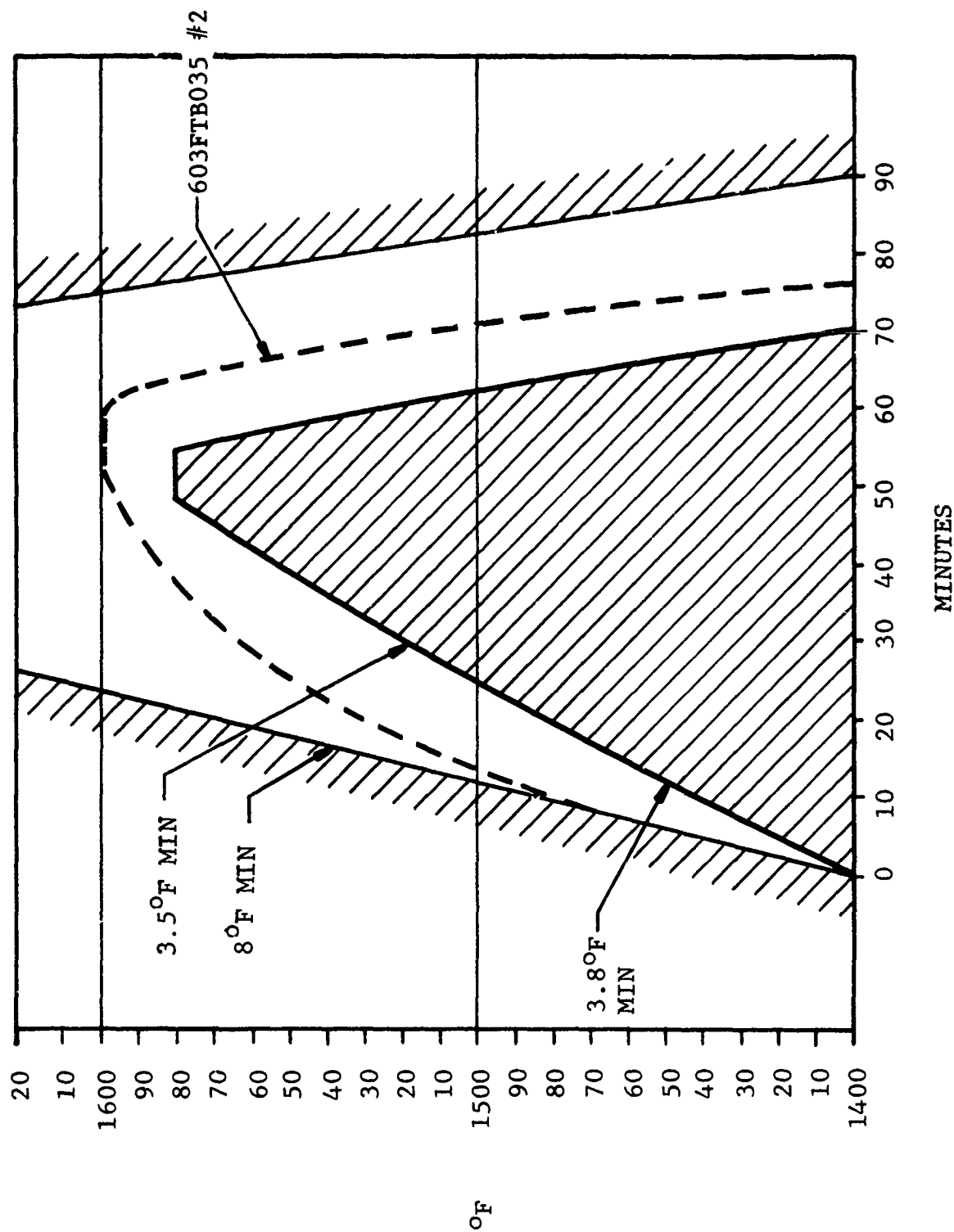


Figure 2-114 AMAVS BRAZING CYCLE TIME-TEMPERATURE BOUNDARIES

allowables and fracture mechanics properties based on this data is shown in Table II-33. The fatigue and crack growth data is included in subsection 2.3 of this report.

Election beam welding of 10 Nickel steel is also desirable for producing joints in thick sections. Welding of 1/2" and 1" thick section has not presented a problem and weld parameters are tentatively established. EB welding of 1.6-inch thick material using present procedures, however, has presented a cracking problem. The cracks are found in the center of the depth of the weld joint. A transverse cross-section of the weld joint shows the width of the center of the joint to be greater than the top or bottom. The heat transfer coefficient for 10 Nickel steel is different than that for D6ac steel which was used for establishing the parameters used to date. The high cobalt content of the 10 Nickel steel changes the heat transfer coefficient and therefore the parameters for heavy sections must be modified. Additional processing parameter studies are required.

2.4.6 Adhesive Bonding Development

Confirmation testing of aluminum adherends using the PL 717B adhesive and PL 718 corrosion inhibiting primer has been completed. Lapshear, peel, and flatwise tension tests were conducted. Data indicated no particular difference in strengths when using primer, and peel data was not sensitive to primer thickness. The peel strength was of interest because some corrosion inhibiting systems reduce peel strength. As noted, this is not the case with PL 717B adhesive and PL 718 primer. No processing problems are anticipated with the system during component fabrication. The test data will be included in the Materials Property Data Report.

2.4.7 Materials and Processes Specifications

A number of specifications are required to cover new materials and processes and speciality items required for the AMAVS program. A list of these which have been written for this program is shown in Table II-34. These documents will be released progressively as the drawings requiring their use are released, however, all but four have been completed.

Table II-33 DESIGN ALLOWABLES FOR WELD JOINTS

	Beta Annealed 6Al-4V Ti	10 Nickel Steel
Weld Joint Efficiency	85%	85%
K_{IC} (KSI $\sqrt{\text{inch}}$) Typ.	72	N.A.
K_{Iscc} (KSI $\sqrt{\text{inch}}$) Typ.	60	N.T.P.

N.A. = Not Available

N.T.P. = No Test Planned

6Al-4V Ti EB Welded

10 Nickel Steel GTA Welded

TABLE II-34
AMAVS SPECIFICATIONS

<u>Number</u>	<u>Title</u>
X7223990	Exterior Finish
X7224194	7050 Aluminum Alloy Special Billet Procurement Specification
X7224195	7050 Aluminum Alloy Billet Special Process Treatment
X7224196	Sealant Application
X7224197	Adhesive Bonded Panel Detail Preparation
X7224198	Identification of Parts
X7224199	Material Traceability Procedures
FMS-1108	Aluminum Alloy, 7050 Sheet and Plate
FMS-1109A	Titanium Alloy, 6Al-4V, Beta Annealed
FMS-1111	Steel Alloy, 10Ni-2Cr-1Mo-8Co (10 Nickel) Bar, Forged Billet and Plate
FMS-1112	Wire, Welding - Type 10 Nickel
FMS-1113	Titanium Alloy, 3Al-8V-6Cr-4Mo-2Zr (Beta C)
FMS-1114	Brazing Alloy, Silver-Aluminum-Manganese, Strip
FMS-1115	Welding Wire, 6Al-4V Titanium Alloy, E.L.I.
FMS-1116	Adhesive, 250°F Cure, 180° Service
FPS-1074	Welding, Electron Beam, General Specification
FPS-1092	Adhesive Bonding Process
FPS-1093	Al-Mn Plating Process
FPS-1094	Furnace Brazing Process
FPS-1095	GTA Welding Process
FPS-1096	Heat Treatment and Processing Requirements, 10 Nickel Steel
FPS-1097	Inspection Processes and Acceptance Standards for Welded Joints

2.4.8 Corrosion Prevention System

The corrosion prevention requirements for the AMAVS program are described in detail in FZM-6183, "Corrosion Prevention Requirements, AMAVS Program, Contract F33615-73-C-3001", dated 23 August 1973. The finishing procedures contained in FZM-6183 comply with the requirements of MIL-E-7179D and MIL-S-5002C and are compatible with those required by Rockwell International for the B-1.

A pilot scale aluminum-manganese alloy plating facility is in operation and has been used to plate approximately 400 high strength H-11 tapered shank fasteners for the AMAVS component test program. The aluminum manganese alloy plating will be used in lieu of cadmium on high strength H-11 fasteners installed in titanium alloy structures.

2.5 WEIGHTS

Weight estimates are shown for the FSIL and NBB configurations in Tables II-35 and II-36 by structural elements. The total weight of 12054.0 pounds for the FSIL is 12.4% less than the baseline. The total weight of 12508.4 pounds for the NBB is 9.1% less than the baseline. These estimated weights are also shown by material breakdown in Figures 2-115 and 2-116.

These reported weights include allowances to provide an aircraft compatible installation. Updated loads, conditions, and interfaces are included in this compatibility.

The impact of individual items on the FSIL configuration weight is shown below.

	<u>Pounds</u>
Phase Ib - AFFDL TR-73-40 p. 2-434 (FSRL)	11168
10% Gross Weight Increase	500*
Update Loads	284*
Fairing Support Ribs	76*
Non-optimum allowance	224
Change to integral lug	<u>-52</u>
Phase II Expected Weight for FSIL	12200
Current Status for FSIL (Fig. 1)	12054
*Remove task change from current status for comparison with Phase Ib target	-860
Current status for comparison with Phase Ib target of 11168.	11194

The current status of the NBB configuration is only 100 pounds above the Phase Ib estimate after incorporating the updated baseline data. However, significant configuration changes were incorporated simultaneously with the baseline update.

Table II-35

GENERAL DYNAMICS
66JF PROCEDURE 41K

CONVAIR AEROSPACE DIVISION
PROBLEM J95482-15

FORT WORTH OPERATION
11/12/73 PAGE J163

FAIL SAFE INTEGRAL LUG(FSIL)-ADV METALLIC WING CARRY THRU STRUCT
DESIGN GROUP 04 TOTAL

WEIGHT SUMMARY

	119 OUTBOARD	84 -119 INTERMEDIATE	J - 84 CENTER	TOTAL STR
STRUCTURAL BOX	1697.9	2494.1	3779.6	8171.5
LOWER PLATE	930.8	887.7	1179.2	2997.7
COVER	0.0	887.7	1179.2	2066.9
LUGS	930.8	J.0	J.0	930.8
UPPER PLATE	493.6	711.6	724.8	1933.9
COVER	0.0	711.6	728.8	1447.3
LUGS	493.6	J.0	J.0	493.6
BULKHEADS	39.4	614.0	1309.9	1953.9
332 BULKHEAD	0.0	277.1	417.6	694.8
347 BULKHEAD	0.0	28.0	269.9	297.9
362 BULKHEAD	0.0	0.0	J.0	J.0
977 BULKHEAD	J.0	38.1	79.3	117.3
992 BULKHEAD	39.4	261.4	543.2	844.0
R135	309.8	240.1	301.2	951.1
J BUTTLINE	0.0	J.0	148.9	148.9
39 BUTTLINE	0.0	J.0	232.3	232.3
84 BUTTLINE	0.0	240.1	J.0	240.1
120 BUTTLINE	309.8	J.0	J.0	309.8
MISCELLANEOUS	124.2	50.1	180.5	354.8
MISCELLANEOUS	124.2	50.1	180.5	354.8
FITTINGS	1967.4	585.9	973.3	3451.5
XF72 TRUNNION	0.0	J.0	160.9	160.9
XF95 TRUNNION	0.0	120.1	J.0	120.1
992 SIDE BRACE	0.0	J.0	242.4	242.4
MLG DRAG BRACE	0.0	J.0	199.6	199.6
WING SWEEP AUT	113.4	386.0	J.0	499.4
PIN/SHLAR/NAC	1446.0	J.0	J.0	1446.0
XF LONGERON WF	0.0	J.0	41.4	41.4
LONGERON LOWER	313.2	J.0	J.0	313.2
LONGERON UPPER	24.4	0.3	J.0	24.7
LONGERON 25 DEG	0.0	J.0	140.0	140.0
LONGERON DORSAL	0.0	J.0	185.0	185.0
LUG RIB	76.4	J.0	J.0	76.4
SUBTOTAL	3865.3	2999.3	4757.9	11623.0
MISCELLANEOUS	2.5	10.3	413.2	431.0
SUBTOTAL	2.5	10.3	413.2	431.0
UPPER FAIRING	0.0	3.0	110.4	113.4
LOWER FAIRING	0.0	3.7	166.4	170.1
EXTERIOR FINISH	0.0	0.0	4.0	4.0
FILLETS	J.0	J.0	15.0	15.0
PROVISIONS-FUEL	2.5	8.0	77.5	88.0
PROVISIONS-HYD	0.0	J.0	2.0	2.0
PROVISIONS-AUX G	0.0	J.0	19.0	19.0
PROVISIONS-ELEC	0.0	J.0	20.0	20.0
TOTAL	3367.8	3315.1	5171.1	12054.0

COPY AVAILABLE TO DDC DOES NOT
PERMIT FULLY LEGIBLE PRODUCTION 2-261

Table II-36

GENERAL DYNAMICS
6657 PROCEDURE R1KCONVAIR AEROSPACE DIVISION
PROBLEM 675465-46FORT WORTH OPERATION
11/12/73 PAGE 0042NO-BOX BOX (N33)-ADVANCE METALLIC WING CARRY THRU STRUCTURE
DESIGN GROUP 34 TOTAL

WEIGHT SUMMARY

	119 OUTBOARD	84 - 119 INTERMEDIATE	0 - 84 CENTER	TOTAL STR
STRUCTURAL 3 X	2423.2	3137.5	3346.1	8937.2
LOWER PLATE	1181.1	928.3	821.1	2929.4
COVER	0.0	928.3	821.1	1748.4
LUGS	1181.1	0.0	0.0	1181.0
UPPER PLATE	506.8	1113.2	431.7	2131.7
COVER	0.0	1113.2	431.7	1544.9
LUGS	506.8	0.0	0.0	506.8
BULKHEADS	0.0	893.3	1600.3	2499.7
932 BULKHEAD	0.0	523.0	597.7	1120.3
947 BULKHEAD	0.0	0.0	182.1	182.1
962 BULKHEAD	0.0	0.0	0.0	0.0
977 BULKHEAD	0.0	0.0	0.0	0.0
992 BULKHEAD	0.0	364.7	826.5	1191.3
RIBS	493.5	171.5	347.1	1012.2
0 BUTTLINE	0.0	0.0	149.2	149.2
39 BUTTLINE	0.0	0.0	197.9	197.9
84 BUTTLINE	0.0	171.5	0.0	171.5
120 BUTTLINE	493.5	0.0	0.0	493.5
MISCELLANEOUS	161.3	31.0	140.9	334.3
MISCELLANEOUS	161.3	31.0	140.9	334.3
FITTINGS	1701.5	511.1	957.7	3170.2
XF72 TRUNNION	0.0	0.0	169.9	169.9
XF95 TRUNNION	0.0	121.1	0.0	121.1
992 SIDE BRACE	0.0	0.0	225.3	225.3
MLG DRAG BRACE	0.0	0.0	199.2	199.2
WING SWEEP ALT	105.6	391.9	0.0	496.5
PIN/SH-AR/NAC	1443.0	0.0	0.0	1443.0
XFJ LONGERON WF	0.0	0.0	39.4	39.4
LONGERON LOWER	55.1	0.0	0.0	55.1
LONGERON UPPER	24.4	0.0	0.0	24.4
LONGERON 25 JEG	0.0	0.0	140.0	140.0
LONGERON DORSAL	0.0	0.0	185.0	185.0
LUG RIB	76.4	0.0	0.0	76.4
SUBTOTAL	4124.7	3643.9	4303.8	12072.4
MISCELLANEOUS	2.5	118.0	310.5	431.0
SUBTOTAL	2.5	118.0	310.5	431.0
UPPER FAIRING	0.0	114.0	0.0	114.0
LOWER FAIRING	0.0	0.0	170.0	170.0
EXTERIOR FINISH	0.0	0.0	4.0	4.0
FILLETS	0.0	0.0	15.0	15.0
PROVISIONS-FUEL	2.5	0.0	81.5	84.0
PROVISIONS-HYD	0.0	0.0	2.0	2.0
PROVISIONS-AUX	0.0	0.0	18.0	18.0
PROVISIONS-ELEC	0.0	0.0	20.0	20.0
TOTAL	4127.2	3766.9	4614.3	12508.4

COPY AVAILABLE TO DDC DOES NOT
PERMIT FULLY LEGIBLE PRODUCTION

FAIL SAFE INTEGRAL LOG (FSIL)-ADV METALLIC RING CARRY THRU STRUCT
DESIGN GROUP 04 TOTAL

MATERIAL	FORM	MATERIAL BREAKDOWN	
		WEIGHT	PERCENT
2024 ALUMINUM		(445.4)	(3.69)
	SHEET	171.4	1.41
	PLATE	275.0	2.28
5052 ALUMINUM		(81.4)	(.68)
	CORE	81.4	.68
7050 ALUMINUM		(1685.2)	(13.98)
	SHEET	217.3	1.80
	PLATE	1467.9	12.18
OTHER ALUMINUM		(66.5)	(.55)
	PLATE	63.5	.53
	FASTENERS	.9	.01
	SHIM STOCK	2.2	.02
6-4 BA TITANIUM		(6024.3)	(54.95)
	PLATE	6024.3	54.95
COMPURE TITANIUM		(32.6)	(.27)
	SHEET	32.6	.27
OTHER TITANIUM		(21.5)	(.18)
	PLATE	13.4	.11
	FASTENERS	8.1	.07
662 TITANIUM		(83.7)	(.69)
	PLATE	83.7	.69
10 NI STEEL		(214.2)	(1.78)
	PLATE	214.2	1.78
AMS 5629 STEEL		(10.7)	(.09)
	PLATE	10.7	.09
OTHER STEEL		(561.8)	(4.66)
	FASTENERS	561.8	4.66
ADHESIVES		(93.5)	(.78)
	FMS-1116 TYPE I	42.0	.35
	FMS-1116 TYPE III	11.4	.09
	FMS-1116 TYPE II	.0	.00
	BRAZING ALLOY	39.0	.33
RUBBERS		(1.0)	(.01)
	SILICONE	1.0	.01
SEALANTS		(28.0)	(.23)
	FMS 1043 GENERAL	28.0	.23
PURCHASED PARTS		(2104.3)	(17.46)
	RING	2104.3	17.46
TOTAL		(12054.3)	(100.00)

Figure 2-115 CONVAIR AEROSPACE DIVISION PROBLEM 005485-05
2-263

NO-80X BOX (N33)-ADVANCE METALLIC WING CARRY THRU STRUCTURE
DESIGN GROUP 64 TOTAL

MATERIAL	FORM	MATERIAL BREAKDOWN WEIGHT	PERCENT
2024 ALUMINUM		(780.0)	(6.24)
	SHEET	242.1	1.94
	PLATE	537.9	4.31
5052 ALUMINUM		(136.1)	(1.09)
	CORE	136.1	1.09
7050 ALUMINUM		(344.2)	(2.75)
	SHEET	14.3	.12
	PLATE	329.9	2.63
OTHER ALUMINUM		(1.2)	(.01)
	FASTENERS	.3	.00
	SHIM STOCK	.9	.01
6-4 BA TITANIUM		(1660.4)	(13.27)
	SHEET	127.0	1.02
	PLATE	1532.9	12.25
COMPURE TITANIUM		(142.5)	(1.14)
	SHEET	21.5	.17
	PLATE	120.9	.97
OTHER TITANIUM		(2.1)	(.02)
	FASTENERS	2.1	.02
18 NI STEEL		(6773.3)	(54.15)
	SHEET	300.4	2.40
	PLATE	6049.9	48.37
	FORGING	423.0	3.38
AMS 5629 STEEL		(10.7)	(.09)
	PLATE	10.7	.09
OTHER STEEL		(448.0)	(3.58)
	FASTENERS	448.0	3.58
PAINT + FINISHES		(1.2)	(.01)
	EPOXY PRIMER	1.2	.01
ADHESIVES		(53.0)	(.42)
	FMS-1116 TYPE I	44.0	.36
	FMS-1116 TYPE III	8.0	.07
	FMS-1116 TYPE II	.0	.00
RUBBERS		(1.0)	(.01)
	SILICONE	1.0	.01
SEALANTS		(20.7)	(.17)
	FMS 1043 GENERAL	20.7	.17
PURCHASED PARTS		(2133.4)	(17.06)
	WING	2133.4	17.06
	TOTAL	(12508.4)	(100.00)

Figure 2-116 CONVAIR AEROSPACE DIVISION PROBLEM 005485-06

2.6 CONFIGURATION RATINGS

The merit rating equation and the grading system developed in Section II, Volume II, of AFFDL-TR-73-40 were applied to the two WCTS configurations. Grades for each major category, with the exception of Technology Advancement, are shown in Tables II-37 through II-40. Technology Advancement was rated equal for the configurations and a grade of 6.0 was assigned for this category.

Table II-37 EFFICIENCY GRADE

CONFIGURATION	% WEIGHT REDUCTION	N_{WT}	% COST REDUCTION	N_{COST}	$N_{EFF.}$
FSIL	12.42	5.97	33.15	7.63	6.97
NBB	9.11	4.64	35.0	8.00	6.66

Table II-38 INTEGRITY AND RELIABILITY GRADE

SUB-CATEGORY GRADES	CONFIGURATION	
	FSIL	NBB
STATIC STRENGTH RESERVE	0	0
N_{STATIC}	1.0	1.0
% FASTENER REDUCTION	69.7	70.8
$N_{FATIGUE}$	7.97	8.08
DAMAGE TOLERANCE SCORES		
MULTIPLE LOAD PATHS	1.5	0.0
PLANE STRESS FRACTURE	2.0	2.0
PLANE STRESS FRACTURE	1.5	2.0
SAFE CRACK GROWTH	2.0	1.2
LEAK BEFORE BREAK	1.0	0.0
FAIL SAFE	1.0	0.0
$N_{SCG} = N_{DAM. TOL.}$	8.0	5.2
N_{INTEG}	6.59	5.22

Table II-39 ILITIES GRADE

SUB-CATEGORY GRADES	CONFIGURATION	
	FSIL	NBB
INSPECTABILITY		
MATERIAL	.3	.6
JOINING PROCESSES	.5	.8
DETAIL PART CONFIG.	.6	.9
SUB-ASSEMBLY CONFIG.	1.3	1.7
EQUIP. & TECHNIQUES	.8	.8
ACCESSIBILITY	1.7	1.7
FIELD INSPEC. CAP.	1.4	1.1
N_{INSPECT}	6.6	7.6
MANUFACTURABILITY		
BASIC MFG.	1.968	1.527
SECONDARY MFG.	2.748	2.835
SUB-ASSEMBLY	1.886	1.28
FINAL ASSEMBLY	1.008	1.364
N_{MFT}	7.61	7.01
MAINTAINABILITY		
ACCESSIBILITY	0.3	0.9
FUEL PURGING	2.2	2.5
MECH. JOINTS-COMPLEXITY	2.2	2.5
RESIST. TO GRD. DAMAGE	0.8	0.9
COMPLEXITY OF REPAIR	1.5	2.0
N_{MAINT}	6.4	8.2
REPAIRABILITY		
LUGS	1.2	1.8
LOWER PLATE/RAILS	2.7	1.5
UPPER COVER/RAILS	1.5	1.8
EXTERIOR PANELS	0.7	0.8
INTERNAL STRUCTURE	0.8	0.8
N_{REPAIR}	6.9	6.7
PREDICTABILITY		
PROCESS	2.5	3.5
MATERIAL	2.8	2.6
ANALYSIS	2.5	2.5
N_{PREDICT}	7.8	8.6

Table II - 40 CONFIGURATION RATINGS

CONFIGURATION			
	FSIL		"NO-BOX" BOX
CATEGORY	Detail Item Grades	Category Grade	Detail Item Grades Category Grade
EFFICIENCY	$\frac{N_{WT}}{N_{COST}} = \frac{5.97}{7.63}$	$N_{EFF.} = 6.97$	$\frac{N_{WT}}{N_{COST}} = \frac{4.64}{8.00}$ $N_{EFF.} = 6.66$
TECHNOLOGY ADVANCEMENT		$N_{TECH ADV} = 6.0$	$N_{TECH ADV} = 6.0$
INTEGRITY AND RELIABILITY	$\frac{N_{STATIC}}{N_{FATIGUE}} = \frac{1.0}{7.97}$ $\frac{N_{SCG}}{N_{DAM.TOL.}} = \frac{8.0}{8.0}$	$N_{INTEG.} = 6.59$	$\frac{N_{STATIC}}{N_{FATIGUE}} = \frac{1.0}{8.08}$ $\frac{N_{SCG}}{N_{DAM.TOL.}} = \frac{5.2}{5.2}$ $N_{INTEG.} = 5.22$
ILITIES	$\frac{N_{INSPECT.}}{N_{MFT}} = \frac{6.6}{7.61}$ $\frac{N_{MAINT}}{N_{REPAIR}} = \frac{6.4}{6.9}$ $N_{PREDICT} = 7.8$	$N_{ILITIES} = 7.03$	$\frac{N_{INSPECT.}}{N_{MFT}} = \frac{7.6}{7.01}$ $\frac{N_{MAINT}}{N_{REPAIR}} = \frac{8.2}{6.7}$ $N_{PREDICT} = 8.6$ $N_{ILITIES} = 7.49$
Merit Rating	$M.R. = 6.57$		$M.R. = 6.11$

2.7 CONFIGURATION SELECTION

Based on the configuration ratings of subsection 2.6, the FSIL configuration was recommended as the configuration to be manufactured in Phase III of the AMAVS Program. A Phase II Design Review, attended by AFFDL, AFML, ASD and contractor personnel, was held to review the two designs and select the configuration to be manufactured. After this review, the NBB was selected for Phase III.

Selection of the NBB configuration was based on the following major points:

1. The two designs were rated equal by AFFDL, AFML, and ASD personnel. Both were considered to be good designs which met the program objectives.
2. There are fewer manufacturing problems anticipated for the NBB configuration. The risk in the development of the brazing process was considered to be high in comparison to the expected pay-off.
3. It was also felt that the stresses induced in the braze line were not sufficiently high to prove the worth of the braze in this application. This concern was the result of the basic design philosophy of using mechanical fasteners at all points of load transfer in the FSIL configuration.

SECTION 3

TESTING

3.1 MATERIALS TESTING

Materials testing as required to support the detail design and analysis effort was started in Phase Ib and was essentially complete at the end of Phase II. This testing is defined in AFFDL-TR-73-40 and AFFDL-TR-73-77. Significant test results are presented in Section 2.4 of this report. The complete results of this testing are being reported to the Air Force Flight Dynamics Laboratory in General Dynamics Report No. FZM-6148.

3.2 COMPONENT TESTING

During Phase II a follow-on component test program was established. This series of tests, called Group II Tests, was established to verify the structural integrity of typical proposed hardware for the two configurations of WCTS, the "No-Box" Box, and the FSIL. A summary of the Group II Component Test Program is shown below.

Group II Tests

Test	Config.	Dwg. No.	No. of Specs.	Type of Test
Crack Growth Test Lower Plate	FSIL	603FTB033	6	Crack Growth
Damage Tolerance Lower Surface	FSIL	603FTB035	1	Damage Tolerance
Upper Surface Compression	FSIL	03FTB034	1	Static
Lower Aft Centerline Splice	"No-Box"	603FTB052	2	Fatigue
Lower Centerline Splice	FSIL	603FTB053	2	Fatigue-Static

3.2.1 Test Results

3.2.1.1 Crack Growth Test Lower Plate (Dwg. No. 603FTB033)

The braze assembly shown on this drawing was cut up to produce several test specimens (Figure 3-1). The purpose of the test was to provide information for the type of flaw to create on the damage tolerance test (603FTB035) and to prove that a crack in the center plate would not cross the braze lines into the reinforcing bars. Specimen A-1 was edge saw-cut as shown in Figure 3-2. The specimen was constant amplitude cycled at a load which caused stress equal to F_{tu} on the edge of the reinforcing bar. After 14 cycles of this loading a crack had initiated at the edge of the saw cut and progressed to the edge of the bar. At this point, constant amplitude cycling was stopped and spectrum cycling was started. Cycling was continued until one service life had been accomplished. The specimen was then static tested to failure. Failing load was 244,000 pounds. This load exceeds the predicted load, based on nominal specimen geometry and a fully plastic bending stress distribution, by about 40%. The larger than predicted failing load was the result of inelastic deformation of the specimen which caused the net section of the specimen to be more nearly in line with the load points.

Examination of the failed specimen showed that the crack in the center plate had progressed approximately two-thirds of the way under the bar, but the crack had not crossed the braze lines into the reinforcing bars.

Specimens B-1 and B-2 contained semi-circular surface cracks in the center plate. Cracks were created by eloxing and flexure of the center plate prior to brazing the assembly. Both specimens were spectrum fatigue tested identically using a 48.22 cycle per flight spectrum.

Specimen B-1 was tested for one service life, after which fatigue cracks were discovered in the load pin hole. The hole was bored out and the width of the center plate was reduced. Testing was resumed with the applied fatigue stresses increased by a factor of 1.33. The specimen failed through the loading hole after 549 flights of this loading.

Specimen B-2 was also reworked after one service life. Testing was resumed with the applied fatigue stresses increased by a factor of 1.33. Failure occurred in the test section after 1031 flights of this loading. Failure was due to independent fatigue of each of the three layers.

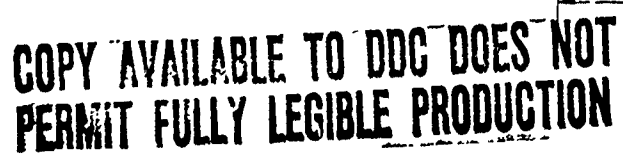
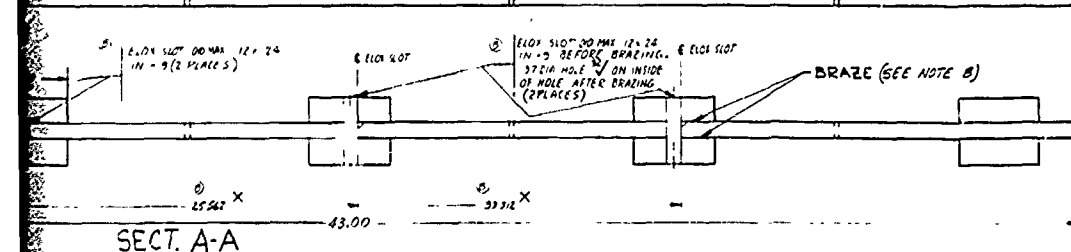
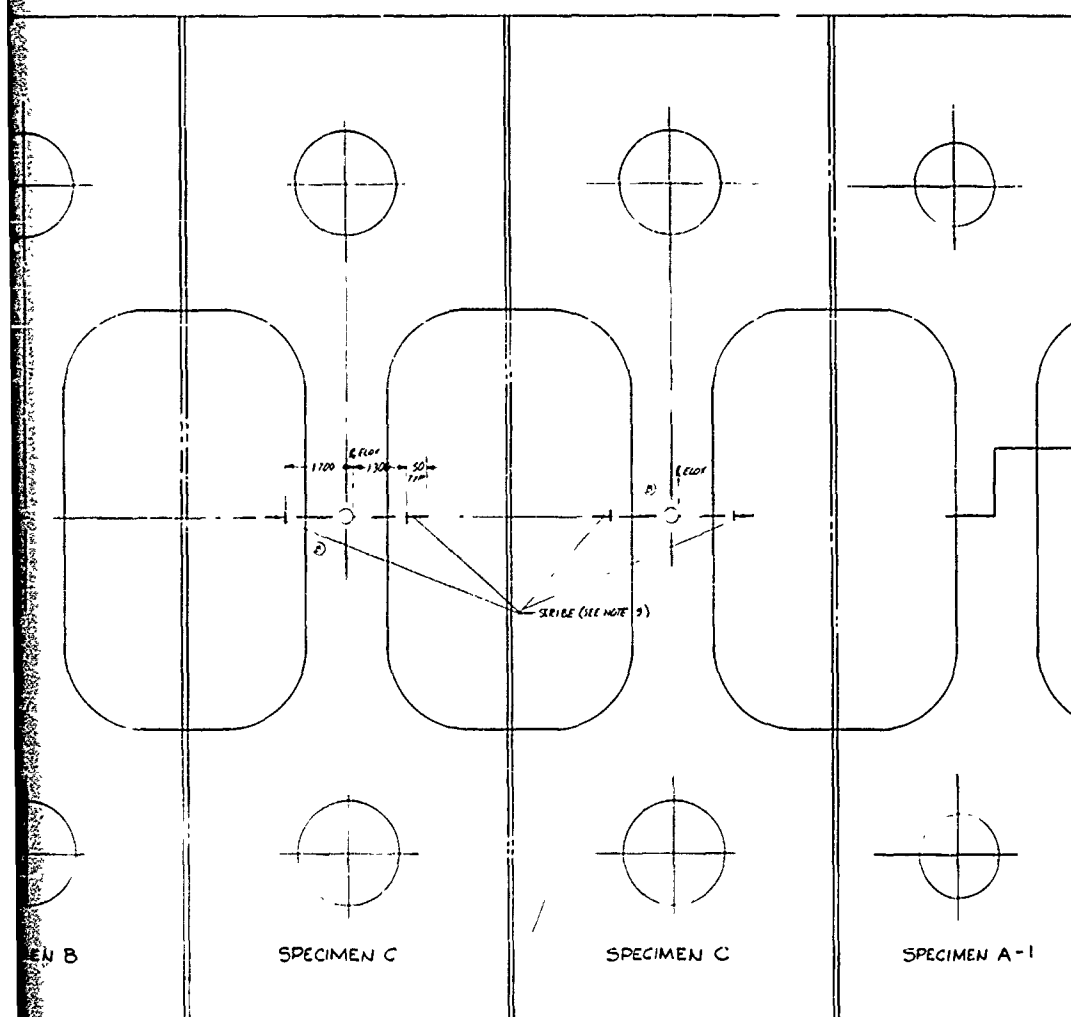


Figure 3-1 TEST SPECIMEN - DAMAGE TOLERANCE.

PLACES
BOTH SIDES
OF HOLE
HOLE

A	REDRAWN WITH CHANGES	DATE	BY
B	ADDED SLOT SLOTS		
C	ADDED S TO 14167		
	ADDED P TO 14167		

COPY AVAILABLE TO DDC DOES NOT
PERMIT FULLY LEGIBLE PRODUCTION



1. X DENOTES DIMENSIONS FOR LOCATING SLOT SLOTS IN-9 (SCRIBE LIGHTLY) & OF SLOT SLOTS ON-9 (CONTINUED W/SPRINT BEFORE Scribing 140E 007)
2. 1/2 OR BETTER ON MATING SURFACES ONLY IF LAMINA BEING BRAZED TOGETHER T-3 FINISH TO BE OBTAINED BY BELT SANDING BEFORE CHAMFERING.
3. STENCIL OUT SIDE ON UNSHARDED SURFACES.
4. FOR BRAZING INFORMATION CONTACT R.E. KEY, ENGR MATERIALS
5. NDI REQUIRED ON BRAZED ASSY
6. NO FINISH REQUIRED FOR -7/-9
7. BETA ANNEALED CAL ANTI-TITANIUM SEE ANR DEV 100 FOR SPECIFICATION.
8. .003 MAX MISMATCH BETWEEN LITTEL PASSES PERMISSIBLE ON OUT-CE SURFACES
9. -9 TO BE PRE-CRACKED 4 PLACES BEFORE BRAZING. CONTACT N.J. DARR, EXT 2071 OR 2078 FOR LOCATIONS.

PART NO	DESCRIPTION	STOCK SIZE	MATERIAL	DATE SPECIFICATION
14167	PLATE	14167	14167	14167
14167	PLATE	14167	14167	14167
14167	PLATE	14167	14167	14167
14167	PLATE	14167	14167	14167
14167	PLATE	14167	14167	14167
14167	PLATE	14167	14167	14167
14167	PLATE	14167	14167	14167
14167	PLATE	14167	14167	14167
14167	PLATE	14167	14167	14167
14167	PLATE	14167	14167	14167

DAMAGE TOLERANCE, BRAZED LOWER PLATE ELEMENT

3-3/3-4

603FTB033-A1

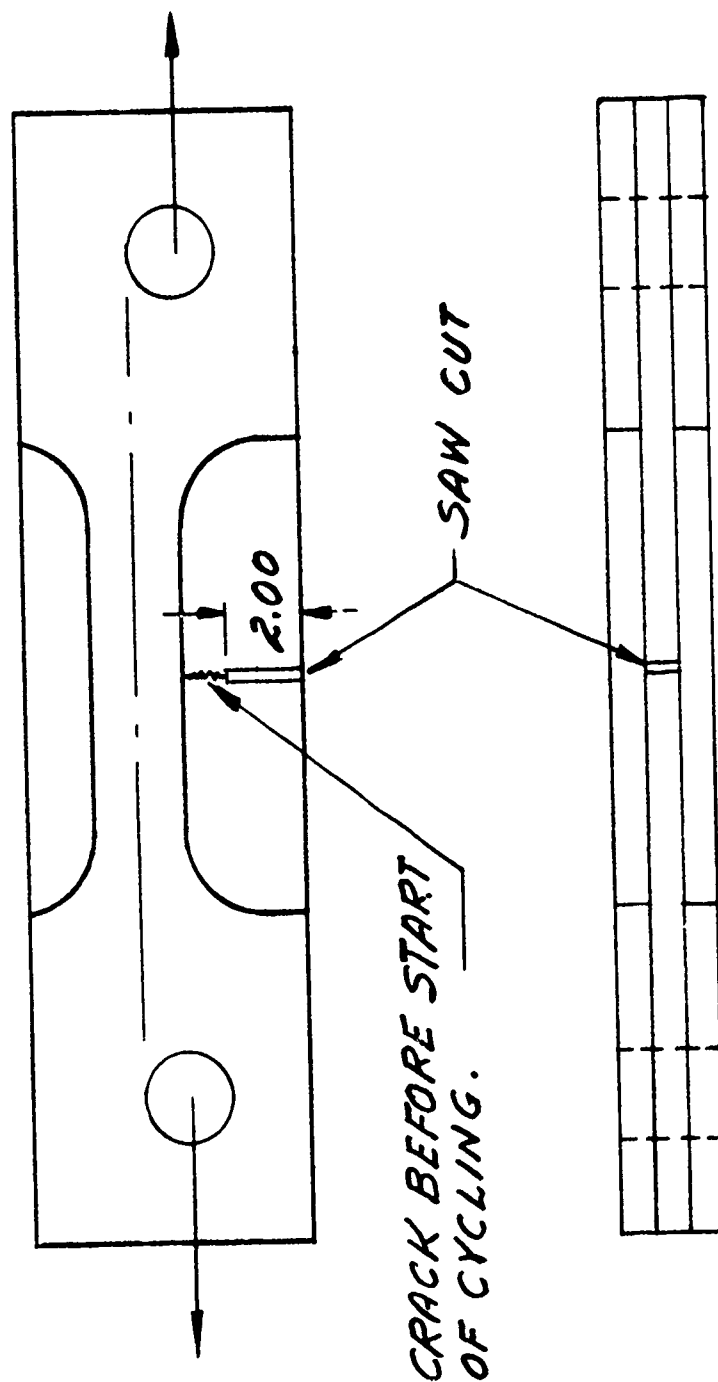


Figure 3-2 EDGE CRACKED CRACK GROWTH TEST

The Type C specimens each contained a corner crack in the center plate in a hole which was drilled through all three thickness. The crack was created by eloxing and flexure of the center plate prior to brazing and drilling the specimen.

The two specimens were tested identically using a 48.22 cycle per flight fatigue spectrum. Specimen C-1 failed through the load pin hole after one service life, plus 1166 flights. Specimen C-2 failed in the test section after one service life, plus 600 flights. Failure was due to independent fatigue of each of the three layers.

3.2.1.2 FSIL - Lower Surface, Damage Tolerance Test (Dwg. No. 603FTB035)

This specimen represented a cross section of the lower surface of the FSIL configuration in the region between $X_f = 84$, and the closure rib. Actual production material thicknesses were used. Because the magnitude of the loads required to test the specimen exceeded the capacity of the General Dynamics testing equipment, the specimen was tested at Southwest Research Institute in San Antonio, Texas. Figure 3-3 shows the specimen installed in the test rig.

The specimen had a 5-inch long elox slot through the web of one of the interior bays. The specimen was cycled 63 times from 0 to 110% of limit load, which resulted in the growth of cracks from the ends of the elox slot to almost the full width of the bay.

The specimen was then cycled to one quarter of a service life, using an accelerated spectrum of 3.22 cycles per flight. This did not result in any further extension of the cracks.

Following the fatigue cycling, the specimen was loaded to limit load. No additional crack growth was observed. Finally, the specimen was loaded to ultimate load, 3×10^6 pounds. During this loading the cracks extended under the bars.

An X-ray inspection following the test showed that the crack had progressed to about 2/3 of the way under the forward bar and about 1/2 of the way under the aft bar. Ultra-sonic inspection also revealed very local delamination of the braze lines in the region of the crack extensions.



Figure 3-3 603FTB035 TEST SPECIMEN IN TEST FIXTURE

3.2.1.2 Upper Surface Compression Test FSIL (Dwg. No. 603FTB043)

The specimen was designed to represent the area of the upper surface of the FSIL between the closure rib and bulkhead 84, and between the front spar and $Y_f = 947$. In order to simulate the normal support given to the upper surface by the spars and bulkheads of the WCTS, a fixture was designed that gives this support, but does not absorb any of the applied axial load. This fixture is shown in Dwg. No. 603FTB034. Figure 3-4 shows the specimen installed in the 1,000,000 pound test machine at General Dynamics

It was estimated that 800,000 to 1,000,000 pounds of applied load would be required to satisfy the requirements of the design. The specimen was loaded to the 1,000,000-pound capacity of the machine with no failure, and with no apparent permanent deformation.

3.2.1.3 Lower Aft Rail, Centerline Splice, "No-Box" Box (Dwg. No. 603FTB052)

This specimen design represented the splice at the centerline of the lower aft rail of an earlier configuration of the "No-Box" Box. Both specimens were tested to four service lives using a 48.22 cycle per flight fatigue spectrum. Figure 3-5 shows the specimen installed in the test fixture.

Following completion of the four lives of testing, the loading was changed on specimen No. 2 to an accelerated spectrum consisting of 3.22 cycles per flight. Testing was continued on this specimen until failure occurred at the equivalent of 9.6 lives.

3.2.1.4 Centerline Splice, Fuel Pump Holes, FSIL (Dwg. No. 603FTB053)

This specimen design represented the centerline splice of the lower surface of the FSIL in the second bay forward of the rear spar in the region of the cutouts for the fuel pump holes. Both specimens were tested to six service lives using a 48.22 cycle per flight spectrum. Figure 3-6 shows one of the specimens installed in the test fixture.

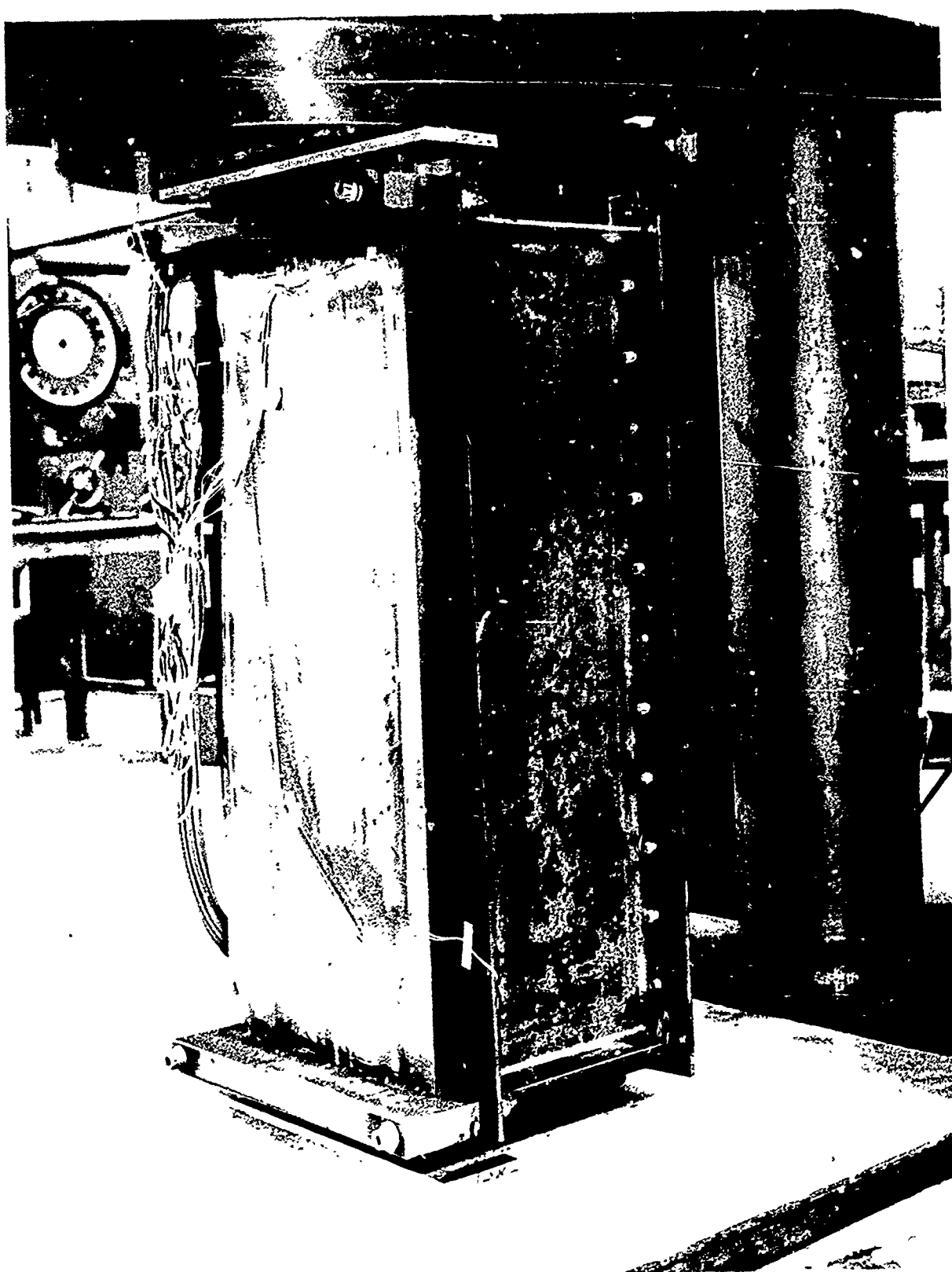


Figure 3-4 UPPER COVER COMPRESSION TEST SPECIMEN IN THE
1,000,000 LB TEST MACHINE

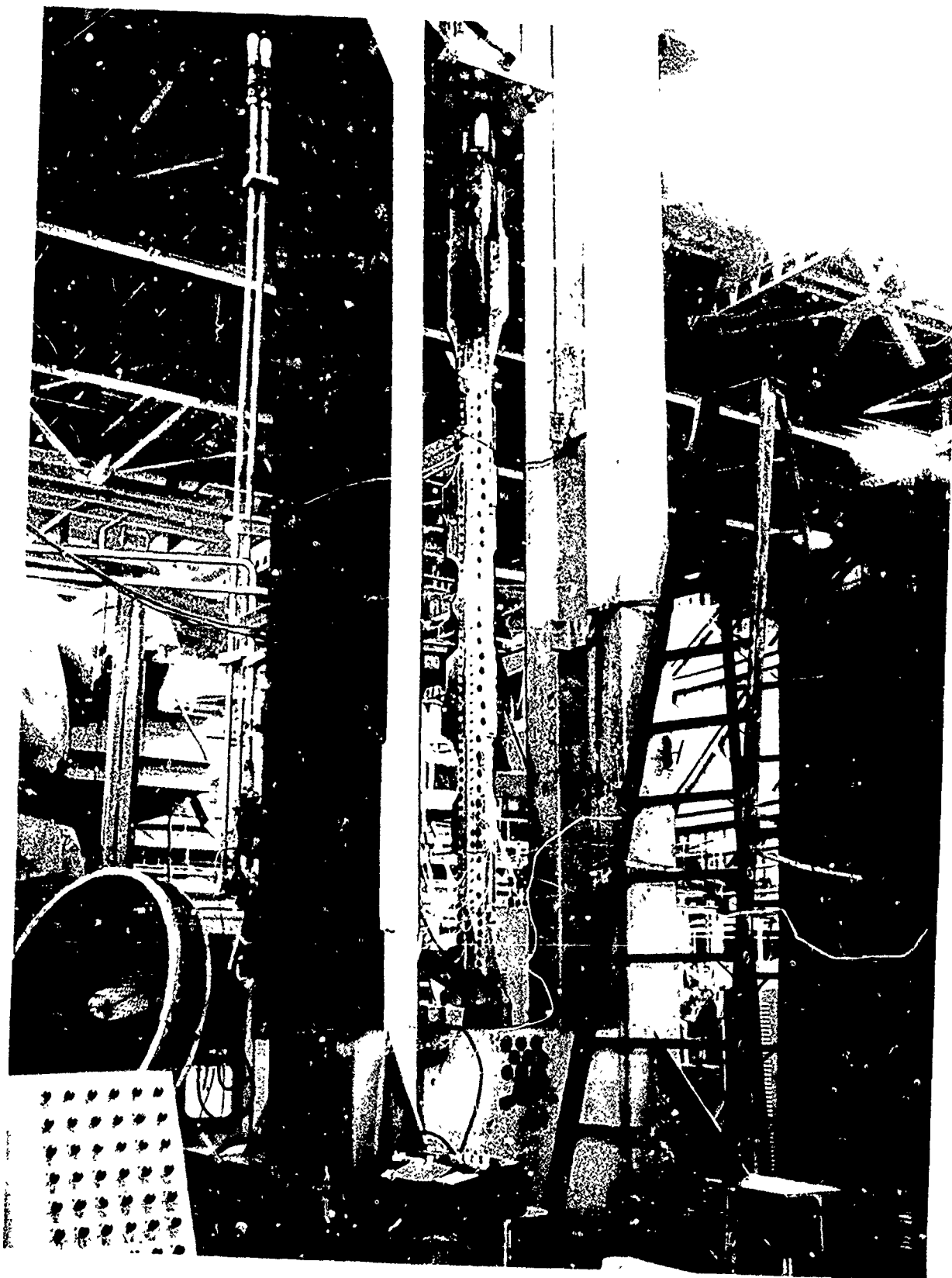


Figure 3-5 TEST SPECIMEN IN TEST FIXTURE (052)

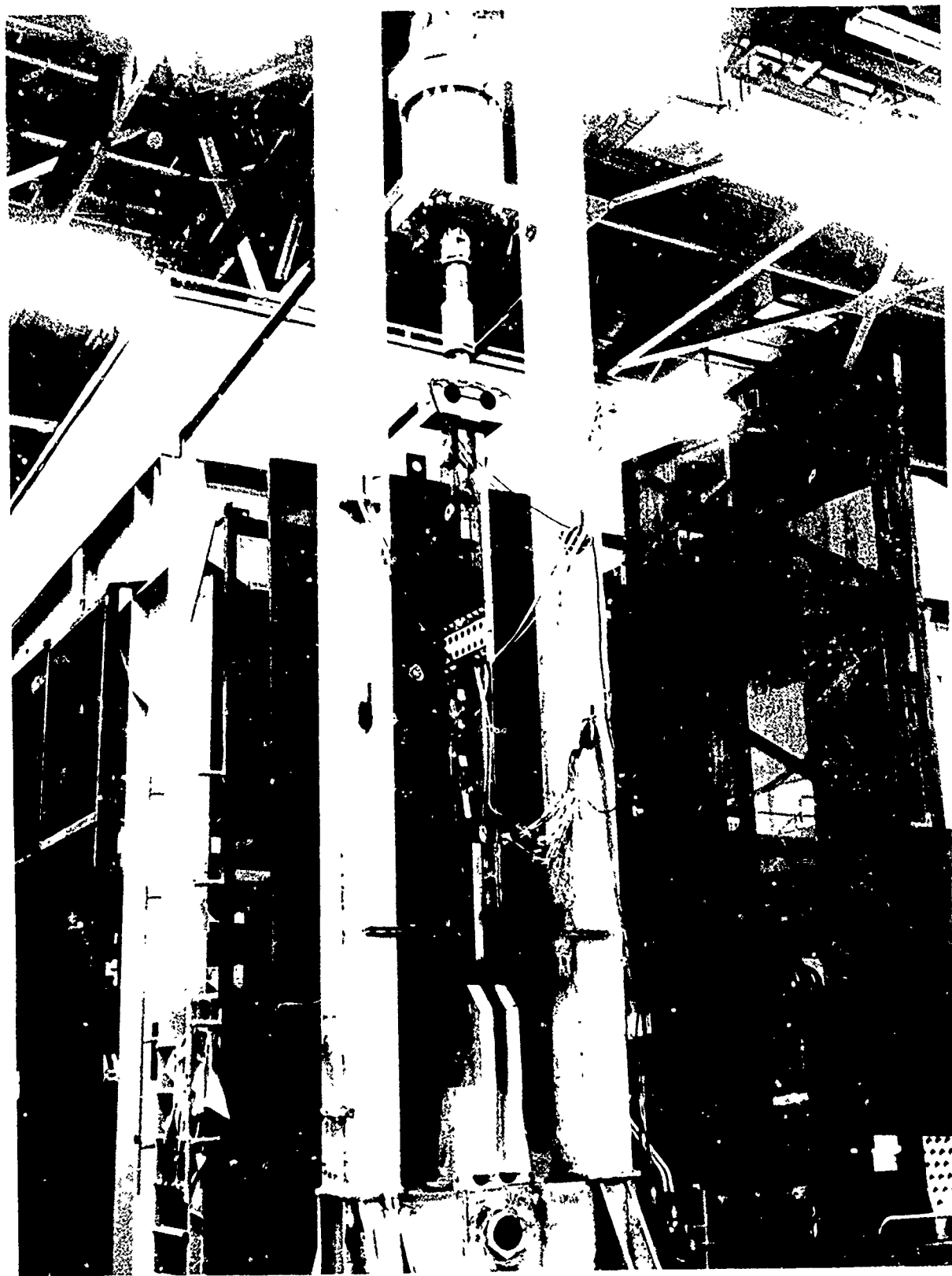


Figure 3-6 FSIL CENTERLINE SPLICE SPECIMEN IN FATIGUE FIXTURE

Specimen No. 2 was then continued in test using an accelerated spectrum of 3.22 cycles per flight for an additional 2.03 service lives at which time a fixture failure stopped the test. The specimen was then installed in the 1,000,000 Lb. test machine for static loading. The required static load capability of the specimen is 750,000 Lbs. The specimen was loaded three times to the 1,000,000 Lb. capability of the test machine. No failure occurred, and no permanent deformation was noted.

3.3 FULL SCALE TESTING

Testing is to be accomplished on a full-scale WCTS of the configuration chosen at the end of Phase II. This testing will be accomplished at AFFDL in the test setup shown in Figure 3-7. General Dynamics will provide test planning, test fixtures, and the test article, and AFFDL will provide test equipment and perform the testing. A definition of the planned testing is presented in AFFDL-TR-73-40 along with a description of the physical setup to be used for this testing.

3.3.1 Progress During Phase II

A plan was developed for manufacturing the full-scale test fixture, shipping it to AFFDL, and reassembling it. This plan involves three shipments of hardware as shown in Figures 3-8, 3-9, and 3-10. The initial shipment will allow early installation and checkout of loading systems and of some data systems elements. The second shipment will allow full preparation for final mating, while the test article is still in manufacture. The final shipment will complete the setup and will facilitate final checkout and testing. Design of the test fixture is nearing completion, as is the procurement of fixture materials and hardware. Manufacture of the test fixture is progressing satisfactorily. Status at the end of the reporting period is shown in Table III-1 for the main elements of the test fixture.

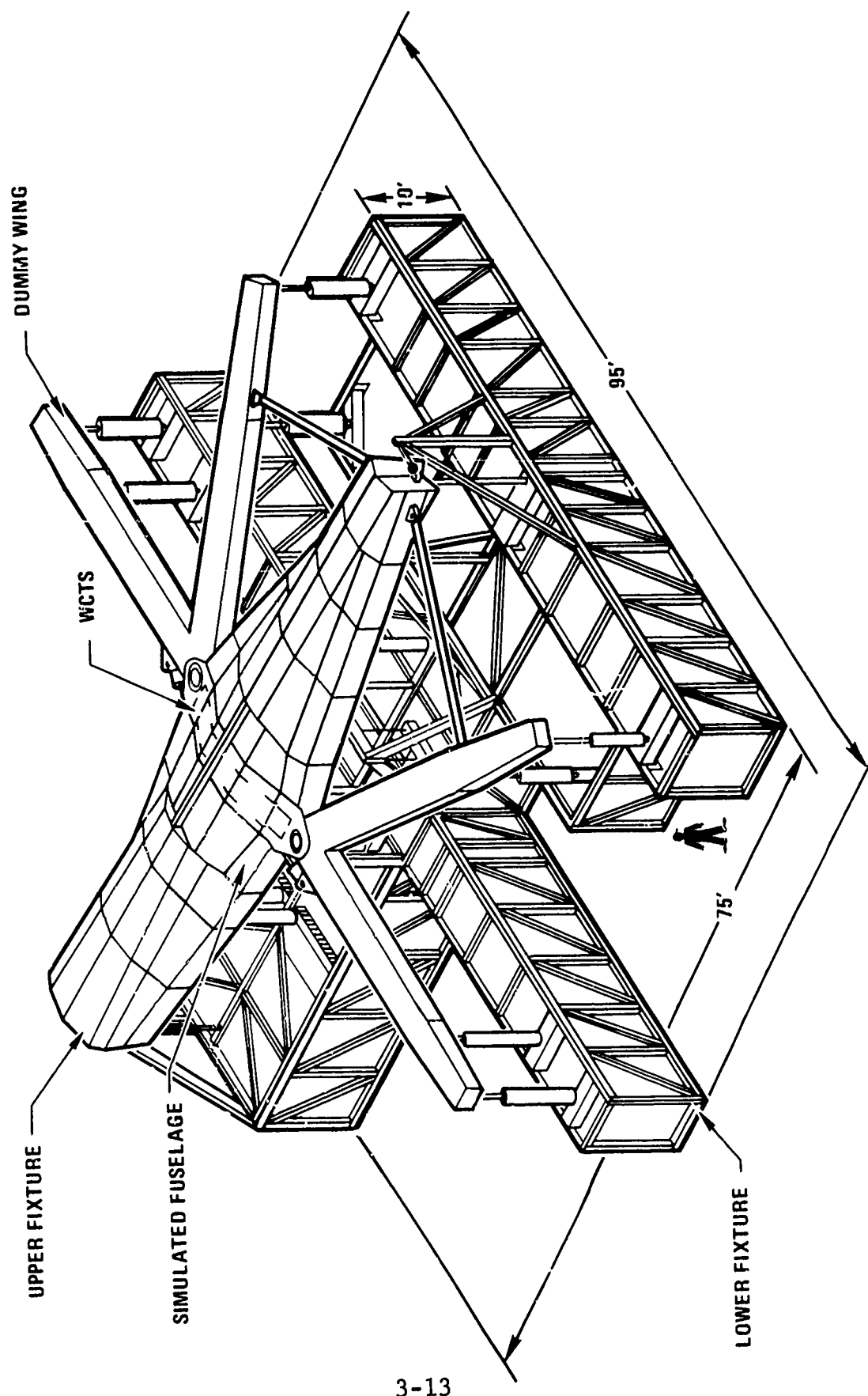


Figure 3-7 AMAVS FULL SCALE TEST

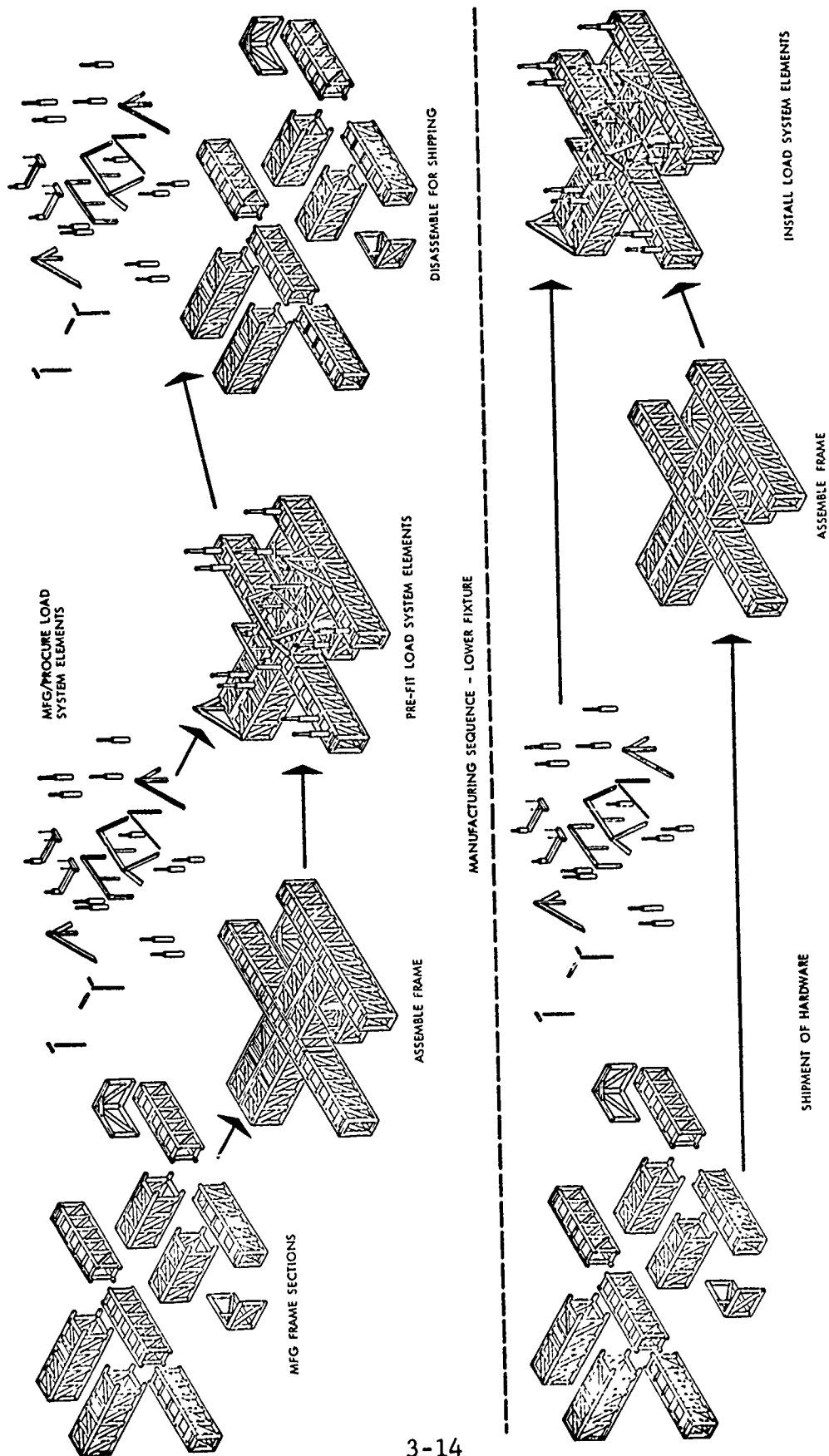
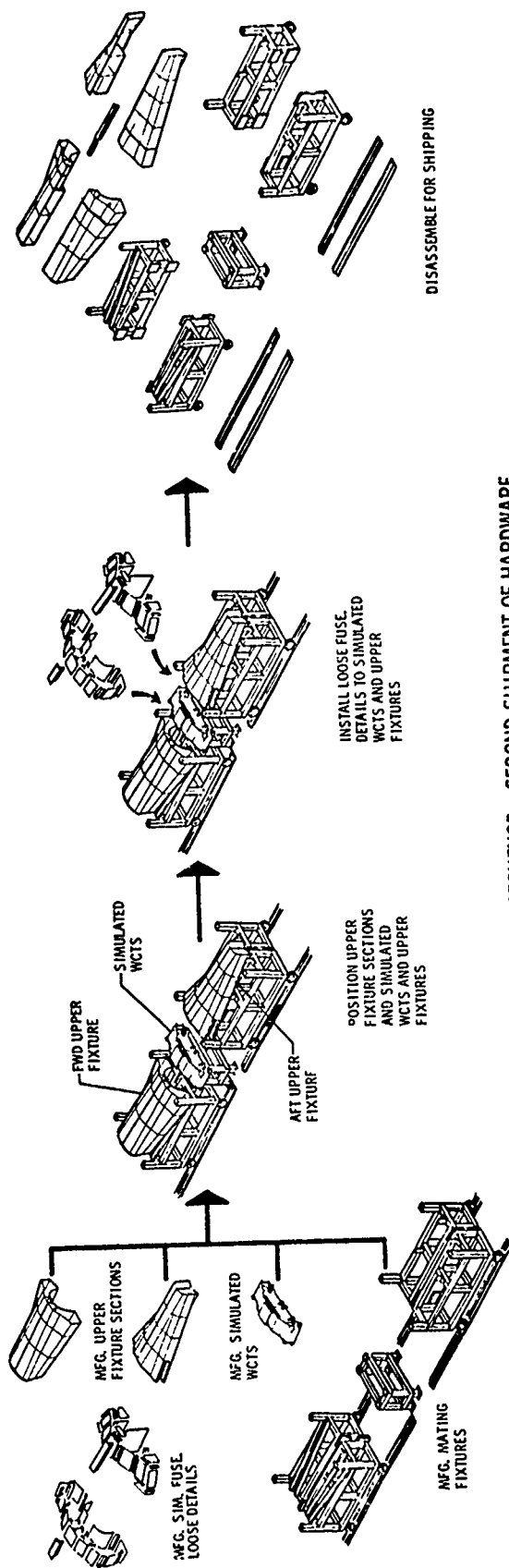


Figure 3-8 REASSEMBLY SEQUENCE - LOWER FIXTURE



MANUFACTURING SEQUENCE - SECOND SHIPMENT OF HARDWARE

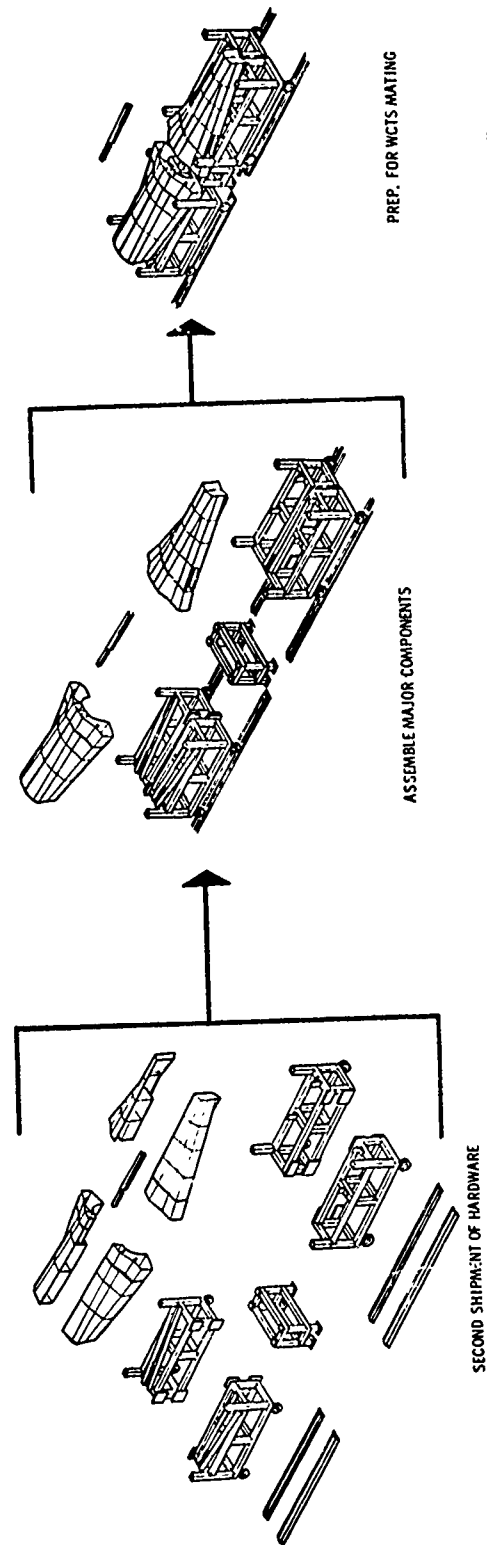


Figure 3-9 REASSEMBLY SEQUENCE - SECOND SHIPMENT OF HARDWARE

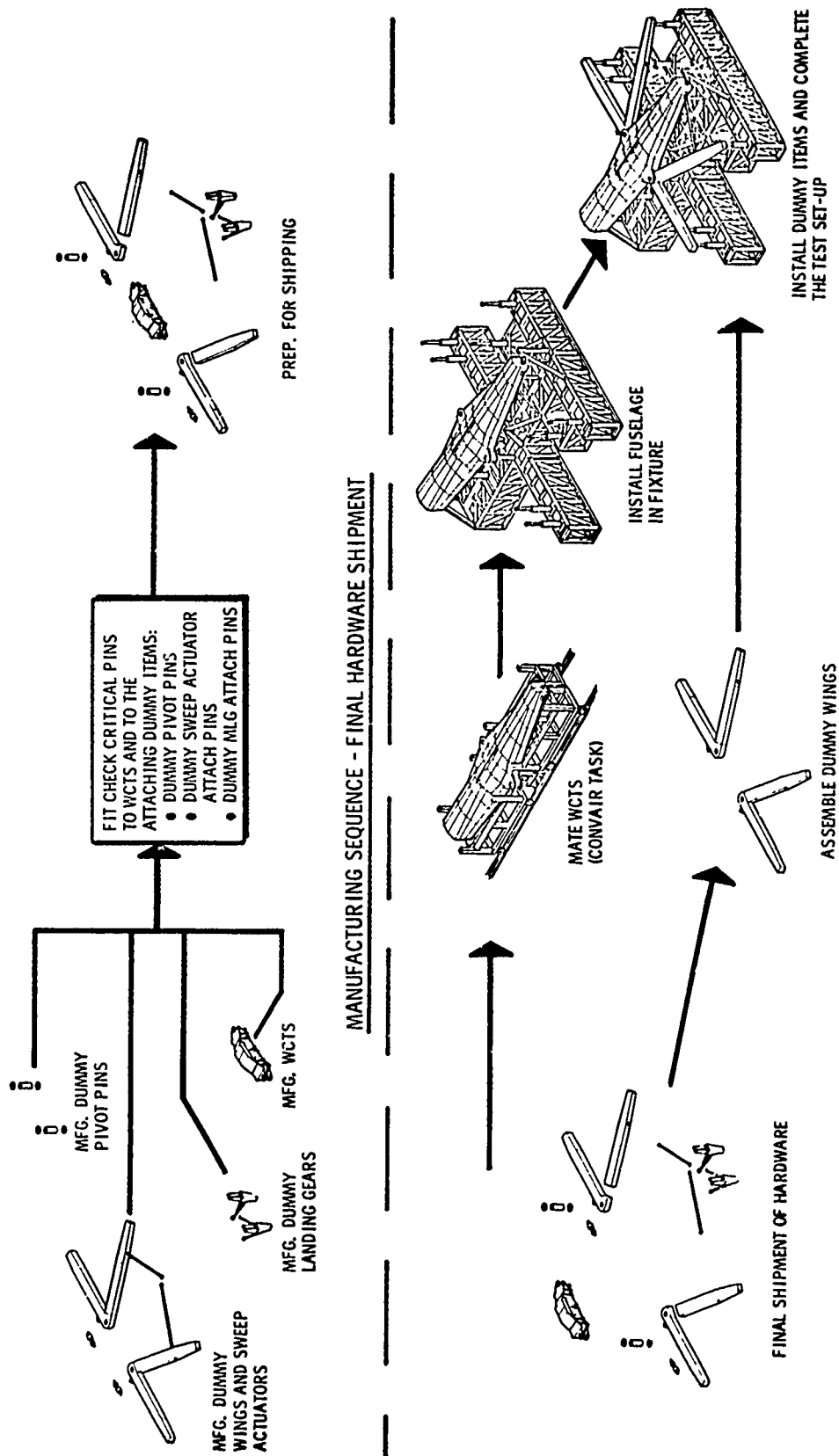


Figure 3-10 REASSEMBLY SEQUENCE - FINAL HARDWARE SHIPMENT

Table III-1 FULL-SCALE TEST FIXTURE STATUS

ITEM	STATUS - PERCENT COMPLETE														
	DESIGN & ANALYSIS					PRCCUREMENT					MFG./ASSEMBLY				
	20	40	60	80	100	20	40	60	80	100	20	40	60	80	100
<u>INITIAL SHIPMENT OF HARDWARE</u>															
Load Systems Hardware															
Flat Trusses for Base Frame															
Assembly of Flat Trusses into Box Section															
Assembly of Box Sections into Base Frame															
Prefit Load Systems Hdw. on Base Frame															
Disassemble for Shipping															
<u>SECOND SHIPMENT OF HARDWARE</u>															
Simulated Fuselage Loose Details															
Upper Fixture Sections															
Simulated WCTS															
Mating Fixtures															
Final Assembly & Mating															
Disassemble for Shipping															
<u>FINAL SHIPMENT OF HARDWARE</u>															
Dummy Wings															
Dummy Pivot Pin System															
Dummy Sweep Actuators															
Dummy Main Landing Gears															
Mating															
Prefit Dummy Hardware															
Disassemble for Shipping															

3.4 ALUMINUM-MANGANESE COATING FOR STEEL BOLTS

The use of cadmium plated steel bolts in titanium structure has been prohibited by USAF because of the possibility of inducing cadmium embrittlement in the titanium. For this reason Convair is investigating the use of Aluminum-Manganese coating for steel bolts in lieu of the cadmium plating for bolts installed in titanium structure.

For the initial investigation of this coating, 10 high strength steel bolts were given the Aluminum-Manganese coating and sent to Mr. Richard Stewart of ASD/ENFSS for stress corrosion investigation. In addition, 12 high strength steel bolts supplied by Omark Industries were coated and returned to Omark for static and fatigue testing.

Results of Testing

The results of four fasteners tested by Mr. Stewart are reported in his paper entitled "Preliminary Results of Stress Corrosion Test of Cadmium and Aluminum-Manganese Coated Taper-Loks in Titanium." While the test results are admittedly preliminary, the report is favorable and states that: "The Aluminum-Manganese Taper-Loks showed no signs of corrosion. There was no visible sign of cracking of the titanium specimen." Testing duration was 1000 hours. Bolts were 260-290,000 PSI heat treated. Figures 3-11 and 3-12 show Taper-Loks installed in the titanium specimens, parallel to each of the three major axis of the material. Note that the two specimens in Figure 3-12 are not joined together, but are merely in close proximity.

Omark Industries conducted three fatigue tests on both 1/2-inch-diameter and 5/8-inch-diameter bolts. The bolts were 220,000 minimum heat-treat.

The bolts tested in fatigue were cycled in axial tension from 3.5% to 35% of the rated axial strength. All bolts withstood 130,000 cycles of loading with no failures.

After completion of the fatigue tests, the bolts were failed statically. All static failing loads exceeded the minimum rated allowables.

Omark is also in the process of conducting alternate immersion salt-spray corrosion testing of Aluminum-Manganese fasteners.

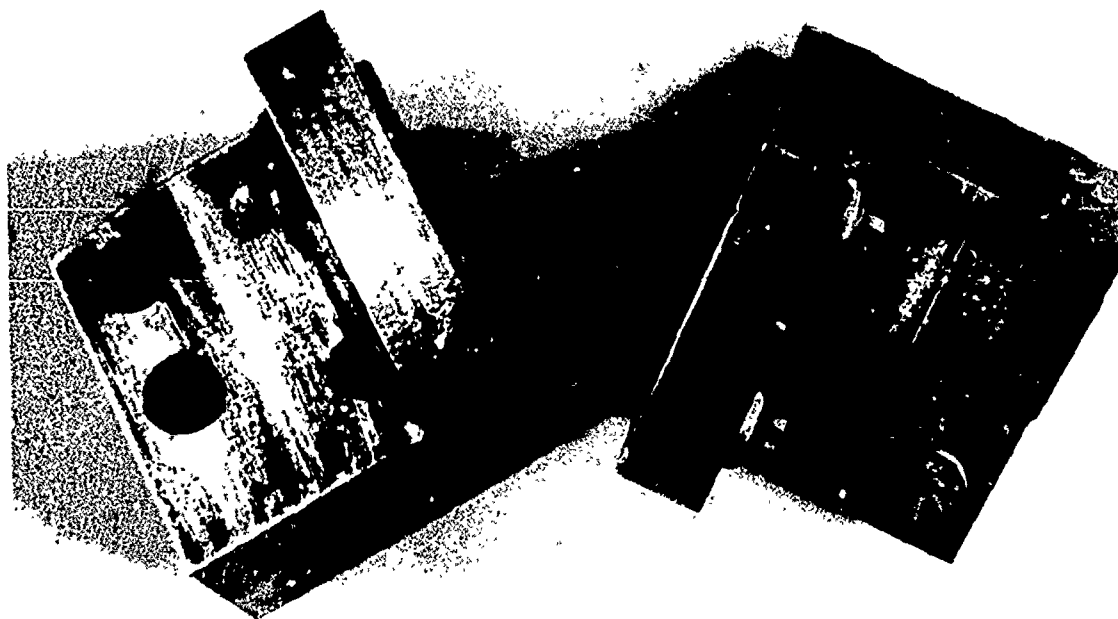


Figure 3-11 TAPER-LOKS, FASTENERS INSTALLED IN
TITANIUM SPECIMENS

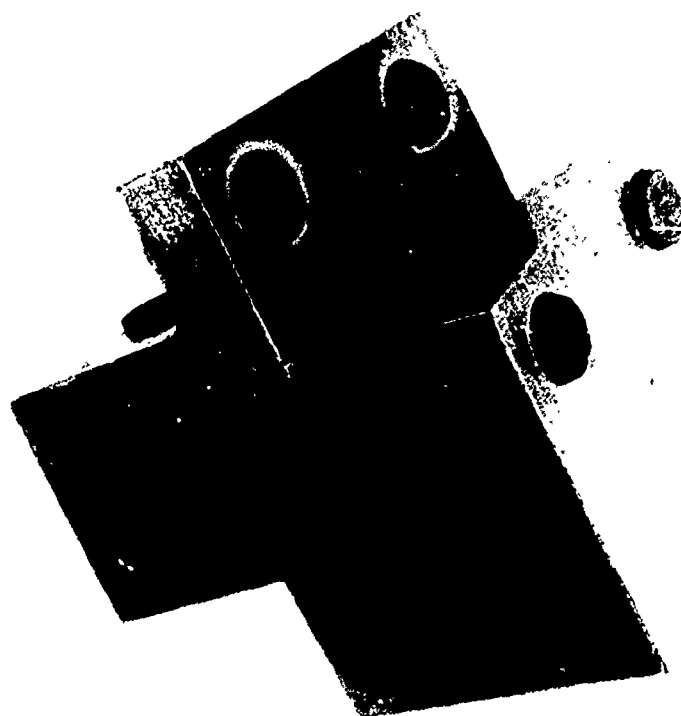


Figure 3-12 TAPER-LOK FASTENERS INSTALLED IN
TITANIUM SPECIMENS

SECTION 4

QUALITY ASSURANCE AND NDI

Quality Assurance and NDI participated in the detail design phase to a large degree. Adhesive bonding, brazing and welding were evaluated as material joining techniques. The results of the activity are covered in the following paragraphs.

4.1 BONDING EVALUATIONS

A total of forty-eight bonded specimens were fabricated to be used in developing NDI techniques. As indicated in Table IV-1, forty-two specimens were titanium and aluminum sandwich structure while six panels (Table IV-2) were of a titanium multilayer laminate construction. These panels were designed to simulate various structures in the preliminary Fail Safe Integral Lug (FSIL) and "No-Box Box" (NBB) configurations. Each panel was bonded with the PL717 adhesive and contained intentional defects. The defects were a combination of the teflon tape insert type and, in some sandwich panels, a local crushed core type.

A through transmission ultrasonic C-scan recording (Figure 4-1) was made for each specimen. The through transmission evaluation was used as a baseline inspection to detect gross deficiencies in the specimens. This system was not considered as a candidate inspection system. The through transmission system detected only about 75% of the intentional defects. Also, extraneous indications were observed on some of the recordings.

Eight laminate-to-laminate type specimens consisting of different skin thicknesses were evaluated using several techniques. The Slik Bond Tester (Energy Summing Ultrasonic System) and Fokker Bond Tester (Resonance System) were evaluated using transducers of various sizes, types and frequencies. Results similar to the through transmission tests were obtained in detecting the induced flaws, but numerous additional areas were also detected with same response as the induced flaws. The destructive examinations provided a very close correlation of induced versus detected flaws. However, the cause of the additional indications were not determined.

Table IV-1
BONDED NDI SANDWICH PANELS

Specimen No.	Material Skin	Skin Thickness T ₁	Core	Skin Thickness T ₂	Quantity Fabricated
MD3266	2024 Alum.	.200	1" Thk	.075	2
MD3256	"	.125	"	.025	2
MD3267	"	.080	"	.025	2
MD3258	"	.035	"	.025	2
MD3268	"	.125	"	.040	2
MD3260	"	.190	"	.032	2
MD3272	"	.130	"	.032	2
MD3269	"	.050	"	.032	2
MD3262	"	.300	"	.050	2
MD3271	"	.250	"	.050	2
MD3270	"	.150	"	.050	2
MD3264	"	.090	"	.050	2
MD3259	"	.300	2" Thk	.063	2
MD3261	"	.213	"	.063	2
MD3263	"	.125	"	.063	2
MD3257	Ti 6AL-4V Mill	.250	1" Thk	.030	2
MD3265	Annealed	.135	"	.030	2
MD3278	"	.060	"	.030	2
MD3279	"	.135	"	.060	2
MD3280	"	.185	"	.060	2
MD3281	"	.300	"	.060	2

Table IV-2
BONDED NDI LAMINATE SPECIMENS

Specimen No.	Material	Laminate Thickness				Quantity Fabricated
		T ₁	T ₂	T ₃	T ₄	
MD3204	Beta C	.125	.125	.125	.125	1
MD3203	Beta C	.062	.125	.125	.062	1
MD3253	Beta C	.100	.100	.100	.100	1
MD3255	Beta C	.100	.100			1
MD3254	Beta C	.06	.06			1
MD3251	Beta C	.125	.125	.05	.100	1

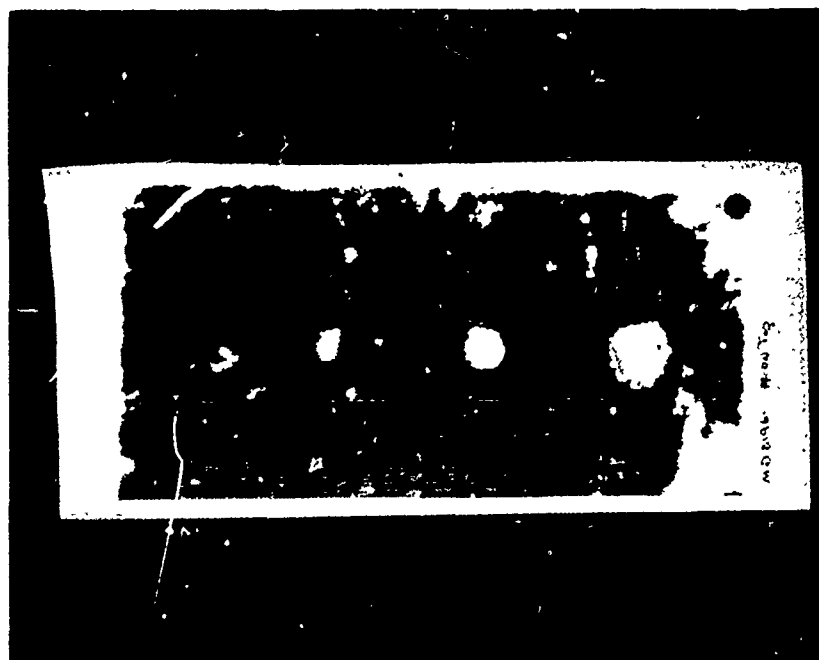


Figure 4-1 Typical Through Transmission C-Scan Recording of an NDI Sandwich Panel

Evaluation of laminate-to-laminate specimens was stopped due to engineering design changes of the FSIL and "No-Box Box" configurations and the cancellation of the titanium laminate configuration. However, the preliminary studies indicate the possibility of using the Energy Summing Ultrasonic System (Slik Bond Tester) to inspect titanium laminates but additional work would be required for production applications.

The sandwich specimens are currently being evaluated using the UM-721 Reflectoscope and Slik Bond Tester. Two different techniques are being considered with the UM-721 Reflectoscope, ring pattern for thick skin specimen and back surface reflection for thin skin specimens.

Each of the three different techniques has produced some favorable results. The Slik Bond Tester using a dual "pitch-catch" type transducer system will detect most of the induced flaws in skin thickness of .125" and greater. However, numerous additional indications have been recorded in some specimens. In most cases these indications are confirmed by the through transmission recordings.

The ring pattern and the energy summing technique results correlate very closely in the detection of both artificial and natural flaws in the thick skinned panels. This lends credit to the preliminary selection of one of these techniques. Final technique selection will depend on flaw configuration in the disassembly of selected panels and the final design of various AMAVS structures.

For the thin skinned panels (skin thickness of .124" and less) a back surface reflection technique application was recently developed. This technique monitors the inside surface of the opposite skin of the sandwich structures. The other standard technique applications have been ineffective in detecting flaws in the thin skinned panels due to the high porosity content in the PL-717 adhesive system.

The preliminary techniques indicated are necessarily tentative. The lack of a specific final design configuration (i.e. skin gage, core thickness, etc.) have delayed the technique selection. As the final production designs are completed, specimens will be fabricated that simulate these designs. The tentative techniques will be verified on the new specimens and production inspection procedures will be prepared.

4.2 BRAZED JOINT EVALUATIONS

4.2.1 NDI Development

NDI development has consisted of the selection and development of both flaw induction technique and a nondestructive inspection technique. Technique selection was made based on NDI data obtained from a series of specimens brazed with the existing optimum manufacturing techniques.

Initially the reference specimens were made using .25 thick 6AL-4V Beta Annealed laminates. These specimens were satisfactory for establishing flaw induction techniques. Specimens having .40 to .60 inch thick laminates were used to develop the NDI inspection technique.

A summary of the flaw induction results is shown in Table IV-3. The overall quality of the brazed specimens was not good, but was satisfactory for the flaw induction program. In addition to the flaw induction media shown in the above table, flat bottom holes were drilled and slots eloxed in a section of panel MD3211 (See Figure 4-2).

Stainless steel spacers, flat bottom holes and stop-off have provided the most uniform, dimensionally controllable flow induction media. Stop-off is a high temperature material used to prevent adherence of the braze alloy to a laminate and is used as a control in the brazing operation.

The size of flaws induced using spacers and stop-off is more difficult to control because of migration of both braze alloy and induction media during the braze operation. Diameters of flat bottom holes are easily controlled, but locating the depth of the braze line exactly is difficult. The time domain responses from each of the flaw types are the same.

Several ultrasonic techniques were evaluated for use in inspecting the brazed specimens. Of the techniques evaluated, five were effective in detecting defective conditions. The most effective technique was pulse echo. It is easy to set up and can be used with a wide variety of transducers. Both flat and focused transducers with frequencies of 5, 10 and 15 MHz were evaluated. The technique was employed strictly in an immersion mode, but can also be applied in the contact mode. Permanent recordings (C-Scan) can be made using existing equipment. Access to only one side of the part is required.

Table IV-3
NDI BRAZED JOINT SPECIMEN

<u>SPECIMEN NO.</u>	<u>FLAW INDICATION MEDIA</u>	<u>OVERALL PANEL QUALITY</u>	<u>REMARKS</u>
MD3188-1-1	Volatiles (corrosives, stop-off)	Fair	Good flaws
MD3187-1-2	Inserts	Poor	Large void area.
MD3189-1	Everlube T-50 Tungsten disulfide	Fair	Fairly good flaws. Used for techniques development.
MD3189-2	Sulfuric acid Nitric-hydrofluoric acids	Poor	Sulfuric flaws - present but large, HF-HNO ₃ - absent.
MD3208	Sulfuric acid, nitric acid	Poor	Large void area, poor induced flaw quality.
MD3209	Stop-off material Tungsten Disulfide	Poor	Naturally occurring flaws.
MD3210	Kerosene Cutting Oil	Poor	Large void areas poor induced flaw quality.
MD3211	Lube Oil HF-HNO ₃ acid	Fair	Poor flaw quality. Excessive areas of naturally occurring flaws.
MD3222	Inserts, stop-off	Poor	Large areas of naturally occurring voids (retort leak)
MD3223	Inserts, stop-off	Poor	Same as MD3222.



Figure 4-2 Flat Bottom Holes and an Elox Slot
Evaluated as Flaw Induction Methods

Through transmission is also effective. It likewise has recording capabilities and is easy to set up. However, because access to both sides of the part is required, it is impractical for large-area brazed panels.

A pitch-catch technique proved effective, but hard to set up. Likewise, the ring pattern technique proved to be very difficult to apply. The Slik Bond Tester (energy summing ultrasonic technique) was only marginally effective and lacked recording capabilities.

The procedure selected to inspect the brazed structures employs a focused 10 MHz transducer. Basically, the procedure is as follows:

- o The transducer is normalized (made perpendicular) to the front surface of the test part.
- o The sound beam is focused on the brazeline under evaluation.
- o An electronic gate is placed on the signal from the brazeline.
- o Gain and accept/reject levels are determined from setting up on a reference part. Figures 4-3 and 4-4 show typical "good" and "bad" signals.
- o The entire part is scanned and a recording (C-scan) made of both the acceptable and unacceptable areas.

The primary problem that has been experienced with the focused transducer method is that the inspection is very dependent on normality and to a lesser degree on the water travel distance (distance between transducer and part). Frequent set-up adjustments are necessary to inspect the large area brazed parts.

A Schlieren study was undertaken to determine if the normality problem was caused by a malfunction in the transducer. Schlieren imaging is a process in which the sound beam emanating from a transducer is made visible. The process is helpful in determining transducer characteristics such as beam strength and beam pattern of the transducer. The Convair imaging equipment allows the operator to rotate the transducer and observe different cross-sections of the soundbeam. A marked difference in the intensity of the soundbeam of the transducer used in the

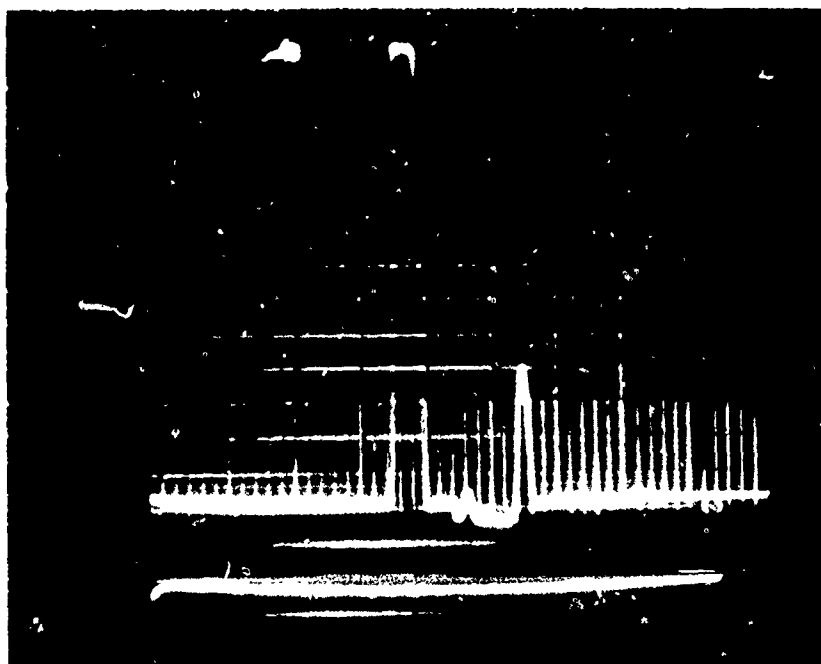


Figure 4-3 A "Good" Area Showed a Relatively Low Signal in the Gate

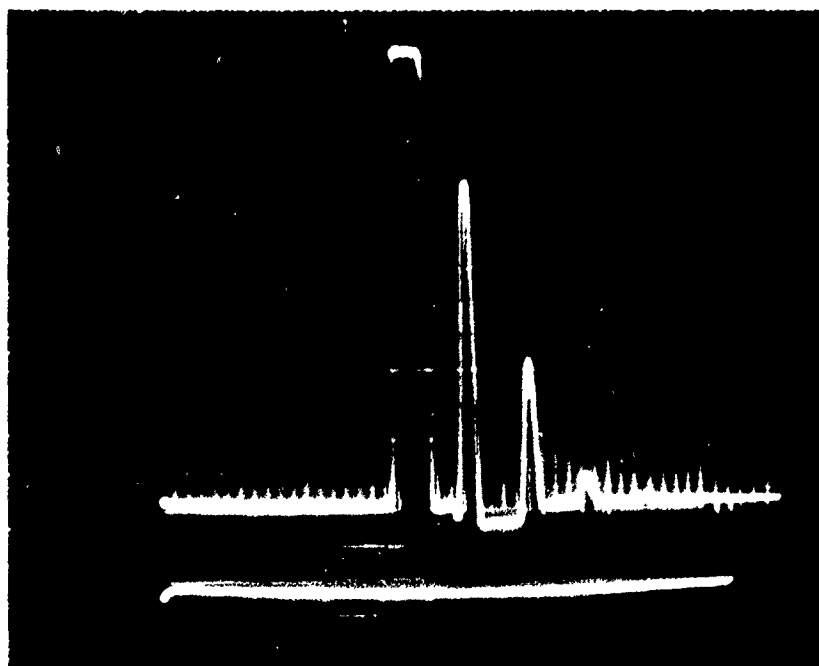


Figure 4-4 A Defective Area Was Indicated by a Relatively High Signal in the Gate

inspection was noted as shown in Figures 4-5 and 4-6. These two photographs depict the effect of a 45° of rotation of the transducer. They show that the normality problem is due to abnormalities in the beam pattern of the transducer. Because the transducer used was the only one of its type on hand at Convair, a new long-focus transducer of the same type would have been purchased to accomplish the inspection of the test part had the FSIL design been selected.

4.2.2 Engineering Specimen Evaluation

All the Group Engineering specimens were inspected using Radiography and the ultrasonic techniques. These specimens were used by manufacturing and engineering to establish manufacturing variables and allowables. They were also used to develop and improve the ultrasonic NDI technique. This preliminary technique was finalized at the end of the Group II portion of the program.

Part 603FTB033 was inspected before test and after two stages of testing. Scattered void areas were found in the panel before test, but did not propagate during test or appear to affect the crack stopping capabilities of the brazeline.

The ultrasonic response from the brazeline of the first 603FTB035 panel (-1, -2) was considerably different from previous brazed parts in that a large signal was present in the assumed "good" areas. Metallographic examinations showed the entire brazeline to be porous and to have a substandard strength. Half of the 603FTB035-1, -2 was rebrazed and tested ultrasonically. The part was found to contain enough defect areas to warrant cancellation of the structural testing of the panel.

The third large specimen, 603FTB035-2, showed to have a very good quality braze. Shown in Figure 4-7 is a photograph of the ultrasonic recording (C-scan) of one side of one end of the part. Subsequent physical testing of the part was successful. The part will be re-inspected when physical testing is completed.

Panel 603FTB053-21 was inspected a total of three times; before test, after four lifetimes, and after six lifetimes of testing. Figure 4-8 shows a photograph of the ultrasonic recordings (C-scan). No void propagation was observed. It should be noted that most of the defective areas present in the specimen before test, shown at the left of Figure 4-8, were machined away in the manufacture of the test specimen.

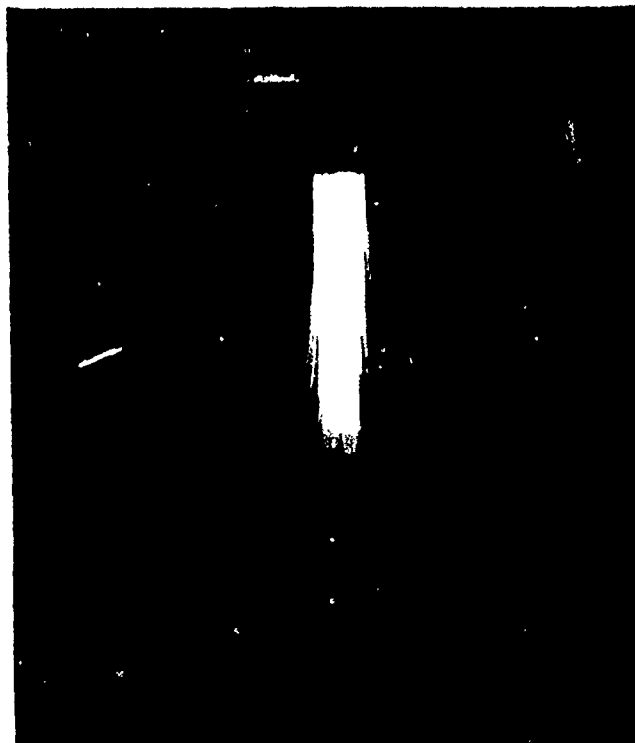


Figure 4-5 The Schlieren System Indicates One Cross Section of the Soundbeam to be Strong

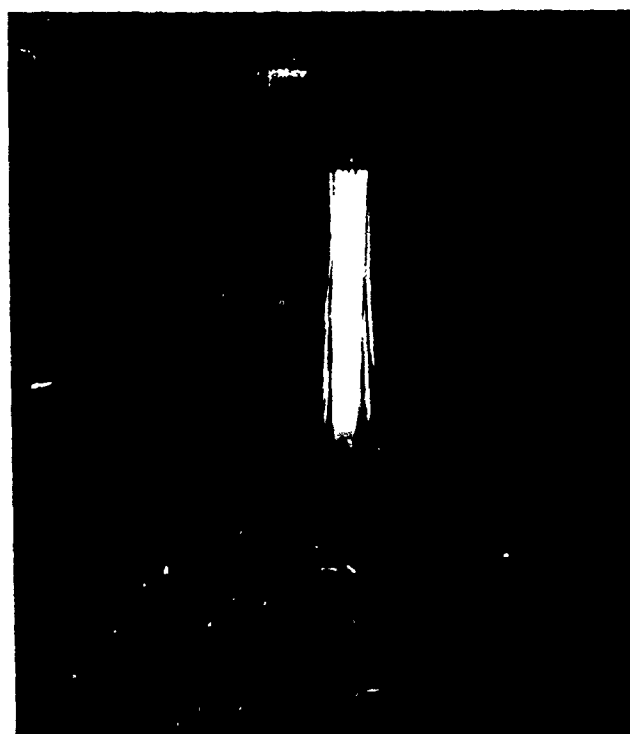


Figure 4-6 Because of a Malfunction in the Transducer, Part of the Soundbeam is Missing.

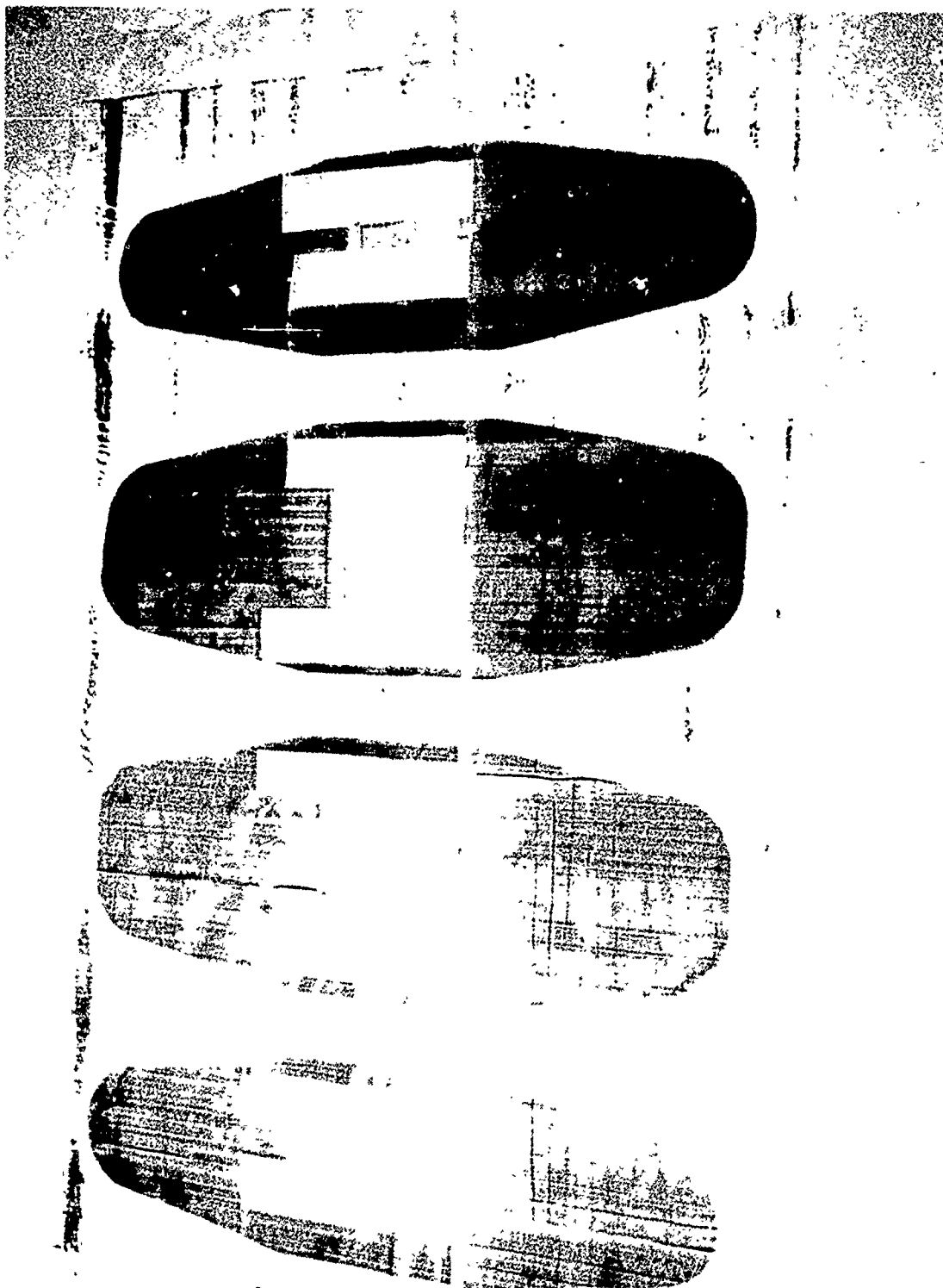


Figure 4-7 The Ultrasonic Inspection of 603FTB035-2 Recorded in a C-Scan Mode

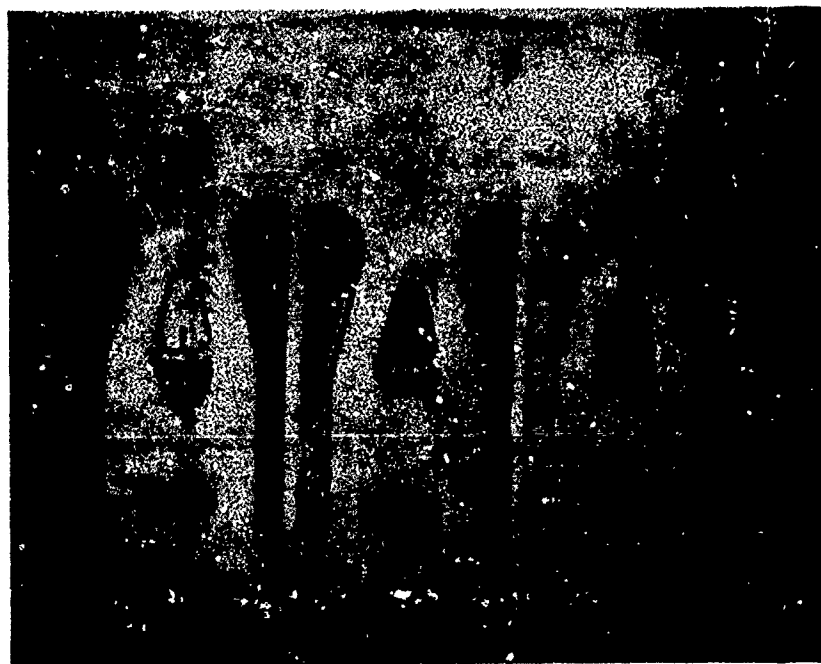


Figure 4-8 Ultrasonic Recording of 603FTB053-21
A) Before Testing (Left),
B) After Four Lifetimes of Testing (Center), and
C) After Six Lifetimes of Testing (Right)

4.3 WELDED JOINT EVALUATIONS

4.3.1 NDI Specimen Design & Fabrication

Under this program provisions were made for the design and fabrication of 6AL-4V Beta Annealed Titanium and 10 Nickel (HY180) steel specimens necessary to provide adequate data to evaluate transducers and techniques for the NDI of weldments made from these alloys.

Configurations MD3190, MD3191 and MD3202 (Figure 4-9) were constructed to provide a titanium thickness range of weld from 0.5 to 1.5 inches. Configurations MD3232 and MD3233 (Figure 4-9) were fabricated with a similar weld thickness range for 10Ni.

4.3.2 Transducer Evaluation

Available transducers in the 5, 10 and 15 MHz range were evaluated. Response profiles were plotted for those transducers demonstrating best sensitivity and resolution for both Ti and 10Ni flat bottom hole (FBH) references. Transducers SIL (15 MHz), 1/2 inch OD, focused, immersion, and transducer A311, (15 MHz), 1/2 inch OD, focused, immersion, manufactured by Automation Industries and Panametrics respectively, were selected on the basis of their response profiles. Further experimentation confirmed their efficiency. Evaluation was performed on the basis of their response to 2/64 flat bottom holes (FBH) drilled at various depths in fabricated reference specimens. (See Figure 4-10).

4.3.3 Engineering Specimen Inspection

Most of the specimens manufactured for engineering testing purposes underwent a "best effort" ultrasonic inspection on a routine basis. Data was recorded and filed for further evaluation. These inspections included both 10Ni and 6AL-4V Ti specimens.

In addition, some of the 10 nickel specimens with natural defects were used to acquire preliminary ultrasonic information on this alloy, since the scheduled receipt of the formal NDI specimens was delayed. Preliminary references were constructed with some of these specimens. (See Figure 4-11).



Figure 4-9 NDI Welded Specimens

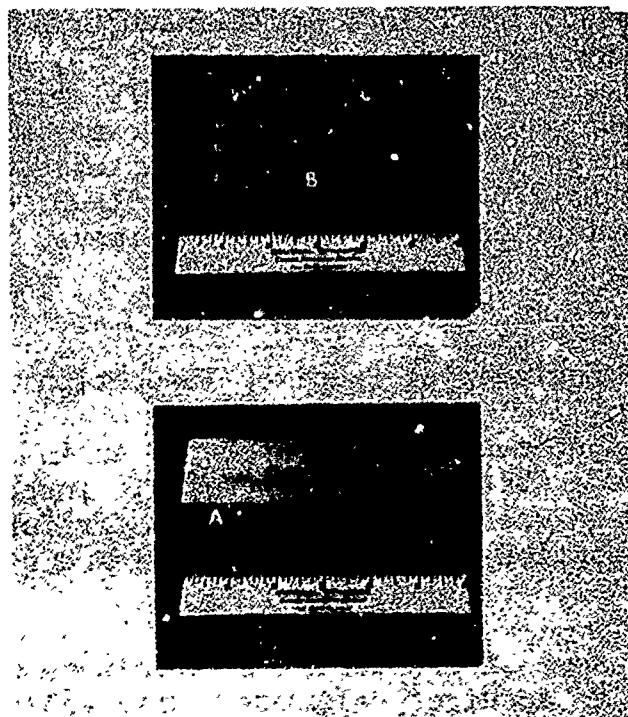


Figure 4-10 6AL-4V(A) and 10 Ni(B) Flat Bottomed Hole References

4.3.4 Shear Ultrasonic Techniques, 6AL-4V Titanium

Evaluation of shear techniques, at 45° and 30° with 2.5, 5 and 10 MHz shear contact transducers was discontinued almost immediately due to unsatisfactory results. At thicknesses from 0.5 to 0.900 inch, #3 electric discharge machined slot responses were detectable. For bottom and top surface slots for 1.5 inch thick materials only bottom surface responses were detectable. It was also noted that natural flaws easily detected with longitudinal techniques were not detectable with the shear transducers evaluated.

4.3.5 Delta Ultrasonic Techniques, 6AL-4V Titanium

Evaluation of ultrasonic delta techniques was completed for Ti 6AL-4V specimens with negative results. Available delta probes, GD/QC 148, 149 and 124 were tested and found unsuitable. Either top or bottom eloxed slots produced satisfactory responses, but not both. Some of the radiographic detected flaws could not be detected or the response amplitudes were less than or equal to the weld structural or surface noise. Attempts were made to produce a working delta probe by using 5, 10 and 15 MHz transducers in various combinations of frequencies, angles and transducer spacing with unsatisfactory results. One of the variable depth and spacing fixtures used is shown in Figure 4-12. A dual 15 MHz transducer combination (focused) produced usable eloxed slot responses for 0.370, 0.425 and 0.620 inch thick weldments; but it also produced spurious responses where metallographic sectioning failed to produce any flaws. In addition, extreme sensitivity to surface conditions was noted.

4.3.6 Pulse Echo Longitudinal Evaluation, 6AL-4V Titanium

Scans of NDI specimens MD3202, MD3191 and MD3190 using 2/64 FBH reference specimens were performed in a series of tests to provide suitable weld responses (Figure 4-13). All radiographic detected flaws in these specimens were detected ultrasonically with additional responses in adjacent areas. This indicates that ultrasonic sensitivity is of an improved degree to that of radiography. Full confidence in the ability to detect flaws in this type of weld is based not only in the correlation of radiograph to ultrasonic responses for the specimens listed above; but also in results obtained in prior company programs.

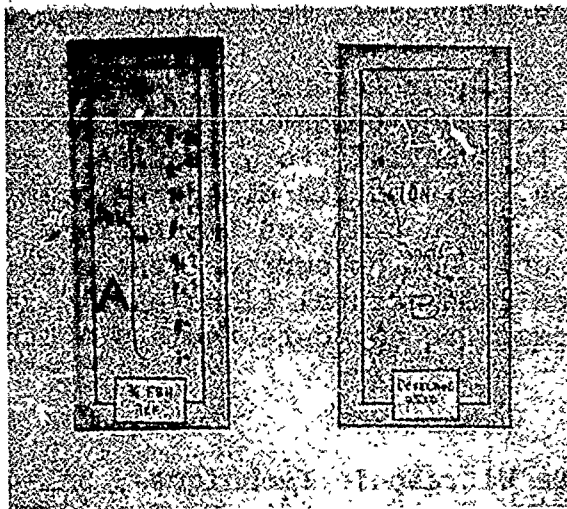


Figure 4-11 Typical Pulse-Echo Recordings of 10 Ni Weld and Preliminary Reference Specimen

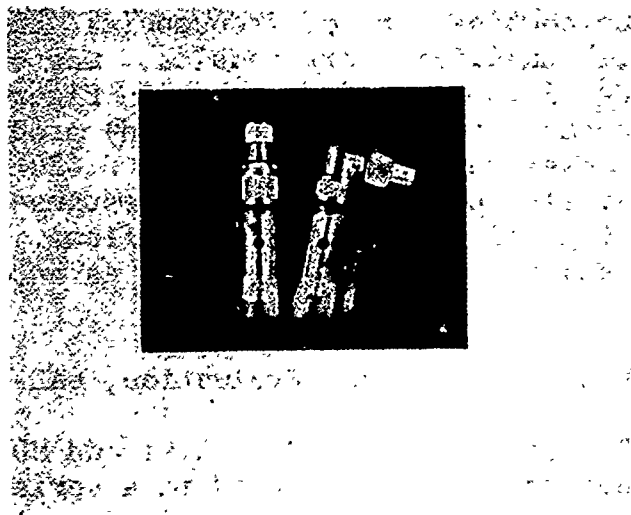


Figure 4-12 Variable Depth/Angle Delta Probe Fixture

4.3.7 Pulse Echo-Longitudinal Evaluation, 10 Nickel Specimens

Late arrival of 10 Nickel material and manufacture of 10 Nickel NDI specimens has precluded any ultrasonic evaluation other than pulse echo-longitudinal techniques. This has been possible only through the availability and use of some defective engineering 10 Nickel weld specimens.

Scans were performed on engineering weld specimens H9 and H27 using a 10 Nickel reference specimen with 2/64 FBH. Sectioning of H9 specimens verified that good ultrasonic response to flaw correlation was obtained. A microsection of a defective portion of engineering specimen H27 supplemented these findings where an equally effective ultrasonic response to flaw correlations was found. (Figure 4-14).

Radiography to ultrasonic response correlations on engineering specimen H9 can be seen in Figure 4-15. This correlation shows the improved sensitivity of ultrasonics over radiography detection.

4.3.8 Evaluation Summary

The following summary is preliminary and subject to re-evaluation as additional work is performed on Weld NDI specimens.

- a. EB welds of 6AL-4V Titanium and 10 Nickel alloys may be ultrasonically inspected using pulse echo-longitudinal methods with water immersion or bubbler techniques.
- b. The thickness range of inspection meets the requirement of the program: 0.5 - 1.6 inch (Ti and 10Ni).
- c. Within the scope of these tests and materials, minimum detectable anomalies are estimated to be between 0.015 to 0.050 in. for 10Ni. No estimate can be made at this time for titanium since insufficient destructive analyses have been performed at this point in the program.
- d. Ultrasonic longitudinal pulse echo and radiography "flaw" detection provide complementary NDI data. Inspection of 10Nickel and 6AL-4V Titanium will require the use of both techniques for the following reasons:

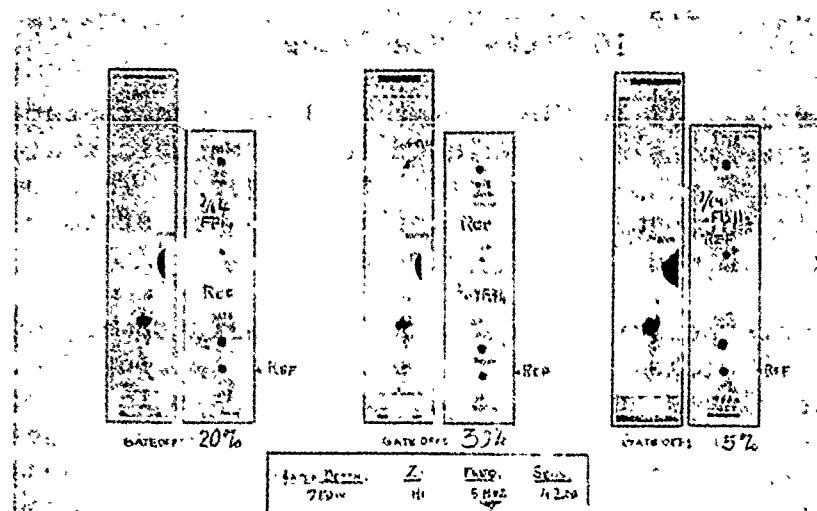


Figure 4-13 Typical 6AL-4V B Weld Responses Using Pulse Echo Longitudinal Technique

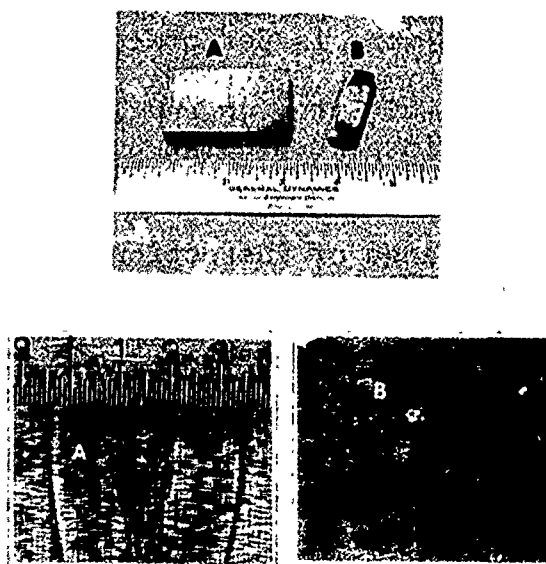


Figure 4-14 Metallographic Sections of Flaws in Specimen H27(A) and H9(B)

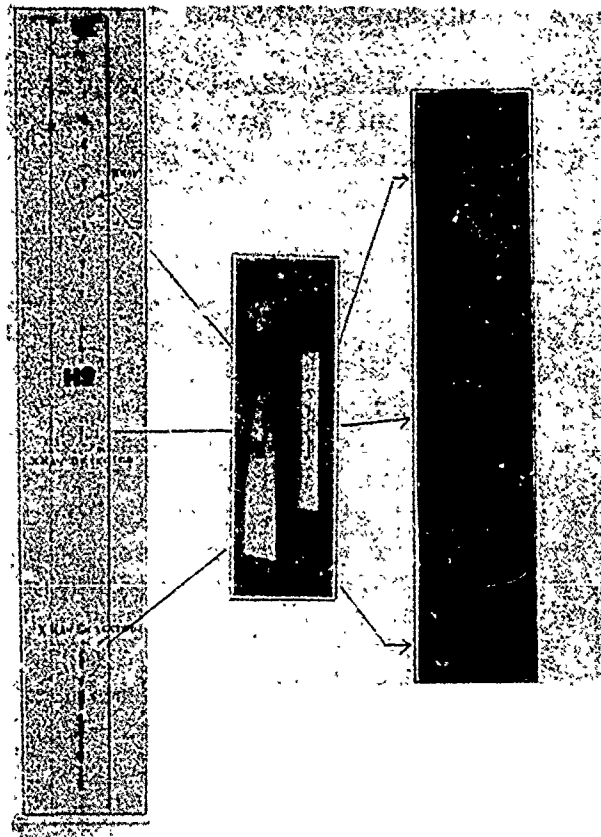


Figure 4-15 Radiographic/Ultrasonic Comparisons for the Inspections of 10Ni Specimen H9

- o Some ultrasonically detected "indications" cannot be detected radiographically. (Figure 4-15).
- o All pulse echo-longitudinal techniques are ultrasonically blind at the near front surface (front surface resolution). Radiography techniques minimize this 0.100 to 0.150 inch deficiency.
- o Radiography and ultrasonic techniques have different accessibility potential for the inspection of different geometries of the specimens.

4.4 NDI PLANS

Drawings 603R234, 603R231, and 603R232 were developed to outline an NDI program on welded, bonded, and brazed specimens. These drawings are shown as Figures 4-16, 4-17, and 4-18, respectively. All of the NDI specimens shown in Figure 4-16 were completed during Phase II. The welded NDI specimens for both 6AL-4V titanium and 10 Nickel steel shown in Figure 4-17 were also completed. Forty-two of the bonded sandwich panel NDI specimens shown in Figure 4-18 were evaluated during the Detail Design Phase.

Additional bonded and welded NDI specimens will be evaluated to assure inspectability of the "No-Box" Box configuration selected for manufacturing during Phase III.

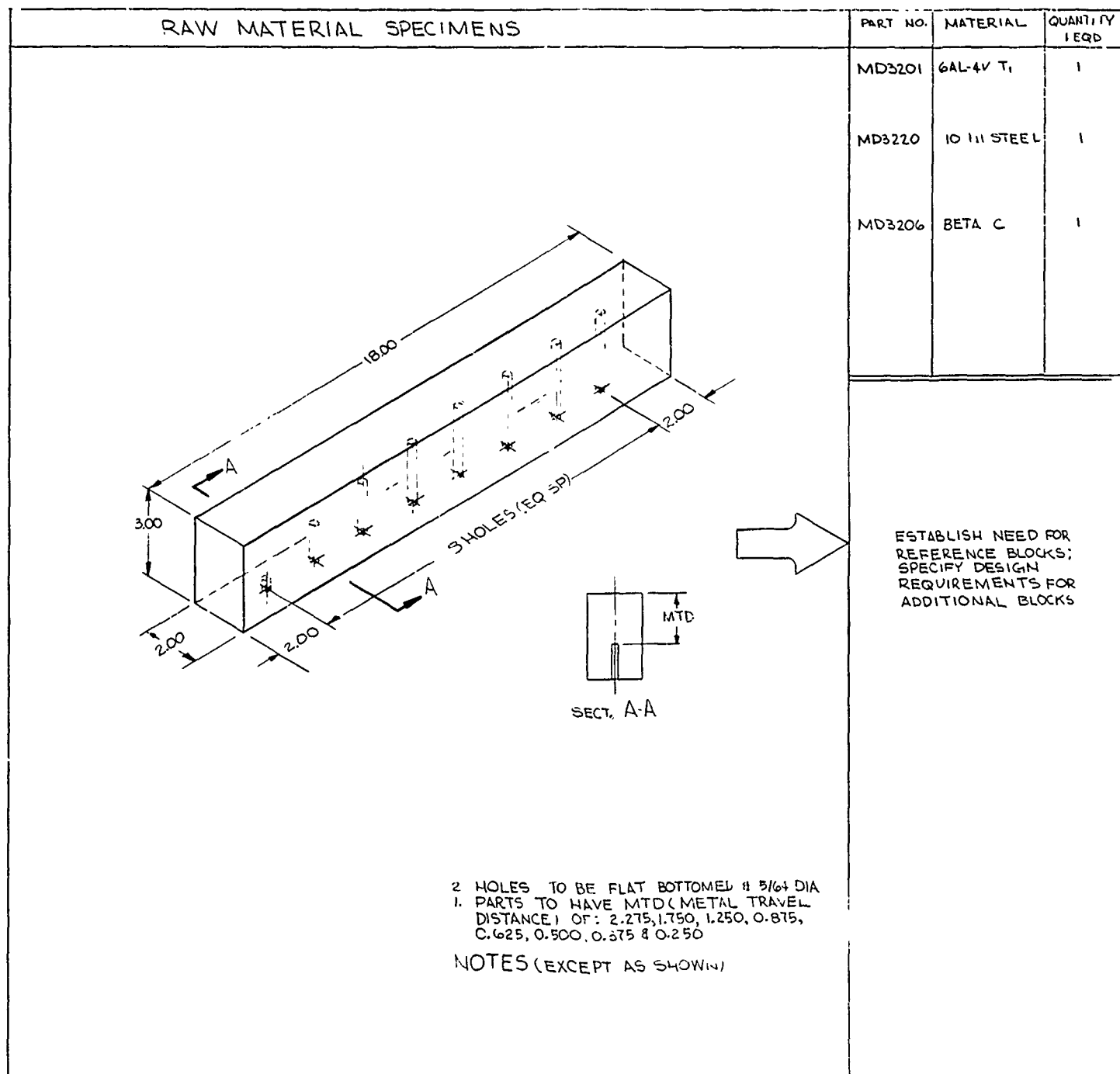
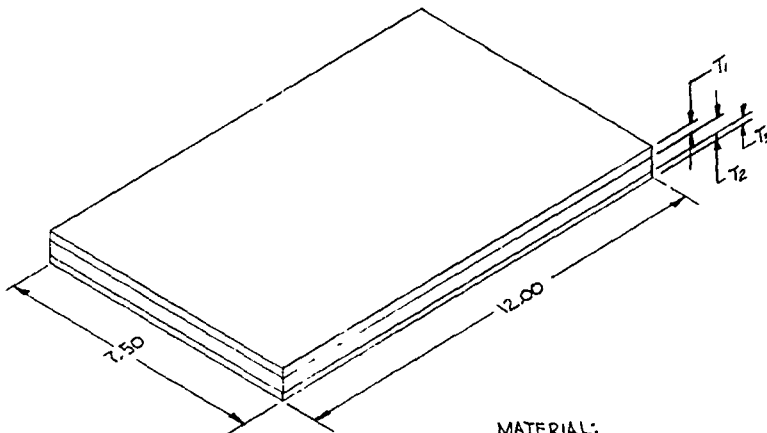


Figure 4-16 RAW MATERIAL AND BRAZED

NO.	MATERIAL	QUANTITY REQD
01	6AL-4V T ₁	1
02	1011 STEEL	1
06	BETA C	1

ESTABLISH NEED FOR
REFERENCE BLOCKS;
SPECIFY DESIGN
REQUIREMENTS FOR
ADDITIONAL BLOCKS

BRAZED SPECIMENS				PART NO.	LAMINA			TYPE FLAW	QTY REQD	
					T ₁	T ₂	T ₃			
 <p>MATERIAL: BETA ANNEALED 6AL-4V TITANIUM</p>					MD3187-1-1	.250	.250		CORROSIVE	1
					MD3187-1-2	.250	.250		INCLUSION	1
					MD3189-1-1	.250	.250		CORROSIVE	1
					MD3189-1-2	.250	.250		INCLUSION	1
					MD3188-1	.250	.250		CORROSIVE	1
					MD3188-2	.250	.250		CORROSIVE	1
					MD3208	.250	.250		CORROSIVE	1
					MD3209	.250	.250		INCLUSION	1
					MD3210	.400	.600		CORROSIVE	1
					MD3211	.400	.600		CORROSIVE	1
					MD3212-1	.250	.250		SEE NOTE 1	1
					MD3213-1	.250	.250			1
					MD3215	.400	.600			1
					MD3222	.400	.400	.400		1
					MD3223	.400	.400	.400	SEE NOTE 1	1

1. FLAW TYPE WILL BE DEFINED AS A RESULT
OF PRELIMINARY STUDIES
NOTES (EXCEPT AS SHOWN)

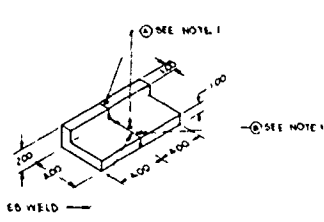
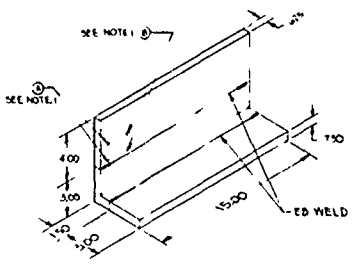
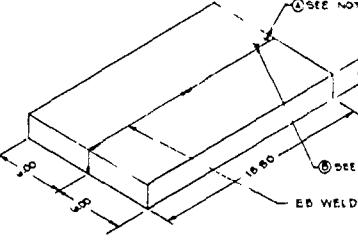
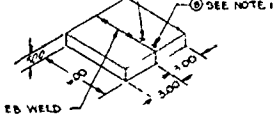
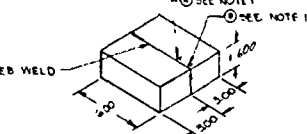
PRELIMINARY DESIGN DRAWING

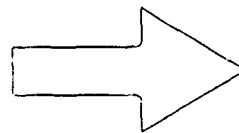
RAW MATERIAL AND BRAZED
NDI SPECIMENS

BY <i>L. Brubaker</i>	APPROVED <i>Robert</i>	SCALE	DATE 5-29-73
GENERAL DYNAMICS		603R234	
Convair Aerospace Division		SHEET 1 OF 1	
Fort Worth, Texas		PDS-8-1	

4-23 / 4-24

MATERIAL AND BRAZED NDI SPECIMENS

SPECIMEN	MATERIAL	REQUIREMENTS	
		NDI	WELD
	GAL-VZ BETA TITANIUM	1	3
	GAL-VZ BETA TITANIUM	1	3
	GAL-VZ BETA TITANIUM	1	
	10 NI STEEL	2	
	10 NI STEEL	2	



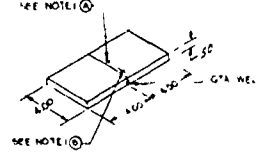
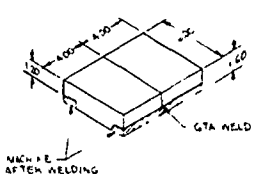
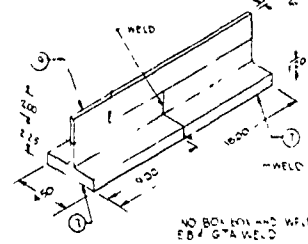
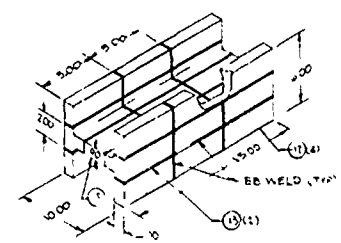
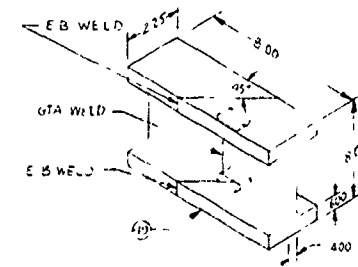


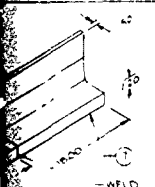
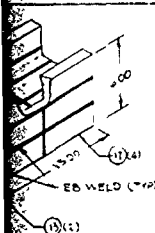
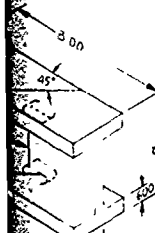
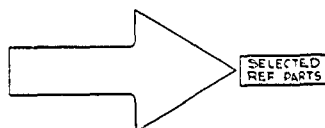
SPECIMEN	MATERIAL	REQUIREMENTS	WELD
			
			
			
			
			

Figure 4-17 EB AND GTA WELDING NDI SPECIMEN

VIEW	MATERIAL	REQUIREMENTS	
		NDI	MFG PRODUCABILITY
 GTAW WELD PART NO. MD3229	0 NI STEEL	2	
 GTAW WELD PART NO. MD3231	0 NI STEEL	2	
 NO BOV ON EB WELD EB / GTAW WELD PART NO. 100 ASSY	0 NI STEEL GTAW WELD 10 NI STEEL EB WELD	2 2	
 EB WELD ("14") EB WELD ("12") PART NO. 101 ASSY	10 NI STEEL	1	SEE NOTE 3
 3.00 45° 4.00 4.00 PART NO. 102 ASSY	10 NI STEEL	2	SEE NOTE 2



3. MFG PRODUCABILITY SPECIMEN WILL BECOME NDI SPECIMEN UPON COMPLETION
2. MFG PRODUCABILITY SPECIMEN MAY BECOME NDI SPECIMEN UPON COMPLETION

1. INDUCED FLAW

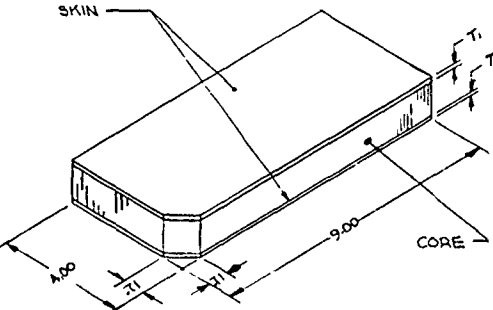
HOLE	PE	SIZE
①	FBH	1/64 DIA
②	FBH	2/64 DIA

NOTES (EXCEPT AS SHOWN)

PRELIMINARY DESIGN DRAWING			
EB AND GTAW WELDING NDI SPECIMENS			
GENERAL DYNAMICS Convair Aerospace Division Fort Worth, Texas	603R231	DATE 1-25-62	DESIGNED BY 101

WELDING NDI SPECIMENS

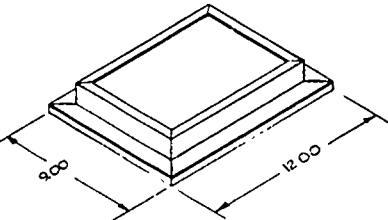
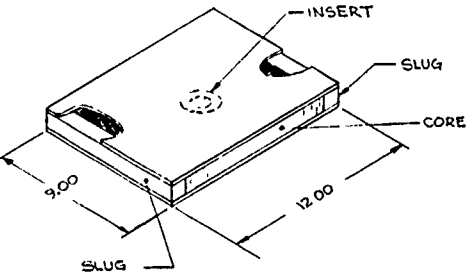
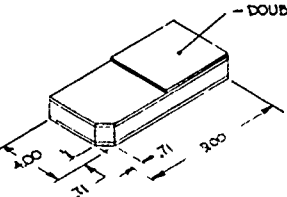
4-25 / 4-26

SPECIMEN	PART NO.	MATERIAL		GAGE		QUANTITY REQUIRED
		SKIN	CORE	T ₁	T ₂	
	MD3196	6AL-4V MILL ANNEALED		.063	.063	1
	MD3195	6AL-4V MILL ANNEALED		.090	.032	1
	MD3249	BETA C		.125	.040	3
	MD3266	2024 ALUMINUM		.200	1" THK .075	3
	MD3256			.125	.025	2
	MD3267			.080	.025	3
	MD3258			.035	.015	2
	MD3268			.125	.040	3
	MD3260			.190	.032	2
	MD3272			.190	.032	3
	MD3269			.050	.032	2
	MD3262			.300	.050	3
	MD3271			.250	.050	2
	MD3270			.150	.050	3
	MD3264			.090	1" THK .050	2
	MD3259			.300	2" THK .063	3
	MD3261			.213	.063	2
	MD3263	2024 ALUMINUM		.125	2" THK .063	3
	MD3257	6AL-4V MIL ANNEALED		.25	1" THK .030	2
	MD3265			.135	.030	3
	MD3278			.060	.030	2
	MD3279			.135	.060	3
	MD3280			.185	.060	2
	MD3281	6AL-4V MIL ANNEALED		.300	1" THK .060	3

PRELIMINARY
TECHNIQUE
SELECTION

Figure 4-18 BONDED SANDWICH NDI SPECIM

QUANTITY
REQUIRED

SPECIMEN	PART NO.	MATERIAL	QUANTITY REQUIRED
		2024 ALUMINUM	30
		6 AL-41 MILL ANNEALED T1	10
		2024 ALUMINUM	10
		TITANIUM AND ALUMINUM AS REQUIRED TO EXTEND PRELIMINARY DEVELOPMENT	15

PRELIMINARY
TECHNIQUE
SELECTION

SELECTED PANELS
FOR INSPECT
REF PARTS

3. DETAILED CONSTRUCTION AND QUANTITY DETERMINED BY PRELIMINARY RESULTS, DESIGN ITERATION AND INSPECTION CRITERIA
 2. FLAW TYPES - TEFLON TAPE INSERTS, OTHER TYPES AS REQUIRED
 1. USE PLTIT ADHESIVE FOR ALL PANELS
- NOTES (EX EPT AS SHOWN)

PRELIMINARY DESIGN DRAWING

BONDED SANDWICH
NDI SPECIMENS

BY <i>Braden</i>	APPROVED <i>Robert</i>	SCALE	DATE 5-10-73
GENERAL DYNAMICS		603R232	
Convair Aerospace Division		SHEET 1 OF 1	
Fort Worth Operation		4-27 / 4-28	

SECTION 5

MANUFACTURING DEVELOPMENT

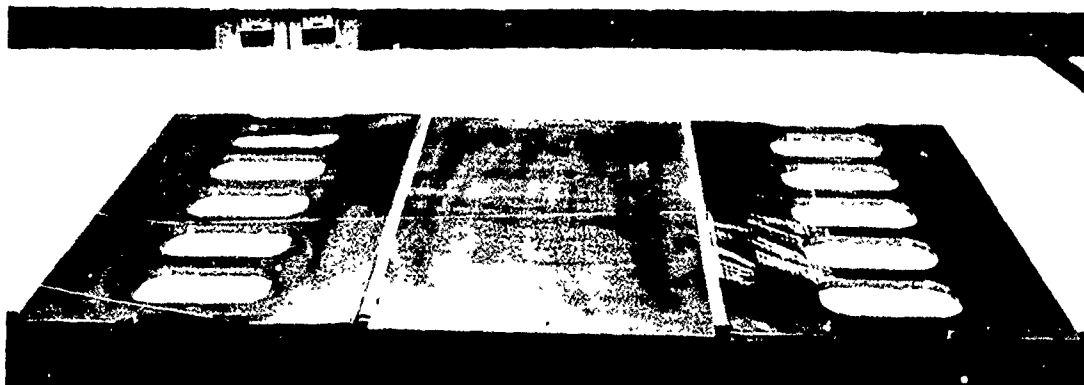
The manufacturing development effort during Phase II was primarily concerned with manufacturing methods development, fabrication of engineering and production verification test specimens, and design support consultation. Phase II tasks accomplished through 15 March 1973 were reported in AFFDL-TR-73-70 and accomplishments through 15 July 1973 were reported in AFFDL-TR-73-77.

5.1 LAMINATED BRAZING PROCESS DEVELOPMENT

Work accomplished since the second interim report, 15 July 1973, includes brazing one 603FTB033 damage tolerance, braze lower plate element test specimen, two 603FTB053 center line splice lower plate brazed test specimens, and two 603FTB035 brazed lower plate damage tolerance test specimens. Also, special brazing parameter tests were run to resolve problems encountered in brazing the large area 603FTB035 parts.

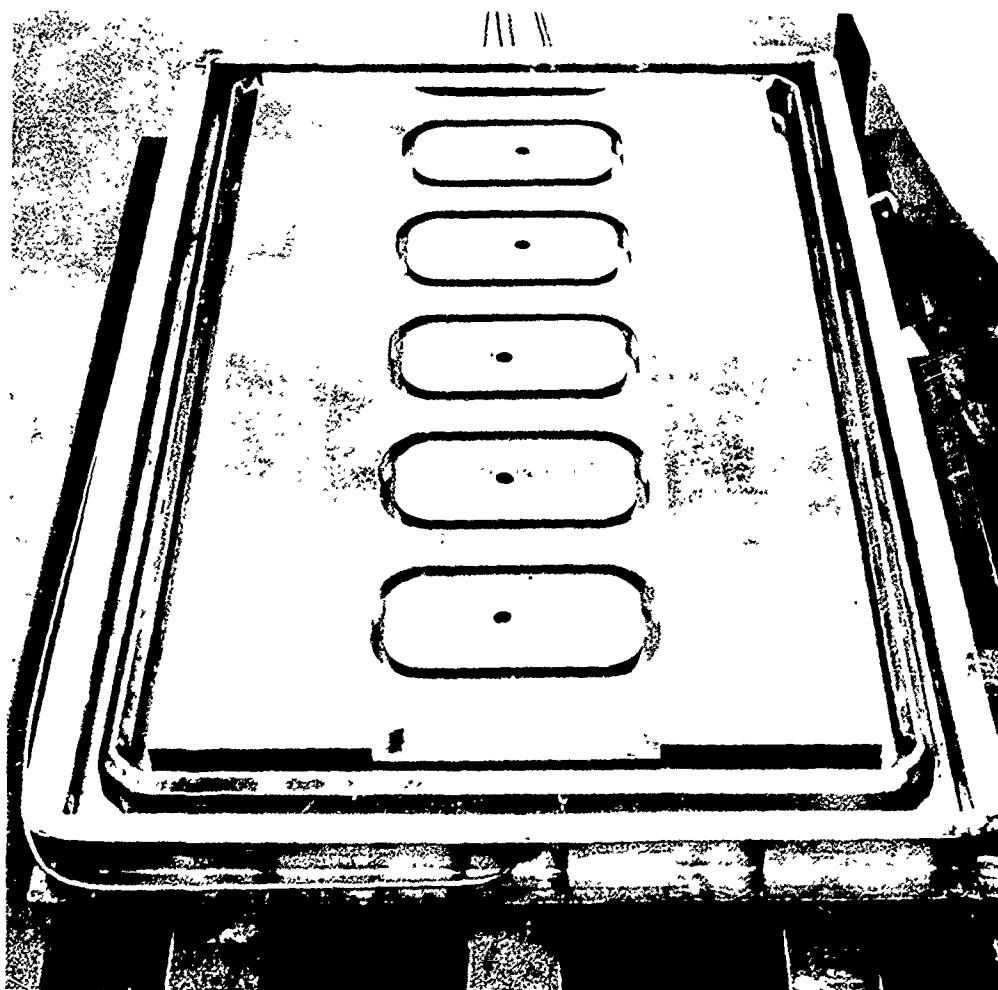
5.1.1 603FTB033 Test Specimen, Damage Tolerance, Braze Lower Plate Element

The engineering test part consisted of three titanium details brazed with Ag-Al-Mn braze alloy. The upper and lower details were 0.600-inch thick with five equally spaced hog-outs and the center detail was a solid plate 0.400-inch thick. Titanium details are shown in the photograph in Figure 5-1. The braze surface of the details were initially machined by face milling, then finished to final dimension by dry belt sanding. The complete detail lay-up in the braze box tooling is shown in Figure 5-2. Brazing was accomplished using standard procedures except a pre-braze cycle was run to flatten the titanium details. The pre-braze cycle and braze cycle are shown in the graphs in Figures 5-3 and 5-4. The part, after brazing is shown in Figure 5-5. Visual inspection of the part showed good alloy wetting and flow and the part relatively free of surface discoloration. X-ray and ultrasonic inspection was made and the part was sent to the engineering test lab for further testing.



4-53437

Figure 5-1 TITANIUM DETAILS FOR 603FTB033 BRAZE TEST SPECIMEN



4-53430

Figure 5-2 TITANIUM DETAILS FOR 603FTB033 BRAZE TEST SPECIMEN ASSEMBLED IN BRAZE BOX

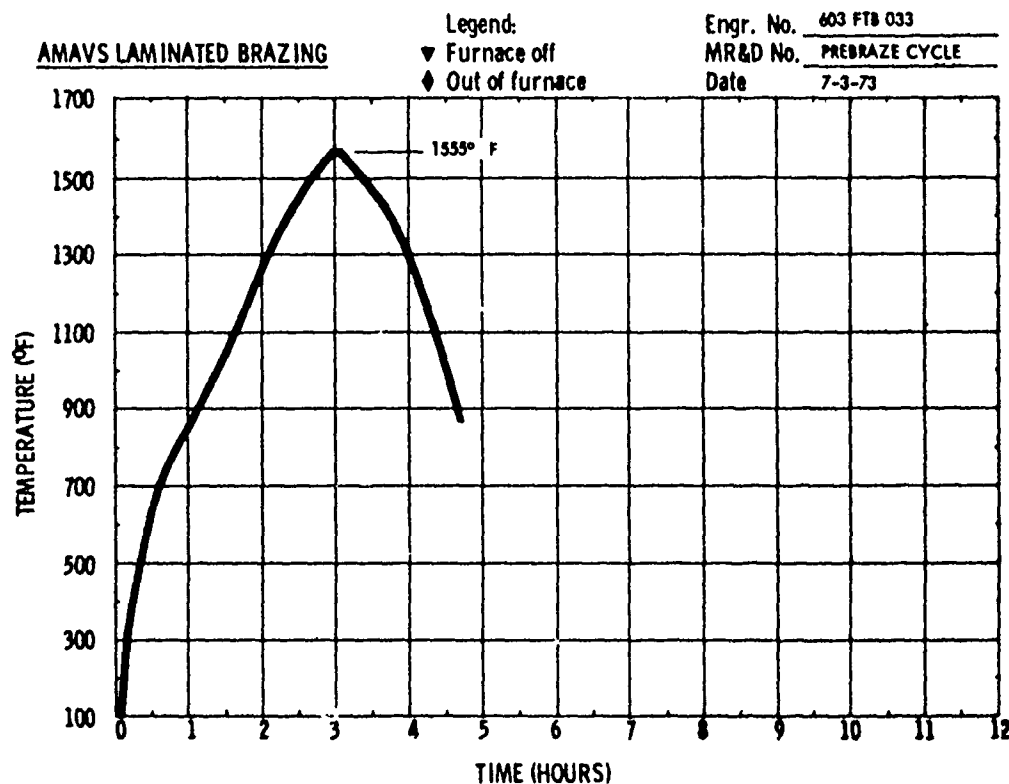


Figure 5-3 PREBRAZE CYCLE FOR 603FTB033 TEST SPECIMEN

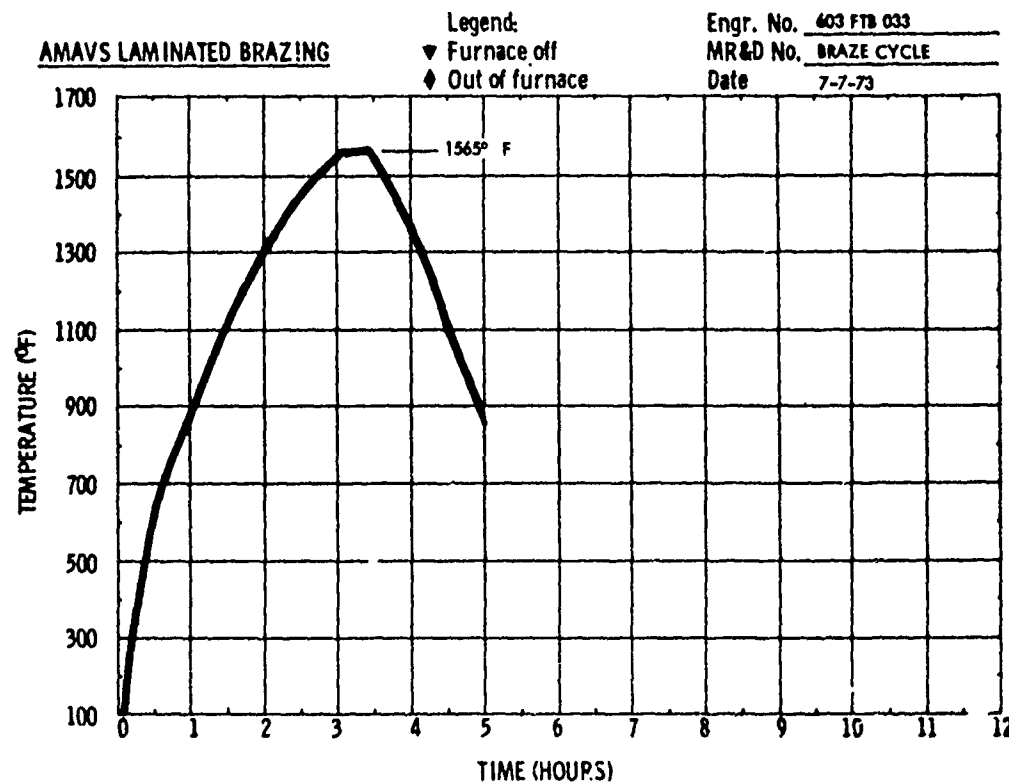


Figure 5-4 BRAZE CYCLE FOR 603FTB033 TEST SPECIMEN



Figure 5-5 603FTB033 BRAZED TEST SPECIMEN AFTER REMOVAL
FROM BRAZE BOX

4-53542

5.1.2 603FTB053 Braze Test Specimen Centerline Splice Lower Plate

Two 603FTB053 test parts were brazed using titanium details that were machined to thickness dimension by face milling followed by dry belt grinding. The part was a two-braze line component consisting of an upper and lower plate of 0.600-inch thick titanium and a center plate of 0.400-inch titanium. Standard cleaning and lay-up procedures were used and no difficulty was experienced throughout the braze operation. The photograph in Figure 5-6 shows the lower plate detail with 0.005-inch thick Ag-Al-Mn braze alloy tack welded in place. The braze cycle time/temperature curves for the two parts are shown in Figures 5-7 and 5-8. A part, after brazing, is shown in the photograph in Figure 5-9. Visual inspection of the parts showed good alloy wetting and flow with little surface discoloration. X-ray and ultrasonic inspection was made and the parts were sent to the engineering test lab for further evaluation.

5.1.3 603FTB035 Brazed Lower Plate Damage Tolerance Test Specimen

The brazed lower plate damage tolerance test specimen (603FTB035) is a double braze line component with dimensions of 1.60 inches x 48.0 inches x 114.3 inches. The part was several times larger in surface area than preceding brazed structures. The increased size and weight of the panel and braze tooling required additional development of both handling and brazing procedures. A pre-braze run and three braze runs established the necessary procedures for the production of a satisfactory brazed part. Each braze run is discussed separately below.

5.1.3.1 Pre-braze Run for 603FTB035

A pre-braze cycle, simulating actual production, was run except that braze alloy was not used in the detail lay-up of the panel. The test was run to determine the effect of scale up on either tooling or the braze cycle. This test and all subsequent braze tests with 603FTB035 parts were run in the gas fired Holden-Pacific furnace shown in the photograph in Figure 5-10. Four .250/.250 x 7.5 x 12 inch test panels were brazed in the retort during the pre-braze cycle. The test panels were inserted in the hog-outs in the upper (-9) detail of the part. Six thermocouples were used in the test and locations are shown in the sketch in Figure 5-11. Time/temperature curves for the pre-braze cycle are shown in Figures 5-12 and 5-13. Components for the pre-braze cycle are shown in Figure 5-14 and the complete pre-braze procedure is shown below:



Figure 5-6 LOWER PLATE TITANIUM DETAIL OF 603FTB033 TEST
SPECIMEN WITH BRAZE ALLOY TACK WELDED IN PLACE

4-30831

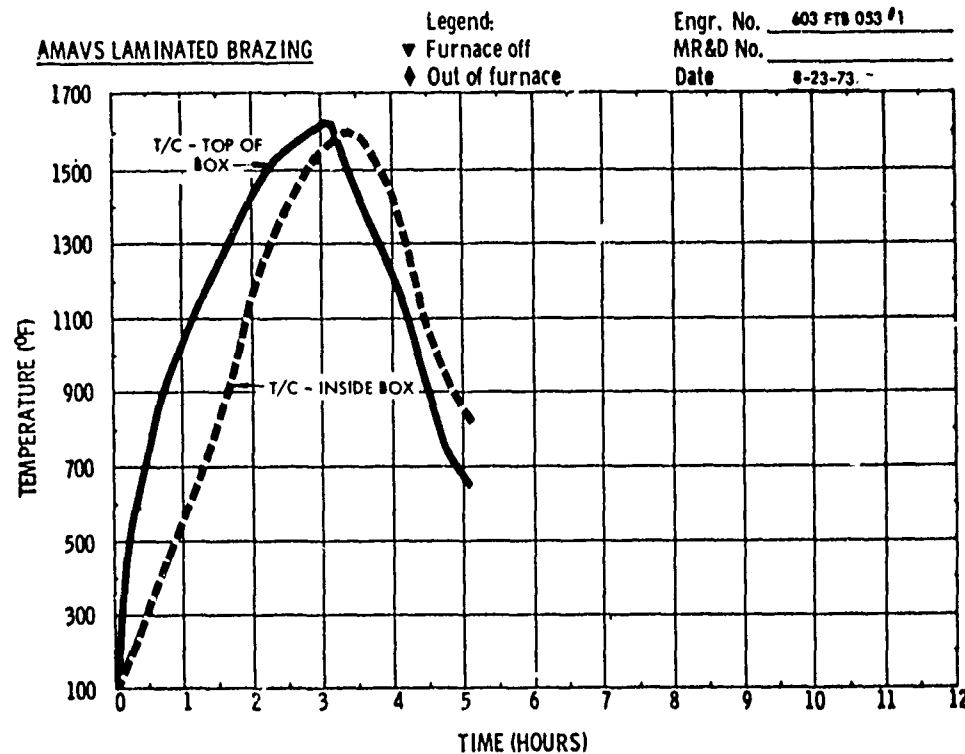


Figure 5-7 BRAZE CYCLE FOR 603FTB053 RUN #1

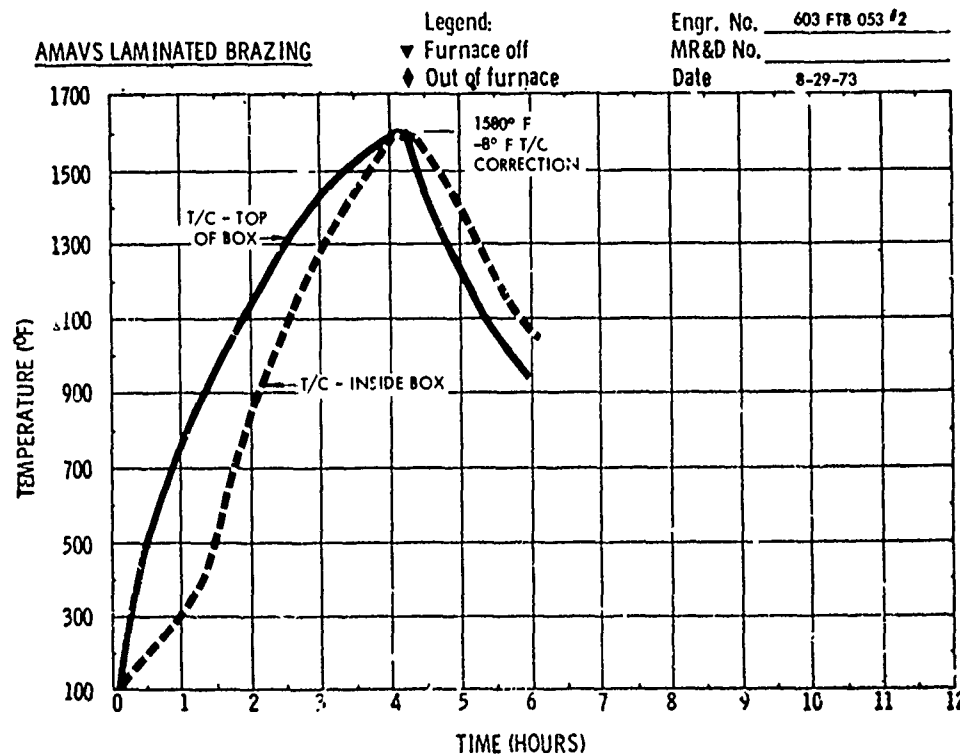


Figure 5-8 BRAZE CYCLE FOR 603FTB053 RUN #2

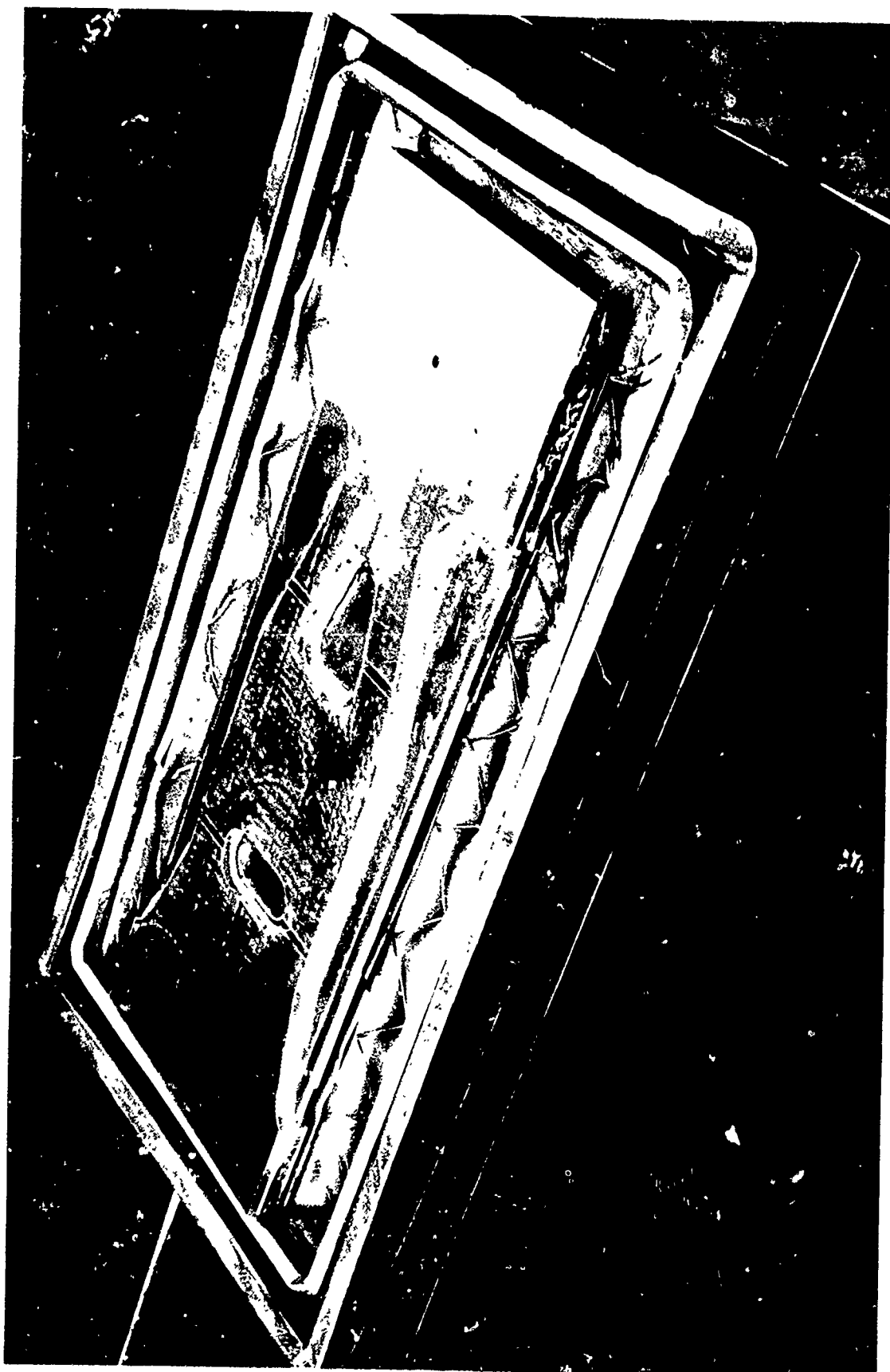


Figure 5-9 BRAZED TEST SPECIMEN 603FTB053 IN BRAZE BOX TOOLING

4-54075

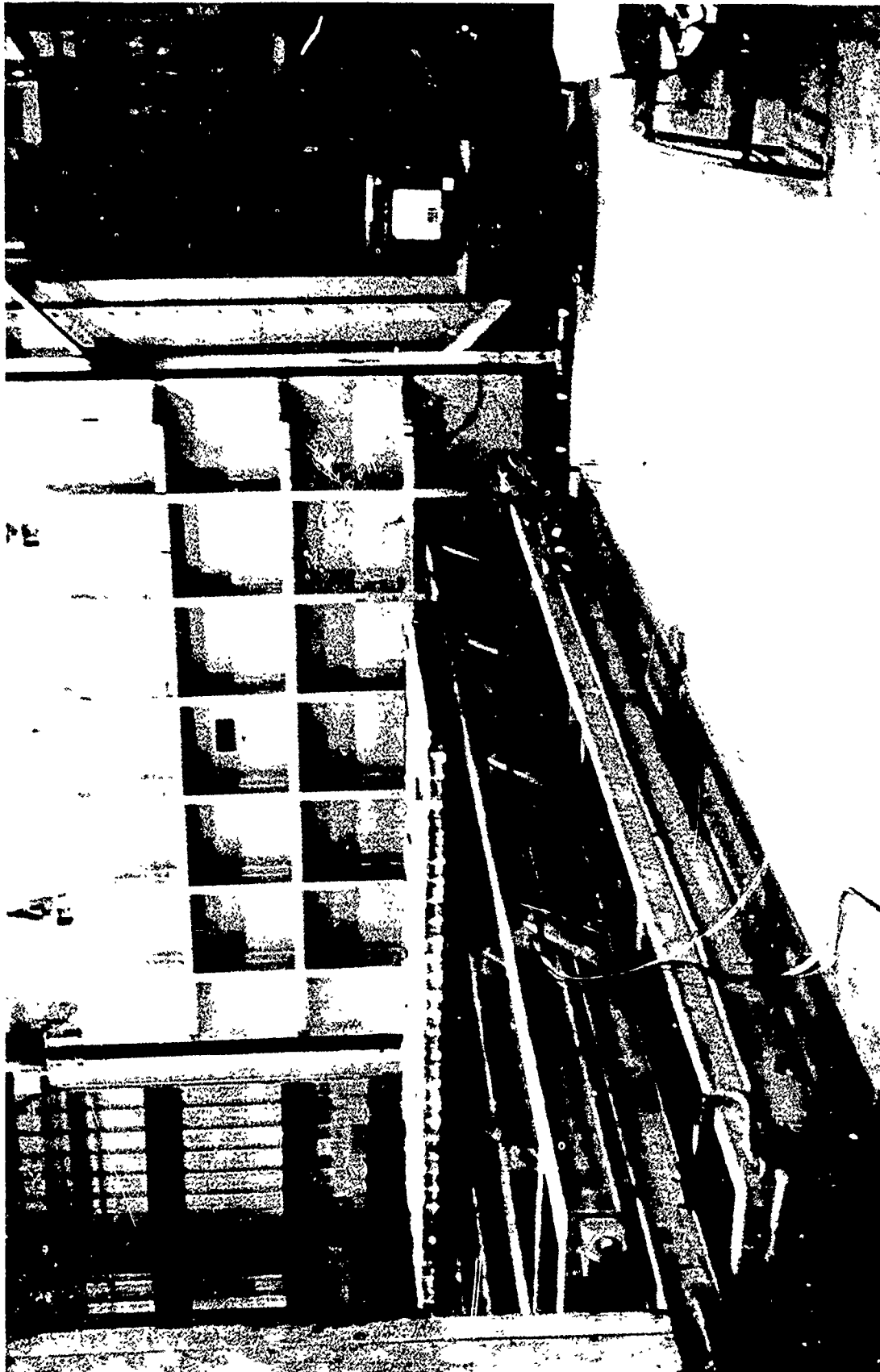
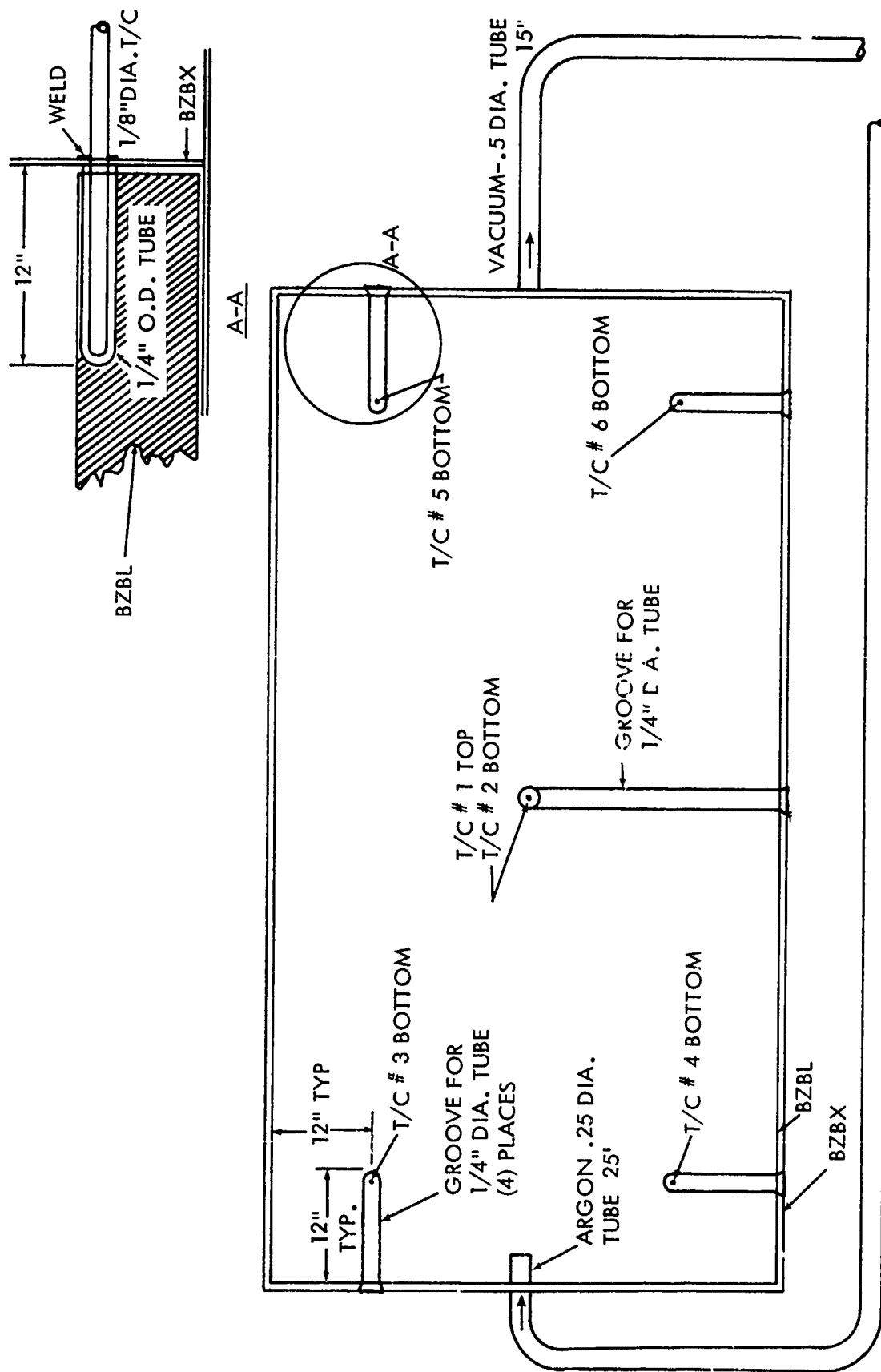


Figure 5-10 GAS FIRED HOLDEN PACIFIC FURNACE FOR BRAZING
603FTB035 TEST SPECIMENS

4-5372



5-10

Figure 5-11 THERMOCOUPLE LOCATIONS FOR 603FTB035
TEST PART PREBRAZE CYCLE

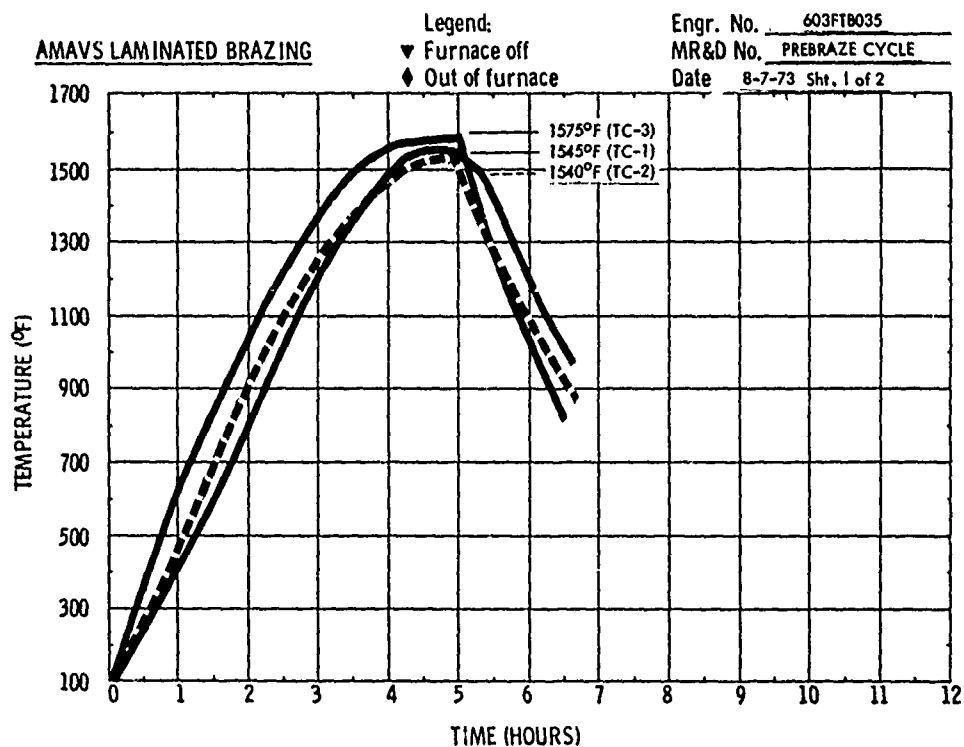


Figure 5-12 PREBRAZE CYCLE FOR 603FTB035 TEST SPECIMEN THERMOCOUPLES 1, 2, AND 3

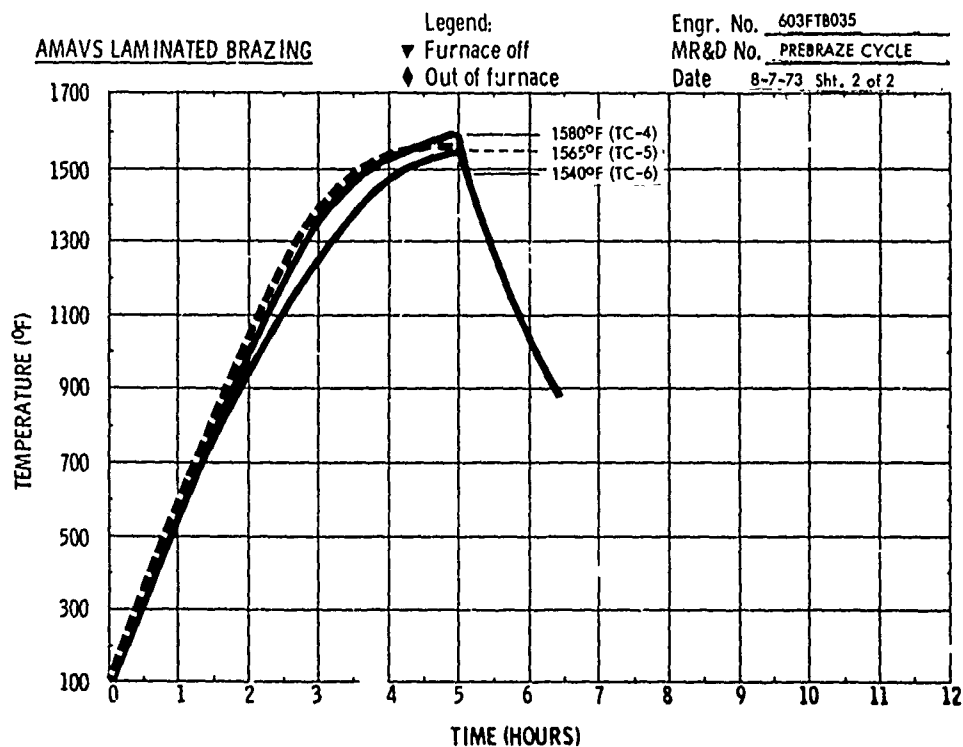


Figure 5-13 PREBRAZE CYCLE FOR 603FTB035 TEST SPECIMEN THERMOCOUPLES 4, 5, AND 6

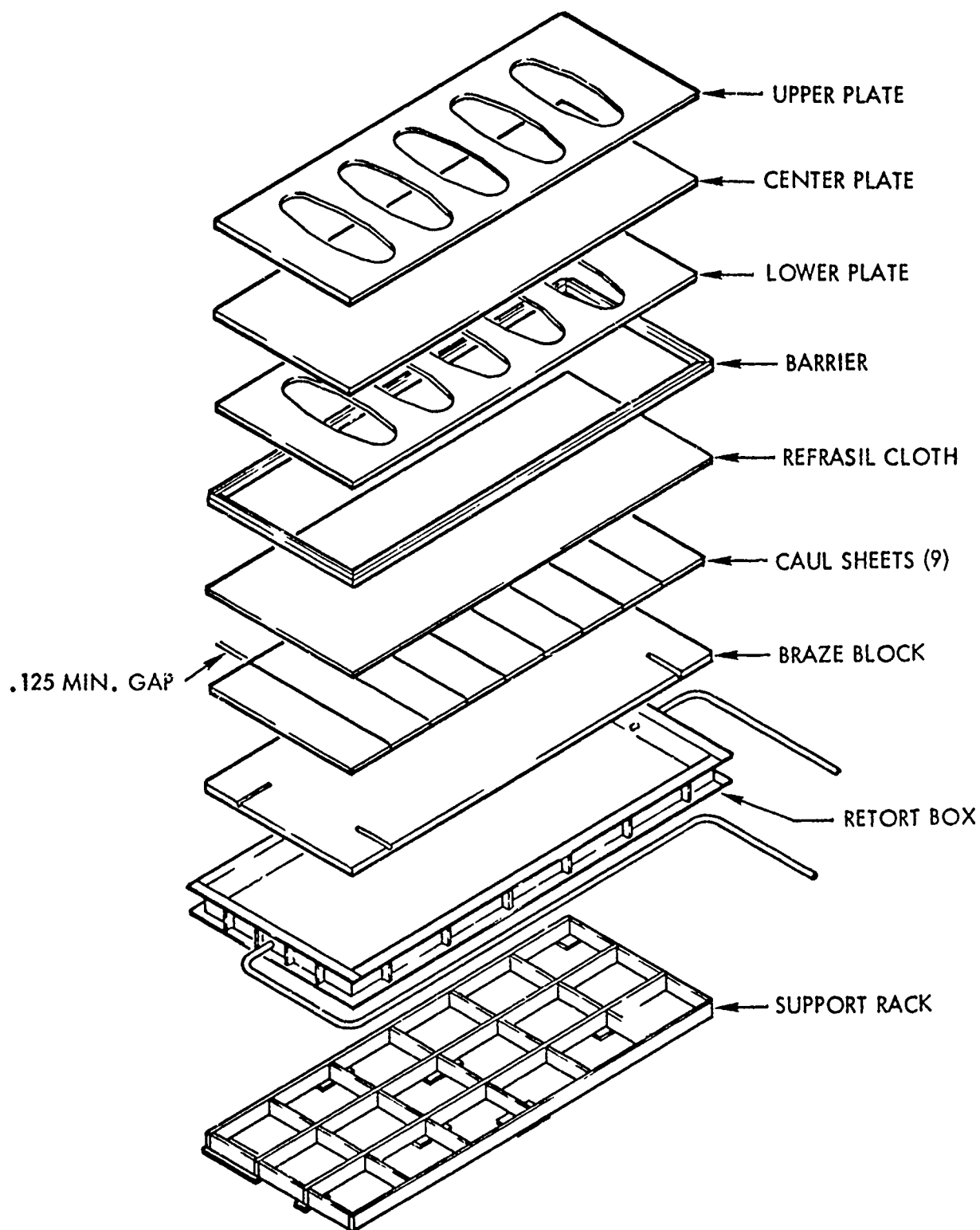
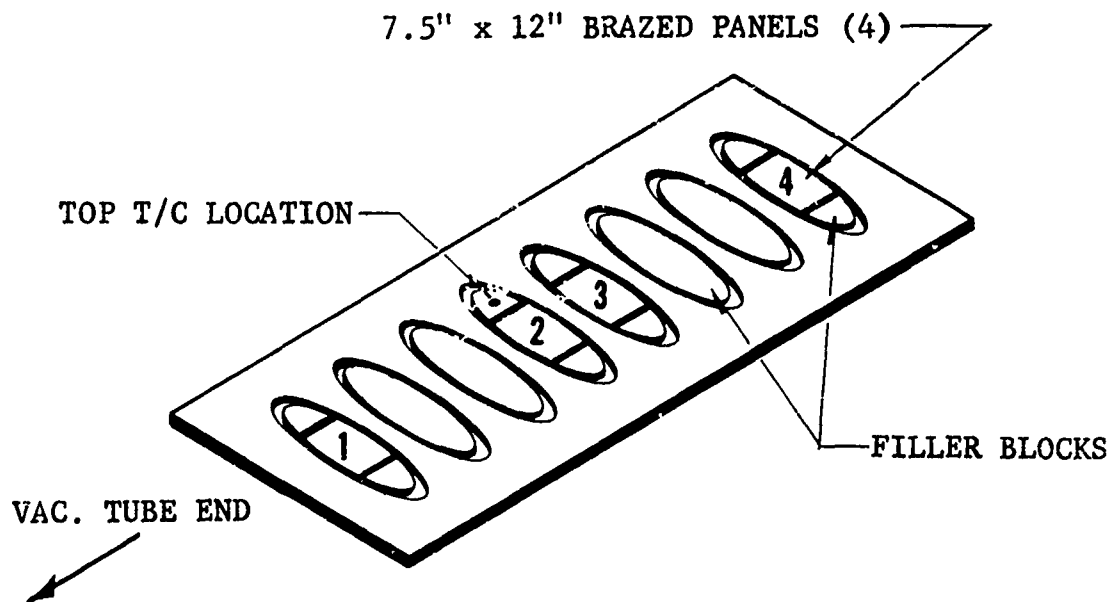


Figure 5-14 TOOLING AND TEST SPECIMEN COMPONENTS OF
603FTB035 PREBRAZE CYCLE

1. Preclean braze box and braze block using cheesecloth and acetone or distilled isopropyl alcohol.
2. Locate braze block in braze box. Use the required thickness shims around the perimeter of the block to prevent slipping.
3. Locate (5) 1/4 inch O.D. tubes in slots of braze block and weld to box.
4. Clean surface of block with cheesecloth and acetone. Use clean cotton gloves.
5. Clean (9) pieces of 0.062-inch thick caul sheets. Use Cheesecloth and acetone. Paint bottom surface of sheets with stop-off.
6. Locate caul sheets on braze block with a minimum of 1/8 inch gap between each sheet. Tack weld sheets together with 0.002 x 0.5-inch stainless steel strips.
7. Place refrasil cloth over caul sheets and braze block.
Note: Refrasil to be the same size as the braze block. This sheet of refrasil cloth does not require prebaking.
8. Clean atmosphere barrier with acetone and cheesecloth. Locate in braze box.
9. Clean 603FTB035-9 detail with acetone or distilled isopropyl alcohol. Locate the -9 plate in box equally spaced inside the atmosphere barrier.
10. Fabricate spacers to fit between the barrier and the -9 plate. Make spacers from 0.100-inch 321 stainless steel.
11. Clean spacers with acetone and cheesecloth. Locate spacers laying flat around the perimeter of the -9 part.
Note: These spacers are to prevent the barrier from warping and pulling in toward the panel.
12. Remove the refrasil cloth from each cutout in -9 detail part.
13. Clean (8) filler blocks with acetone and cheesecloth. Locate filler block in hog-outs in the -9 detail.
14. Locate refrasil cloth over the -9 detail.
Note: This refrasil cloth must be baked out at 1550°F for 5 minutes prior to lay-up.

15. Clean the -11 detail with acetone or alcohol and cheesecloth. Locate on top of the -9 detail.
16. Locate refrasil cloth over the -11 detail.
Note: This refrasil cloth must be baked out at 1550°F for 5 minutes prior to lay-up.
17. Clean the top -9 detail with acetone or distilled isopropyl alcohol and cheesecloth. Locate on top of the -11 detail.
18. Clean (12) filler blocks with acetone and cheesecloth. Locate in slots per following sketch. Place 0.002-inch thick stainless steel foil under each 7.5 x 12 inch panel and crimp up the corners to trap any excess alloy run out.



19. Clean (8) detail parts 0.250 x 7.5 x 12 inch 6Al-4V titanium with acetone and cheesecloth. Acid clean details per cleaning procedure for brazing.
20. Prefit alloy and punch 5/32 diameter holes on 3 inch centers for spacers.
21. Clean alloy to remove any oxides. Use steel wool or silicon carbide 320 grit sand paper. Note: When using steel wool, accomplish cleaning on table away from titanium details.

22. Clean alloy with acetone and cheesecloth.
23. Lay-up alloy and locate spacer buttons in four panels 7.5 x 12 inch. Tack weld a 0.002 x 0.375-inch stainless steel strip around the perimeter of each panel. Vibro etch number each panel No. 1-2-3-4-.
24. Locate panels in the hog outs of the -9 plate per above sketch. Place 1-inch sine wave strips of titanium inside and outside of the atmosphere barrier.
25. Locate refrasil cloth on top of panel. Cut the refrasil cloth into strips to match the steel caul sheets under the panel, leave a minimum of 1/8-inch gap between the strip. Note: Refrasil cloth to be the same size as the panel. This sheet of refrasil does not require prebaking.
26. Locate vacuum sheet and trim to size.
27. Weld vacuum sheet to braze box.
28. Check for leaks.
29. Argon purge braze box 15 cycles (hold maximum vacuum 3 minutes each cycle, then back fill with argon) and then maintain maximum vacuum.
30. Locate (5) 1/8-inch diameter Inco sheath chromel-alumel thermocouples 25 feet long into tubes in sides of braze box. Wedge thermocouples into the 1/4-inch diameter tubes. Locate and secure a 25-foot thermocouple in the 1/4-inch diameter 20.400-inch tube on top of the box.
31. Place (2) layers of 1/4-inch fiberfrax on top of vacuum sheet. Secure by placing several pieces of 1/4 or 3/8-inch steel on top of fiberfrax. Note: Wind turbulence is fairly strong inside the furnace.
32. Furnace should be leveled out at 1000°F to 1200°F. Place retort in furnace and increase furnace controls to 1600°F. Make individual recordings on each thermocouple.
33. Preheat at 1550°F for 5 minutes. Note: When lowest thermocouple reaches 1545°F turn furnace control back to 1000°F. When lowest thermocouple reaches 1550°F open furnace door. Maintain a vacuum of 15 in. HG and 5 C.F.H. argon. Turn argon off at 800°F.

34. Furnace cool to 1400°F.
35. Remove from furnace and cool to room temperature.
36. Remove assembly from retort box.
37. Save the reffrasil cloth for use in the braze cycle. Remove all filler blocks from hog-outs and clean for use in the braze cycle.
38. Do not remove the 0.100-inch thick caul sheets, the bottom layer of reffrasil cloth, or the atmosphere barrier.
39. Remove all thermocouples and forward to the cal. lab for calibration.
40. Grind flanges of the braze box. Make a new vacuum sheet for use on the braze cycle.

Braze Surface Preparation for 603FTB035 and 603FTB053

The braze surfaces of titanium details for 603FTB035 were prepared by face milling to within $0.060 + .030 - .000$ inch of nominal blueprint dimension and finished to final dimension by wet precision belt sanding. Sanding was done at Mill Polish Corp., Del Air, N. J. Final detail thickness was within $+.008 - .000$ of nominal blueprint dimension. Surface finish was measured at 38 to 50 RMS.

Details for 603FTB053 were also face milled, then finished to final dimension by dry belt sanding using 80 to 180 grit belts. Parts were face milled to $+.010 - .000$ inch of nominal blueprint dimension and about .002 inch removed from each surface by dry sanding.

The pre-braze cycle test demonstrated that the tooling, furnace, and support equipment functioned properly and indicated that there would be no serious problems in brazing a 603FTB035 part.

5.1.3.2 First Braze Run - 603FTB035

The braze surfaces of the three titanium details for 603FTB035 were prepared by face milling to within $0.060 + 0.030 - 0.000$ inch of nominal blueprint dimension and finished to final dimension by wet precision belt grinding. Grinding was done at Mill Polish Corp., Del Air, N. J. Final detail thickness was within $+ 0.008$

-0.00 of nominal blueprint dimension. Surface finish was measured at 38 to 50 RMS. The remaining procedure and braze cycle was accomplished as follows:

Procedure and Braze Cycle for First 603FTB035 Braze

1. Remove all oxides from surfaces of the -9 and -11 details. Use vibro sander with 320 grit paper.
2. Acetone clean details - use clean cheesecloth.
3. Acid clean details, reference P.S. 40.01-25 section 2, using the following cleaning procedure.
 - a. Wipe with clean cheesecloth and acetone to remove light oils and fingerprints. Handle parts with clean cotton gloves after this operation until brazing has been completed.
 - b. Attach parts to cleaning rack then complete the following operations:
 - o Alkaline soak* $-180 \pm 10^{\circ}\text{F}$, 15 minutes.
 - o Hot rinse $-180 \pm 10^{\circ}\text{F}$, 5 minutes.
 - o Nitric-hydrofluoric pickle** - Room temperature, 1 minute.
 - o Cold rinse - Room temperature, 45 seconds.
 - o Repeat the pickling and rinsing operations until a total of 5 cycles have been completed.
 - o Nitric acid desmut*** - Room temperature, 5 minutes.
 - o Deionized water rinse - Room temperature, 5 minutes.
 - o Allow parts to drip dry. Clean cheesecloth may be used, as a wick, to remove water from depressions that will not drain easily.
 - o Remove wires from parts. Wrap in clean brown paper, and forward to lay-up area.

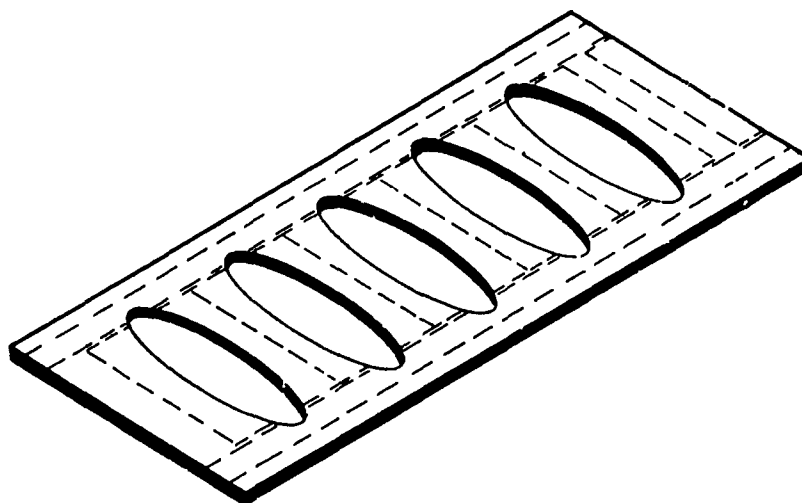
* Sodium hydroxide 32-48 oz./gal.

** Nitric acid (29-31% by wt.) + hydrofluoric acid (2.4-3.2% by wt.)

Note: The hydrofluoric content stated above is contained in the initial tank charge. A periodic test of the active fluorides is made by etching titanium test coupons. Weight loss from the etched coupons is converted to thickness. The solution is maintained in a range that removes titanium at the rate of .022 to .028 mils/side/minute.

*** Nitric acid 35-64% by wt.

4. Check braze box to see that the caul sheets and refrasil cloth are in the correct location.
5. Prefit and trim the brazing alloy to fit the lower -9 plate. Punch 5/32-inch diameter holes on three-inch centers in the brazing alloy for the 1/8-inch diameter 0.002-inch thick stainless steel spacers.
6. Locate and tack the braze alloy and spacers to the -9 plate. Reference the following sketch for layout of the alloy. Do not overlap the alloy joints.



7. Locate the -9 plate in braze box. Equally space the plate inside the atmosphere barrier.
8. Locate the 0.100-inch thick shims around the perimeter of the -9 plate to prevent the atmosphere barrier from warping in toward the panel.

9. Locate filler blocks in hog-outs of -9 plate. Place refrasil cloth on top of each filler block.
Note: All refrasil cloth used in the braze cycle must be baked before using in braze box. Do not use stainless steel retainer strips around the perimeter of the hog-outs.
10. Inspect the -11 plate for water marks or other contamination. Remove any contamination with distilled isopropyl alcohol and clean cheesecloth.
11. Locate the -11 plate on top of the -9 lower plate.
12. Punch 5/32-inch holes in the alloy. Tack alloy to the surface of -11 plate. Locate and tack 0.002-inch thick x 1/8 inch dia. stainless steel spacers in each hole in the alloy.
13. Locate the -9 upper plate on top of the -11 center plate. Scribe the braze alloy around the perimeter of each hog-out in -9 plate. Remove -9 plate and trim out alloy to the scribe lines.
14. Relocate the -9 upper plate in the braze box.
15. Tack weld a 0.002 x 1-inch stainless steel strip over the braze joints around the perimeter of the parts.
16. Place prebaked refrasil cloth in the bottom of each hog-out. Do not use 0.002-inch stainless steel retainer strips around the inside of the hog-outs.
17. Acetone clean the filler blocks and locate in the center of the hog-outs.
18. Preform a 1 inch wide titanium ribbon into a sinewave configuration and place in braze box. Ribbon is required both inside and outside of the atmosphere barrier.
19. Locate refrasil cloth on top of panel. Cut the refrasil cloth into strips to match the steel caul sheets under the panel; leave a minimum of 1/8-inch gap between the strips. This refrasil cloth must be prebaked.
20. Locate vacuum sheet and trim to size.
21. Weld vacuum sheet to braze box.
22. Check for leaks.

23. Argon purge braze box 15 cycles. Hold maximum vacuum 3 minutes each cycle, then back fill with argon. Hold at maximum vacuum.
24. Locate (5) 1/8"-diameter Inco sheath chromel-alumel thermocouples 25 feet long into tubes in sides of braze box. Wedge thermocouples into the 1/4-inch diameter tubes. Locate and secure a 25 foot thermocouple in the 1" x 8" x 8" steel block on top of box.
25. Place (2) layers of 1/4 inch fiberfrax on top of vacuum sheet. Secure by placing several pieces of 1/4 or 3/8-inch steel on top of fiberfrax.
Note: Wind turbulence is fairly strong inside the furnace. Place one layer of fiberfrax inside the "C" channels of the braze box.
26. Furnace should be leveled out at 900°F. Place retort in furnace and increase furnace controls to 1600°F. Make individual recordings on each thermocouple.
27. Preheat at 1550°F for 5 minutes.
Note: When lowest thermocouple reaches 1545°F turn furnace control back to 1000°F. When lowest thermocouple reaches 1550°F open furnace door. Maintain a vacuum of 15 in. Hg and 5 C.F.H. argon. Turn argon off at 800°F.
28. Furnace cool to 1400°F.
29. Remove from furnace and cool to room temperature.
30. Remove assembly from retort box.

The entire brazing procedure was completed with little difficulty and no apparent problems; however, tests of the part showed an inadequate braze. X-ray and NDI inspection indicated a heavy concentration of braze line irregularities, especially between the middle and lower details in the area of the hog-outs. Destructive testing showed what appeared to be a "cold braze" with a lack of alloy flow and insufficient melt. The braze surface of the titanium details also appeared to be contaminated. All thermocouples indicated sufficient temperature for brazing based on results of previous tests. Thermocouple locations are shown in the sketch in Figure 2. Braze cycle time/temperature graphs are shown in Figures 5-15 through 5-20.

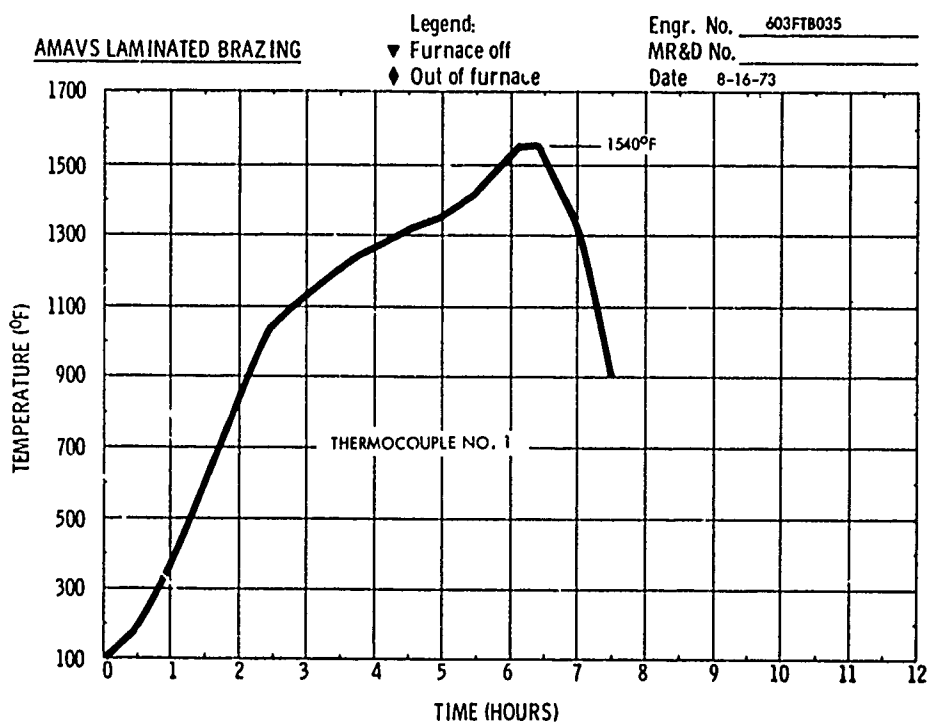


Figure 5-15 BRAZE CYCLE FOR 603FTB035 TEST SPECIMEN
 RUN #1 THERMOCOUPLE NO. 1

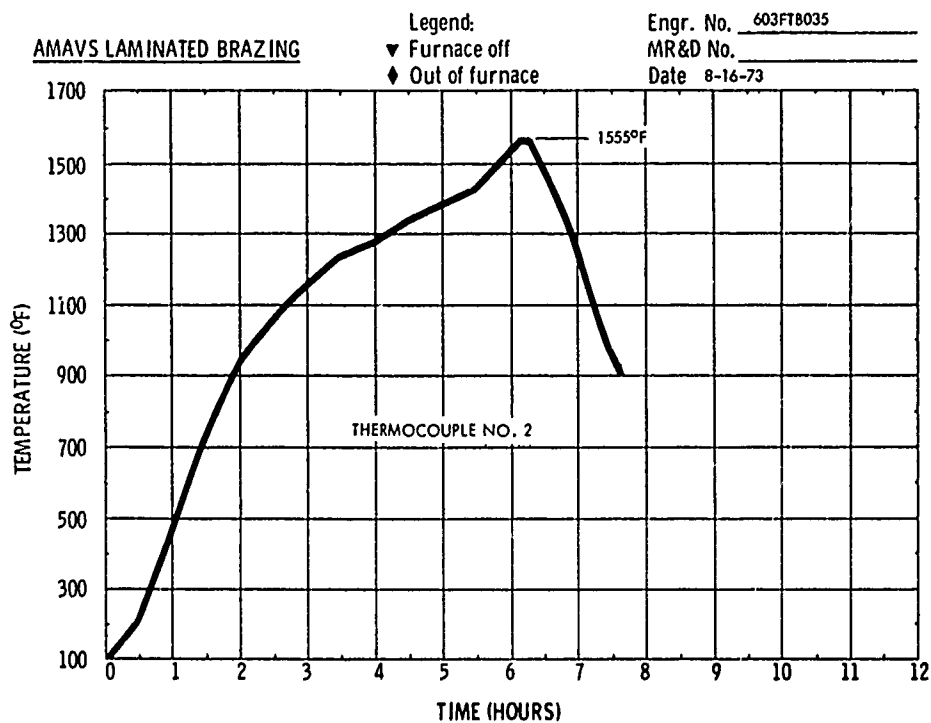


Figure 5-16 BRAZE CYCLE FOR 603FTB035 TEST SPECIMEN
 RUN #1 THERMOCOUPLE NO. 2

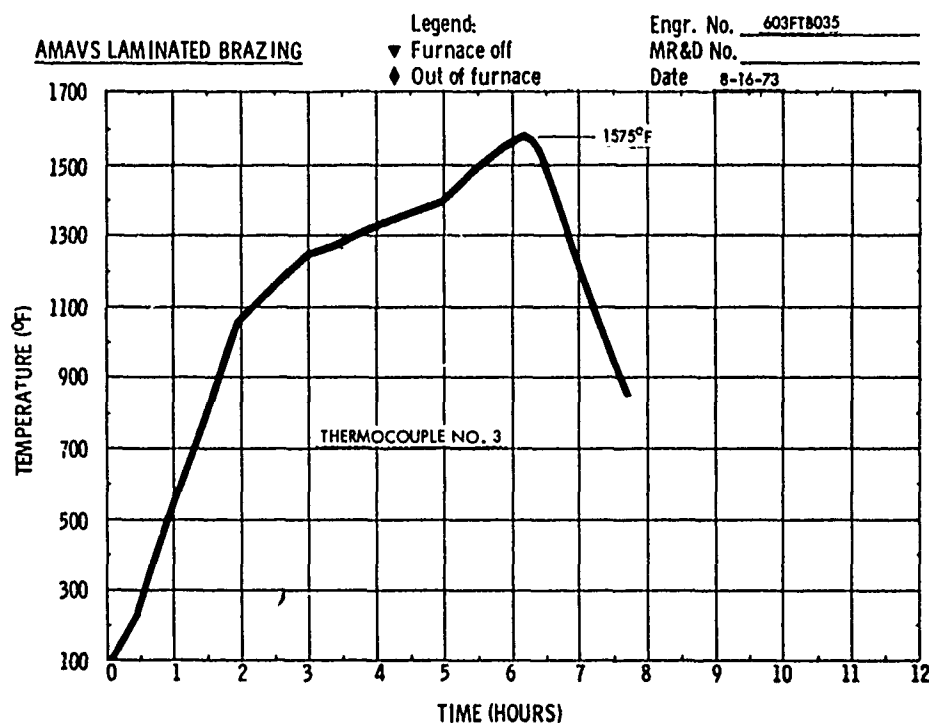


Figure 5-17 BRAZE CYCLE FOR 603FTB035 TEST SPECIMEN
 RUN #1 THERMOCOUPLE NO. 3

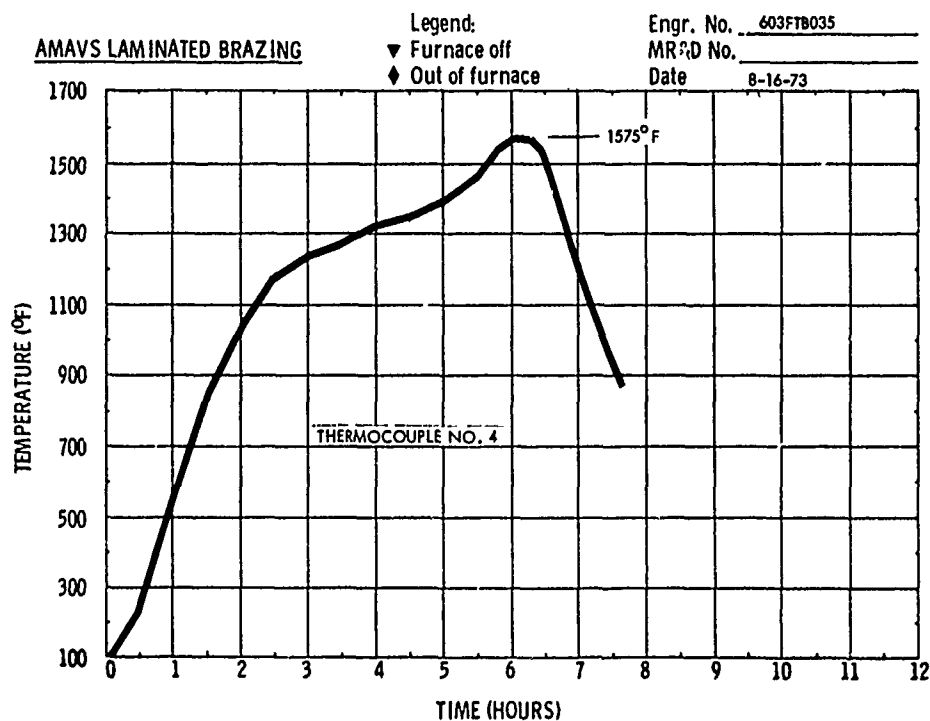


Figure 5-18 BRAZE CYCLE FOR 603FTB035 TEST SPECIMEN
 RUN #1 THERMOCOUPLE NO. 4

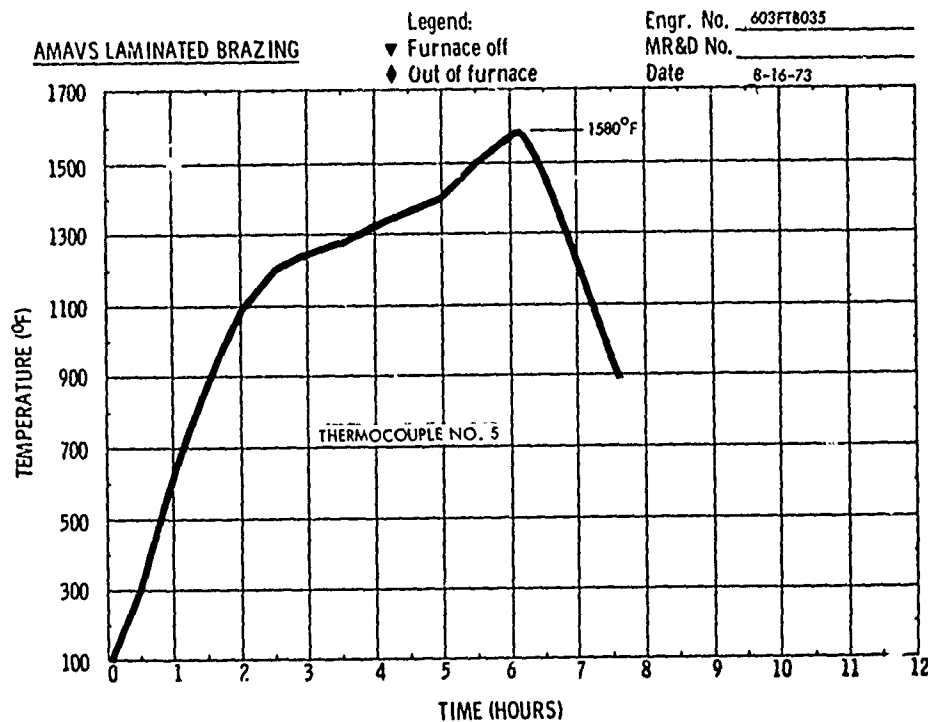


Figure 5-19 BRAZE CYCLE FOR 603FTB035 TEST SPECIMEN
 RUN #1 THERMOCOUPLE NO. 5

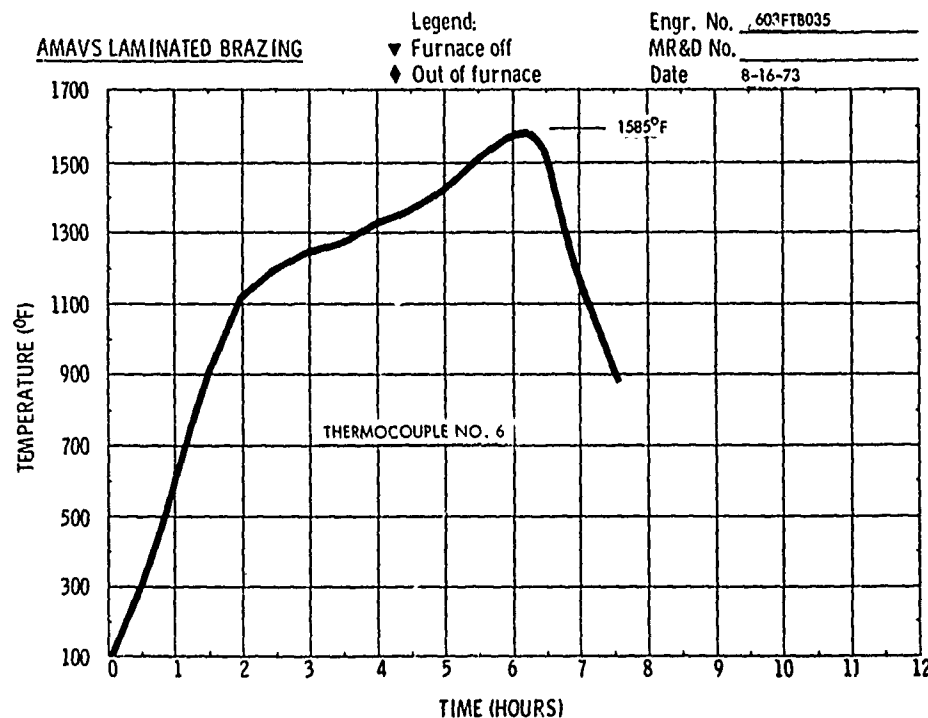


Figure 5-20 BRAZE CYCLE FOR 603FTB035 TEST SPECIMEN
 RUN #1 THERMOCOUPLE NO. 6
 5-23

5.1.3.3 Rebrazed of the First 603FTB035 Test Specimen (603FTB035-3C)

The first 603FTB035 brazed test specimen was sawed in half in the transverse direction, disassembled at each braze line, and prepared for a second braze operation. Disassembly was relatively easy because of an inadequate braze. The braze alloy was chemically stripped from the details prior to the standard pre-braze cleaning operation.

The second braze operation (603FTB035-3C) was run to refine the braze cycle, to further determine temperature distribution within the panel, to determine the requirements for an increased heat-up rate in the braze cycle, and to establish potential of rebrazing salvaged details.

After the braze alloy from the first braze operation was stripped, the titanium details were vibro sanded to provide a smooth surface and remove intermetallics that may have been present. Chemical cleaning the details was by standard procedure. Only one-half of the part (about 4' x 5') was prepared for brazing. The remaining half of the panel was installed in the braze box, without braze alloy, to provide a uniform load. Two 1/4" x 1/4" x 7 1/2" x 12" braze test panels were placed in the hog-out areas as illustrated in Figure 5-21. A total of ten thermocouple locations were planned for this test run. During the braze box leak detection test a leak was found in thermocouple tube No. 5. Attempts to repair the leak failed; therefore, the tube entry was welded and the thermocouple omitted. Complete tooling, detail layup and thermocouple entry locations are shown in Figure 5-22.

The braze time/temperature cycle for 603FTB035-3C is shown in the graphs in Figures 5-23 through 5-31. It is believed that thermocouples 3 and 9 (Figures 5-29 and 5-30) showed faulty readings due to shorting out on the braze box. Both of these thermocouples were insulated with a soft material and it is possible that the insulation was scraped off in localized areas in initial installation.

After brazing, visual inspection of the part showed only a small amount of alloy flow at the panel edges. Also, discoloration was evident around the periphery of the part and in the hog-out areas. The part was inspected by NDI and sent to the engineering test lab for further evaluation.

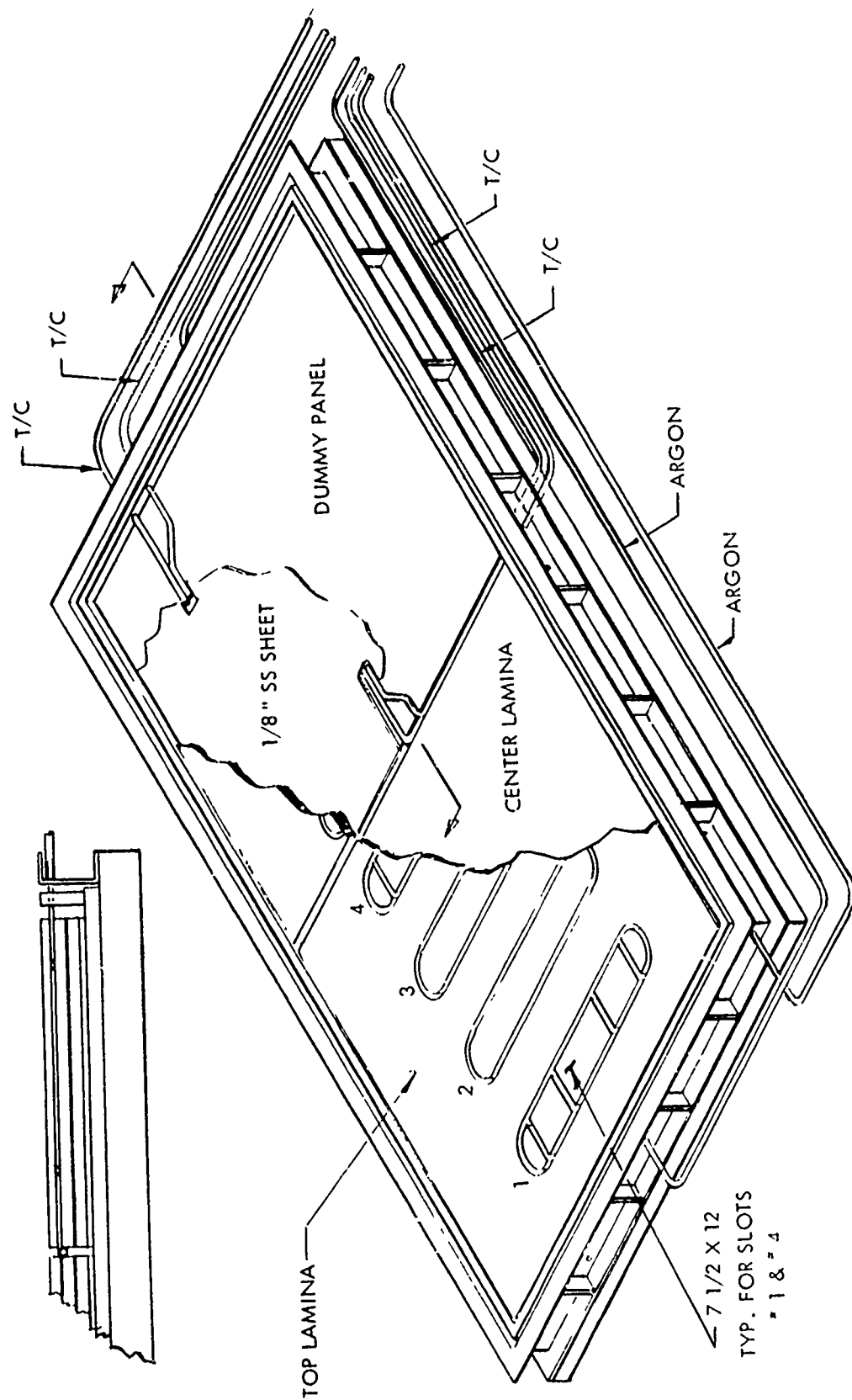


Figure 5-21 LAY-UP OF 603FTB035-3C ILLUSTRATING DUMMY PANEL, CENTER LAMINA AND 7 1/2 X 12" TEST SPECIMEN LOCATIONS

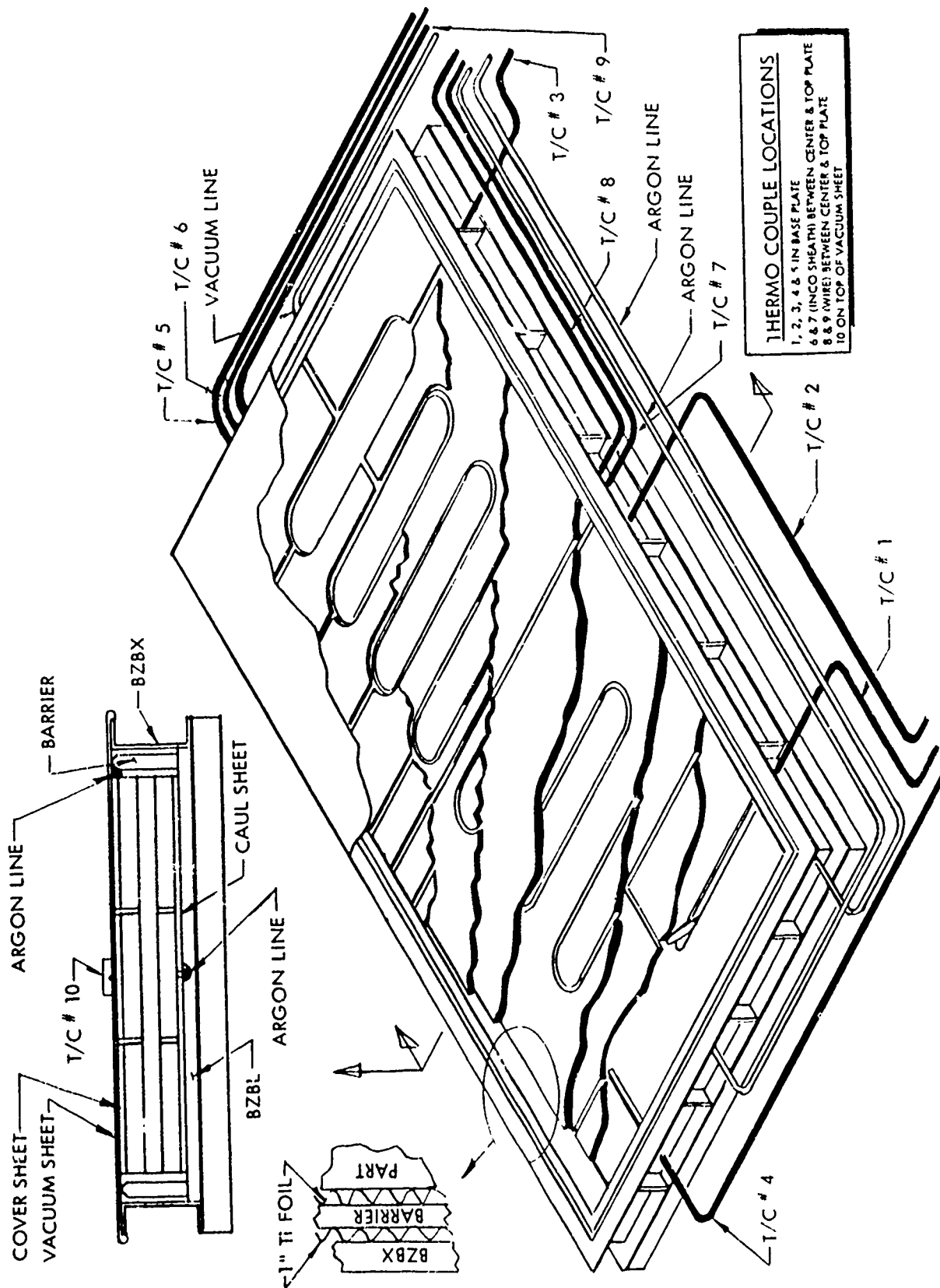


Figure 5-22 TOOLING, LAY-UP AND THERMOCOUPLE ENTRIES FOR 603FTB035-3C

Engr. No. 603FTB 035-3C
 MR&D No. _____
 Date 9-22-73

AMAVS LAMINATED BRAZING

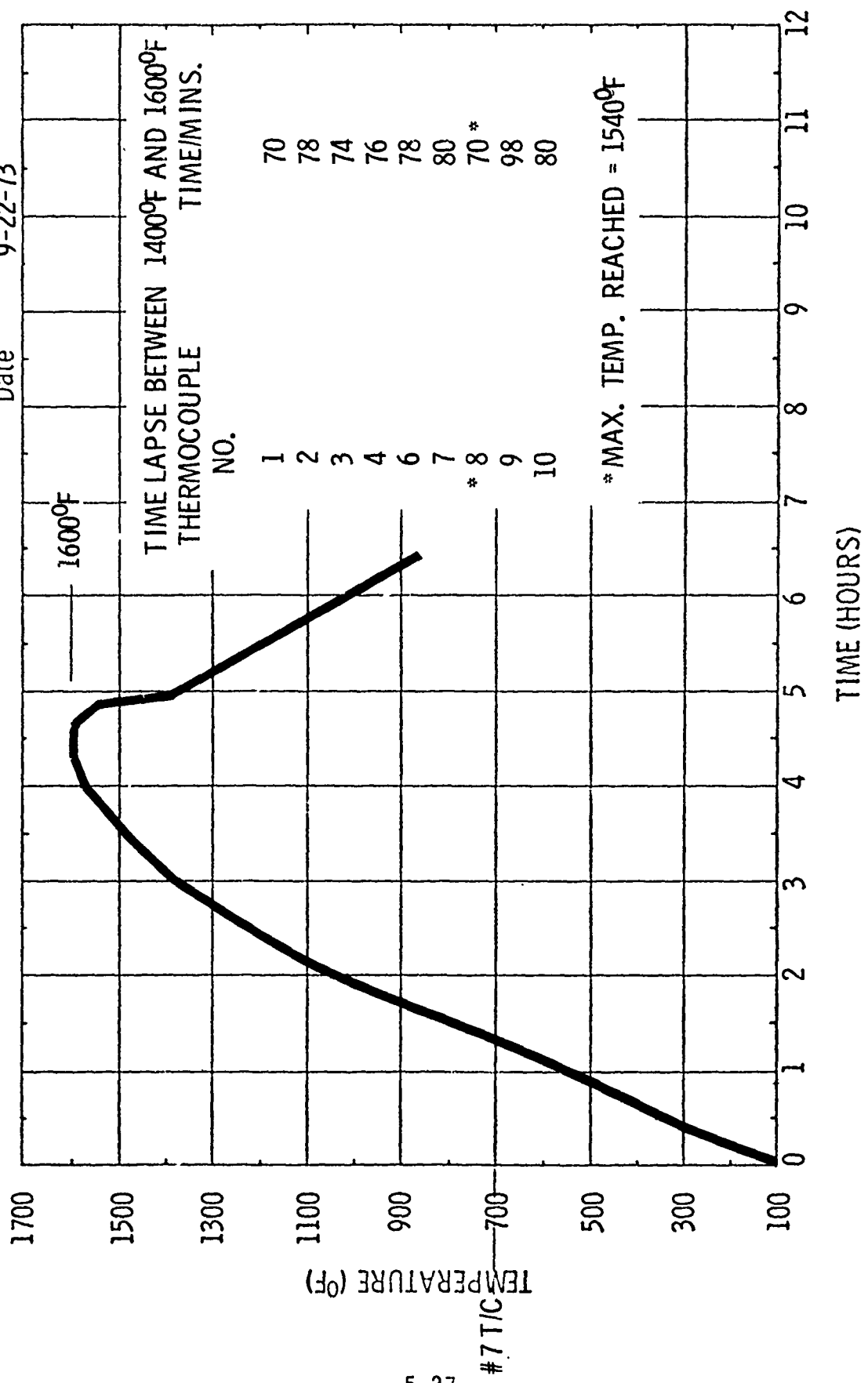


Figure 5-23 BRAZE CYCLE FOR 603FTB035-3C THERMOCOUPLE NO. 7

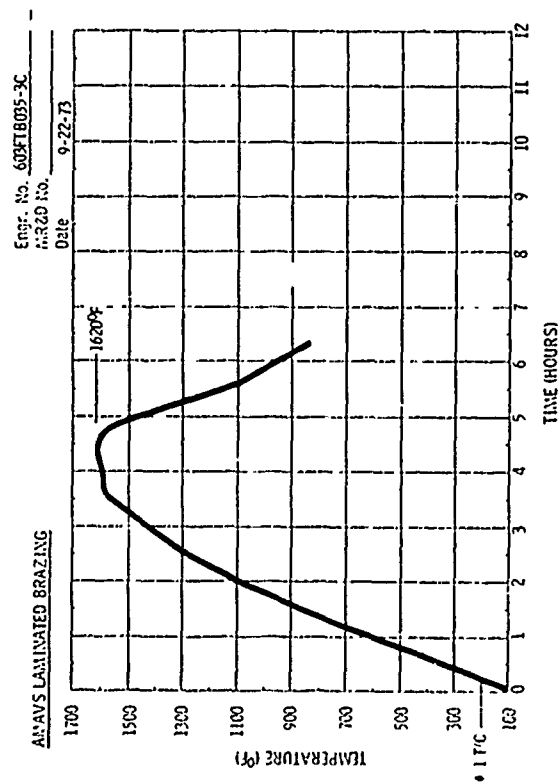


Figure 5-24 BRAZE CYCLE FOR 603FTB035-3C
 THERMOCOUPLE NO. 1

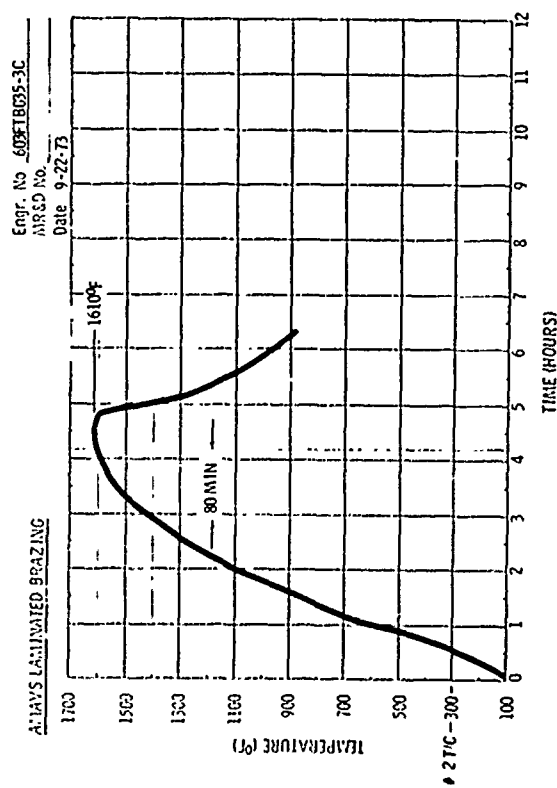


Figure 5-25 BRAZE CYCLE FOR 603FTB035-3C
 THERMOCOUPLE NO. 2

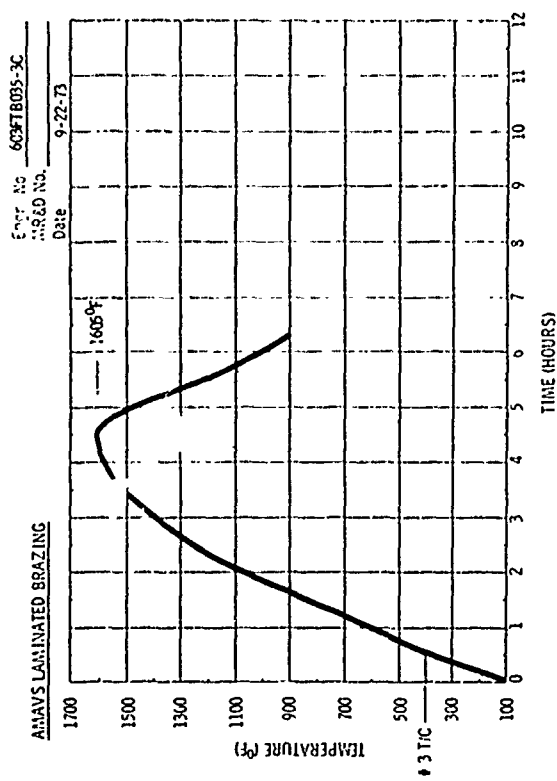


Figure 5-26 BRAZE CYCLE FOR 603FTB035-3C
 THERMOCOUPLE NO. 3

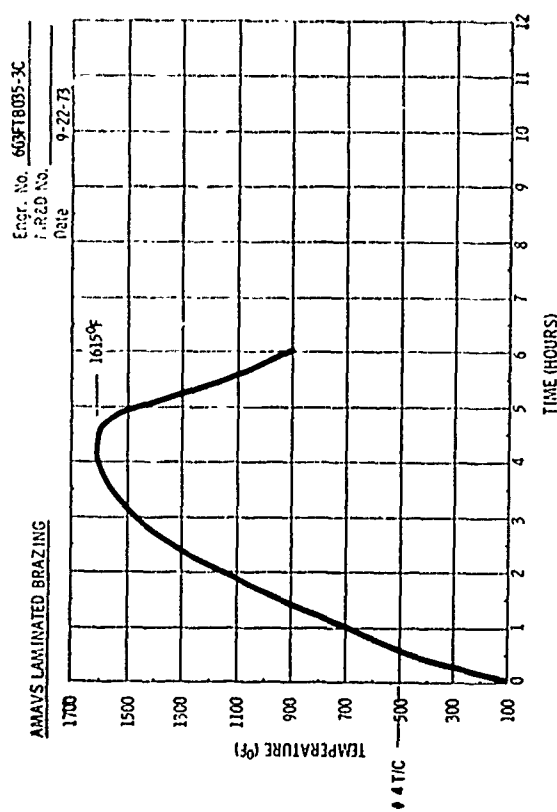


Figure 5-27 BRAZE CYCLE FOR 603FTB035-3C
 THERMOCOUPLE NO. 4

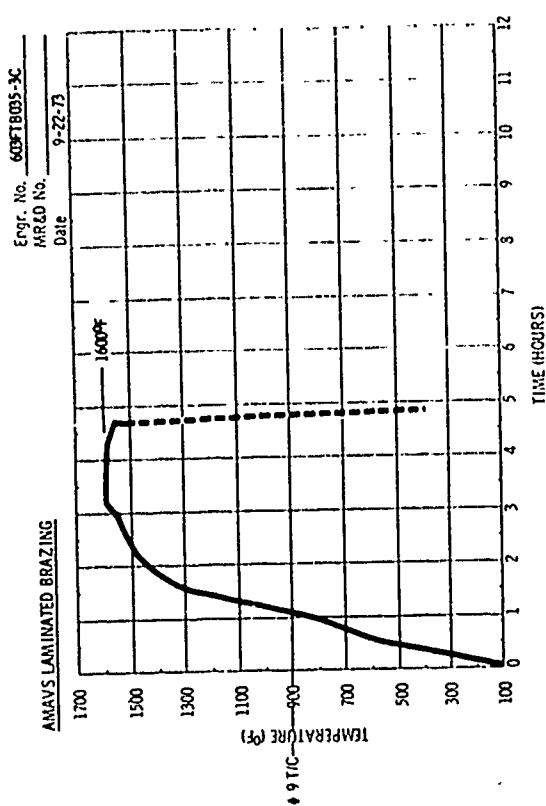


Figure 5-28 BRAZE CYCLE FOR 603FTB035-3C
THERMOCOUPLE NO. 6

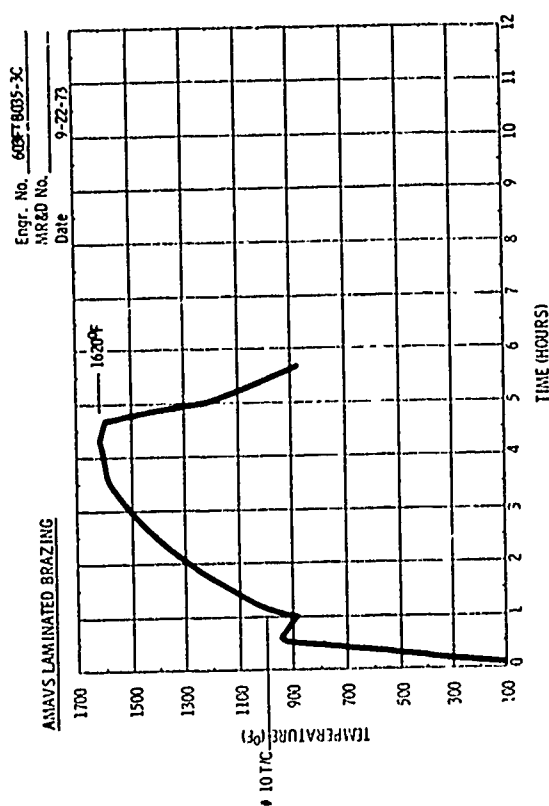


Figure 5-29 BRAZE CYCLE FOR 603FTB035-3C
THERMOCOUPLE NO. 8

Figure 5-30 BRAZE CYCLE FOR 603FTB035-3C
THERMOCOUPLE NO. 9

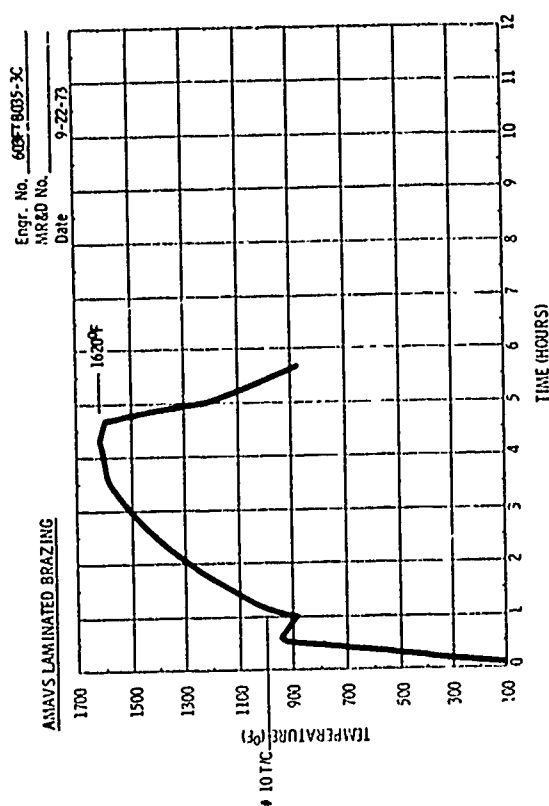


Figure 5-31 BRAZE CYCLE FOR 603FTB035-3C
THERMOCOUPLE NO. 10

5.1.3.4 Brazing of the Second Lower Plate Damage Tolerance Test Specimen 603FTB035-7A

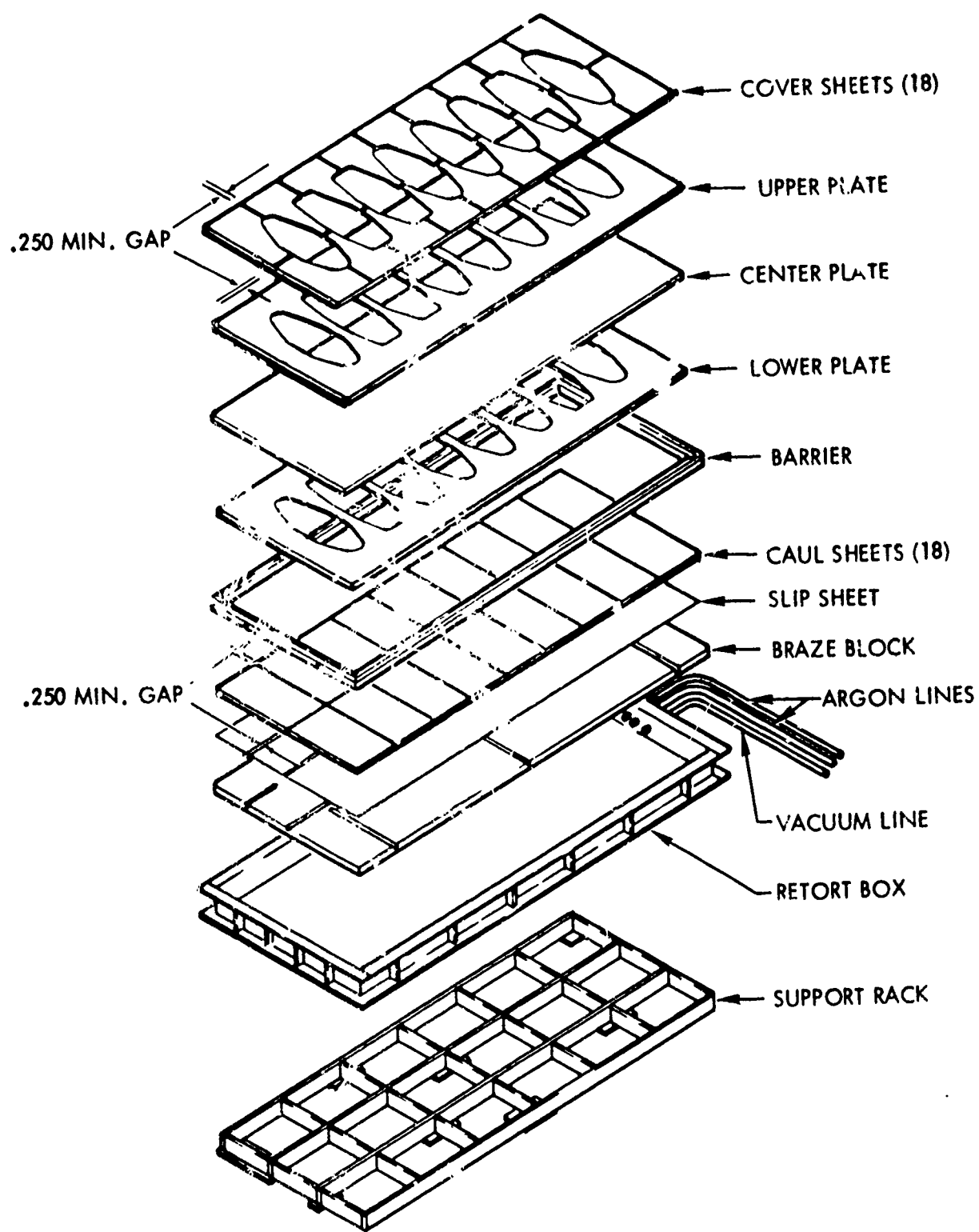
Before brazing the 603FTB035-7A test specimen, special braze tests were run using 1/4" x 1/4" x 6" x 6" test parts. These specimens were run to refine brazing parameters. Specifically, the variables investigated were effect of time delay between cleaning and brazing, the effect of sanded braze alloy vs. as-received alloy, heating rate, and the effect of using titanium plate previously subjected to a braze cycle.

Based on results of the previously brazed 603FTB035 parts and results of special tests several tooling and process changes were incorporated into the procedure for brazing the 603FTB035-7A test specimen. The major changes include:

- (1) Central location of argon supply tubes to improve purging in upper and lower hog-out areas. (Figure 5-37)
- (2) Elimination of insulation on top of braze box during braze heat cycle (to increase heating rate).
- (3) Higher furnace temperature in initial stage of braze cycle (to increase heating rate).
- (4) Increased energy input into furnace during braze cycle (to increase heating rate).

Tooling, thermocouple inlet locations, and lay-up procedure are illustrated in Figures 5-32 through 5-37 and a complete tooling, layup and braze check off list for 603FTB035-7A is shown below:

1. Clean braze block with isopropyl alcohol and clean cheesecloth.
2. Bake braze block at 1600°F for 15 minutes.
3. Clean braze box
 - a. Vacuum
 - b. Isopropyl alcohol and clean cheesecloth.
4. Insert braze block in braze box.



603FTB035

Figure 5-32 BRAZE COMPONENTS FOR 603FTB035-7A

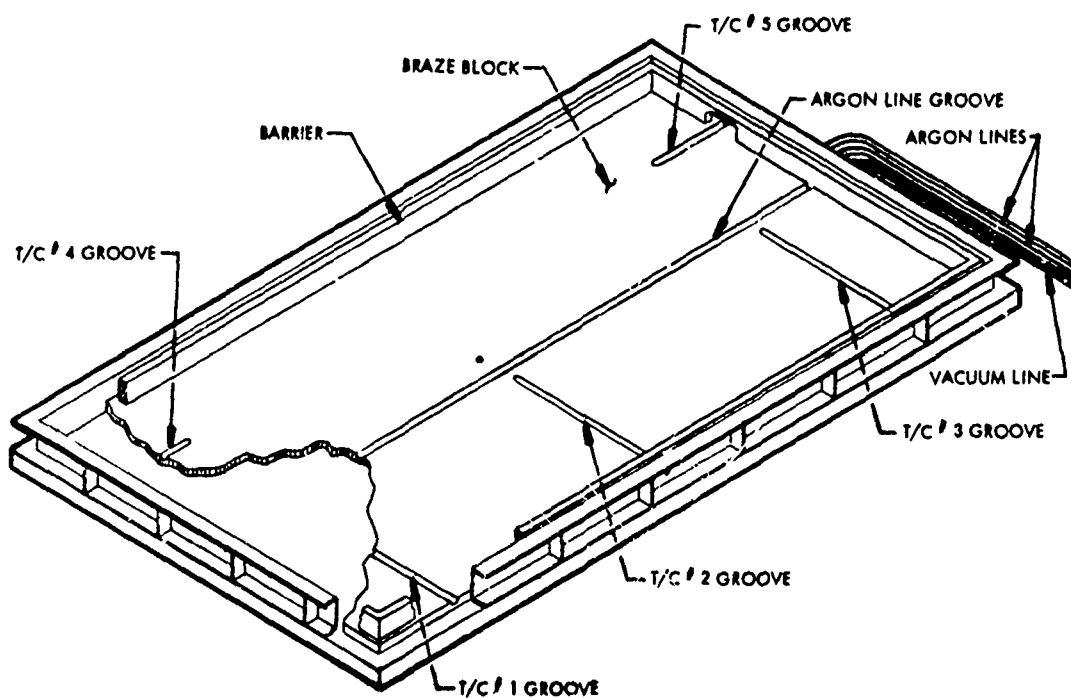


Figure 5-33 BRAZE BOX TOOLING ILLUSTRATING THERMOCOUPLE LOCATIONS

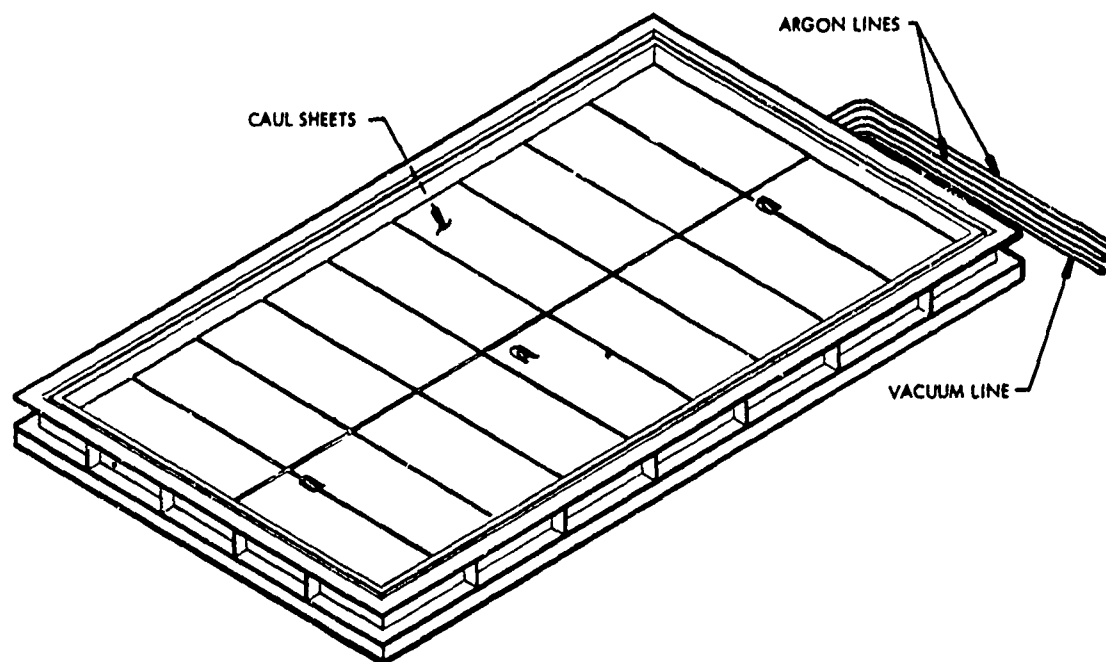


Figure 5-34 BRAZE BOX TOOLING ILLUSTRATING CAUL SHEETS, ARGON LINES AND VACUUM LINE

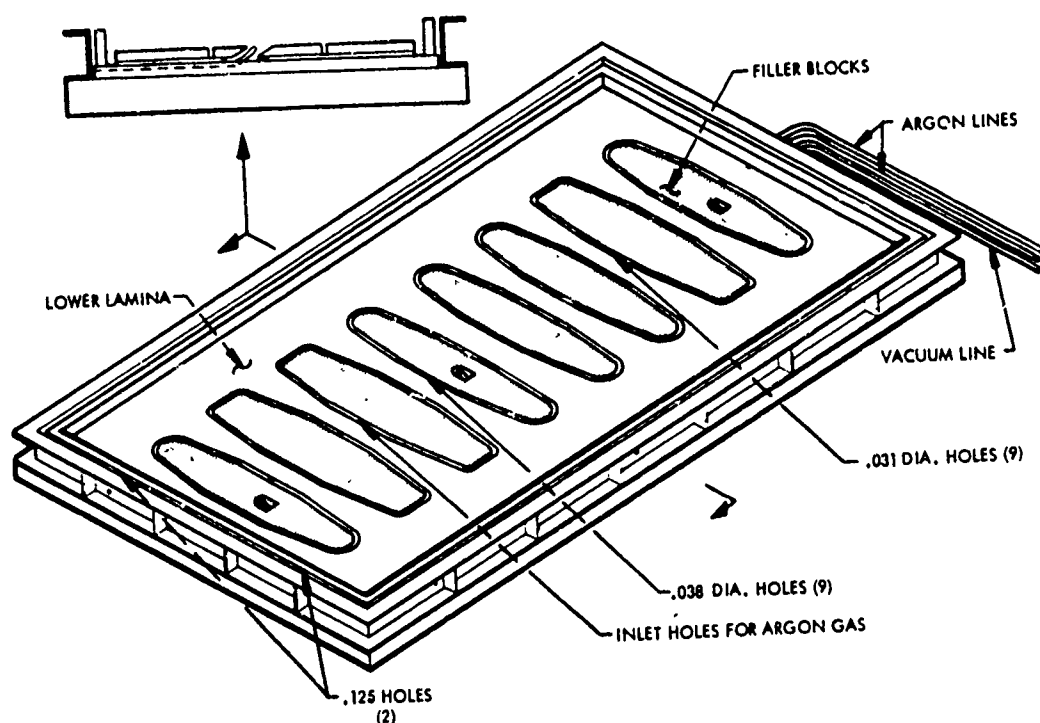


Figure 5-35 BRAZE BOX ILLUSTRATING ARGON GAS LINES FOR PURGING LOWER LAMINA HOG-OUTS

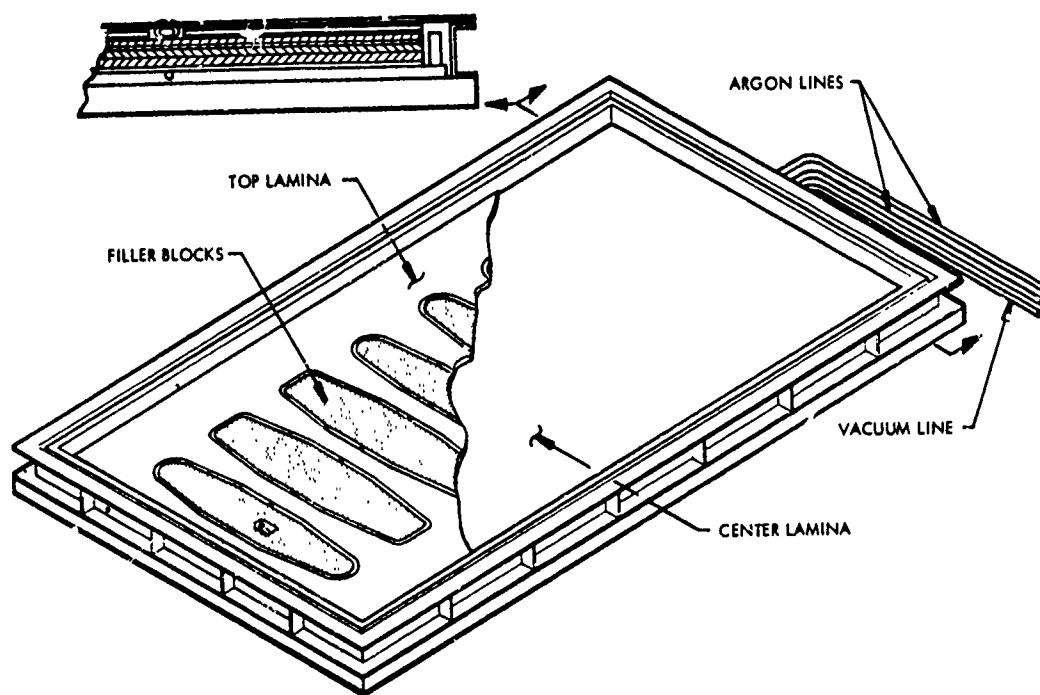
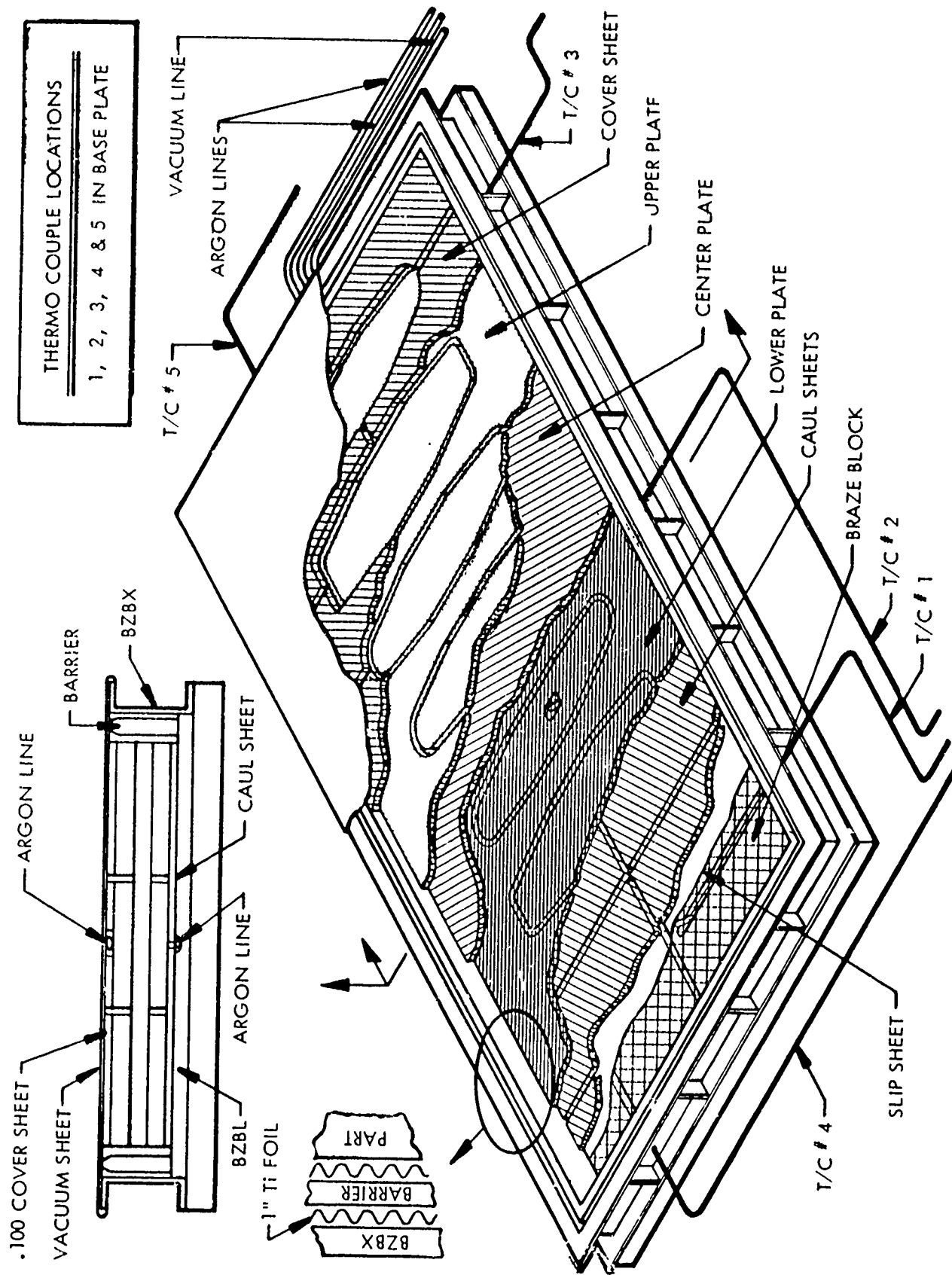


Figure 5-36 BRAZE BOX ILLUSTRATING TITANIUM LAMINA AND FILLER BLOCKS



603FTB035-7A

Figure 5-37 COMPLETE LAY-UP FOR 603FTB035-7A

5. Fabricate thermocouple tubes.
6. Leak check thermocouple tubes.
7. Clean thermocouple tubes - vapor degrease (150°F tank).
8. Weld thermocouple tubes in braze box.
9. Fabricate caul sheets.
10. Disc grind surface of caul sheets to remove oxides and manufacturer's identification (ink stencil).
11. Clean both surfaces of caul sheets with alcohol and clean cheesecloth.
12. Paint upper surface of caul sheets with stop-off (Stopyt), air dry, bake at 800°F for 10 minutes.
13. Fabricate lower argon line of 0.250-inch diameter, 0.020" wall, 321 stainless steel tube.
 - a. Drill (9) 0.038-inch holes and (9) 0.031-inch holes in tube using prepared template for hole spacing. Smaller holes will be at argon entry end.
 - b. Deburr holes and flare one end.
 - c. Clean argon supply line using vapor degrease (150°F tank).
 - d. Plug weld end of argon line.
 - e. Drill 1/4-inch hole in braze box to receive lower argon line.
 - f. Locate and weld tube to braze box. Holes to be normal to top surface of braze plate.
14. Seal weld the argon and (5) T/C tubes directly beneath the atmosphere barrier. Grind welds flush with top of base plate.
15. Locate slip sheets (2) on top of braze block.
16. Locate caul sheets in braze box on top of slip sheets. Maintain 1/4 inch minimum gap between each caul sheet. Tack weld one place, each sheet on end near argon line.

17. Drill (1) hole for upper argon line in the vacuum end of barrier.
18. Drill (2) 1/8" vent holes in the opposite end of atmosphere barrier located 8" in from the corners.
19. Fabricate picture frame type spacer (0.100-inch thick 321 stainless steel) and locate in braze box.
20. Place atmosphere barrier in braze box (on top of picture frame).
21. Mill T/C slot in (3) filler blocks. Paint one surface and all edges of 16 filler blocks with (Stopyt) and bake off at 800°F for 30 minutes.
22. Prepare upper argon supply line.
 - a. Flatten 1/4-inch diameter 321 stainless steel tube to 0.200-inch height.
 - b. Drill argon exit holes with size, location, and pattern as described in 13a. Flare one end of tube.
 - c. Clean argon line using vapor degrease (150°F tank).
 - d. Crimp end of upper argon line and seal weld.

Reference Material

CSA 760-8-6-1	603FTB035-9	Plate
CSA 760-8-7-1	603FTB035-9	Plate
CSA 760-8-8-1	603FTB035-11	Plate (center plate)

23. Inspect and log test tag.
24. Prefit details and rough trim braze alloy to details.
25. Remove all oxides from surfaces of the -9 and -11 details. Use vibro sander with 320 grit paper.
26. Acid clean details (P.S. 40.01-25 section 2) Reference the following cleaning procedure.
 - a. Wipe with clean cheesecloth and acetone to remove light oils and fingerprints. Handle parts with clean cotton gloves after this operation until brazing has been completed.

b. Attach parts to cleaning rack then complete the following operations.

- o Alkaline soak at $180 \pm 10^{\circ}\text{F}$, 15 minutes, tank 650.
- o Hot rinse at $180 \pm 10^{\circ}\text{F}$, 5 minutes, tank 651.
- o Nitric-hydrofluoric pickle at room temperature, 1 minute, tank 652.
- o Cold rinse at room temperature, 45 seconds, tank 653.
- o Repeat the pickling and rinsing operations until a total of 5 cycles have been completed.
- o Nitric acid desmut at room temperature, 5 minutes, tank 721.
- o Deionized water rinse at room temperature, 5 minutes, tank 722.
- o Allow parts to drip dry. Clean cheesecloth may be used, as a wick, to remove water from depressions that will not drain easily.

27. Inspect

28. Remove wires from parts and wrap in clean brown paper. Handle parts with clean cotton gloves.

29. Forward parts to lay-up area, Col. 41 C-D.

Note: All succeeding operations shall be accomplished per instructions from L. I. Burnett, extension 4461 and will be monitored by the assigned MR&D brazing engineer.

30. Check braze box to see that the caul sheets are in correct location.

Note: Paint top sides of caul sheets with stop-off and bake at 800°F 10 minutes prior to location.

31. Prefit and trim the brazing alloy to fit the lower -9 plate. Punch 9/32-inch holes on four inch centers in the brazing alloy for the 0.250 x 0.002-inch thick stainless steel spacers.

32. Sand braze alloy with 240 grit paper.
33. Wipe braze alloy and -9 plate with distilled isopropyl alcohol and clean cheesecloth to remove fingerprints or other contamination. Handle parts only with white cotton gloves.
34. Locate and tack the braze alloy and spacers to the -9 plate. Do not overlap the alloy joints.
35. Locate the -9 plate in braze box. Equally space the plate inside the atmosphere barrier.
36. Locate filler blocks in hog-outs of -9 plate. Paint all surfaces with stop-off and bake at 800°F 30 minutes prior to locations. Do not use stainless steel retainer strips around the perimeter of the hog-outs.
37. Inspect the -11 plate for water marks or other contamination. Remove any contamination with distilled isopropyl alcohol and clean cheesecloth. Use cotton gloves for handling part.
38. Locate the -11 plate on top of the -9 lower plate.
39. Punch 5/32-inch holes in the alloy. Remove contamination with distilled alcohol and clean cheesecloth. Handle parts only with cotton gloves. Tack alloy to the surface of -11 plate. Locate and tack 0.002 thick x 1/8 inch dia. stainless steel spacers in each hole in the alloy (holes to be 4" centers).
40. Remove contamination with distilled alcohol and clean cheesecloth. Handle parts only with cotton gloves. Locate the -9 upper plate on top of the -11 center plate. Scribe the braze alloy around the perimeter of each hog-out in -9 plate. Remove -9 plate and trim out alloy to the scribe lines.
41. Relocate the -9 upper plate in the braze box.
42. Tack weld a 0.002 x 1 inch stainless steel strip over the braze joints around the perimeter of the parts.
43. Locate the filler blocks in the center of the hog-outs.
Note: Paint surfaces with stop-off and bake at 800°F 30 minutes prior to location.
44. Preform a 1 inch wide titanium ribbon into a sinewave configuration and place in braze box. Ribbon is required both

inside and outside of the atmosphere barrier.

45. Locate 0.100-inch thick cover sheets on top of panel.
Note: Paint lower surfaces with stop-off and bake at 800°F 10 minutes prior to location. Locate and weld upper argon line in braze box.
46. Locate vacuum sheet and trim to size.
47. Weld vacuum sheet to braze box.
48. Check for leaks.
49. Argon purge braze box 15 cycles, hold maximum vacuum 3 min. (accomplish at furnace with liquid argon).
50. Locate (5) 1/8" diameter Inco sheath chromel-alumel thermocouples 25 feet long into tubes in sides of braze box. One (1) T/C on top of box in 1 x 8 x 8-inch steel block.
51. Place one layer of fiberfrax inside the "C" channels of the braze box. Purge box 5 minutes at 17" Hg vacuum and 10 CFH argon.
52. Set furnace temperature at 1400°F prior to locating panel in furnace. Place panel in furnace and turn furnace heat controls to 1650°F. Allow low T/C to reach 1600°F and adjust controls to hold for 15 minutes.
Note: Turn argon off at 900°F on heat up. Adjust vacuum to 17" Hg vacuum.
53. Turn furnace control off and cool until T/C #2 reads 1200°F.
54. Remove retort from furnace and place two layers of fiberfrax on top of box. Cool to room temperature.
55. Forward to pilot shop, Col. 47J on mezz.
56. Open retort - remove brazed assembly and remove all oxides and alloy from surfaces.
57. Identify with assembly part number.
58. X-ray inspect.
59. Ultrasonic inspect (Attention: D. L. Duncan) (Col. 47J Mezz.)

60. Record all data.

61. Forward to stock room No. 1000.

5.1.3.5 Lay-up of Details for 603FTB035-7A Test Specimen

To avoid excessive contamination of the clean titanium details and braze alloy effort was made to minimize the time between acid cleaning and brazing. Also, handling of details was kept to a minimum and clean white cotton gloves were used at all times. In periods of inactivity during the lay-up procedure, all details were covered with brown kraft paper. A pictorial history of lay-up through sealing the braze box is shown in the photographs in Figures 5-38 through 5-45.

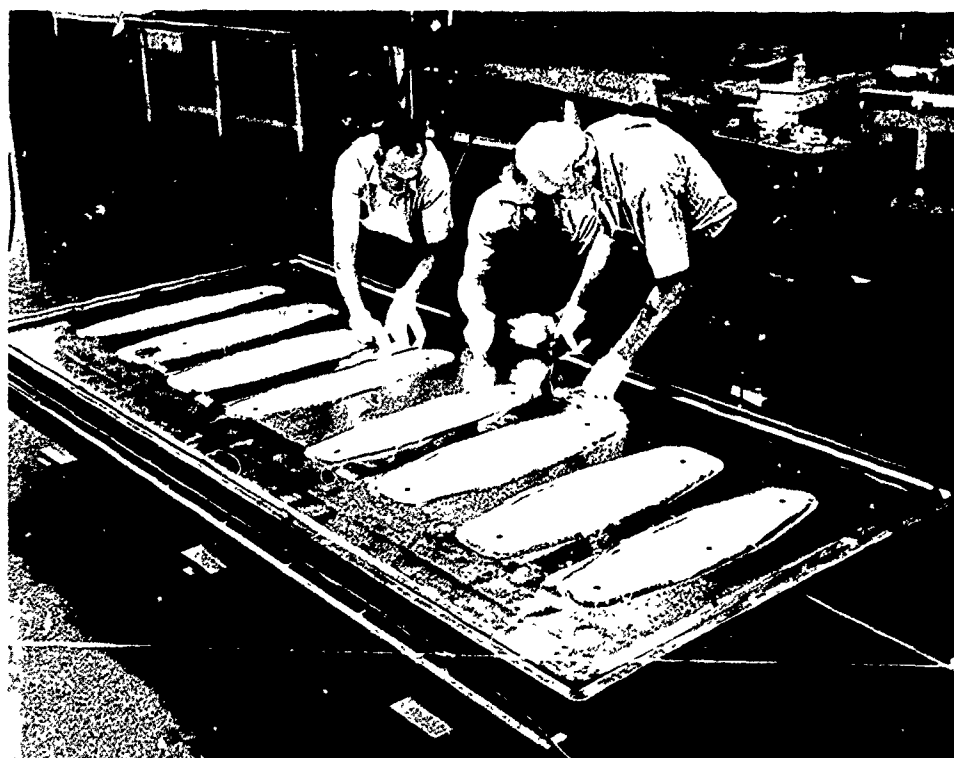
Other precaution taken in lay-up procedure included an increased cure cycle for the stop-off material (Stopyt) used on caul sheets, cover sheets, and filler blocks and an elimination of the use of refrasil cloth in the braze box. Smoke originating in the braze box in previous runs was traced, by tests, to uncured stop-off material. Tests also demonstrated that a thermal treatment of 800°F for 10 minutes was sufficient to eliminate the smoke. It was also believed that refrasil cloth contributed to contamination, therefore its use was discontinued.

The braze box containing 603FTB035-7A was placed in a furnace operating at 1400°F. After placement in the furnace the temperature controller was raised to 1650°F. At about 1500°F (furnace temperature) input was automatically reduced to 95 to 98%. As furnace temperature increased the furnace automatic controller decreased BTU input. To avoid a slowing down in the heat-up rate of the braze panel, BTU input was controlled manually to maintain 100%. Manual control was continued until the furnace reached 1645°F. At this temperature BTU input was cut to zero for three minutes then gradually increased to maintain 1650°F. The manual input control, coupled with the effect of the omitted insulation on top of the braze box, increased heat-up rate considerably as compared to previous braze runs with similar panels. (See Figure 5-46.) The braze time/temperature cycle for 603FTB035-7A is shown in the graphs in Figures 5-47 through 5-51. Thermocouple locations are the same as shown previously in Figures 5-11 and 5-37. The planned heating rate for 603FTB035-7A was 4°F per minute in the range between 1400°F and maximum braze temperature. A heating rate 3.8°F per minute was attained.



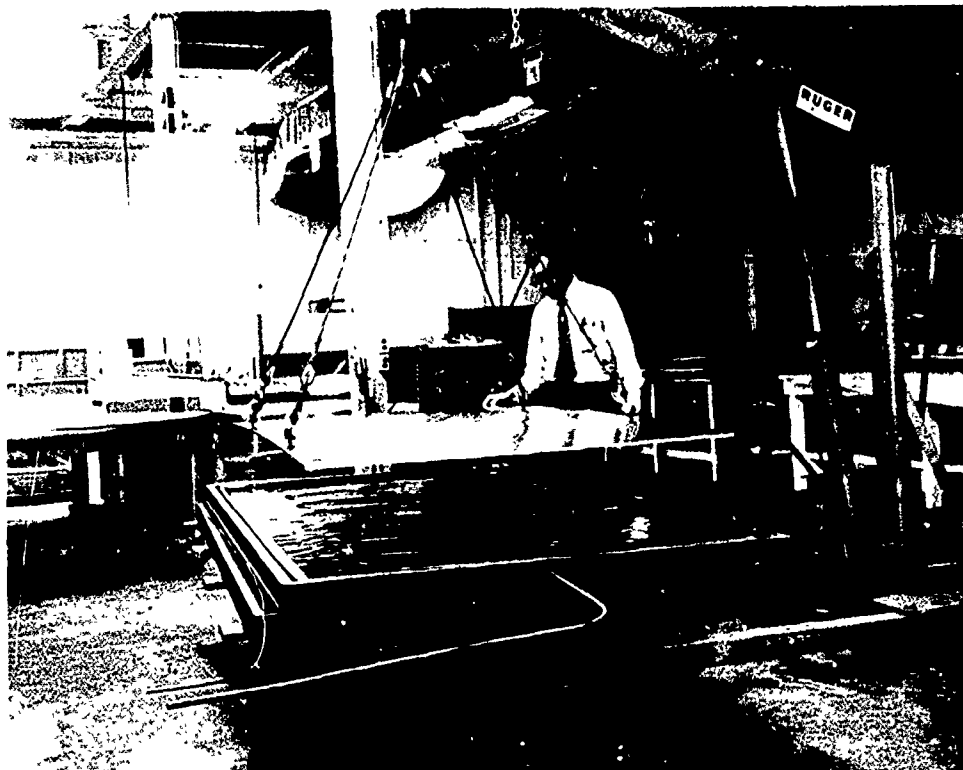
4-53802

Figure 5-38 UPPER TITANIUM DETAIL FOR 603FTB035-7A BRAZE TEST SPECIMEN IMMEDIATELY AFTER ACID CLEAN



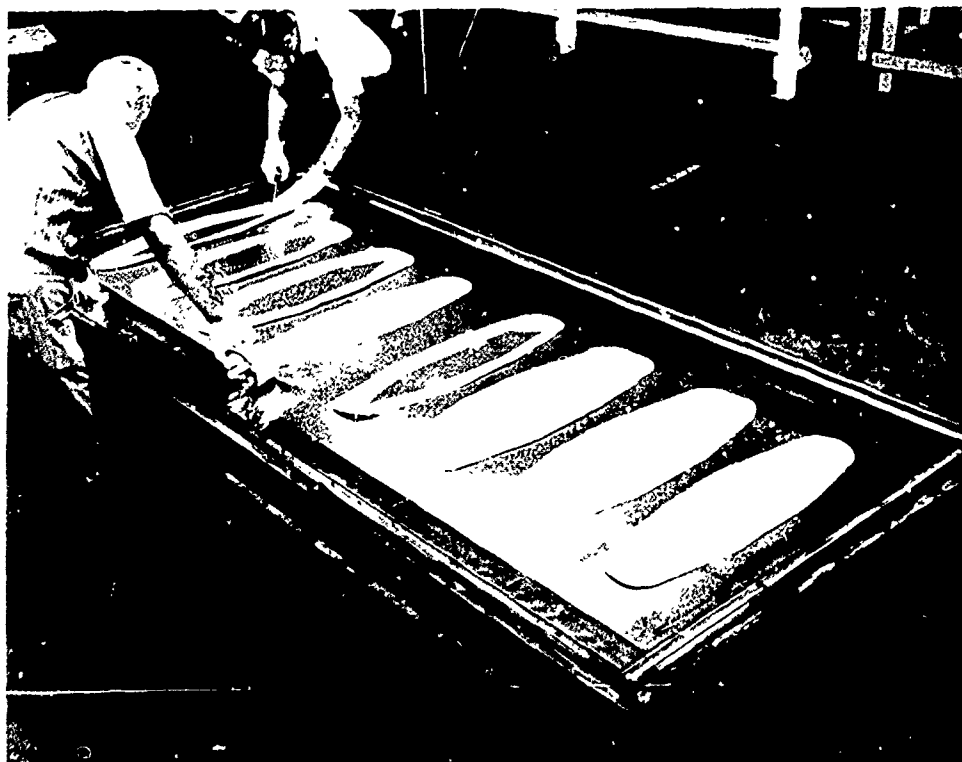
4-53794

Figure 5-39 LAY-UP OF BRAZE ALLOY ON LOWER PLATE OF 603FTB035-7A TEST SPECIMEN



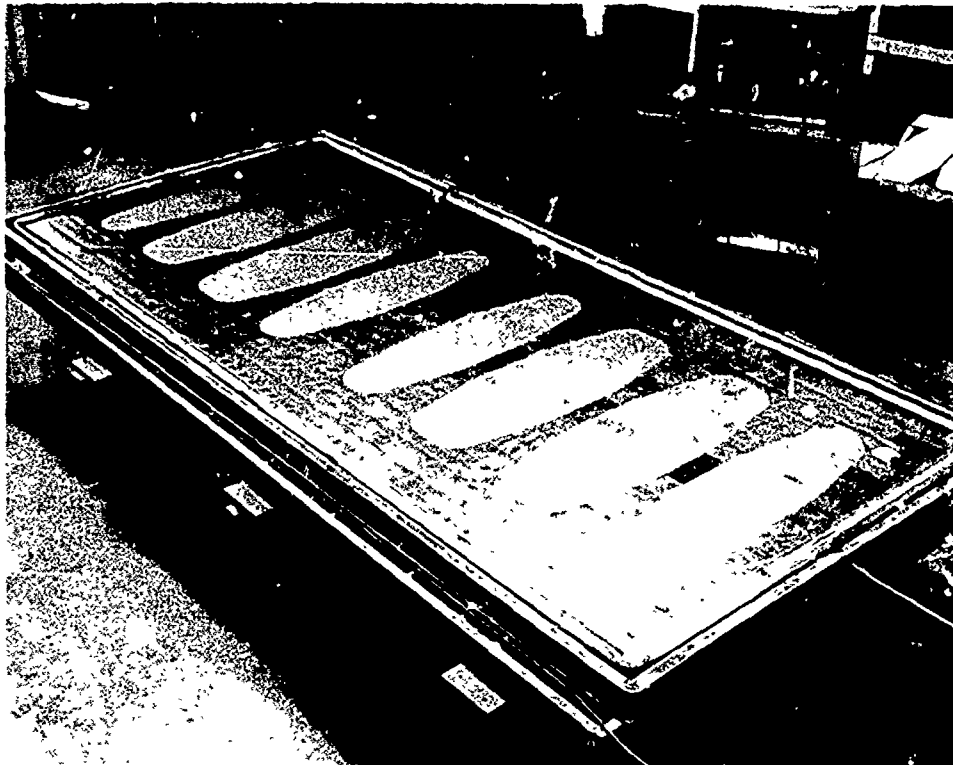
4-53793

Figure 5-40 PLACEMENT OF CENTER TITANIUM DETAIL AFTER LAY-UP OF BRAZE ALLOY ON LOWER TITANIUM DETAIL -603FTB035-7A



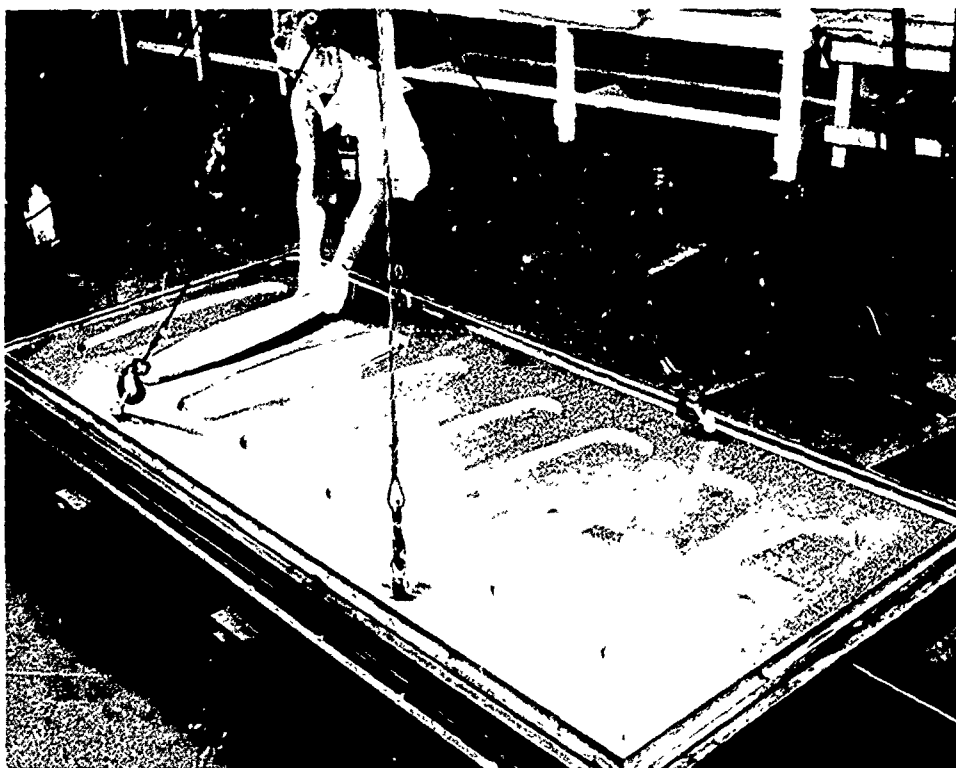
4-53807

Figure 5-41 LAY-UP OF BRAZE ALLOY ON UPPER SURFACE OF CENTER TITANIUM PLATE (TOP BRAZE LINE) FOR 603FTB035-7A



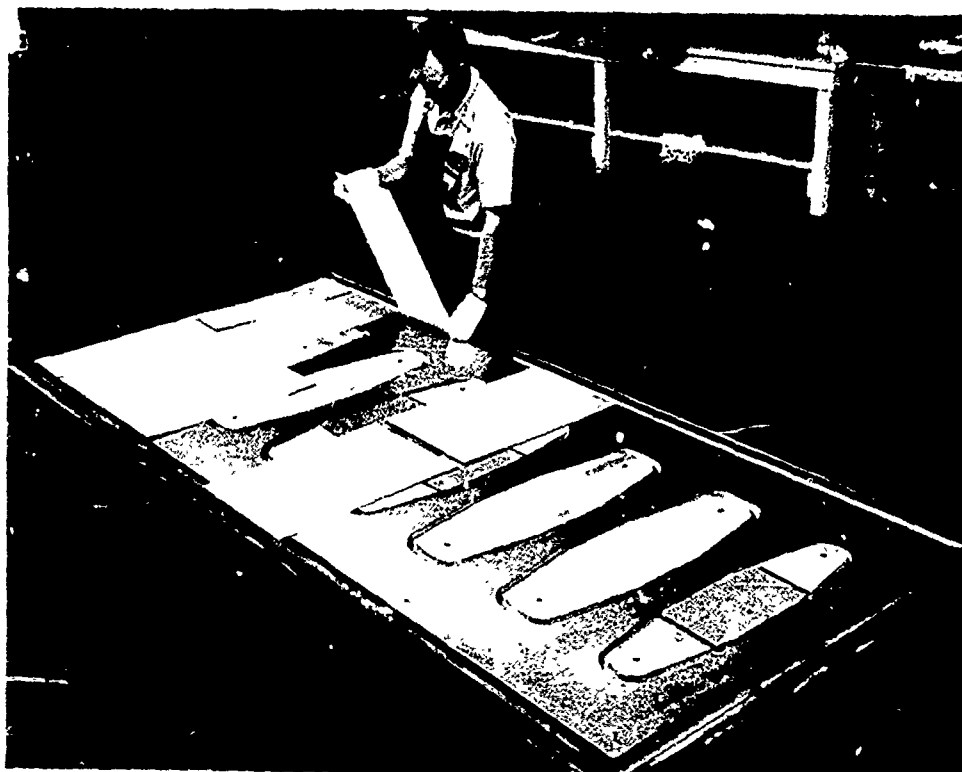
4-53805

Figure 5-42 FINAL ALLOY LAY-UP ON CENTER TITANIUM DETAIL
OF 603FTB035-7A



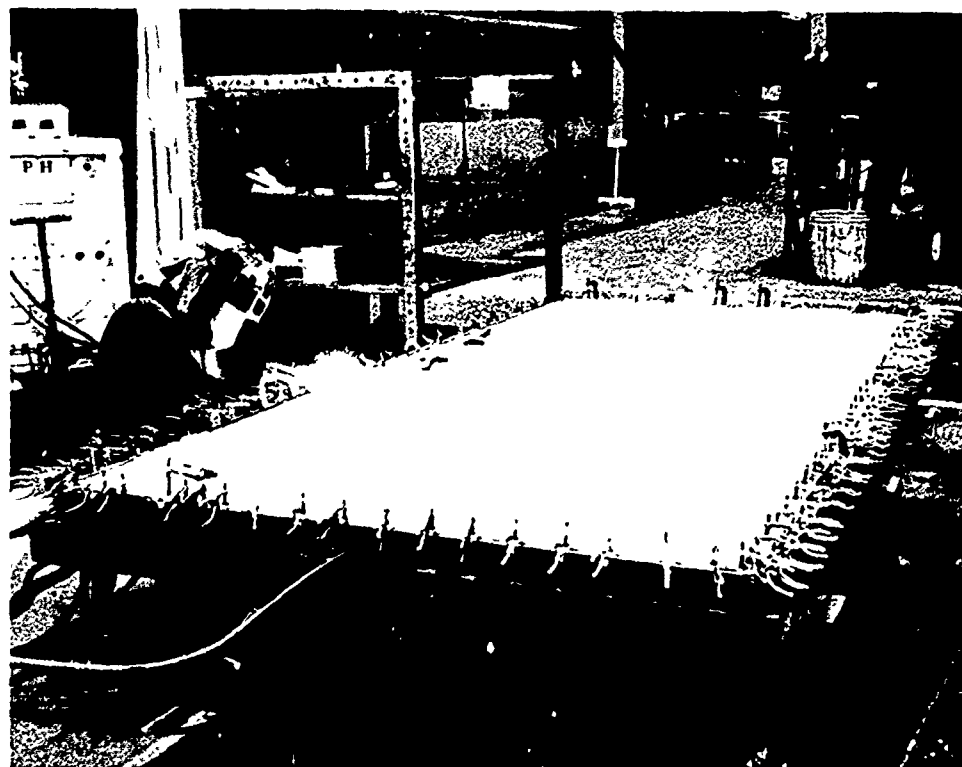
4-53806

Figure 5-43 INSERTION OF FILLER BLOCKS IN HOG-OUTS OF UPPER
TITANIUM DETAIL OF 603FTB035-7A



4-53804

Figure 5-44 PLACEMENT OF COVER SHEETS ON TOP OF LAID-UP ASSEMBLY OF 603FTB035-7A



4-53799

Figure 5-45 WELDING VACUUM SHEET ON BRAZE BOX RETORT FOR 603FTB035-7A

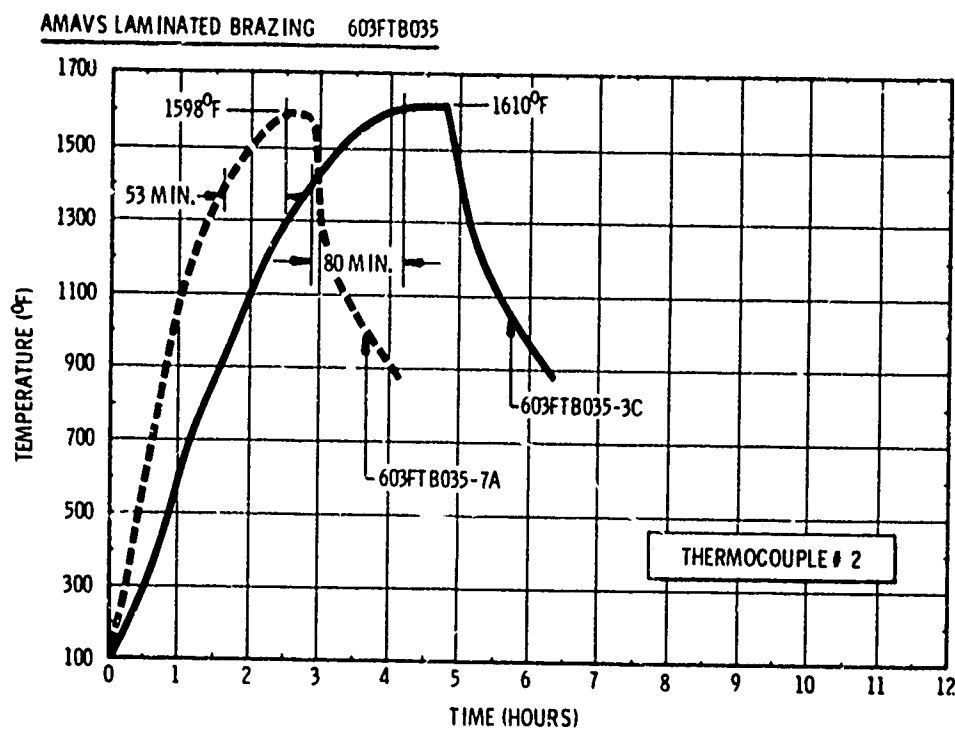


Figure 5-46 HEAT-UP RATE COMPARISON OF 603FTB035-3C AND -7A

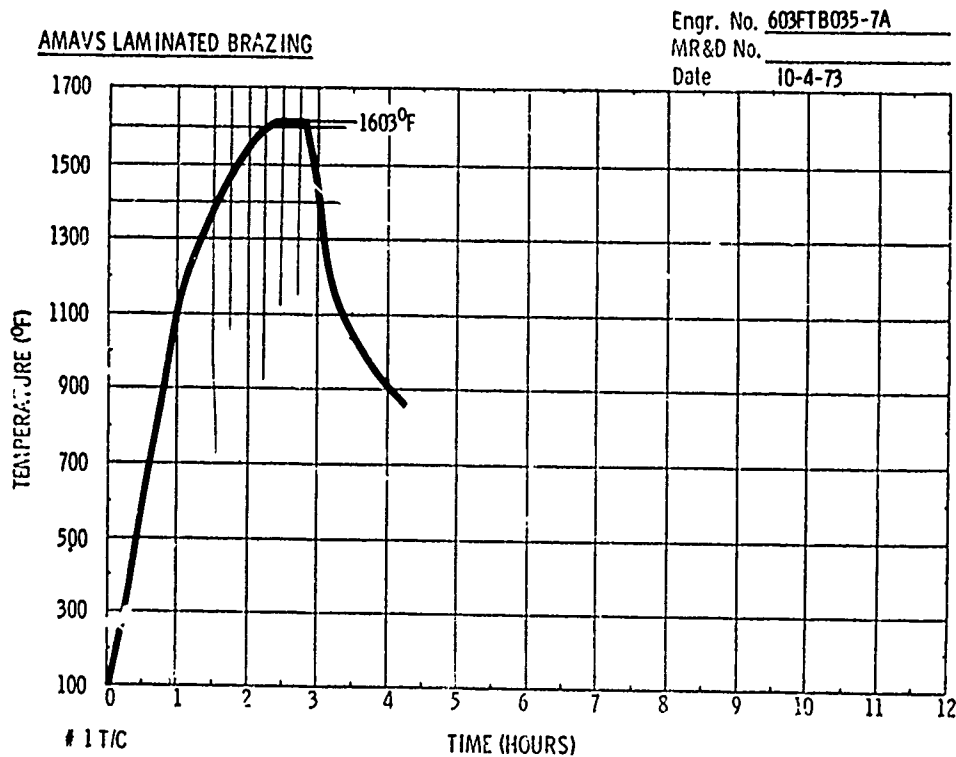


Figure 5-47 BRAZE CYCLE FOR 603FTB035-7A THERMOCOUPLE NO. 1

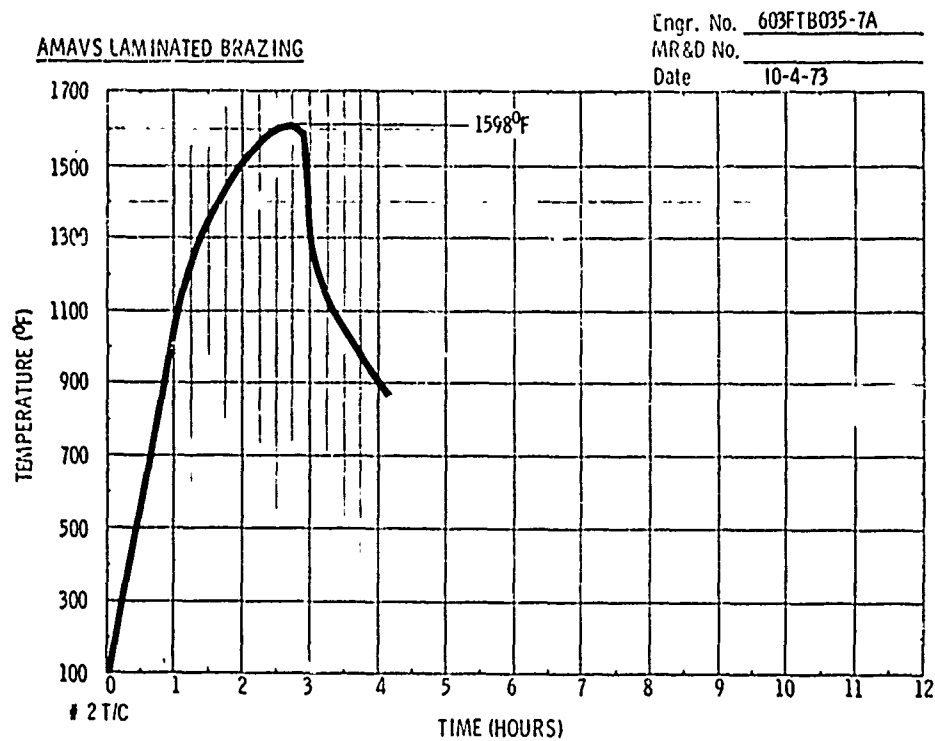


Figure 5-48 BRAZE CYCLE FOR 603FTB035-7A THERMOCOUPLE NO. 2

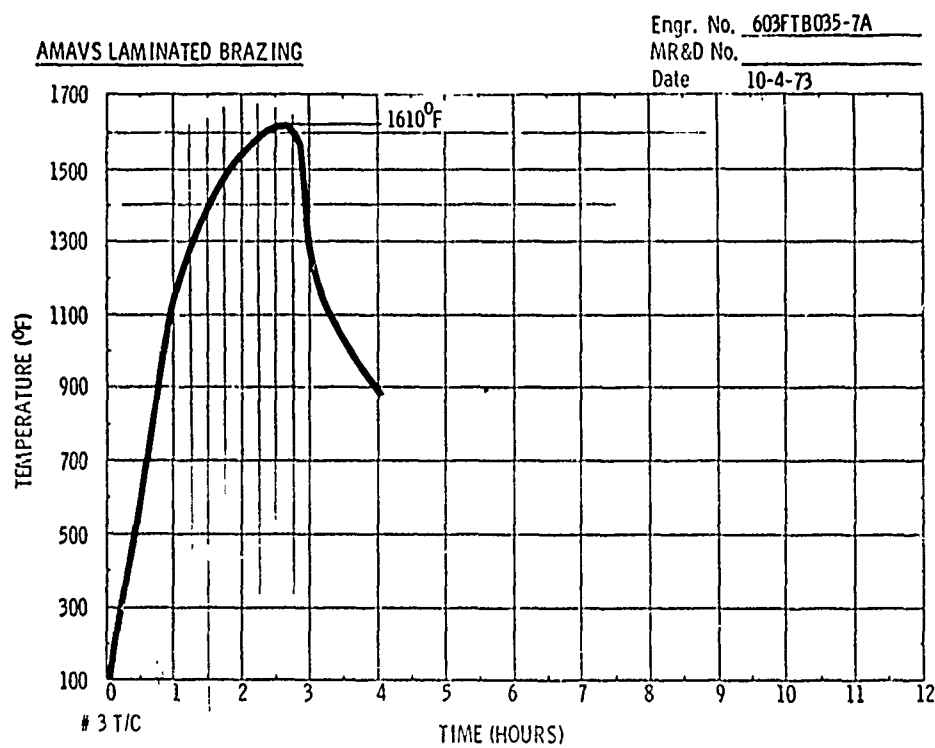


Figure 5-49 BRAZE CYCLE FOR 603FTB035-7A THERMOCOUPLE NO. 3

AMAVS LAMINATED BRAZING

Engr. No. 603FTB035-7A

MR&D No.

Date 10-4-73

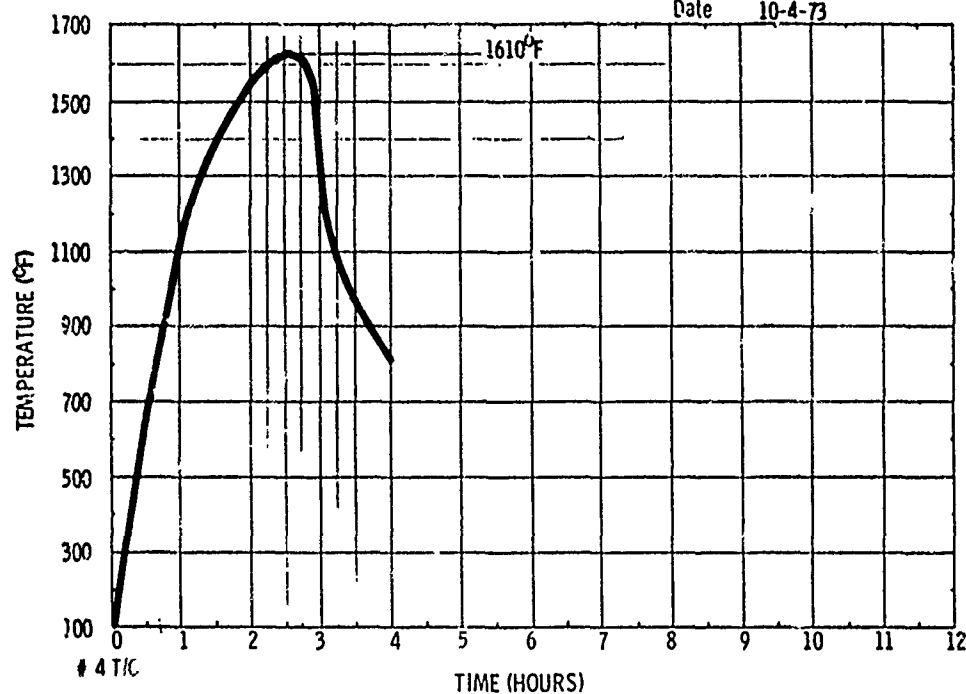


Figure 5-50 BRAZE CYCLE FOR 603FTB035-7A THERMOCOUPLE NO. 4

AMAVS LAMINATED BRAZING

Engr. No. 603FTB035-7A

MR&D No.

Date 10-4-73

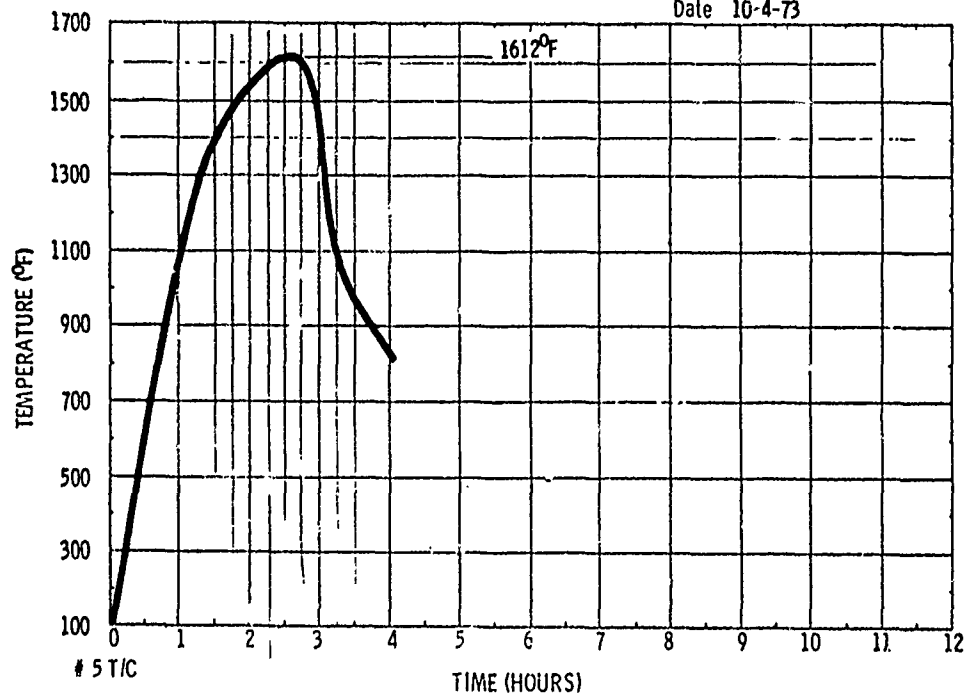


Figure 5-51 BRAZE CYCLE FOR 603FTB035-7A THERMOCOUPLE NO. 5

Visual inspection of the brazed part showed good filleting, alloy wetting, and flow in both braze lines around all exposed edges. There was little discoloration on the titanium details. Examples of alloy filleting and flow are shown in the photographs in Figures 5-52 and 5-53. The upper and lower surfaces of the brazed part are shown in the photographs in Figures 5-54 and 5-55.

Ultrasonic inspection showed narrow, intermittent light voids extending in the longitudinal direction the entire length of the part. It is believed that these voids resulted from longitudinal depressions in the braze surface of the titanium details. The titanium braze details for this part were finished for brazing by wet precision belt grinding after rough machining both surfaces. Previous inspection of the details after grinding had detected longitudinal depressions running the length of the part (see Figure 5-56). The most severe depressions had a maximum depth of 0.001-inch over a width of 1.5-inches. This condition was apparent in varying degrees in all three titanium details.

Braze Alloy Used in 603FTB035-3C and -7A

The braze alloy used in test parts 603FTB035-3C and -7A was an Ag-Al-Mn alloy supplied by Western Gold and Platinum Co. of Belmont, California. After receipt of the alloy liquidus-solidus tests were run to verify the compatibility of the alloy with the projected brazing temperature. Curves from which liquidus-solidus determinations were made are shown in Figures 5-57 and 5-58.

5.2 WIDE-AREA ADHESIVE BONDING

Large Beta C titanium adhesive bonded, metal laminate (3 and 4 ply) bulkhead panels were required for both the FSRL and "No Box" box designs.

Details for a typical bulkhead panel (Figure 5-59) were prepared to determine if machining cutouts, pockets and "finger strips" would cause distortion detrimental to bonding. In addition, a 1/8 x 36 x 40 inch sheet of Beta C titanium was chemically etched to evaluate this method of metal removal as an alternate to machining.



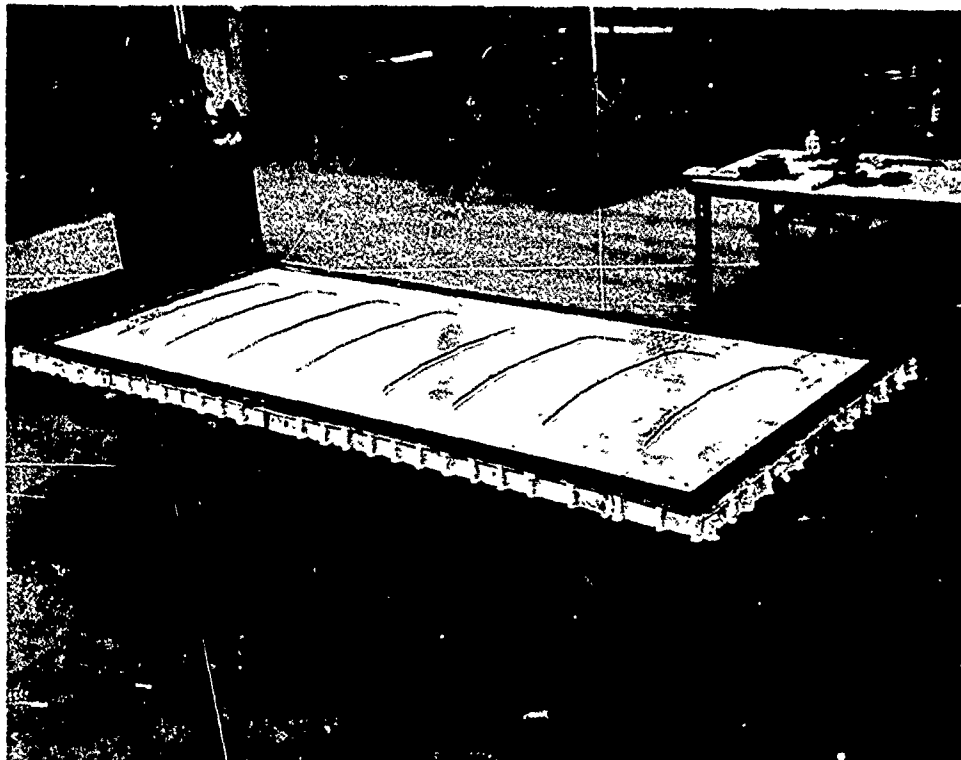
4-54298

Figure 5-52 UPPER PLATE SURFACE OF BRAZED 603FTB035-7A-
NOTE ALLOY FILLETING IN HOG-OUT AREA



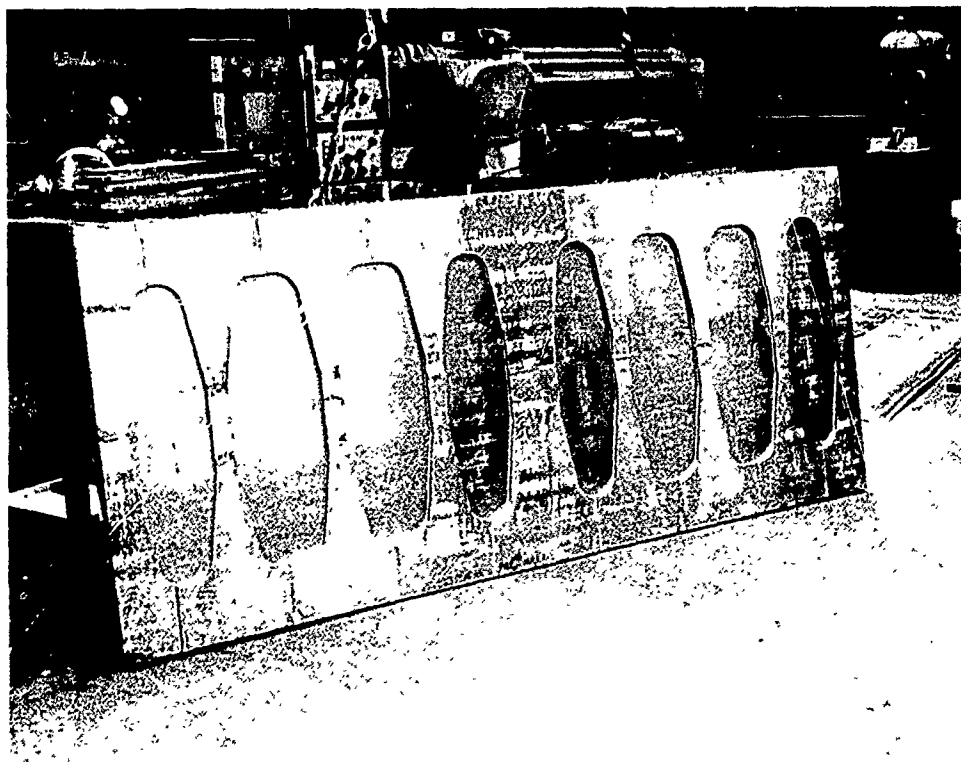
4-54299

Figure 5-53 LOWER PLATE SURFACE OF BRAZED 603FTB035-7A-
NOTE ALLOY FILLETING IN HOG-OUT AREA



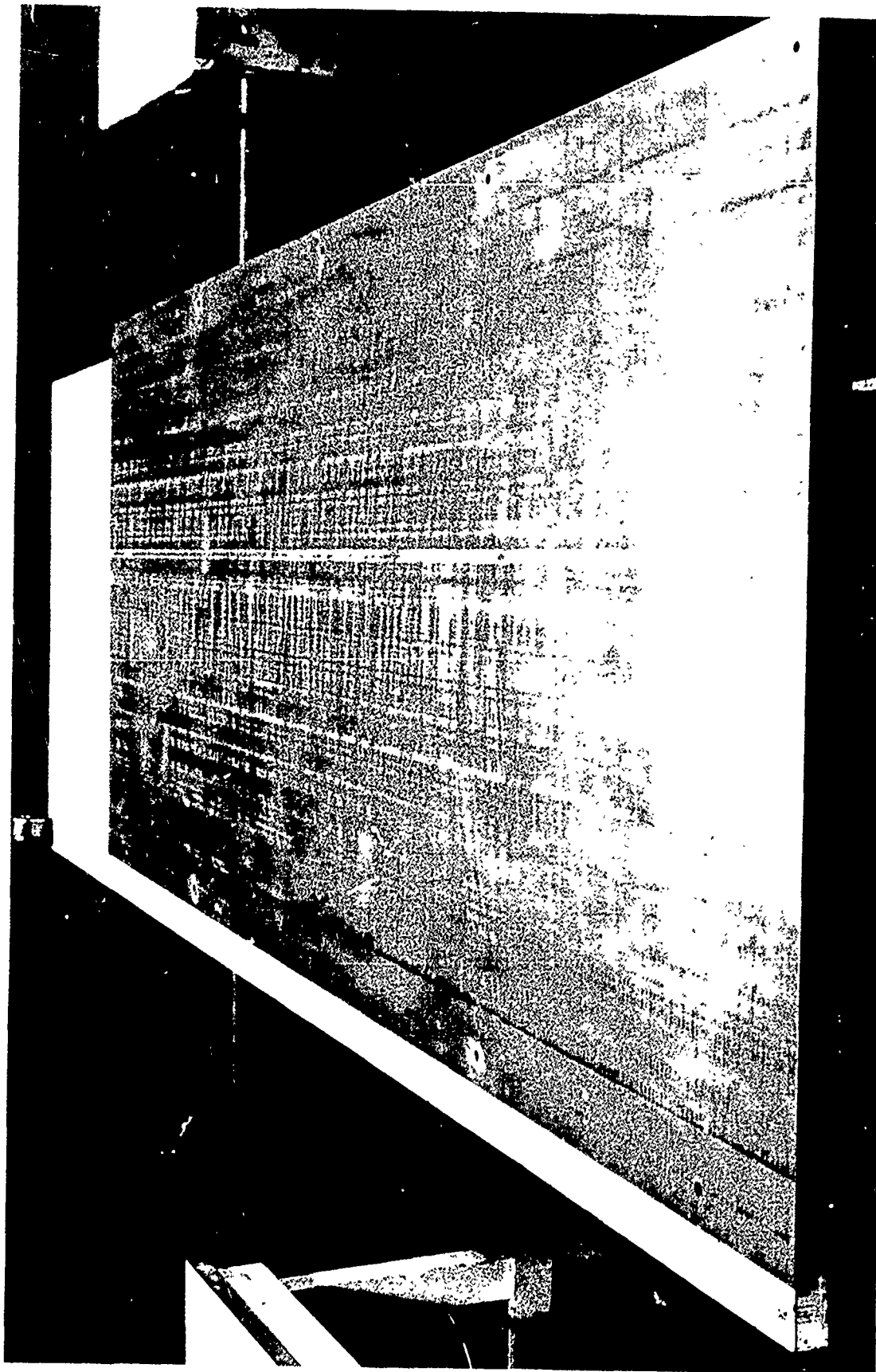
4-54302

Figure 5-54 BRAZED TEST SPECIMEN 603FTB035-7A READY FOR REMOVAL FROM BRAZE BOX (UPPER SURFACE)



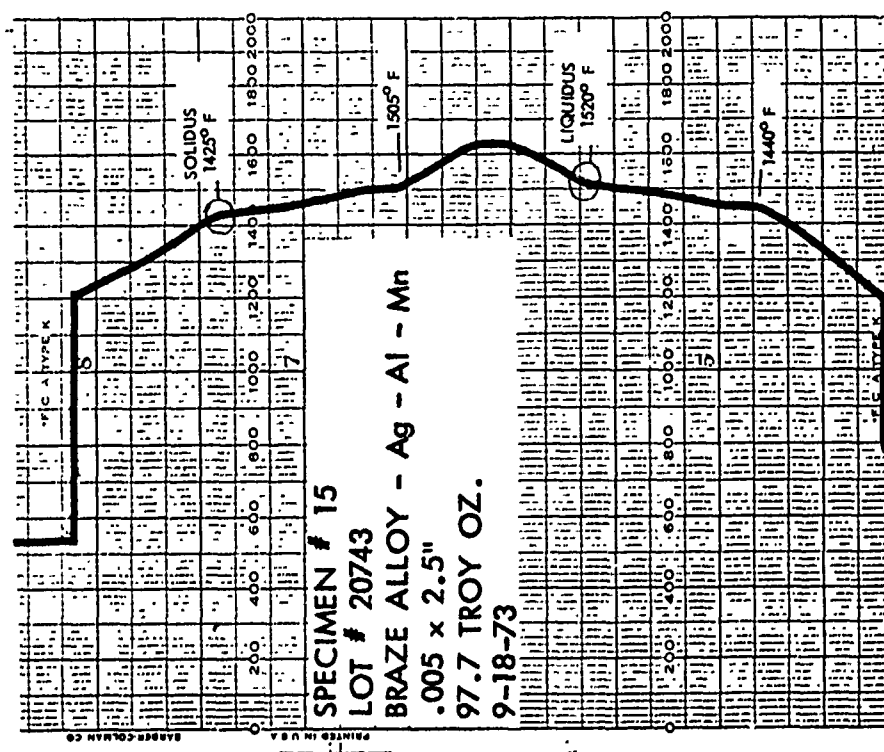
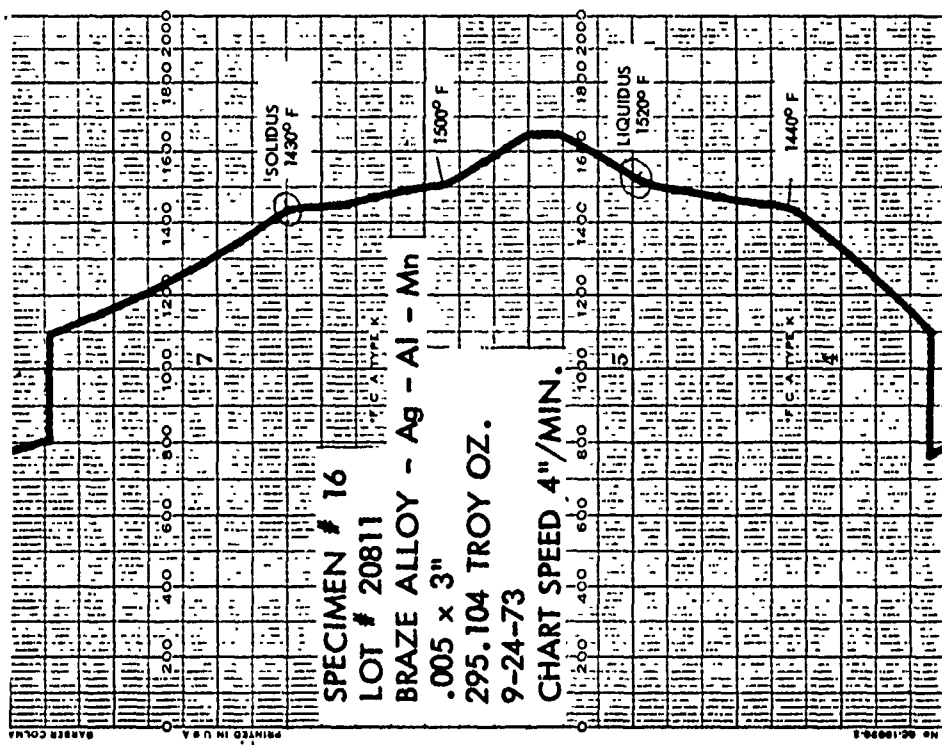
4-54300

Figure 5-55 LOWER SURFACE OF BRAZE TEST SPECIMEN 603FTB035-7A



4-50198

Figure 5-56 BRAZE SURFACE OF CENTER TITANIUM PLATE FOR
603FTB035-7A



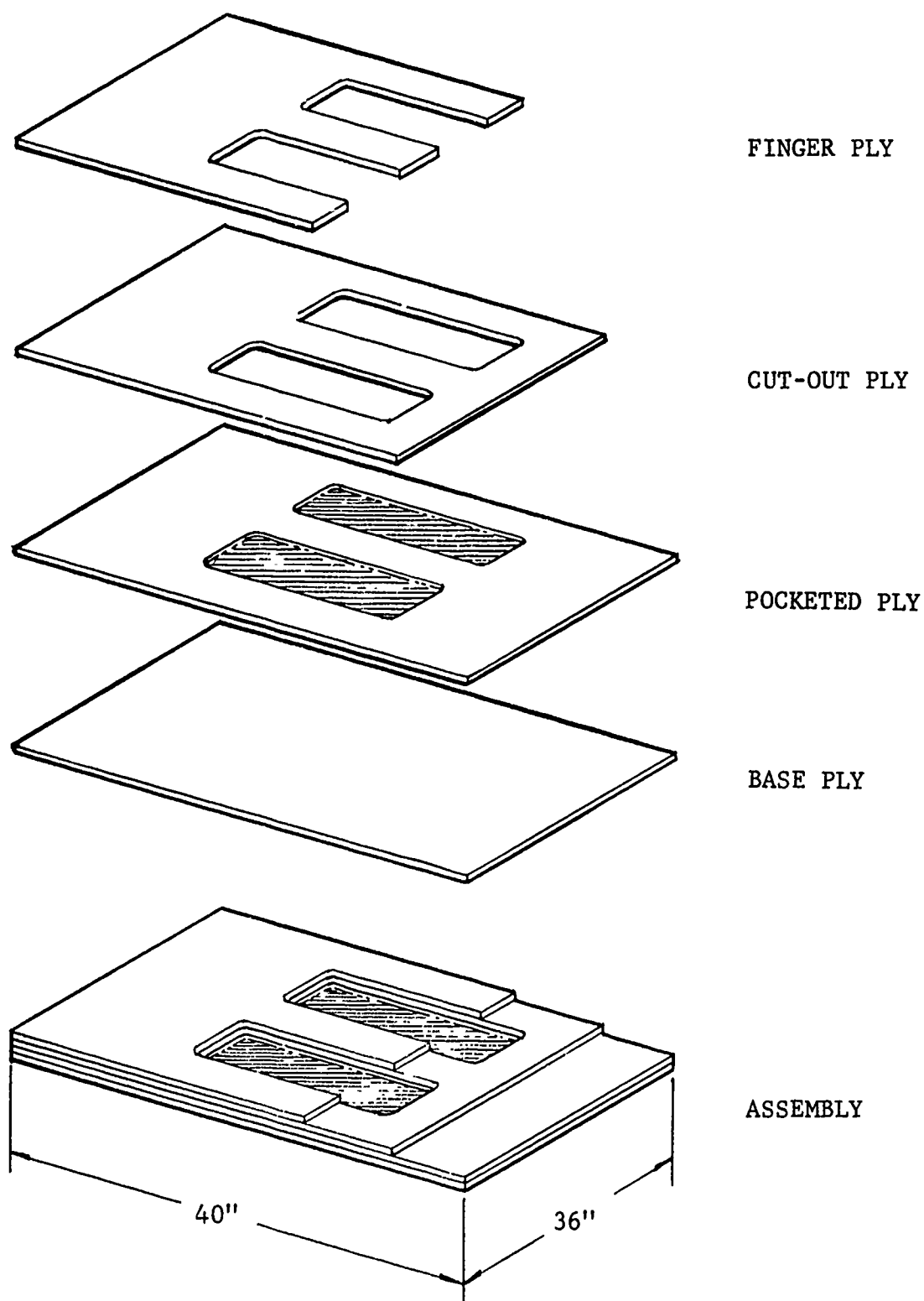


Figure 5-59 SIMULATED 4 PLY BULKHEAD PANEL (ADHESIVE BONDED BETA C TITANIUM)

Machining and bonding tests were not completed. Failure of the Beta C titanium to meet critical engineering requirements deleted the material from the carry-through structure design and the machining and bonding tests were terminated. However, the chemical etching test was completed and significant data obtained.

Pockets and cutouts were etched from the 1/8 inch Beta C titanium alloy sheet as shown in Figure 5-60. The pockets were approximately 0.060-in. deep. Etching operations drastically changed the sheet contour, making it unsuitable for bonding. Curvature greater than one inch occurred along the 40 inch sheet length as shown in Figure 5-61. In addition, the etched pocket areas "canned" 0.100 inch or greater, away from area where the material was removed. Figure 5-62 shows this distortion on the material side opposite of the etched pockets (areas that contact the straight edge).

Analysis of specimens taken from selected areas in the panel showed extremely high hydrogen pickup by the Beta C alloy from chemical etching.

<u>Area</u>	H ₂ (PPM)
No chemical etch	78
Edge etched	150
Bottom of pocket 1	534
Bottom of pocket 2	573

Chem etching thickness results are shown in Figure 5-63.

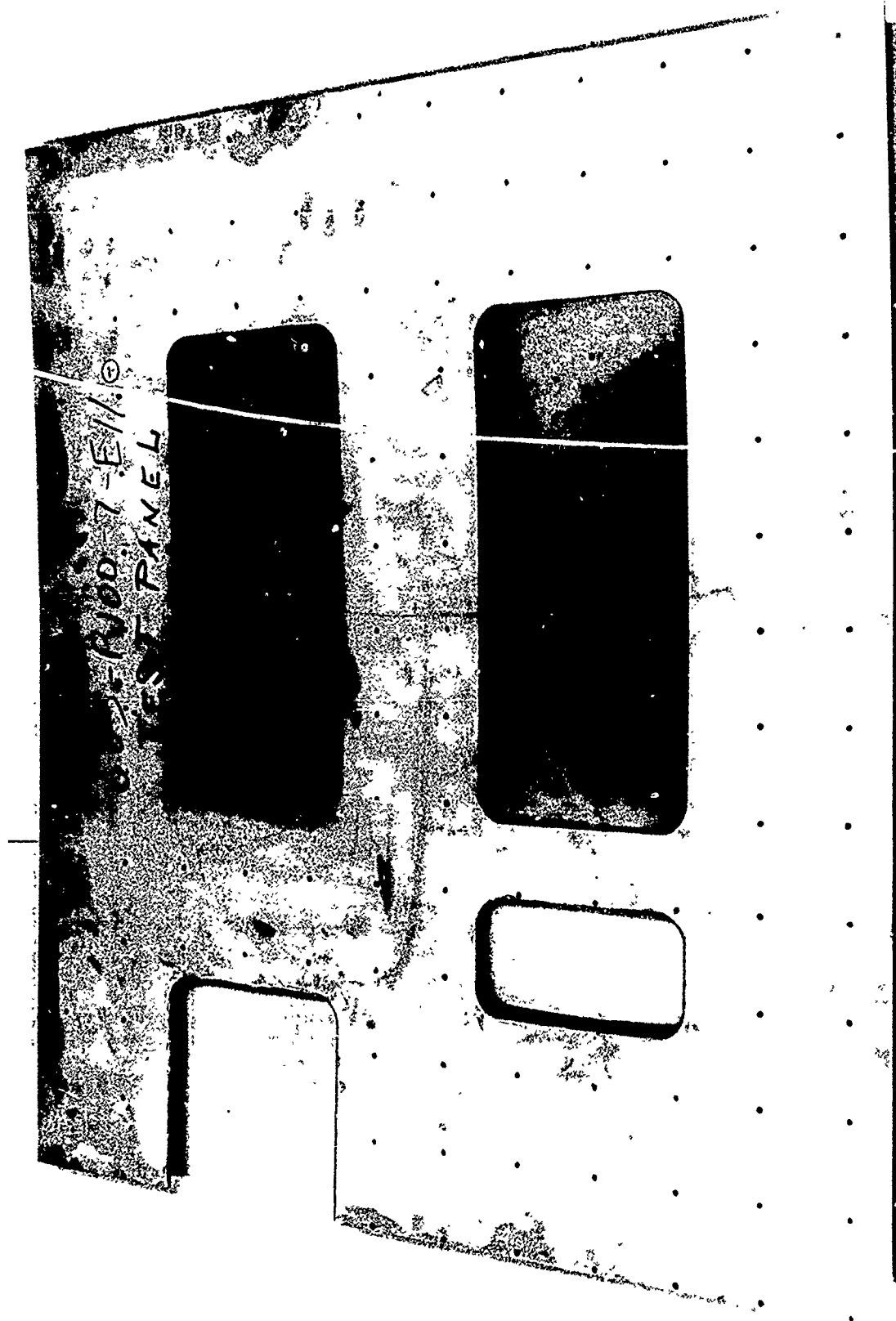
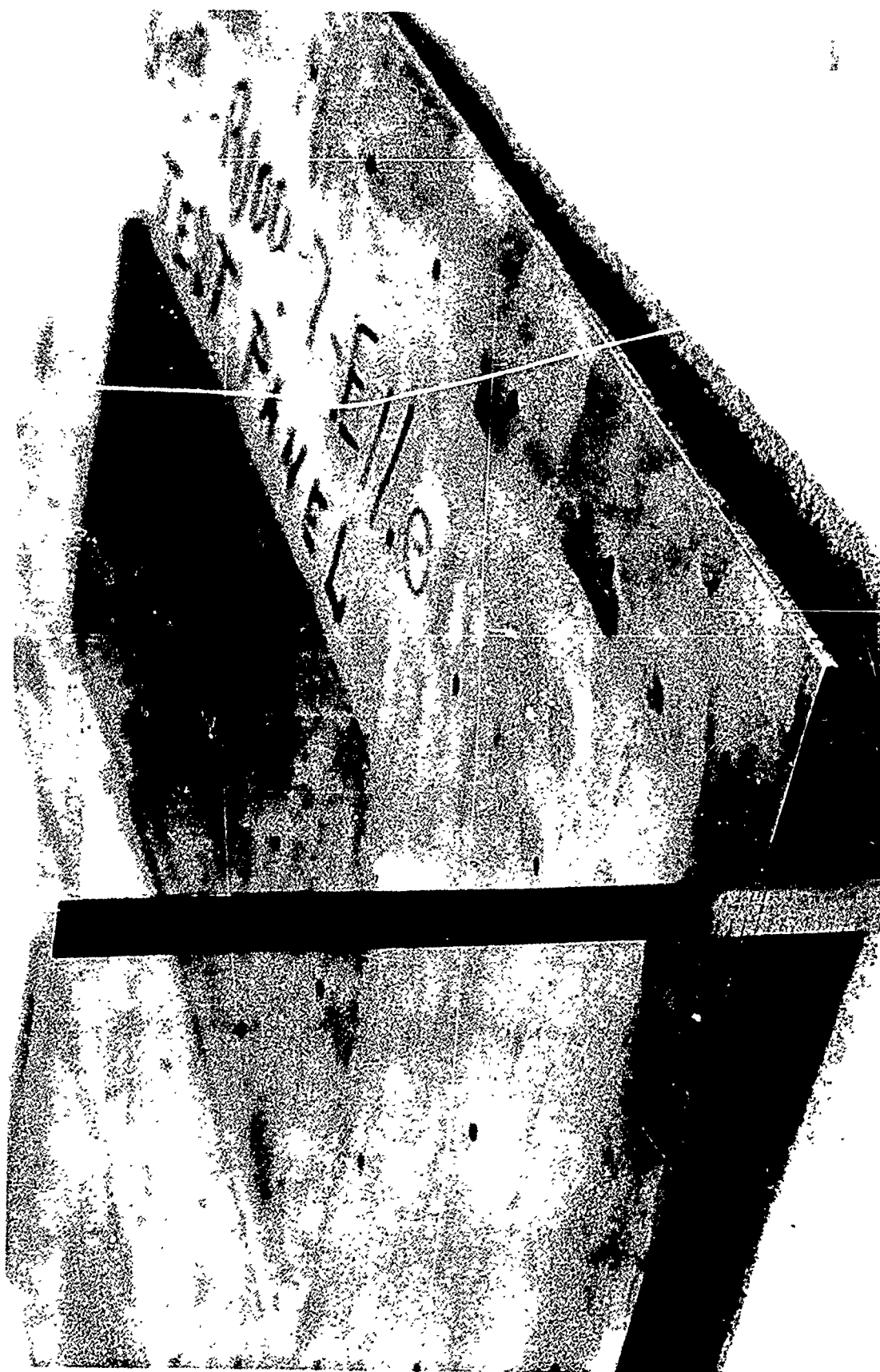


Figure 5-60 CHEMICALLY ETCHED TEST PANEL (1/8 X 36 X 40 IN)
BETA C TITANIUM)



4-5303

Figure 5-61 OVERALL WARPAGE OF 1/8 INCH BETA C TEST PANEL
FROM CHEMICAL ETCHING



Figure 5-62 WARPAGE RESULTING FROM CHEMICAL ETCHING .060 INCH
DEEP POCKETS IN 1/8 INCH BETA C TITANIUM

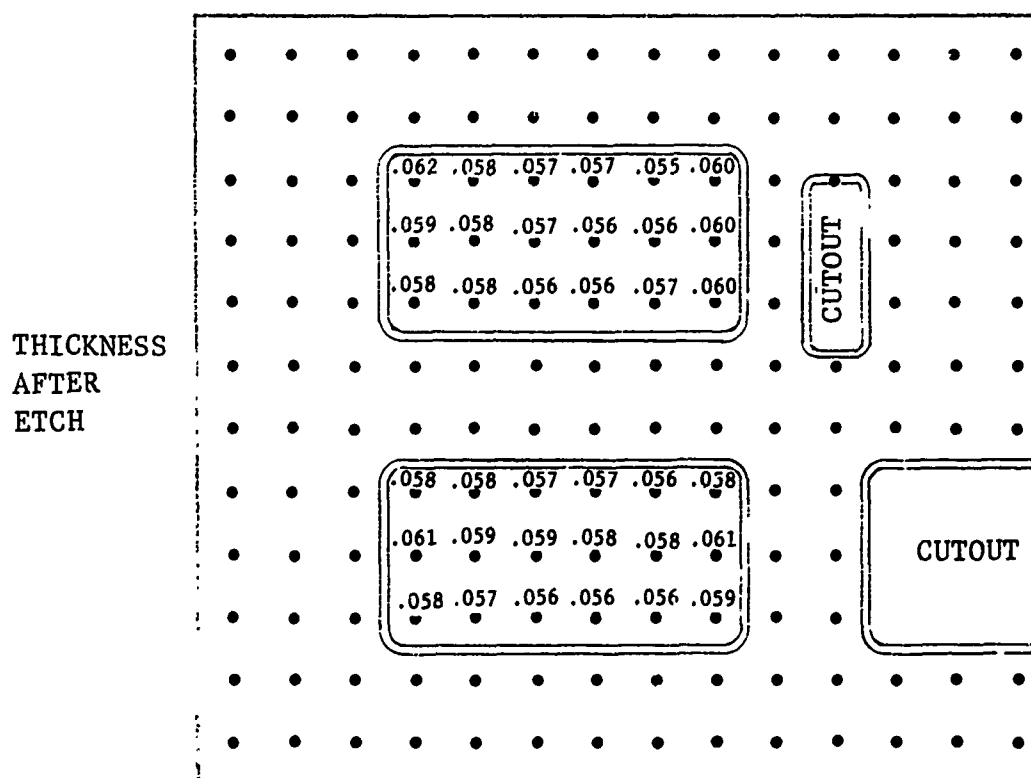
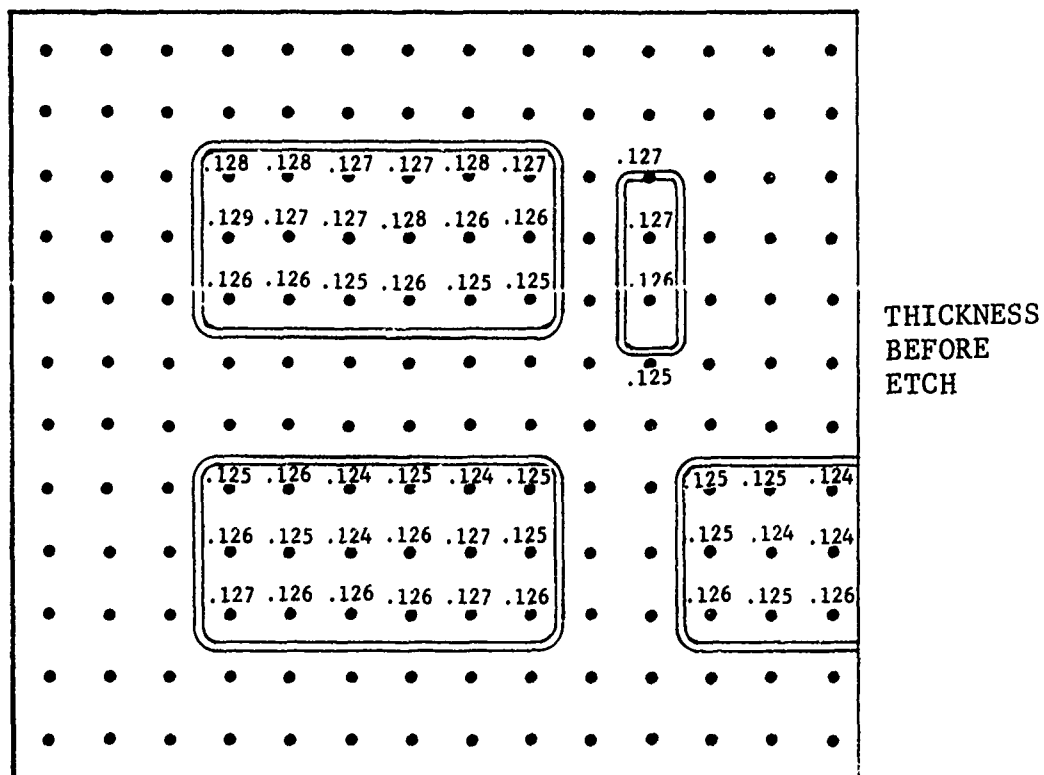


Figure 5-63 THICKNESS MEASUREMENTS BEFORE AND AFTER CHEMICAL ETCHING OF BETA C TITANIUM SHEET

5.3 WELDING 10 NI STEEL

The NBB configuration includes several 10 Ni steel welded joints in relatively thick material. An industry survey disclosed very limited information on gas tungsten arc (GTA) welding of 10 Ni steel, and no data on electron beam (EB) welding. Development programs were initiated to provide the necessary data on both processes.

5.3.1 Electron Beam Welding

The objectives of the EB weld program were to establish capability and process limitations for joining various thicknesses of 10 Ni (HY-180) steel.

Requirements for EB butt welds on the NBB design were originally in 0.375, 0.90 and 2.10-inch thick 10 Ni steel. Subsequent design refinements changed the maximum section thickness to 1.6 inches. EB weld parameters were successfully developed for 0.50-inch thick 10 Ni steel and consistently good welds produced. Efforts to EB weld 1.6-inch thick 10 Ni were unsuccessful. Defect free welds could not be consistently made with the limited available material. This does not mean that thick sections of 10 Ni steel cannot be EB welded, however, considerable time and material will be required to achieve consistent, good quality welds on 1.0-inch and thicker material.

5.3.1.1 Development of Weld Parameters for Thick 10 Ni Material (1.0 and 1.6 inch)

Based on previous EB welding experience with other materials, the ideal EB weld nugget is parallel-sided with a uniform crown on the face of the weld. Full (100%) penetration welds should have a uniform root, the width of which is dependent on the welding parameters and material heat transfer characteristics.

In EB welding thick sections of material, the face and root surface condition is dependent upon surface tension supporting the column of molten metal as the weld is being made. Insufficient surface allowed the 10 Ni material to flow and form an extremely heavy globular underbead (Figure 5-64) when welding speed was decreased or beam power increased to get full penetration. The sag of these globules caused a severe underfill on the face of the weld and even with added filler metal, produced gross internal voids as shown by the longitudinal X-ray in Figure 5-65.

Weld parameter adjustments to eliminate this condition consisted of a careful increase in speed to reduce the time at melting temperature or a reduction of beam current density. Balance of the welding parameters became more sensitive as the material thickness increased. The effect of small changes is illustrated in Figure 5-64 where a change of 2 inches per minute weld speed drastically altered the weld root shape.



UNIFORM-
PENETRATION

GLOBULAR-
PENETRATION

Figure 5-64 EB WELD ROOT OF 1.6 INCH THICK 10 Ni STEEL
SHOWING GLOBULAR AND UNIFORM PENETRATION

4-54719

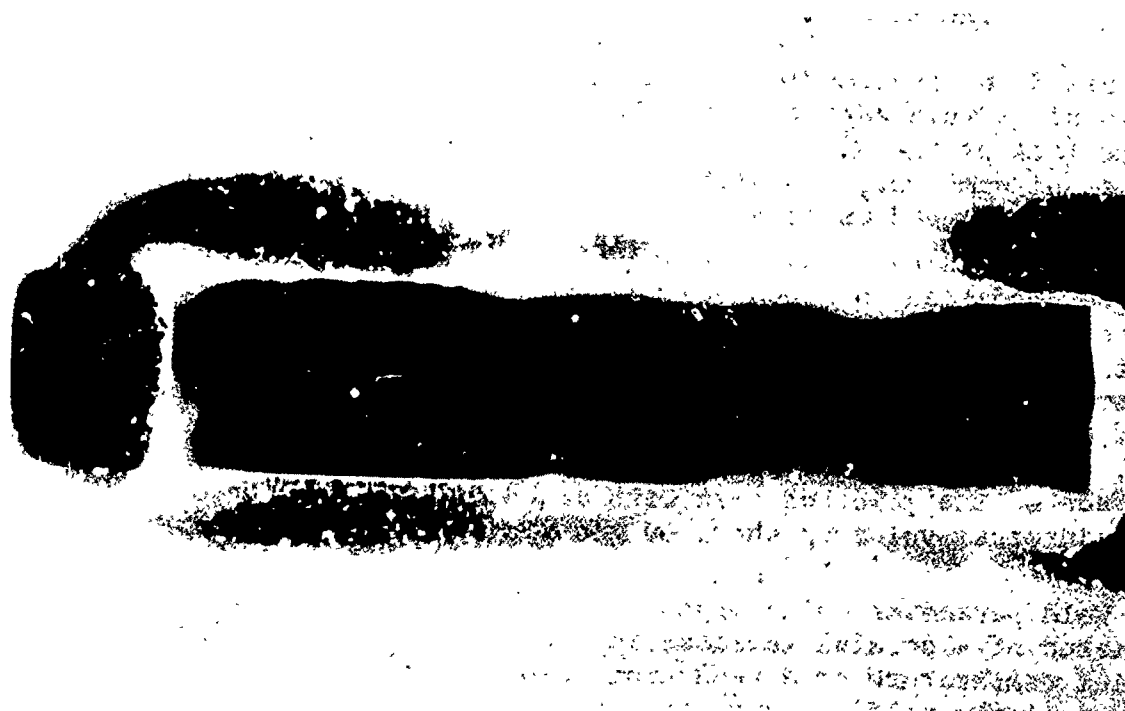


Figure 5-65 X-RAY OF WELD SPECIMEN FROM FIGURE 5-64
SHOWING VOIDS AND MICROFISSURES

The longitudinal X ray (Ref. Figure 5-65) of this particular weld shows voids above the globules and micro fissures above the uniform root. The microfissures shown are typical for thick section EB welds on low alloy steels. In many cases, they are impossible to detect by conventional X-ray techniques because of the small size and location. However, ultrasonics was successfully used to inspect EB welds on 10 Ni in the "as welded" condition after the weld reinforcement was removed. Ultrasonic inspection results were verified by macro section and longitudinal section X ray.

Beam Focus

Heat input for electron beam welding is controlled by four basic parameters; voltage, beam current, weld travel speed and the diameter of the beam at the surface or within the workpiece. This beam crossover point location is usually referred to as face, midpoint or root focus and simply indicates the point of maximum beam current density. The work accomplished to date indicates that very close control of the beam focal point and its resulting weld profile is extremely important in obtaining sound EB welds in 10 Ni steel.

Initial bead-on-plate studies on 2.0-inch thick 10 Ni consisted of determining the effect of the focal point on the weld geometry. Midpoint focus resulted in the best weld cross section geometry. However, the parallel side weld geometry obtained with 0.500-inch thick material (Figure 5-66), was not obtained on the thicker sections. Macro sections of 1.6-inch thick welds shown in Figure 5-67 (A, B and C) are typical examples of microfissures that occurred in the center of non-parallel sided welds. This indicates that solidification occurred last in that area, forming a crack when the relatively weak hot metal attempted to contract and pull the adjacent strong cold metal with it. Figure 5-67 (D) shows a defect free macrosection.

Beam Oscillation

Beam oscillation is sufficient to produce parallel-sided weld geometry on thinner sections, such as the 0.500-inch thick weld shown in Figure-5-68. Attempts to spread the weld with beam oscillation in the thicker sections were unsuccessful.

Multipass Welding

Welds were made using both single and multipass techniques, but no appreciable difference could be noted on the weld quality.

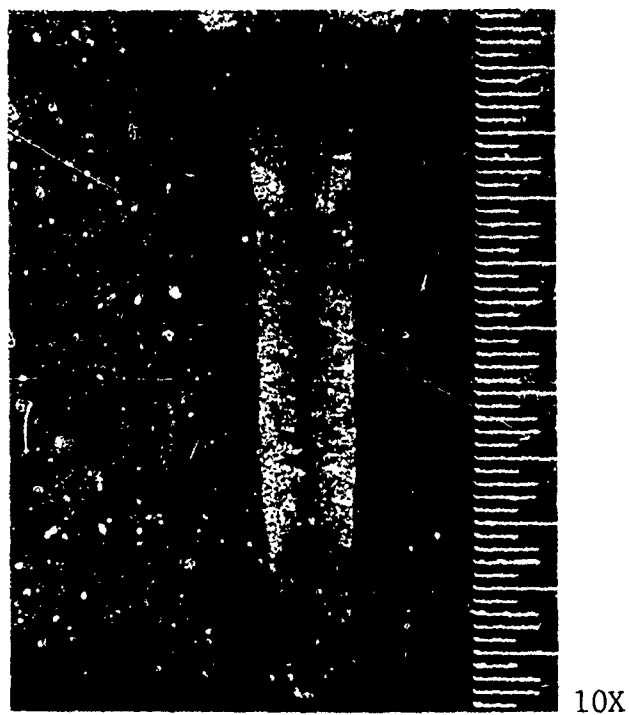
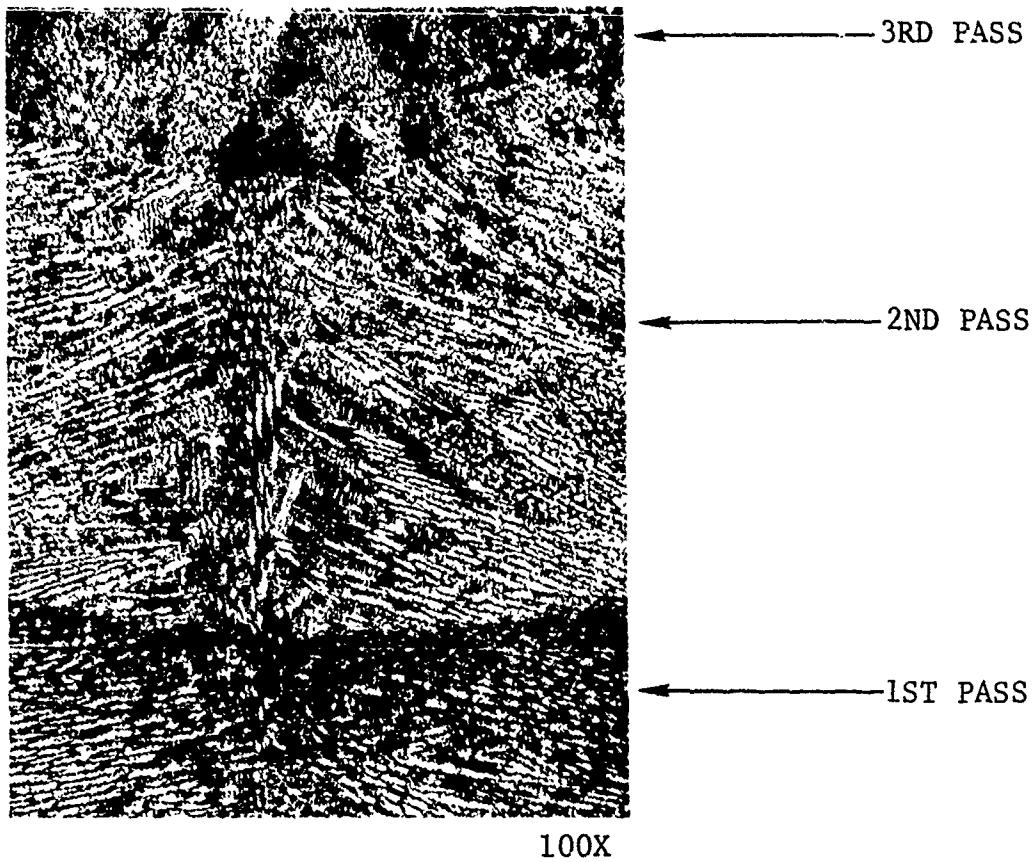
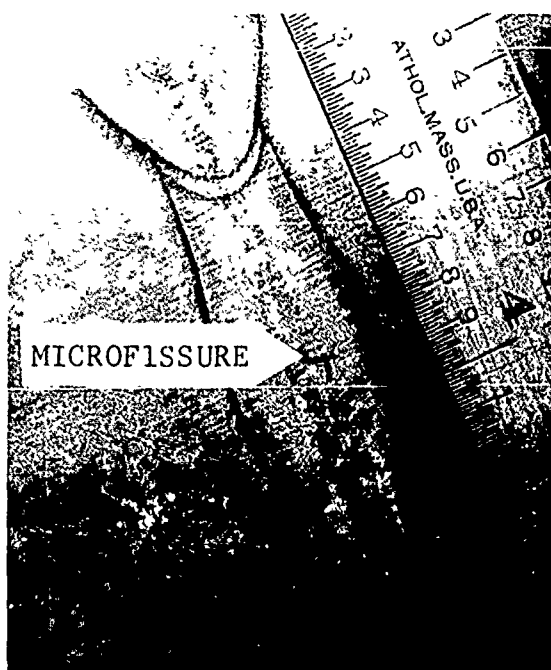
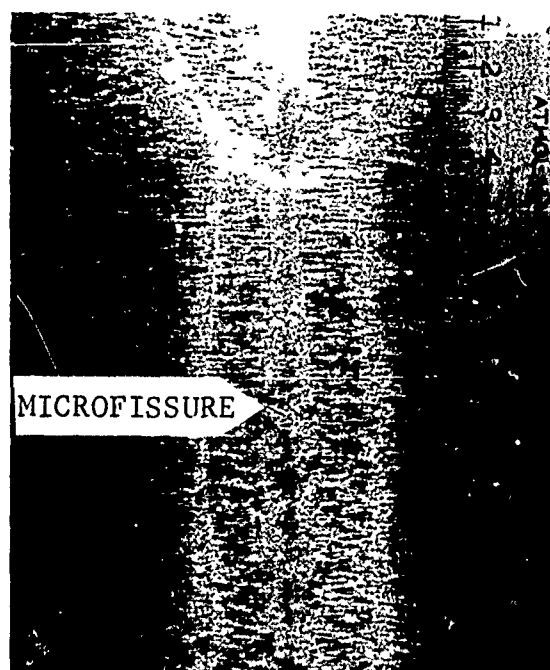


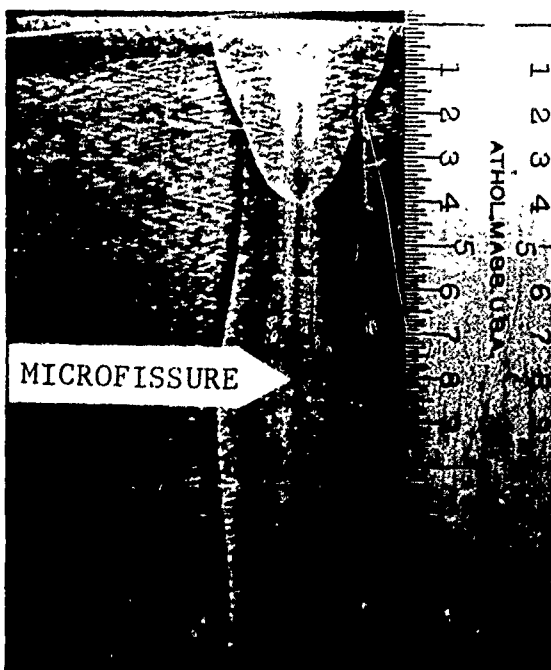
Figure 5-66 MACRO AND MICRO STRUCTURE OF EB WELDED .500 INCH THICK 10 Ni STEEL (WELD NO. H10)



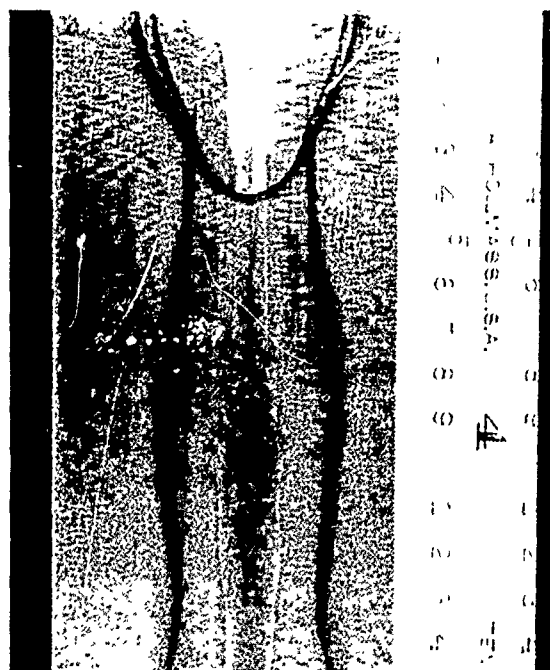
A - DEFECTIVE WELD



B - DEFECTIVE WELD



C - DEFECTIVE WELD



D - GOOD WELD

Figure 5-67 MACROS OF EB WELDS ON 1.61 INCH THICK 10 Ni STEEL SHOWING TYPICAL MICROFISSURES AND GOOD WELD

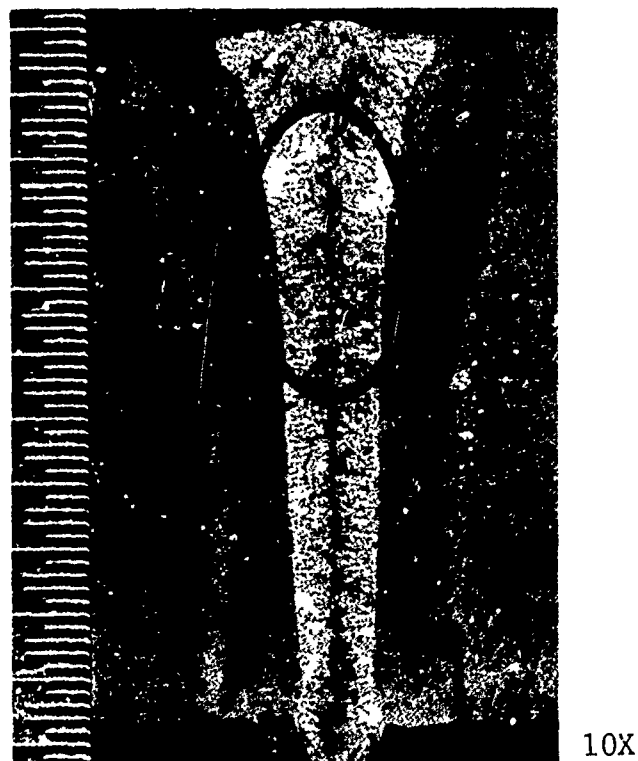
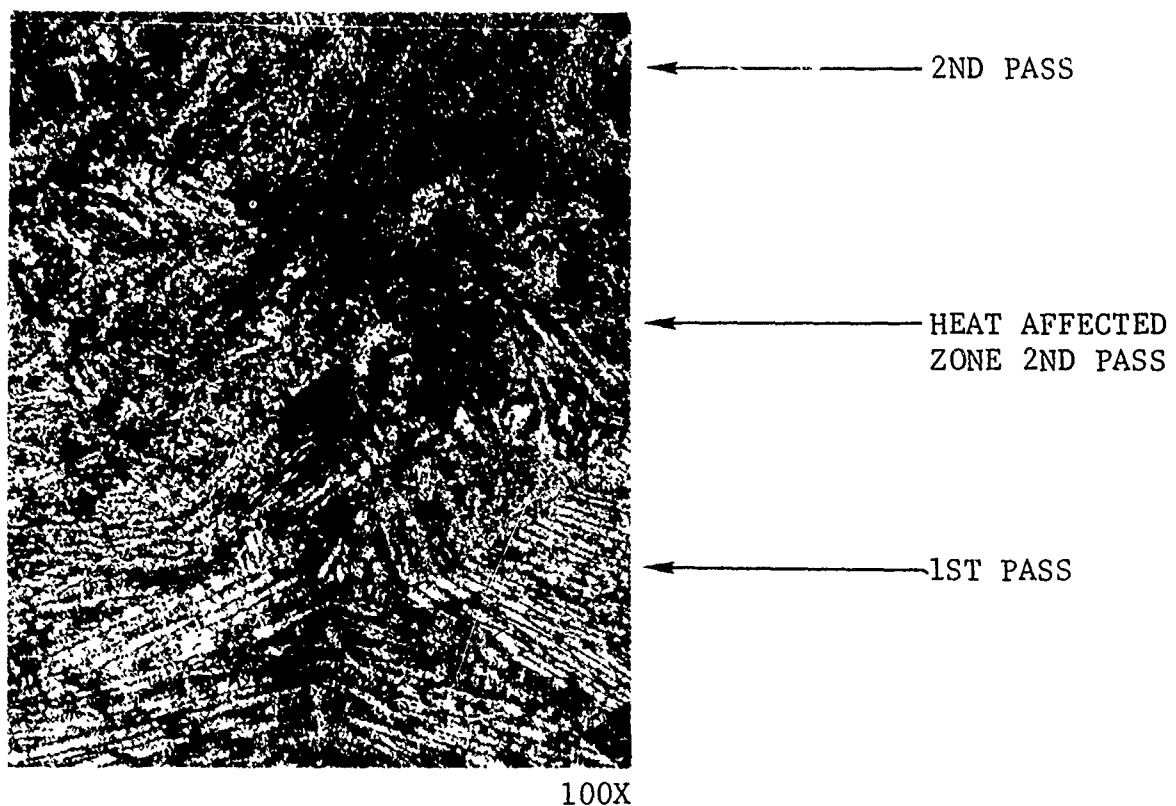


Figure 5-68 MACRO AND MICRO STRUCTURE OF EB WELDED .500
INCH THICK 10 Ni STEEL (WELD NO. H11)

It is significant that defects found in the cross-section macros could not be attributed to the multipass technique since defects are not near the root of the filler pass.

Filler Wire

Welds were made with and without filler wire to study the effects of added filler metal. The results of several bead-on-plate welds with added filler did not solve the cracking problems but did increase the gap allowance from ± 0.005 inch to ± 0.020 inch. Machine cleanup of both face and root beads was also reduced from 0.090 inch per surface to less than 0.030 inch per surface by using filler wire.

Weld Shrinkage

Transverse shrinkage measurements were made across two 1.6-inch thick welds and are shown in Table V-1. These measurements were made on 15-inch long welds to represent conditions that would be found in full scale parts. The shrinkage was small and uniform, indicating very little movement in the transverse plane.

Backup Plates

A backup plate of the same material is used for EB welding thick sections when the root geometry cannot be controlled by adjusting weld parameters. Backup plates have been used successfully on materials that are not producers of high vapor pressures. In the case of 10 Ni steel, the backup plates acted as a thermal barrier and vapor trap instead of supporting the molten metal column. This condition caused the molten steel to boil and form an uncontrollable weld puddle. Metal expulsion, in the form of splatter and a heavily ionized vapor column back streaming into the EB gun, caused high voltage discharges or arc outs. Weld root porosity resulted from the use of backup plates and no satisfactory welds could be made.

5.3.1.2 EB Welding of 0.500-Inch Thick 10 Ni Steel

Engineering design on the main landing gear drag fitting (common to both WCT designs) requires EB welds on 0.375, 0.400 and 0.500-inch thick 10 Ni steel.

A limited number of 0.500-inch thick welds were made to determine joint efficiency, weld shrinkage and inspection methods. Weld shrinkage on 0.500-inch thick welds is shown in Table V-2

Table V-1 TRANSVERSE SHRINKAGE OF ELECTRON BEAM
WELDS WITH 1.6 INCH THICK 10 Ni STEEL

Location	SPECIMEN WIDTH (INCHES)		Transverse Shrinkage	
	Before Welding	After Welding		
1	5.970	5.956	.014"	Weld No. H-28 Average weld shrinkage .0015"
2	5.970	5.956	.014	
3	5.970	5.955	.015	
4	5.970	5.955	.015	
5	5.970	5.955	.015	
6	5.970	5.955	.015	
7	5.970	5.955	.015	
8	5.970	5.955	.015	
9	5.971	5.955	.016	
10	5.970	5.955	.015	
11	5.971	5.955	.016	
12	5.971	5.955	.016	
13	5.971	5.915	.016	
14	5.971	5.955	.016	
15	5.970	5.956	.014	
16	5.971	5.957	.014	
<hr/>				
1	5.998"	5.982"	.016"	Weld No. H-29 Average weld shrinkage .0016"
2	5.998	5.591	.017	
3	5.997	5.980	.017	
4	5.997	5.979	.018	
5	5.998	5.980	.018	
6	5.998	5.980	.018	
7	5.998	5.980	.018	
8	5.998	5.980	.018	
9	5.998	5.980	.018	
10	5.998	5.981	.017	
11	5.998	5.981	.017	
12	5.998	5.981	.017	
13	5.998	5.982	.016	
14	5.998	5.982	.016	
15	5.998	5.983	.015	
16	5.998	5.984	.014	

All measurements taken at 1 inch spacing.

Table V-2 TRANSVERSE SHRINKAGE OF ELECTRON BEAM
WELDS WITH .500 INCH THICK 10 Ni STEEL

SPECIMEN WIDTH (INCHES)				
Location	Before Welding	After Welding	Transverse Shrinkage	
1	5.500	5.493	.007	Weld No. H-11 Average weld shrinkage .0082"
2	5.501	5.494	.007	
3	5.501	5.493	.008	
4	5.501	5.493	.008	
5	5.501	5.493	.008	
6	5.501	5.493	.008	
7	5.502	5.493	.009	
8	5.502	5.493	.009	
9	5.502	5.493	.009	
10	5.502	5.493	.009	
11	5.502	5.493	.009	
12	5.502	5.494	.008	
13	5.502	5.494	.008	
1	5.820	5.817	.003	Weld No. H-10 Average weld shrinkage .0064"
2	5.820	5.816	.004	
3	5.821	5.816	.005	
4	5.822	5.816	.006	
5	5.822	5.816	.006	
6	5.823	5.816	.007	
7	5.823	5.816	.007	
8	5.824	5.817	.007	
9	5.824	5.816	.008	
10	5.825	5.817	.008	
11	5.826	5.818	.008	
12	5.826	5.818	.008	

All measurements taken at 1 inch spacing.

with an average of 0.0064 inch for weld No. H-10 and 0.0082 inch for weld No. H-11.

The two welded plates were machined into tensile specimens and tested to determine weld integrity. The mechanical properties of the two welds are shown in Table V-3. All failures were in the base metal except weld No. H-11-4 which had a termination crack caused by a missed joint. It is significant that this specimen pulled 174 KSI before failure. Both welds were made with the same parameters (see weld schedules in Appendix A) except that the face pass was oscillated on weld No. H-11 and the beam defocused on weld No. H-10. X-ray inspection of both plates shows only termination flaws.

Figure 5-69 shows the tensile specimens after they had been tested. Note that all failures are in the base metal. The elongation averaged 16.2 percent and 17 percent for the two welds. The type of fracture surfaces of these specimens are typical for 10 Ni steel.

Welding schedules and beam current traces of parameter development welds are included in the appendix.

5.3.1.3 Conclusions from EB Weld Tests

1. Satisfactory EB welds can be made on 0.375, 0.500, 0.625-inch thick 10 Ni to Class I quality standards.
2. One-inch thick 10 Ni steel can be EB welded, but further work is required to achieve reproducibility and maintain quality.
3. EB welding thicknesses greater than 1.0 inch will require extensive additional development including both welding and metallurgical considerations.
4. Transverse weld shrinkage is consistent and can be predicted on both thick and thin sections.
5. Added filler wire can be used to minimize the amount of post weld machining requirements and to increase the gap tolerance from ± 0.005 inch without wire to $+ 0.020$ inch with filler wire.
6. 10 Ni steel details must be thoroughly demagnetized just prior to welding. Any magnetized areas, with a field strength in excess of 1 gauss on a field strength meter, can cause

Table V-3 MECHANICAL PROPERTIES OF EB WELDED .500 INCH THICK 10 Ni STEEL TENSILE TEST SPECIMEN

10 Ni STEEL (HY-180) ELECTRON BEAM WELD						
IDENT. S/N	YIELD STRENGTH Fty at 0.2 Offset	ULTIMATE		ELONGATION % of 2 Inches	HARDNESS	
		Ftu	KSI		Rc	KSI
H-10-1 (2,3)	183.2 KSI	186.2		16	41.8	193
-2	183.7	186.9		16	42.0	194
-3	183.5	186.0		16	42.8	198
-4	184.1	186.9		16	43.0	200
-5	182.3	185.6		16	42.2	195
-6	183.2	186.2		17	41.5	191
AVG.	183.3	186.3		16.2	42.2	195.2
H-11-1 (4)	185.9	195.3		17	42.8	198
-2	182.5	194.7		18	43.8	205
-3	-	193.3		16	44.8	212
-4		174.8 (1)			44.2	208
AVG.	183.9	193.4		17.0	43.9	205.7
						(5)

1. Approximately 0.100 inch weld joint at root was not fusion welded.
2. H-10, heat treatment was as follows: Austenitized: 1500°F for 2 hours, WQ, 950° Aged, 8 hours.
3. H-10, only initial weld pass plus cosmetic weld pass.
4. H-11, heat treatment was as follows: Austenitized: 1500°F for 2 hours, WQ, 950° Aged, 8 hours.
5. Impact tests were made in the Engineering Department Test Laboratory.



Figure 5-69 FAILED TENSILE SPECIMENS FROM EB WELDED .500
INCH THICK 10 Ni STEEL SHOWING FRACTURES

4-54718

serious beam deflection

7. The longitudinal cross-section method of EB weld inspection must be used for parameter development because of the small size of flaws in thick section welds.

5.3.1.4 Recommendations for EB Welding of 10 Ni Steel

1. EB welding on 10 Ni steel should be restricted to joint thickness less than 1.0 inch until satisfactory procedures are developed for thicker sections.
2. Use of EB welding of 10 Ni steel on the wing carrythrough test structure should include the following procedures:
 - o Witness lines should be scribed on both face and root side of the weld joint and included on the engineering design.
 - o Beam current traces should be required on all EB welds to assure reproducibility and to provide a permanent record.

5.3.2 Gas Tungsten Arc Welding

5.3.2.1 Weld Parameter Development

The first attempt at GTA welding 0.500-inch thick 10 Ni steel plate was accomplished using information supplied by Linde and U. S. Steel. The information indicated that the best fracture toughness resulted from very low heat input (KJ) values during welding. Weld test plates were machined with standard J-grooves as shown in Figure 5-70. The plates were set up and welded in the weld fixture shown in Figures 5-71 and 5-72. Recommended values did not achieve 100 percent root penetration and severe lack of fusion resulted. The weld current was incrementally increased 100 percent above the recommended level without adequate root penetration. To conserve material, the weld was cut out of the plate and the J-Grooves remachined. Weld travel speed was reduced from 6 ipm to 2.5 ipm and the plate was

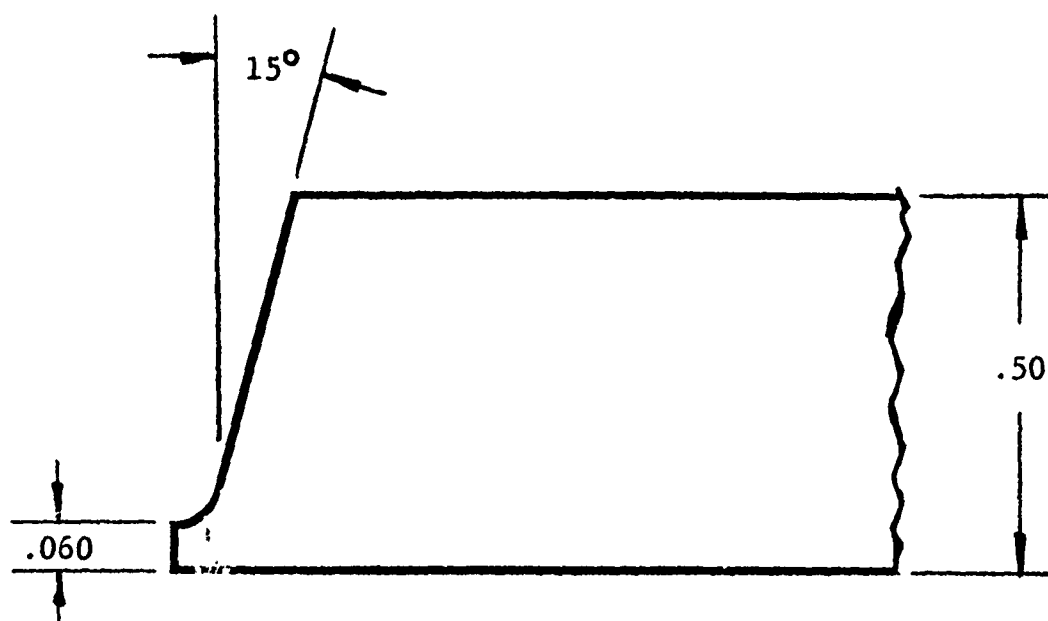


Figure 5-70 TEST PLATE J-GROOVE CONFIGURATION

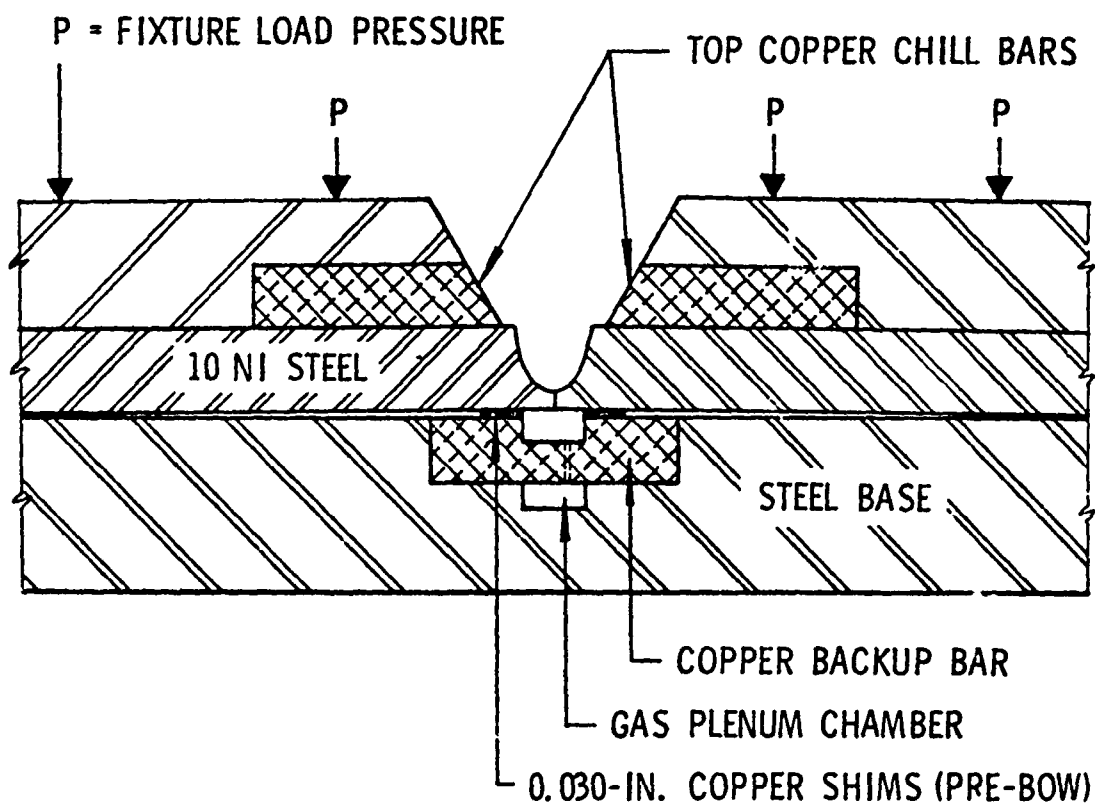


Figure 5-71 SECTION OF GTA WELD FIXTURE

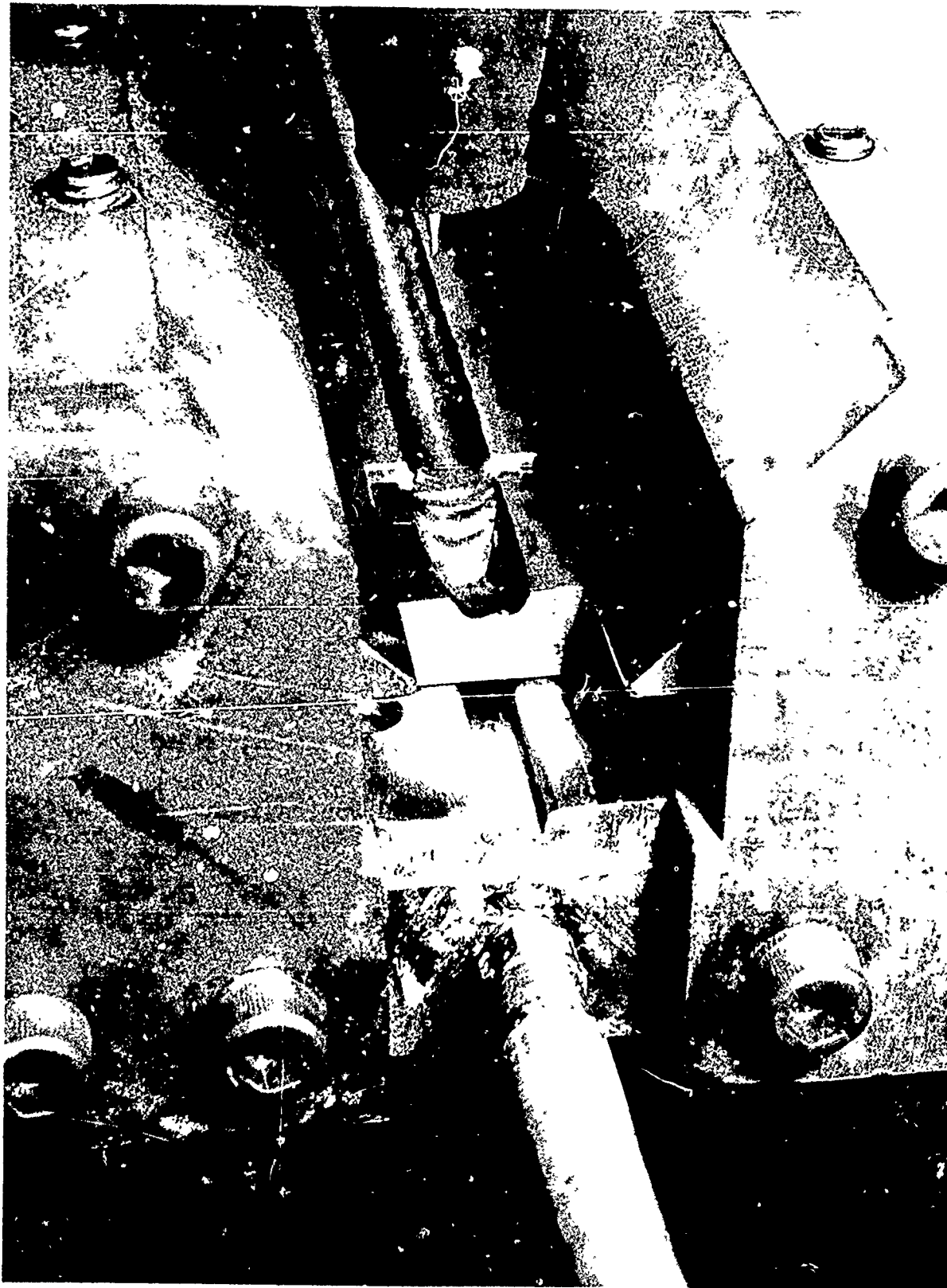


Figure 5-72 SETUP FOR USING WELD TABS

rewelded. Penetration was achieved. Further refinements were made in the weld parameters to obtain the weld schedule shown in Table V-4.

The root pass required higher heat input than the subsequent filler passes. The total joules/inch input was:

$$H = \frac{E \times I \times 60}{S}$$

H = Heat Input (Joules/inch)

E = Arc Voltage arc

I = Total pulsed current for level 1 and level 2

therefore:

$$H = 13.0 \left(\frac{225 \times 10 + 180 \times 5}{15} \right) \times 60 = 75,600 \text{ Joules/inch}$$

The subsequent filler pass heat input is expressed as:

$$H = 13 \left(\frac{160 \times 15 + 200 \times 5}{20} \right) 60 = 33,200 \text{ Joules/inch}$$

The capping pass which is used solely to refine the previous weld pass grain structure, is expressed as:

$$H = 13.5 \left(\frac{120 \times 15 + 160 \times 5}{20} \right) 60 = 26,300 \text{ Joules/inch}$$

As can be seen from the above data, it is very easy to alter the pulsed arc heat input by either varying the current level or the duration of current. However, the heat input values as expressed above can be used only as a reference. It does not take

Table V-4 GTA WELDING SCHEDULE FOR 10 NI STEEL

WELDING SCHEDULE FOR MECHANIZED FUSION WELDING

PROGRAM AMAVS DATE 4-4-73
 MATERIAL 10 NI STEEL THICKNESS 0.500 IN. CONDITION AUST. QUENCH & AGE
 EQUIPMENT NO. 36911 PART NO. 603 R 100-2
 PREHEAT TEMP. 100°F INTERPASS TEMP. 150-180°F
 PRECLEANING MACHINED EDGE, WIRE BRUSH, MEK-WIPED
 NOZZLE SIZE NO.10 TUNGSTEN: Type 2%TH Diameter 0.125 IN.
 TUNGSTEN: Extension 0.500 IN. Shape 15° ANGLE
 FILLER WIRE: Type 10 NI Diameter 0.045 IN.
 TORCH GAS: Type HE Flow 90 cfh; BACKUP GAS: Type HE Flow 15 cfh

Weld Pass No.	1	2	3	4	5	6	7	8	9	10	11	12
Voltage	13	13	13	13	13	13	13	13	13	13.5	13.5	13.5
Weld current (amperage)												
Level 1	225	160	160	160	160	160	160	160	160	160	160	120
Level 2	180	200	200	200	200	200	200	200	200	200	200	160
Number of cycles												
Level 1	10	15	15	15	15	15	15	15	15	15	15	15
Level 2	5	5	5	5	5	5	5	5	5	5	5	5
Wire speed (ipm)	32	32	32	32	32	32	32	32	32	32	32	16
Weld speed (ipm)	2	4	4	4	4	4	4	4	4	4	4	4

into consideration variations of preheat or the unit volume of filler wire additions. Also, if transverse arc oscillation is used, another dimensional factor must be considered. Therefore, data reported as heat input alone is totally inadequate. Another important consideration in the documentation of welding variables is that of the basic tooling configuration. It was later found that some of the recommended welding parameters were used to weld 10 Ni steel on a flat metal table using a solid copper backup plate. Hence, no penetration was expected or achieved. Back grinding or chipping was used to clean the back side root area. A weld bead was then applied to the back side. The preferred method is to use backup bars for inert gas shielding whenever possible, thus eliminating the back grinding or chipping operation. This, however, may be necessary on thicknesses in excess of 1/2 inch.

5.3.2.2 Weld Set-Up Procedure

The test plates were positioned in the weld fixture (Ref. Figure 5-71). A 0.030 x 0.375-inch copper strip was used for shims to provide prebowl to compensate for weld distortion. Weld run off tabs (Ref. Figure 5-72) were installed so that arc initiations and terminations would not be included in the weld plate test zones. The test plates were stainless steel wire brushed and MEK wiped. An oxy-acetylene torch was used to preheat the test plates to approximately 100°F. Weld passes were then made keeping the interpass temperature between 150 - 180°F.

5.3.2.3 Weld Shrinkage

Transverse weld shrinkage was measured after the weld parameters were established. A ground gage block was placed on top of the unwelded plates, and lines were scribed along the edges of the gage block at each end of the plate. The distance between the scribe lines was measured and recorded. The test plates were welded and the scribe lines were remeasured. The net difference is the actual transverse weld shrinkage. As shown in Table V-5, the average shrinkage for the starting end of the weld was 0.019 inch and the finished end of the weld was 0.027 inch. The average weld shrinkage was 0.023 inch. The shrinkage experienced is approximately half that of most other high strength materials welded in the same manner. The low shrinkage most likely resulted from the pulsed arc welding mode. Further work should be pursued to define the benefits from using the pulsed arc welding technique.

Table V-5 TRANSVERSE GTA WELD SHRINKAGE DATA
1/2" THICK 10 Ni STEEL

TEST PLATE	S/N	START END SHRINKAGE	FINISH END SHRINKAGE	AVG START	AVG FINISH	TOTAL AVG
W-6	F467195	-.015	-.035			
W-7	F528036	-.010	-.015			
W-8	F528033	-.015	-.020			
W-9	F467193	-.025	-.030			
W-10	F528032	-.010	-.020			
W-11	F528031	-.030	-.030			
W-12	F528034	-.020	-.040			
W-13	F467196	-.015	-.025			
W-14	F528030	-.025	-.030			
W-15	F528035	-.020	-.025			
W-16	F467197	-.025	-.025			
				-.019"	-.027"	-.023"

5.3.2.4 Weld Producibility Test Specimen

The NBB designs were reviewed and evaluated with Engineering Design on the usage of GTA welding. Because of the thicknesses involved in the bulkhead T-members, it was decided these members would best be electron beam welded. GTA welds were thus limited to the bulkhead web areas. The weld joints were designed to make the final welds by GTA because the assembly was too large for available electron beam weld chambers.

A simulated test detail was designed to represent the web to T-member joint. The weld fixture design is shown in Figure 5-73. This fixture provides side load pressure to assure tight fit up of the details. Downward pressure for alignment is also provided. Copper chill bars are provided to control bead shape and heat buildup. A copper gas backup bar is also used to control root penetration and provide inert gas shielding.

The weld fixture was designed for both the GTA and electron beam welding tests. The GTA backup bar and support block (details -4 and -8) are removable and replacement bars can be added to facilitate electron beam welding.

Two sets of test details were machined but were not welded. These specimens are representative of both the Yf 992 and Yf 932 outboard bulkheads (Ref. X7224071 and X7224091 respectively).

5.4 METALLURGICAL EVALUATION OF 10 NI STEEL

Data on heat treatment was generated as a result of the EB/GTA welding and machining programs. Weldments produced in establishing GTA/EB weld parameters were cross sectioned after X-ray inspection. Defects that were picked up by X ray were evaluated by metallographic examination. Macro and microphotographs were made for records.

5.4.1 Thermal Treatment

Several pieces of 10 Ni steel were austenitized at 1500°, 1550°, 1650°F and double austenitized at 1650° and 1550°F and water quenched. Aging was accomplished at 950°F for 3, 4, 5 or 8 hours with air cool. Aging was also accomplished at 950°F for 4 or 5 hours and water quenched. Other age temperatures were 1050° and 1150°F. Hardness tests were conducted on welded and base metal specimens after welding and the various thermal treatments. GTA and EB weldments plus base metal specimens were thermally pro-

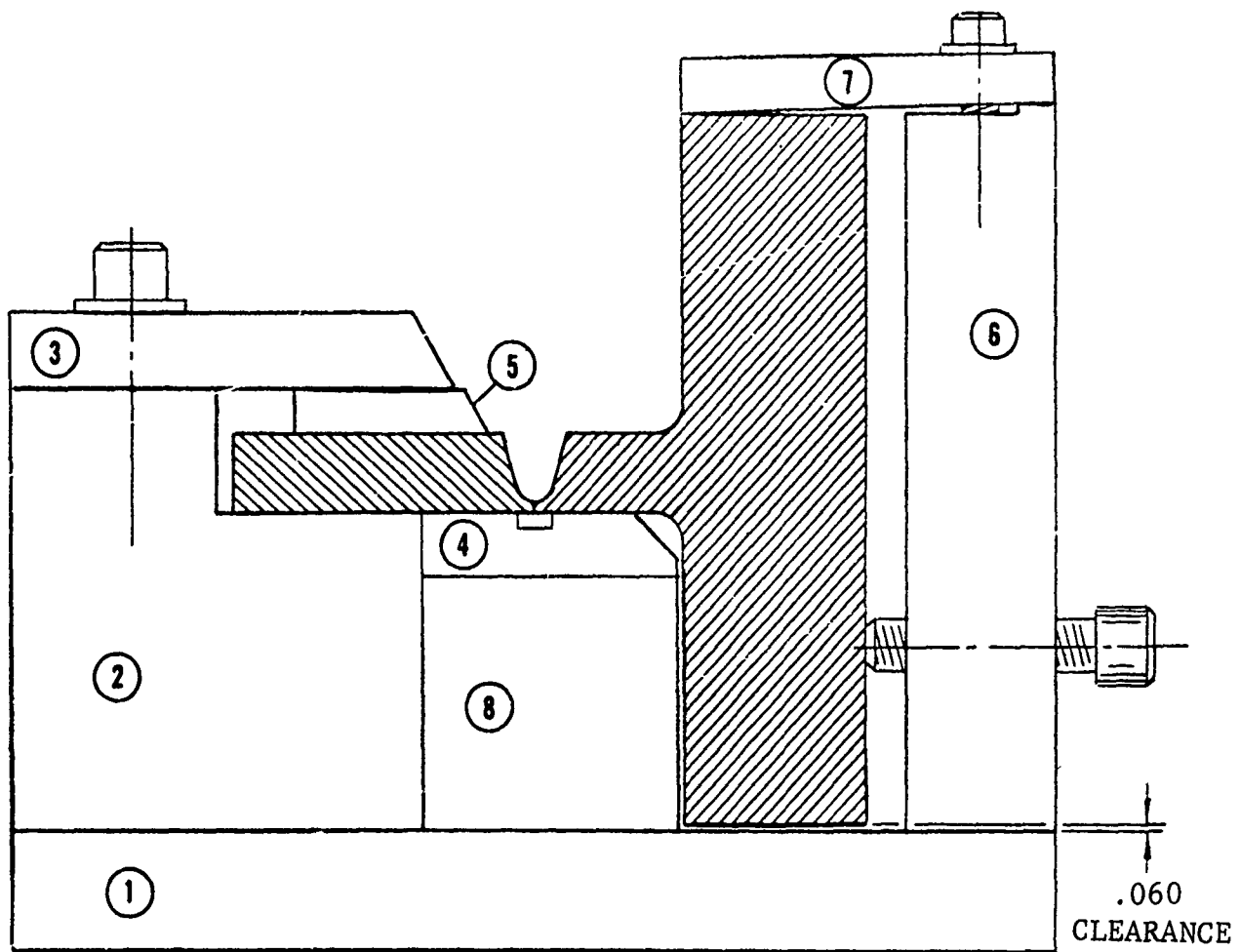


Figure 5-73 COMBINATION GTA AND EB WELD FIXTURE FOR WELDING BULKHEAD TEST SPECIMENS

cessed. Several small plates were austenitized and water quenched for machining tests.

Plate stock in the as-received, "austenitized and aged" condition and "re-austenitized plus water-quenched" condition were utilized in the machining tests previously reported.

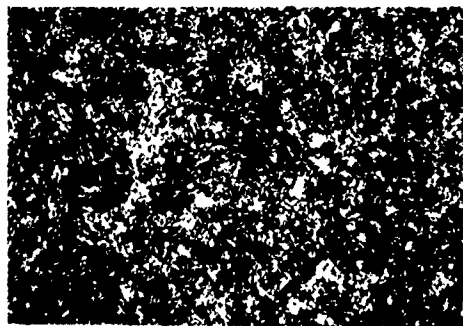
5.4.2 Microstructure Evaluation

Metallographic examination of the 10 Ni steel base metal and GTA/EB weldments, involved five different etchants. U. S. Steel Corp. and Linde recommended a three-step etch procedure. Etchant (I) - Use 25% HNO_3 + ethanol for 10 to 30 seconds to reveal solidification structure, etchant (II) - use 40% sodium bisulfite in water for 30 to 120 seconds to reveal the transformation structure, etchant (III) - use 1% picric + 5% HCl in ethanol for 10 to 30 seconds to reveal grain boundary contrast. These etchants were evaluated separately and jointly. Microstructure obtained is shown in Figure 5-74. It was found that the 40 percent sodium bisulfite reaction was too severe. A 10 percent sodium bisulfite etchant for 30 to 120 seconds developed a better surface. Also, Nital etchant (either 2 or 10 percent solution) may be utilized to show the grain structure.

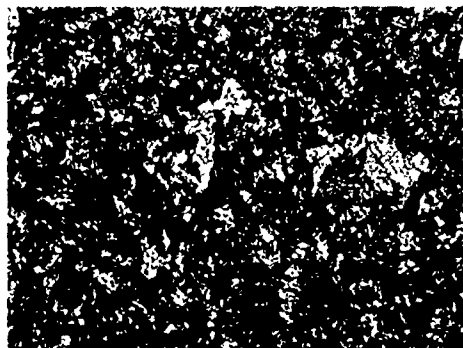
The 1650° and the 1650 + 1550°F solution treated (ST) and water quenched specimens showed a banded structure after polish and etch, but this type structure disappeared after the aging operations. (Figure 5-75 A and B). The 950°F age for 5 hours plus water-quenched versus the 950°F age for 8 hours and air-cooled to room temperature shows that the grain size varies. The water-quenched specimen had a grain size of 6 to 8 and the air-cooled specimens had a grain size of 8 or finer. There was a drastic difference in the microstructure after the 1500°F solution treated (Figure 5-75 B and C). There was no banding in the 1500°F austenitized specimens. Double solution treated (ST) and aged (STA) microstructure is shown in Figure 5-75D.

5.4.3 Microhardness Tests

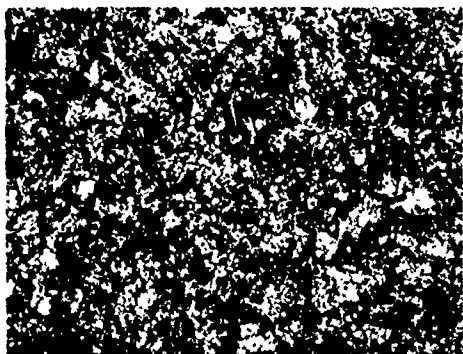
Test specimens taken from GTA weldments, that utilized 10 Ni steel purchased in the solution treated and aged condition, were evaluated for microhardness and microstructure. A traverse microhardness was made on specimens from the center of the final GTA weld pass, through the multipass welds, heat affected zones, and the base metal. Weldments were aged at 950°, 1050° and 1150°F for four hours and air-cooled. The Knoop hardness was converted to R²c". The 950°F reaged test specimens had a minimum hardness



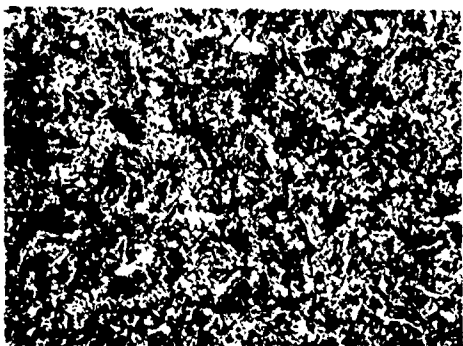
BASE METAL



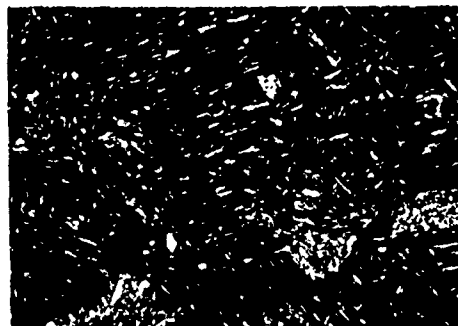
BASE METAL



BASE METAL



BASE METAL



WELD METAL
(2ND WELD PASS)

ETCHANT NO. I



WELD METAL
(2ND WELD PASS)

ETCHANT NO. II
OVER ETCHANT NO. I



WELD METAL
(2ND WELD PASS)

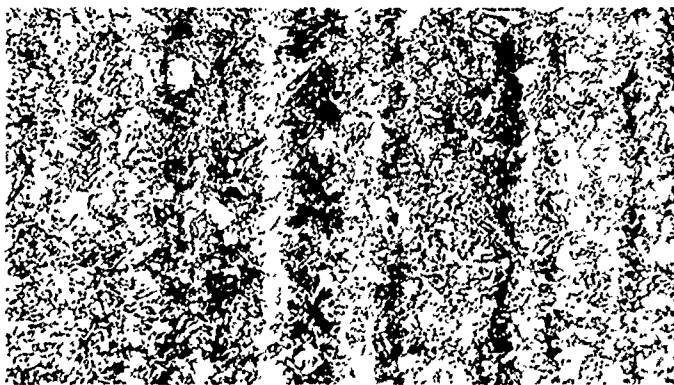
ETCHANT NO. III
OVER ETCHANT I & II



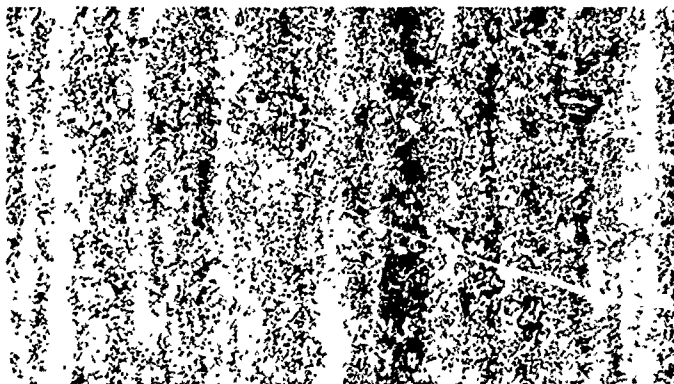
WELD METAL
(2ND WELD PASS)

ETCHANT NO. III

Figure 5-74 COMPARISON OF MICROSTRUCTURE OF 10 Ni STEEL USING VARIOUS ETCHANTS
ON BASE AND GTA WELD METAL (200X)



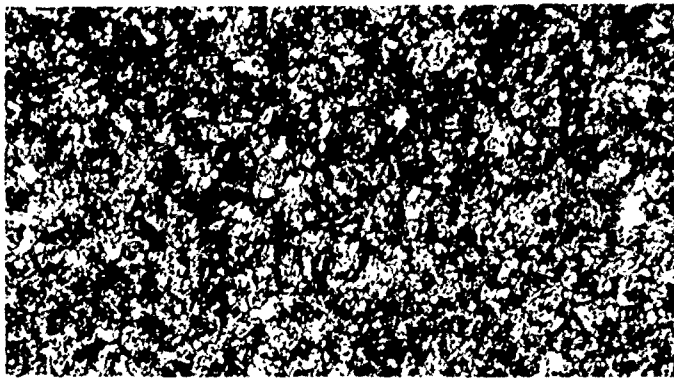
A -
1650 \pm 25°F SOLUTION
TREATMENT (1½ HRS)
AND WATER QUENCH



B -
1650°F + 1550 \pm 25°F
SOLUTION TREATMENT (1½
HRS) AND WATER QUENCH



C -
1500 \pm 25°F SOLUTION
TREATMENT (1½ HRS)
AND WATER QUENCH



D -
SOLUTION TREATMENT
A + B + 950 \pm 10°F
AGE (8 HRS) AND AIR
COOLED

Figure 5-75 MICROSTRUCTURE OF SOLUTION TREATED AND SOLUTION TREATED AND AGED
10 Ni STEEL - 2% NITAL ETCHANT (200X)

of R" c" 37.9 in the center of the final GTA weld pass to a maximum hardness of R" c" 44.9 in the primary heat affected zone. The secondary heat affected zone had a hardness of R" c" 40 to 42. The base metal hardness ranged from R" c" 39 to 41. Hardness values for the third through fifteenth weld passes are shown in Table V-6. Macrostructure of the multipass weld is shown in Figure 5-76 B. Microstructure of the base and weld metal is shown in Figure 5-76 A and C.

5.5 MACHINING

5.5.1 Machinability Evaluation of 10 Ni Steel

Machinability tests conducted during Phase II encompass the basic metal removal operations anticipated for fabricating the wing carrythrough test structure. The machinability test data is segregated into the following categories of machine operations.

1. Band sawing and cut-off sawing
2. Turning and boring
3. Machine drilling and reaming
4. End milling
5. Skin milling

5.5.1.1 Band Sawing

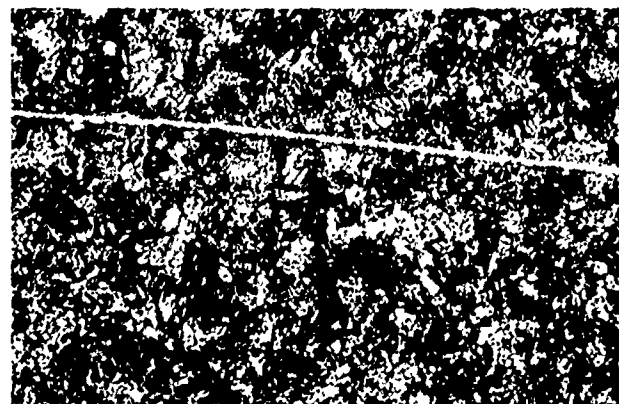
Band sawing tests were conducted on 10 Ni steel plate specimens, 1.0-inch thick x 4.8-inches wide x 17.5-inches long. Based on the 1.0-inch plate thickness a 6 pitch (tooth) blade was selected. A standard 1 inch x 6P Simonds "Weld Edge" premium HSS blade was used for the test. A band speed of 90 surface feet/minute (SFM) was initially used and failed after 0.5 square inch of cut.

A new blade was installed and adjusted to maximum recommended band tension. A band speed of 55 SFM produced good cuts at an average sawing rate of 0.5 sq. in./min. A DoAll variable speed contourmatic power feed band saw was used for all tests to simulate the sawing speeds and feed rates of other sawing operations. All sawing test cuts were accomplished without coolant.

Table V-6 HARDNESS VALUES OF GTA WELDED AND
AGED 10 Ni STEEL 1/2 INCH PLATE

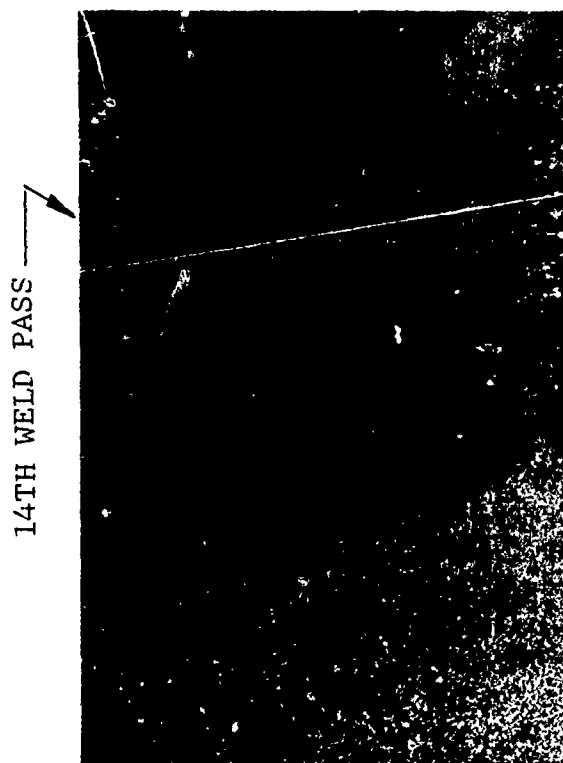
STA. FUSION WELD (2)	AGED @ 950°F (3)		AGED @ 1050°F (3)		AGED @ 1150°F (3)	
LOCATION OF TEST	RC (1)		RC (1)		RC (1)	
Center of 14th Weld Pass	42.0	37.9	40.0	36.9	35.5	36.2
Bottom of 14th Weld Pass	41.8	41.6	41.7	36.9	36.8	36.8
Center of 13th Weld Pass	44.9	44.7	44.8	38.9	39.7	39.3
WM 12th Weld Pass	41.9	44.2	43.0	36.9	39.2	38.0
WM 11th Weld Pass	43.8	44.2	44.0	38.8	39.2	39.0
WM 10th Weld Pass	41.8	42.6	42.2	36.8	37.6	37.2
FZ 9th Weld Pass	44.2	44.9	44.5	39.2	39.2	39.2
HAZ-FZ 8th Weld Pass	42.6	42.6	42.6	37.6	37.6	37.6
HAZ- 7th Weld Pass	44.7	44.2	44.2	39.2	39.4	39.3
HAZ- 6th Weld Pass	44.2	43.8	44.0	39.2	38.8	39.0
HAZ- 5th Weld Pass	40.0	40.0	40.0	35.0	35.0	35.0
BM/HAZ 4th Weld Pass	41.9	41.9	41.9	36.9	36.9	36.9
BM/HAZ 3rd Weld Pass	41.8	41.6	41.7	38.8	36.6	37.7
				28.0	26.0	27.0
				26.0	26.0	26.0
				28.8	28.3	28.5
				28.3	29.5	28.9
				28.3	28.8	28.6
				28.8	28.8	28.8
				28.8	28.8	28.8
				30.0	29.5	29.7
				28.8	28.8	28.8
				30.3	30.3	30.3
				30.3	30.0	30.0
				29.1	30.0	30.1
				30.0	29.1	29.5

- (1) Microhardness (KNOOP) Values Converted to Rockwell "C"
(2) 10 Ni Steel Condition STA Prior to GTA Fusion Welding
(3) Material Was Aged for 4 Hours After Welding at 950°, 1050°,
or 1150°F



(200X)

A - BASE METAL
(REAGED)



(6X)

B - GTA MULTIPASS WELD OF
SOLUTION TREATED AND AGED
MATERIAL (REAGED AT 950°F
FOR 4 HOURS)



(200X)

C - WELD METAL
(REAGED)

Figure 5-76 MACRO AND MICRO STRUCTURE OF MULTIPASS GTA WELDED AND REAGED 10 Ni STEEL (ETCHANT - 25% HNO₃ + ETHANOL)

5.5.1.2 Boring and Turning

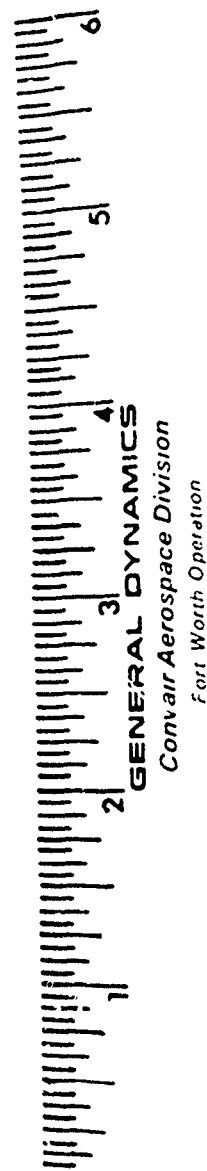
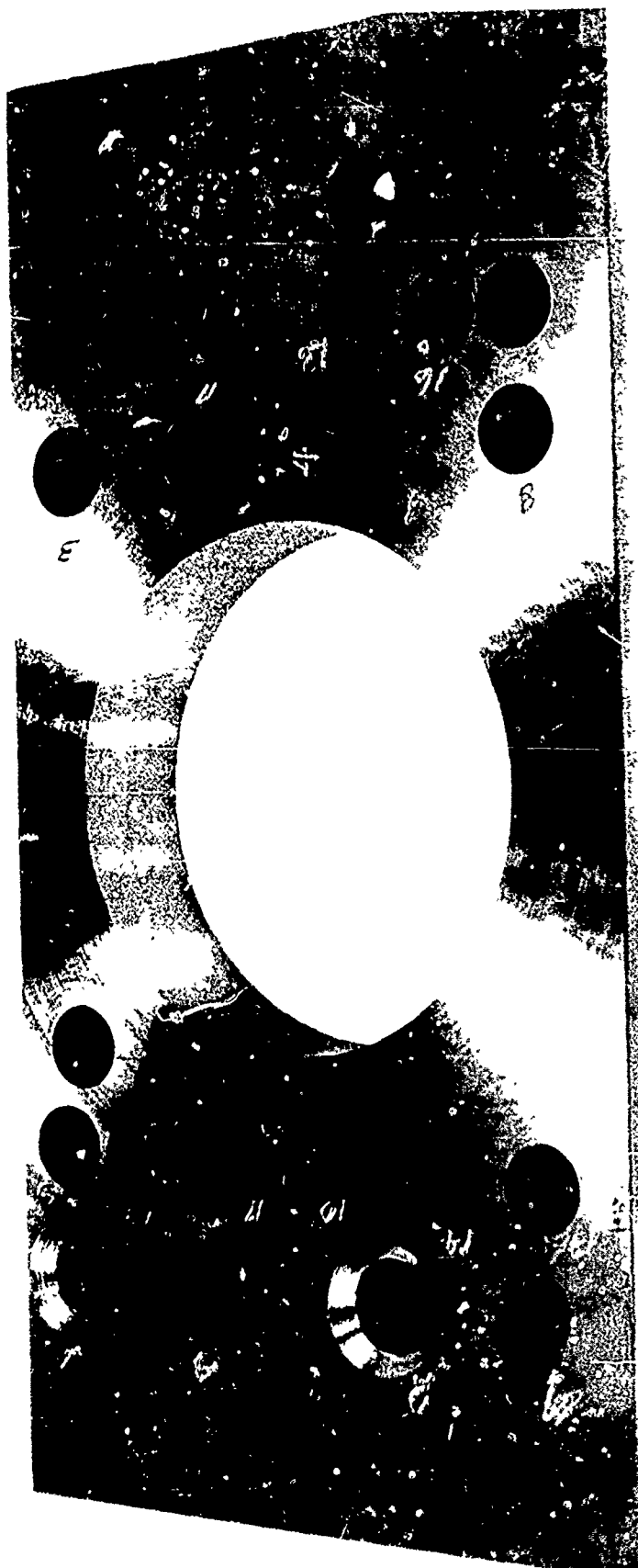
A series of single tool boring tests were conducted on a Monarch engine lathe in the MR&D machining test center. The lathe is equipped with an infinitely variable spindle speed selector with visual readout of spindle speeds. Availability of 10 Ni steel for this test was limited to (2) pieces 1.0 inch thick x 5 inches wide x 10 inches long. Tests were conducted by boring a series of holes, starting with a 1.5-inch hole in 1.0-inch plate material. Figure 5-77 shows one of the 1.0-inch thick machined specimens after boring tests. The plate was also used for drilling and reaming tests discussed in the next section. Table V-7 presents the boring test results conducted on the two test plates. The data developed during the boring test is representative and adequate for turning, as both operations employ the same cutting principle.

The boring test results reveal that 100 SFM for roughing and 150 SFM for finishing is adequate. Feed rates of 0.0075 inch per revolution (IPR) for rough boring and 0.005 IPR for finishing were best when using C-6 grade carbide throwaway inserts with positive rake angles.

5.5.1.3 Machine Drilling and Reaming

Drilling and reaming tests were conducted on 1.0-inch thick, aged 10 Ni steel plate material. The tests were performed on a power feed drill press in the MR&D machining center using Gulf HD51 water soluble coolant. The drills tested were 0.4846 diameter oil hole types of HSS and cobalt. The C15002-4844 test drill shown in Figure 5-78 is a 20 degree helix type cobalt normally used for drilling high strength steel. The C15013-4844 test drill in Figure 5-79 is a 30 degree helix high speed steel type normally used for aluminum and mild steel.

Test results presented in Table V-8 reveal that the C15013-4844 30 degree helix HSS drill performed better than the C15002-4844 20 degree helix cobalt drill, except for tolerance control. It is assumed that the resulting tolerance is adequate to allow for subsequent reaming operations. The reaming tests proved that the C15481 (GD/FW specification) carbide tipped reamer (Figure 5-80) performed better than the C15014 (GD/FW specification) cobalt reamer (Figure 5-81) for producing finished holes in 10 Ni steel.



1-51974

Figure 5-77 10 Ni STEEL PLATE USED FOR BORING, DRILLING AND REAMING TESTS

Table V-7 BORING TEST DATA - 1 INCH THICK 10 Ni STEEL

MATERIAL	HEAT TREAT CONDITION	HARDNESS	DEPTH OF CUT	FPM SPEED	IPR. FEED	TOOL MAT'L.	REMARKS
HY180 (10 Ni)	Solution treated and aged (S.T.A.)	200-205 KSI	.062	100	.0075	C-5 Carbide	Poor finish 140-160 micro inches chip blue
HY180 (10 Ni)	S.T.A.	200-205	.062	150	.0050	C-5 Carbide intent	Fair finish tool chipped
HY180 (10 Ni)	S.T.A.	200-205	.125	100	.0050	C-5 Carbide	Excessive chatter tool chipped
HY180 (10 Ni)	S.T.A.	200-205	.062	100	.0040	C-5 Carbide	Good finish 125 micro inches chip bronze
HY180	S.T.A.	200-205	.032	100	.0040	C-6 Carbide	Good finish 60-80 micro inches slight tool wear
HY180	S.T.A.	200-205	.032	75	.0045	C-6 Carbide	Good finish 60-80 micro inches negligible tool wear
HY180 (10 Ni)	Solution treated only	186 KSI	.062	100	.0075	C-6 Carbide	Chip blue 140 micro inch finish
HY180 (10 Ni)	Solution treated only	186 KSI	.125	100	.0075	C-6 Carbide	Chip blue excessive chatter tool chipped
HY180 (10 Ni)	Solution treated only	186 KSI	.062	150	.0045	C-6 Carbide	Chip bronze 125 finish slight tool wear
HY180 (10 Ni)	Solution treated only	186 KSI	.032	150	.0045	C-6 Carbide	Chip bronze 60-80 micro inch finish min. tool wear



4-53073

Figure 5-78 C15002 - 4844 COBALT,
20° HELIX DRILL
(NORMALLY USED FOR
HIGH STRENGTH STEEL)

4-53072

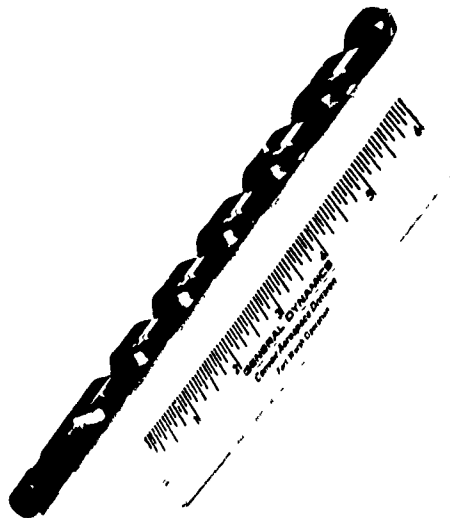
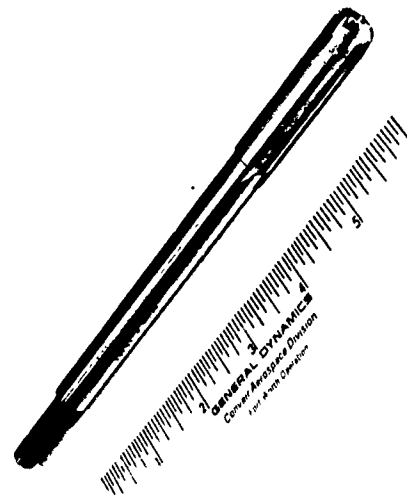


Figure 5-79 C15013 - 4844 HSS,
30° HELIX DRILL
(NORMALLY USED FOR
ALUMINUM AND MILD STEEL)



4-53074

Figure 5-80 C15481 CARBIDE
TIPPED REAMER

4-53075

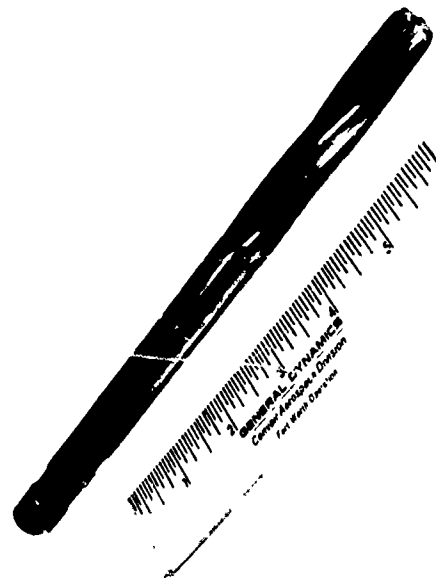


Figure 5-81 C15014 COBALT REAMER

Table V-8 DRILL TEST DATA - 1 INCH THICK 10 Ni STEEL

MATERIAL = 10 Ni - AGED @ 205 KSI (1" THICK)

DRILL	RPM	FEED	HOLE NO	HOLE SIZE	FINISH RMS	COMMENT
C15002-4844	250	.001	1	.4846	50-80	TOO SLOW
COBALT	250	.001	2	.4846	50-80	
20° HELIX	250	.002	3	.4856	50-80	
	250	.002	4	.4857	50-80	BURR ON FAR SIDE
	250	.002	5	.4851	50-80	LARGE BURR ON FAR SIDE - LIP WORN CHIP BUILD UP ON CUTTING EDGE VISIBLE
C15013-4844	250	.002	6	.4884	50-80	
HSS	250	.002	7	.4882	50-80	
30° HELIX	250	.002	8	.4883	50-80	
	250	.002	9	.4885	50-80	
	250	.002	10	.4884	50-80	
	250	.002	11	.4885	50-80	
	250	.002	12	.4882	50-80	DRILLS SMOOTH WITH NO CHIP
	250	.002	13	.4883	50-80	REMOVAL PROBLEM
	250	.002	14	.4888	50-80	
	250	.002	15	.4885	50-80	DRILL SHARP AFTER 15 HOURS
	250	.002	16	.4884	50-80	
	250	.002	17	.4886	50-80	
	250	.002	18	.4885	50-80	
	250	.002	19	.4884	50-80	
	250	.002	20	.4886	50-80	
C15013-4844	250	.004	21	.4849		
	250	.004	22	.4849		GALLED AND BROKE IN HOLE #23
	250	.004	23	-		FEED TOO GREAT

5.5.1.4 End Milling

Preliminary end milling tests were performed on a small test block of 10 Ni steel material using 1 1/2-inch diameter 8 flute HSS end mill cutters. (See Figure 5-82.) The test consisted of multipasses at various feeds and speeds to determine the cutting rate for milling Group II detail parts. A 1 1/2-inch diameter 8 flute 30 degree helix end mill performed best using 75 SFM speed and 0.002 inch per tooth (IPT) feed at 0.21 inch depth of cut. Test cuts at 0.35 inch and 0.50-inch depth of cut exceeded the 125 microinch surface finish requirement. The preliminary end milling data was used to establish machine shop milling procedures for the fabrication of the large detail parts for Group II production verification test components. Figure 5-83 is a profile milling operation on a 10 Ni steel part of thin flange design. Figure 5-84 is an end milling operation on a thick 10 Ni steel splice plate using an 8-flute 2-inch diameter end mill cutter.

5.5.1.5 Skin Milling

Skin milling 10 Ni steel represents one of the more difficult metal removal operations. The difficulty is associated with the rapid breakdown of the cutter edges causing high machining stresses and the subsequent warpage of large plate material. Initial face milling tests were conducted using negative rake carbide inserted face milling cutters. The negative rake cutters produced rapid buildup of the 10 Ni steel on the cutter edges causing premature cutter failure and rough surface finishes. Positive shear angle cutters were then tested. Initial test data using positive rake carbide inserted face mills (Table V-9), proved that positive shear angle cutters perform satisfactorily. A round throwaway carbide insert (7 degrees axial, 2 degrees radial) face milling cutter (Figure 5-85), produced best results at 100 SFM and .004 feed per tooth. This cutter was used for skin milling 10 Ni plate stock in the production machine shop during fabrication of Group II production verification test specimens.

5.5.1.6 Flame Cutting 10 Ni Steel

A 2 3/8 x 60 x 135 inches 10 Ni steel plate was flame cut using oxygen and Mapp gas. Fifty-eight details were removed from the plate using the Airco automatic tracing flame cutting machine. The plate was in the austenitized and quenched condition before flame cutting. After solution treating, the plate



Figure 5-82 PRELIMINARY END MILLING
TEST ON 10 Ni STEEL -
1 1/2 INCH DIAMETER,
8 FLUTE, HSS CUTTER



Figure 5-84 END MILLING 10 Ni STEEL
SPLICE PLATE (603FTB052
PRODUCTION VERIFICATION
TEST SPECIMEN)



Figure 5-83 PROFILE MILLING
10 Ni STEEL, THIN FLANGE,
PRODUCTION VERIFICATION
TEST PART (603FTB052)

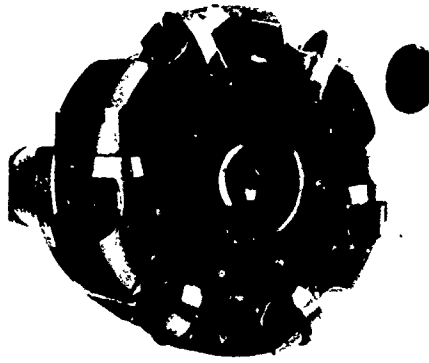


Figure 5-85 FACE MILLING CUTTER WITH
ROUND CARBIDE INSERTS

Table V-9 FACE MILLING TESTS ON 10 NI STEEL

MATERIAL	SURFACE FT/MIN.	CHIP/ TOOTH	CUT	RPM	FEED MIN.	CUTTER	# TEETH	TOOTH CONFIG.	FINISH	TOOTH CONDITION	CHIPS
1. 10 Ni @ 200-205 KSI (AGED)	60	.003	.10 x 2.5 x 12	28	1.0	8" DIA. @ 25° POS.	12	.12 x 45° @ 30° POS.	GOOD	2 CHIPPED	SMOOTH, BRIGHT, COOL
2. "	60	.003	.12 x 2.5 x 12	45	1.0	5" DIA. @ 70° POS.	6	1/2" RAD. @ 15° RELIEF	GOOD	GOOD	SMOOTH, BRIGHT, COOL
3. "	100	.003	.12 x 2.5 x 12	71	1.4	5" DIA. @ 70° POS.	6	1/2" RAD. @ 15° RELIEF	GOOD	GOOD	SMOOTH, BRIGHT, COOL
4. "	130	.003	.12 x 2.5 x 12	90	1.6	5" DIA. @ 70° POS.	6	1/2" RAD. @ 15° RELIEF	GOOD	GOOD	SMOOTH, BRIGHT, COOL
5. "	130	.003	.25 x 2.5 x 12	90	1.6	5" DIA. @ 70° POS.	6	1/2" RAD. @ 15° RELIEF	FAIR	GOOD	STARTING TO TURN BROWN
6. "	100	.008	.31 x 2.5 x 12	71	3.5	5" DIA. @ 70° POS.	6	1/2" RAD. @ 15° RELIEF	FAIR	CHIPPING	SOME BROWN AND PURPLE
7. "	100	.008	.25 x 2.5 x 12	71	3.5	5" DIA. @ 70° POS.	6	1/2" RAD. @ 15° RELIEF	FAIR	CHIPPING	SOME LIGHT BROWN
8. "	100	.006	.25 x 2.2 x 12	71	2.56	5" DIA. @ 70° POS.	6	1/2" RAD. @ 15° RELIEF	GOOD	GOOD	SMOOTH, BRIGHT, WARM
9. "	100	.006	.31 x 2.5 x 12	71	2.56	5" DIA. @ 70° POS.	6	1/2" RAD. @ 15° RELIEF	FAIR	CHIPPING	SOME BROWN
10. 10 Ni @ 186-202 KSI (NON-AGED)	100	.006	.25 x 1.0 x 9.0	71	2.56	5" DIA. @ 70° POS.	6	1/2" RAD. @ 15° RELIEF	GOOD	FAIR	SOME LIGHT BROWN
11. 10 Ni @ 186-202 KSI (WITH SCALE)	100	.006	.25 x 4.5 x 9.0	71	2.56	5" DIA. @ 70° POS.	6	1/2" RAD. @ 15° RELIEF	GOOD	CHIPPING	SOME PURPLE
12. 10 Ni @ 186-202 KSI (SCALE RE- MOVED)	100	.006	.25 x 4.5 x 10	71	2.56	5" DIA. @ 70° POS.	6	1/2" RAD. @ 15° RELIEF	FAIR	CHIPPING	SOME PURPLE
13. 10 Ni @ 200-205 KSI (AGED)	95	.006	.25 x 2.5 x 12	45	2.15	8" DIA. RADIAL POS. 4° NORMAL POS. 5 1/2°	8	.12 x 45°	FAIR	CHIPPING	CHIPPING BAD AFTER ONLY 1" OF TRAVEL - BROWN CHIPS -
14. 10 Ni @ 200-205 KSI (AGED)	105	.006	.25 x 2.5 x 12	45	3.25	9" DIA.	12	.12 x 45° #10	FAIR	CHIPPING	HEAVY CHIPPING
15. 10 Ni @ 200-205 KSI (AGED)	100	.006	.25 x 2.5 x 6.0	71	.4	5" DIA. @ 70° POS.	1	1/2" RAD. CHIP- BREAK @ 15°REL	FAIR	CHIPPED	ALL DARK BLUE CHIPS WRINKLED-BROWN-BLUE CHIPBREAKER CHIPPED OUT
16. 10 Ni @ 200-205 KSI (AGED)	100	.006	.25 x 2.5 x 6.0	71	.4	5" DIA. @ 70° POS.	1	1/2" Rad. CHIP- BREAK @ 12° REL.			WRINKLED-BROWN-BLUE CHIPBREAKER CHIPPED OUT SLIGHTLY CHIPPED
17. 10 Ni @ 200-205 KSI (AGED)	100	.005	.25 x 2.5 x 6.0	71	.35	5" DIA. @ 70° POS.	1	1/2" RAD. @ 15° REL.	FINE	LIGHT WEAR	SMOOTH, BRIGHT, COOL
18. 10 Ni @ 200-205 KSI (AGED)	100	.004	.25 x 2.5 x 6.0	71	.29	5" DIA. @ 70° POS.	1	1/2" RAD. @ 15° REL.	FINE	LIGHT WEAR	SMOOTH, BRIGHT, COOL
19. 10 Ni @ 190-200 KSI (AGED)	95	.005	.12 x 2.5 x 12	90	.44	4" DIA. 6°POS NOR 10°POS RAD	1	SQUARE .03R 10°REL T-15	FINE	GOOD	SMOOTH, BRIGHT, COOL
20. 10 Ni @ 190-200 KSI (AGED)	95	.004	.25 x 2.5 x 10	90	.36	4" DIA. 6°POS NOR 10°POS RAD	1	SQUARE .03R 10°REL T-15	FINE	GOOD	SMOOTH, BRIGHT, COOL NO CHIPPING OF INSERT BUT SHOWS SLIGHT WEAR
21. 10 Ni @ 190-200 KSI (AGED)	95	.005	.25 x 2.5 x 10	71	.35	5" DIA. @ 7° POS.	1	1/2" RAD. @ 10° RELIEF	POOR	GOOD	BROWN AND BLUE - NOT ENOUGH RELIEF HEEL DRAGGING
22. 10 Ni @ 190-200 KSI (AGED)	120	.004	.25 x 2.5 x 10	90	.36	5" DIA. @ 7° POS.	1	1/2" RAD. @ 15° RELIEF	FINE	GOOD	SOME BROWN/BLUE SLIGHT CHIPPING

was machined on both sides; therefore, all flame cutting was accomplished on clean machine cut surfaces.

Difficulty was encountered in the initiation of the cut. A preheat temperature of approximately 150°F was used. This was accomplished by allowing the cutting torch to follow the cutting pattern four times before turning on the cutting oxygen. Occasional blowout at the cut initiation was experienced. The flame would cut through two-thirds of the plate and then expel the molten metal at 90° as shown in Figure 5-86A. It was found that by preheating the lower edge of the plate with a manual torch (Figure 5-86 B), successful cutting starts were consistently achieved without blowouts. When good cutting starts were made no problems were encountered in maintaining the cut.

Manual edge preheating was used on long, thin details at the edge of the plate to eliminate warpage from cutting. Two details were 4 inches wide by 80 inches long. Because of material limitation, a waster strip could not be removed to equalize cutting stresses. The preheating technique is depicted in Figure 5-86C.

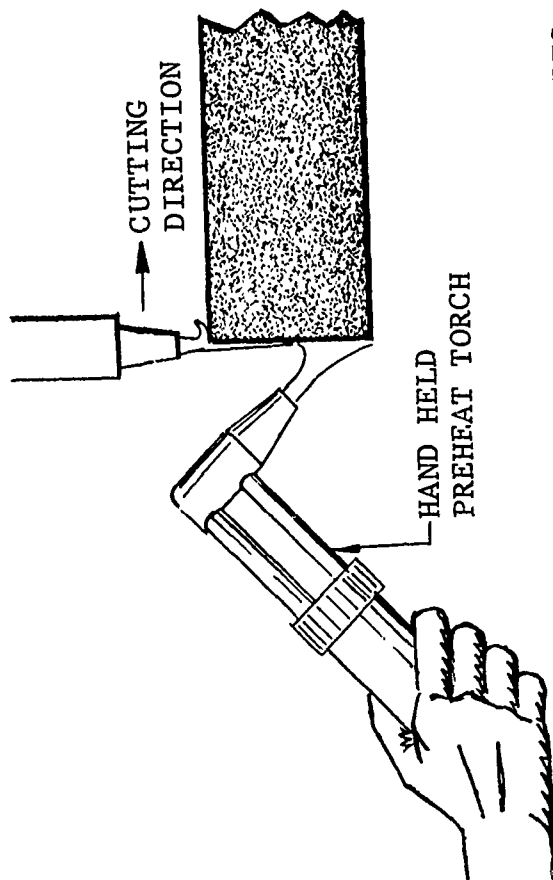
The heat affected zone obtained on the 2-3/8-inch thick plate is shown in Figure 5-86D. The allowance for heat affected zones was established at 0.100-inch per inch of thickness. However, other plate thicknesses should be checked in the same manner, if a significantly different cutting speed is used.

This was the first thick plate that was torch cut on this program. It is felt that further improvements can be made in the area of flame cutting. This plate was cut at 7 inches per minute. Satisfactory cuts were achieved at this speed, therefore, no other speeds were evaluated. The 1/2-inch per side cut allowance proved to be adequate and assured stock clean up around 90° corners and profiled shapes.

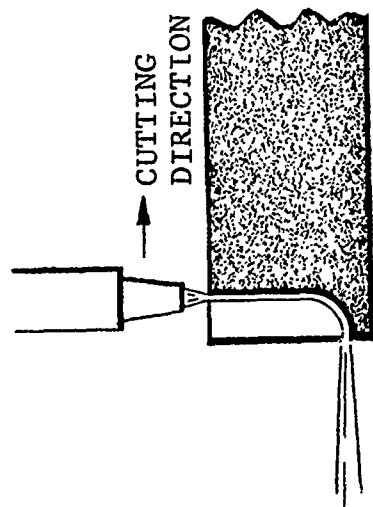
It is recommended that plasma arc cutting be investigated for use on thick plates. The higher velocity of the cutting gases may overcome the edge starting problem and eliminate the requirement for manual preheating.

5.5.1.7 Stress Relief Test on Machined 10 Ni Steel

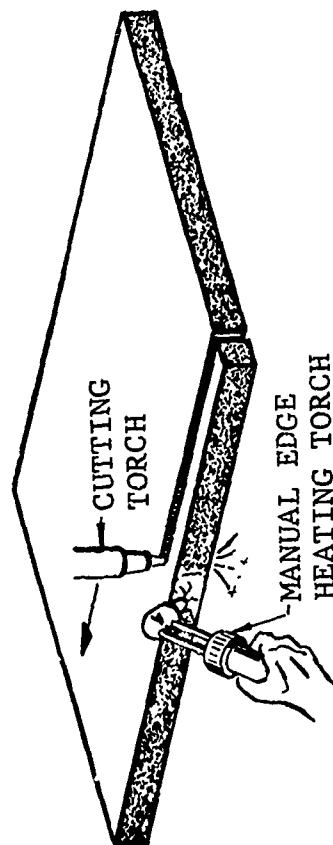
A preliminary stress relief test was conducted on a machined 10 Ni steel part. The purpose of this test was twofold; to determine if appreciable machining stresses were retained in the part and to determine if the part would warp when subjected to



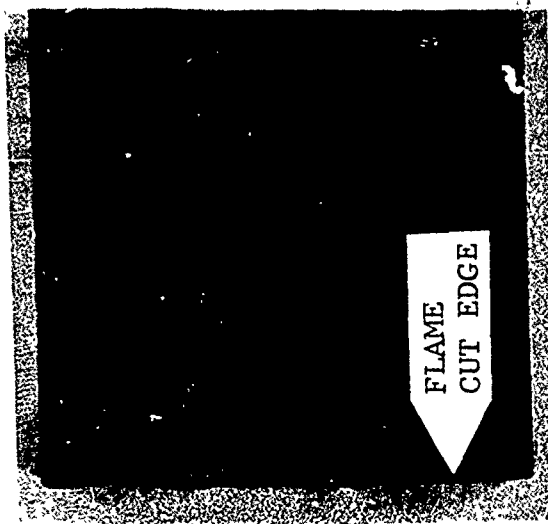
B. PREHEATING TECHNIQUE FOR EDGE STARTS



A. TYPICAL BLOW-OUT CONDITION



C. EDGE HEATING TO MINIMIZE WARPAGE



D. MACRO OF HEAT AFFECTED ZONE

Figure 5-86 FLAME CUTTING TECHNIQUES FOR 2 3/8 INCH THICK 10 N1 STEEL

stress relief temperatures. The part shown in Figure 5-87 was free-state stress relieved at 950°F for one hour and dimensional changes noted. A second 950 F stress relief was accomplished for four hours. The dimensional changes per side are shown. These readings were dial indicated and the net change by location is given. It should be noted that although only 0.002 inch movement was detected on this part, it may not be representative of large machined wide flanged or deep pocketed configurations. Subsequent to the above tests an engineering specification is being published. Since the age temperature was established at $950 \pm 10^\circ\text{F}$ for 8 hours, the post stress relieve treatment must heat at least 50°F below the age temperature to prevent over-aging; therefore, stress relieve at 900°F maximum. The producer indicates that such a stress relief will not affect material properties.

5.6 ASSEMBLY OF GROUP II PRODUCTION VERIFICATION

TEST SPECIMENS

5.6.1 603FTB052 Lower Lug to Rail Splice Assembly

A combination assembly and drill fixture was designed and fabricated to accurately locate and secure all detail parts for drill and ream operations. Two fixtures were necessary, one for the -A10 subassembly (consisting of details -31, -15, and -21) and another for the -A1 assembly (consisting of the -A10 subassembly and the remaining six detail parts). Prior to design of the fixtures, portable tooling kit accessories were selected from available stock to eliminate manufacture of special bushing, nosepieces, etc. The portable equipment power kits were altered using present motor kits to increase torque and reduce spindle speed.

The 603FTB052-A10 subassembly fixture is shown in Figure 5-88. Forty-nine $0.375 + 0.002/-0.000$ -inch diameter holes were drilled and reamed using the subassembly fixture. The detail parts were removed from the fixture, cleaned and deburred. FMS1043 sealant was applied to the faying surfaces of the parts and the Hi-lok fasteners were installed. After the sealant had cured, the Hi-lok fasteners were removed in areas of interference with other bolts and for fixture clearance.

The 603FTB052-A1 assembly fixture was loaded with the detail parts shown in Figure 5-89 plus the -A10 subassembly. Before any holes were drilled, detail part locations and hole edge distances were checked and detail parts were securely clamped. The first holes drilled were selected for threaded

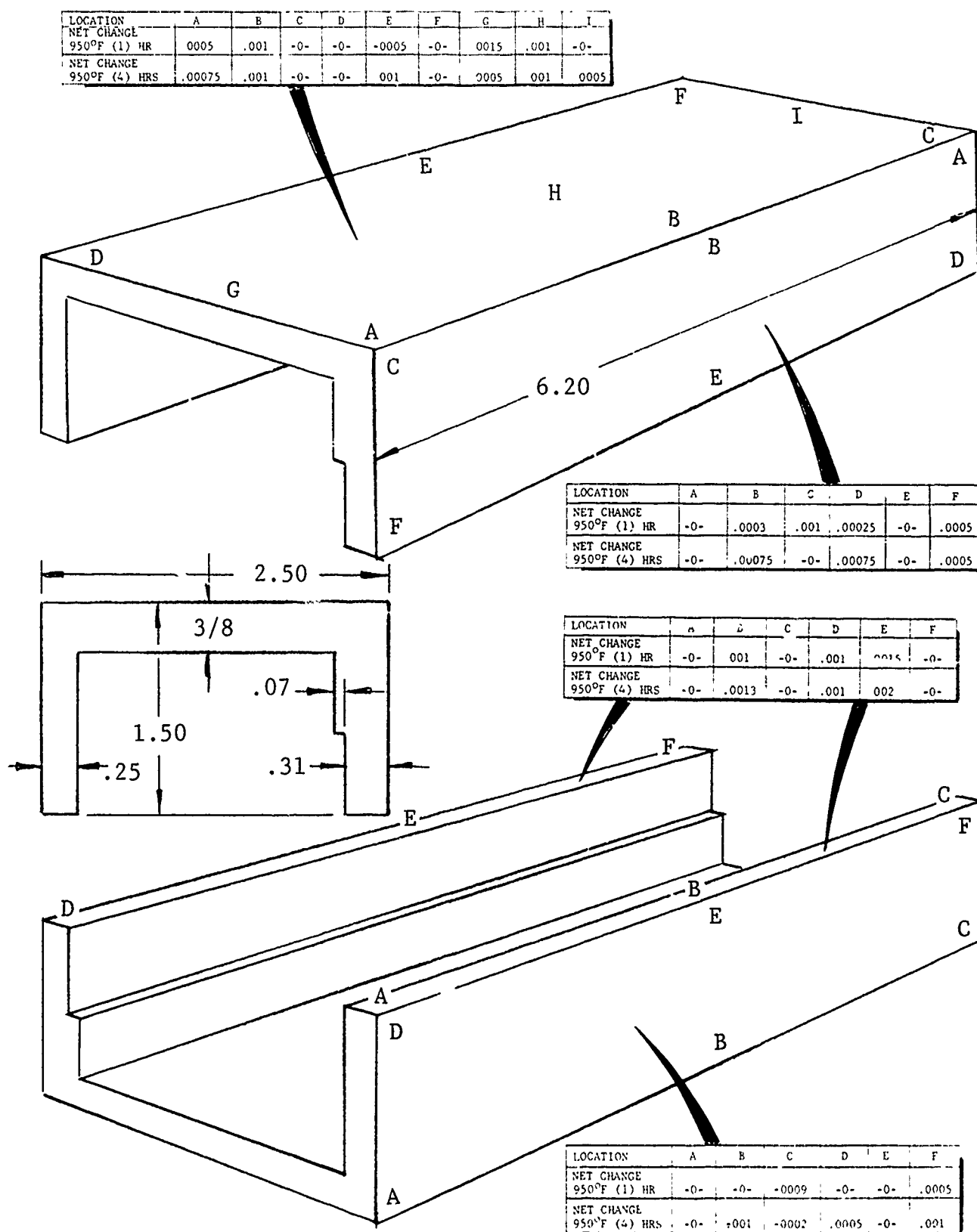


Figure 5-87 POST STRESS RELIEF DIMENSIONAL SURVEY

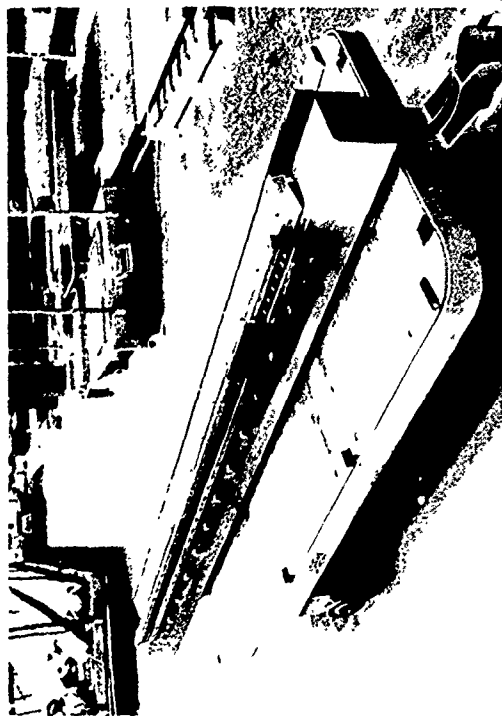


Figure 5-88 -A10 SUBASSEMBLY FIXTURE
FOR 603FTB052 TEST
COMPONENT

4-51110



4-54124

Figure 5-89 603FTB052 10 Ni STEEL
DETAILS (UNPAINTED PART
IS 6AL-4V TITANIUM)

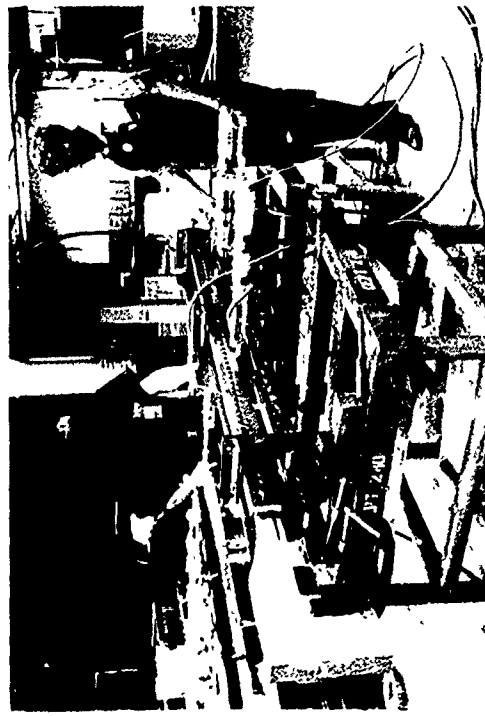


Figure 5-90 FIXTURE FOR
INSTALLING BOLTS IN
603FTB052-A1 ASSEMBLY
(-A10 ASSEMBLY SIDE)

1-51138



4-51139

Figure 5-91 FIXTURE FOR
INSTALLING BOLTS IN
603FTB052-A1 ASSEMBLY
(OPPOSITE SIDE)

tooling pin locations. The tooling pins clamped the fixture to the assembly in all splice and end locations. Undersize holes were drilled for Taper-lok bolts in 128 places in the assembly. All holes were drilled in accordance with Process Standard PS-22.02-6. Figures 5-90 and 5-91 show the drilling operation in the 603FTB052-A1 assembly fixture. The undersize holes drilled in the -A1 assembly included (58) 0.3594-inch diameter, (20) 0.4844-inch diameter and (50) 0.6094-inch diameter for piloted Taper-lok rough reamer operations.

The -A1 assembly fixture was disassembled and all detail parts were removed for cleaning and deburr operations. Figures 5-92 and 5-93 show the complete assembly after undersize holes were drilled and the fixture removed. After final deburr and cleaning operations were complete, FMS1043 sealant was applied to all faying surfaces in a reassembly sequence. Close tolerance tooling pins and setup bolts were installed in all even number holes. All setup bolts were torqued, the sealant allowed to cold flow, and all bolts were then retorqued.

After final sealant cure, the assembly was reloaded in the assembly fixture for Phase 1 taper-ream operation. Alignment was maintained using tapered tooling pins in the rough taper reamed holes before removing the undersize tooling pins. All odd numbered holes were rough taper reamed with depth controlled pre-set portable tool kits.

The drill and assembly fixture was removed from the assembly and final hole preparation was made on all open holes. This included multiflute reaming for proper hole finish, maintaining the correct head protrusion. After final inspection on the Phase 1 holes, the taper-lok bolts were installed. Prior to bolt installation, all bolts were cetyl alcohol coated. All of the bolts were torqued to maintain M263 Engineering Standard.

Phase 2 hole preparation and bolt installation was made identical to the Phase 1 operation sequence. Figures 5-94 and 5-95 show the 603FTB052 final assembly ready for instrumentation and test.

5.6.2 603FTB053 Lower Plate Centerline Splice Assembly

A drill plate was designed and fabricated for drilling and rough taper reaming twenty-five holes for 5/8-inch diameter taper-lok fasteners. The drill plate included locators for the splice plates and provisions to control the gap between the lower plates. Straight and taper tooling pins were also fur-

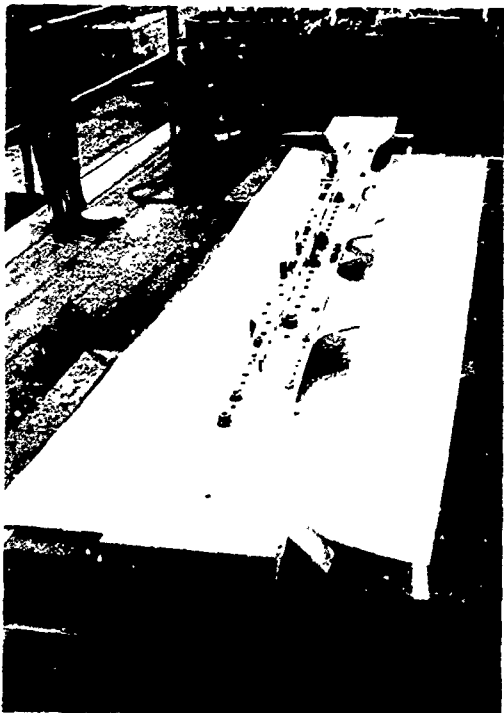


Figure 5-92 PARTIALLY ASSEMBLED
603FTB052 TEST COMPONENT
(-A10 ASSEMBLY SIDE)

Figure 5-93 PARTIALLY ASSEMBLED
603FTB052 TEST COMPONENT
(OPPOSITE SIDE)

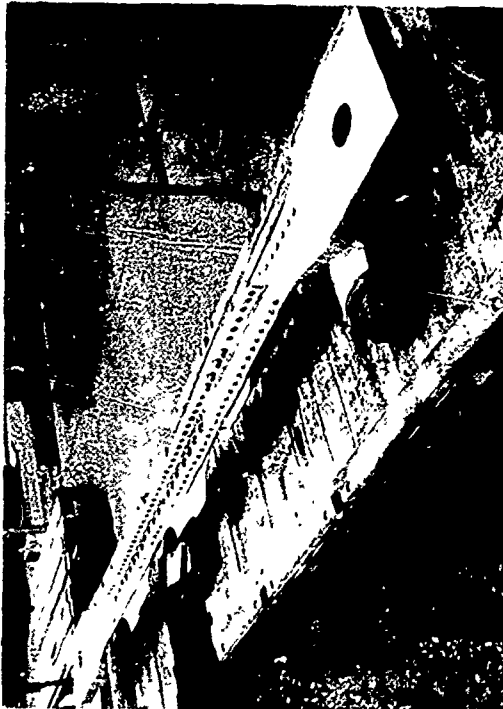


Figure 5-94 COMPLETED 603FTB052
TEST COMPONENT



Figure 5-95 COMPLETED 603FTB052
TEST COMPONENT
(OPPOSITE SIDE)

nished since the drill plate was moved from upper to lower surface several times during the drilling and reaming operations. The portable equipment kits and all accessories were identical to the ones used on the 603FTB052 assembly.

The drill plate was located on the assembled 603FTB053 details, rigidly secured, using large C-clamps. Inspection before any holes were drilled disclosed voids or gaps between the detail parts caused by accumulative tolerances in the lap splice design. FMS1048 liquid shim was applied to the splice plates to compensate for this mismatch. The four corner holes were then drilled. Threaded tooling pins were installed to secure the drill plate to the assembly and the remaining seven holes were drilled through the upper surface.

Close tolerance set-up bolts were installed in the assembly at four locations and the drill plate repositioned on the lower surface using tooling pins in the same holes to secure the drill plate. Fourteen holes were then drilled in the lower surface and all detail parts were marked to assure correct reassembly.

The drill plate was removed and the assembly was disassembled for cleaning and deburring. FMS1048 liquid shim was applied to the faying surfaces of the splice plates and parting agent applied to the lower plates at the splice areas. The reassembly sequence was made using twenty-five close tolerance set-up bolts torqued from center to outer edge to allow excess liquid shim to squeeze out. Final torque was made in one hour. After liquid shim cure, the parts were disassembled again for removal of the parting agent and final cleaning for FMS1043 sealant. Figure 5-96 shows detail parts ready for sealant application.

FMS1043 sealant was applied to all faying surfaces and final assembly of the 603FTB053 was made using set-up bolts in all odd numbered holes. The set-up bolts were retorqued and the sealant allowed to cure. All locators were removed from the drill plate for ease of locating and to reduce weight. Figure 5-97 shows the drill plate and the portable equipment kit used for Phase 1 rough taper reaming. All open holes were power reamed from the upper and lower surfaces and the drill plate removed. Phase 1 holes were final reamed and taper-lok bolts were installed.

Set-up bolts were removed from the even numbered holes and Phase 2 rough taper reaming, final carbide reaming and bolt installation was made in the same sequence as for Phase 1. Hole preparation and bolt installation was made in accordance with

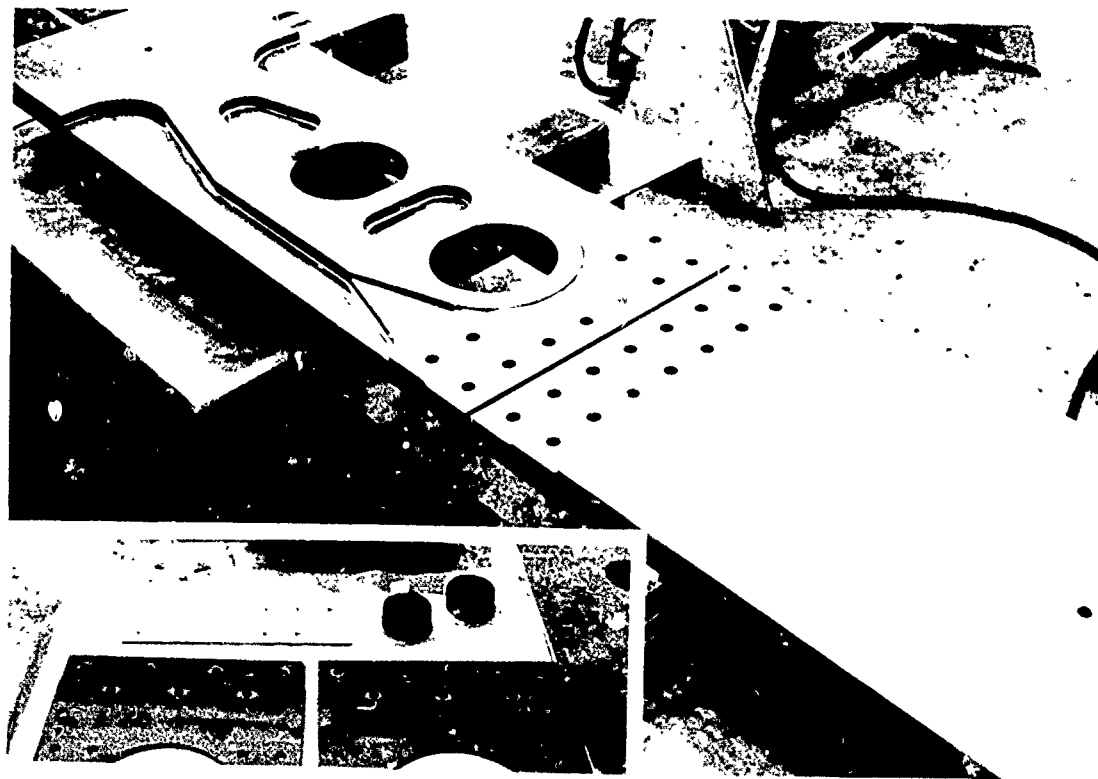


Figure 5-96 603FTB053 DETAIL PARTS READY FOR SEALING APPLICATION AND ASSEMBLY

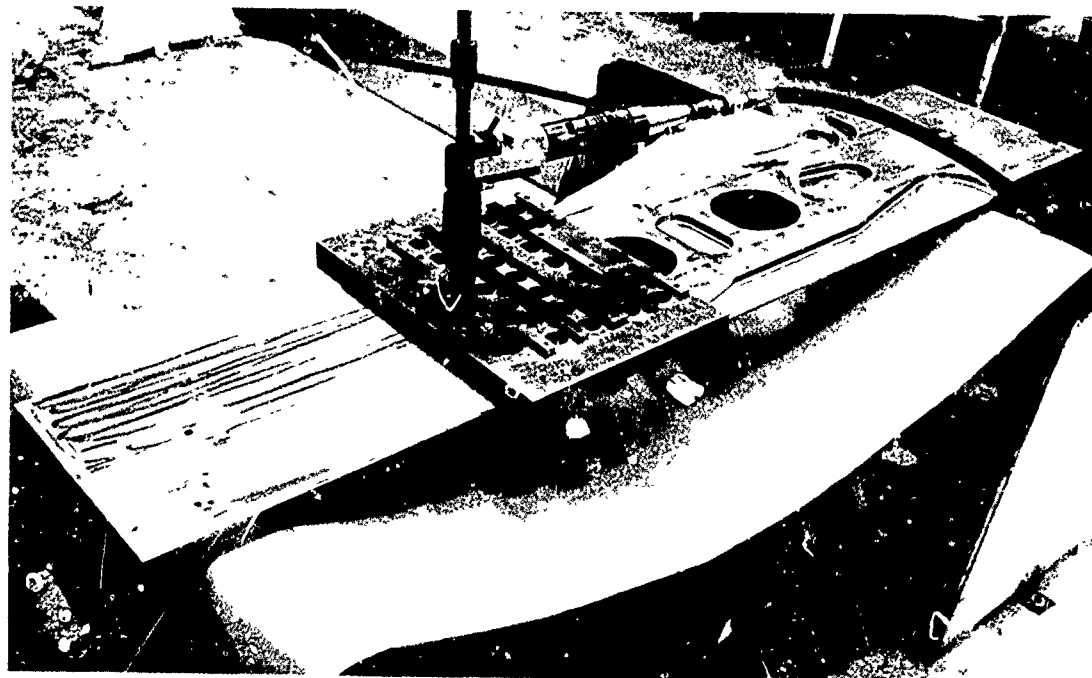


Figure 5-97 DRILL PLATE AND PORTABLE EQUIPMENT KIT USED TO POWER REAM TAPER-LOK HOLES IN 603FTB053

M263 Engineering specification. Figure 5-98 shows the completed 603FTB053-2 assembly.

5.6.3 603FTB035 Brazed Lower Plate Assembly

A one-piece picture frame drill plate was designed and fabricated for drilling and rough reaming the twelve 5/8-inch diameter taper holes in the brazed assembly. The fixture attached to four corner bolt holes used for mounting the support lugs. All twelve holes were drilled and power reamed complete, without removing the fixture, since no deburr or sealant operations were required. The drill plate was then removed and the final carbide reaming was completed in all twelve holes. The hole finish and protrusion was verified by Quality Control. The twelve taper-lok bolts were installed and torqued per M263 Engineering specification.

The end lugs were attached with straight shank bolts in matched hole patterns that were drilled in the detail parts using a N/C tape controlled American drill press. The assembled 603FTB035 is shown in Figure 5-99 prior to boring the test fixture attach holes.

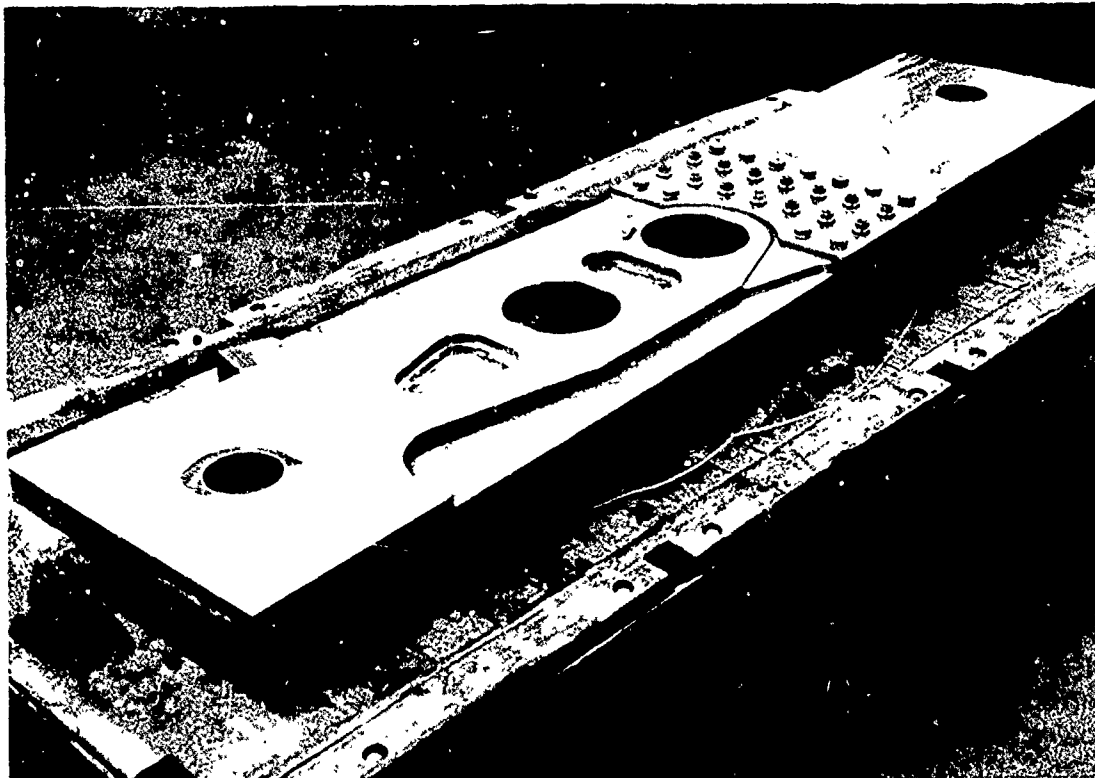
5.7 MACHINING OF 603FTB043 UPPER COVER

GROUP II TEST SPECIMEN

The 603FTB043 test specimen was numerically control (N/C) machined from a 6Al-4V beta annealed titanium billet. Excess material was face milled from all surfaces of the billet and starter holes drilled in the pocket areas prior to N/C machining. Figure 5-100 shows the part completely machined except for tooling tab removal.

Pocket milling starter holes (2.5-inch diameter by 3.170-inch depth) were N/C drilled on an American radial arm drill press. A 2.5-inch diameter spade drill was operated at 31 RPM and a feed rate of .004 inch per revolution.

Milling was accomplished on an Onsrud N/C milling machine. Surface material was removed using a 6-inch diameter face mill with 6 inserted carbide teeth. Feeds and speeds were 50 RPM (80 SFM) 2.0-IPM feed rate and 0.0065-inch feed per tooth. The pockets were profiled with 8-flute, 2-inch diameter end mills. Feeds and speeds were 100 RPM (52 SFM), 3.5-IPM feed, and 0.0044-inch feed per tooth.



4-54295

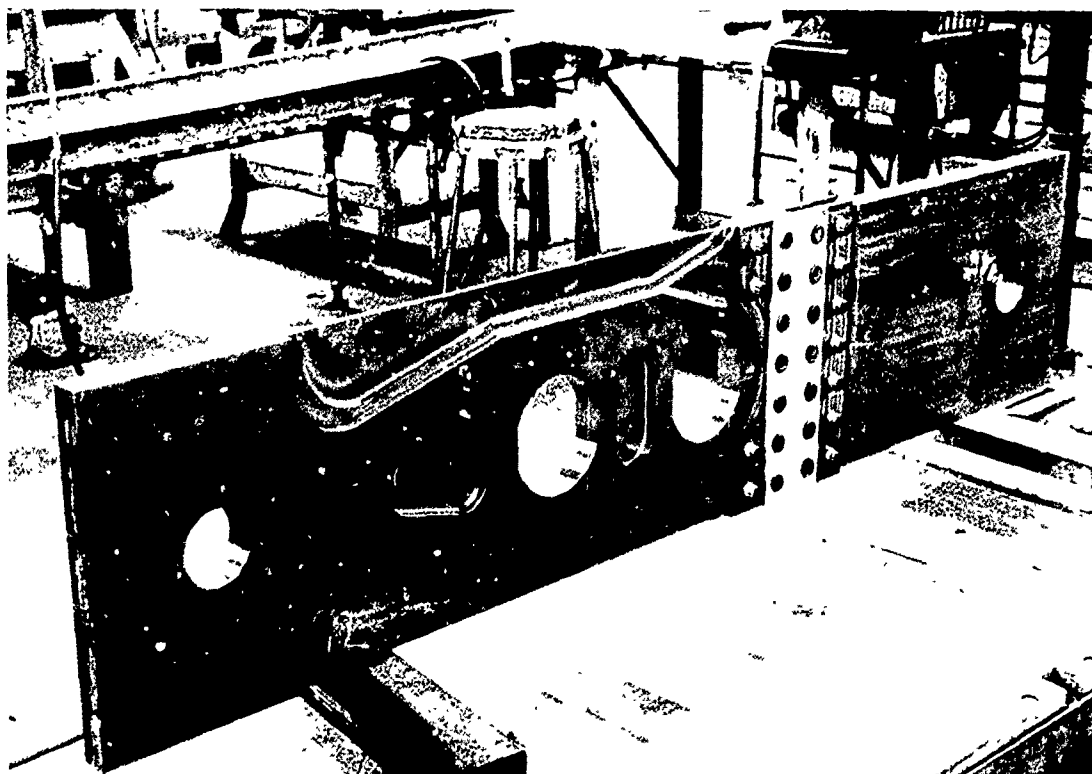


Figure 5-98 ASSEMBLED 603FTB053 (TOP SIDE AND BOTTOM SIDE)

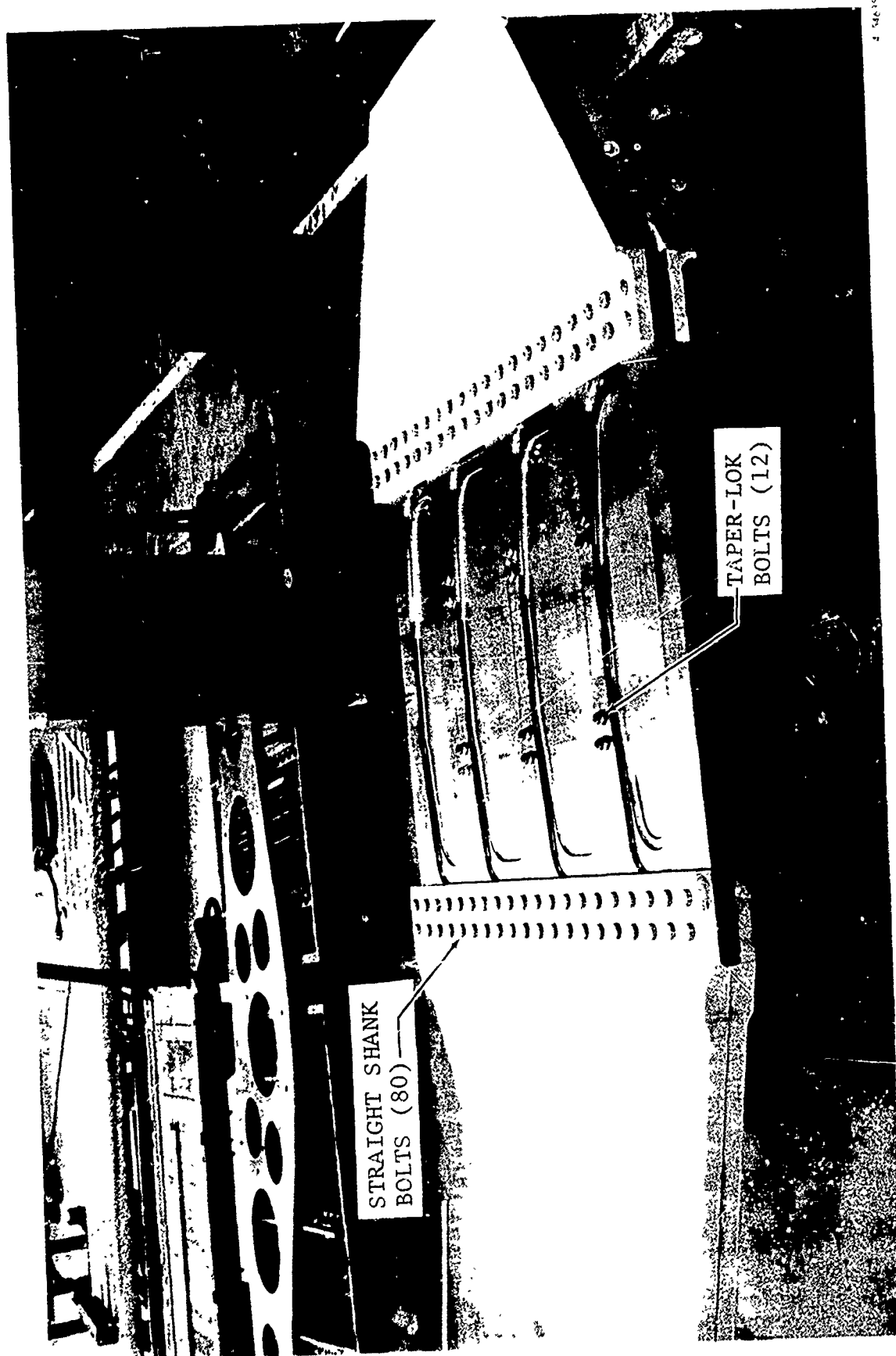
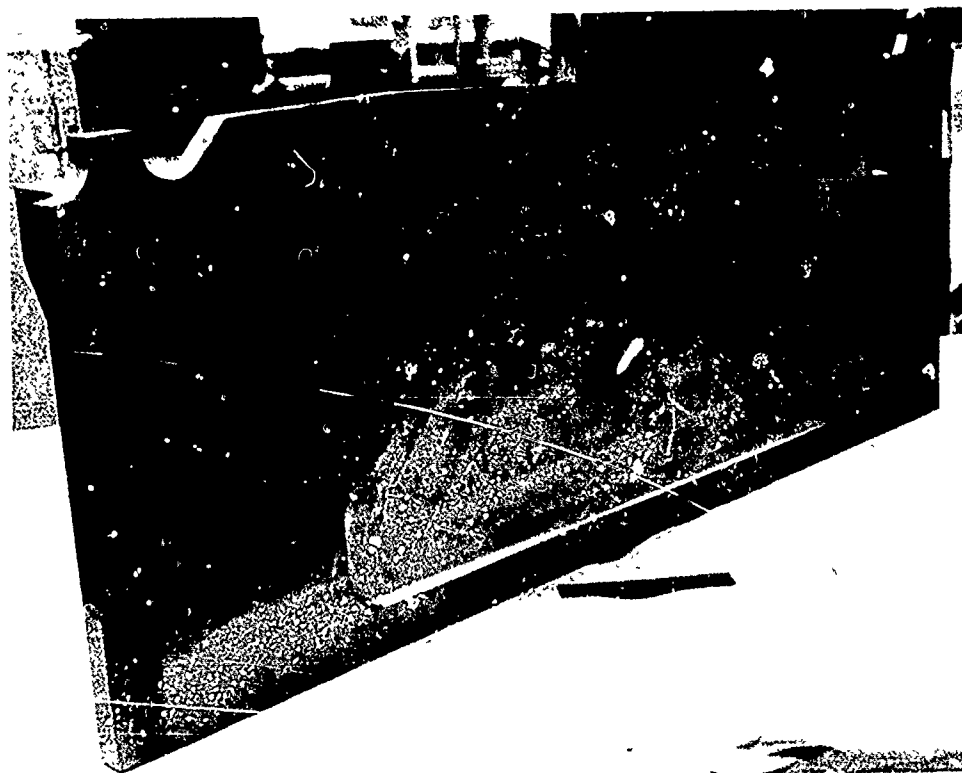


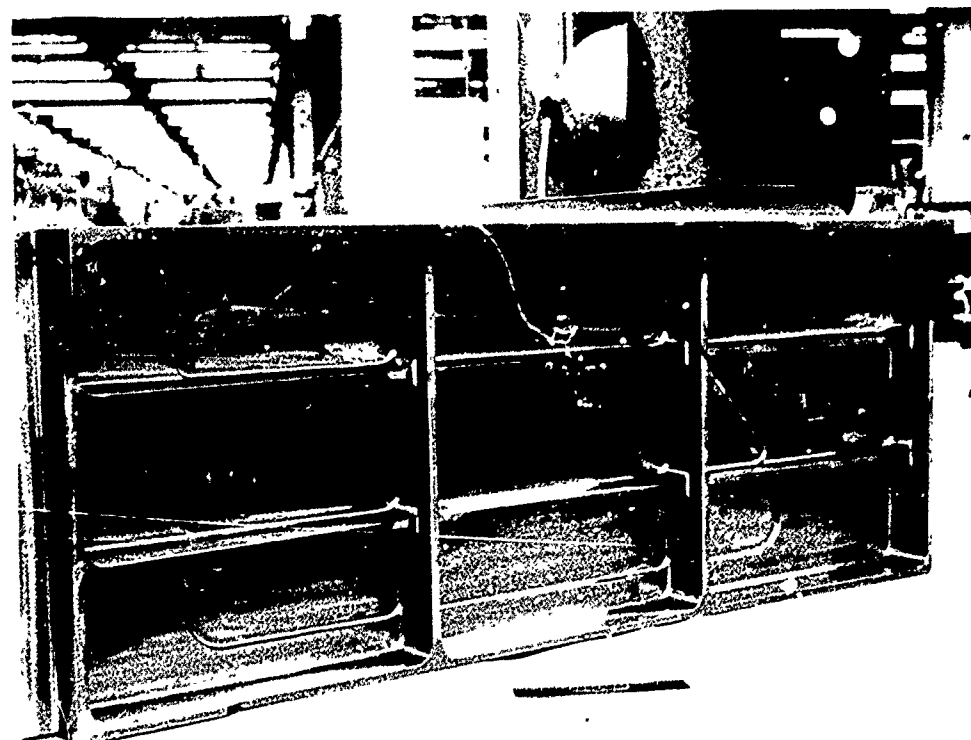
Figure 5-99 ASSEMBLED 603FTB035 TEST COMPONENT



4-54156

(OUTER SURFACE)

(OPPOSITE SIDE)



4-54157

Figure 5-100 603FTB043 UPPER COVER GROUP II TEST SPECIMEN

Cutter life was reduced approximately 20 percent in machining the beta annealed 6Al-4V titanium as compared to conventionally annealed material.

A P P E N D I X A

- o ELECTRON BEAM WELD SCHEDULES
- o ELECTRON BEAM CURRENT TRACES

ELECTRON BEAM SCHEDULES

Date 9-25-73

Gun-to-Work Distance 3.5 Inches

Weld No.	Mat'l	Thickness inch	Weld Type	Wire Feed ipm	Weld Speed ipm	Weld Axis	Current ma	Voltage kv	Focus Pot.	Oscillator Freq.	Attenu.	Current Trace	Filament	Remarks
(1)	D6ac	1.00	BOP	30	15	X	460	34.5	5.22	5Kc	-9	✓	66 amps.	
(2)	"	"	"	30	15	X	180	18.0	5.22	5Kc	-7	✓	"	
			Parameter development weld - (good setting)											
(1)	10Ni.	1.00	BOP	30	15 / 20	X	400	34.5	5.22	5Kc	-9	✓	66 amps.	
(2)	"	"	"	30	12 / 18	X	160	18.0	5.22	5Kc	-7	✓	"	
			Parameter development weld.											
(1)	10Ni.	1.00	BOP	30	18 / 15	X	440	34.5	5.22	5Kc	-9	✓	66 amps.	
(2)	"	"	"	30	15	X	160	18.0	5.22	5Kc	-7	✓	"	
			Appearance Fair -											
			Parameter development weld.											
(1)	10Ni.	1.00	BOP	30	18	X	400	34.5	5.22	5Kc	-9	✓	66 amps.	
(2)	"	"	"	30	18	X	160	18.0	5.22	5Kc	-7	✓	"	
(3)	"	"	"	30	15	X	160	16.0	5.22	5Kc	-7	✓	"	
			Root uniform, face underfilled, required 3 passes.											

ELECTRON BEAM SCHEDULES

Gun-to-Work Distance <u>3.5</u> Inches										Date <u>10-4-73</u>			
Weld No.	Mat'l	Thickness	Weld Type	Wire Feed ipm	Weld Speed ipm	Weld Axis	Mid Point		Remarks	Current Trace	Filament	Oscillator Freq.	Attenu.
							Weld	Current					
		inch		ipm				ma	kv			Focus Pot.	
X-1(1)	10Ni.	1.00	BOP	30	18	x		460	34.5	5.22	5Kc	-9	68 amps
(2)	"	"	"	30	15	x		180	18.0	5.22	5Kc	-8	"
			Root good, face underfilled.										
X-2(1)	10Ni.	1.00	BOP	30	18	x		460	34.5	5.22	5Kc	-9	68 amps
(2)	"	"	"	30	18	x		180	18.0	5.22	5Kc	-7	"
			Root good, face fair.										
X-3(1)	10Ni.	1.00	BOP	30	18	x		420	34.5	5.22	5Kc	-9	68 amps
(2)	"	"	"	35	18	x		160	18.0	5.22	5Kc	-9	"
			Root good, face irregular.										
			Parameter development welds.										
H-17(1)	10Ni.	1.6	Butt	30	12.8	x		680	47.5	5.22	5Kc	-7	67 amps
(2)	"	"	"	30	15.8	x		200	20.0	5.22	5Kc	-7	"
			X-ray - porosity - cracks.										
			Weld cut out and inspection through the longitudinal plane.										

ELECTRON BEAM SCHEDULES

Date 8-7-73

Gun-to-Work Distance 3.5 Inches

Weld No.	Mat'l	Thickness	Weld Type	Wire Feed	Weld Speed	Weld Axis	Current	Voltage	Focus Pot.	Oscillator Freq.	Atten.	Current Trace	Filament	Remarks
X-1(1)	10Ni.	2.00"	BOP	30	28	X	700	47.5	5.22	8Kc	-9	✓	65 amps	
(2)	"	"	"	30	26	X	200	20.0	5.22	"	-6	✓	"	
		appearance -	Face good,	root globular,	cutout for inspection	- X-ray shows								
		very fine cracks	- 5/8 inch	from face.										
X-2(1)	10Ni.	2.00"	BOP	30	30	X	700	47.5	5.22	8Kc	-9	✓	65 amps	
(2)	"	"	"	30	26	X	200	20.0	"	"	-6	✓	"	
		Face underfilled	because of heat buildup.											
		Root globular	- cutout for NDI - X-ray - cracks.											
X-3(1)	10Ni.	2.00	BOP	30	30	X	630	46.0	5.22	8Kc	-9	✓	65 amps	
(2)	"	"	"	30	26	X	200	20.0	5.22	8Kc	-6	✓	"	
		Face good -	Root globular -											
		X-ray shows	porosity and hairline cracks.											
X-4(1)	10Ni.	2.00	BOP	OPP	30	X	620	45.0	5.22	8Kc	-9	✓	65 amps	
(2)	"	"	"	30	26	X	200	20.0	"	8Kc	-6	✓	"	
		BOP =	Bead on plate.				X-ray	cracks.						

ELECTRON BEAM SCHEDULES

Gun-to-Work Distance 3.5					Inches			AMAVS			Date 3-27-73			
Weld No.	Mat'l	Thickness	Weld Type	Wire Feed ipm	Weld Speed ipm	Weld Axis	Current ma	Voltage kv	Focus Pot.	Oscillator Freq.	Atten.	Current Trace	Filament	Remarks
		inch		ipm	ipm									
H-1(1)	Hyl80 (10Ni)	1.00	Butt	30	28	X	560	34.5	5.22	8Kc	-9	✓	65 amps	
(2)	"	1.00	Butt	30	30	X	380	25.0	"	"	-9	✓	"	
(3)	"	1.00	Butt	0	30	X	220	18.0	"	"	"	✓	"	
(4)	"	1.00	Butt	30	28	X	160	16.0	"	"	-6	✓	"	
		4th pass made to determine effects of tempering pass.												
H-2(1)	10Ni.	.500	Butt	30	28	X	380	27.5	5.22	8Kc	-9	✓	65 amps	
(2)	"	.500	Butt	30	28	X	180	16.0	"	"	-7	✓	"	
(3)	"	.500	Butt	30	28	X	160	16.0	"	"	-7	✓	"	
				(Good Setting)										
H-3(1)	10Ni.	.500	Butt	30	28	X	340	27.5	5.22	8Kc	-9	✓	65 amps	
(2)	"	.500	Butt	30	28	X	160	16.0	"	"	-7	✓	"	
(3)	"	.500	Butt	30	27	X	160	16.0	"	"	-6	✓	"	
H-4(1)	10Ni.	.500	Butt	30	28	X	340	27.5	5.22	8Kc	-9	✓	65 amps	
(2)	"	.500	Butt	30	27	X	160	16.0	"	"	-7	✓	"	

ELECTRON BEAM SCHEDULES

Gun-to-Work Distance 3.5 Inches														Date 5-14-73	
Weld No.	Mat'l	Thickness inch	Weld Type	Wire Feed ipm	Weld Speed ipm	Weld Axis	Current ma	Voltage kv	Focus Pot.	Oscillator Freq.	Attenu.	Current Trace	Filament	Remarks	
H-5(1)	10Ni.	.500	Butt	30	30	X	350	27.5	5.22	8Kc	-9	✓	65 amps		
(2)	"	.500	Butt	30	25	X	140	16.0	"	"	-6	✓	"		
(3)	"	.500	Butt	30	25	X	140	15.0	"	"	-6	✓	"		
(4)	"	.500	Butt	30	25	X	150	16.0	"	"	-4	✓	"		
		X-ray OK - Weld area cut out for NDI.													
H-10(1)	10Ni.	.500	Butt	30	30	X	330	27.5	5.22	8Kc	-8	✓	65 amps		
(2)	"	.500	Butt	30	28	X	160	16.0	4.90	OFF		✓	" (Defocused)	pass.	
		(Weld Shrinkage measurements)													
		X-ray OK - Magnaflux OK													
		Will be used for impact and tensile test.													
H-11(1)	10Ni.	.500	Butt	30	30	X	340	27.5	5.60	8Kc	-9	✓	68 amps		
(2)	"	.500	Butt	30	28	X	160	16.0	5.60	8Kc	-6	✓	"		
		(Weld shrink measurements).													
		X-ray OK. Ultrasonics OK. - 2 defects													
		will be used for impact and tensile test.													

ELECTRON BEAM SCHEDULES

Gun-to-Work Distance 3.5 Inches													Date 8-22-73	
Weld No.	Mat'l	Thickness	Weld Type	Wire Feed ipm	Weld Speed ipm	Weld Axis	Current ma	Voltage kv	Focus Pot.	Oscillator Freq.	Atten.	Current Trace	Filament	Remarks
H-12(1)	10Ni.	.500	Butt	30	30	X	320	27.5	5.22	8Kc	-9	✓	66 amps.	
(2)	"	"	"	30	28	X	140	16.0	"	"	-7	✓	"	
		Appearance fair - root narrow.												
		Wire feed intermittent - 1st pass.												
								N.D.I.	Specimen	MD-3232-1				
H-13(1)	10Ni.	.500	Butt	30	30	X	300	27.5	5.22	5Kc	-9	✓	67 amps.	
(2)	"	"	"	30	26	X	160	18.0	5.22	5Kc	-6	✓	"	
		Appearance - face good, root narrow.												
								N.D.I.	Specimen	MD-3232-2				
H-14(1)	10Ni.	2.00	Butt	30	28	X	680	47.5	5.22	5Kc	-8	✓	66 amps.	
(2)	"	"	"	30	25	X	160	18.0	5.22	5Kc	-6	✓	"	
		Arc out first pass. Repaired -												
		Face good - root globular -												
		X-ray shows gross voids.												

ELECTRON BEAM SCHEDULES

Date 8-21-73

Gun-to-Work Distance 3.5 Inches

or noted.

Weld No.	Mat'l	Thickness	Weld Type	Wire Feed	Weld Speed	Weld Axis	Current	Voltage	Focus Pot.	Oscillator Freq.	Atten.	Current Trace	Filament	Remarks
		inch		ipm	ipm		ma	kv						
Fatigue	10Ni.	.900	Butt	OFF	26	X	440	34.5	5.22	5Kc	-8	✓	66 amps	
Specimen	10Ni.	.900	Butt	30	24	X	160	18.0	5.22	5Kc	-6	✓	"	
E.T.L.		Appearance	- Face good, root good.											
		Bolt hole failure	- new end welded on to complete											
		fatigue test.	X-ray OK.											
		3.5 inch focal point	- 3 inch gun to work distance											
H-15(1)	10Ni.	1.6	Butt	30	13	X	660	47.5	5.22	5Kc	-7	✓	67 amps	
(2)	"	"	"	30	13	X	200	20.0	5.22	5Kc	-6	✓	"	
		Appearance	face wide .375 inch, root uniform.											
		Weld cut out,	- longitudinal X-ray shows porosity and cracks.											
H-15A(1)	10Ni.	1.6	BOP	30	13	X	660	47.5	5.22	5Kc	-7	✓	67 amps	
(2)	"	"	"	30	13	X	200	20.0	5.22	Kc	-7	✓	"	
		Appearance	- face good, root good.											
		X-ray scattered	porosity, mid point cracks.											

ELECTRON BEAM SCHEDULES

Date 10-9-73

Gun-to-Work Distance 3.5 Inches MP

Weld No.	Mat'l	Thickness	Weld Type	Wire Feed ipm	Weld Speed ipm	Weld Axis	Current ma	Voltage kv	Focus Pot.	Oscillator Freq.	Attenu.	Current Trace	Filament	Remarks
H-18(1)	10Ni.	.900	Butt	30	18	x	440	34.5	5.22	5Kc	-9	✓	65 amps.	
(2)	"	"	"	30	18	x	180	18.0	5.22	5Kc	-9	✓	"	
(3)	"	"	"	30	18	x	160	18.0	5.22	5Kc	-7	✓	"	
		Part No. 603R-100-11-5	-H-18											
		Magnaflux shows	root crack -											
		X-ray rejection,	processing stopped.											
H-19(1)	10Ni.	.900	Butt	off	18	x	440	34.5	5.22	5Kc	-9	✓	65 amps.	
(2)	"	"	"	30	18	x	160	18.0	5.22	5Kc	-9	✓	"	
(3)	"	"	"	30	18	x	160	18.0	5.22	5Kc	-7	✓	"	
		Part No. 603R-100-11-5	-H-19											
		Appearance	face-good, root - good.											
		Magnaflux shows	indications on weld face of surface cracks but this											
		inspection is inconclusive	because dye penetrant shows an acceptable weld.											
		X-ray shows starting	and termination cracks-remainder of weld acceptable.											

ELECTRON BEAM SCHEDULES

Gun-to-Work Distance 3.5 Inches														Date 10-10-73	
Weld No.	Mat'l	Thickness	Weld Type	Wire Feed	Weld Speed	Weld Axis	Current	Voltage	Focus Pot.	Oscillator Freq.	Atten.	Current Trace	Filament	Remarks	
		inch		ipm	ipm		ma	kv							
H-20(1)	10Ni.	1.6	Butt	off	13	x	700	47.5	5.22	5Kc	-8	✓	65 amps.		
(2)	"	"	"	30	13	x	200	20.0	5.22	5Kc	-8	✓	"		
		Parameter development joint.													
H-21(1)	10Ni.	1.6	BOP	30	10 18	x	540	41.0	5.22	5Kc	-9	✓	65 amps.		
(2)	"	"	"	30	18	x	200	20.0	5.22	5Kc	-7	✓	"		
(3)	"	"	"	30	15	x	200	20.0	5.22	5Kc	-6	✓	"		
		Weld bend cross section shows bulge and included cracks.													
		Gun to work distance changed to 2.7 inches.													
H-22(1)	10Ni.	1.6	BOP	30	10	x	540	41.0	5.22	5Kc	-9	✓	65 amps.		
(2)	"	"	"	30	10	x	200	20.0	5.22	5Kc	-8	✓	"		
(3)	"	"	"	30	10	x	200	20.0	5.22	5Kc	-7	✓	" Osc. too wide.		
H-23(1)	10Ni.	1.6	Butt	30	10	x	560	41.0	5.22	5Kc	-9	✓	65 amps	Arc out	
(2)	"	"	"	30	10	x	200	20.0	5.22	5Kc	-9	✓	"		
(3)	"	"	"	30	10	x	200	20.0	5.22	5Kc	-8	✓	"		

ELECTRON BEAM SCHEDULES

Date 10-12-73

Gun-to-Work Distance 3.5 Inches Fx

[illegible]

ELECTRON BEAM SCHEDULES

Date 10-17-73

Gun-to-Work Distance 3.5 Inches

Weld No.	Mat'l	Thickness	Weld Type	Wire Feed	Weld Speed	Weld Axis	Current	Voltage	Focus Pot.	Oscillator Freq.	Attenu.	Current Trace	Filament	Remarks
H-26(1)	10Ni	1.6	Butt	30	12	x	480	41.0	5.22	5Kc	-9	✓	65 amps.	
(2)	"	"	"	30	12	x	200	20.0	5.22	5Kc	-10	✓	"	
(3)	"	"	"	30	12	x	200	20.0	5.22	5Kc	-7	✓	"	
		Appearance	face good,				root good.							
		Macro	of run out				show cross	section	bulge					
		5/8 inch	from face				surface.							
		Ultrasonic	inspection -				immersion,	C scan	recording					
		show	cracks.											
H-27(1)	10Ni	1.6	Butt	30	12	x	460	41.0	5.22	5Kc	-9	✓	65 amps.	
(2)	"	"	"	30	12	x	200	20.0	5.22	5Kc	-9	✓	"	Wire fouled
(3)	"	"	"	30	12	x	200	20.0	5.22	5Kc	-8	✓	"	
		Macro	of tab				shows cross	section	bulge with	micro-fissure		in the		
		vertical	plane.											
		Ultrasonic	inspection -				shows intermittent	cracks.						

ELECTRON BEAM SCHEDULES

Date 10-7-73Gun-to-Work Distance 3.5 Inches

Weld No.	Mat'l	Thickness inch	Weld Type	Wire Feed ipm	Weld Speed ipw	Weld Axis	Current ma	Voltage kv	Focus Pot.	Oscillator Freq. Atten.	Current Trace	Filament	Remarks
M-1(1)	10Ni.	.500	Butt	30	24	x	340	27.5	5.22	5Kc	✓	65 amps.	
(2)	"	"	"	30	24	x	180	18.0	5.22	5Kc	✓	"	
			Appearance - face good, root good.										
			X-ray OK. Send to ETL for fatigue test.										
H-28(1)	10Ni.	1.6	Butt	30	14	x	560	41.0	5.22	5Kc	✓	65 amps.	Wire fouled
(2)	"	"	"	30	12	x	180	20.0	5.22	5Kc	✓		because of
			Appearance, face under cut on high side.										
			Root good, Weld shrink measurements.										
			Mismatch of .050 inch.										
			Ultrasonics show intermittent cracks										
			verified by macrosection.										
H-29(1)	10Ni.	1.6	Butt	30	15	x	580	41.0	5.22	5Kc	✓	65 amps.	
(2)	"	"	"	30	15	x	200	20.0	5.22	5Kc	✓	"	
(3)	"	"	"	30	12	x	200	20.0	5.22	5Kc	✓	"	
			Weld shrink measurements.										
			Ultrasonics shows intermittent cracks										
			verified by macrosection.										

ELECTRON BEAM SCHEDULES

Date 10-22-73

Gun-to-Work Distance 3.5 Inches

Weld No.	Mat'l	Thickness	Weld Type	Wire Feed ipm	Weld Speed ipm	Weld Axis	Current ma	Voltage kv	Focus Pot.	Oscillator Freq.	Atten.	Current Trace	Filament	Remarks
H-30(1)	10Ni.	1.6	Butt	30	15	x	540	41.0	5.22	5Kc	-9	✓	65 amps.	
(2)	"	"	"	30	15	x	180	20.0	5.22	5Kc	-9	✓	"	
(3)	"	"	"	30	12	x	180	20.0	5.22	5Kc	-8	✓	"	
		Push up tabs			Appearance face good.									
		Root good			Ultrasonics shows cracks.									
		Macrosection verifies			hot cracking									
H-31(1)	10Ni.	1.6	Butt	30	15	x	580	41.0	5.22	5Kc	-9	✓	65 amps.	
(2)	"	"	"	30	15	x	200	20.0	5.22	5Kc	-9	✓	"	
(3)	"	"	"	30	12	x	200	20.0	5.22	5Kc	-8	✓	"	
		Welded tabs.												
		Appearance face good			root good.									
		Ultrasonics show cracks.												
		Macrosection show good geometry,			and no defects.									
H-32(1)	10Ni.	1.6	Butt	0	10	x	450	38.0	5.22	5Kc	-8	✓	65 amps.	
(2)	"	"	"	0	10	x	380	30.0	5.22	5Kc	-7	✓	"	
(3)	"	"	"	30	10	x	200	20.0	5.22	5Kc	-6	✓	"	

ELECTRON BEAM WELDING SCHEDULE

Schedule Number _____ Date 10-12-73
 Part Number MD 32.33 Part Name _____ Material Type 10Ni (Hy 180)
 Serial Number F 530647 Tool Number _____ Mat'l. Thick 1.6"
-H-24 Filler Wire Type Low alloy Hy180/220 Diameter .062
 (10Ni Chr.-Mo. Co)

UPPER CONTROL PANEL			
HV START Delay	MOTOR START Delay	HIGH VOLTAGE Initial KV	SPEED ADJUSTMENT Initial and Final
0 0 2	0 0 2	4 0 0	0 5 9
Seconds	Seconds	Slope	Run
<input checked="" type="checkbox"/> 15 30 60 120	<input checked="" type="checkbox"/> 15 30 60 120	0 1 4	0 4 5

OSCILLATOR			
AXIS X <input checked="" type="checkbox"/> Y <input type="checkbox"/>	FREQUENCY, KC	0 5 0	RANGE X 1 0 0
ATTENUATION, Db 0 0 0	METER RANGE	2 0	METER READING - 9

CENTER CONTROL PANEL			SKETCH OF JOINT
BEAM CURRENT, MA	HIGH VOLTAGE, KV	TRAVEL, IPM	
Pass 1 5 8 0	4 1. 0	1 2. 0	
Pass 2 2 0 0	2 0. 0	1 2. 0	
Pass 3			
FOCUS CURRENT METER 5 2 2 DC Amps.	GUN FILAMENT METER 0 6 5 AC Amps.	FILAMENT ADJUST POT. 0 7 6	TYPE OF JOINT BUTT

GUN ELEMENTS			
GUN TYPE, KV	6 0	BIAS	On <input type="checkbox"/> Off <input checked="" type="checkbox"/> 2
FILAMENT, MA	5 0 0	METER, AC VOLTS	
CATHODE, MA	7 5 0	VOLTAGE ADJUST.	
ANODE, KV/MA	7 5 0	Mid-point focus	
SPACER, Inches	0 0 0	GUN-TO-WORK DISTANCE, Inches 3 . 5	

OPERATOR'S STATION CONTROL			
X-AXIS	On <input checked="" type="checkbox"/> Off <input type="checkbox"/>	Y-AXIS	On <input type="checkbox"/> Off <input type="checkbox"/>
DIRECTION	Fwd. <input type="checkbox"/> Rev. <input checked="" type="checkbox"/>	DIRECTION	Fwd. <input type="checkbox"/> Rev. <input type="checkbox"/>
TRAVEL SPEED, IPM	1 2. 0	TRAVEL SPEED, IPM	
WIRE FEED	On <input checked="" type="checkbox"/> Off <input type="checkbox"/>	INCH PER MINUTE	3 0. 0
BEAM ALIGNMENT	<input type="checkbox"/> NA <input type="checkbox"/>	FOCUS ADJUST.	5 2 2
HIGH VOLTAGE ADJUST.	<input type="checkbox"/> NA <input type="checkbox"/>	AVR	Lock <input type="checkbox"/> Unlock <input checked="" type="checkbox"/>

X-Ray Serial Number _____ Operator _____
 Mag. Inspection _____ MR&D Engineer J. C. Collins
 Acceptance Standard _____ Process Control _____
 Metallurgical Exam. _____

ELECTRON BEAM WELDING SCHEDULE

Schedule Number	FMR 60-2154	Date	8-7-73
Part Number		Part Name	
Serial Number		Material Type	10Ni. (Hy 180)
		Tool Number	
		Mat'l. Thick	2.00"
PARAMETER		Filler Wire Type	Low alloy Hy 180/220
Development		Diameter	0.062"
			(10Ni. - Chr., Mo., Co.)

UPPER CONTROL PANEL

HV START Delay			MOTOR START Delay			HIGH VOLTAGE				SPEED ADJUSTMENT Initial and Final								
						Initial KV		Final										
0	0	2	0	0	5	4	5.0	0	5	9								
Seconds			Seconds			Slope		Slope		Run								
20	15	30	60	120	20	15	30	60	120	0	0	2	0	4	5			

OSCILLATOR

AXIS X	X	Y		FREQUENCY, KC	0	8	0	RANGE X	1	0	0
ATTENUATION, Db			0	METER RANGE	2	0		METER READING		-	9

CENTER CONTROL PANEL

BEAM CURRENT, MA			HIGH VOLTAGE, KV			TRAVEL, IPM					
Pass 1	7	0	0	4	7.	5	3	0	0		
Pass 2	2	0	0	2	0.	0	3	0.	0		
Pass 3											
FOCUS CURRENT METER			GUN FILAMENT METER			FILAMENT ADJUST POT.			TYPE OF JOINT		
5	2	2	DC Amps.	0	6	6	AC Amps.	0	7	6	BUTT

GUN ELEMENTS

GUN TYPE, KV	6	0		BIAS	On		Off	X
FILAMENT, MA	5	0	0	METER, AC VOLTS				
CATHODE, MA	7	5	0	VOLTAGE ADJUST.				
ANODE, KV/MA	7	5	0	MID point, and as noted				
SPACER, inches	0	0	0	GUN-TO-WORK DISTANCE, inches	3		.5	

OPERATOR'S STATION CONTROL

X-AXIS	On	<input checked="" type="checkbox"/>	Off	<input type="checkbox"/>	Y-AXIS	On	<input type="checkbox"/>	Off	<input type="checkbox"/>
DIRECTION	Fwd.	<input type="checkbox"/>	Rev.	<input checked="" type="checkbox"/>	DIRECTION	Fwd.	<input type="checkbox"/>	Rev.	<input type="checkbox"/>
TRAVEL SPEED, IPM	<input type="text" value="3"/> <input type="text" value="0"/> <input type="text" value="0"/>				TRAVEL SPEED, IPM	<input type="text" value=""/> <input type="text" value=""/> <input type="text" value=""/>			
WIRE FEED	On	<input checked="" type="checkbox"/>	Off	<input type="checkbox"/>	INCH PER MINUTE	<input type="text" value="3"/> <input type="text" value="0"/> <input type="text" value="0"/>			
BEAM ALIGNMENT	<input type="text" value=""/> <input type="text" value=""/> <input type="text" value=""/>				FOCUS ADJUST.	<input type="text" value=""/> <input type="text" value=""/> <input type="text" value=""/>			
HIGH VOLTAGE ADJUST.	<input type="text" value="N"/> <input type="text" value="A"/> <input type="text" value=""/>				AVR	Lock	<input type="checkbox"/>	Unlock	<input checked="" type="checkbox"/>

X-Ray Serial Number _____
Mag. Inspection _____
Acceptance Standard _____
Metallurgical Exam. _____

Operator _____
MR & D Engineer J. C. Collins
Process Control _____

ELECTRON BEAM WELDING SCHEDULE

Schedule Number _____ Date 8-22-73
 Part Number MD-3232-2 Part Name _____ Material Type 10Ni, Hy180
 Serial Number H-13 Tool Number _____ Mat'l. Thick .500
 Filler Wire Type Low alloy Hy180/220 Diameter .062
 (10Ni, Cr. Mo-Co)
 Heat No. 51361

UPPER CONTROL PANEL

HV START Delay <div style="border: 1px solid black; padding: 2px;">0 0 2</div>	MOTOR START Delay <div style="border: 1px solid black; padding: 2px;">0 0 2</div>	HIGH VOLTAGE Initial KV <div style="border: 1px solid black; padding: 2px;">4 7. 5</div>	Final <div style="border: 1px solid black; padding: 2px;">0 0 9</div>	SPEED ADJUSTMENT Initial and Final
Seconds <div style="border: 1px solid black; padding: 2px;">X 30 60 120</div>	Seconds <div style="border: 1px solid black; padding: 2px;">X 15 30 60 120</div>	Slope <div style="border: 1px solid black; padding: 2px;">0 1 2</div>	Slope <div style="border: 1px solid black; padding: 2px;">0 4 5</div>	Run <div style="border: 1px solid black; padding: 2px;">3 0 0</div>

OSCILLATOR

AXIS X <input type="checkbox"/> Y <input checked="" type="checkbox"/>	FREQUENCY, KC <div style="border: 1px solid black; padding: 2px;">0 0 5</div>	RANGE X <div style="border: 1px solid black; padding: 2px;">1 0 0</div>
ATTENUATION, Db <div style="border: 1px solid black; padding: 2px;">0 0 0</div>	METER RANGE <div style="border: 1px solid black; padding: 2px;">2 0</div>	METER READING <div style="border: 1px solid black; padding: 2px;">0 0 9</div>

CENTER CONTROL PANEL

SKETCH OF JOINT

BEAM CURRENT, MA	HIGH VOLTAGE, KV	TRAVEL, IPM	
Pass 1 <div style="border: 1px solid black; padding: 2px;">3 0 0</div>	<div style="border: 1px solid black; padding: 2px;">2 7. 5</div>	<div style="border: 1px solid black; padding: 2px;">3 0. 0</div>	
Pass 2 <div style="border: 1px solid black; padding: 2px;">1 6 0</div>	<div style="border: 1px solid black; padding: 2px;">1 8. 0</div>	<div style="border: 1px solid black; padding: 2px;">2 6. 0</div>	
Pass 3 <div style="border: 1px solid black; padding: 2px;"></div>	<div style="border: 1px solid black; padding: 2px;"></div>	<div style="border: 1px solid black; padding: 2px;"></div>	
FOCUS CURRENT METER <div style="border: 1px solid black; padding: 2px;">5. 2 2</div> DC Amps.	GUN FILAMENT METER <div style="border: 1px solid black; padding: 2px;">0 6 5</div> AC Amps.	FILAMENT ADJUST POT. <div style="border: 1px solid black; padding: 2px;">0 7 7</div>	TYPE OF JOINT BUTT

GUN ELEMENTS

GUN TYPE, KV <div style="border: 1px solid black; padding: 2px;">6 0</div>	BIAS On <input type="checkbox"/> Off <input checked="" type="checkbox"/>
FILAMENT, MA <div style="border: 1px solid black; padding: 2px;">5 0 0</div>	METER, AC VOLTS <div style="border: 1px solid black; padding: 2px;"></div>
CATHODE, MA <div style="border: 1px solid black; padding: 2px;">7 5 0</div>	VOLTAGE ADJUST. <div style="border: 1px solid black; padding: 2px;"></div>
ANODE, KV/MA <div style="border: 1px solid black; padding: 2px;">7 5 0</div>	Mid-point focus
SPACER, Inches <div style="border: 1px solid black; padding: 2px;">0 0 0</div>	GUN-TO-WORK DISTANCE, Inches <div style="border: 1px solid black; padding: 2px;">3. 5</div>

OPERATOR'S STATION CONTROL

X-AXIS On <input checked="" type="checkbox"/> Off <input type="checkbox"/>	Y-AXIS On <input type="checkbox"/> Off <input checked="" type="checkbox"/>
DIRECTION Fwd. <input type="checkbox"/> Rev. <input type="checkbox"/>	DIRECTION Fwd. <input type="checkbox"/> Rev. <input type="checkbox"/>
TRAVEL SPEED, IPM <div style="border: 1px solid black; padding: 2px;">3 0. 0</div>	TRAVEL SPEED, IPM <div style="border: 1px solid black; padding: 2px;"></div>
WIRE FEED On <input checked="" type="checkbox"/> Off <input type="checkbox"/>	INCH PER MINUTE <div style="border: 1px solid black; padding: 2px;">3 0. 0</div>
BEAM ALIGNMENT <div style="border: 1px solid black; padding: 2px;">NA</div>	FOCUS ADJUST. <div style="border: 1px solid black; padding: 2px;">5. 2 2</div>
HIGH VOLTAGE ADJUST. <div style="border: 1px solid black; padding: 2px;">NOTED</div>	AVR Lock <input type="checkbox"/> Unlock <input checked="" type="checkbox"/>

X-Ray Serial Number _____ Operator _____
 Mng. Inspection _____ MR&D Engineer J. C. Collins
 Acceptance Standard _____ Process Control _____
 Metallurgical Exam. _____

ELECTRON BEAM WELDING SCHEDULE

Schedule Number FMR 60-2154 Date 10-9-73
 Part Number 603R-100-11-5-H18 Part Name _____ Material Type 10Ni (Hy180)
 Serial Number 473943 Tool Number _____ Mat'l. Thick .900
CSC 1000-1-2-4 thru 7 Filler Wire Type _____ Diameter .062"

UPPER CONTROL PANEL

HV START Delay	MOTOR START Delay	HIGH VOLTAGE		SPEED ADJUSTMENT Initial and Final
0 0 5	0 0 3	Initial KV 4 4 0	Final 0 5 9	004
Seconds 15 30 60 120	Seconds 15 30 60 120	Slope 0 0 7	Slope 0 4 5	Run 0 1 4

OSCILLATOR

AXIS X <input checked="" type="checkbox"/> Y <input type="checkbox"/>	FREQUENCY, KC 0 0 5	RANGE X <input type="checkbox"/> 1 0 0
ATTENUATION, Db 0 0 0	METER RANGE 2 0	METER READING <input type="checkbox"/> - <input type="checkbox"/> 9

CENTER CONTROL PANEL

SKETCH OF JOINT

BEAM CURRENT, MA	HIGH VOLTAGE, KV	TRAVEL, IPM	TYPE OF JOINT BUTT
Pass 1 4 4 0	3 4. 5	1 8. 0	
Pass 2 1 8 0	1 8. 0	1 8. 0	
Pass 3 1 6 0	1 8. 0	1 8. 0	
FOCUS CURRENT METER 5. 2 2 DC Amps.	GUN FILAMENT METER 0 6 5 AC Amps.	FILAMENT ADJUST POT. 0 7 6	

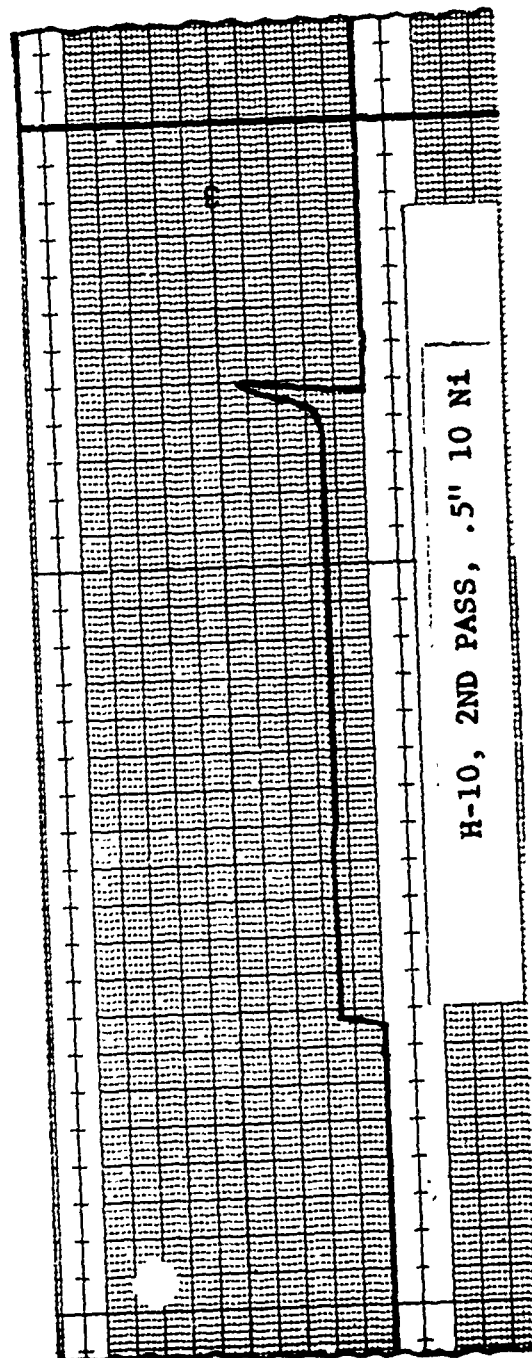
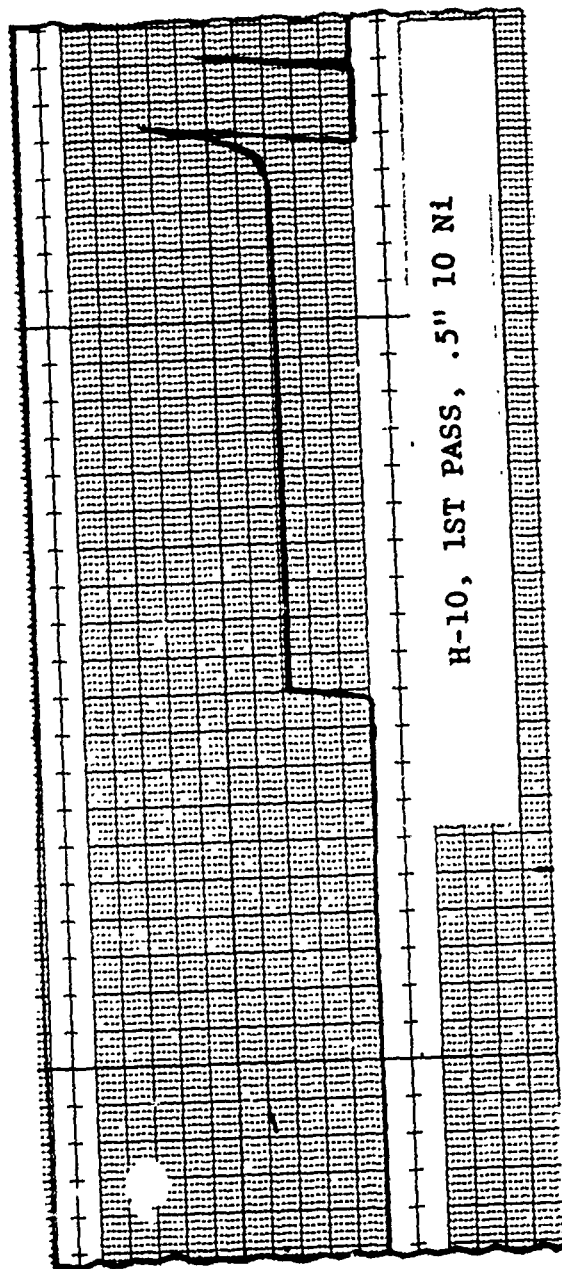
GUN ELEMENTS

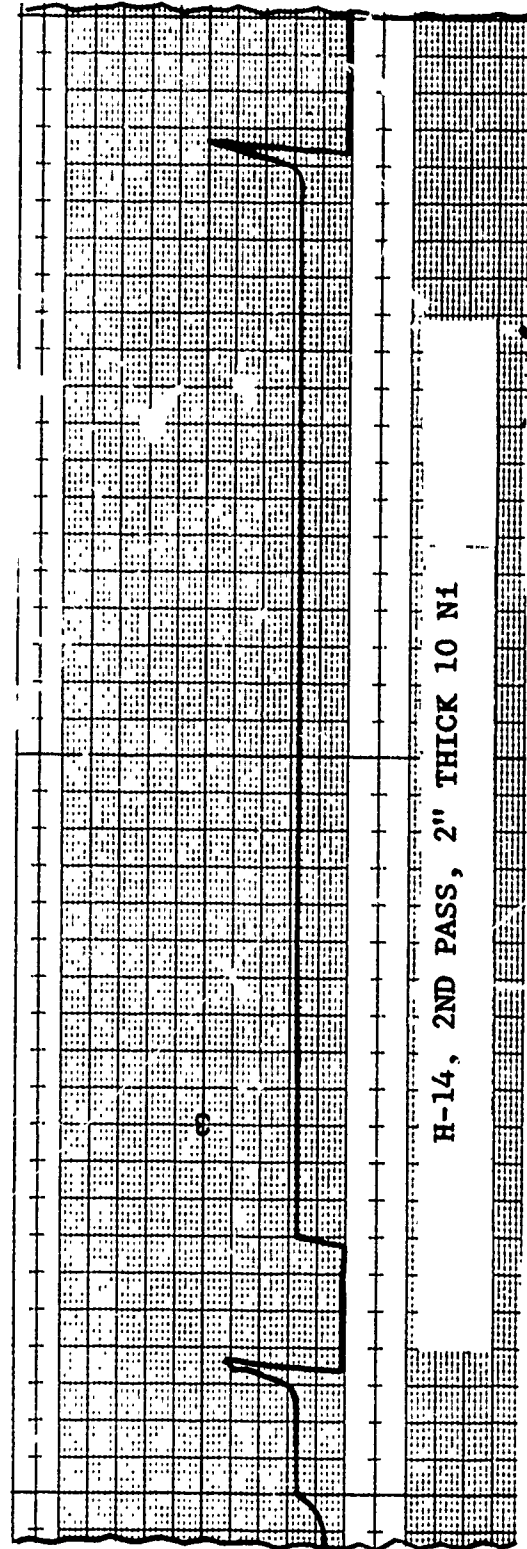
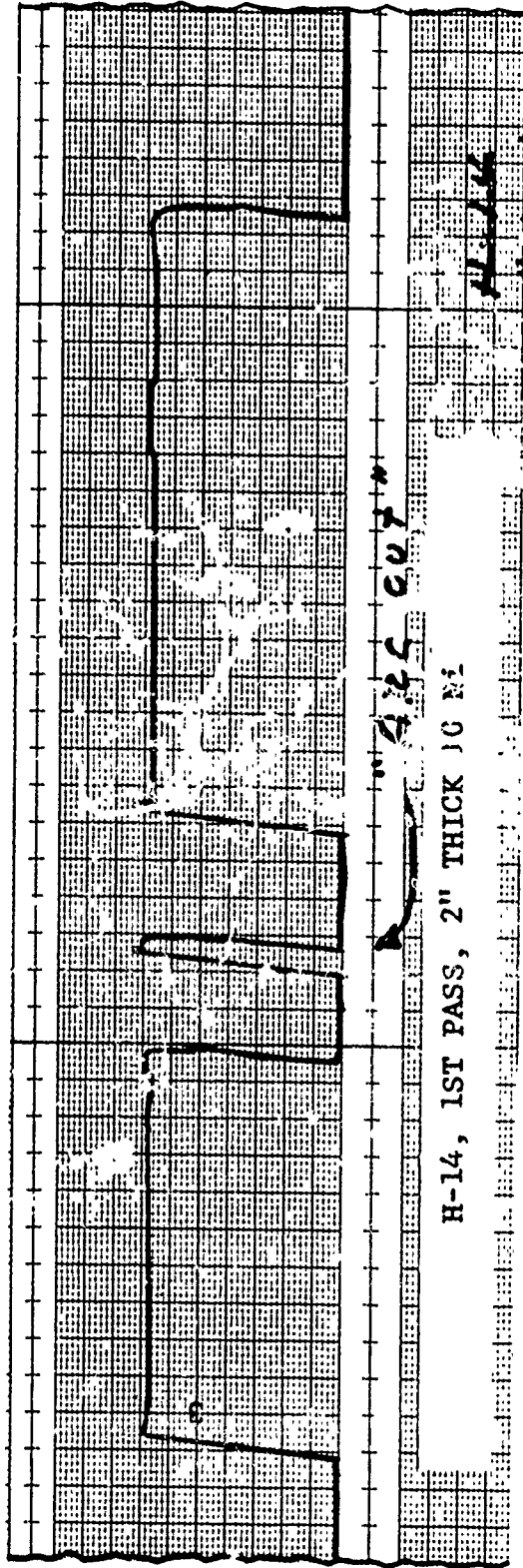
GUN TYPE, KV 6 0	BIAS On <input type="checkbox"/> Off <input checked="" type="checkbox"/>
FILAMENT, MA 5 0 0	METER, AC VOLTS <input type="checkbox"/> <input type="checkbox"/> <input type="checkbox"/>
CATHODE, MA 7 5 0	VOLTAGE ADJUST. <input type="checkbox"/> <input type="checkbox"/> <input type="checkbox"/>
ANODE, KV/MA 7 5 0	Mid-point focus _____
SPACER, Inches 0 0 0	GUN-TO-WORK DISTANCE, inches 3. 5

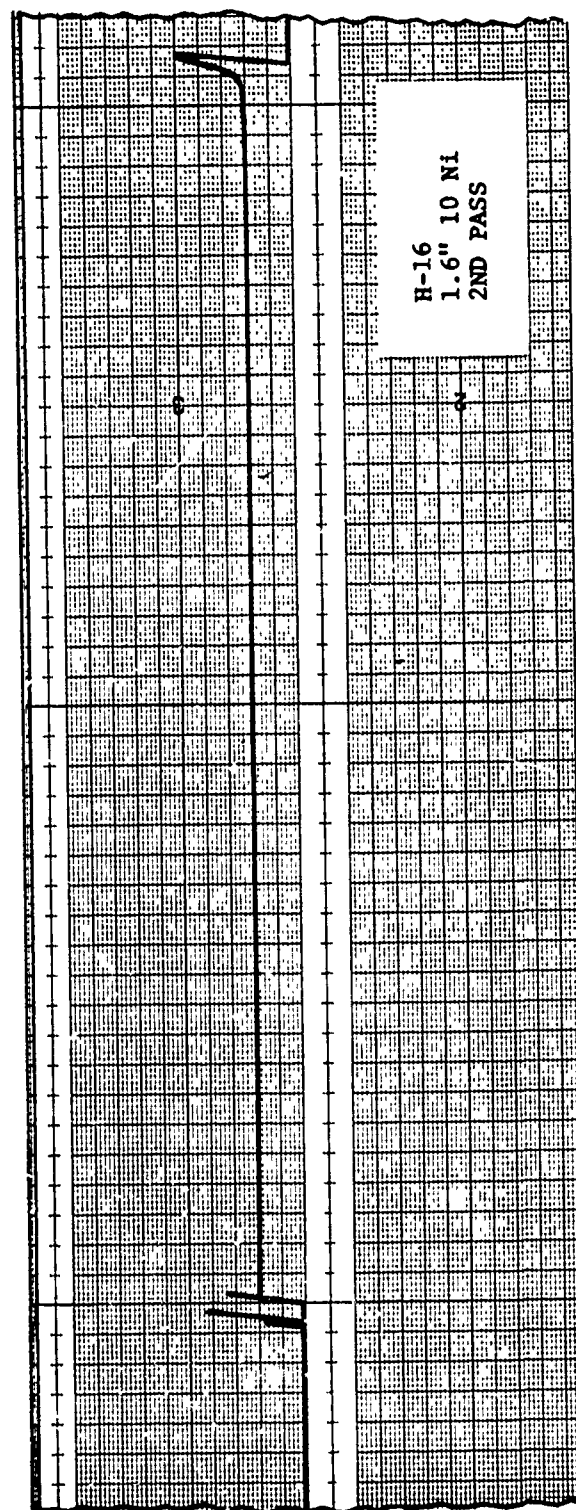
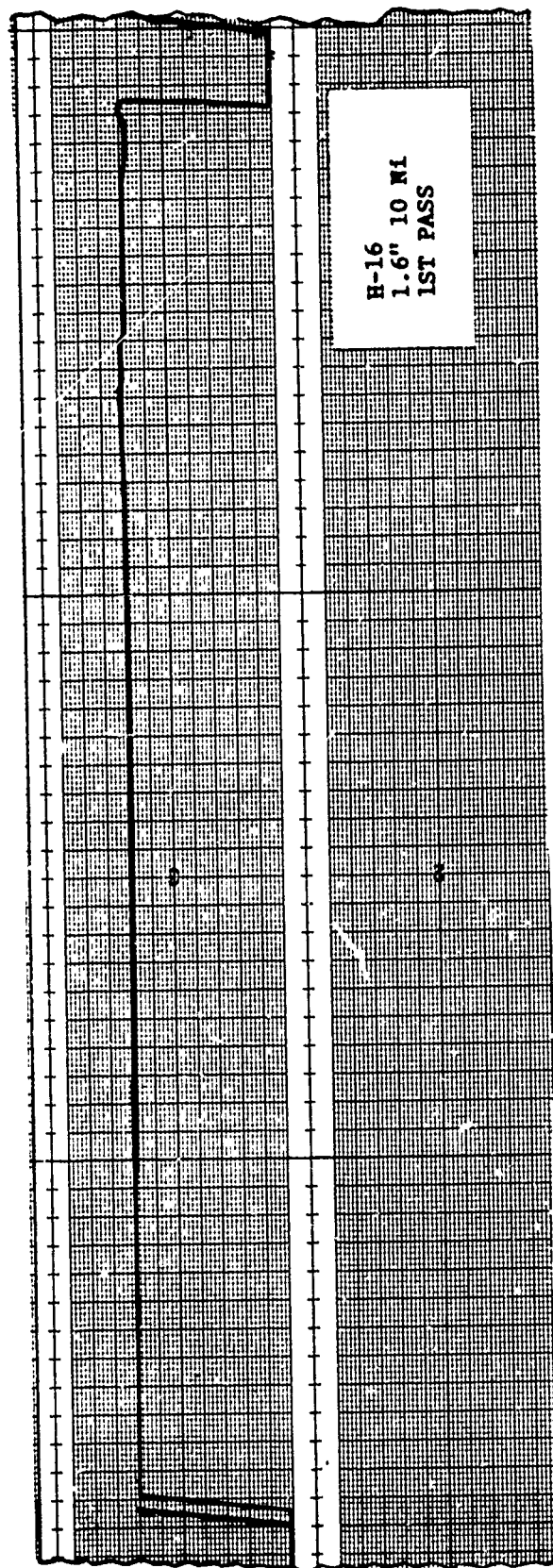
OPERATOR'S STATION CONTROL

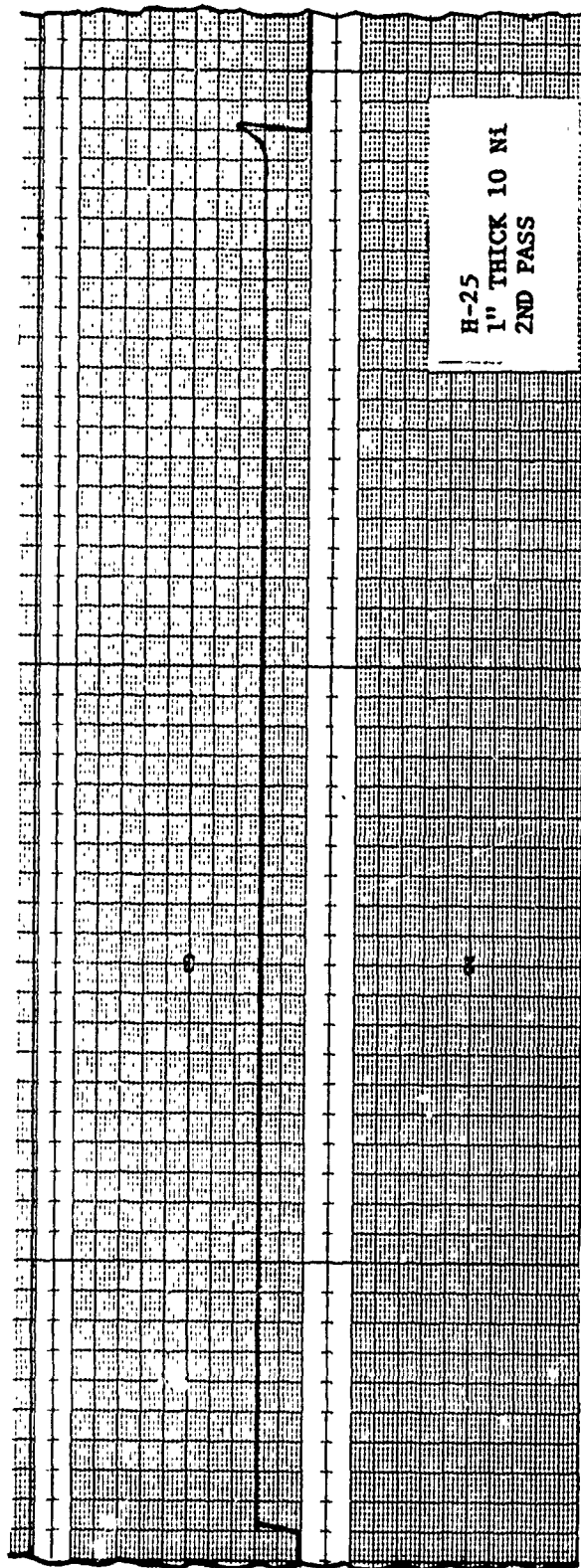
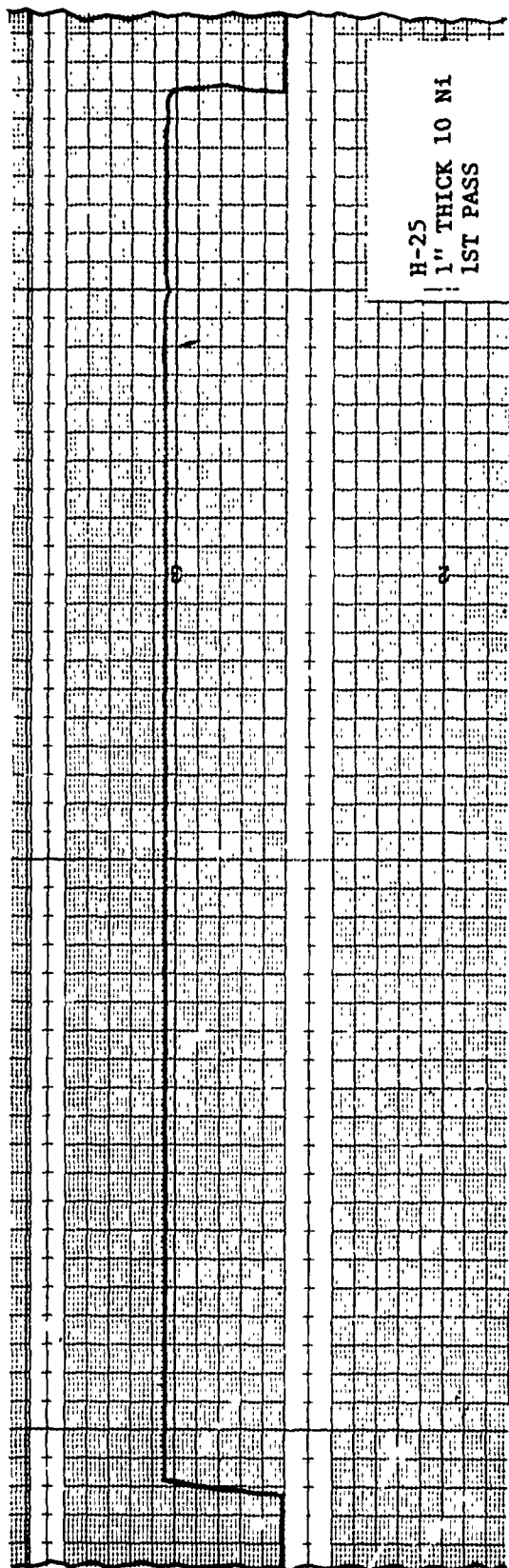
X-AXIS On <input checked="" type="checkbox"/> Off <input type="checkbox"/>	Y-AXIS On <input type="checkbox"/> Off <input type="checkbox"/>
DIRECTION Fwd. <input type="checkbox"/> Rev. <input checked="" type="checkbox"/>	DIRECTION Fwd. <input type="checkbox"/> Rev. <input type="checkbox"/>
TRAVEL SPEED, IPM 1 8. 0	TRAVEL SPEED, IPM <input type="checkbox"/> <input type="checkbox"/> <input type="checkbox"/>
WIRE FEED On <input checked="" type="checkbox"/> Off <input type="checkbox"/>	INCH PER MINUTE 3 0. 0
BEAM ALIGNMENT <input type="checkbox"/> <input type="checkbox"/> <input type="checkbox"/>	FOCUS ADJUST. 5. 2 2
HIGH VOLTAGE ADJUST. NOTED	AVR Lock <input type="checkbox"/> Unlock <input checked="" type="checkbox"/>

X-Ray Serial Number _____ Operator _____
 Mag. Inspection _____ MR&D Engineer J. C. Collins
 Acceptance Standard _____ Process Control _____
 Metallurgical Exam. _____









Unclassified

Security Classification

DOCUMENT CONTROL DATA - R & D		
(Security classification of title, body of abstract and indexing annotation must be entered when the overall report is classified)		
1. ORIGINATING ACTIVITY (Corporate author) Air Force Flight Dynamics Laboratory (FBA) Air Force Systems Command Wright-Patterson Air Force Base, Ohio 45433		2a. REPORT SECURITY CLASSIFICATION Unclassified
		2b. GROUP
3. REPORT TITLE Advanced Metallic Air Vehicle Structure Program		
4. DESCRIPTIVE NOTES (Type of report and inclusive dates) Phase II - Detail Design and Analysis Summary Report - Technical		
5. AUTHOR(S) (First name, middle initial, last name) C. E. Hart, et al.		
6. REPORT DATE	7a. TOTAL NO. OF PAGES 476	7b. NO. OF REFS
8a. CONTRACT OR GRANT NO F33615-73-C-3001	9a. ORIGINATOR'S REPORT NUMBER(S) AFFDL-TR-74-17	
b. PROJECT NO. 486U		
c.	9b. OTHER REPORT NO(S) (Any other numbers that may be assigned this report)	
d.		
10. DISTRIBUTION STATEMENT Distribution limited to U.S. Government Agencies only. Reason: Test and Evaluation. Other requests for this document must be referred to Air Force Flight Dynamics Laboratory/FBA, Wright-Patterson Air Force Base, Ohio 45433.		
11. SUPPLEMENTARY NOTES		12. SPONSORING MILITARY ACTIVITY Air Force Flight Dynamics Laboratory Air Force Systems Command Wright-Patterson AFB, Ohio 45433
13. ABSTRACT <p>This report covers the design, analysis, manufacturing and testing done during Phase II, Detail Design, of the Advanced Metallic Air Vehicle Structure (AMAVS) program. The objectives of Phase II were to complete the detail design work for two configurations of a wing carrythrough structure for a movable-wing aircraft, to complete materials and component testing in support of the two configurations, to select one of the configurations for manufacture in Phase III and to continue design and manufacture of a fixture for full-scale testing of the carrythrough structure.</p> <p>Additional trade studies and design optimization studies were conducted in the early part of Phase II for the two configurations selected in Phase Ib: Fail Safe Integral Lug (FSIL) and "No-Box" Box (NBB). An updated baseline data package was received during Phase II and the configurations were revised to meet the modified baseline requirements.</p> <p>Material testing and component testing were completed. Beta annealed 6Al-4V and Beta C titanium and 10Ni steel (HY180) were used in these tests.</p> <p>Some detail design work remains on the full-scale test fixture but manufacturing has started. Manufacture of the simulated fuselage structure has also begun.</p> <p>The NBB configuration which utilizes the outstanding fracture toughness and good crack growth characteristics of 10Ni steel has been selected for manufacture in Phase III.</p>		

DD FORM 1473
1 NOV 65

Unclassified

Security Classification

Unclassified
Security Classification

14	KEY WORDS	LINK A		LINK B		LINK C	
		ROLE	WT	ROLE	WT	ROLE	WT
	Structural Design Stress Analysis Fracture Mechanics Materials Manufacturing Technology Damage Tolerance						

Unclassified
Security Classification